

90-M-0225

①

100% COPY

Third International Workshop on

Gravel-Bed Rivers

"DINAMICS OF GRAVEL-BED RIVERS"

Firenze - Poggio a Caiano - 24-28 September 1990

Florence July 31, 1990

DTIC  
ELECTE  
AUG 20 1990  
S B D

Your reference: AMXSN-UK-RE/R&D 6510-EN-02 (70-1s)

Following your letter of April 2, 1990, I enclose a first set with the agreed 8(eight) copies of the paper presentations. Unfortunately very few authors haven't yet submitted their paper. As they arrive to me I'll send you a second set with 8(eight) copies of them.

Thank you for your support.

Sincerely yours

3rd International Workshop  
on  
Gravel - Bed Rivers  
Firenze, 24-28 September 1990

Dr. Paolo BILLI

*Paolo Billi*

DISTRIBUTION STATEMENT A

Approved for public release  
Distribution is unlimited

AD-A225 520



## "DINAMICS OF GRAVEL-BED RIVERS"

Firenze - Poggio a Caiano - 24-28 September 1990

### DISTRIBUTION STATEMENT A

Approved for public release;  
- Distribution Unlimited

#### SCIENTIFIC COMMITTEE

P. Billi, University of Florence, Italy (Treasurer)  
P. Canuti, University of Florence, Italy (Secretary)  
P. Tacconi, University of Perugia, Italy (Chairman)  
C. R. Thorne, University of Nottingham, U.K.

#### HONOUR COMMITTEE

W.W. Emmett, U.S. Geological Survey, Denver, U.S.A.  
L.B. Leopold, University of Berkeley, U.S.A.  
F. Mancini, University of Florence, Italy  
E. Marchi, University of Genoa, Italy  
L. Ubertini, University of Perugia, Italy  
G.W. Wolman, Johns Hopkins University, Baltimore, U.S.A.

#### ORGANIZING INSTITUTIONS

Dipartimento di Ingegneria Civile, University of Florence  
Dipartimento di Scienze della Terra, University of Florence  
Istituto di Ingegneria Ambientale, University of Perugia

#### SPONSORS

C.N.R. - Gruppo Nazionale Difesa Catastrofi Idrogeologiche  
C.N.R. - Comitato Nazionale Scienze Geologiche e Minerarie  
CONSIAG - Azienda Consorziale Acqua e Gas, Prato  
Università di Firenze  
U.S. Army - Research Development and Standardisation Group, London, UK

#### PATRONAGE

Azienda di Promozione Turistica Firenze  
Ministero dell'Ambiente  
Ministero dell'Università e della Ricerca Scientifica  
Provincia di Firenze  
Regione Toscana

#### SECRETARIAT

Dipartimento di Ingegneria Civile  
Via S. Marta, 3 - 50139 Firenze, Italy  
Phone (055) 4796225  
Fax (055) 404375

## VENUE

The workshop will be held in the Hotel Hermitage, Via Ginepraia 112, Poggio a Caiano, phones: (055) 877040-877244-8777085-8777045.

### How to reach Poggio a Caiano:

From 13:00 to 22:00 <sup>if Sunday don't</sup> a Workshop Reception Point will be specially set up in the Florence main station (Firenze Santa Maria Novella). On your arrival, please, look for it. During the same hours a shuttle service between Santa Maria Novella Station and the workshop hotel will be held by minibus; please, meet at the reception point. The organizers invite the attending people to take this chance as it is not easy to reach the conference site by public bus services.

Alternatively the workshop hotel can be reach privately by taxi at an approximate rate of Lit. 50,000.

Florence has only a small airport, while there are good train links from Rome (2 hours of travel), Milan (3 hours), and Pisa (1 hour) to Florence Santa Maria Novella.

However, for any problem please contact the workshop secretariat at the conference hotel (see above) which will be working from 9:00 am of Sunday 23rd.

## USEFULL INFORMATIONS

- Obviously bank offices are closed on sunday 23rd. Currency can be changed at the hotel reception desk.
- The weather in september is commonly mild, but recent years experiences suggest to consider a wide range of conditions from rather hot and bright to relatively cool and rainy.
- No programme for accompanying persons is scheduled
- A registration desk will operate at Hermitage Hotel (Poggio a Caiano) on Sunday 23 from 9:00 am to 9:00 pm and on Monday 24 from 8:00 am to 9:00 am.
- A minibus shuttle service will operate from the conference hotel arriving to Firenze Santa Maria Novella Station on the evening of Friday 28 at 8:00 pm and on the morning of Saturday 29 at 9:00 am.
- The field trip on Tuesday 25 will start from the conference hotel at 3:00 pm. The return to the hotel is forecast at about 11:00 pm. Accompanying persons are mostly welcomed (a sweater could be usefull!).
- The field trip on Saturday 29 will start from the conference hotel at 7:00 am and will end at the conference hotel at about 9:00. On the way back, a stop at Firenze Santa Maria Novella station can be scheduled on request (again don't forget your sweater!).

## RESPONSABILITY

The organizing committe takes no responsability for any damage to attending people, baggage and properties.

Accession For	
NTIS GRA&I	<input checked="checked" type="checkbox"/>
DTIC TAB	<input type="checkbox"/>
Unannounced	<input type="checkbox"/>
Justification	
By _____	
Distribution/	
Availability Codes	
Dist	Avail and/or Special
A-1	



## TECHNICAL PROGRAMME

Scientific sessions will usually start at 9.00 a.m and will end at 5.30 p.m.

In the conference room a 5X5 slide projector and a overhead projector will be available.

Those having produced scientific videos on gravel-bed rivers and related aspects are kindly invited to present them on the evening of Wednesday 26 using the standard european VHS and the Video 8 systems.

### **Monday 24 September**

#### **Morning**

##### **I INTRODUCTION AND KEYNOTE ADDRESSES**

1. G. Wolman: Gravel-bed rivers. Some possible keynotes
2. M. Newson: Gravel-bed rivers, floods and thresholds

##### **II SEDIMENT YIELD DYNAMICS**

3. J. Bathurst, S. White: Modelling sediment yield
4. S. Moretti, F. Brunori, L. Chiarantini: Modelling sediment supply
5. G. Leeks: Fluvial sediment transport and plantation forestry: monitoring and application - Case studies from upland Mid-Wales, UK

#### **Afternoon**

##### **III DEBRIS FLOW DYNAMICS**

6. F. Iseya, H. Ikeda, H. Maita: Fluvial deposits in a torrential gravel-bed stream by extreme sediment supply: sedimentary structure and depositional mechanism
7. P. Canuti, C. Garzonio, G. Rodolfi: The historical and catastrophic debris flow phenomena of Mt. Falterona (Tuscany, Italy)
8. D. Rickenmann: Analysis of massive sediment transport processes in torrents

##### **IV ALLUVIAL FAN AND STEEP STREAM SEDIMENT PROCESSES**

9. A. Harvey: Sediment transport processes on alluvial fans: influence on fan morphology
10. A. Schick, J. Lekach: Bed material conveyance in a flash-flood system: magnitude, frequency, mechanics
11. P. Carling, A. Kelsey, M.S. Glaister: Effect of bed roughness, particle shape and orientation on initial motion criteria

## **Tuesday 25 September**

### **Morning**

#### **V CHANNEL MORPHOLOGY DYNAMICS**

- 12. C.R. Thorne: Flow processes in gravel-bed bends
- 13. M. Colombini, M. Tubino, P. Whiting: Topographic expression of bars in meandering channels
- 14. L.B. Leopold: The sediment size that determines channel morphology

#### **VI BRAIDED CHANNEL DYNAMICS**

- 15. R.I. Ferguson, P.J. Ashworth: Spatial pattern of bedload transport and channel change in braided and near-braided rivers
- 16. J. Laronne, M.J. Duncan: Bedload transport path and gravel bar formation
- 17. P. Ashworth, M. Powell: The mode of medial bar formation or the sorting processes in braided rivers.

### **Afternoon**

#### **VII DOWNSTREAM FINING**

- 18. A. Werritty: Downstream fining in a gravel-bed river in S. Poland: lithologic controls and the role of abrasion
- 19. A. Armanini: Variation of bed and transport mean diameters in erosion-deposition processes

- Field trip to Virginio stream

## **Wednesday 26 September**

### **Morning**

#### **VIII GRAIN-SIZE DISTRIBUTION**

- 20. H. Ibbeken: The mystery of bimodality: falsification of current concepts, proposal of a new one
- 21. I. Becchi, P. Billi, A. Moro: Grain-size distribution characteristics: an advanced problem for statistical tools
- 22. K. Bunte: Counting instead of weighing: grain-size composition of coarse material bedload in a mountain stream expressed in particle number transport rate

#### **IX ENTRAINMENT AND MOVEMENT AT LOW TRANSPORT RATES**

- 23. E. Andrews: Marginal bedload transport rates
- 24. P. Diplas, G. Parker: Deposition and removal of fines in gravel-bed streams
- 25. M. Kondolf: Salmonid spawning gravels: size distribution and modification by spawning fish

## **Afternoon**

### **X ARMOURING**

- 26. B.B. Willetts, S.J. Tait, J.K. Maizels: Laboratory observation of bed armouring and changes in bed load composition
- 27. E. Paris, A. Lamberti: Analysis of armouring processes through laboratory experiments
- 28. T. Lisle, M.A. Madej: Spatial variation in armouring in a channel with high sediment supply

### **XI MOVEMENT OF MIXED-SIZED SEDIMENT**

- 29. P.D. Kumar, Shyue-Ming Shih: Equal grain mobility versus changing bedload grain size in gravel-bed streams
- 30. P.R. Wilcock: Bed-load transport of mixed-size sediment
- 31. R.A. Kuhnle: Fractional transport rates of bed load on Goodwin Creek

## **Evening**

- Video session: informal projection of videos on gravel-bed rivers

## **Thursday 27 September**

### **Morning**

### **XII MONITORING OF PARTICLE MOVEMENT: NEW TECHNIQUES**

- 32. P. Tacconi, M. Rinaldi, S. Moretti, M. Matteini: Monitoring of particle movement on Virginio gravel-bed stream.
- 33. M.A. Hassan, M. Church: The movement of individual grains on the stream bed
- 34. W. Emmett: Movement of coarse particles monitored by micro radio transmitters

### **XIII MODELLING SEDIMENT TRANSPORT**

- 35. G. Di Silvio: Modelling sediment transport: dominant features to be simulated in different hydrological and morphological circumstances
- 36. R.R. Copeland, W.A. Thomas: Numerical modelling of gravel movement in concrete channels
- 37. A. Lamberti, L. Montefusco: Sediment transport in steep plane beds: a general model.

## **Afternoon**

### **XIV BED DYNAMICS**

- 38. I. Reid, L. Frostick, A.C. Brayshaw: Microform roughness elements and the selective entrainment and entrapment of particles in gravel-bed rivers
- 39. P. Ergenzinger: River bed adjustments in a step-pool system (Lainbach, Upper Bavaria).

40. R. Hey, D.J. Needham: Dynamic modelling of bed waves

### **Evening**

- Workshop banquet

### **Friday 28 September**

#### **Morning**

#### XV ANALYSIS OF HISTORICAL CHANGES

- 41. C. Fritz, G. Giada, V. Villi (IT): Long term sediment budget in an alpine catchment
- 42. J. Hooke, C.E. Redmond: Causes and nature of river planform changes
- 43. M.G. Macklin, B.T. Rumsby, M.D. Newson: Historic floods and vertical accretion of fine-grained alluvium in the lower Tyne valley, North East England

#### XVI HUMAN IMPACTS

- 44. M. Jaeggi: Effect of engineering solutions on sediment transport
- 45. D. Sear: The effect of river regulation for hydro-electric power on sediments and sediment transport within riffle-pool sequences
- 46. B.R. Hall, W.A. Thomas, M.L. Pearson: Computing bed-load discharge and channel adjustment in a cobble bed river for flood control channel design

#### CONCLUDING REMARKS

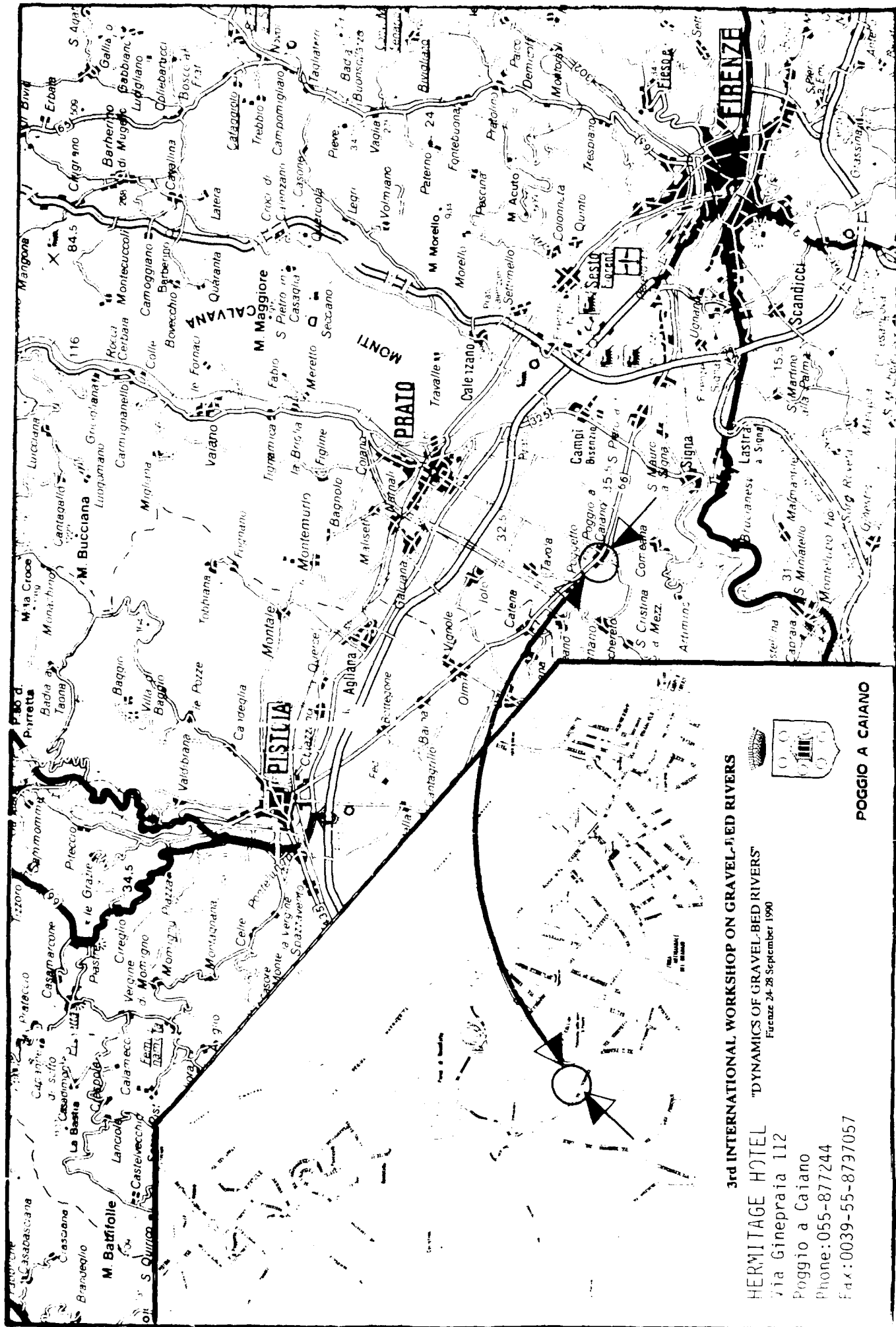
- 47. L. Leopold: Overview of gravel-bed river dynamics.

#### **Afternoon**

- Departure for people not going on the field trip

### **Saturday 29 September**

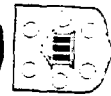
- Field trip: Gravel-Bed River Dynamics in Southern Tuscany



# 3rd INTERNATIONAL WORKSHOP ON GRAVEL-BED RIVERS

HERMITAGE HOTEL "DYNAMICS OF GRAVEL-BED RIVERS"

Firenze 24-28 September 1990



POGGIO A CAIANO

Via Gineproia 112

Poggio a Caiano

Phone: 055-877244

Fax: 0039-55-8797057

Gravel-Bed Rivers  
Some Possible Keynotes  
M. Gordon Wolman  
The Johns Hopkins University  
June, 1990

Everyone knows what a gravel-bed river is, yet describing the particle size distribution on the bed of a river tells only a small part of the story. The patterns of gravel-bed rivers range from braided channels with many branches to straight flumes or canal-like natural rivers. The banks of gravel-bed rivers may be composed of gravel or a wide variety of materials and particle sizes ranging from clay and clay sizes to mosses and sedges. The gradients of gravel-bed rivers may be very steep or quite gentle as in many trout streams treasured by local fly fishermen.

Not only do gravel-bed rivers range in size, plan, profile, and cross section, but our interest in them spans a similar range. At one extreme human concern for gravel-bed rivers focuses upon attempts to maintain the "natural" river and riparian system in a world dominated by human activity. At the opposite extreme, the concept of control is evoked to fix the position and form of an unruly natural stream to prevent it from behaving in a "natural" fashion, to preserve the adjacent lands from erosion, or to assure a fixed channel to speed the passage of floods or to assure navigability.

Given the variety of gravel-bed rivers and the range of objectives inspiring interest in such rivers, few specific topics clearly warrant priority of inquiry over others. In the preface to the remarkable volume representing the deliberations of the Second International Workshop on gravel-bed rivers it is noted that at the First International Workshop in 1980, "the major obstacle to achieving goals [of better management guidelines] was identified as a lack of knowledge concerning sediment transport processes..." Both understanding of process and its application to management require continuing work refining the understanding of transport processes which control the behavior of gravel-bed rivers. The second conference made major contributions to this understanding. Despite such progress, uncertainties remain about sediment transport even when "gravel" alone is transported in the bed of the river channel. As the papers in the 1987 volume made clear, the full range of hydrologic and hydraulic complexities is also reflected in the behavior of gravel-bed rivers.

Papers in the second workshop contain careful evaluations of transport models along with cautions about the variety of materials in gravel-bed rivers, possible effects of ranges in particle size including suspended load, and the relative confidence in the application of transport equations to conditions where the channel geometry is assumed and water flow and sediment movement calculated, as opposed to those conditions estimates of channel features are to be derived from principles of hydrology and hydraulics in channels with mobile boundaries. Has a consensus emerged on the present

state-of-the-art of sediment transport estimation and observation? Is it premature to provide confidence intervals for the estimation of sediment movement in gravel-bed rivers, qualified or structured according to a rough classification of the variety of gravel-bed rivers?

Equilibrium concepts applied channel form and plan have assumed steady state and uniform flow in characterizing the relationship between geometry and flow in specific reaches. From the outset, it has been known that these assumptions are simplifications of the natural world. Analogies between regime canal systems and natural rivers have recognized the disparity in hydrologic regimen between the two while marveling at the apparent similarity of the resulting river features. Design criteria for river control mimicking canal design have sought to minimize problems associated with the variability of flow and transport in natural rivers. "Dominant" and "channel-forming" discharge are surrogates for a more complex reality, and recognized as such. Is sufficient information now available to do without the single flow concept implied in dominant, channel-forming or bankfull discharge in the hydrology relating to river form or pattern? The literature on flow and transport variability grows, but the association of flow variability and channel behavior is more weakly supported. The time history of channel behavior coupled with flow variation is poorly known and hence models of temporal change are hard to verify. Perhaps it is time for a structured inquiry designed at an international level to monitor carefully both flow and channel behavior in a well chosen sample of gravel-bed rivers.

As one moves from interest in the geomorphic characteristics and behavior of gravel-bed rivers to a focus upon society's demands and interest in such rivers, the scope of inquiry expands. A simple classification of the range of interest can be shown based on an artificial dichotomy between the natural and the controlled river (Table). The dichotomy is artificial because even the so-called natural channel is beginning to require management either because human beings really do not like the "natural", or because the natural channel system is being markedly altered by human activities on most areas of the drainage basin which control the downstream fluvial system. In addition, one cannot separate the channel itself from the riparian margin. The channel alone, however, has received the lion's share of attention in research and management. Moreover, in each domain, the aquatic and terrestrial, there are plants and animals whose habitat and behavior are essential features of the management of both natural and controlled river systems.

The spatial and temporal characteristics of fish habitats are receiving increasing attention. Riparian terrestrial vegetation, particularly trees, have been the subject of intense study; first from the standpoint of evapotranspiration and water loss, and more recently because of the relationship between water loss and instream flow requirements. Aquatic plants, rooted and lotic are vital to the habitat and to the quality of the river waters themselves and, of course, vegetation has long been recognized as an important component of boundary material confining the channel cross-section. Relatively few observations, however, quantify these effects. While not new, emphasis upon the riparian scene as a whole, including the biota as well as upon the channel, appears to be critical for understanding and hence, management of gravel-bed rivers. The humorist Robert Benchley discussed an

international fisheries agreement from the standpoint of the fish. Perhaps a view of the gravel-bed river from the standpoint of a fish, a bird, or a tree plant might be useful in suggesting hypotheses to be tested of observations to be made of different parameters in different ways. What are the interactions of biota, channel, and riparian margin?

Managing the controlled or regulated natural channel whether for navigation, erosion control, gravel extraction or recreation faces the same issues as those encountered in a natural scene. Further, multiple use, while sometimes a euphemism glossing over conflicting objectives, dominates in many gravel-bed rivers. Such multiple objectives can be seen where groins are used in bank control and the habitat for birds within the slack water between the groins becomes a major environmental objective issue. A habit of visualizing the controlled or natural river from the standpoint of the fish, the birds, and the trees might mitigate the likely regret associated with failure to satisfy a variety of social values expressed by society as such values change over the years. The relationship between bank erosion control, floodway design, and habitat for biota might provide a framework for review and summary in a more sophisticated handbook for the management of some gravel-bed rivers than currently exists.

As noted earlier, the words gravel-bed rivers encompass an enormous range of channel and riparian characteristics. The continuum represented by both the downstream channel system within a drainage basin and by the variety of channel forms and patterns is well known. At the same time, the challenge of classification based on quantitative measures remains. We are hard pressed to quantify the description of bank material in the natural scene, let alone relate the full range of hydrologic behavior, geologic setting, and temporal variations to one another as determinants of channel form and pattern. Yet, in the absence of quantitative classification, it is difficult to transfer information derived from experience and observation in one place to that in another. In theory, it is correctly assumed that understanding and hence modelling based upon first principles is the basis for transferability. But, we also recognize the nearly infinite variability of the natural scene which requires reasoning by analogy as well as by the application of principles. Any classification of a continuum will require arbitrary "splitting or lumping", as the paleontologists recognize, but diagrammatic representation of channel forms would be much improved if the axes were quantitative rather than qualitative. Can this be achieved today for gravel-bed rivers?



SOCIETY'S INTEREST IN GRAVEL-BED RIVERS

Objective	Maintaining the Natural Scene	Controlling the River
Specific Uses	Preservation of Ecosystem Recreation Fishing Hunting Hiking Walking Viewing	Navigation Erosion Control Floodway Gravel Mining Recreation Fishing Hiking Biking Walking
Location	Channel Riparian Margin	Channel Riparian Margin
Biota	Aquatic Terrestrial	Aquatic Terrestrial

GEOMORPHIC THRESHOLDS  
IN GRAVEL BED RIVERS-  
REFINEMENTS FOR AN ERA OF ENVIRONMENTAL CHANGE

by  
Malcolm Newson  
Professor of Physical Geography  
University of Newcastle upon Tyne  
NE1 7RU. (U.K)

Contents

1. Introduction
2. Thresholds: original scales and definitions
3. Thresholds: developing doubts and criticisms
4. Field evidence of basin-scale threshold behaviour during extreme floods: Northern England
5. Thresholds and the spatial and temporal pattern of sediment throughput in river basins
6. Conclusions and implications for managed fluvial environments

## 1. Introduction

In 1973 Schumm introduced geomorphologists to the concept of thresholds in the fluvial sediment system. The concept has spread to all facets of the subject, often without question as to its true applicability; those who work with gravel-bed rivers, with flood effectiveness and with engineering applications of geomorphology are prone to unquestioning acceptance. The present author is therefore particularly vulnerable to "threshold spotting", and at the outset it is essential to list the qualitative appeals of the concept to the geomorphologist:

- a. Threshold concepts work best at the basin scale. Intrinsic "geomorphic" thresholds establish the value of geomorphological study as a valid, even crucial, contribution to the multidisciplinary field of fluvial systems,
- b. Thresholds are paradigmatic, representing a useful philosophical template for observations, located between catastrophic and uniformitarian explanations of the landscape. Thresholds normalize the role and relations of fluvial studies with other sciences which have employed the concept with great success.

The prospect of an impending era of marked changes in extrinsic climatic variables and of a determined anthropogenic response makes this a good time to evaluate the validity and utility of threshold concepts in gravel-bed systems (these two values are not perfectly correlated!) . River systems appear to have caught the imagination of politicians and planners concerned with environmental management; possibly the river basin outline represents a helpful circumscription to "the problem". The balance between anthropogenic and climatic influences in river basins is highly debated (Newson & Lewin, in press); if the former already dominate, there is less apparent need to "prepare" for global warming and, if the latter dominate, we need to decide urgently whether and how to increase the anthropogenic imprint in order to conserve human resource systems. A new alternative has also emerged: that of a sustainable, mainly natural response in which we largely withdraw from some or all of the hazardous locations in river basins in favour of the conservation of nature (Newson, in press). To all of these scenarios there attends the need for predictions of the "where and when" of river responses.

The threshold concept has impinged on the public debate on climate change, notably through the spectacular example of the potentially threshold-like behaviour of the West

Antarctic Icesheet and the results of its melting (Grove, 1987). However, in the decade since the highly enthusiastic Binghampton Symposium devoted to the subject, (Coates & Vitek, 1980) thresholds in geomorphology have been increasingly questioned (e.g. Carlson, 1984; Ferguson, 1987), either because threshold behaviour at one scale becomes progressive at another or because the abruptness of change implied by the concept itself becomes questionable after the arrival of observations of intermediate conditions and forms.

The dust-jacket of the volume containing papers from the 9th Annual Geomorphology Symposium at Binghampton (Coates & Vitek, 1980) proclaims that "critical limits, boundary conditions, and yield points - indeed thresholds" are important in many fields of science and technology. Although a stricter definition was offered at least once inside the covers ("within the natural system boundary conditions exist that when exceeded can cause sudden and vast changes") such definitions have been little refined, and even less adhered to. Table 1 lists the alternative definitions of thresholds found in the Binghampton volume; it is not offered as supercilious criticism, but instead to demonstrate that the threshold concept is very compelling - indeed those criticising it often fall to using it within their critical writing (e.g. Ferguson, 1986). Coates and Vitek (1980) themselves tacitly admit to a lack of rigidity in definition when they say that "'the judgment criteria that are adopted may determine whether to label an event on landform change as a true threshold" (p 11). Nevertheless, they are in optimistic mood, finding that "thresholds are present in all geomorphic processes" and that, in an era of increasing application for geomorphology "ignoring thresholds invites tragedies in every aspect of human utilization of the surface" (p 21). It is the latter remark which now needs some substantiation in this review.

TABLE 1: Definitions of thresholds offered at the  
1980 Binghampton Symposium

"The point at which a stimulus begins to produce a response"  
McKerchar (1980) p 171

"a threshold is a turning point or boundary condition that separates two distinct phases of interconnected processes, a dynamic system that is powered by the same energy source"  
Fairbridge (1980) p 48

"That critical distance from equilibrium at which unstability may occur therefore represents a thermodynamic threshold beyond which a perturbation introduced to the system does not decay to the steady state ..."  
Karcz (1980) p 220

"Although thresholds are generally defined as an abrupt temporal change in morphology or dynamics of landforms, similar abrupt spatial transitions are common (stream banks, escarpment brinks, riffles and pools, stream junctions etc.)."  
Howard (1980) p 227

"A threshold may be regarded as a balance between opposing tendencies"  
Bull (1980) p 260

"'Threshold' or 'threshold concept' are employed as self-explanatory terms to denote existence of zones or critical conditions at which change in topographic form or process occurs"  
Ford (1980) p 345  
quoting Frederking & Vilek.

"The Nile seems to be a classic example of a hydrologic threshold"  
Fairbridge (1980) p 45

## 2. Thresholds: original scales and definitions

Schumm (1973) began his influential paper on the threshold phenomena of river basins with the words, "The alluvial and morphologic details of drainage systems are much too complex to be explained by progressive erosion alone." (p 299). He wrote as a geologist and geomorphologist - about alluvium and landform. At our last gathering in Pingree Park (Thorne, Bathurst & Hey, 1987) the present author made a plea that each contribution be accompanied by a time- and space-scale cartoon locating its disciplinary origins in space and time - to avoid fruitless debate between the "zones" of Schumm and Lichty's (1963) table of dependent and independent river basin variables. Such attention to detail is also a requirement of any review of the origins and subsequent critiques of the threshold concept. To place this (geomorphological) contribution on the working diagram we need to refer to Schumm's original definition of geomorphic thresholds:

"A geomorphic threshold is one that is inherent in the manner of landform change; it is a threshold that is developed within the geomorphic system by changes in the system itself through time" (Schumm, 1973, p301)

In Schumm's treatment the external variables change progressively (much of the work having been done experimentally in the CSU basin-scale "facility"), but a complex response is evoked by the interaction of sediment supply and transport processes within the fluvial system. Refining the concept, Schumm (1977) is quick to point out that the alternating phases of erosion and deposition he defines as comprising complex response do not simply represent the system hunting for an equilibrium: "the complexity is not simply negative feedback that restores a former condition: rather it involves the crossing of a threshold to a new equilibrium state" (p 77). Schumm tends to restrict the utility of geomorphic thresholds and complex response to areas of high sediment production or of "rugged, youthful topography".

In view of these apparent restrictions the main task of the present review becomes one of investigating whether the original constraints placed on the applicability of threshold concepts have been validly breached or not and, if not, whether it is important that we now localise genuine threshold phenomena further in time and space because of their practical potential in interpreting and responding to environmental change.

The main extensions to the threshold concept appear to have been largely away from the fluvial system itself; thresholds are applied particularly to processes which include mechanical failures or overflow of storages (or a

mixture of both). Graf (1982) examining the potential of catastrophe theory in geomorphology concluded that, with the possible exception of arroyo formation, rapid system changes were much more likely in mass movement, aeolian processes, glacial surges and breaking waves; in other words, where the mechanical action of failure is critical. Thresholds have also been associated with the magnitude/frequency spectrum of extrinsic variables (and we may include anthropogenic activity as well as storms and floods). More in-keeping with Schumm's geomorphic thresholds has been the extension of threshold concepts to the interface between processes leading to sediment production/supply and those producing sediment transport. Intrinsic thresholds, in particular, may be associated with many of the multitude of storages associated with cascading natural systems such as those of river basins: "Where catchment processes incorporate storages a new mode of operation commences, or a new process is included when a storage is filled" (McKerchar, 1980, p 172). Kirkby (1980) writes of "domains of dominance" for particular processes, with the changeover from one to another commonly progressive, but which "in several important cases involves an instability which sharpens the transition" (p 53). Even if the processes operate in a linear fashion, says Kirkby, the change of domain produces a non-linearity and this is especially true of storage/release processes.

To the present author's knowledge there has been but one attempt in geomorphology to refine a working definition of threshold behaviour in terms of generic attention to process behaviour (one of Graf's objections to the application of catastrophe theory in the subject was our ignorance of control processes). At our last Workshop Hey (1987) suggested that the normal interaction of load and transport in rivers could produce threshold effects whilst Pitlick in his discussion of Hey's paper concluded that a reach downstream from a catastrophic dam burst had not shown threshold responses! However, Chappell (1983) draws attention to an important divergence in the nature of thresholds; defining a threshold as the boundary between different states of a system, he goes on to define them as transitive or intransitive according to whether the new state represents a persistent or short-lived change of external boundary conditions. Chappell implies that the "perturbation of boundary conditions" which occurs over an intransitive threshold is one "within the normal magnitude - frequency spectrum". "Bistable behaviour" can occur in some systems containing intransitive thresholds, as defined by the process-resultant curve. The crossing of transitive thresholds is, however, more akin to Karcz's (1980) thermodynamically-defined perturbation which does not decay to steady state.

Chappell stresses the need to identify thresholds at the process level because apparent boundaries in geomorphological systems can masquerade as thresholds. Concluding, he says that any study of geomorphological change must involve

- a) the boundary magnitude - frequency distribution
- b) the range of sensitivity of the threshold process
- c) the system lag and feedbacks

### 3. Thresholds: developing doubts and criticisms

Threshold interpretations may now be said to have come to occupy a number of niches in the fluvial system, as shown by Table 2:

---

Table 2 Summary table of threshold interpretations within the time and space scales of the fluvial system

---

PARTICLES	SEDIMENT YIELDS	PATTERNS	FORMS
Initiation/cessation of transport			
	sedimentation features/zones		
		channel pattern/metamorphosis	
		climatic geomorphology	

---

One may consider three factors which have helped extend the popularity of the concept:

- a. In hydraulics there are thresholds between sub- and supercritical flow regimes; thresholds also said to describe the entrainment, transport and deposition of sediment grains, indeed there are "threshold channels" designed to throughput sediment whilst retaining form. Hydrologists have produced more evidence for non-progressive behaviour of runoff processes and the "rare, great" flood event has been a major focus of geomorphological study.
- b. The methods available to those studying the fluvial system may have influenced the adoption of threshold concepts; geomorphology is rooted in descriptive classifications and "classic" forms dominate over intermediate states. "Snapshot" historical evidence of fluvial change from maps, air photos etc. is an essential methodological component. In process studies, trapping of sediments has necessarily discretized what may be continuous properties.



- c. There has been something of a cultural proclivity in late 20th century science to interpret rapid change - for example catastrophe theory (Woodcock and Davis, 1980), Chaos (Gleick, 1988) and mass extinction (Albritton, 1989).

By the mid 1980's, however, doubts were growing over the application of threshold concepts, especially to the transformation of channel planform.

Leopold and Wolman's (1957) location of planform domains for channel patterns on a slope/discharge plot attracted Schumm's attention as a candidate for the threshold concept; however, his 1973 paper does not expressly classify the transition from meandering to braided planforms as representing a process threshold. Clearly the importance of slope attracted him to the potential for a true geomorphic threshold but he did this only at a valley scale, not at a single site through time. The temporal reference in the paper is to valley metamorphosis such as that which occurred in the Cimmaron River (Schumm and Lichty, 1963); it therefore implies a change in sediment load calibre as the result of crossing the threshold.

Ferguson (1987) says of the Leopold and Wolman paper: "Despite its authors' emphasis that natural channel patterns form a continuum..... the paper is remembered mainly for its graphical discrimination between braided and meandering channels in terms of just two controlling variables, discharge and slope" (p 129). Ferguson also writes, "Surprisingly, few fluvial scientists have paused to ask whether Leopold & Wolman's threshold between meandering and braiding is quantitatively, conceptually or even morphologically correct. Ferguson is firmly of the view that "we should think in terms of transitions in channel pattern rather than sharp thresholds". The evolution of bar forms, leading eventually to channel change, is also said to involve transitions rather than thresholds, although the shift in chute location across point or lateral bars might well be considered by Chappell to be worthy of the "intransitive threshold" classification. Furthermore, any channel observed in the field, says Ferguson, is likely to be recovering from the last major flood during which an essentially equilibrium channel form resulted. Again, the Chappell terminology would label the flood channel and recovering low flow channel as existing either side of an intransitive threshold unless the flood had set up entirely new catchment or reach dynamics (e.g. by creating a new river cliff source of sediments). A similar point was made by Harvey, Hitchcock and Hughes (1982) - see Section 4 below.

Carson and Griffiths' (1987) impressively practical review (from the perspective of the management of New Zealand's extensive gravel-bed systems) incorporates a criticism of two threshold concepts - the initiation (and cessation) of gravel movement and meandering/braiding channel planforms. They vindicate Ferguson's view that a more complete field survey of channel types would yield considerable evidence of intermediate forms, for example the "wandering" channels classified by Neill (1973). Carson and Griffiths stress (p 119), "in attempts to differentiate meandering and braided channels in terms of some 'threshold', care is needed not to include such channels misclassified as one of the two end-members".

Turning to the mechanisms of the "wandering" channel, Carson and Griffiths report that the locus and pattern of secondary flows in the asymmetric bends of many gravel-bed meandering reaches produce both upvalley migration between bends and local shoaling of the thalweg in the bend-entry zone. As is demonstrated below for northern England, such "fill and cut" behaviour, producing a new thalweg is an important aspect of channel change both laterally and vertically. The lateral activity is far less likely to cross a transitive threshold than the vertical activity if it occurs.

Carson and Griffiths restate Carson's (1984) conclusions that channel classification into threshold types is illusory, that the conventional discharge/slope threshold is one of particle size and that there is weak support for an association between braiding and high slope-discharge values.

In terms of the initiation of movement the New Zealand review supports the view that "the critical mean velocity for the onset of bed material movement is significantly higher than that needed to maintain movement once particles have been entrained by the flow". (p 10). There are now significant proofs from the field that bed condition (overloose/underloose - Church, 1978), bedforms (Reid & Frostick, 1986) and particle exposure (Andrews, 1983) all produce this (intransitive) threshold-like effect. However, particularly in the wider channels reviewed by Carson and Griffiths, it is clear that whilst there is theoretical support for grain transport thresholds, the inter-relationships between mean and convective stresses and variability of particle size on the bed mean that bed movement may in reality be progressive.

There is clearly a dire need to measure the specific location of bed material entrainment and routes taken during bed material transport so as to confirm or refute the hypothesis that the apparent thresholds observed by trapping do not result from spatial variability of a bed material

source and of the trajectory of movement. Thus the bed material discharge may be more or less progressive but the yield from a reach may be represented by apparent thresholds. Meigh (1987) pointed out that channel storage and confinement of transport routes within the cross-section of a "near threshold" gravel-bed channel produced a temporal record of irregular throughput. Of equal relevance to the argument is the role of the supply-limited "throughput" material (Carson & Griffiths' term); because it is supply-limited and because bank collapses are a key mode of supply, its transport will appear quasi-threshold. If we have erred in applying threshold concepts to channel patterns because of classification problems we may have made errors in assigning sediment transport phenomena on the basis of observations which must be highly dependent upon sampler design and sampling position within a reach.

#### 4. Field evidence of basin-scale threshold behaviour during extreme floods: Northern England

At the outset of this review we considered the importance of the threshold concept to an era in which climatic change scenarios seem destined to force river basin managers into a greater familiarity with equilibrium and instability concepts. It seems reasonable, therefore, for the case of Northern Britain (in which both average rainfall and "storminess" are likely to increase) to examine the recent flood record for geomorphological changes which might fit the more rigorous of the threshold definitions presented above. It is of particular interest in the two field areas discussed below to consider the additional problems of anthropogenic effects, especially via biogenic controls on the important feedback loops which may control the transitive or intransitive nature of a threshold event. The relationship between lateral and vertical responses is also of interest.

The "Hurricane Charley" floods in Northern England in August 1986 were remarkable for their geomorphological effectiveness throughout major drainage basins (Newson, 1989), with vertical channel adjustments dominating over planform change (by incision in the headwaters and floodplain accretion down-river). Geomorphological studies of the affected headwater areas were made to investigate the process thresholds which might have resulted in incision during the event. Schumm, Harvey and Watson (1984) have referred to the fact that "when geomorphic thresholds are exceeded incision will occur" (p 11/12).

The conclusions reached by Newson and Macklin (1990) are that, although the Charley event may have been relatively common in the hydrological record (estimated 50-

year return period) it produced very high rates of coarse sediment transport, partly because of the availability of mining wastes in some valleys. Although large fan-like depositional zones were created where headwaters joined larger valleys, incision through valley fill and bedrock predominated. Bedrock incision appears to have been lithologically-controlled and intrinsic thresholds were crossed as alternating sandstone and shale strata were breached in the narrower, confined reaches of the affected valleys. A basic process leading to incision in broader valley reaches appears to be the "fill and cut" sequence which occurs at minor depositional storage sites, for example in the short meandering reaches. At the upstream end of such reaches flood deposition causes afflux which causes incision across the valley floor; if the incision(s) headcut successfully within the duration of the peak flow there is positive feedback to further incision and this proceeds to the upstream reach. Coxon, Coxon and Thorn (1989) describe an identical sequence of channel blocking, chute cutting in the Yellow River (Ireland) floods of 1986 (return period several hundred years). After the event, the sediment supply to the flood-torn channels in such valleys is entirely changed; in the bedrock reaches it may be reduced because the weathering profile has been stripped, but elsewhere the incised stream flows between unconsolidated banks and there are fresh bluffs and slope failures to form additional point sources of glacial material. A transitive threshold has clearly been crossed in respect of the "normal" magnitude/frequency relationship.

The rapidity of the incision by these northern Pennine streams is confirmed by small terraces which have been dated by lichenometry performed on the flood boulders which mantle them. Both this positioning of boulders and the concordance of lichenometric dates with large floods from the documentary record lead to the conclusion that phases of incision represent transitive threshold changes in processes operating in these systems. These are non-engineered fluvial environments and the prime human influence appears to be on the intrinsic threshold behaviour of the basins where mining waste has been redistributed by fluvial action. Mining has had another influence in that much of the waste is polluted with metals and this prevents the biogenic stabilization of near-channel sediment storages between threshold-crossing events.

The Forest of Bowland study by Newson and Bathurst (1990) was prompted by severe, costly management problems resulting from both erosion and deposition within two Victorian water supply schemes - the Brennand and Whitendale catchments. The North West Water Authority was alerted to the possible impact of land-use and land-management factors on the catchments by the fact that sedimentation rates to the nearby Abbeystead Reservoir had almost doubled since

approximately 1932; drainage, roading, vegetation control and afforestation seemed to be the most likely factors. They needed a remedial explanation for the damaging instability, particularly in the Brennand catchment, and Newson & Bathurst (1990) conclude that the explanation may be the crossing of a sediment transfer threshold by a spectacular flood in August 1967.

The flood-producing rainfall of August 8th totalled 109 mm. in the Brennand catchment and 89 mm. in the Whitendale, with a duration of approximately 90 minutes. The estimated discharge peak in the Brennand was 15-16 times the mean annual flood, equivalent in this region to a return period in excess of 10,000 years! Accounts written at the time speak of mudslides, landslides, boulder dams, channel diversions, severe erosion, "phenomenal" movement of bed material and, significantly, heavily-scoured channels of enlarged dimensions. Aerial photographs for 1945, 1948 and 1968 confirm almost complete valley-floor adjustment by channel switching or overbank deposition. New exposures of sediment include a large number of river cliffs created by mass movement and incision (but maintained by the latter process) and extensive moorland gullies stripped of their peat cover.

The present-day channel network of the Brennand catchment has, therefore, as a result of the one event, much larger sources of sediment supply than at any time since the growth of the present vegetation cover. A transitive process threshold was apparently crossed in that both supply and transfer of gravel material became adjusted to new conditions through a number of feedback processes.

Without more detailed study, however, particularly of catchment conditions prior to the 1967 flood, it would be difficult to judge the significance of the estimated 10,000-year+ return-period of the event. In the neighbouring Whitendale catchment the morphological legacy of the flood is minimal (flood peak approx. 7 times the mean annual flood). The evidence of incision in the Brennand headwaters and of the "wandering" channel which now occupies the transfer-zone is that lesser events would not cross the threshold. Indeed, in the neighbouring Langden Brook catchment Thompson (1987) concluded that channel planform fluctuations could be accommodated within a dynamic equilibrium framework despite the repeated crossing of (intransitive) channel thresholds. Valley-floor widths are important to this discussion - in the "Charley" flood areas it was the alternation of severe confinement and storage zones which set up the threshold conditions; in Bowland the wider valley floors are influenced only by a much higher magnitude event.

It is interesting to note in this respect that, in writing of a number of similar upland British catchments, Harvey, Hitchcock and Hughes (1982) see no evidence of recent approach to a major system threshold. They identify process thresholds and quote time intervals for events controlling overall channel morphology (2 - 4 per year) and adjustment of channel forms (14 - 30 per year). They observe that "there is no evidence that any past events larger than those occurring during the study period have had any lasting influence on the contemporary morphology of the active landforms" (p165).

However, in one of their study areas a 100yr + storm in June 1982 crossed major slope stability thresholds as well as those for a range of processes of fluvial transport (especially debris flows) to produce profound landscape and, on the resulting fan features a potential instability during subsequent fluvial action (Harvey, 1987; Wells and Harvey, 1987). There was on this occasion a "semi-permanent" change to braided channels sustained by a large number of new sediment sources. Channel slopes were also influenced by the calibre of the new inputs and presumably, therefore, an almost entirely new set of process-response relationships now exists.

At the slightly longer timescale there is considerable overlap between the catchments on which "rare, great" floods have been documented in Britain (Acreman, 1989) and the regions in which channel instability is pronounced in downstream, piedmont reaches (Hooke and Redmond, 1989)

One further conclusion by Newson and Bathurst is relevant; that is the contribution of land management practices to restricting biogenic recovery mechanisms in the Forest of Bowland catchments. The use of all-terrain vehicles, bracken control, heather burning and failure to control an infestation of burrowing animals (rabbits) has helped keep the process system in its current state of relative instability.

From these field studies we may conclude that, from the standpoint of long-lasting process switches induced by flood events there are a number of regularities:

- a. If the extrinsic signal is a "rare, great" flood initiating slope changes (note the channel/slope flood demarcation of Newson, 1980), there are likely to be transitive threshold changes, during recovery
- b. Sediment storage in headwater valley floors permits the development of intrinsic thresholds
- c. When they are crossed the processes of incision represents the transitive threshold change, involving positive feedbacks to sediment supply and stream power during lesser events

- d. Biogenic and land-use influences are important if they influence recovery by colonisation of deposits, maintain sediment supply sources or impinge directly on valley floor sediment stores.

## 5. Threshold behaviour and the spatial and temporal patterns of sediment throughput in river basin systems

Lewin (1989) has described the background to the domination of the "fluvial processes" school in the 1960's in terms of the availability of a spatially-restricted fluvial database, i.e. one derived largely from gauged alluvial channels in large basins. "Belief in systems that equilibrated in the short term allowed students to look at functional inter-relationships between discharge and other environmental variables such as slope, soil and drainage network parameters" (p 266). The origins and emphasis of data widely used in the subject are also considered by Lewin as of significance in forming what he describes as the "unorthodox challenges" to the process school. "There appears to be a growing impression that some environments are more prone to long-lasting landforming effects of exceptional events than others" (p 273): Lewin quotes semi-arid environments and small headwater catchments as susceptible; in both of these environments sediment supply processes are significantly altered by "rare great" floods and the growth curve of flood frequency is steep.

It is important to remember that Schumm's treatment of threshold phenomena in "The Fluvial System" (1977) was also spatially limited; he restricts thresholds to those parts of the system dominated by highly stratified climate, proclivity to large flood events, steep relief and neotectonics. These are the regions of high sediment production and storage, i.e. "The drainage basin", "valleys and valley fills" and "the piedmont" (largely alluvial fans).

Warner (1987) has confirmed a predictable spatial variability in channel response to the pronounced climatic variability of New South Wales. "Gorge", "armoured" and "backwater" zones react little and slowly to the alternation of flood- and drought-dominated regimes; "transition" and "mobile" zones react profoundly and rapidly (zones after Pickup, 1984). Because the mobile zone is composed of sand-bed rivers we restrict ourselves here largely to the transition zone, where-ever it may occur (as with many zonal schemes the individual units of this one may repeat throughout the fluvial system; this is a point further confirmed by Maizels (1985) for a major Scottish river.

It may be preferable to remain less specific about labelling zones of the river long-profile in relation to their susceptibility to threshold response and instead to refer to those parts of any drainage basin where considerable sediment storage occurs either on slopes or in channels, the result of either current, or as Church, Kellerhals and Day (1989) have shown, long-past, processes. Clearly, therefore, we can include both the apparently different valley fills of the narrow British upland headwaters and Warner's gorge zone - see Nanson's (1986) "floodplain stripping" mechanisms.

It may well be that the proper definition of geomorphic thresholds needs to reconcile the spatial distribution, volume and erodibility of basin storages with the magnitude/frequency concept. Not only is the perturbing event of importance here, but also the recovery process. Pitlick (1988) has a "zone-free" classification of the recovery process from the impact of large floods; the reach factors which control recovery (if it is to occur) include:

- magnitude of the initial perturbation
- sediment storage potential of the reach
- continuity of sediment supply from upstream
- frequency of flows subsequent to the big event

The storages, too, need a formal classification. Kelsey, Lamberson and Madej (1986) describe the movement of a "slug" of sediments introduced by a flood to the 720 km Redwood Creek basin; it traversed the active storages of the basin in 18 years but the important contribution made by this study is that of a model which simulates the role of active, semi-active, inactive and stable sediment stores in the basin. Not all valley-floor storages will respond in the classic threshold fashion. Macklin and Lewin (1989) describe the 115-year fluctuations of five "sedimentation zones" in a 22 km reach of the South Tyne. These zones, which average 1.69 km long appear to be largely a glacial inheritance; the more stable zones which link them are controlled by bedrock or by confining Quaternary fills and have much steeper channel gradient. Key controls are operated by the ability of the intervening "stable" (i.e. laterally stable - Lewin & Macklin's study is primarily from maps) reaches to temporarily store coarse sediments and by the ability of major floods to transfer such sediments (in-channel) to the downstream sedimentation zone. Once again the relationship between storage location, volume and flood frequency is confirmed.

Obviously the emerging hypothesis that vulnerability to transitive threshold behaviour during the extreme events which may typify climate change can be localised and predicted in drainage basin systems can be partially tested by reference to past climate changes, such as those of the



Holocene. From this perspective Rose and Boardman (1983), comparing the sedimentological response of two contrasting rivers of the same order to the same climatic deterioration (the lowland, alluvial, Gipping and the upland, boulder-bed, Mosedale Beck), conclude that gradient-controlled valley floor energy conditions explain why upland basins exhibit continuing complex response following a perturbation. Nevertheless, in both river systems there are alternating phases of incision and aggradation at first because of the delay between climate change and the sediment supply response. Richards et al (1987) review the major phases of anthropogenic sediment-supply changes in the British environment; they too contrast the sediment size and supply cycles of the lowland and upland headwater sites which have been reported and dated. The upland catchments are notable for the additional influence of localized meteorological events and for their episodic use and abandonment by agriculture.

Green and McGregor (1987) describe the significance of the thresholds implicit in dynamic metastable equilibrium for the formation of Holocene valley floors. Thus "relatively shortlived conditions of environmental change" can produce a terrace whose detail is then added by longer spells of quiescence and "morphostasis". Thanks to the temporal and spatial variability of threshold conditions, they claim that geomorphological response, even to global change is unlikely to be synchronous.

## 6. Conclusions and implications for managed fluvial environments.

Acceptance or rejection of the threshold concept by those disciplines and environments represented at this Workshop may either confirm the paradigmatic nature of thresholds or support the contention that thresholds are poorly defined. However, we might also consider that their proper investigation refers us to an new emphasis on sediment storage in river basins.

Geomorphologists are beginning to lay down guidance on the techniques for properly locating and evaluating basin storage, for example Laronne and Duncan (1989) have measured the storage potential and duration for braided river sections; channel sediment delivery ratios (Phillips, 1989) are also a conceptual advance and can be modelled. One of the most influential recent workshops on the topic of fluvial sediment storage concluded (Kelsey, 1982) that there was considerable potential in the division of drainage basins on the basis of supply- and transport-limited sediment fluxes and the appropriate magnitude/frequency growth curve. At the same meeting Reid formalised an

approach to sediment routing through drainage basins on a "from", "to" and "process" matrix. Swanson, Janda and Dunne (1982) concluded that "geomorphic recovery from a sediment-routing standpoint could be viewed as the refilling of storage sites and their readiness to fail again".

Knox (1989) suggests that the tendency for net storage in modern drainage systems implies a degree of disequilibrium in the erosional and depositional system. Furthermore, "the effectiveness to erode, transport and store sediment in watersheds is subject to considerable spatial variation within drainage hierarchies and the zone of maximum effectiveness may shift with changing processes over time" (p158). It required a complete change of climatic conditions to remove the colluvial deposits of the Late Pleistocene in the Upper Mississippi; this was then followed by a disjointed sequence of anthropogenic sedimentation from agriculture and removal of these storages once conservation treatments were applied to the headwaters. Humid environments can exhibit significant volumes of sediment storage within small basins, for example 90% of the material excavated by modern gullying is stored within the 13.8km Fernances Creek basin in south-east Australia (Melville and Erskine, 1986).

In terms of management of fluvial systems it is significant to note that certain characteristics of human manipulation of both land and water resource systems set up transitive or intransitive geomorphic thresholds. For instance, in the release of large volumes of Quaternary sediments by ploughing steep land for afforestation in Britain, or by closing off an impoundment to remove sediment from the downstream reaches we produce a hiatus which may or not recover (see Petts, 1979, 1987). Urbanisation can produce a discontinuity between the release of large amounts of sediment (during building) and the release of increased flood flows (after completion) - see Roberts, 1989.

However, management should now be concentrating on the sensitive zones of each major basin and the current condition of the anthropogenic/ biogenic controls on sediment stores in relation to the effect of climate change in either filling or emptying those stores. Brown (1987) writes of the importance of storage zones in middle and lower basins and suggests that up to 3,000 years' volume of stored sediments may be removed from the Severn basin (UK) were it not for extensive flood- and erosion-protection works on the river. Burrin (1985), writing about rivers in Sussex (UK) concludes that their valley floors have been artificially separated from formative fluvial action for up to 500 years as a result of engineering. If the response to climate change is further structural protection we further delay the time during which these sediments will be remobilised. Because of the popularity of sustainable

design and accounting timescales nowadays these are considerations which are politically and, through geomorphology, practically relevant.

Clearly the threshold concept has already had some practical utility; even the now discredited threshold of channel planform has encouraged a more sympathetic engineering treatment of channels in the field (Newson, 1986; Leeks, Lewin and Newson, 1988). However geomorphologists are now contemplating the benefits of thirty years of process measurements designed to elucidate the controlling variables in river dynamics. Richards (1990) has concluded that we should now judge results on the basis of their ability to explain the development of landforms. "Real" geomorphology, writes Richards, is emerging in which "criteria for acceptance of a theory are not based on predictive success but on explanatory power".

The critical phase now entered "must involve the emergence of new structures and relationships employing the identified mechanisms". Richards advocates the most likely line of progress as "the development of iteratively and spatially-distributed form-process-form feedback models".

A properly-defined, spatially-discrete threshold approach to the fluvial landforms created by sediment storage in river basins would conform to Richards' wishes. "Threshold spotting" now has to enter a new era and the signals for its methodologies have come from those working with both historical and contemporary storages in a variety of climatic zones.

## 7. REFERENCES

ACREMAN M C 1989 Extreme historical UK floods and maximum flood estimation. J, IWEM, 3, 404-412.

ALBRITTON C C 1989 Catastrophic episodes in Earth history. Chapman and Hall, London.

ANDREWS E D 1983 Entrainment of gravel from naturally sorted riverbed material. Bull. Geol. Soc. Amer., 94, 1225-1231.

BILLI P 1987 Sediment storage, bed fabric and particles features of two mountain streams at Plynlimon (mid Wales). Institute of Hydrology Report 97, Wallingford UK, 39pp.

BRADFORD J M & PIEST R F 1980 Erosional development of valley-bottom gullies in the upper midwestern United States. in D R Coates & J D Vitek (eds) Thresholds in Geomorphology, George Allen and Unwin, London, 75-101.

- BRAGA G & GERVASONI S 1989 Evolution of the Po River: an example of the application of historic maps. In G E Petts (ed) Historical change of large alluvial rivers: western Europe, John Wiley and Sons, Chichester, 113-126.
- BROWN A G 1987 Long term sediment storage in the Severn and Wye catchments. In K J Gregory, J. Lewin and J.B. Thornes (eds) Palaeohydrology in practice. John Wiley and Sons, Chichester, 302-332
- BULL W B 1980 Geomorphic thresholds as defined by ratios. In D R Coates and J D Vitek (eds) Thresholds in Geomorphology, George Allen & Unwin, London, 259-263.
- BURRIN P J 1985 Holocene alluviation in SE England and some implications for palaeohydrological studies.. Earth Surface Processes and Landforms, 10, 257-271.
- CARSON M A 1984 the meandering-braided river threshold: a reappraisal. J. Hydrol. 73, 315-334.
- CARSON M A & GRIFFITHS G A 1987 Bedload transport in gravel channels. Journal of Hydrology (New Zealand), 26(1), 151pp.
- CHAPPELL J 1983 Thresholds and lags in geomorphic changes. Australian Geographer, 15(6), 357-366.
- CHURCH M 1978 Paleohydrological reconstructions from a Holocene valleyfill. In A D Miall (ed), Fluvial Sedimentology. Canadian Soc. Petr. Geol. Memoir 5, 743-772.
- CHURCH M, KELLERHALS R & DAY T J 1989 Regional clastic sediment yield in British Columbia. Can. J. Earth Sci., 26(1), 31-45.
- COATES D R & VITEK J D 1980 Perspectives on geomorphic thresholds. in D R Coates and J D Vitek (eds) Thresholds in geomorphology. George Allen and Unwin, London, 3-23.
- COXON P, COXON C E & THORN R H 1989 The Yellow River (County Leitrim, Ireland) flash flood of June 1986. In K Beven & P Carling (eds) Floods: hydrological, sedimentological and geomorphological implications, John Wiley and Sons, Chichester, 199-217.
- FAIRBRIDGE R W 1980 Thresholds and energy transfer in geomorphology. In D R Coates and J D Vitek (eds), Thresholds in Geomorphology, George Allen and Unwin, London, 43-49.
- FERGUSON R 1981 Channel form and channel changes. In J Lewin (ed) British Rivers, George Allen and Unwin, London, 90-125.

- FERGUSON R 1987 Hydraulic and sedimentary controls of channel pattern. In K.S.Richards (ed) River channels: environment and process, Oxford, Blackwells, 129-158.
- FORD D C 1980 Threshold and limit effects in karst geomorphology. In D R Coates & J D Vitek (eds) Thresholds in Geomorphology, George Allen and Unwin, London, 345-362.
- GLEICK J 1988 Chaos: making a new science. Heinemann, London.
- GRAF W L 1979(1982) Catastrophe theory as a model for change in fluvial systems. In D D Rhodes & G P Williams (eds) Adjustments of the fluvial system, George Allen and Unwin, London, 13-32.
- GREEN C P & MCGREGOR D F M 1987 River terraces - a stratigraphic record of environmental change. In V Gardiner (ed), International Geomorphology, I, 977-987.
- GRIFFITHS G A 1979 Recent sedimentation history of the Waimakariri River, New Zealand. J Hydrol (NZ), 18, 6-28.
- GROVE J M 1987 Glacier fluctuations and hazards. Geog. J., 153(3), 351-369.
- HARVEY A M 1987 Sediment supply to upland streams: influence on channel adjustment. In C R Thorne, J C Bathurst and R D Hey (eds) Sediment transport in gravel-bed rivers. John Wiley and Sons, 121-150.
- HARVEY A M, HITCHCOCK D H & HUGHES D J 1982 Event frequency and morphological adjustment of fluvial systems in upland Britain. In D D Rhodes and G P Williams Adjustments of the fluvial system, George Allen and Unwin, London, 139-167
- HEY R D 1987 River dynamics, flow regime and sediment transport. In C R Thorne, J C Bathurst and R D Hey (eds) Sediment transport in gravel bed rivers, John Wiley and Sons, 17-40.
- HOOKE J M & REDMOND C E 1989 River channel changes in England and Wales. J. IWEM, 3, 328-335.
- HOWARD A D 1980 Thresholds in river regimes. In D R Coates & J D Vitek (eds) Thresholds in Geomorphology, George Allen and Unwin, London, 227-258.
- KARCZ I 1980 Thermodynamic approach to geomorphic thresholds. In D R Coates & J D Vitek (eds) Thresholds in Geomorphology, George Allen and Unwin, London, 209-226.

- KELSEY H M 1982 Influence of magnitude, frequency and persistence of various types of disturbance on geomorphic form and process. In F J Swanson et al (eds) Sediment budgets and routing in forested drainage basins. USDA Forest Service, General Tech. Rept. PNW 141, 150-153.
- KELSEY H M, LAMBERSON R & MADEJ M A 1986 Modelling the transport of stored sediment in a gravel bed river, northwestern California. IAHS Publ. 159, 367-391.
- KIRKBY M J 1980 The stream head as a significant geomorphic threshold. In D R Coates & J D Vitek (eds) Thresholds in Geomorphology, George Allen and Unwin, London, 53-73.
- KNOX J C 1989 Long- and short-term episodic storage and removal of sediment in watersheds of southwestern Wisconsin and northwestern Illinois. IAHS Publ. 184, 157-164.
- LAIRD J R & HARVEY M D 1986 Complex response of a chaparral drainage basin to fire. IAHS Publ. 159, 165-183.
- LARONNE J B & DUNCAN M J 1989 Constraints on duration of sediment storage in a wide, gravel-bed river, New Zealand. IAHS Publ. 184, 165-172.
- LEEKES G J, LEWIN J & NEWSON M D 1988 Channel change, fluvial geomorphology and river engineering: the case of the Afon Trannon, mid-Wales. Earth Surface Processes and Landforms, 13, 207-223.
- LEOPOLD L B & WOLMAN M G 1957 River channel patterns: braided, meandering and straight. US Geol. Survey, Prof. Paper 282-B.
- LEWIN J 1989 Floods in fluvial geomorphology. In K Beven & P Carling (eds) Floods: hydrological sedimentological and geomorphological implications. John Wiley and Sons, Chichester, 265-284.
- MACKLIN M G & LEWIN J 1989 Sediment transfer and transformation of an alluvial valley floor: the river South Tyne, Northumbria, UK. Earth Surface Processes and Landforms, 14, 233-246.
- MAIZELS J K 1985 The physical background of the River Dee. In D Jenkin. (ed) Biology and management of the River Dee. Institute of Terrestrial Ecology.
- McKERCHAR A I 1980 Thresholds in deterministic models of the rainfall-runoff process. In D R Coates & J D Vitek (eds), Thresholds in Geomorphology, George Allen and Unwin, London, 171-177.

- MEIGH J R 1987 Transport of bed material in a gravel-bed river. Unpub. PhD Thesis, University of East Anglia.
- MELVILLE M D & ERSKINE W 1986 Sediment remobilization and storage by discontinuous gullyng in humid southeastern Australia. IAHS Publ. 159, 277-286.
- NANSON G C 1986 Episodes of vertical accretion and catastrophic stripping: a model of disequilibrium flood-plain development. Geol. Soc. Amer. Bull., 97, 1467-1475.
- NEWSON M D 1980 The geomorphic effectiveness of floods. A contribution stimulated by two recent events in mid-Wales. Earth Surface Processes, 5, 1-16.
- NEWSON M D 1986 River basin engineering - fluvial geomorphology. J IWES, 40(4), 307-324.
- NEWSON M D 1989 Flood effectiveness in river basins: progress in Britain during a decade of drought. In K Beven & P Carling (eds) Floods: hydrological, sedimentological and geomorphological implications. John Wiley and Sons, Chichester, 151-183.
- NEWSON M D 1990 River conservation and catchment management - UK perspectives. Proc. Int. Conf. on Conservation Management of Rivers, John Wiley and Sons.
- NEWSON M D & BATHURST J C 1990 Sediment movement in gravel-bed rivers: applications to water supply and catchment management problems, River Dunsop, Forest of Bowland, Lancs. University of Newcastle upon Tyne, Department of Geography, Seminar Paper 59, 45pp.
- NEWSON M D & LEEKS G J 1987 Transport processes at the catchment scale. In C R Thorne, J C Bathurst & R D Hey (eds) Sediment transport in gravel-bed rivers. John Wiley and Sons, Chichester, 187-223.
- NEWSON M D & LEWIN J 1990 Climate change, river flow extremes and fluvial erosion - scenarios for England and Wales. Progress in Physical Geography.
- NEWSON M D & MACKLIN M G 1990(in press) The geomorphologically-effective flood and vertical instability in river channels - a feedback mechanism in the flood series for gravel-bed rivers. In W R White (ed) Flood Hydraulics, John Wiley and Sons, Chichester.
- PETTS G E 1979 Complex response of river channel morphology subsequent to reservoir construction. Progress in Physical Geography, 3(3), 329-362.

- PETTS G E 1987 Timescales for ecological change in regulated rivers. In J Craig & J B Kemper (eds) Regulated streams - advances in ecology. Plenum, New York, 257-266.
- PHILLIPS J D 1989 Hillslope and channel sediment delivery and impacts of soil erosion on water resources. IAHS Publ. 184, 183-190.
- PICKUP G 1984 Geomorphology of tropical rivers. Catena Suppl. 5, 1-17.
- PITLICK J 1988 The response of coarse-bed rivers to large floods in California and Colorado. Unpub. PhD Thesis, Colorado State University, Fort Collins.
- REID I & FROSTICK L E 1986 Dynamics of bedload transport in Turkey Brook. Earth Surface Processes and Landforms, 11, 143-155.
- REID L M 1982 The use of flow charts in sediment routing analysis. In F J Swanson (ed) Sediment budgets and routing in forested drainage basins. USDA Forest Service, General Tech. Rept. PNW 141, 154-156.
- RICHARDS K S 1982 Channel adjustment to sediment pollution by the china clay industry in Cornwall, England. In D D Rhodes & G P Williams (eds) Adjustments of the fluvial system. George Allen and Unwin, London, 309-331.
- RICHARDS K 1990 "Real" geomorphology. (editorial) Earth Surface Processes and Landforms, 15, 195-197.
- RICHARDS K S, PETERS N R, ROBERTSON-RINTOUL M S E & SWITSUR V R 1987 Recent valley sediments in the North York Moors: evidence and interpretation. In V Gardiner (ed) International Geomorphology I, John Wiley and Sons, Chichester, 869-883.
- ROBERTS C 1989 Flood frequency and urban-induced channel change: some British examples. In K Beven & P Carling (eds) Floods: hydrological, sedimentological and geomorphological implications, John Wiley and Sons, Chichester, 57-82.
- ROSE J & BOARDMAN J 1983 River activity in relation to short-term climatic deterioration. Quaternary Studies in Poland, 4, 189-198.
- SCHUMM S A 1973 Geomorphic thresholds and the complex response of drainage systems. In M Morisawa (ed) Fluvial Geomorphology, State University of New York, Binghamton, 299-310.
- SCHUMM S A 1977 The fluvial system. John Wiley and Sons, New York,



SCHUMM S A 1980 Some applications of the concept of geomorphic thresholds. In D R Coates and J D Vitek (eds) Thresholds in Geomorphology, George Allen and Unwin, London, 473-485.

SCHUMM S A & LICHTY R W 1963 Channel widening and floodplain construction along Cimarron River in southwest Kansas. US Geol. Survey, Prof. Paper 352-D.

SCHUMM S A & LICHTY R W 1965 Time, space and causality in geomorphology. Amer. J Sci., 263, 110-119.

SCHUMM S A, HARVEY M D & WATSON C C 1984 Incised channels: morphology, dynamics and control. Water Resources Publications, Littleton, Colorado, 200pp.

SWANSON F J, JANDA R J & DUNNE T 1982 Summary: sediment budget and routing studies. In F J Swanson et al (eds) Sediment budgets and routing in forested drainage basins. USDA Forest Service, General Tech. Rept. PNW141, 157-165.

THORNE C R, BATHURST J C & HEY R D 1987 Sediment transport in gravel-bed rivers. John Wiley and Sons, Chichester.

VAN URK G & SMIT H 1989 The Lower Rhine: geomorphological changes. In G E Petts (ed) Historical change of large alluvial rivers: Western Europe, John Wiley and Sons, Chichester, 167-182.

WARNER R F 1987 Spatial adjustments to temporal variations in flood regime in some Australian rivers. In K S Richards (ed) River channels, environment and process, Basil Blackwell, Oxford, 14-40.

WELLS S G & HARVEY A M 1987 Sedimentologic and geomorphic variations in storm-generated alluvial fans, Howgill Fells, northwest England. Geol. Soc. Amer. Bull., 98, 182-198.

WOODCOCK A & DAVIS M 1980 Catastrophe theory. Penguin Books.

**ANALYSIS OF MASSIVE SEDIMENT TRANSPORT PROCESSES IN TORRENTS**

---

D. Rickenmann,

in collaboration with M. Zimmermann,

Laboratory of hydraulics, hydrology and glaciology,  
ETH - Zentrum, CH-8092 Zürich, Switzerland

**Abstract**

As a result of a laboratory study, new formulae are proposed to calculate bed load transport rates and velocities of torrent flows with high suspended fine material concentrations. Using the bedload transport equation in a case study, sediment volumes of flood events are determined and compared with independent estimates. In a second part, several empirical equations are compared which were developed to estimate the total sediment volume that may be mobilized in a torrent catchment during an extreme rainstorm event by either a debris flow or by fluvial sediment transport.

**1 INTRODUCTION**

With increasing population densities and with increased tourist activities in mountain areas, the problem of sediment hazards from mountain torrents has to be given more attention. A flood event involving massive sediment transport can endanger human life, property and traffic routes particularly on the fan area. If a lot of material is deposited at the mouth of the torrent, the main stream in the valley may be dammed which will cause trouble for the next village downstream. In order to plan countermeasures against such disasters, it is therefore important to know more about massive sediment transport processes in torrents and to develop methods to estimate sediment volumes resulting from flood events.

Torrent catchments are characterized by steep gradients, and thus the sediment transport capacity in the channels can be very large. During periods with no major flood events, however, a lot of debris and sediment may be stored in and along the channel. In addition, there are often steep side slopes composed of loose material (e.g. moraines). If an intense rainstorm occurs over such a catchment, the resulting flood may mobilize major parts of these sediment resources, and under certain conditions the transport can also be in form of a debris flow. Accompanying landslides enhance both the sediment supply into the torrent and the probability that a dangerous debris flow will form.

## 2 FLUVIAL SEDIMENT TRANSPORT

### Bed load transport experiments

During a flood event a lot of fine material may enter the channel from the side slopes. If this material is suspended in large quantities by the water flow, a slurry of fine material will result which can eventually form the fluid matrix of a debris flow. In order to examine the transition region between "normal" (fluvial) sediment transport and debris flows, an experimental study was performed (Rickenmann, 1990). A clay suspension of increasing concentrations was used to simulate the fine material slurry. In a steep flume with slopes between 5 and 20 %, the bed load transport capacity ( $q_b$ ) and the flow behaviour of the slurry were determined, looking at the effect of the increasing fluid density and viscosity with increasing clay concentration of the flow.

The main results of this study can be summarised as follows: As long as viscous effects remained negligible (particle Reynolds numbers above approximately 10) the bed load transport rates increased with increasing fluid density. As compared to the corresponding clear water flow (having the same flow rate and the same slope), the increase in the experiments reached up to 300 %. Once the flow around the grains became laminar (particle Reynolds numbers below 10), however, a marked decrease of  $q_b$  with further increasing clay concentration could be observed. All the experiments were performed with steady uniform flow. The fact that the transport capacity of debris flows is still much greater than in these slurry flows, is probably associated with the unsteady flow behaviour and the different rheologic behaviour of such grain-water mixtures.

The majority of the experiments were performed under flow conditions with negligible viscous effects. The analysis showed that this experimental data can be described by a similar bed load transport formula as proposed by Smart and Jäggi (1983), only the density factor had to be adjusted. Since these authors had performed similar experiments in the same steep flume facilities, using clear water as transporting fluid, both data sets were analysed together (totalling 115 tests). The resulting calculation procedure is shown in Fig. 1.

At steep slopes ( $> 10\%$ ) the bed load transport capacity becomes so large that the concentration of moving grains increases the flow depth. Therefore a distinction is necessary between the mixture flow depth  $h_m$  and the fictitious fluid depth  $h_f$  (fictitious depth in the case of no transport). For the same reason two different calculation procedures were proposed, depending on whether the flow rate ( $q$ ) or the flow depth ( $h_m$ ) is given or assumed. In the following case studies we start from the flow rate, therefore only the first procedure (labelled "design case") is presented here. The second calculation procedure can be found in Rickenmann (1990).

As mentioned, equ. (2) is the result of a regression analysis of both the clay suspension experiments of the author and the tests of Smart and Jäggi (1983). Equ. (1) represents a slight modification of a formula proposed by Bathurst et al. (1987), to include also density effects. This equation is partly based on steep flume experiments (up to  $20\%$  slope) and it applies essentially to beds with more or less uniform grain size distribution. From the flow resistance analysis of the steep flume tests, a formula very similar to equ. (3) had been developed. Interestingly, the measured velocities fitted even better to equ. (3) which was adapted from Takahashi (1978); his formula is based on theoretical considerations, and a "calibration" with his experimental debris flows results in the constant 1.3. Equ. (4) is a purely empirical relation that was developed from the steep flume data of the author and of Smart and Jäggi (1983).

The channel bed of a torrent is often composed of an armour layer containing very coarse pebbles and boulders. The main difficulty in assessing the sediment transport is to determine the critical discharge above which substantial transport will occur. For rivers with flat slopes, full sediment transport (close to the calculated transport capacity) may be assumed after the armour layer is destroyed. In a torrent, however, the coarsest boulders (grains sizes above about 1 m) may not be moved even at higher flow rates. Since transport formulae

were developed with comparatively uniform grain sizes, effective sediment transport rates in torrents might only make up for a part of the calculated values.

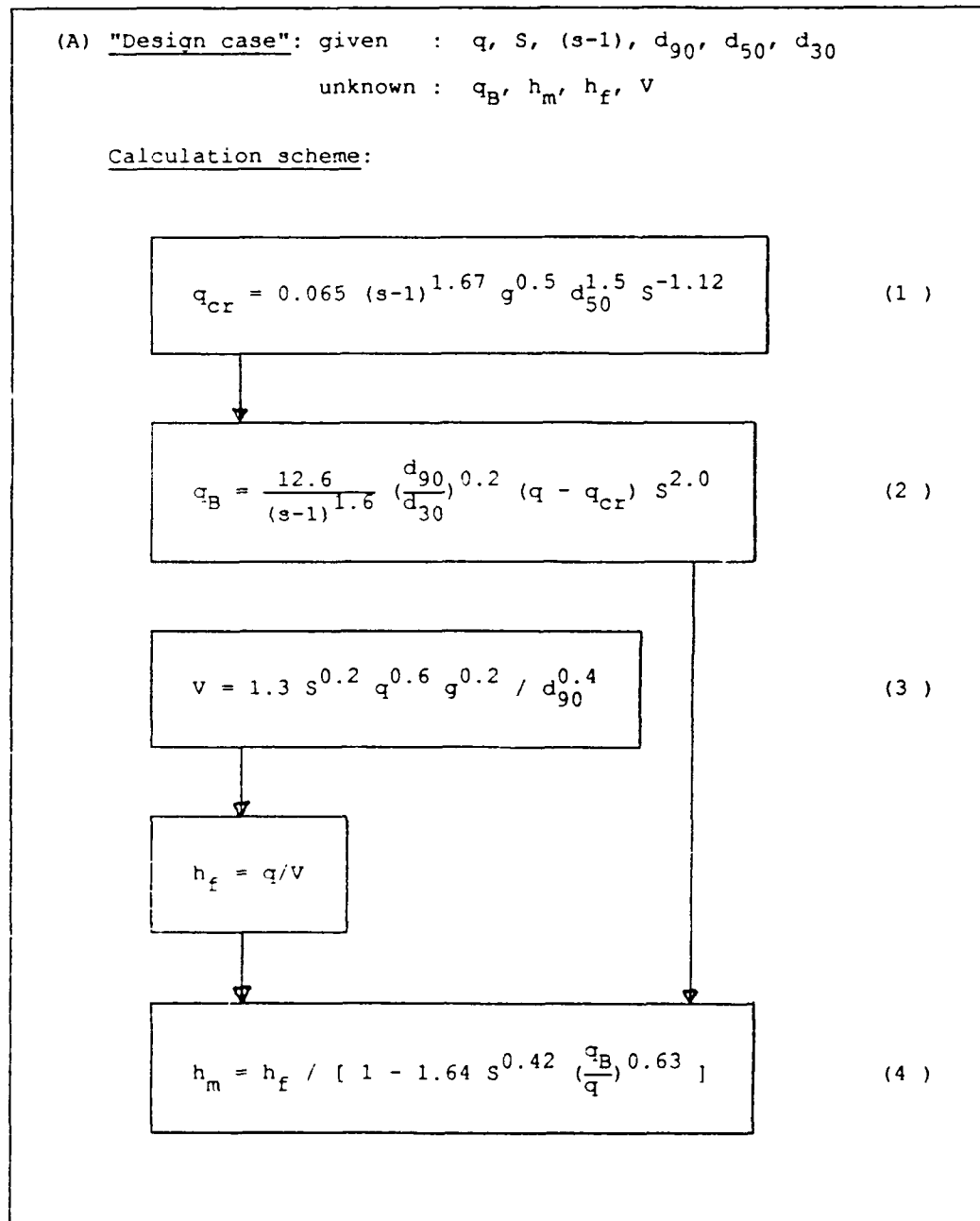


Fig. 1: Calculation procedure for the "design case". Recommended range of application:  $5 \leq S \leq 20$ ,  $q \geq 5 \cdot q_{cr}$ ,  $h_m/d_{90} \leq 20$ .

In Fig. 1, the following notation is used:

$q$  : fluid flow rate per unit width [ $m^3/(s \cdot m)$ ]  
 $S$  : slope  
 $s = \rho_s/\rho_f$  : ratio of sediment to fluid density  
 $d_{90}$  : characteristic grain size than which 90 weight percent is finer  
 $d_{50}$  : characteristic grain size than which 50 weight percent is finer  
 $d_{30}$  : characteristic grain size than which 30 weight percent is finer  
 $q_B$  : bed load transport rate per unit width [ $m^3/(s \cdot m)$ ]  
 $q_{cr}$  : critical flow rate at initiation of motion  
 $h_{cr}$  : mixture flow depth (including part occupied by moving grains)  
 $h_m^f$  : (fictitious) fluid flow depth ( $= q/V$ )  
 $V^f$  : mean fluid velocity

Günter (1971) performed experiments to study the effect of a wide grain size distribution on the critical dimensionless shear stress to break up the armour layer,  $\theta_{cr,D}$ , which can be expressed as follows:

$$\theta_{cr,D} = \theta_{cr} \left( \frac{d_{90}}{d_m} \right)^{0.67} \quad (5)$$

where  $\theta_{cr}$  is the critical dimensionless shear stress at initiation of motion for a uniform sediment ( $\theta_{cr} = 0.05$ ), and  $d_m$  is the mean grain size. If equ. (5) is combined with the formula of Manning-Strickler, a critical discharge for the destruction of the armour layer,  $q_{cr,D}$ , can be determined. Comparing this relation with equ. (1), the following first approximation results (putting  $d_{50} = d_m$ ):

$$q_{cr,D} = \frac{d_{90}}{d_m} q_{cr} \quad (6)$$

For the bed material of the examples in the following case studies the ratio  $(d_{90}/d_m)$  varies between 2 and 2.6. In this case it may be concluded that the critical discharge to destroy the armour layer is about 2 to 3 times larger than the one for initiation of motion with a relatively uniform sediment (with the same mean grain size  $d_m$ ).

In the bed load transport equ. (2), the effect of a wide grain size distribution is accounted for by the factor  $(d_{90}/d_{30})$ , and the density effect by the factor  $(s-1)$ . These influences may be replaced by a single factor  $F$ . Putting  $F = 1$  for clear water with  $(s-1) = 1.65$  and for a uniform sediment with  $(d_{90}/d_{30})^{0.2} = 1.05$  (Smart and Jäggi, 1983), equ. (2) can be simplified to:

$$q_B = 5.9 F (q - q_{cr}) s^{2.0} \quad (7)$$

The respective influence of these two effects is as follows (if both effects are to be taken into account, the two factors have to be multiplied):

$$\frac{d_{90}}{d_{30}} = \frac{5}{10} \quad \text{----> increase of } q_B \text{ by factor } F = \frac{1.3}{1.5}$$

$$p_f = \frac{1.15 \text{ t/m}^3}{1.28} \quad \text{----> increase of } q_B \text{ by factor } F = \frac{1.5}{2.0}$$

### Case Study

During the summer of 1987 two heavy rainstorm events occurred in July and August, resulting in large floods and widespread debris flow activity. These natural events killed one car driver and caused a lot of damage to traffic routes, buildings and cultivated land. In order to study the causes and the processes associated with these events, a national research program was initiated by the Swiss Federal Board of Water Resources Management. In one subproject, the debris flow and flood events in torrent catchments were studied (Haeberli et al., 1990).

Four flood events in torrent catchments were studied in more detail. The sediment volumes transported to the mouth of the catchment were between 30'000 m<sup>3</sup> and 250'000 m<sup>3</sup>. In all these torrent catchments there was both a flood event and debris flow activity during long-lasting precipitation of about 1 1/2 to 3 days. Based on field observation and eyewitness accounts, an attempt was made to distinguish between the sediment volumes resulting from fluvial transport and those volumes associated with the debris flows.

The following Table 1 gives the main characteristics of the catchment and the transported sediment volumes:

name	date	catchment area	mean creek gradient	fluvial sed. volume [m <sup>3</sup> ]	debris flow sed. volume [m <sup>3</sup> ]
Varuna	18.7.87	6.6 km <sup>2</sup>	37 ‰	max. 20'000 <sup>1)</sup>	200'000 <sup>2)</sup>
Plaunca	18.7.87	3.8 km <sup>2</sup>	34 ‰	?	240'000 <sup>2)</sup>
Zavragia	18.7.87	13.0 km <sup>2</sup>	26 ‰	?	30'000 <sup>3)</sup>
Münster	24.8.87	15.3 km <sup>2</sup>	16 ‰	max. 20'000 <sup>4)</sup>	30'000 <sup>4)</sup>

Table 1: Observed sediment volumes resulting from fluvial transport or debris flows, for four flood events in torrent catchments.

In Table 1, the sediment volume estimates are based on:

- 1) sediment retention capacity of channels in the fan area, with no deposition outside channels according to eyewitnesses
- 2) analysis of aerial photographs before and after the event
- 3) damming of the main stream within about 15 to 45 minutes
- 4) debris flow occurred clearly before flood event; photographic documentation of deposition in the village area before and after the flood

In all four creeks, information on the characteristic grain sizes of the bed material was obtained from several frequency-by-number transect samples of the armour layer. Subsequent transformation into a sieve-by-weight distribution of the whole grain mixture was performed according to a procedure given by Fehr (1987). The following values represent the bed material characteristics near the head of the fan; also listed are the bed slope of the fan head and the mean width B of the channel there:

name	$d_{90}$ [m]	$d_m$ [m]	$d_{30}$ [m]	$d_{90}/d_{30}$	slope of fan head	B [m]
Varuna	0.46	0.18	0.05	9.2	0.24	5
Plaunca	0.29	0.14	0.025	11.6	0.11	4
Zavragia	0.52	0.21	0.04	13.0	0.083	10
Münster	0.42	0.16	0.04	10.5	0.13	7

Table 2: Grain size and channel characteristics.

Since no discharge measurements (during the flood events) exist for any of the four creeks, flood hydrographs were constructed from rainfall intensity data for three hour intervalls (based on interpolation from nearby raingauge stations). Runoff coefficients were varied between 0.25 and 0.7, depending on catchment characteristics and preceding rainfall conditions. The combination of the flood hydrograph with the bed load transport equation (7) yielded fluvial sediment volumes.

Preliminary calculations showed that these volumes depend to a great extent on both the value of the critical discharge for initiation of motion and the time during which substantial sediment transport is



assumed to have occurred. A breaking up of the armour layer can be expected with increasing discharge, but what is the effect of the largest boulders not moved by the flow ? And the armour layer will probably be rebuilt during the receding part of the hydrograph. Calculations of the flow depth at peak discharge according to the procedure in Fig. 1 resulted in values less than 1 m at the time of the flood peak. In view of the uncertainties related to the beginning and ceasing of transport, it was decided to neglect any correction for sidewall friction effects, and a rectangular flow cross section was assumed. Thus, discharge values over the whole width were obtained as:  $Q = B \cdot q$ ,  $Q_{cr} = B \cdot q_{cr}$ ,  $Q_B = B \cdot q_B$ .

In a first case (A), the critical discharge  $q_{cr}$  (and  $Q_{cr}$ ) was determined with  $d_m$ . A comparison of the resulting sediment volumes with the observed ones (Varuna and Münster creek) showed a clear overestimation (although with  $d_m$  a larger grain size was already used than with  $d_{50}$  according to equ. 1). A considerable higher critical discharge for the breaking up of the armour layer is obtained by equ. (6), the increase is a factor  $d_{90}/d_m$ . For a second set of calculations (case B), it was decided to choose an even larger upper extreme value: Using  $d_{90}$  instead of  $d_m$  in equ. (1), there is an increase in  $q_{cr}$  by a factor  $(d_{90}/d_m)^{1.5}$ .

The combined effects of an increased fluid density and of a wide grain size distribution are taken into account by the factor  $F$ . For the Varuna, Zavragia and Münster creek this factor was varied between 1.0 and 1.5. Extremely high fine material concentrations were indicated for the flood event in the Plaunca creek, muddy and humid deposits could be observed even some days after the event. In this case the factor  $F$  was varied between 1.5 and 2.0. Several combinations between the cases A or B and different values of  $F$  were introduced in the bed load transport calculations. Case 1 refers to the greater, case 2 to the smaller  $F$  value. Here, only the two extreme combinations are considered. The results are given in Table 3 and in the Figures 2(a)-(d) showing the constructed hydrographs and the calculated sediment graphs.

A further assumption concerns the onset of substantial sediment transport during the event. For three creeks (Varuna, Zavragia, and Münster) this time is mainly based on eyewitness accounts. The flood event in the Plaunca creek was not observed by anybody. There it was assumed that substantial transport began either at the flood peak (linear increase from 14<sup>00</sup>h to 15<sup>30</sup>h) or after the presumed time of debris flow occurrence (21<sup>30</sup>h). For the Varuna creek, no substantial bed load transport was reported for the time before 17<sup>00</sup>h. In the Zavragia

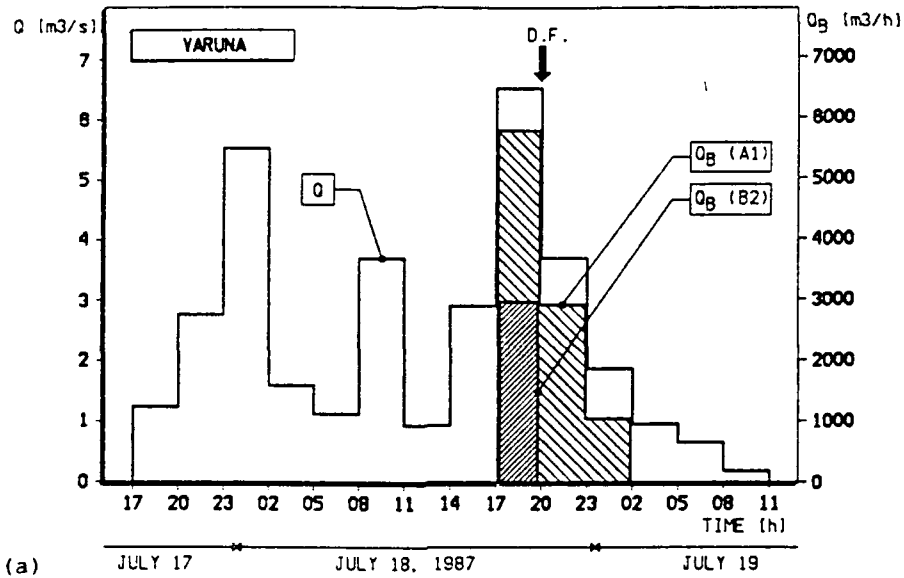


Fig. 2(a)

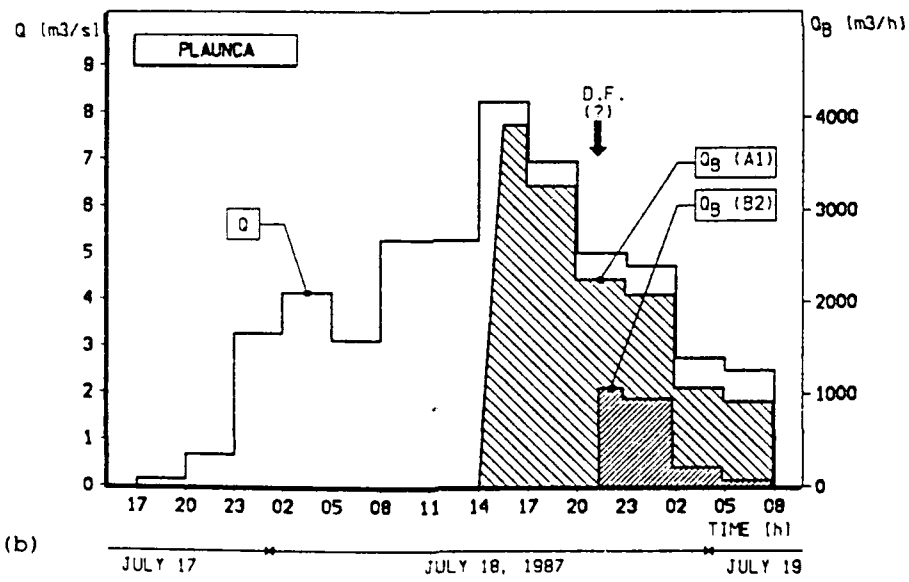


Fig. 2(b)

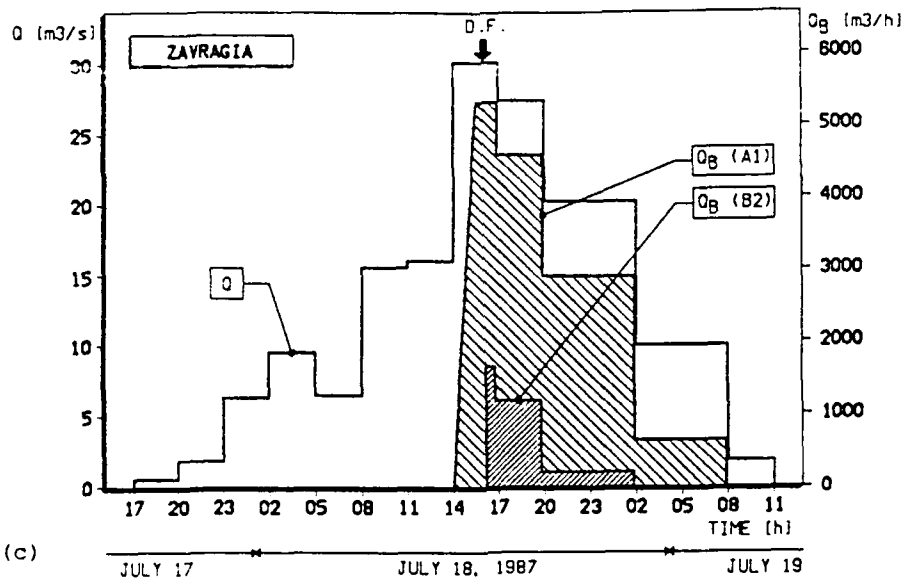


Fig. 2 (c)

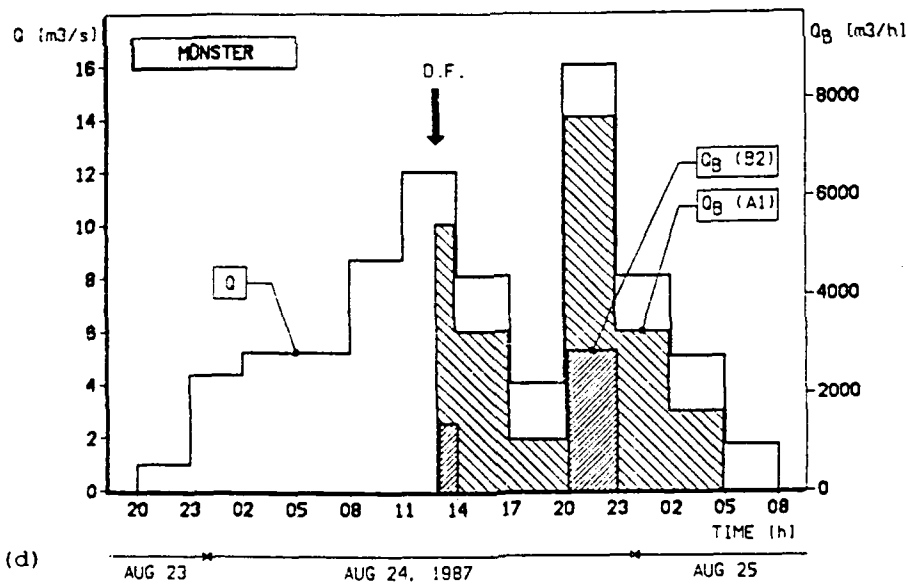


Fig. 2 (d)

Fig. 2: Flood hydrographs constructed from rainfall data and sediment graphs calculated by equ. (7), for four torrent catchments: (a) Varuna, (b) Plaunca, (c) Zavrágia, and (d) Münster. The arrow with D.F. marks the time of the (first) debris flow occurrence.

case, bed load transport is said to have started in the afternoon. With Münster, the debris flow (13<sup>00</sup>h) occurred clearly before the flood peak. It may be assumed that the armour layer was destroyed afterwards, and that some bed load transport occurred in the afternoon, although the eyewitnesses reported substantial transport during the evening (of August 24) and overnight.

name	case	d [m]	$Q_{cr}$ [m <sup>3</sup> /s]	F	Fluvial sed. volume [m <sup>3</sup> ]
Varuna	A1	0.18	0.9	1.5	45'000
	B2	0.46	3.6	1.0	11'000
Plaunca	A1	0.14	0.8	2.0	37'000
	B2	0.29	2.3	1.5	5'000
Zavragia	A1	0.21	7.4	1.5	48'000
	B2	0.40*	19.3	1.0	6'000
Münster	A1	0.16	2.1	1.5	57'000
	B2	0.40	8.2	1.0	10'000

\* With  $d_{90} = 0.52$  m the critical discharge becomes larger than the peak flow rate, and no bed load transport would result. Therefore a smaller characteristic grain size is assumed in case B.

Table 3: Range of calculated fluvial sediment volumes.

The figures for the Varuna and Münster creeks can be compared with the observed sediment volumes given in Table 1. It is seen that the predicted volumes based on  $d_{90}$  (to determine  $Q_{cr}$ , case B) are closer to the observations (s. Table 1) than those based on  $d_m$  (case A). This is in general agreement with equ. (6) which indicates that a larger critical discharge is required to break up the armour layer than the one for initiation of motion of a relatively uniform sediment (equ. 1).

A torrent bed is characterised by a very wide grain size distribution. A complete destruction of the armour layer is probably very rare and might not even be reached after the passage of a debris flow. During a flood event, sediment enters the channel also from undercutting and failure of side slopes; however, it cannot be expected that this supply

is sufficient to satisfy the (calculated) transport capacity of the flow. It may therefore be concluded that direct application of bed load transport formulae, developed under idealized laboratory conditions, tend to overestimate effective transport rates in a torrent.

### 3 DEBRIS FLOW OR TOTAL SEDIMENT VOLUMES

During flood events, enormous masses of sediment can be delivered to the mouth of a torrent catchment. In many cases, only minor parts of all the material is transported in fluvial form (as bed and suspended load) and large portions are moved in the form of a debris flow which may consist of one or several waves or pulses. Then it is no longer sufficient to estimate the sediment volumes transported from the catchment by using a bedload transport formula and a hydrograph (as done in the previous section). Instantaneous peak discharges of debris flow pulses can be one or two orders of magnitude higher than the peak water discharge during the same flood event (Haeberli et al., 1990). In such cases, the approach discussed above could clearly underestimate resulting sediment volumes.

Therefore numerous debris flow events of the summer 1987 in Switzerland were analysed on a statistical basis. As a result, a new empirical formula was developed to estimate the debris potential associated with such events. This relation is compared with similar equations which were developed in Austria and in Japan.

#### Analysis of Swiss debris flow events

The two major rainstorm events (July 18/19 and August 24/25) of the summer 1987 caused flooding (s. also case study of previous section) and debris flows in several regions in the Swiss alps. A large concentration of debris flows could be observed in the scree and moraine slopes of the periglacial belt, because warm temperatures resulted in rain- instead of snowfall at high altitudes. Most of the debris flows analysed in this study deposited between 1000 m<sup>3</sup> and several 10'000 m<sup>3</sup> of material on the fan. However, there was also a number of events in which up to several 100'000 m<sup>3</sup> of sediment were eroded in and along torrent channels and transported down to the main valley (s. also Table 1).

A detailed analysis was performed with 82 of these debris flow events (Haeberli et al., 1990). It was examined whether any general relationships exist between simple parameters such as total debris volume, average debris yield rate per unit channel length, catchment area, mean channel slope and fan slope. The most clear dependency was found on a diagram of channel debris yield rate versus fan slope. From this diagram, an upper limit defining the maximum debris yield rate,  $EL$  [ $m^3/m$ ], could be determined as a function of the fan slope in percent,  $J_K\%$  :

$$EL = 110 - 2.5 J_K\% \quad (8)$$

For the examined cases, the fan slope varied between 8 and 45%, and the largest value of the average debris yield rate was about 100  $m^3/m$ . (It may be noted that negative values of  $EL$  result, if  $J_K$  is greater than 45%). Since the debris yield rate  $EL$  is defined as the ratio of the total debris volume,  $M$  [ $m^3$ ], to the channel length,  $L$  [ $m$ ], equ. (8) can be transformed into:

$$M = (110 - 2.5 J_K\%) \cdot L \quad (9)$$

These equations express an upper limit of erosion to be expected in the case of a debris flow event. To illustrate the degree of overestimation, the ratios of calculated to observed debris volumes ( $M_{cal}/M_{obs}$ , termed "estimation error") are plotted in Fig. 3 as a function of the observed volumes. Also included are some Austrian events (taken from Hampel, 1977, 1980) to enhance the number of debris flows with large volumes. It is seen from Fig. 3 that very large estimation errors can result for events with smaller observed volumes, while for large events (with  $M_{obs} \geq 100'000 m^3$ ) the error is less than a factor of 2.

#### Comparison with similar formulae

In Austria and in Japan, similar formulae were proposed to estimate the maximum debris potential that can be moved during extreme flood and debris flow events. Also with these equations, the maximum debris volume is estimated as a function of simple parameters characterising certain elements of the torrent catchment.

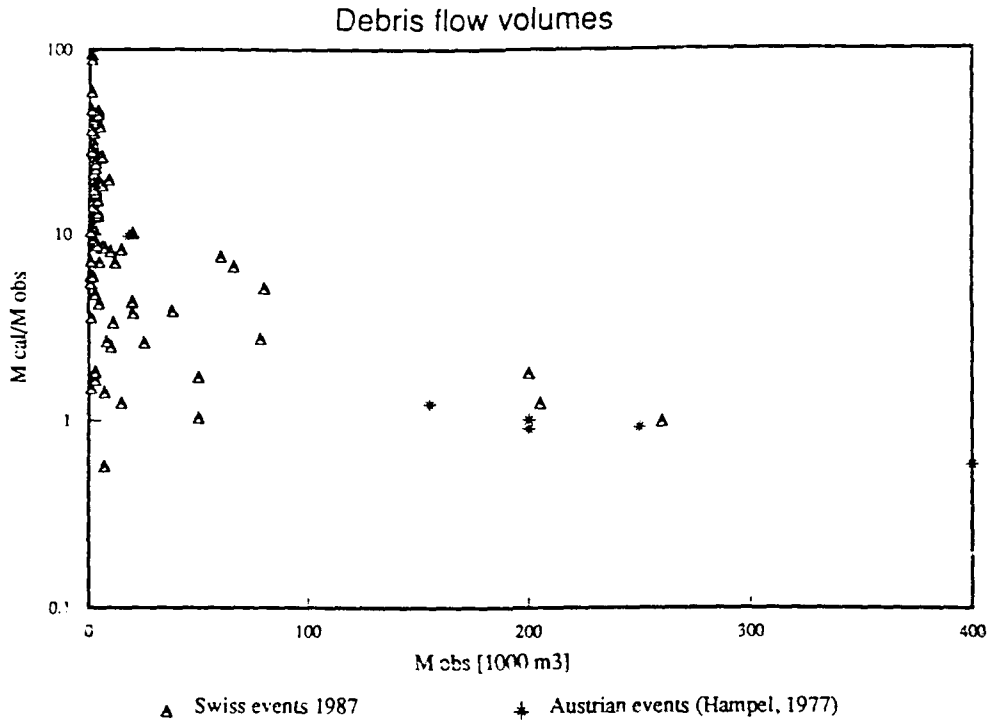


Fig. 3: Performance of Equ. (9) in comparison to 82 Swiss debris flow and some Austrian events, showing the ratio of calculated to observed debris volumes ( $M_{cal}/M_{obs}$ ) as a function of the (observed) event magnitude ( $M_{obs}$ ).

Hampel (1977) developed an equation to estimate the debris volume  $M$  in  $[m^3]$  as a function of the parameters catchment area,  $EG$  in  $[km^2]$ , and fan slope  $J_K\%$  :

$$M = 150 EG (J_K\% - 3)^{2.3} \quad (10)$$

The exponent of the slope term is partly based on laboratory experiments, and the constant 150 was "calibrated" with 15 debris flow events with volumes between 4000 and 500'000  $m^3$ ; the corresponding fan slopes vary between 6 and 14%.

Another formula was proposed by Kronfellner-Krauss (1982), expressing the debris volume,  $M$  in  $[m^3]$ , in terms of the catchment area  $EG$   $[km^2]$  and the mean creek slope,  $J_m\%$  in  $[\%]$ :

$$M = K EG J_m\% \quad (11)$$

where  $K$  is a torrential erosion coefficient which varies between 500 (large catchments, with sediments already eroded) and 1500 (steep torrents with large sediment sources). In this study, a value  $K = 1500$  was used. For the calibration of the coefficient  $K$ , Kronfellner-Krauss (1982, 1985 Tsukuba) used a part of over 100 events with volumes between 5000 and 20'000 m<sup>3</sup> and several events with more than 20'000 m<sup>3</sup>. The corresponding catchment areas vary between about 1 and 80 km<sup>2</sup>.

A third empirical equation is presented in Japanese planning and design guidelines against debris flow events (Public Works Research Institute, 1988). Using some coefficients given in this publication, the formula can be simplified to:

$$M = 1100 \Psi_o R_{24} EG \quad (12)$$

where  $R_{24}$  in [mm] is the accumulated rainfall 24 hours prior to the event, and  $\Psi_o$  is a runoff coefficient (given in a diagram), which decreases with increasing catchment area ( $\Psi_o = 0.55$  for  $EG = 0.1$  km<sup>2</sup>, and  $\Psi_o = 0.1$  for  $EG = 10$  km<sup>2</sup>); again,  $EG$  is in [km<sup>2</sup>] and  $M$  in [m<sup>3</sup>]. There is no mentioning of the range of the parameters used in the development of this equation.

For comparison with equ. (9) and with the corresponding data set, the three formulae (10) to (12) were applied to 82 Swiss debris flow events of the summer of 1987. The results are shown again in terms of the "estimation error" ( $M_{cal}/M_{obs}$ ) as a function of the observed debris volume, s. Fig. 4(a)-(c). The largest ratio  $M_{cal}/M_{obs}$  shown in Fig. 4 is 100; even larger "estimation errors" result for small events (around 1000 m<sup>3</sup>) according to equ. (10) of Hampel (up to a factor of 530).

It is seen that the three formulae (10) to (12) show a similar pattern in the diagrams as equ. (9) in Fig. 3. Again, there is a clear overestimation of the debris volumes for small events, while the error becomes smaller for larger events. It is noted that the three later formulae also underpredict observed volumes by up to a factor of about 5 (s. Fig. 4), whereas equ. (9) was developed on the basis of the presented data set to give an upper limit. The range of the estimation error is similar for all equations, except for the formula of Hampel (equ. 10) which yields a somewhat larger overestimation for some cases.



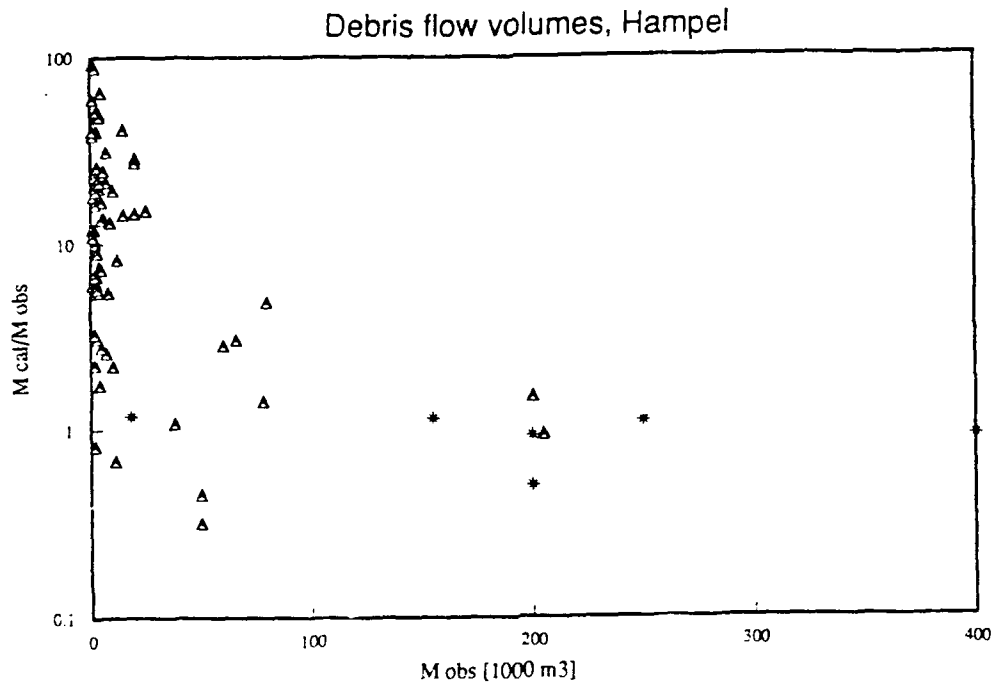


Fig. 4 (a)       $\Delta$  Swiss events 1987       $+$  Austrian events (Hampel, 1977)

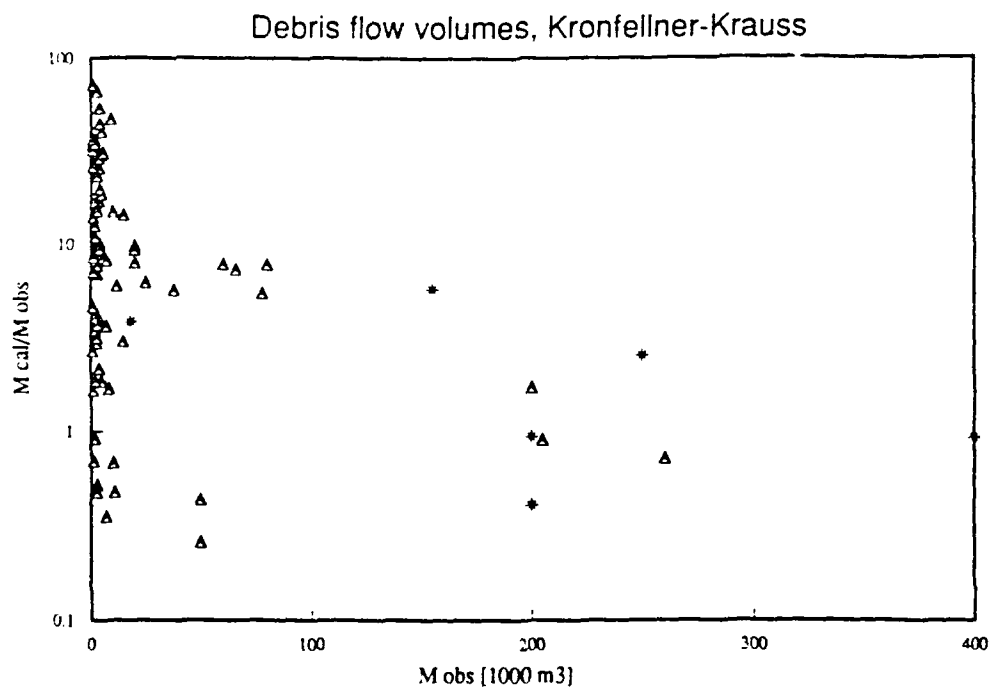


Fig. 4 (b)       $\Delta$  Swiss events 1987       $+$  Austrian events (Hampel, 1977)

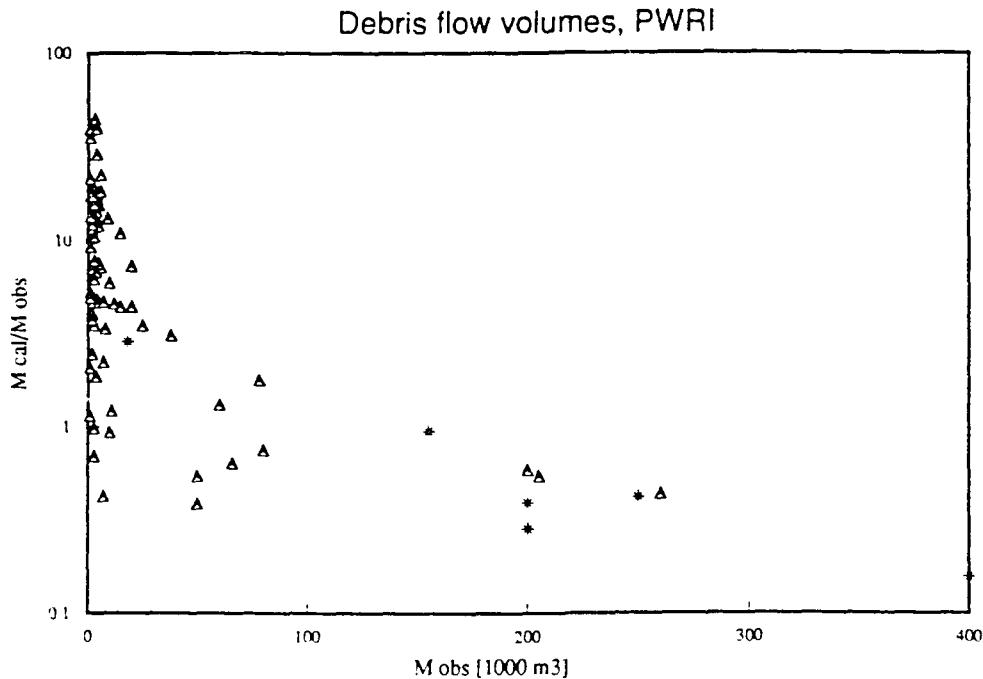


Fig. 4(c)       $\Delta$  Swiss events 1987       $+$  Austrian events (Hampel, 1977)

Fig. 4: Application of several empirical formulae to the same debris flow events as in Fig. 3, showing the ratio of calculated to observed debris volumes ( $M_{cal}/M_{obs}$ ) as a function of the (observed) event magnitude ( $M_{obs}$ ).  $M_{cal}$  was determined according to (a) Hampel's equ. (10), (b) Kronfellner-Krauss' equ. (11), and (c) the Japanese equ. (12).

For the considered debris flow events, the parameter  $R_{24}$  varied in a relatively narrow range (about 50 to 250 mm), so that it may be neglected in a first comparison of the four empirical formulae (in view of the much larger overall estimation error). Then it is not so much surprising that there is a similar estimation error for all four equations. For there are mainly two effects that are considered: First, a parameter characterising the catchment area ( $EG$ ,  $L$ ) represents the overall debris and water potential. Second, there is a "correction" factor ( $J_K$ ,  $J_m$ ,  $\Psi_o$ ) which decreases with increasing catchment area. With equ. (9), the effect of an increasing  $EG$  does not seem sufficiently accounted for by the parameter  $L$  (instead of  $EG$ ); this is probably the reason why  $J_K$  has a negative sign, and thus the correction works in the opposite direction (as compared for example to Hampel's equ. 10).

It appears that the maximum debris potential can be very roughly estimated considering simple parameters that characterise the potential debris and water supply. This simplified view seems to hold approximately for larger catchment areas ( $> 1 \text{ km}^2$ ), involving still an estimation error up to a factor of the order of 10. With smaller catchments, other factor related to the initiation of debris flows become relatively much more important, and thus the error increases drastically. An upper limit of application may be given by the debris flow process as such, since with increasing catchment area and decreasing slopes, channel yield rates decrease markedly and furthermore a debris flow might not reach the mouth of the catchment. In alpine regions, a catchment area of about  $25 \text{ km}^2$  may be suggested as this upper limit.

#### 4 CONCLUSIONS

Based on laboratory experiments, a new procedure is proposed to determine bedload transport rates and flow resistance in steep channels. For four torrents, fluvial sediment volumes transported to the fan were calculated by combining the proposed bedload transport formula with an (estimated) flood hydrograph. A comparison with observed volumes shows that a relatively high critical discharge at initiation of motion should be selected, using rather  $d_{90}$  than  $d_m$  as characteristic grain size of the bed material. It seems likely that in a torrent the armour layer is very rarely completely destroyed. Thus full transport capacity (as determined from idealized experimental conditions) may be reached only during short periods of a flood event, since no continuous sediment supply can be expected from side slope failures.

To estimate the maximum debris potential of a torrent catchment, several empirical formulae are available. They are based on parameters characterising the water and sediment to be possibly discharged during a flood event. Such a simple approach gives a first, very rough estimate of the maximum debris volume that can be removed from the catchment during an extreme rainstorm event. An application to 82 debris flow events of the summer 1987 in Switzerland showed that the error of estimation decreases with increasing catchment area; observed debris volumes were overestimated by up to a factor 10 in catchments larger than about  $1 \text{ km}^2$ .

REFERENCES:

- Bathurst, J.C., Graf, W.H., Cao, H.H. (1987):**  
"Bed load discharge equations for steep mountain rivers", in: Sediment transport in gravel bed rivers, eds. Thorne, Bathurst, Hey, John Wiley and Sons, p.453-477.
- Fehr, R. (1987):**  
"Geschiebeanalysen in Gebirgsflüssen", Mitteilung Nr. 92 der Versuchsanstalt für Wasserbau, Hydrologie und Glaziologie, ETH Zürich.
- Günter, A. (1971):**  
"Die kritische mittlere Sohlenschubspannung bei Geschiebemischungen unter Berücksichtigung der Deckschichtbildung und der turbulenzbedingten Sohlenschubspannungsschwankungen", Mitteilung Nr. 3 der Versuchsanstalt für Wasserbau, Hydrologie und Glaziologie, ETH Zürich.
- Haeberli, W., Rickenmann, D., Rösli, U., Zimmermann, M. (1987):**  
"Murgänge 1987: Dokumentation und Analyse", Mitteilung der Versuchsanstalt für Wasserbau, Hydrologie und Glaziologie, ETH Zürich, in preparation.
- Hampel, R. (1977):**  
"Geschiebewirtschaft in Wildbächen", Wildbach- und Lawinenverbau, Jg. 41, H. 1, p. 3-34.
- Hampel, R. (1980):**  
"Die Murenfracht von Katastrophenhochwässern", Wildbach- und Lawinenverbau, Jg. 44, H. 2, p. 71-102.
- Kronfellner-Krauss, G. (1982):**  
"Ueber den Geschiebe- und Feststofftransport in Wildbächen", Oesterr. Wasserwirtschaft, Jg. 34, H. 1/2, p. 12-21.
- Kronfellner-Krauss, G. (1985):**  
"Quantitative estimation of torrent erosion", Int. Symp. on Erosion, Debris Flow and Disaster Prevention, Tsukuba, Japan, p. 107-110.
- Public Works Research Institute [PWRI] (1988):**  
"Technical standard for measures against debris flow (draft)", Technical Memorandum of PWRI No. 2632, Ministry of Construction, Japan.
- Rickenmann, D. (1990):**  
"Bedload transport capacity of slurry flows at steep slopes", Mitteilung Nr. 103 der Versuchsanstalt für Wasserbau, Hydrologie und Glaziologie, ETH Zürich.
- Smart, G.M., and Jäggi, M.N.R. (1983):**  
"Sediment Transport on Steep Slopes", Mitteilung Nr. 64 der Versuchsanstalt für Wasserbau, Hydrologie und Glaziologie, ETH Zürich.
- Takahashi, T. (1978):**  
"Mechanical characteristics of debris flow", ASCE, J. Hydr. Div., Vol. 104, No. HY8, p. 1153-1169.

Sediment Transport Processes on Alluvial Fans:  
Influences on Fan Morphology and Development

A.M. Harvey, University of Liverpool, England

INTRODUCTION

Alluvial fans are important depositional landforms composed predominantly of coarse sediments, laid down where stream systems issue from steep mountain catchments into zones of reduced stream power. They are transitional between dominantly erosional upland or mountain catchments, within which the transporting capacity exceeds the rate of sediment generation, and valley, piedmont, or lowland areas where transporting capacity is much closer to, and least during the deposition of the fan is or has been exceeded by the rate of sediment supply. This situation has been described by Bull (1979) as one where effective stream power falls below critical stream power i.e. that required to transport the available sediment (Figure 1). This typically occurs in mountain-front locations but fans may also occur where steep tributary streams join major valleys (Harvey 1989a). They are common in arid and semi-arid regions (Bull 1977, Harvey 1989a), but also occur in humid environments especially in mountain areas where sediment generation is high in relation to transport capacity (Rachocki and Church 1990).

Because the streams feeding alluvial fans are at or near the threshold of critical stream power (Bull 1979) they are especially important to the geomorphology of mountain or upland regions for two reasons. First, they are sensitive to changes in run-off and sediment generation from the mountain catchments and preserve in their constituent sediments the most complete record of the erosional history of the mountain catchment. Second, from a functional point of view, they may act as major sediment stores within the fluvial system, trapping most or all of the coarse sediment generated within the mountain catchments and therefore buffering the system downstream from the effects of changes in sediment production. The effectiveness of this buffering role will depend upon the processes on the fan itself. An aggrading fan may trap all the coarse sediment generated within the mountain catchment and therefore effectively break the continuity of the system, but if the fan surface becomes dissected then channel continuity and sediment transport continuity from mountain areas to mainstream systems may be restored.

The factors controlling alluvial fan behaviour are firstly those controlling water and sediment supply to the alluvial fan and secondly the transport efficiency through the fan. The first group depend on catchment characteristics, on for example the tectonic context, the geological and geomorphological history, relief, erosion rates, climate and hydrology. The second group depend in part on the transport mechanism through the fan environment but also on the fan morphology, itself the product of previous alluvial fan deposition. This paper examines the

influence of catchment characteristics on the sediment transport characteristics and in turn their influence on fan morphology paying special attention to progressive changes in fan morphology resulting from environmental change. It draws on examples from a wide range of climatic environments from the arid Mojave Desert, California, to semi-arid Mediterranean region fans in Spain and Greece, to humid region fans in northwest England, over a range of timescales from the mid Quaternary to the present day.

#### SEDIMENT TRANSPORT PROCESSES ON ALLUVIAL FANS

Classically sediment transport processes on alluvial fans have been grouped into three (Blissenbach 1954); debris flow, stream flow and sheet flow processes. More recent work by Wells and Harvey (1987), on the basis of the characteristics of sediments produced by a major storm on small alluvial fans in the Howgill Fells, northwest England, has identified four types of depositional environment and therefore four types of sediment transport mechanism. These are: (i) true debris flow deposits, characterised by a matrix supported fabric showing push structures, including vertical clasts, aligned parallel with lobe fronts, and surface pressure ridges; (ii) transitional deposits, characterised by clast-supported, structureless gravels with matrix only in the lower part of the deposit. These deposits have been interpreted as transported and deposited by hyperconcentrated flows (Pierson and Scott 1985) whereby transport takes place as a very wet mass flow but on deposition the wet fluid matrix drains, or at least partially drains. Sediment concentration in the fluid gives the material sufficient strength for mass transport but on deposition is sufficiently dilute to drain, causing the clasts to settle and giving the deposit its almost structureless clast-supported fabric. (iii) fluvial bar deposits, showing a well developed fluvialite imbrication and a clearly developed nose to tail sorting. These deposits show clear evidence of fluvial transport, often with a strongly developed 'bar and swale' relief. They include features similar to those described as sieve deposits (Hooke 1967). (iv) fluvial sheet deposits: these are well sorted thin sheets of fluvialite gravels locally showing a weak bar and swale topography on the surface.

Matrix particle size varies between these four types of deposit. The matrix of the true debris flows has an abundance of silt and clay, whereas the matrix in the fluvial deposits is almost wholly of sand. Where present, that in the transitional deposits has particle size characteristics mid-way between those of the true debris flows and of the fluvial deposits (Wells and Harvey 1987).

In that study a general model was proposed relating the transport and depositional processes to the relative fluidity of the water sediment mix fed in from the catchment, and identifying the controlling catchment characteristics. (Fig.2) Although based on the response of the Howgill fans to one major storm, the same general principles should apply to the dominant mode of deposition over a period of time on any group of fans. The

Howgill fans were then grouped into two groups; fans dominated by debris flow/transitional deposits and fluvial fans, and the two groups were successfully discriminated on the basis of a variety of catchment characteristics relating, on one axis, to drainage area, and on the other to various measures of catchment steepness (Wells and Harvey 1987). The results accord in a general sense with the trends identified by Kostachuk et al. (1986) working in the Canadian Rockies, and with those identified by Harvey (1984a) working in Spain. In all cases debris flow fans with Trollheim-type sedimentary sequences (Miall, 1977) are associated with small steep catchments, whereas fluvial fans with Scott-type sedimentary sequences (Miall 1977) are associated with larger and less steep catchments.

In this paper the catchment characteristics discriminating between debris flow and fluvial fans are examined for fans in a variety of climatic environments and over a range of timescales.

#### STUDY AREAS

##### Zayzix fans, California.

The Zayzix fans (Fig.3) issue from the eastern flank of the Soda Mountains in the Mojave Desert, California, an arid region with c.100mm mean annual precipitation. Geology of the source area comprises Mesozoic granites and metamorphic rocks. The fans occur along a faulted, but long since stabilised, mountain front and backfill into the mountain catchments. They toe out at the margins of Pleistocene Lake Mojave, now a dry playa, Soda Lake. The fan surfaces have been mapped and segments assigned to late Pleistocene and late Holocene ages on the basis of desert varnish and soil development (Wells et al., in preparation), and their relations to dated late Pleistocene and Holocene lake shorelines (Wells et al. 1987). The fans (Fig.4) range from debris flow fans issuing from small steep basin to fluvial fans issuing from larger and less steep basins, but there is an overall trend towards increasing fluvial activity and decreasing debris flow activity from Pleistocene to Holocene times. On the larger fans this has been associated with the development of fanhead trenches and the progradation of the distal fan area (Wells et al., in preparation; Harvey and Wells, in preparation).

##### Southeast Spain

Numerous fan groups occur in south east Spain (Fig. 3) issuing from mountains of the Betic Cordillera into adjoining lowland areas or at the margins of adjoining Neogene sedimentary basins. The region has a semi-arid climate with mean annual precipitation ranging from c.350mm in the northern part of the area in Alicante Province to less than 200mm in the south in Almeria. The fan surfaces range in age from mid-Pleistocene to Holocene and most are dissected by deep fanhead trenches, some also by mid-fan trenching, and some are dissected throughout (Harvey, 1987a, 1989, 1990).

For the purposes of this paper the fan groups are divided into three: (i) those in southern Alicante and northern Murcia provinces, which issue from catchments on Mesozoic limestones and on tough low grade metamorphic rocks. They include both debris flow (Fig. 4) and fluvial fans. These areas have had a more complex aggradation and dissection history during the Pleistocene

than areas further south (Harvey, 1984b), (ii) fans in southern Murcia and Alicante provinces issuing from schist catchments, mostly simple fans (Fig. 4) which are dominated by fluvial deposits (Harvey 1984a), (iii) other fans in southern Murcia and Almeria provinces issuing from non-schist catchments which include debris flow fans but have a less complex Pleistocene history than those in the area to the north (Harvey 1984a).

#### Methana, Greece

Around the margins of the Methana peninsula (Fig. 3) fans issue from catchments on early to mid-Quaternary Dacite/Andesite volcanic rocks. They include both debris flow and fluvially dominated fans of late Quaternary age. The larger fans have been dissected by deep fanhead trenches (Fig. 7) and in some cases Holocene fan segments prograde in the distal areas. The climate is a dry Mediterranean climate, with mean annual total of strongly seasonal rainfall of  $\approx 400$ mm.

#### Howgill and Bowland Fells, Northwest England

Holocene alluvial fans have been studied in two upland areas of northwest England, the Howgill and Bowland Fells, humid regions with mean annual precipitation ranging from  $\approx 1500$ mm in the Howgills to  $\approx 1900$ mm in Bowland (Harvey 1986). In both areas the fans date from the younger Holocene (Harvey et al 1981; Harvey and Renwick 1987; Harvey 1985), apparently resulting from accelerated hillslope erosion induced by vegetation changes in Bowland at  $\approx 2000$ BP and in both areas at  $\approx 1000$ BP. Source area geology in the Howgills is of late Pleistocene periglacial hillslope sediments overlying tough Silurian mudrocks. In Bowland the source area geology is of late Pleistocene periglacial hillslope sediments overlying very coarse massive sandstones of Carboniferous age. Both areas include both fluvial fans and debris cones. Some composite fans occur in the Howgills (Fig. 4). In both areas sedimentation on the fan surfaces has effectively ceased, apart from sedimentation induced by rare catastrophic flood events, with a return period perhaps of  $\approx 100$  years (Harvey 1986, Wells and Harvey, 1987).

In each study area fan surfaces have been mapped and assigned to dominantly fluvial or dominantly debris flow origins, for the older fan surfaces on the basis of the sedimentology of the deposits exposed in fanhead trenches, and for modern fan surfaces on the basis of surface sedimentary features. For each fan surface segment identified, the fan slope has been measured by profiling along the axial slope of the fan segment. For each fan or fan segment the drainage area has been delimited in the field onto large scale topographic maps, then from these maps catchment morphometric data, drainage area, basin length, basin relief, the latter two giving mean basin slope, have been derived from these topographic maps. This provided the primary data set for the consideration of the influence of catchment characteristics on sediment transport and deposition processes, and the implications for fan morphology and development.

#### CATCHMENT CONTROLS OVER DOMINANT PROCESSES

The previous work, referred to above, has identified that for given climatic and geological context the water:sediment mix fed to the fan environment from the mountain catchment may act



as a major control over sediment transport and deposition processes. If we plot drainage area as an index of water discharge from the mountain catchment, against some measure of slope steepness as an index related to potential sediment supply, it may be possible, on any one group of fans, to identify threshold combinations of these two variables to differentiate between debris flow and fluvial processes. Two immediate problems arise in this simple methodology. First, it only relates to conditions at the fan apex and does not take into account down-fan variations in the water:sediment mix which lead to the proximal to distal facies variations on many alluvial fans (Harvey 1989a). This may not be too great a problem in simple mountain-front fans, where there is little extra water or sediment supply away from the fan apex and down-fan facies changes may be predictable. However on back filled fans, drainage area increases down-fan and this must be taken into account. Furthermore, there may be addition of proximal type sediments in mid-fan from adjacent side slopes, which may otherwise complicate simple thresholds. This problem is considered below especially in the context of the Zzyzx fans.

#### Zzyzx fans

The Zzyzx fans were mapped in the field grouping the fan surface segments into late Pleistocene, Holocene or active modern age categories (see above). For each segment the dominant depositional process, debris flow or fluvial, was inferred either from exposures in fanhead trenches or at the margins of incised channels, or by the sedimentary characteristics of the exposed surfaces. For each fan segment, drainage area was then plotted against drainage basin slope, the latter being the steepness-related variable, which when plotted against drainage basin area gave the clearest separation of plotting position.

Three separate plots were derived for the Zzyzx fans. The first (Figure 5a), deals only with fan apex environments and is therefore directly comparable with true mountain front, rather than backfilled fans. Also shown on this plot are data derived from other fans in the Mojave and Sonoran deserts (Harvey 1987). The fan surfaces shown all relate to late Pleistocene deposition. The Zzyzx fans (shown by the solid symbols on Figure 5a) are nearly all dominated by debris flow deposition at their apices, and contrast with the other, dominantly fluvial fans. It is clear that the Zzyzx debris flow fans are associated with small steep catchments, contrasting with the much larger and less steep catchments for the fluvial fans, but because of an absence of data relating to drainage areas of between 0.2 and 1 km<sup>2</sup>, the pecked line shown on Figure 5a, suggesting the approximate threshold between debris flow and fluvially dominated systems, can only be very approximate.

To examine this threshold more precisely and specifically in relation to the Zzyzx fans, drainage area characteristics feeding the mid-point of all mapped fan segments have been determined and plotted on Figure 5b. Here three types of fan surface are shown, Pleistocene, debris flow and fluvial fan surfaces and Holocene fluvial fan surfaces. The pecked line on Figure 5b suggests a threshold between debris flow and fluvial depositional environments, one about which there are relatively few anomalies. The plotting positions of the Holocene

fluviatile surfaces, dominantly to the lower right of the graph reflect the tendency for Holocene fanhead trenching and distal aggradation by fluvial processes (Wells et al. in preparation).

It has also been possible to consider the controls over modern, active processes on the Zyzx fans (Figure 5c). Five categories of modern processes can be recognised. In some fan apex areas and locally further downfan there are recent debris flow deposits. Two fans show little evidence of any geomorphic activity, and these are classified as 'passive', in contrast to deep narrow channels actively incising into older fan surfaces. Two styles of fluvial transport or depositional activity are apparent, either within wide shallow channels, identified here as 'fluvial transport', or as sheets of fluviatile gravels deposited in the distal zones of the modern fans, described here as 'fluviatile fan deposition'. Two thresholds can be suggested here (shown by pecked lines on Figure 5c) one between debris flow deposition and channel incision, both associated with relatively steep catchments, but with incision occurring only on fans draining the larger catchments, presumably as a result of higher stream power. The other threshold, approximately defines the upper limit for fluvial transport and deposition processes. Its position when compared with that on Fig. 5b suggests that at the present day fluvial processes are dominant in some areas which were producing debris flows during the late Pleistocene. This reflects a progressive trend from the Pleistocene through the Holocene of increasing fluvial dominance on these fans apparently reflecting increased aridity, and presumably associated with a reduced sediment supply from the mountain slopes but an increased stream power during flood events typical of arid regions (Baker 1977).

#### Mediterranean fans, Greece, Spain.

Similar methodology has been used for the Mediterranean region fans in an attempt to identify the catchment controls over debris flow and fluvial processes. For the Methana fans (Fig. 6a) data relating only to Pleistocene fan surfaces are included. Most of the fans are deeply trenched and Holocene fan segments are restricted to small distal areas. The dominant sedimentary process in each case has been identified from exposures in fan trenches. The fans are not simple mountain-front fans, but a back-filled fan complex at Kipseli, and coalescent, multi-sourced fan aprons in the other areas. (Fig. 3). Despite the problems of drainage area delimitation a reasonable threshold can be identified on Figure 6a with only two apparently anomalous fan segments.

Previous work on the Spanish fans (Halvey 1984a, 1987b, 1990) has shown that different groups of fans have had rather different Pleistocene aggradation and dissection histories and show rather different morphometric characteristics. For this reason the Spanish fans are treated here as three separate groups. The fans issuing from the limestone Pre-Betic mountains in Alicante and those issuing from the massive low grade metamorphic rocks of the Sierra de Carrasoy and the coastal Sierras in northern Murcia all show strongly calcreted Pleistocene fan surfaces, deep fanhead trenches and a relatively complex history of Pleistocene aggradation and dissection. Some are simple mountain front fans, others are back-filled fans.

For individual fan apices (Figure 6b) a reasonably clear threshold discriminates between debris flow and fluvial fans with few major exceptions. One of the exceptions relates to a small fan in the Torre group (location, Fig. 3) which produces a sediment sequence dominated by stratified fluviatile gravels rather than the debris flows that would be expected on the basis of the steep mountain catchment, however, this source area is in a relatively high grade fissile schist which may not be conducive to the production of debris flows.

On the basis of previous work, fans in southern Murcia and Almeria are sub-divided into those issuing from high grade fissile schist catchments and those from non-schist areas. For the non-schist areas (Fig. 6c), with the exception of fans from the Cabo de Gata volcanics, a reasonably clear threshold can be identified, despite the wide range of bedrock geologies. Most of these fans are simple mountain front fans with well developed calcrete crusted fan surfaces, shallow fanhead trenches and Holocene fluviatile distal fan deposits. Only the Pleistocene upper fan segments are included here.

In the schist areas (Fig. 6d) only two small fans are dominated by debris flow deposits, but three others show occasional debris flow deposits at the base of the sedimentary sequences. If these are grouped with the two debris flow fans a threshold can be identified separating this group from the majority fluviatile fans. Some of these fans are simple mountain front fans, but many, especially issuing from the Sierra de los Filabres are back-filled fan complexes. The fan sequences are relatively simple, with aggradation often until late Pleistocene, often with little calcrete development, limited fan trenching and Holocene distal aggradation. Again only proximal fan surface segments are included here.

#### Northwest England, Howgills and Bowland Fells

The sedimentary style for Howgill and Bowland fans has been determined either from exposed sections or from fan surface morphology. For the Howgill fans there is a contrast between debris flow fans or debris cones, composed of ill-sorted matrix-rich debris flow deposits whose surfaces preserve lobate debris flow morphology, and fluviatile fans composed of stratified, better sorted matrix-poor cobbles whose surfaces are either smooth or lightly channelled. Some of the Howgill fans are composite forms with proximal debris flow deposits from which distal fluvial fan segments have been flushed. If these are considered primarily as debris flow fans a reasonably clear threshold with few anomalies can be identified (Fig. 7a). Two anomalous fluvial fans issue from steep catchments, both in the same valley, Upper Bowderdale; both are small fans and could be younger than the main group of fans.

The debris cones in Bowland show ill-sorted largely unstratified boulder or cobble deposits with a sandy matrix whereas those classified as fluvial fans show better sorting and clear stratification. Because of the coarse sandy nature of the periglacial hillslope parent materials the debris cones were probably deposited by transitional rather than true debris flow deposition. Despite the limited number of fans in Bowland an approximate threshold can be suggested (Fig. 7b).

### Catchment controls: summary

When the thresholds suggested on Figs. 5 to 7 are plotted together (Fig. 3), it is clear that within the various regions different catchment characteristics influence the relative importance of fluvial and debris flow processes. The most "fluvial" fans are those in the arid American southwest. In that area modern fan processes are more "fluvial" than they were during the Pleistocene. The Mediterranean region fans are more debris flow rich, though it must be remembered that these fans relate to Quaternary climates rather than present day Mediterranean climates. Climates during Pleistocene "glacial" phases appear to have been cold, dry, with relatively high rates of weathering in the mountain catchments but higher storm-induced seasonal run-off than today (Sabelberg 1977). It may be due to climatic or geological control that fans in the more arid south of Spain are more "fluvial" than those further north. Not surprisingly for a humid region, the Bowland fans are the least "fluvial", but the strongly "fluvial" plotting position of the threshold for the Howgill fans appears to be little anomalous. Perhaps the reason may relate to the low infiltration capacities and steep slopes in the Howgills coupled with the fact that the fans are the product of a major phase of gully erosion, whereas in Bowland slope failure appears to be more important in sediment supply, and with the sandier parent material run-off rates may have been lower.

A major implication of these results is that, not only do drainage basin characteristics, drainage area and slope characteristics, and presumably at a local scale geology, influence the threshold between debris flow and fluvial processes, but climate may also be a major control. This may be important not only in the context of contrasts between regions but also in the context of geomorphic responses to climatic changes. The major reason behind this appears to involve the relationship between stream power and critical stream power in the mountain front zone, or in more general terms the relationship between sediment and water generated in the mountain catchment during flood events.

### MORPHOLOGICAL IMPLICATIONS

Previous work on alluvial fan morphology (Bull 1962b, Hooke 1968, Harvey 1989a) has indicated that sediment transport processes on alluvial fans influence fan morphology, especially through their influence on depositional slope. Deposition by debris flows takes place at greater slopes than deposition by fluvial processes, and within fluvial processes deposition by unconfined sheet flow takes place on greater slopes than deposition by channel processes. Therefore, as catchment characteristics influence sediment transport processes so do they influence fan morphology. In addition to this influence, controlled by the water : sediment mix, fed to the fan environment, is an influence related to particle size, itself partly dependent on catchment topography and partly on catchment geology (Blissenbach 1952, Bluck 1964, Lustig 1965, Denny 1965, Hooke and Rohrer 1979). Coarser sediments will be deposited on steeper slopes than finer sediments. Furthermore, these influences are likely to change downfan from proximal to distal environments with selective deposition of coarse material at the

fan apex and possibly dilution downfan, leading to a general concavity in the longitudinal profile of the fan. This tendency is accentuated on backfilled as opposed to mountain-front fans, where drainage area increase downfan. For particular groups of fans the simplest of these relationships can often be expressed by a regression equation in the form:

$$G = aA^b$$

where  $G$  is fan slope and  $A$  is drainage area, but the strength of the correlation can often be improved by taking into account some measure of catchment steepness (Harvey 1987a). In this paper these relationships are considered for the several study areas, taking into account the differences between debris flow and fluvial fans. For simple mountain front fans the fan slope is measured for the proximal third of the fan but for backfilled and composite fans slopes are measured and appropriate drainage basin characteristics derived for individual fan segments in proximal, mid-fan and distal fan locations, thereby taking into account the increase in drainage areas downfan.

For the American fans (Fig. 9a), there is a clear distinction between debris flow and fluvial fans, with the debris flow fans having much higher gradients per drainage area. Given the moderate correlations no real difference is apparent in the slopes of the regression lines. When the Zzyzx fan surfaces are treated separately (Fig. 9b) there is again a clear separation between the debris flow segments and the fluvial segments. The correlation for the Pleistocene fluvial surfaces on their own is not significant and only becomes so when all fluvial fan surfaces, Pleistocene and Holocene are considered together.

For the Mediterranean region fans (Fig. 10), in all cases there are again clear separations between debris flow and fluvial fans. On Methana (Fig 10a), the slope of the regression line for the debris flow fans is less than that for the fluvial fans. For the Spanish northern group (Fig. 10b) the correlation for the fluvial fans is not significant. This group includes a wide range of fan types from basins with a wide range of geology and topography (Harvey 1987a) and includes the tectonically disturbed Carrascoy fans (Harvey 1988). However, the debris flow fans clearly have higher gradients per drainage area than do the fluvial fans, and when an all-fan regression is calculated for this group, although still not significant the 5% level, residuals for the debris flow fans are in all cases but one positive and for all but four of the fluvial fans are negative. The mean residuals for the debris flow and fluvial fans are significantly different at the 1% level on the basis of Student's  $t$  test. For the two southern Spanish groups there are again clear distinctions between debris flow and fluvial fans, and in both cases the slopes of the regression lines for the debris flow fans are less than those for the fluvial fans.

There is a similar picture for the two groups of English fans (Fig. 11), with higher gradients per drainage area for the debris flow fans, and lower slopes to their regression lines. Although there are only four fluvial fans in the Bowland group it is clear that they follow a similar behaviour to those in the Howgill group.

Considering these regression analysis together (Fig. 12, Table 1), several patterns emerge. In some, but not all cases, the correlations are stronger for the fluvial fans. As would be expected, in all cases the fan gradient per drainage area for the debris flow fans is greater than that for the fluvial fans. In most cases the slopes of the fluvial regression lines are greater than those for the debris flow regression lines, suggesting that the fluvial fans are more sensitive to selective sediment transport either within the mountain source areas or within the fan environment itself. The overall differences in plotting position (approximately equivalent to 'a', Table 1) do not seem to reflect climatic differences, and are probably related to geology and relief differences within the source area.

In order to examine the influence of relief characteristics within each fan group, multiple correlation and regression analyses were carried out (Table 2), using drainage basin relief and drainage basin slope as measures of the basin steepness. In almost all cases correlation coefficients significantly improve and standard errors of the estimate significantly decrease when one or other of the two steepness characteristics are taken into account together with drainage area. In most cases basin relief gives better results than basin slope. For most of the major relationships multiple correlation coefficients are at least 0.7; even those relationships that had non-significant correlation coefficients for drainage area alone improve to significance and correlation coefficients of at least 0.5. With two exponents involved it is a little difficult to make direct comparisons between the multiple regression equations, but for the all-fans relationship there are still major differences between the residuals for the debris flow and fluvial fans, reflecting the different nature of the catchment controls over each process.

## DISCUSSION

It is clear that drainage basin characteristics influence the sediment transport processes on alluvial fans which in turn influence fan morphology, especially fan slope. The most important drainage basin characteristics can be divided into three groups, those related to topography, geology, and climate/vegetation. The topographic controls, dealt with in this paper, are the size of the drainage basin influencing the volume of water supplied to the alluvial fan, and the steepness of the drainage basin relating to the potential for sediment supply. Geological controls may account for differences between fan groups within any climatic environment, and include the availability of fine sediment, hence the propensity for debris flow processes, and the particle size characteristics of the coarse sediments which influence depositional slope. The climate/vegetation controls influence the generation of water and sediment on the hillslopes of the drainage basin, and the transport efficiency through the drainage net to the alluvial fan environment. Particularly important are the effectiveness of storm rainfall, and the rate and style of sediment generation, whether by slope failure or by overland flow processes. Of these groups the third is the most likely to change with time,

therefore the most likely to cause changes in alluvial fan morphology.

If climate or vegetational cover were to change in such a way that altered the effective water: sediment ratio during storm events, the sediment transport processes on the alluvial fan would also change (essentially involving a lateral shift in the position of a distribution curve on Fig.2). As the new process would be operating on fan slope or fan channel slope created by former processes a change in the aggradation/dissection regime of the fan could occur. This would be especially important if a change took place from debris flow to fluvial processes in that fan dissection could be initiated. There are three zones within alluvial fans that may be prone to dissection. The first zone is at the apex of an undissected fan where dissection could lead to the development of a fanhead trench (Schumm et al. 1987). The second zone is in mid-fan on a fan whose proximate areas are dissected by a fanhead trench, and where the fan channel emerges onto the fan surface at an intersection point (Hooke 1967). On most fans deposition occurs here (Wasson 1974), but on some dry-region fans, especially where the fan surface is cemented by calcrete, mid-fan incision may occur (Harvey 1987a). The third zone is at the fan toe, but this is related to different controls, either to base level changes causing incision or to the lateral migration of a mainstream to which the fan is tributary.

The relationship between process change and morphological change has two important implications for fan dynamics, first in the context of the history of fan development, and second in the context of the vulnerability of alluvial fans to contemporary environmental change. Providing it can be distinguished from the general long term trend of fanhead incision and distal progradation (Eckis 1928), sequential changes in fan dynamics produce a suite of fan profile types (Fig.13, and Harvey 1987a), ranging from type C for an aggrading fan, types A and B for fanhead trenched but distally aggrading fans, type C for fan with mid-fan scour, but no substantial incision, types D and E for fans subject to mid-fan erosion, type F for a wholly dissected, fan and type G for a fan subject to fan toe incision. Harvey (1987a) has attributed mid-fan erosion to conditions where unit stream power increases rather than decreases in mid-fan, on fans where the channels are relatively narrow and there is a major slope difference between fan surface slope and channel slope (Fig.13). Profile types for the study fans (Table 3) can be compared with the changes in the dominant processes during fan development (Table 4). For the American and Mediterranean groups these trends relate to timescales from the Pleistocene into the Holocene, and for the English fans for environmental changes during the Holocene. The Zyzx fans show a trend away from debris flow processes and a wide range of profile types. The dominantly fluvial other American fans characteristically have A/E profiles. The Methana fans show some shift from debris flow towards fluvial processes, but the most important profile type is type F where dissection is base-level induced (Type G). Similarly the Spanish northern group show some trend from debris flow towards fluvial processes and include many examples of mid-fan scour or dissection (Types C, D and E), but the southern

Spanish groups are overwhelmingly fluvial and dominated by A/B type profiles. The Howgill fans include many simple aggrading fans (Type C) and many of types A/B often associated with a switch from debris flow to fluvial processes, involving the flushing of the deposits towards distal fan environments. This is very similar to some fans in western Scotland, an area more recently glaciated than the Howgills, where late Pleistocene to early Holocene paraglacial debris cones have been flushed out later in the Holocene to produce distal alluvial fans (Brazier et al 1998). Many of the Eowland fans have been dissected at the toe by lateral erosion by the mainstream. Putting these two data sets together it is possible to see some association between process trend and profile type (Table 5). Active and stabilised debris cones are largely of type O. Fans which have seen a switch from debris flow to fluvial processes show profiles dominated by fanhead trenching (types A/B) or mid-fan scour or dissection (type C,D,E). Dominantly fluvial fans show a range of profile types similar to those which have switched from debris flow to fluvial processes. No fans show a switch from dominantly fluvial to debris flow processes and on most of those fans which have switched from deposition, either by debris flow or fluvial processes, to incision, the incision has been primarily related to incision at the toe (type G).

Interestingly, though the Pleistocene to Holocene process and morphological trends are similar in both the American and Mediterranean study areas, the underlying climatic causes do differ. In the American case the Holocene aridification has been associated with the cessation of debris flow activity on the hillslopes, the reduction of sediment supply to the fan environment, the increasing effectiveness of flood run off and the trend towards fan dissection. In the Mediterranean case, cold arid 'glacial' climates produced abundant sediment from the hillslopes, but an apparent decrease in aridity during the Holocene (Harvey 1984a, Sabelberg 1977) has been associated with some switch from debris flow to fluvial activity and an overall dissection trend. This is presumably in response to a reduction in weathering rate within the mountain catchments. The British fans were initiated apparently by human induced vegetation changes, with some subsequent trend from debris flow to fluvial processes or to stabilisation, presumably as revegetation took place within the source areas.

Because alluvial fans are dynamic features, susceptible to environmental change, it is relevant to consider their potential response to currently postulated climatic changes resulting from global warming (Harvey 1989b). Climatically induced vegetation change could influence hillslope erosion rates and therefore sediment supply to the fan environment. In dry regions the climatic trend could be to increasing aridity and a reduction in vegetation cover and an increase in sediment supply, but in humid areas accelerated vegetation growth could lead to stabilisation and a reduction in sediment supply (Fig 14). In most regions an increased storm frequency or storm severity could increase runoff rates and hence stream power. These two changes could cause a shift in the position of the curves on Figure 2, representing a change in transport process and/or erosion/deposition relationships. The cones particularly



susceptible to change are the fan apex, especially on undissected fans, but fanhead trenches themselves could be subject to further dissection, and the intersection point/mid-fan zone. In addition a change in mainstream behaviour, where present, at the fan toe could alter the local base level.

In conclusion, alluvial fans are critical zones within the fluvial system, situated between mountain source areas and main drainages. Processes on alluvial fans influence the continuity of sediment movement through the system. Furthermore, fan morphology is both a product of sediment transport processes and influences the effectiveness of sediment transport through, or deposition on the fan. That these processes may change through time makes it especially important that both the morphology and the processes are studied within their temporal contexts.

#### ACKNOWLEDGEMENTS

I am grateful to the Royal Society for a grant towards the costs of the fieldwork in USA, to the University of Liverpool Research and Development Fund for grants towards the costs of fieldwork in Spain. Fieldwork in USA was carried out in association with Professor S.G.Wells of the University of New Mexico. Fan profile measurement for the Methana and Bowland fans was carried out, under supervision, by Angela Morrow and Rachael Fairburn respectively, both former students at the University of Liverpool. I am grateful to the Drawing Office and Photographic sections of the Department of Geography, University of Liverpool, for producing the diagrams.

## REFERENCES

- Baker, V.R. 1977. Stream channel response to floods, with examples from central Texas. Geological Society of America, Bulletin, 88: 1057-1071.
- Blissenbach, E. 1952. Relation of surface angle distribution to particle size distribution on alluvial fans. Journal of Sedimentary Petrology, 22: 25-28.
- Blissenbach, E. 1954. Geology of alluvial fans in semi arid regions. Geological Society of America, Bulletin, 65: 175-190.
- Bluck, B.J. 1964. Sedimentation of an alluvial fan in Southern Nevada. Journal of Sedimentary Petrology, 34: 395-400.
- Bluck, B.J. 1987. Bed forms and clast size changes in gravel-bed rivers. In Richards K. (ed.), River channels: Environment and process. Blackwell, Oxford: 159-178.
- Brazier, V., Whittington, G. and Ballantyne, C.K. 1988. Holocene debris cone evolution in Glen Etive, West Grampian Highlands, Scotland. Earth Surface Proc. and Landforms, 13: 325-331.
- Bull, W.B. 1962. Relations of alluvial fan size and slope to drainage basin size and lithology in western Fresno County, California. United States Geological Survey, Professional Paper, 430B, 51-53.
- Bull, W.B. 1977. The alluvial fan environment. Progress in Physical Geography, 1: 222-270.
- Bull, W.B. 1979. Threshold of critical power in streams. Geological Society of America, Bulletin, 90: 453-464.
- Denny, C.S. 1985. Alluvial fans in Death Valley region, California and Nevada. United States Geological Survey, Professional Paper, 466.
- Eckis, R. 1928. Alluvial fans of the Cucamonga district, Southern California. Journal of Geology, 36:, 225-247.
- Graf, W.L. 1982. Downstream changes in stream power in the Henry Mountains, Utah. Annals Assoc. Amer. Geogr. 72: 372-387.
- Harvey, A.M. 1994a. Aggradation and dissection sequences in Spanish alluvial fans: influence on morphological development. Catena, 11: 289-304.
- Harvey, A.M. 1994b. Debris flows and fluvial deposits in Spanish Quaternary alluvial fans: implications for fan morphology. In Foster B.H. and Steel R. (eds), Sedimentology of gravels and conglomerates. Canadian Society of Petroleum Geologists, Memoir 10, 123-132.

- Harvey, A.M. 1985. The river system of North-west England. In Johnson R.H. (ed.), The Geomorphology of North-west England, Manchester 122-142.
- Harvey, A.M. 1986. Geomorphic effects of a 100 year storm in the Howgill Fells, North-west England. Zeits. fur Geomorph. 30, 71-91.
- Harvey, A.M. 1987a. Alluvial fan dissection: relationships between morphology and sedimentation. In Frostock L. and Reid I. (eds.) Desert sediments, ancient and modern Geol. Soc. of London. Sp. Publ. 35, 87-103.
- Harvey, A.M. 1987b. Patterns of Quaternary aggradational and dissectional landform development in the Almeria Region, southeast Spain: a dry-region tectonically active landscape Die Erde. 118, 193-215.
- Harvey, A.M. 1988. Factors influencing alluvial fan development: the Sierra de Carrascoe, Murcia, Spain. In, Harvey, A.M. and Sala M. (eds.) Geomorphic process in environments with strong seasonal contrasts Volume II, Geomorphic Systems, Catena, Suppl. 13, 123-137.
- Harvey, A.M. 1989a. The occurrence and role of arid-region alluvial fans. In, Thomas D. (ed.) Arid-region geomorphology. Belhaven/Frances Pinter Publ. 136-158.
- Harvey, A.M. 1989b. The role of Alluvial fans in mountain fluvial systems of southeast Spain. Landscape - Ecological Impact of Climatic Change: Mediterranean systems, Conference volume, Wageningen, Netherlands.
- Harvey, A.M. 1990. Factors influencing Quaternary alluvial fan development in southeast Spain. In, Rackocki A.H. and Church M.J. (eds.) Alluvial fans: a field approach, Wiley, 247-268.
- Harvey, A.M., Oldfield, F., Baron, A.F. & Pearson, G.W. 1991. Dating of post-glacial landforms in the central Howgills, Earth Surf. Processes and Landforms, 6: 401-412
- Harvey, A.M. and Renwick, W.H. 1987. Holocene alluvial fan and terrace formation in the Bowland Fells, northwest England. Earth Surface Proc. and Landforms, 12: 249-257.
- Harvey, A.M. and Wells, S.G. (in preparation) Changing morphometric controls of the sedimentology and geomorphology of late Quaternary Alluvial fans, Soda Mountains, Mojave Desert, California.
- Hooke, R. le B. 1967. Processes on arid region alluvial fans. Journal of Geology, 75: 439-460.

- Hooke, R. le B. 1963. Steady state relationships on arid-region alluvial fans in closed basins. American Journal of Science, 266: 609-629.
- Hooke, R. le B. and Rohrer, W.L. 1979. Geometry of alluvial fans: effect of discharge and sediment size. Earth Surface Processes, 4: 147-166.
- Lustig, L.K. 1965. Classic sedimentation in Deep Springs Valley, California. United States Geological Survey, Professional Paper, 352F, 131-192.
- Miall, A.D. 1977. A review of the braided river depositional environment. Earth Science Reviews, 13: 1-62.
- Pierson, T.C. and Scott, K.M. 1985. Downstream dilution of a lahar: Transition from debris flow to hyperconcentrated streamflow. Water Resources Research, 21: 1151-1124.
- Rachocki, A.W. and Church, M. 1990. Alluvial fans, a field approach, Wiley, 391p.
- Sabelberg, U. 1977. The stratigraphic record of late Quaternary accumulation series in southwest Morocco and its consequences concerning the pluvial hypothesis. Catena, 4: 204-215.
- Schumm, S.A., Mosley, M.P. and Weaver, W.E. 1987. Experimental Fluvial Geomorphology, Wiley, New York, 413p.
- Wasson, R.J. 1976. Intersection point deposition on alluvial fans: and Australian example. Geografiska Annaler 56A, 83-92.
- Wells, S.G. and Harvey, A.M. 1987. Sedimentologic and geomorphic variations in storm generated alluvial fans, Howgill Fells, northwest England. Geological Society of America, Bulletin, 98: 192-98.
- Wells, S.G., Harvey, A.M. and Moissac J.L., (in preparation), late Quaternary alluvial fan development, relations to climatic change, Soda Mountains, Mojave Desert, California.
- Wells, S.G., McFadden, L.D. and Dohrenwend, J.C. 1987. Influence of Late Quaternary Climatic Changes on Geomorphic and Pedogenic Processes on a Desert Piedmont, Eastern Mojave Desert, California.

Table 1

Correlation and regression analysis for the relationships:-  
 $G = aA^b$  (where G is fan gradient, A is drainage area km<sup>2</sup>, R is correlation coefficient, SE is standard error of the estimate, log units)

Fan group		n	r	SE	a	b
American	Debris flow	19	-0.798	0.061	0.161	-0.169
	Fluvial	19	-0.779	0.024	0.036	-0.141
Japan	Debris flow	36	-0.691	0.056	0.146	-0.101
	Fluvial flow	15		no correlation		**
	Hot flow	10	-0.839	0.064	0.081	-0.064*
	All flows	15	-0.478	0.057	0.062	-0.134
Madras	Debris flow	10	-0.765	0.047	0.171	-0.071
	Fluvial flow	9	-0.611	0.099	0.131	-0.009*
	All flows	10	-0.680	0.110	0.100	-0.071
Spain - N	Debris flow	11	-0.648	0.111	0.103	-0.003*
	Fluvial	15		no correlation		**
	All fans	17	-0.001	0.198	0.034	-0.001*
Spain - S non-estuarine	Debris flow	11	-0.408	0.101	0.074	-0.066*
	Fluvial	10	-0.651	0.071	0.051	-0.071
	All fans	11	-0.499	0.140	0.031	-0.196
Spain - S Estuarine	Debris flow	5	-0.886	0.059	0.111	-0.151*
	Fluvial flow	15	-0.801	0.060	0.036	-0.150
	Hot flow	7	-0.611	0.116	0.008	-0.101*
	All flows	17	-0.771	0.010	0.036	-0.026
	All fans	11	-0.108	0.016	0.040	-0.056
Newquill	Debris flow	11	-0.647	0.166	0.161	-0.010
	Fluvial	19	-0.744	0.161	0.066	-0.071
Bowland	Debris flow	8	-0.617	0.036	0.015	-0.090*
	Fluvial	9	-0.891	0.195	0.106	-0.094**
	All fans	10	-0.811	0.101	0.016	-0.489

\* significant levels <0.05

\*\* Non-significant <0.05

Table 1. Logarithmic multiple correlation and regression analyses of Drainage area,  $\text{km}^2$ , A, Basin relief in m, H, and Fan slope, S, on fan gradient, G. R is correlation coefficient, SE is standard error of the estimate, log units.

Fan Group		A - G		A,H - G		A, S - G		'Best' Equation
		R	SE	R	SE	R	SE	
American	Debris flow	+0.798	0.031	0.798	0.031	<u>0.806</u>	0.031	$G = 0.038A^{0.15}H^{0.16}$
	Fluvial	+0.778	0.031	0.810	0.031	<u>0.807</u>	0.031	$G = 0.038A^{0.15}H^{0.16}$
Oregon	Debris flow	+0.661	0.036	0.663	0.036	<u>0.692</u>	0.036	$G = 0.038A^{0.15}H^{0.16}$
	Pleist. flow	+0.197	0.101	0.170	0.101	<u>0.618</u>	0.101	$G = 0.038A^{0.15}H^{0.16}$
	Hol. flow	+0.033	0.134	<u>0.870</u>	0.136	0.411	0.131	$G = 0.01018A^{0.05}H^{0.01}$
	All fans	+0.473	0.137	<u>0.893</u>	0.134	<u>0.896</u>	0.134	$G = 0.038A^{0.15}H^{0.16}$
Mediana	Debris flow	+0.769	0.047	0.790	0.048	<u>0.861</u>	0.041	$G = 0.038A^{0.15}H^{0.16}$
	Pleist. flow	+0.610	0.099	0.671	0.100	<u>0.676</u>	0.100	$G = 0.038A^{0.15}H^{0.16}$
	All fans	+0.691	0.117	0.691	0.116	<u>0.701</u>	0.116	$G = 0.038A^{0.15}H^{0.16}$
Spain - N	Debris flow	+0.848	0.010	<u>0.859</u>	0.010	0.708	0.035	$G = 0.000548A^{0.50}H^{0.88}$
	Fluvial	+0.801	0.010	<u>0.887</u>	0.036	0.584	0.110	$G = 0.0002A^{0.44}H^{0.84}$
	All fans	+0.801	0.030	<u>0.761</u>	0.110	0.787	0.116	$G = 0.00028A^{0.44}H^{0.88}$
Spain - S non adjust	Debris flow	+0.408	0.101	<u>0.786</u>	0.077	0.751	0.078	$G = 0.00178A^{0.36}H^{0.60}$
	Fluvial	+0.850	0.170	<u>0.704</u>	0.147	0.560	0.174	$G = 0.00188A^{0.44}H^{0.68}$
	All fans	+0.698	0.168	<u>0.778</u>	0.144	0.580	0.168	$G = 0.00192A^{0.44}H^{0.60}$
Spain - S sorted	Debris flow			S fans only				
	Pleist. flow	+0.800	0.090	<u>0.801</u>	0.099	0.878	0.077	$G = 0.00066A^{0.31}H^{0.58}$
	Hol. flow	+0.611	0.116	<u>0.801</u>	0.190	0.806	0.097	$G = 0.00411A^{0.17}H^{0.59}$
	All fans	+0.770	0.101	<u>0.887</u>	0.190	0.806	0.096	$G = 0.00878A^{0.31}H^{0.54}$
	All fans	+0.838	0.106	<u>0.840</u>	0.137	0.801	0.101	$G = 0.01548A^{0.27}H^{0.48}$
Atapalla	Debris flow	+0.699	0.056	0.791	0.054	<u>0.843</u>	0.074	$G = 0.048A^{0.15}H^{0.16}$
	Fluvial	+0.647	0.056	<u>0.781</u>	0.050	0.690	0.055	$G = 0.01038A^{0.08}H^{0.60}$
Lowland	Debris flow	+0.617	0.038	<u>0.781</u>	0.054	0.619	0.051	$G = 0.00038A^{0.15}H^{0.46}$
	Fluvial			S fans only				
	All fans	+0.888	0.001	<u>0.902</u>	0.150	0.874	0.034	$G = 0.0000801A^{0.64}H^{0.56}$

Figures in brackets are for non-significant > 5% correlations

Table 3: Occurrence of various styles of fan/channel profile relationships for the study areas.

<u>Fan Group</u>	<u>Profile Style</u> (see Fig. 13)						
	O	A/B	C	D	E	F	G*
Zzyzx	7	5	-	3	4	-	6
Other American	-	6	1	-	-	-	-
Methana	-	3	-	1	-	4	4
Spain, North	1	8	2	10	2	1	1
Spain, South (non-schist)	4	11	3	1	-	3	4
Spain, South (schist)	-	21	1	1	-	6	2
Howgill	14	12	-	-	-	4	5
Bowland	6	-	-	-	-	6	8

\* numbers showing toe incision, also included in other groups

Table 4 Progressive changes in dominant fan processes, for American and Mediterranean fans changes relate to Pleistocene to Holocene timescales, for English fans changes relate to the Holocene. D Debris flow, P Passive i.e. non erosive/non depositional, F Fluvial Deposition, I Incision.

<u>Fan group</u>	<u>Dominant Process Change</u>							
	DD	DP	DF	DI	FD	FP	FF	FI
Zyzak	4	4	6	3	-	-	2	1
Other American	-	-	1	-	-	-	6	-
Methana	-	-	3	1	-	-	4	-
Spain North	-	-	8	2	-	-	15	1
Spain South (non-schist)	-	2	3	3	-	1	11	2
Spain South (schist)	-	-	-	2	-	-	26	1
Howgill	9	5	7	1	-	-	6	3
Bowland	-	3	-	5	-	-	3	1



Table 5    Relation of dominant process change (see Table 4) to Profile Change (see table 3, Fig.13), Number of occurrences.

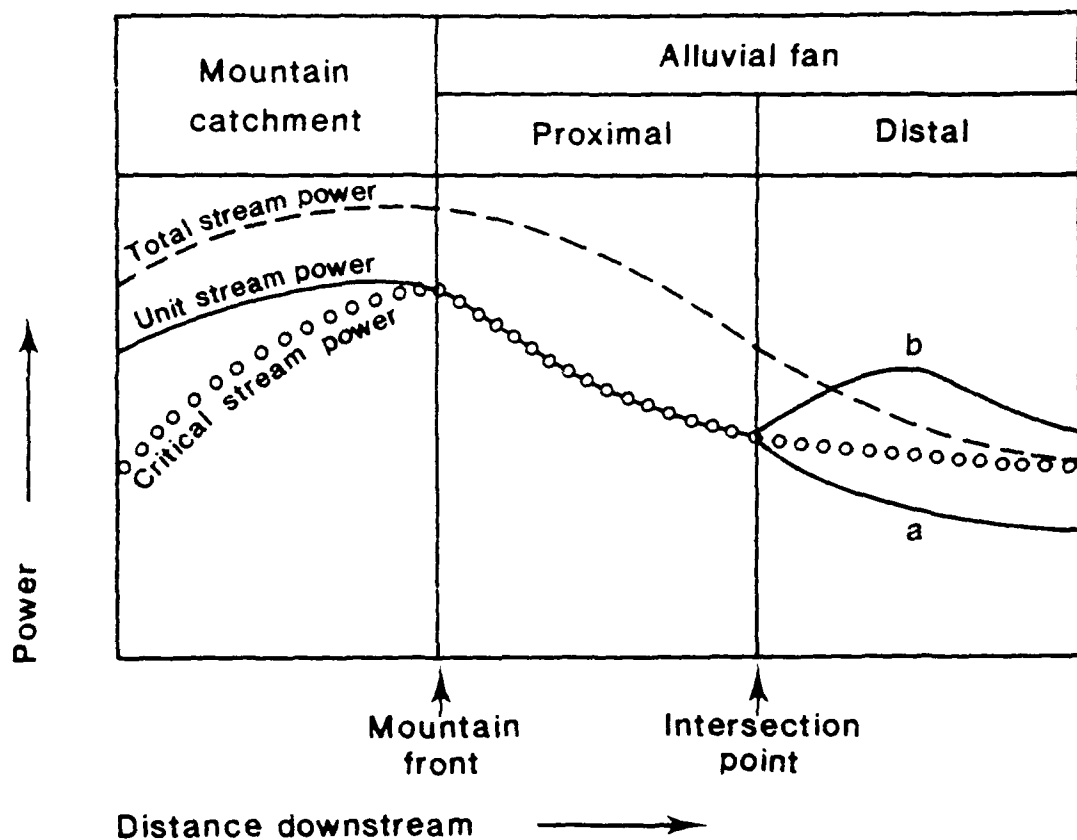
<u>Profile style</u> (see table 3, Fig 13)	Dominant Process Change**							
	DD	DP	DF	DI	FD	FP	FF	FI
O	7	14	1	2	0	1	6	1
A/B	4	0	16	1	0	0	47	0
C	0	0	5	1	0	0	1	0
D/E	2	0	4	6	0	0	11	1
F	0	0	3	7	0	0	9	6
G*	2	2	1	13	0	0	8	8

\* Indicates number of fans subject to (local) base-level induced top incision, also included in other groups.

\*\*D,P,F,I, as defined on Table 4.

# List of Figures

- Fig. 1 Postulated relationships between total stream power, unit stream power and critical stream power through incision front alluvial fan cones. Modified from ideas presented by Swil (1979) and Graf (1981).
- Fig. 2 Conceptual model showing influence of catchment geomorphology on water, sediment ratios and hence on dominant sediment transport processes in alluvial fan environments. Modified after Wells and Harvey (1987). 1, 2, 3, 4 represent typical depositional responses.
- Fig. 3 Study areas & locations
- Fig. 4 Examples of alluvial fan types within the study areas: a) Bayan fans, California; b) Kypseli fan, Methana, Greece; c) steep dissected fanhead, Carrassey fans, Murcia, Spain; d) low angle fluvial fan, Sierra de los Filabres, Spain; e) steep debris cone, Howgill Falls, England; f) fluvial fan, Howgill Falls, England.
- Fig. 5 American fans: differentiation between debris flow and fluvial fans on the basis of drainage basin area and slope.
- Fig. 6 Mediterranean fans: differentiation between debris flow and fluvial fans on the basis of drainage basin area and slope.
- Fig. 7 English fans: differentiation between debris flow and fluvial fans on the basis of drainage basin area and slope.
- Fig. 8 Summary of differentiations between debris flow and fluvial fans on the basis of drainage basin area and slope.
- Fig. 9 American fans: relation of fan slope to drainage area. D Debris flow fans; P Pleistocene fluvial fans; H Holocene fluvial fans; F All fluvial fans; A All fans. Fine lines and brackets indicate correlations of low significance, or where the relationship has been estimated by eye.
- Fig. 10 Mediterranean fans: relation of fan slope to drainage area. D Debris flow fans; P Pleistocene fluvial fans; H Holocene fluvial fans; F All fluvial fans; A All fans. Fine lines and brackets indicate correlation of low significance, or where the relationship has been estimated by eye.
- Fig. 11 English fans: relation of fan slope to drainage area. D Debris flow fans; P Pleistocene fluvial fans; H Holocene fluvial fans; F All fluvial fans; A All fans. Fine lines and brackets indicate correlations of low significance, or where the relationship has been estimated by eye.
- Fig. 12 Summary of regression relationships of fan slope to drainage area. Fine lines and brackets indicate correlations of low significance, or where the relationship has been estimated by eye. 1- Bayan group; A- other American fans; M- Methana; SN- Spain North; SO- Spain South; non correct; SS- Spain South; Sonnet; H-Howgill; I-Ireland; -D Debris flow fans; -P Pleistocene fluvial fans; -H Holocene fluvial fans; -F All fluvial fans; -A all fans.
- Fig. 13 Schematic fan surface channel profile relationships and model partially differentiating profile types. Modified from Harvey (1987a). Open triangles represent additional data for truncated fans.
- Fig. 14 Potential response of alluvial fan environments to climatic change.



a distally aggrading fans

b distally trenched fans

(see text)

Fig 1

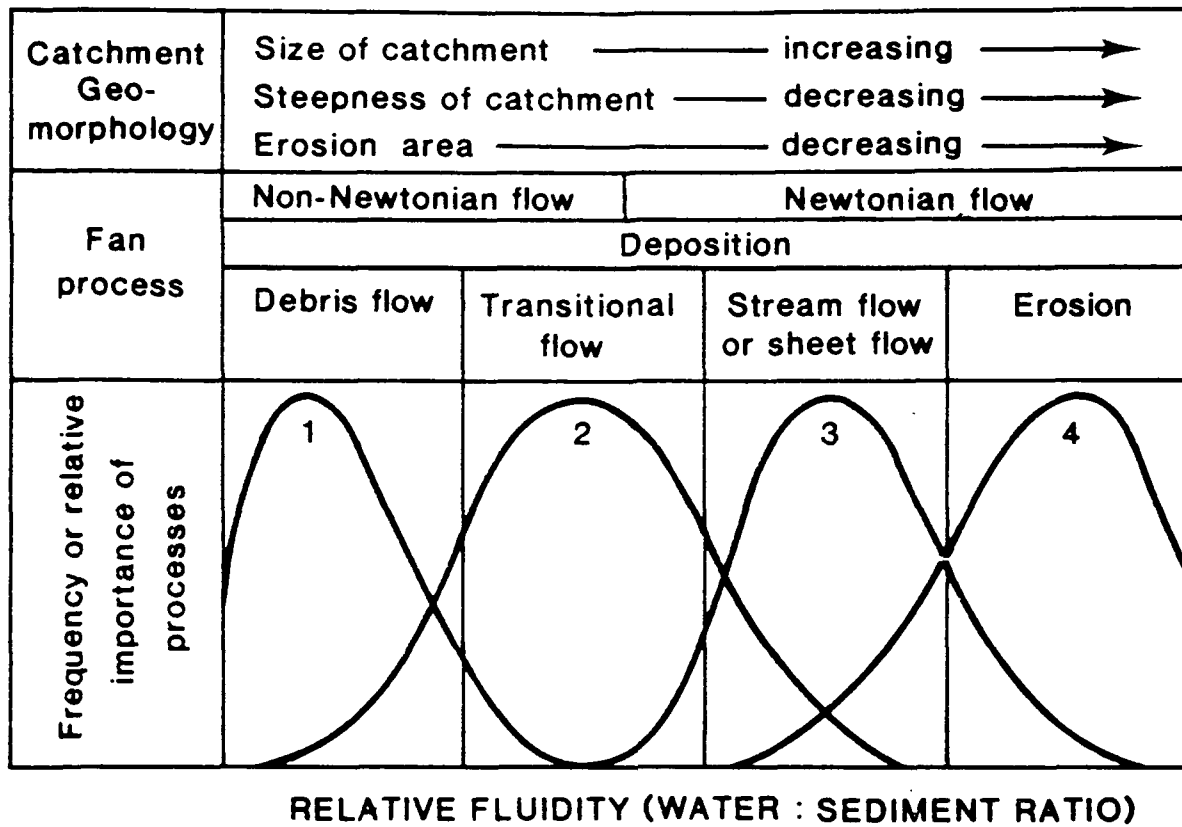
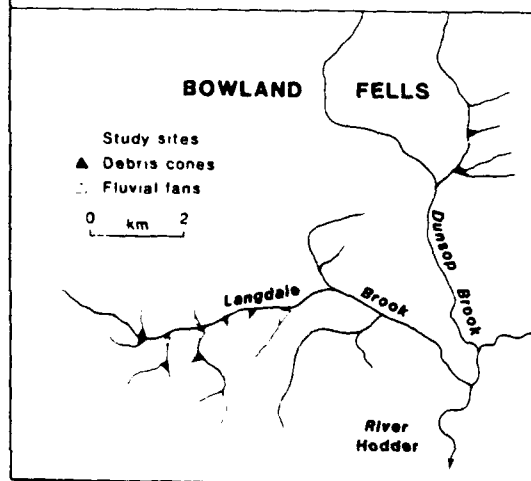
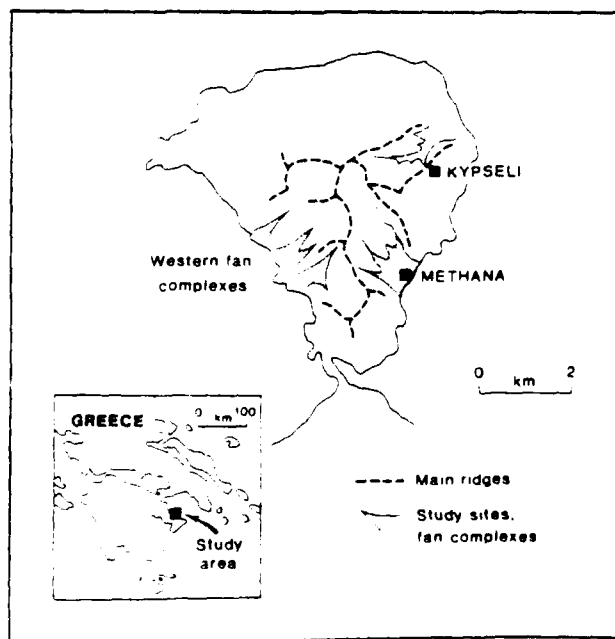
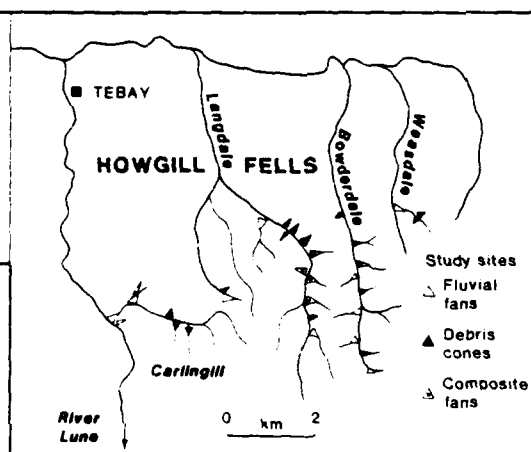
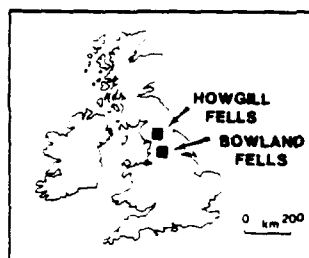
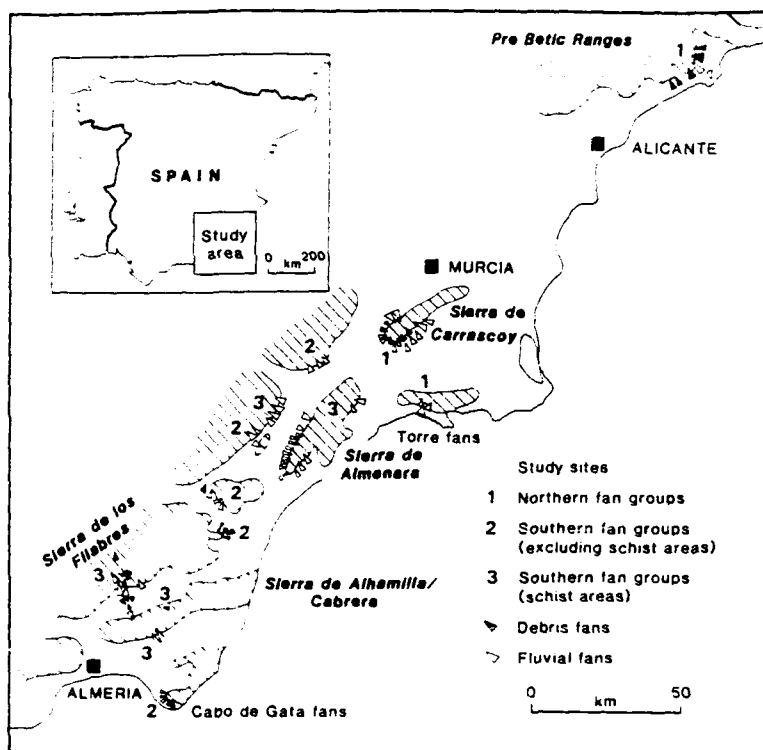
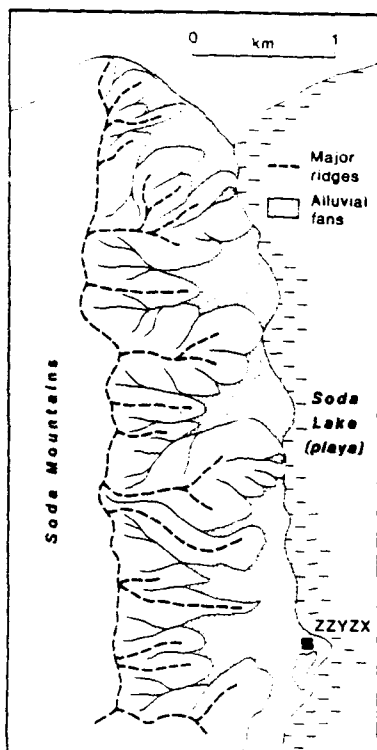
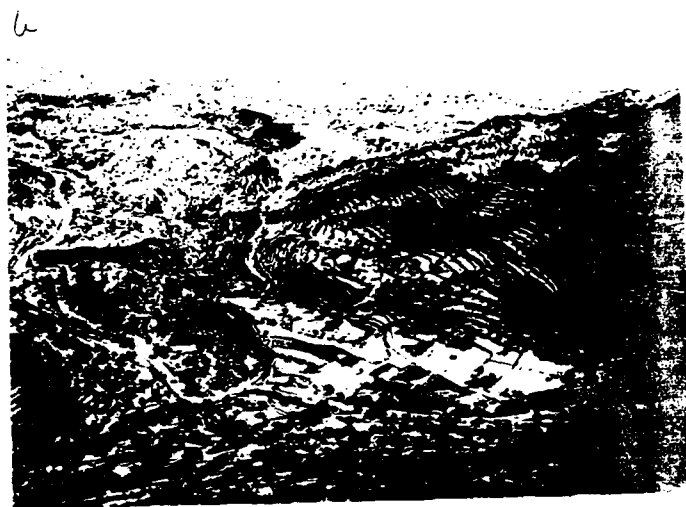
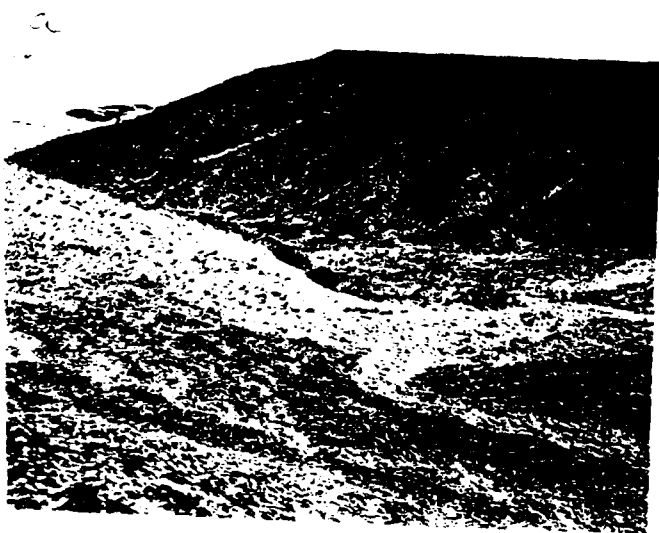
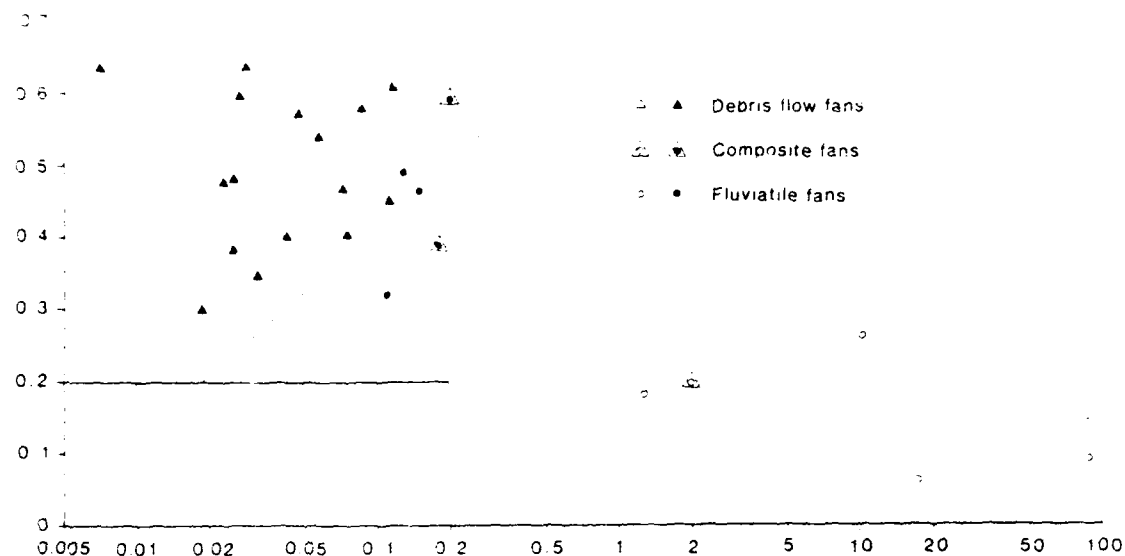


Fig 2

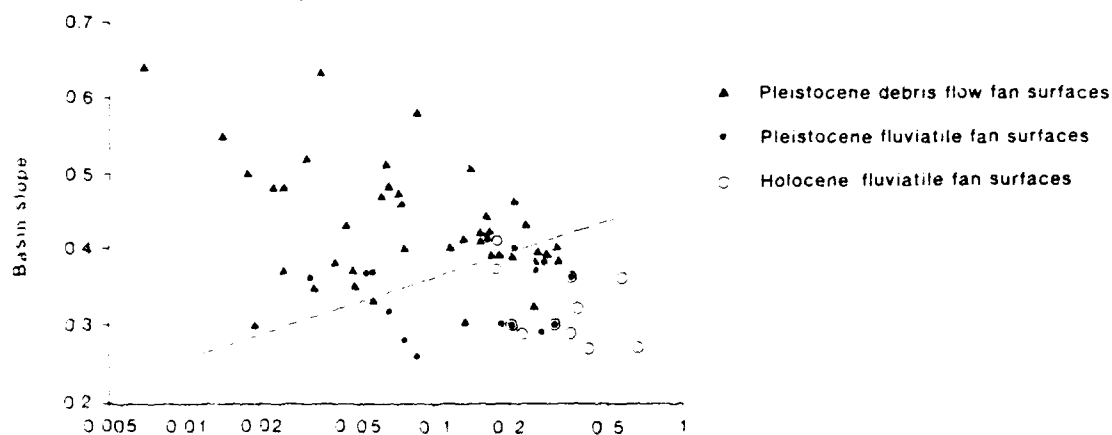




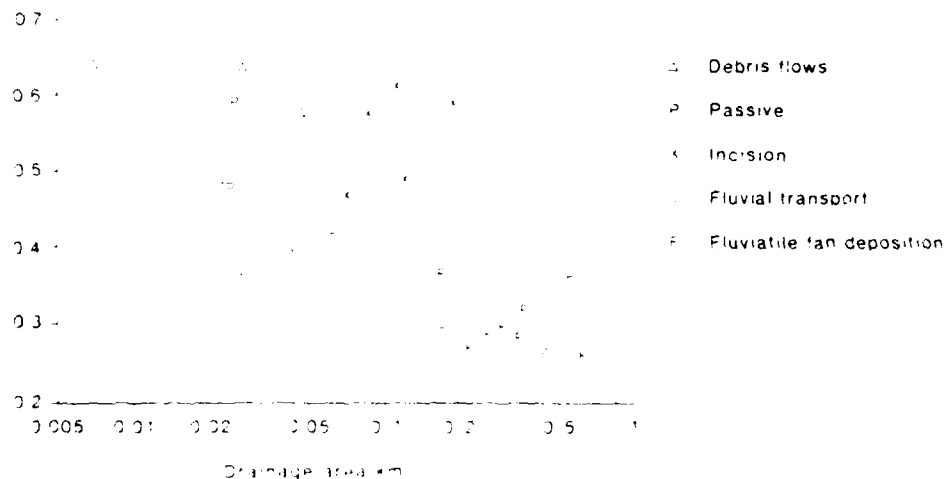
(a) AMERICAN FANS (General)



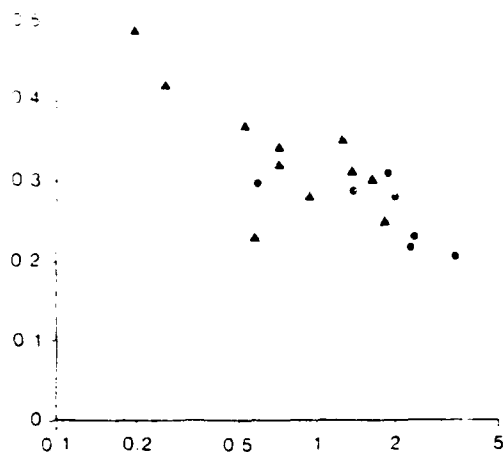
(b) ZZZX (Quaternary fans)



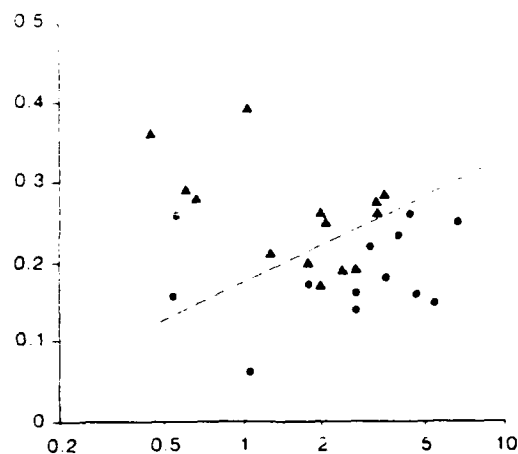
(c) ZZZX (Modern processes)



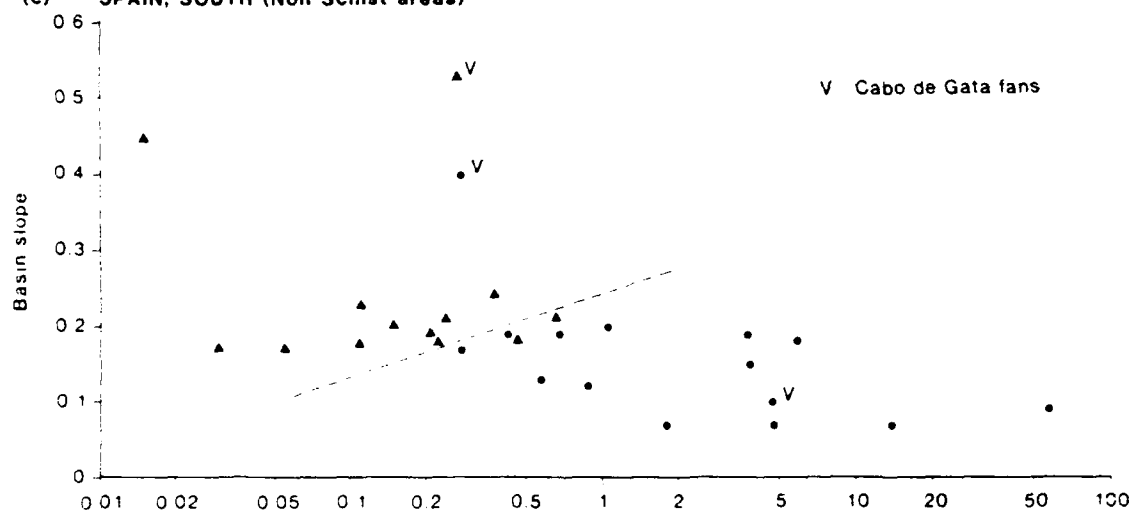
(a) GREECE (Methana)



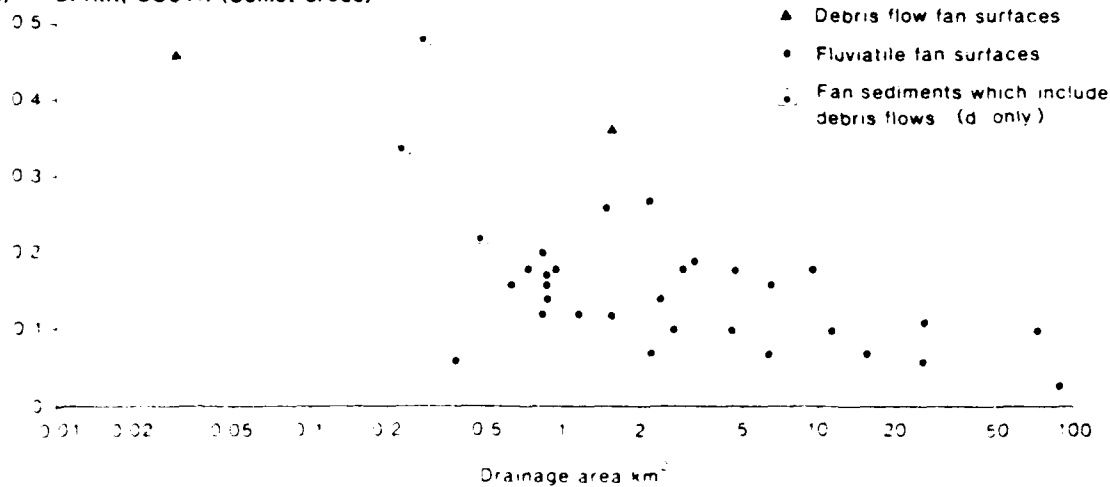
(b) SPAIN (Alicante, Murcia North)



(c) SPAIN, SOUTH (Non Schist areas)

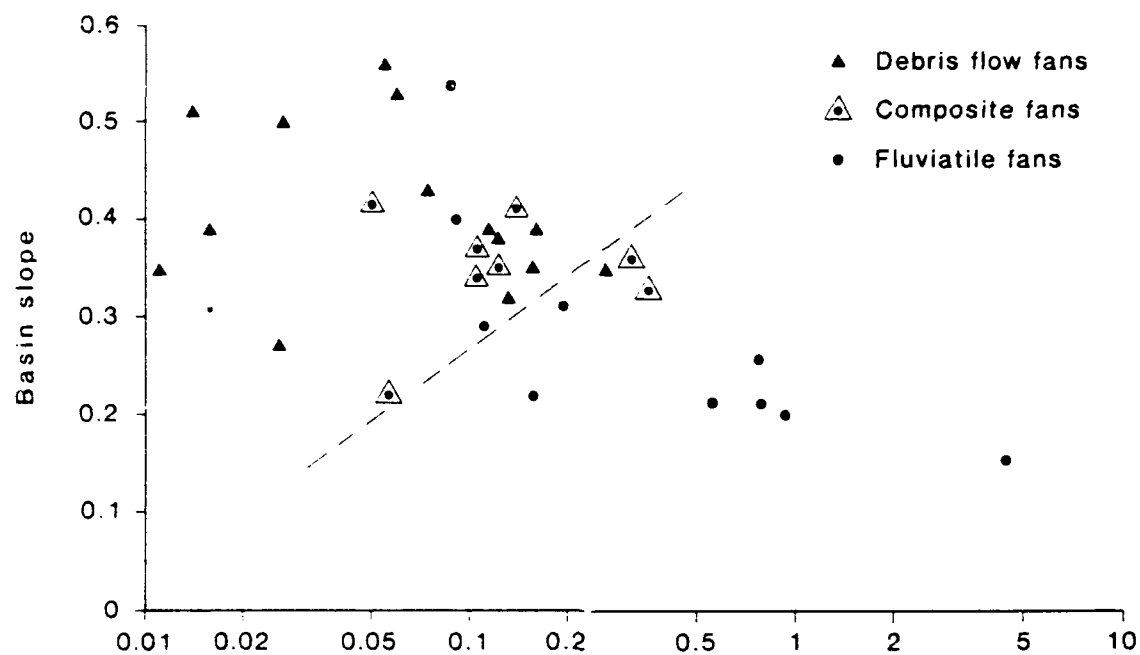


(d) SPAIN, SOUTH (Schist areas)

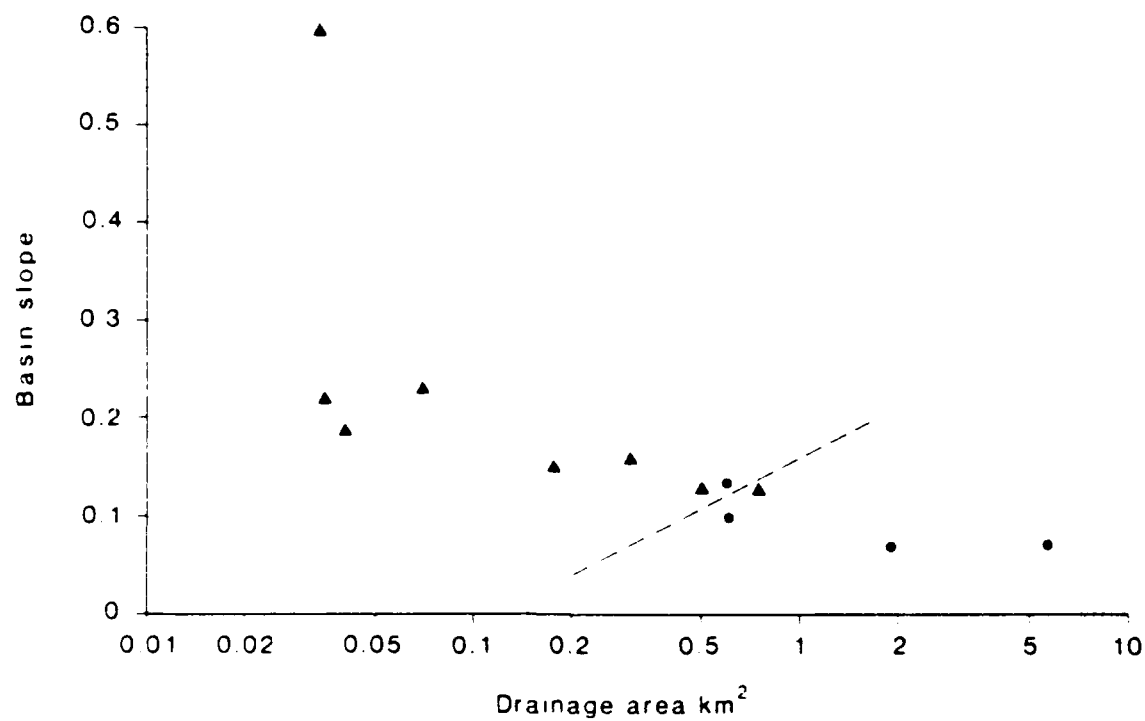




(a) HOWGILL FELLS



(b) BOWLAND



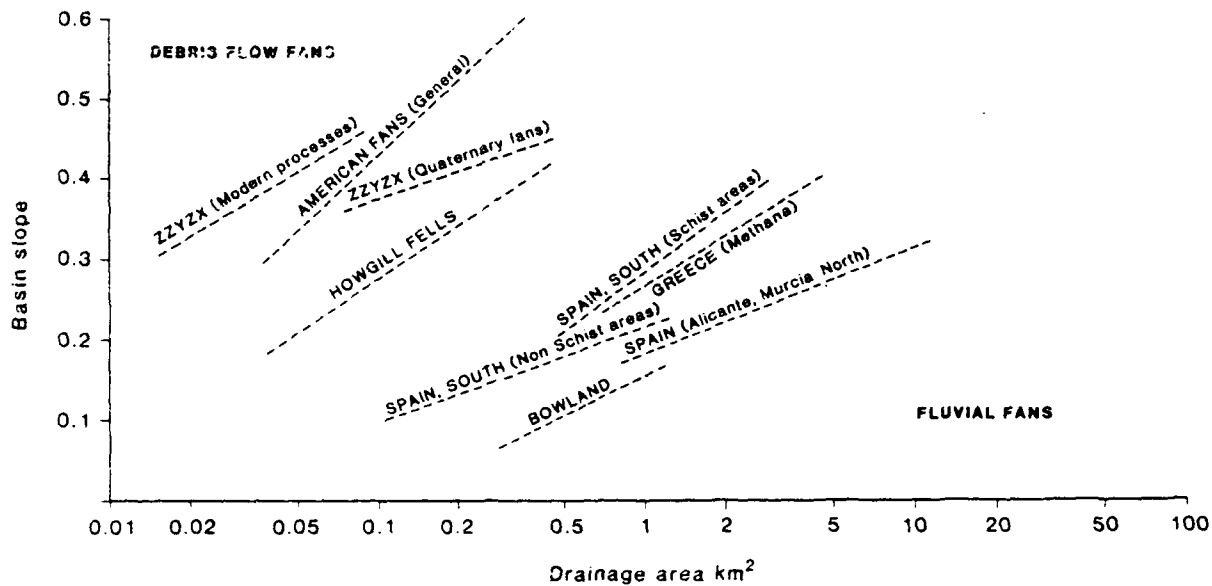
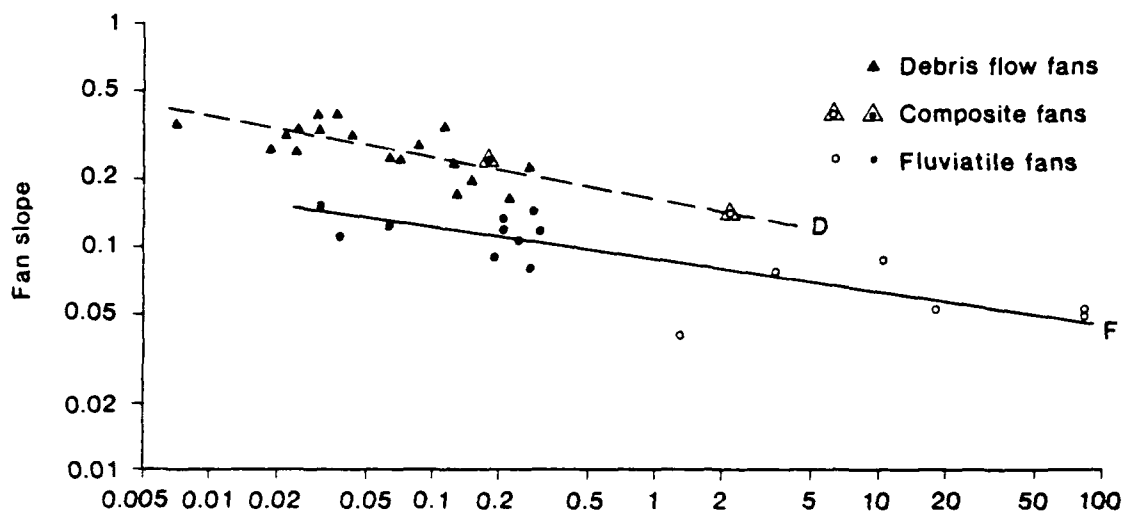
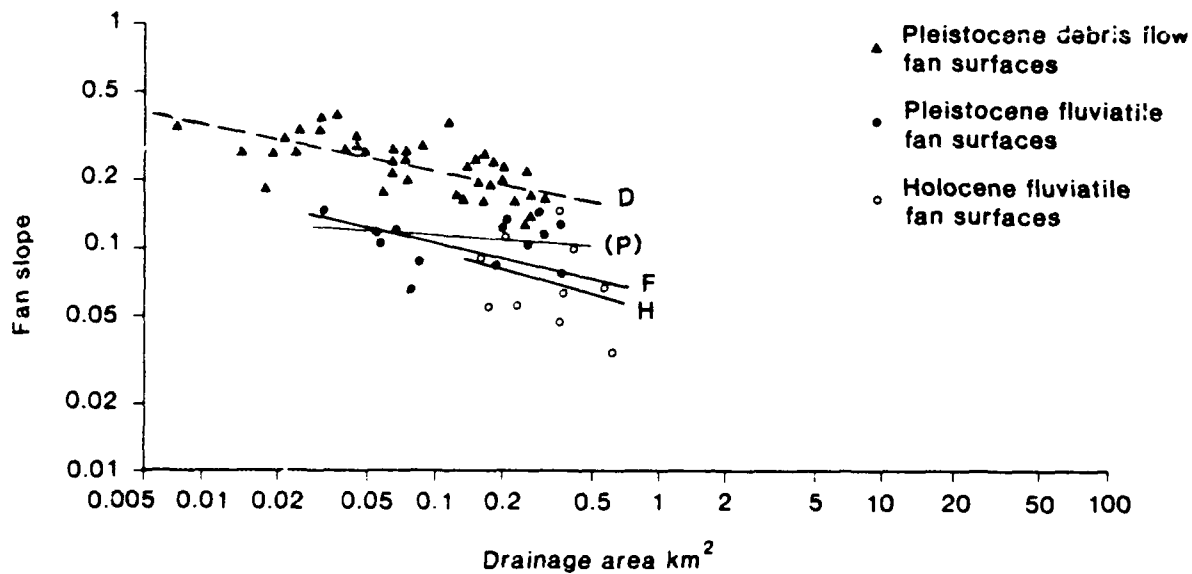


Fig 8

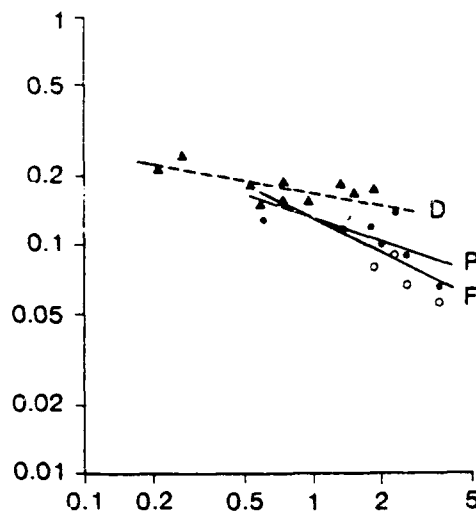
(a) AMERICAN FANS



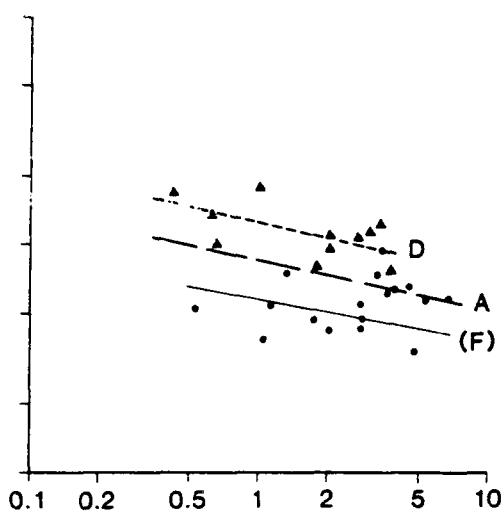
(b) ZZZZX



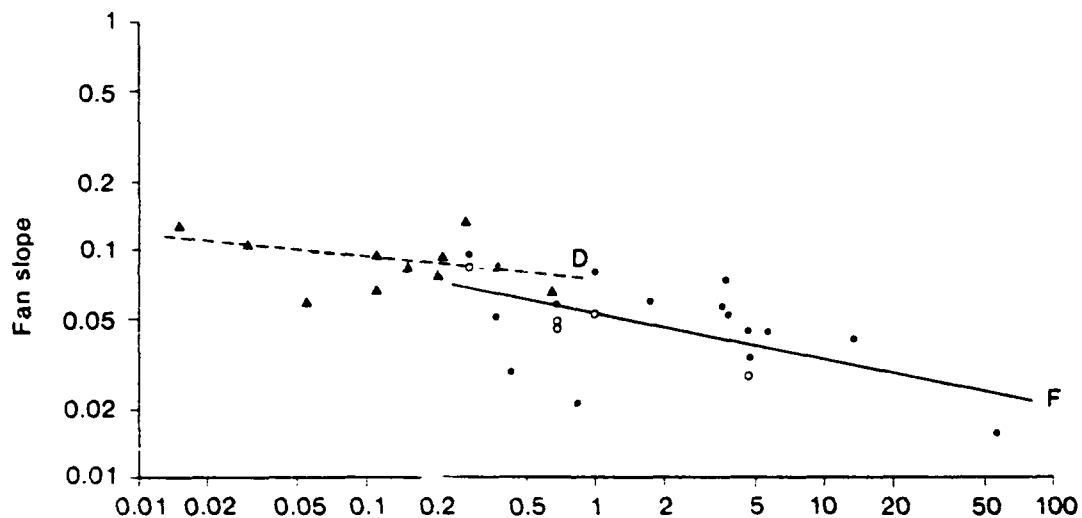
(a) GREECE (Methana)



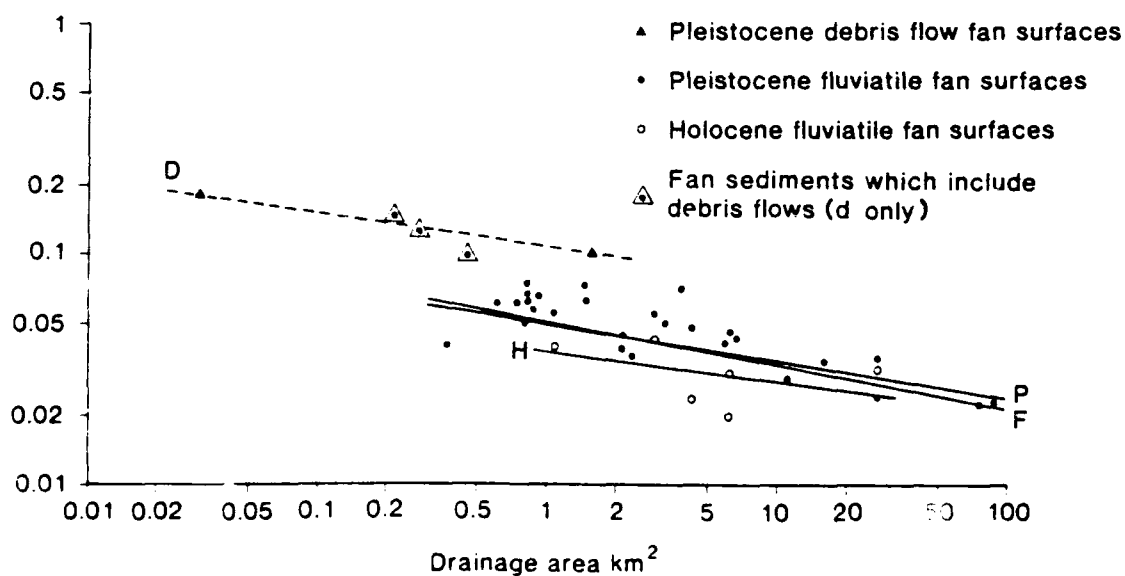
(b) SPAIN (Alicante, Murcia North)



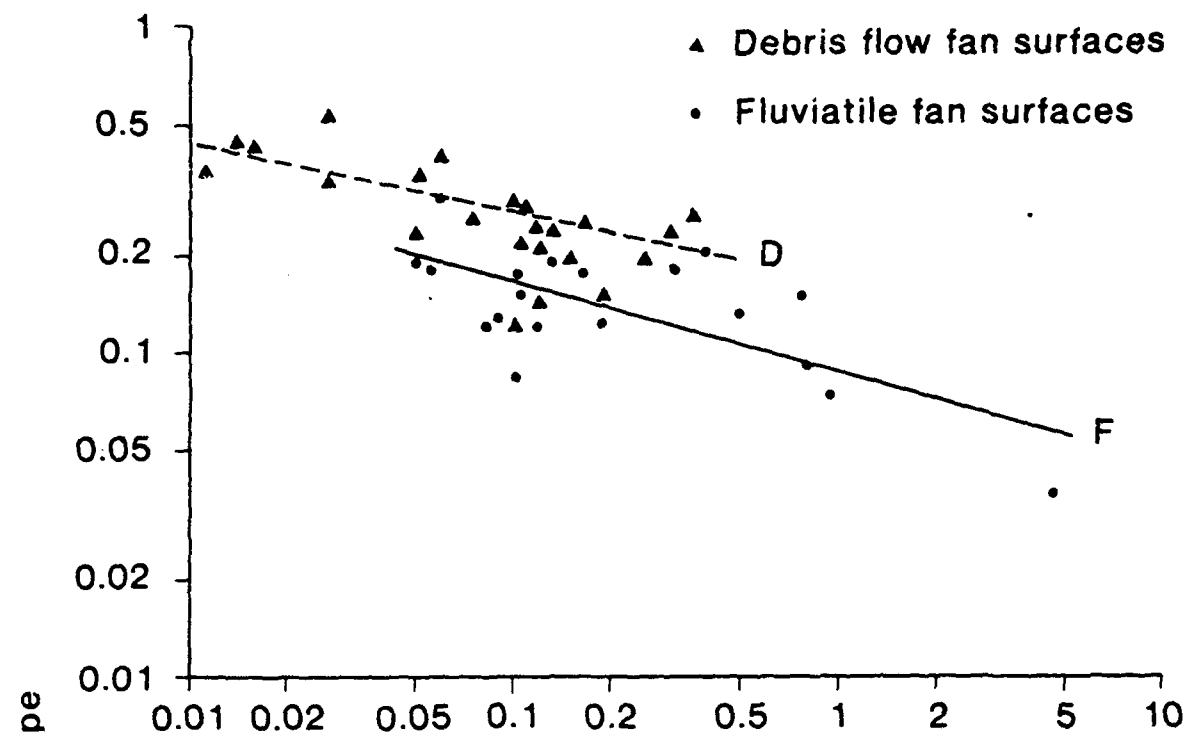
(c) SPAIN, SOUTH (Non Schist areas)



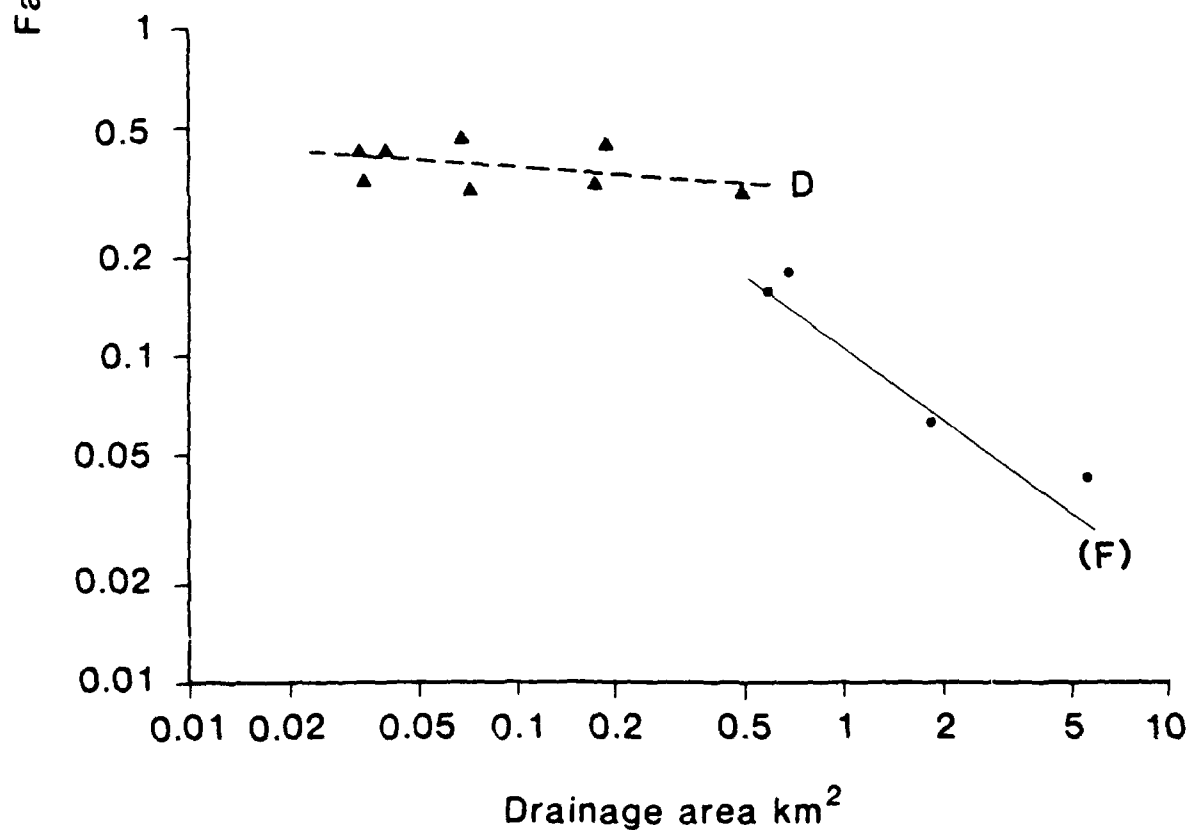
(d) SPAIN, SOUTH (Schist areas)

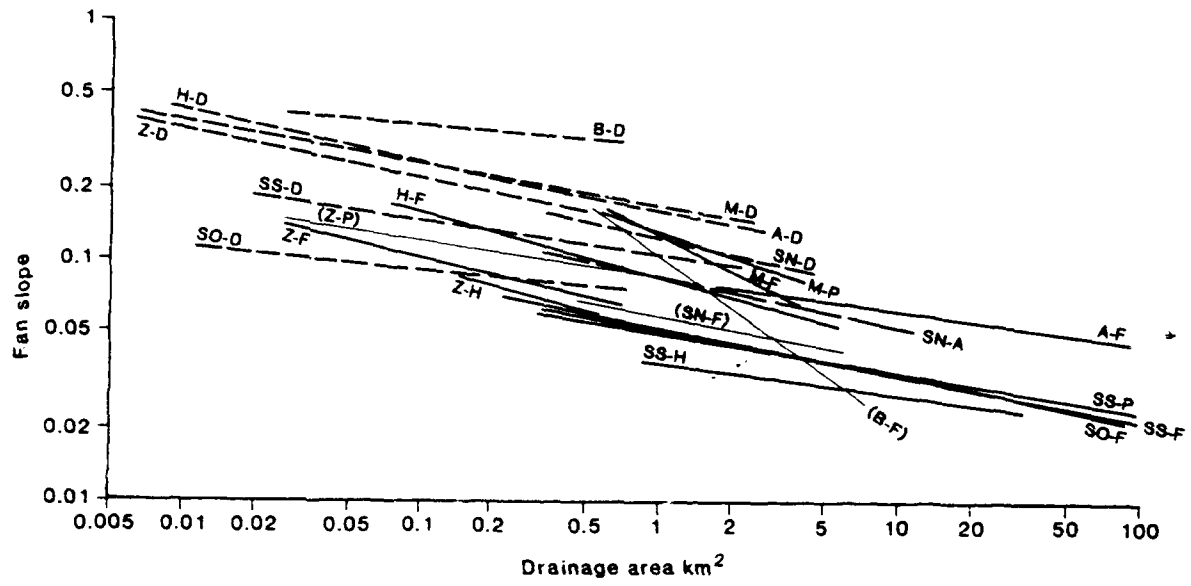


# **HOWGILL FELLS**

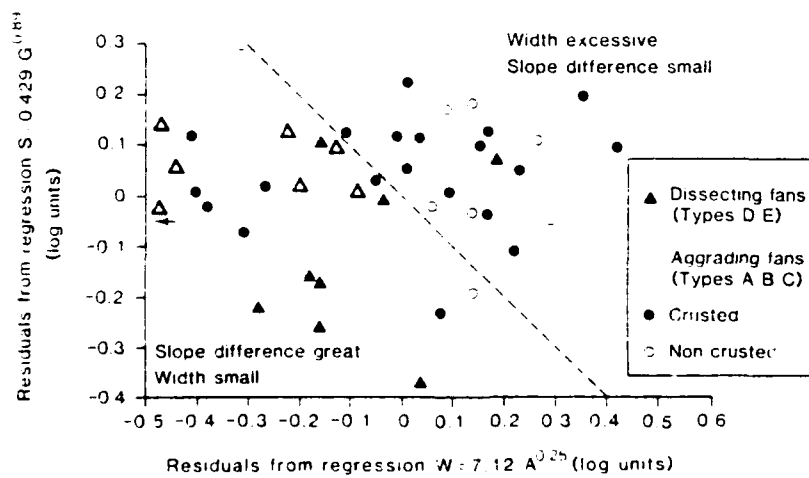
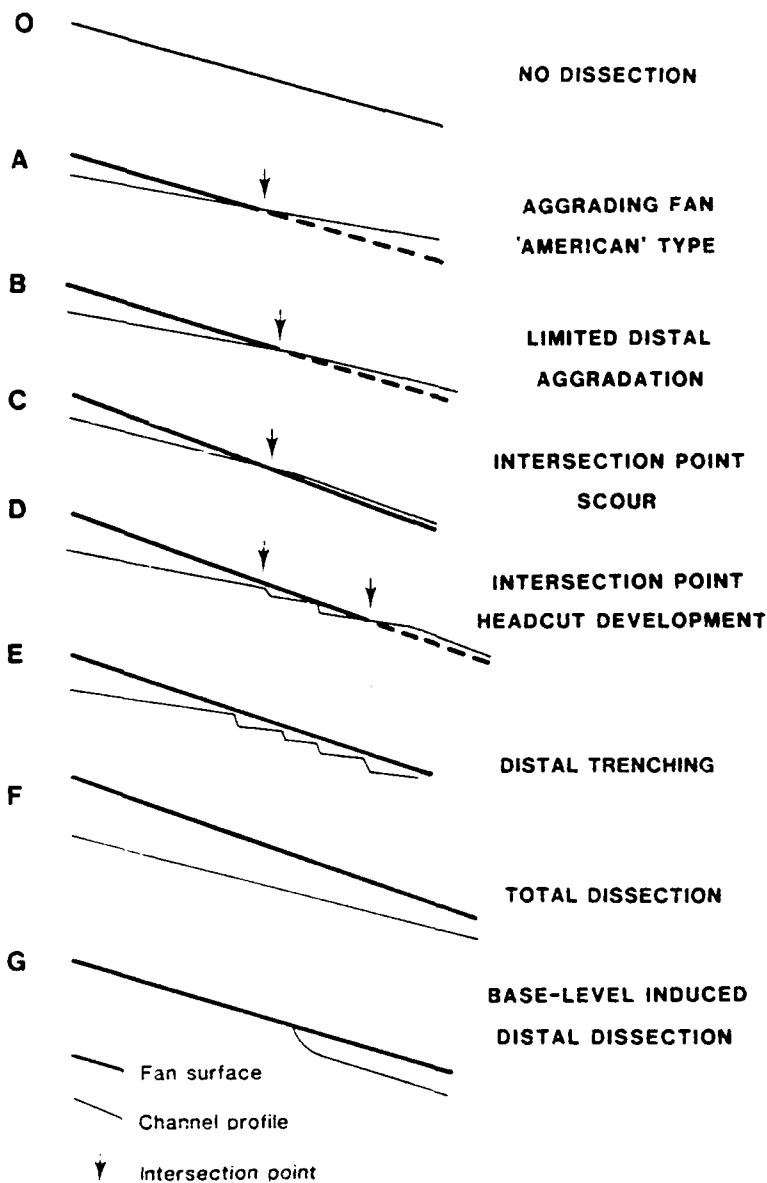


# **BOWLAND FELLS**





21 12



		Effectiveness of storm runoff DECREASE ← → INCREASE	
Vegetation cover DECREASE ↔ INCREASE	Hillslope erosion rate DECREASE	Decrease sediment supply Decrease stream power  STABILISATION	Decrease sediment supply Increase stream power  D' FLOW → FLUV OR INCISION
	INCREASE	Increase sediment supply Decrease stream power  FLUV → D' FLOW OR AGGRADATION	Increase sediment supply Increase stream power  ACCELERATE ACTIVITY (DIRECTION DEPENDS ON RELATIVE INCREASES)



**Effect Of Bed Roughness, Particle Shape and Orientation  
On Initial Motion Criteria**

*Paul A. Carling<sup>1</sup>, Adrian Kelsey<sup>2</sup> & Mark S. Glaister<sup>1</sup>*

Institute Of Freshwater Ecology<sup>1</sup>,  
Windermere Laboratory,  
Ambleside, Cumbria LA22 OLP, UK.

Institute Of Environmental & Biological Sciences<sup>2</sup>,  
Lancaster University,  
Lancaster, Lancashire

## Introduction.

Considerable attention has been given to defining the initial motion criteria for spherical particles perched on planar beds composed of similar particles. In contrast, there is little information on entrainment thresholds and the mechanics of entrainment for non-spherical particles resting in natural positions on beds composed of particles dissimilar in size and shape to the entrained grain. This is surprising as data from gravel-bed rivers has shown that at a given shear velocity, a mix of grain-sizes and shapes can be entrained.

From this evidence it might be surmised that there is no size selection at all from certain bed fabrics or that selective entrainment is dependant on the characteristics of the bed-material fabric. The presence of an armour-layer is an evident structural element of the bed-fabric in many rivers and may act to impart a degree of equal mobility to the bed-material population but other factors have not been fully evaluated. For example, other than density differences, the nature of the over-all grain-size distribution will influence particle packing and bed roughness. In addition, particle shape influences packing and the probability of entrainment as does the exact position and orientation of the individual particles. Each of these various factors can be parameterized and the variability in entrainment thresholds evaluated. In addition, to some extent, these factors can be incorporated into models of the initial motion process which can be used to explain the equal mobility of divers particles at threshold conditions.

A proper consideration of equal mobility should apply only to initial motion conditions and not to material in transport. Consequently in this paper the variability in entrainment is explored and an initial motion criterion developed which reflects these observations.

In the first part of this paper the preliminary results of a laboratory flume experiment are reported. These data primarily concern the initial motion of individual particles of similar weight in natural mixtures, wherein particle shape and orientation on the bed are variables as is the roughness of the bed. The critical shear velocity associated with initial motion of the test particles was ascertained for each case and the range of threshold values determined for combinations of shape, orientation and bed roughness.

In the second part of the paper, the geometric relationship of ellipsoidal particles (ranging from spheroids to discs) perched on a bed of grains of dissimilar size or shape, is considered in the light of the observations obtained from the flume experiments. Contact angles and critical pivoting angles are derived and an example presented graphically. These data provide input to an initial motion criterion which caters for a variety of ellipsoidal shapes and orientation.

## Methods

A series of test runs were conducted in a recirculating glass-walled flume which had an over-all length of 13m, a width of 0.79m and a maximum depth of 0.5m. Near uniform flow, with a discharge up to  $0.3\text{m}^3\text{s}^{-1}$ , could be maintained 6m from the inlet baffles over a 5m section. Flow from the channel was controlled by a vertical louvre gate and bed slope was altered by electric motor from zero gradient to  $3.75^\circ(0.066)$  with a precision in the vertical elevation of 0.5mm. Artificial stable bed-roughness was created by lining the flume bed with concrete slabs into which ellipsoidal river gravels had been tightly packed with their long axes transverse to the flow such that approximately 50% of each cobble was submerged in the concrete. Three grades of gravel (one phi interval apart) were used (16-32mm; 40-64mm and 125-250mm) to create three roughness types. The largest roughness was similar in size to the test particles whilst the smaller roughness elements represented smoother beds over which coarse gravel is observed to roll in natural streams.

Four sets of test runs were designed to represent idealized bed particle shapes and particle orientations, which nevertheless resemble geometries encountered in natural gravel-bed rivers. In the first series, four artificial well-rounded particles of similar weight (1kg) and density (2.65) were compared. These were a rod, an ellipse, a disc and a spheroid; dimensions of which are given in Table 1. Each particle was placed in exactly the same

position on the col between four adjacent bed particles such that initial motion would be by displacement over the col between the two downstream particles. Three particle orientations were considered; long axis parallel to flow, transverse and oblique, so that the projected area and stability of the perched particles varied with orientation and bed roughness. For a given discharge, the bed slope was increased steadily until the test particle was entrained into the flow. The velocity profile over the pivot point was then measured using four simultaneously recording Ott C2' flow meters (positioned between 22mm and 100mm above the base of the col) and the local shear stress computed using the log-profile method for rough turbulent flow. The test was repeated five times for each particle, orientation and roughness type.

Notes were made with respect to the mode of entrainment (eg. whether the particle vibrated, swiveled, imbricated, slid or rolled etc). The disc and ellipsoid displayed a tendency to imbricate on the roughest bed and so the shear velocity required to imbricate the particle and that required to entrain the particle into the flow were recorded as appropriate.

The second series of runs compared the entrainment characteristics of a sphere and a cuboid of similar weight (2.4kg) and density (2.65), whilst the third series examined the differences in the threshold shear stress for two natural cobbles (of similar shape but contrasting weight - Table 1), when the orientation and bed roughness were varied. There was little variability amongst the shear velocity values for the five replicates in the first test series, and so for the latter two series, three replicate runs

were conducted for each set of test conditions.

The final series of experimental runs dealt solely with influences of flow velocity and bed roughness on particle velocity once entrainment had occurred. The mean velocity conditions were established and the velocity of the particle was measured over a distance of 5m.

## **Experimental Results**

### *Mode Of Initial Motion*

Particles frequently vibrated in situ before entrainment occurred. This was less vigorous in the case of the disc, but occurred with all roughness types. In the case of roughness types 1 & 2, all particle shapes (excluding the rod) placed with their A-axes parallel to the flow, tended to rotate out of place without assuming a transverse attitude first. This observation was true even for the disc which never slid out of place but instead flipped over; turning around a pivot point located near the edge of the disc. However, on the smoothest bed (Roughness 1) the ellipse and disc placed parallel or oblique to the flow, swiveled to a transverse attitude before rolling out of place. Only the rod, placed parallel or oblique to the flow always swiveled to a transverse attitude before becoming entrained. The sphere was entrained by rolling in all cases, whilst the cuboid always slide out of it's resting position but then rolled about it's A-axis. Rolling about the A-axis was the usual mode of travel once entrained for all shapes. The exception to this was the disc, at the highest velocities, when motion could be by rolling

along either of the three axes or by sliding. On the roughest bed (Roughness 3) the ellipse and disc always slid to an imbricated position before being entrained by rolling.

*Initial motion on the smoothest bed (Roughness 1)*

The shear velocity data for the various particle shapes and attitudes are summarized in Fig. 1. On the smoothest bed the most stable attitude is for an ellipse positioned with the A-axis parallel to the flow, whilst the least stable is the rod, placed transverse to the flow. It is evident from the range of data values, that particle orientation is as important as particle shape and relative mass in dictating the critical threshold. Orientation alters the cross-sectional area of the particle exposed to the main stream-line and to a lesser extent effects particle stability vis-a-vis the contact points of the particle with the under-lying bed particles. For example, not only does turning a rod from parallel to oblique to the flow increase the cross-sectional area exposed to the flow, but the rod must be tilted and rested across both a bed particle and a col position rather than assume a horizontal attitude over two col locations. The threshold shear velocity for the parallel rod is more than double that for the transverse rod; the ratio being 2.16 which is greater than any ratios comparing shapes rather than orientation. A similar difference applies to the ellipse (1.86) but the differences for the spheroid and disc are not so acute (1.33 and 1.26 respectively) but still remain as important as differences in shape. The sphere of course can have only one orientation, and despite the difference in mass (2.4kg), compared with the other artificial particles (1kg), a small pivoting angle

ensures entrainment occurs at a low threshold value ( $9.8 \text{ cm s}^{-1}$ ) equal to that required to entrain the transverse ellipsoid. The cuboid, although the same weight as the sphere, requires a higher shear velocity for entrainment by sliding, than is needed to entrain the sphere, but even here the entrainment shear velocity is not dissimilar to that associated with the rod, ellipse and spheroid in a variety of orientations.

*Initial motion on the intermediate roughness (Roughness 2).*

Roughening the bed with coarser material, which results in moving the pivot points further apart, provided an opportunity for the test cobbles to assume a more stable attitude, sitting deeper into the col between the bed particles. Consequently, the pivoting angle in all cases is increased and the necessary applied critical shear velocity to dislodge the cobbles also increases (Fig. 2). As might be expected the relative difference between the critical shear velocity for the parallel and transverse orientations changes little. However, the change in the relationship between shear velocity, roughness and test cobble size is not independent of the cobble shape. Whereas on the smoothest bed the parallel ellipse was the most stable, on the rougher bed the parallel rod is the most stable. More importantly, as the amplitude of the bed roughness increases, the tilt of the oblique particles also increases so that they are less stable than on Roughness 1 and easily roll to a transverse orientation. Consequently there is very little difference between the threshold values for oblique or transverse orientations for any individual shape. Whereas the sphere was very unstable on Roughness 1, increasing the roughness



amplitude provides an increasingly stable base. This increase in stability is not reflected in the case of the cuboid which cannot sit in the col between the bed particles selected but largely bridges across the gap and still sits on the tops of the bed particles, as it did on Roughness 1. Consequently, the difference between critical values for sphere and cube are now diminished.

*Initial motion on the roughest bed (Roughness 3)*

Selection of a roughness similar in dimensions to the test particles, meant that up to 17% of the cobble in some cases was not protruding into the flow. More importantly, for particle stability, the greater roughness amplitude provided an opportunity for cobbles to rotate within the col position and to imbricate. This latter series of tests shows quite clearly the importance of flattening of the C-axis to the initiation of imbrication and enhanced bed stability. Only the rod was entrained from any orientation without imbrication occurring first. The spheroid always rotated into an imbricated position ( $22^{\circ}$ - $32^{\circ}$ ) before entrainment. The high shear velocities needed to entrain particles on the rough bed, resulted in high initial particle momentum so that oblique (unstable) cobbles did not roll into new transverse (potentially more stable) locations but were entrained at lower threshold values than the parallel or transverse particles (Fig.3). This result is at variance with the observations from the two less-rough beds (Figs. 1 & 2). The ellipse could only be entrained when placed in the oblique orientation, whilst in other attitudes both it and the disc rotated into imbricated ( $18^{\circ}$ - $24^{\circ}$ ), stable positions. The shear velocity required to induce

imbrication was greatest for parallel orientations and for the disc. Typically, the velocity required varied between 19 and 32 cm s<sup>-1</sup>, which is in excess of that required to entrain the same particles from the smoother beds. The maximum shear velocity that could be generated was 44 cm s<sup>-1</sup>, but this was insufficient to break-up the imbricated structures.

### *Particle Velocities*

On the smoothest bed the rod exhibited the fastest particle velocity, followed by the spheroid, ellipse and disc (Fig.4). On the rougher beds, the motion of the spheroid was retarded by the roughness of the bed more so than any of the other shapes (Fig. 5 & 6). Oblate and flattened particles rolled more easily and directly over the roughness elements whilst the spheroid meandered around obstacles. Consequently on the rougher two beds the relative particle speeds were ranked: rod, ellipse, disc and spheroid.

The difference in particle velocities is maintained over the range of current velocities examined. Particle velocity increases as a linear function of current velocity over the range examined; the rate of particle velocity increase being somewhat less than that of the stream current (Table 2).

### **Entrainment Model**

All of the particles, excluding the cuboid, moved by rolling and so this analysis is restricted to a consideration of entrainment

by pivoting.

In a fuller exposition (Carling & Kelsey, in prep.) geometric relationships are advanced which calculate the grain contact angle and the pivoting angle for any isolated ellipse (2-D case) or ellipsoid (3-D case) positioned over the col between two (or four) bed-particles. The perched grain may be of dissimilar size and shape to the bed-particles and may be in a transverse or parallel orientation. Entrapment may be either by grain-top rotation (2-D case) or by pivoting over a col (3-D case). The geometry is a reasonably exact description of natural bed geometries where clustering of perched particles is not significant but for brevity the full details are not reported here.

Contact angles ( $\theta$ ) and pivoting angles ( $\phi$ ) calculated for the 2-D geometry of the test particles and the three bed roughnesses are summarized in Table 3. In addition the roughness parameter ( $z_p$ ) and the relative degree of exposure ( $\psi$ ) of the test particle are also tabulated. Because calculation of the pivoting angle for a test particle overlying a bed of particles of dissimilar size may be tedious without a computer routine, it is convenient to summarize typical data graphically. An example is given in Fig. 7.

Other parameters can also be presented graphically but for brevity these relationships are not presented here. Appropriate values (as in Table 3) can be selected for insertion in an initial motion function.

Consideration of the usual force balance (Fig 8) acting on the area of an ellipse exposed to the flow gives an expression for the drag force,

$$F_d = \frac{C_d}{2} \rho A U^2 \quad (1)$$

where for the coefficient of drag data used  $A = \pi(a_2 b_2 c_2)^{2/3}$

The force due to the mass of the particle is

$$F_g = V (\rho_s - \rho) g \quad (2)$$

where for an ellipsoid  $V = \frac{4}{3} \pi a_2 b_2 c_2$

and as

$$F_d = F_g \frac{\sin(\phi - \beta)}{\cos(\phi)} \quad (3)$$

then including the relative exposure term ( $\psi$ ) and the drag coefficient ( $C_d$ ) the critical entrainment velocity is given by

$$U_c^2 = \frac{2 V (\rho_s - \rho) g \sin(\phi - \beta)}{\psi C_d \rho \pi (a_2 b_2 c_2)^{2/3} \cos(\phi)} \quad (4)$$

As the velocity at height  $z$  above the bed is given by

$$U = 5.75 u_* \log(30z / k_s) \quad (5)$$

then the critical shear stress for any shaped ellipse can be given by,

$$\tau_c = \frac{2 V (\rho_s - \rho) g \sin(\phi - \beta)}{\psi C_d \pi (a_2 b_2 c_2)^{2/3} \cos(\phi)} \frac{1}{[5.75 \log(30z_p / k_s)]^2} \quad (6)$$

The appropriateness of equation 6 can be checked by comparing the calculated threshold shear velocity ( $u_* = \tau_c / \rho$ ) and the observed threshold shear velocity. For the transverse rod on roughness 3 the observed threshold shear velocity was  $17.29 \text{ cm s}^{-1}$  (Fig.1). Given  $\phi = 28.28^\circ$ ,  $\beta = 0.57^\circ$ ,  $\psi = 0.84$ ,  $(\rho_s - \rho) / \rho = 1.65$ ,  $g = 981 \text{ cm s}^{-2}$  and  $z_p = 4.53 \text{ cm}$ ,  $k_s = 11.3 \text{ cm}$  it remains to select a value for  $C_d$ . As a critical evaluation is required it would be inappropriate to calculate  $C_d$  from the hydraulic test data, but it is expected to be large and so can be set to 1.0 in the first instance. Introduction of the parameters into equation 6 gives a critical entrainment velocity of  $17.08 \text{ cm s}^{-1}$ ; a result in excellent agreement with observation. For roughness 2 the calculated result was  $12.97 \text{ cm s}^{-1}$  (observed =  $10.50 \text{ cm s}^{-1}$ ) and for roughness 1,  $9.61 \text{ cm s}^{-1}$  and  $6.92 \text{ cm s}^{-1}$  respectively.

## Discussion

The flume tests demonstrate that, within a limited size range, variation in cobble shape and orientation for a given bed

roughness are as important variables in the initial motion criteria as is the mass of the particle defined by weight or diameter. This variability means that a range of particles of varying size, shape or orientation may be entrained from a bed of mixed grains under identical flow conditions. These *susceptible* particles may be regarded as 'equally mobile' but other particles may not be entrained for the given hydraulic conditions because of their particular size shape or attitude on the bed.

Attention needs to be given to the influence of the complete size distribution and packing of the bed materials in individual rivers as field data (eg. Carling, 1989) show conclusively that where a wide gradation of particle sizes exists, then selective entrainment (defined by size) is an important process such that the probability of encountering larger particles in motion increases as the shear velocity increases. Any robust deterministic initial motion expression must include realistic definitions of the geometry and packing of the particles on the bed such that the mechanics of initial motion can be correctly specified. Further work is in progress and will explore the mechanics of imbrication and initial motion by sliding.

### **Acknowledgements**

The authors would like to thank Prof. P. Ergenzinger of the Free University of Berlin for permission to use the flume facilities. Ralph Busskamp and Dorothea Gintz gave freely of their time in laboratory assistance. One of us (A.K.) is in receipt of a NERC research studentship and an enabling grant from the British

Council to PAC facilitated travel. For all this support we are grateful.

Table 1 . Dimensions of test particles

Shape	A-axis	B-axis	C-axis	Weight
	(mm)	(mm)	(mm)	(kg)
Rod	225	60	60	1
Ellipse	159	100	47	1
Disc	155	137	40	1
Spheroid	122	95	63	1
Sphere	116	116	116	2.4
Cuboid	129	96	75	2.4
UP60	81	60	49	0.35
UP130	158	130	115	3.2



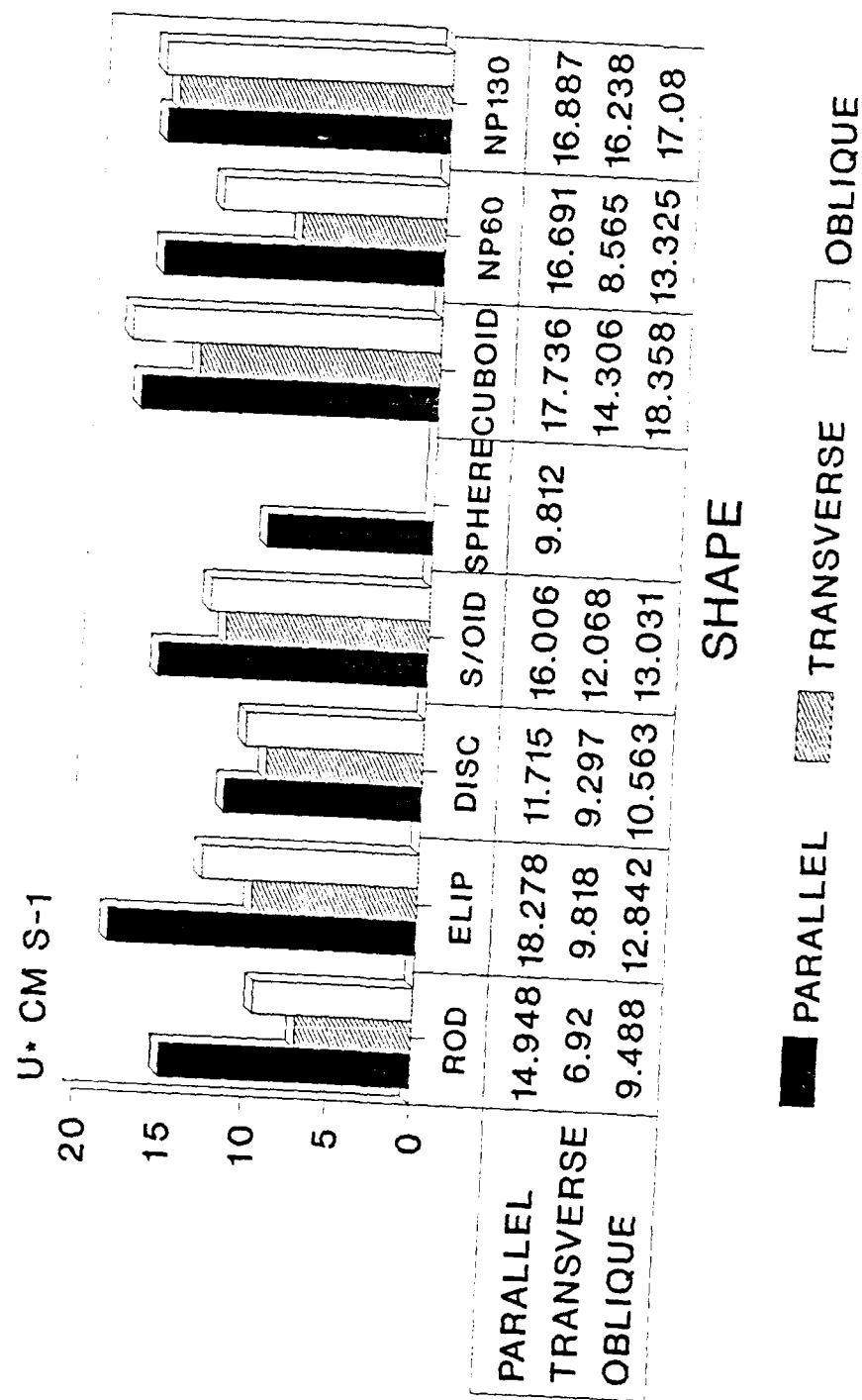
Table 2. Constants and coefficients for particle velocity ( $U_p$ ) as function of near-bed velocity ( $U_b$ ).  $U_p = a + bU_b$

	Roughness 1		Roughness 2		Roughness 3	
	(a)	(b)	(a)	(b)	(a)	(b)
Rod	-43.20	0.66	-41.57	0.73	-43.36	0.70
Ellipse	-69.22	0.76	-42.25	0.69	-55.84	0.75
Disc	-98.68	0.87	-37.10	0.68	-54.79	0.73
Spheroid	-54.16	0.71	-56.93	0.75	-69.56	0.80

Table 3. Calculated entrainment parameters for test particles.

	Roughness	Rod	Ellipse	Disc	Spheroid
$\theta$ (deg.)	1	20.93	10.20	5.57	13.24
	2	23.24	10.99	5.81	14.64
	3	28.28	16.05	9.59	21.11
$\phi$ (deg.)	1	20.93	39.17	48.83	28.14
	2	23.24	41.32	50.06	30.71
	3	28.28	52.82	63.23	41.28
$z_p$ (mm)	1	39	34	32	41
	2	44	36	34	42
	3	45	35	34	39
$\psi$ (-)	1	0.96	0.975	0.985	0.97
	2	0.95	0.96	0.97	0.95
	3	0.84	0.84	0.87	0.83

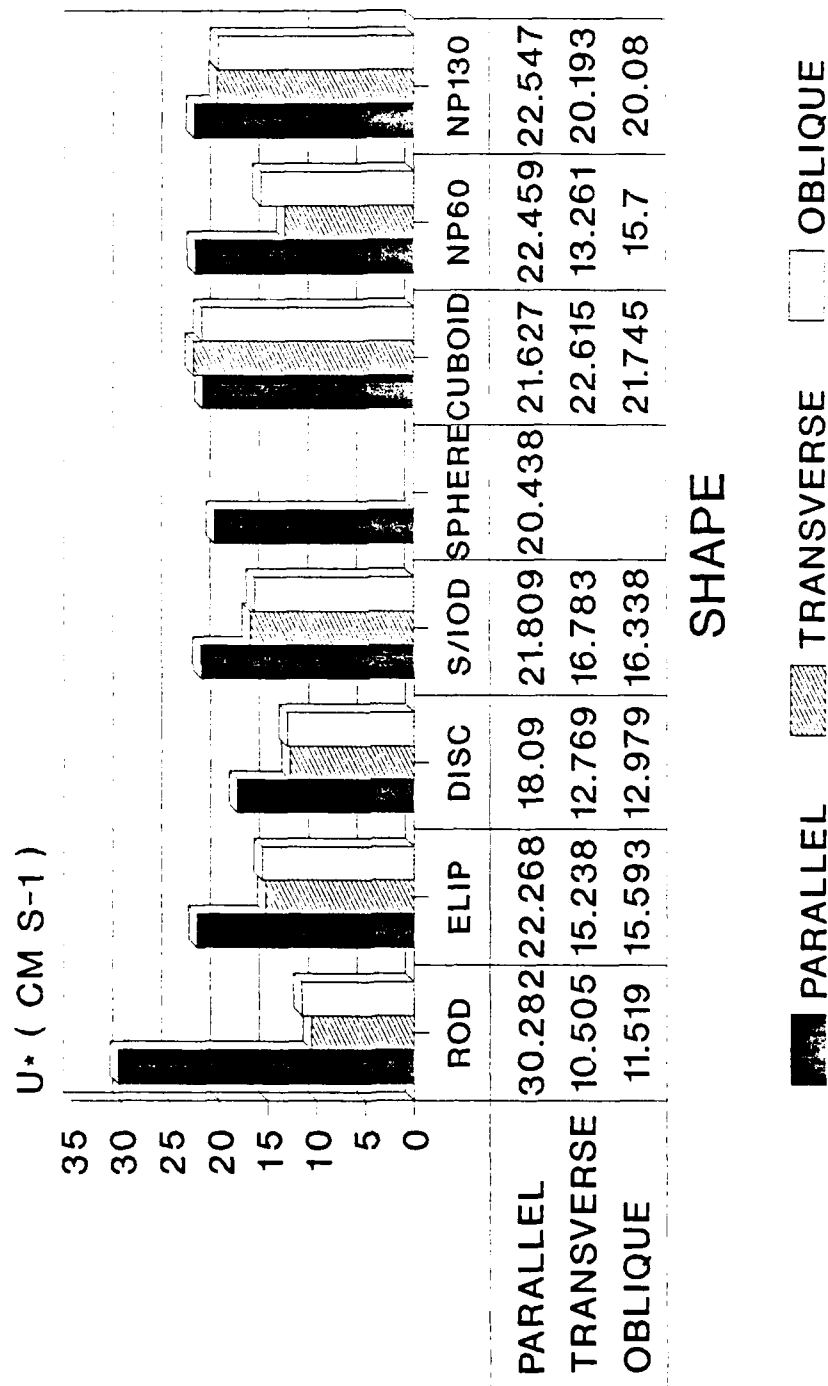
Fig. 1  
Rough 1 Shape/Orientation v.U\*



Mean U\* ( n=5 )

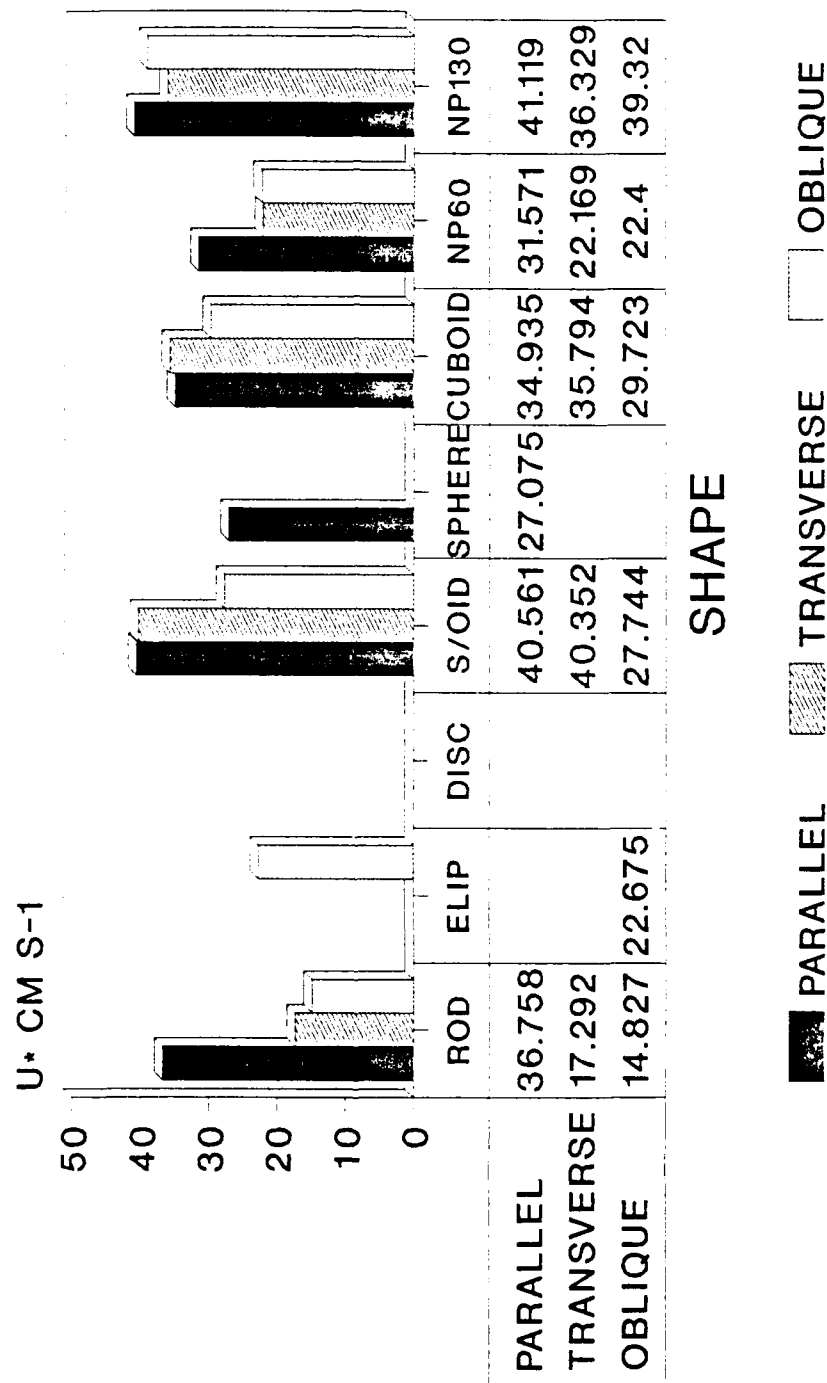
# Fig. 2

Rough 2. Orientation/Shape v.  $U^*$



MEAN  $U^*$  VALUES USED (  $n=5$  )

Fig. 3  
Rough 3 Shape/Orientation v.U\*



Mean U\* ( n=5 )

# Fig. 4. Particle Velocity

## Roughness 1

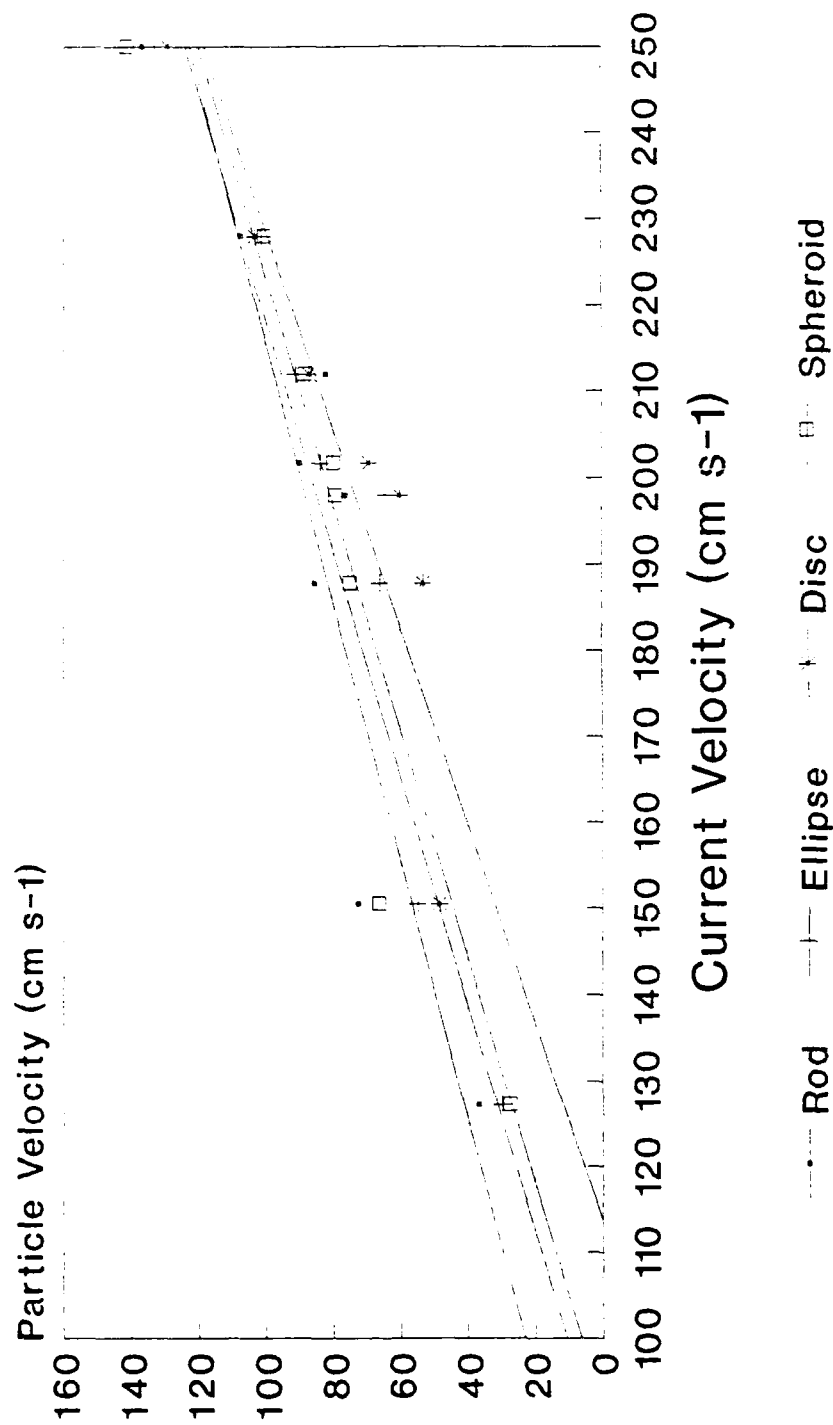
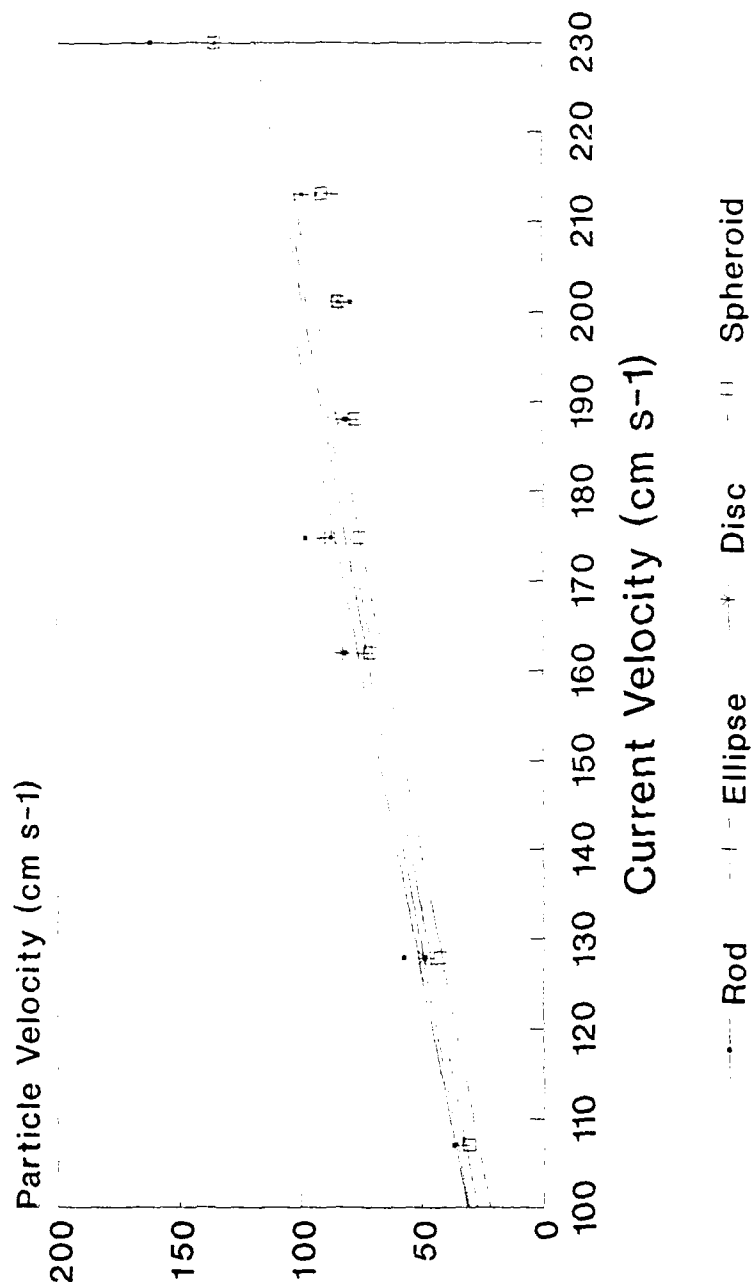


Fig. 5. Particle Velocity  
Roughness 2



# Fig. 6. Particle Velocity

## Roughness 3

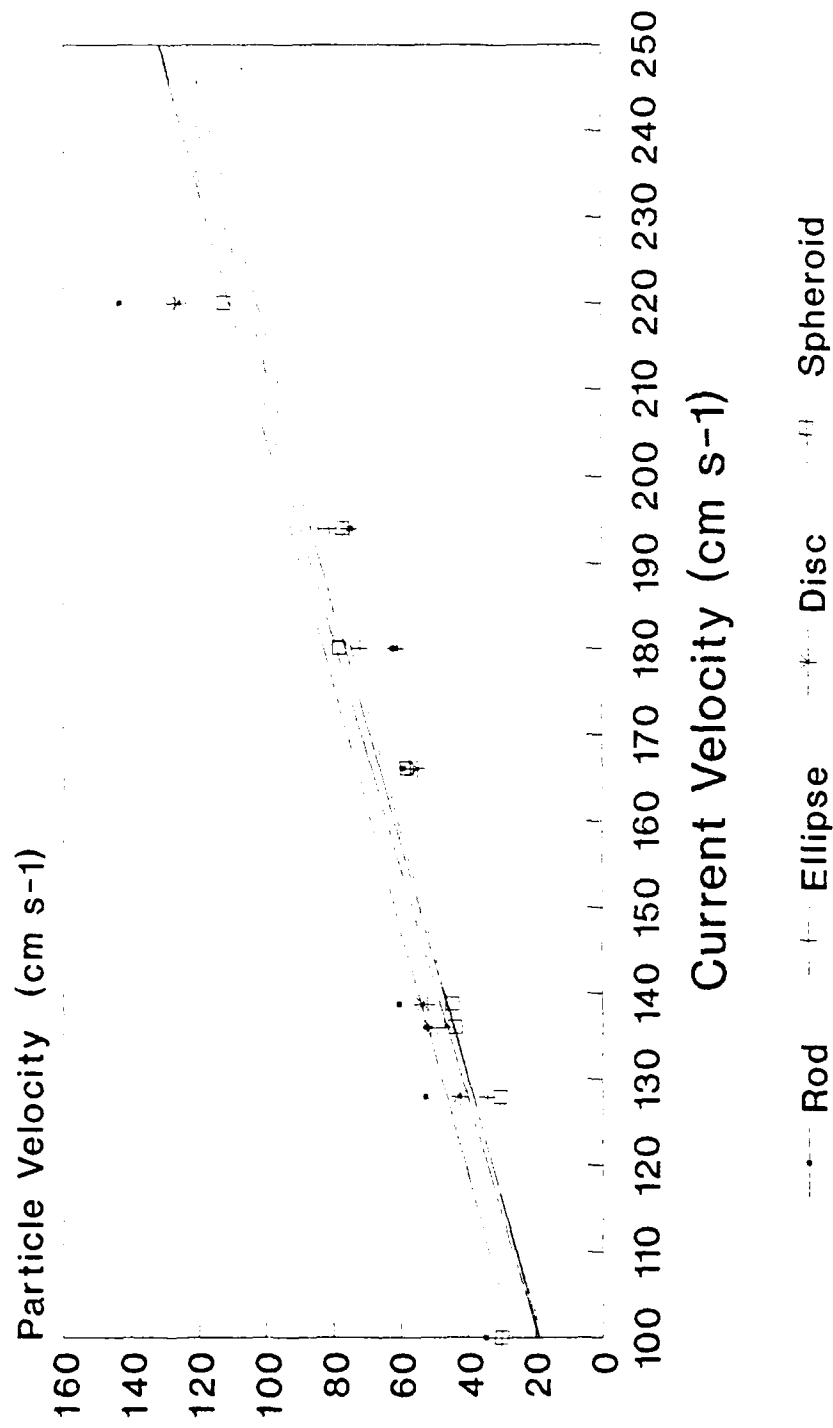
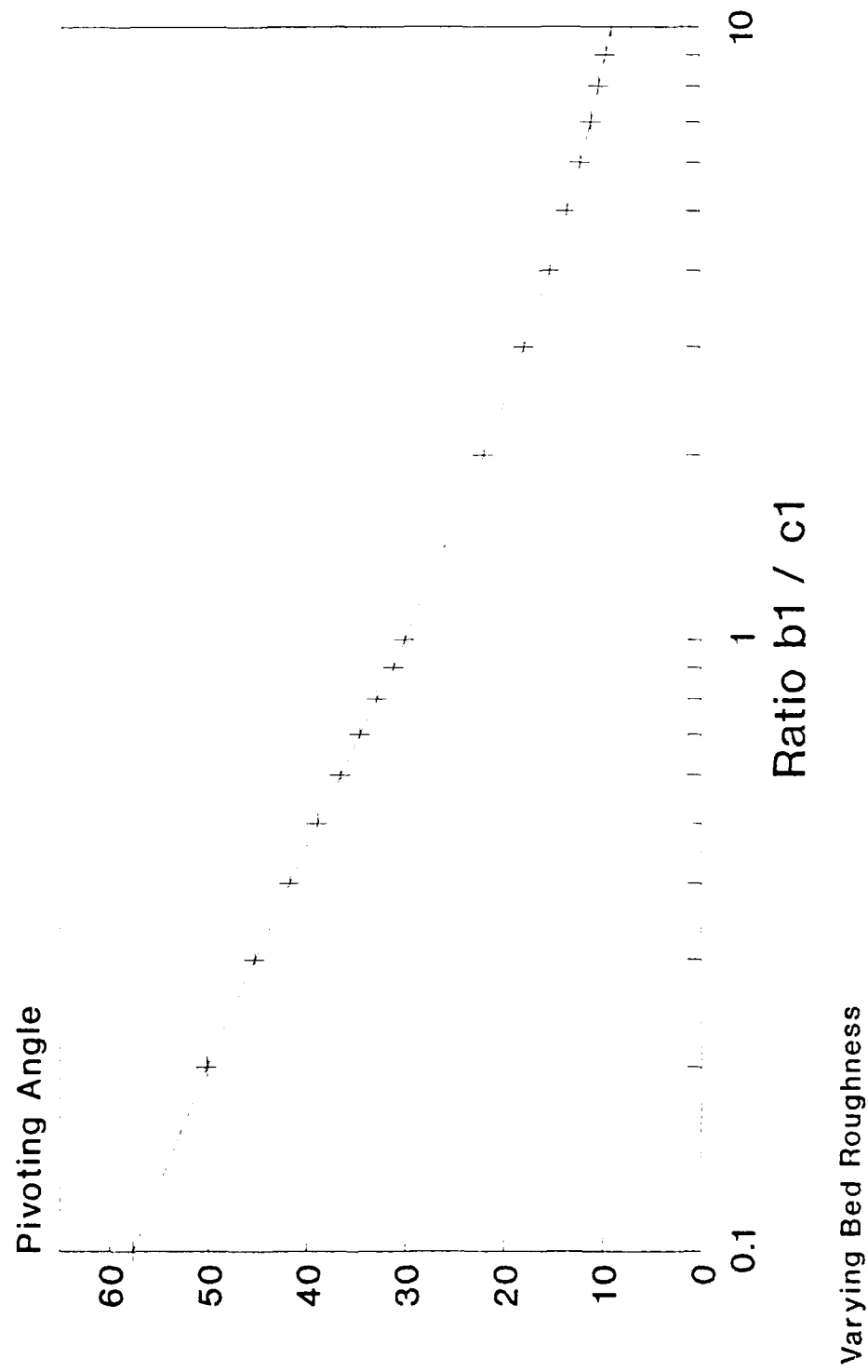




Fig. 7.  
Pivot Angle vs. Bed Form



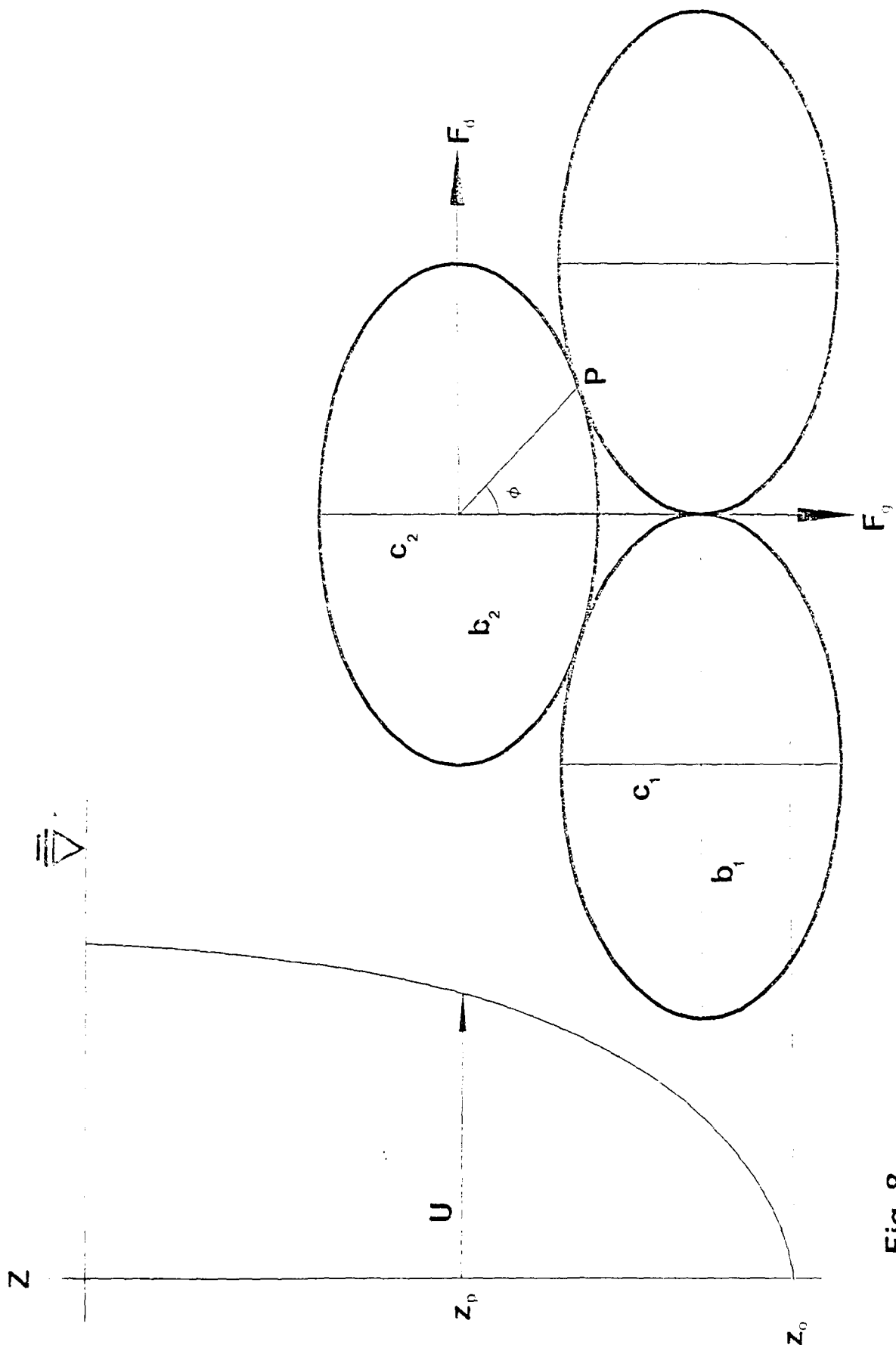


Fig. 8.

THIRD INTERNATIONAL WORKSHOP ON GRAVEL-BED RIVERS  
Florence, 24-28 September, 1990

TOPOGRAPHIC EXPRESSION OF BARS IN MEANDERING CHANNELS

Marco Colombini (\*), Marco Tubino (\*) and Peter Whiting (\*\*)

(\*) Hydraulic Institute, University of Genoa, Italy

(\*\*) Dept. of Geology and Geophysics, Univ. of California, Berkeley, USA

**ABSTRACT** - Bar morphology in meandering channels has been investigated through an extensive set of controlled experiments in fixed side-walls channels with erodible bottom. Different meander configurations have been tested under the same set of flow conditions, with values of channel wavelength and width to depth ratio falling within the range usually found in nature. Results of experiments may shed some light on the fundamental question concerning the triggering mechanism of bend instability which leads to meandering. It appears that within the range of wavelengths examined the experimental trend is far from being satisfactorily predicted by linear theories which have been so far employed to investigate bed topography in meandering channels.

## 1 - INTRODUCTION

Bars are prominent features of alluvial channels. They develop as a results of an instability process that arises from the coupling between flow and sediment transport in mobile channels, on a spatial scale typically of the order of channel width, and grow at a rate that is associated with the bed erosion-deposition process. The presence of bars exerts a strong influence on the flow field and sediment transport process; the resulting patterns greatly enhance the erosion of channel banks and consequently induce bend growth and channel shift. Thus, the presence of bars mainly determines the morphology of alluvial channels.

Besides the practical relevance of the subject (the development of bars affects several aspects of fluvial engineering), modelling flow and bed topography associated with bar development has attracted the interest of many researchers since it stands as the essential step towards the understanding of river meandering.

As a consequence of many theoretical works on meandering, supplemented by various field studies (Bridge and Jarvis, 1982; Dietrich and Smith, 1983, 1984, Thorne et al., 1985) and flume investigations (Friedkin, 1945; Hooke, 1975; Gottlieb, 1976; Fujita and Muramoto, 1982), a fairly advanced knowledge of the process has been reached. Based on these analyses, it is now possible to draw a consistent picture of various phenomena involved in the process of meander formation, even though recent applications of nonlinear mechanics to river systems seem to suggest that the state of the subject can by no means considered as fairly settled.

In single-thread alluvial channels two classes of bars are typically identified that arise from both natural and forced responses. Migrating free bars develop spontaneously in straight channels and persist in gently curved channels unless channel curvature exceeds a threshold value above which bar migration is suppressed. Forced (point) bars are nearly steady features that develop in response to the curvature of the channel and give rise in meandering channels to an alternate sequence of shoals on the inside of the bends and pools along the outer banks.

Research developed in the seventies and in the early eighties on flow and bed topography in meandering channels focussed mainly on linear theories of point bars. However further theoretical investigations have shown a clear connection between free and forced bars. Blondeaux and Seminara (1985), within the context of a unified approach, found that the amplitude of point bars in sinuous channels is likely to be controlled by the interaction between curvature and free bars. In particular they showed that the linear response of flow and bed topography to the forcing effect of curvature exhibits a resonant behaviour and peaks when meander wavelength and width to depth ratio of the channel attain values at which curvature forces a natural response consisting of steady free bars. When coupled with a bend stability analysis of the kind proposed by Ikeda et al. (1981), where meandering is explained in terms of a planimetric instability of the channel activated by secondary flow driven by bed topography in sinuous channels, the above theory shows that resonance controls meander initiation and leads to selected meander wavelengths falling in the resonant range.

The picture that emerges from the linear analyses has been recently questioned by Seminara and Tubino (1990) who derived a nonlinear analytical solution valid within the resonant range; preliminar results of the above analysis show that for a relatively wide range of values of meander wavelength and width to depth ratios centered at resonance the linear solution does no longer apply and nonlinear effects lead to a solution which exhibits a sharply different behaviour.

Validation of the above theoretical findings through the existing experimental data is not possible since they refer to different experimental conditions and are not systematic. Thus a further progress in the understanding of meandering initiation and development preliminarily requires a detailed comparison with experimental data obtained through controlled experiments designed so as to cover the range of wavelengths and width to depth ratios close to the resonant values. To this end flume experiments have been carried out in fixed-sidewalls sinuous channels in the laboratory of the Hydraulic Institute of Genoa University. Experimental conditions have been chosen so as to examine bar development as channel wavelength varies within the resonant range, for the same set of flow conditions. Measurements have focussed mainly on bed topography: during experiments bed evolution in each pool has been documented and detailed altimetric surveys have been carried out at the end of each run.

A detailed description of experimental procedure and results is deferred to sections 3 and 4 respectively, and follows a brief review of previous theoretical results that is given in section 2.

Section 5 is devoted to a discussion of results along with some concluding remarks.

## **2 - THEORETICAL FRAMEWORK**

To investigate the development of bed topography in cohesionless sinuous channels a large number of theoretical studies has been developed by various authors (e.g. Engelund, 1974; Gottlieb, 1976; Ikeda et al., 1981; Smith and Mc Lean, 1984; Kitanidis and Kennedy, 1984; Blondeaux and Seminara, 1985; Seminara and Tubino, 1985; Ikeda and Nishimura, 1986; Odgaard, 1986). A detailed discussion of the mathematical framework and the physical basis of these analyses, which are linear and employ both two-dimensional and three-dimensional flow models, can be found in some recent review papers (Parker and Johannesson, 1989; Seminara and Tubino, 1989; Seminara, 1989; Tubino, 1990). However, a

brief description of the main theoretical assumptions and results may help the reader to locate the experimental results reported in this work in the field of the present status of the theoretical research on river meandering.

Since the original work of Langbein and Leopold (1966) the problem has been treated by assuming that the channel axis follows a 'sine-generated curve'. Thus, denoting by  $R_o^*$  twice the radius of curvature at the bend apex and by  $\lambda_m^*$  the intrinsic meander wavenumber, the longitudinal distribution of channel curvature can be expressed by

$$\frac{1}{r_o^*} = \frac{1}{R_o^*} \exp[i\lambda_m^* s^*] + \text{c.c.} \quad (2.1)$$

where  $r_o^*$  is the local radius of curvature of channel axis, c.c. denotes complex conjugate, and a curvilinear orthogonal coordinate system is adopted such that  $s^*$  is the intrinsic longitudinal coordinate denoting the arclength and  $n^*$  is the transverse coordinate measuring the radial distance from the axis (figure 1).

The mathematical problem, posed by Reynolds equations coupled with sediment continuity equation, can be reduced to a dimensionless form by employing the half width of the channel  $B^*$  as the relevant spatial scale of channel topography and referring to a basic uniform flow, with given discharge and slope, such that  $D_o^*$  and  $U_o^*$  denote the average flow depth and speed respectively. Thus, the solution for the dependent variables (velocity field, flow depth and bed elevation) can be sought in terms of five dimensionless parameters which account for both geometric and hydraulic characteristics:

- the curvature ratio

$$\nu = \frac{B^*}{R_o^*} \quad (2.2)_c$$

- the width ratio

$$\beta = \frac{B^*}{D_o^*} \quad (2.2)_t$$

- the dimensionless meander wavenumber

$$\lambda_m = \lambda_m^* B^* \quad (2.2)_s$$

- the Shields parameter

$$\theta = \frac{\tau_o^*}{(\rho_s - \rho)g d_s^*} \quad (2.2)_a$$

- the roughness parameter

$$d_* = \frac{d_s^*}{D_o^*} \quad (2.2)_r$$

where  $\tau_o^*$  is bed shear stress associated with the reference uniform flow,  $\rho_s$  and  $\rho$  are sediment and water density respectively,  $g$  is gravitational acceleration, and  $d_s^*$  is the diameter of the sediment (modelled as uniform).

Since the timescale of the process under investigation is that associated with bed erosion, which is typically  $10^3 - 10^4$  larger than the flow timescale, a quasi-steady approach can be used, whereby the flow field is assumed to adapt instantaneously to changes in the bottom configuration. Moreover, taking advantage of commonly observed features of natural streams, the mathematical problem can be simplified assuming the channel to be wide and its curvature to be small.

The first assumption, namely  $\beta \gg 1$ , allows one to analyse the flow only in the 'central' region of the channel neglecting the effect of sidewall boundary layers. It also suggests that a two-dimensional depth-averaged flow model can be suitable enough to describe the main features of solution, provided the dispersive effects associated with the helical component of secondary flow, which vanishes when performing the process of depth-averaging, are somewhat accounted for in the model. Following the lead of Engelund (1974), Seminara and Tubino (1989) have incorporated these dispersive effects into a two-dimensional model by decomposing the transverse secondary flow associated with curvature into a helical component with no net flux and a depth-averaged component, and feeding into the 2-D equations for the latter component dispersive (redistribution) terms obtained by the fully three-dimensional solution for the helical component.

The second assumption, namely  $\nu \ll 1$ , applies conveniently to the stage of incipient meandering and suggests the opportunity to investigate the flow field and bed topography in sinuous channels by means of a suitable perturbation expansion in terms of the curvature ratio  $\nu$ . Thus, a linear solution of the problem can be determined in the form

$$U = 1 + \nu U_1(n) e_1(s) + c.c. \quad e_1 = \exp[i\lambda_m s] \quad (2.3)_c$$

where  $U$  is the dimensionless depth-averaged component of longitudinal velocity, scaled by the average speed  $U_0^*$ , the longitudinal and transverse coordinate  $s$  and  $n$  are scaled by the half width  $B^*$ , and similar expansions hold for the other variables.

As shown by Blondeaux and Seminara (1985) the solution of the linear depth-averaged problem can be obtained in a closed form without requiring further assumptions on the transverse structure of solution (Engelund, 1974; Ikeda et al., 1981; Odgaard, 1986). A comparison between two- and three-dimensional predictions shows that both models lead to results of comparable accuracy (Seminara and Tubino, 1985, 1989).

The linear model for flow and bed topography in sinuous channels can be incorporated into a bend instability analysis of meander formation following a procedure originally proposed by Ikeda et al. (1981). The procedure is based on the assumption that, bank erosion being a process acting at a larger timescale than that associated with bed development, the steady solution obtained in sinuous channels can be used to build up a model of bend growth in term of the amplification in time of a small-amplitude sinusoidal perturbation of the channel axis. Assuming the original straight channel to be in equilibrium, a perturbation of the channel axis can induce a flow perturbation in the near-bank region able to produce bank erosion (accretion), i.e. bend growth (decay).

Thus, the preferred meander wavenumber selected by bend instability is determined, for given values of  $\theta$ ,  $d_s$  and  $\beta$ , from the value of  $\lambda_m$  where the near-bank flow perturbation reaches its peak. As shown by Blondeaux and Seminara (1985), the linear solution exhibits a sharp peak in a fairly wide range of values of wavenumber and width ratio, thus showing a resonant (or quasi-resonant) response of flow and bed topography (figure 2). The peak in the linear response occurs whenever  $\beta$  and  $\lambda_m$  fall in a range close to some resonant values  $(\beta_R, \lambda_R)$ , for a given set of flow and sediment parameters; within this range the wavenumber of the forcing curvature is close to the wavenumber of free bars which are steady and not freely growing either in space or in time. Thus curvature provides the forcing for a particular set of natural responses consisting of steady alternate bars.

The resonant behaviour of the linear solution, missed by previous theoretical models where the full coupling between the flow, sediment transport and bed topography was not retained, has been further confirmed within the context of a three-dimensional model (Seminara and Tubino, 1985) and recently recovered also by Johannesson and Parker (1989). Resonance implies that meander wavenumbers selected by bend instability fall within the resonant range, where the bend growth maximizes. When compared with meander wavenumbers observed both in the laboratory and in the field the above prediction appears

fairly satisfactory (Blondeaux and Seminara, 1985, figure 8; Johannesson and Parker, 1989, figure 7). Moreover, for given values of  $\theta$  and  $d_a$ , the resonant values  $\beta_R$  fall in the range physically sensible for meander formation.

However, further theoretical and experimental results suggest that a direct experimental evidence of resonance in sinuous channels in the form predicted by linear models can hardly be expected.

Unless channel curvature exceeds a threshold value, migrating alternate bars may coexist and interact nonlinearly with steady point bars forced by curvature, as observed by Kinoshita and Miwa (1974) and explained theoretically by Tubino and Seminara (1990). The above coexistence, which clearly emerges both in fixed-sidewalls experiments (Gottlieb, 1976) and in free-meandering experiments (Fujita and Muramoto, 1982), is neglected in all the existing linear models, but is responsible for some nonlinear effects that affect the bed topography in sinuous channels (see Seminara and Tubino, 1989). Notice that meandering initiation is invariably found to operate in a channel where migrating free bars have already formed and undergone a finite-amplitude development.

Moreover the linear expansion breaks down when the resonant conditions are exactly met, the solution exhibiting an infinite peak. A recent attempt to remove the above singularity has been introduced by Seminara and Tubino (1990) by means of a nonlinear analysis developed in the range of  $\lambda_m$  and  $\beta$  close to resonant conditions. The above theory shows that within this range nonlinear effects are able to smooth out the infinite peak of the linear solution and shift the maximum response (i.e. the maximum bend growth) towards larger values of  $\lambda_m$  (figure 2). It also appears that as the curvature ratio  $\nu$  increases, the solution is largely controlled by nonlinear effects in a quite wide range of values of  $\lambda_m$  and  $\beta$ .

Then, for larger values of the curvature ratio  $\nu$ , when migrating bar-perturbations are suppressed, linear models are no longer significant and a nonlinear analysis is needed to properly describe the bed topography in sinuous channels for values of  $\lambda_m$  and  $\beta$  which cover the range of values usually found in natural meanders. In particular, within this range the correct order of magnitude of solution is  $O(\nu^{1/3})$  rather than  $O(\nu)$  as in a linear theory. This implies that, even for small values of the curvature ratio  $\nu$ , the contribution of higher harmonics of bed topography can affect the solution in a non-negligible way and lead to the reproduction of distinctive asymmetries that characterize bed topography in natural meanders. This also implies that, within the above range, the finite amplitude evolution of meander bends is likely to be governed by higher harmonics of flow and bed topography induced by flow nonlinearities.

### 3 - METHODS

The experiments were carried out on a large indoor platform measuring 29.6 m long and 2.3 m wide. The concrete platform had a longitudinal slope of approximately 0.006 and was overlain by a 2 cm thick veneer of painted wood. Along both sides of the platform was an approximately 0.40 m high railing that supported a carriage used for leveling the bed and measuring bed and water surface topography. The railing had a constant slope of 0.006 that was carefully checked every 1.5 m.

The 0.35 m wide sinuous flume was constructed by attaching 2 m long and 0.15 m high strips of clear polycarbonate to the wooden platform base. Three or four right-angle braces of bent polycarbonate were glued to the 2 m strips. Screws anchored the base of the braces to the platform forming vertical flume walls. The channel centerline followed a sine curve. The trace of each bank in the series of bends was established by plotting on oversize paper at a 1:1 scale. This paper was tacked to the wooden platform and the banks positioned to follow this trace. Once the banks were correctly located the paper was removed and the polycarbonate sealed to the platform with silicon caulk. The caulk gave additional rigidity to the banks. Once the channel was laid out, local variations in width associated with the

banks not standing at right angles to the platform were eliminated by placing additional braces along the banks. The platform was long enough to allow the modeling of more than seven consecutive bends also for the configuration with maximum wavelength.

The flume was filled with a well sorted 0.76 mm quartz sand. The  $D_{84}$  of the sediment was 0.87 mm and the  $D_{16}$  was 0.65 mm. These percentages correspond to the grain diameter such that 84 or 16 percent were finer.

Flow entered the flume through a 0.35 cm wide notch in the headtank at the upstream end of the flume. A fine mesh screen served as a baffle to surface waves that might have been engendered in the head tank. The inlet pipe's submergence 0.20 m under the free surface minimized disturbance. Two narrow vertical sills, one 0.10 m and one 0.30 m into the flume, prevented inlet scour and thus maintained a constant inlet elevation.

At the downstream end of the flume a tailgate was constructed to maintain the outlet elevation. The tailgate was a plastic strip whose ends were recessed into a wooden enclosure. A ramp with glued-on sand, partially buried in the sand, met the tailgate at the height of the tailgate. This ramp was designed to prevent scour associated with the vertical sill. Above the sill setting the tail elevation a second plate could be lowered to set the height of the free surface. Flow spilled through a tipped trough into the weir box. The weir box was 2.50 m long and .70 m wide and was partitioned into two sections. In the first section, a mesh bag for collecting sediment was placed. The two sections were connected through a slot at the base of the partition. The downstream end of the box had a 90° weir plate. Flow spilled out of the weir box into a large reservoir. A pump submerged in the reservoir returned water to the headtank. A valve along the pipe connecting the pump to the head gate could be turned to vary discharge.

Sediment was fed into the upstream end of the flume with a sediment shaker. The sediment flux out of the shaker was difficult to calibrate so was monitored frequently and adjusted to give the appropriate feed rate set equal to the observed average tailgate flux. The sediment discharge at the end of the flume was measured by collecting the sand in a 0.40 m wide, 0.60 m long and 0.35 m deep mesh draped frame submerged in the weir box. The submerged collector was suspended from an overhead beam and attached to a strain-gage. The cumulative submerged weight was noted every 5 to 10 minutes during the experiment.

The bed of the channel was prepared by using 0.34 m wide scraper that was attached to a carriage that ran along the rails. The bed was smoothed flat to a constant slope of 0.0060 before each experiment. A very low discharge was passed over the bed prior to the experiments to prepare a smooth saturated surface. The bed elevation at 1.0 meter intervals was measured with a point gage attached to the carriage. Once flow was begun the required discharge was achieved by slight adjustments to the valve. The flow discharge was determined with a point gage attached to the weir box.

During experiments the position and maximum depth in each pool was noted periodically and the sediment water interface at the concave bank was traced to document initial bed evolution. After the stable discharge was reached early in the experiment, water surface topography was measured in order to calculate the average depth unperturbed by developing topography. Every 45 minutes later water surface elevation was remeasured. After the pools and bars had become stabilized in position and once water surface slope and discharge were average on the long term indicating equilibrium conditions, the experiment was terminated. This generally took 3-4 hours.

The bed topography was preserved at the end of the experiment as flow waned by carefully placing damp newspapers on bar tops near steep slopes. This prevented dissection of the sideslopes and consequent filling of the pools. The bed topography was measured with a laser scanning device mounted on the carriage. The precision of the scanner was 0.01 mm. The scanner was driven by a stepper motor which stopped every 2 mm across the channel for a measurement. The system was run of an Olivetti M21 computer. The data was later



converted into elevation data for presentation. Traverses of the topography were made every 0.10 to 0.20 m along the channel depending on the channel wavelength; for the configurations studied this corresponds to 36-44 cross-sectional surveys per channel wavelength. Typically two to two-and-a-half wavelengths were scanned. The portion of the channel studied began at least 8 m downstream of the inlet and ended at least 7 m from the flume exit.

#### 4 - RESULTS

To simplify as much as possible the drawing of the channels and the data flow between the intrinsic curvilinear coordinate system ( $s^*$ ,  $n^*$ ) and the Cartesian system ( $x^*$ ,  $y^*$ ) (see figure 1), we decided to have a purely sinusoidal channel axis given, in nondimensional form, by

$$y = a \sin(\lambda x) \quad (4.1)$$

where  $x$ ,  $y$  and the amplitude  $a$  are scaled by the half width  $B^*$  and  $\lambda$  denotes the Cartesian wavenumber, normalized by  $1/B^*$ . The curvature ratio  $\nu$  retains exactly the same meaning as before while the longitudinal distribution of curvature differs from (2.1) of terms of order  $O(a^2\lambda^2)$ .

As was outlined in section 2, the number of parameters present in the problem is high, so that many experiments would be needed to clarify the influence of each variable on the phenomenon. We therefore decided to keep the value of  $\nu$  constant through all the experiments while varying conversely channel wavenumber  $\lambda$  and width ratio  $\beta$  in a range as broad as possible. As mentioned before the slope of the channel and the sand diameter were fixed once and for all to be respectively 0.006 and 0.76 mm.

The choice of  $\nu$  results from a compromise between the requirement of a small  $\nu$  due to theory validation purposes and space limitations, and the need for having a relatively high value of  $\nu$  to minimize the presence of propagating bedforms. On the basis of theoretical estimates of the threshold conditions for migrating bars suppression, the value of  $\nu$  was therefore chosen to be 0.05; this corresponds to a channel curvature characteristic of natural meanders in the initial-intermediate stage of evolution.

Four different channels were built up with four values of  $\lambda$  and the same width (35 cm). The selected range of wavenumbers ( $0.15 \div 0.3$ ) comprises the resonant range ( $\lambda \sim 0.15 \div 0.2$  accordingly with a linear theory) and extends towards higher values of  $\lambda$  which are better representative of natural situations. Once  $\lambda$  was fixed, the amplitude  $a$  of each channel was determined through the relationship

$$\nu = \frac{a\lambda^2}{2} \quad (4.2)$$

In table 1 the geometric characteristics of the channels are shown ( $L^*$  and  $a^*$  are the dimensional Cartesian wavelength and amplitude of channel axis respectively).

Four to five experiments were performed in each channel at different flow rates that were chosen so as to produce almost the same set of values of average flow depth ( $D_o^*$ ) for each configuration. Working in this way we were able to analyse the behaviour of each measured quantity both as a function of  $\beta$  (at  $\lambda = \text{const}$ ) and of  $\lambda$  (at  $\beta = \text{const}$ ). An exact reproduction of the same values of  $\beta$  for each experiment was not possible since flow depth was indirectly obtained by setting a prescribed flow discharge; this led to minor variations in the average value of flow depth that resulted in larger differences in the value of  $\beta$ . Thus a small work of interpolation was needed to obtain iso- $\beta$  curves. It might be useful for the reader to stress here the fact that on these iso- $\beta$  curves Shields stress  $\theta$  and roughness parameter  $d_s$  are constant too.

Table 1: Geometrical characteristics of channels.

Channel	B* (m)	L* (m)	a* (m)	$\lambda$	a	$\nu$
W 15	.175	7.33	0.77	0.15	4.44	0.05
W 20	.175	5.49	0.43	0.20	2.5	0.05
W 25	.175	4.4	0.28	0.25	1.6	0.05
W 30	.175	3.66	0.19	0.30	1.11	0.05

Table 2: Flow and sediment transport parameters.

Run	$Q_o^*$ (l/s)	$D_o^*$ (cm)	$\beta$	$d_s$	$\theta$	Fr
W15Q07	0.76	0.89	19.66	0.085	0.043	0.82
W15Q10	1.01	1.01	17.33	0.075	0.048	0.91
W15Q14	1.42	1.36	12.87	0.056	0.065	0.82
W15Q16	1.56	1.51	11.59	0.050	0.072	0.77
W20Q07	0.76	0.92	19.02	0.083	0.044	0.79
W20Q10	1.01	1.13	15.49	0.067	0.054	0.77
W20Q12	1.23	1.19	14.71	0.064	0.057	0.86
W20Q14	1.42	1.34	13.06	0.057	0.064	0.84
W20Q16	1.56	1.50	11.67	0.051	0.072	0.77
W25Q07	0.76	0.82	21.34	0.093	0.039	0.93
W25Q10	1.01	1.11	15.77	0.068	0.053	0.79
W25Q12	1.21	1.21	14.46	0.063	0.058	0.83
W25Q14	1.39	1.40	12.50	0.054	0.067	0.77
W25Q16	1.56	1.52	11.51	0.050	0.073	0.76
W30Q07	0.76	0.94	18.62	0.081	0.045	0.76
W30Q10	1.01	1.05	16.67	0.072	0.050	0.86
W30Q12	1.20	1.19	14.71	0.064	0.057	0.84
W30Q14	1.42	1.39	12.59	0.055	0.066	0.79
W30Q16	1.56	1.51	11.59	0.050	0.072	0.77

Hydraulic conditions and flow and sediment transport parameters of the experimental runs are summarized in table 2 where  $Q_o^*$  and Fr are flow discharge and Froude number respectively.

Flow and sediment characteristics were chosen so as to obtain relatively high values of width ratio, as is typical of natural conditions, and to prevent the occurrence of small-scale sand waves as ripples or dunes. In spite of the relative smallness of Shields stress  $\theta$  (always less than 0.075) sediment transport was indeed appreciable in all the experiments, the critical value of Shields stress being around 0.035 for the values of particle Reynolds number characteristic of the experiments.

The bed time development was almost similar for all the experiments. After approximately 45 minutes a scour hole appeared, typically located downstream of the bend apexes. While deepening the scour was seen to migrate downstream or upstream depending on experimental conditions until an equilibrium configuration was reached which remained reasonably unchanged until the end of the experiment. This regime topography was fairly stable with the only exception of small propagating sand waves that were often seen to born within the scour hole and vanished at the downstream end of the pool.

Runs at  $\lambda = 0.15$  showed the existence of more pronounced migrating alternate bars, clearly detectable in the straight reaches between two bends, whose amplitude was however smaller than that of fixed bars. It seems that the steady scour hole acts as a source and sink for bar-like disturbances. When the straight reaches between two consecutive bends are long enough, as in the case of runs at  $\lambda = 0.15$ , bar perturbations emerging out of the apex pools are able to develop finite amplitude fronts which spread on the cross section and form conjugate (alternate) fronts. These fronts propagate in the straight reaches between bends and then interact with steady pools when reaching the bend apexes. The latter interaction strongly modifies the alternate pattern; fronts are considerably slowed down while sediment transport concentrates within the pools along the outer bank forming narrow fronts which are stalled and then sped up again when coming out of the pools.

In run W15Q16 free perturbations showed a relatively large amplitude and were often seen to propagate through the bend keeping a distinct alternate pattern. The characteristic wavenumber of these alternate bars was remarkably higher, namely three times larger than that of the meandering channel.

To grasp the main features of bar topography which emerges from the experiments we considered two measured quantities to be representative of each experiment: the former is the value  $\eta$  of the maximum scour with respect to the average (initial) bed, made non-dimensional with the uniform flow depth  $D_o^*$ , the latter is the position of the scour hole with respect to the bend apex. Both quantities were averaged over the series of bends within the scanned reach. Position of scour hole is given in terms of the dimensionless quantity  $\delta = \Delta x^*/(L^*/2)$ , where  $\Delta x^*$  is the longitudinal distance of the scour hole from the bend apex, so that  $\delta$  ranges from -0.5 (scour hole  $L/4$  upstream of bend apex) to 0.5 (scour hole  $L/4$  downstream of bend apex).

Experimental findings are shown in figures 3<sub>a-b</sub> and 4<sub>a-b</sub> where  $\eta$  and  $\delta$  are given as functions of channel wavenumber  $\lambda$  and width ratio  $\beta$ . It may be noticed from figure 3<sub>b</sub> that  $\eta$  exhibits a relative maximum that moves towards larger values of  $\lambda$  as  $\beta$  increases. Moreover figures 4<sub>a-b</sub> show a fairly regular behaviour for  $\delta$  which is decreasing with  $\beta$  (the scour hole moving upstream as discharge decreases) and increasing with  $\lambda$  (the scour hole moving downstream as wavelength decreases).

The maximum scour  $\eta$  and phase lag  $\delta$  are given in table 3 along with the values of the difference between maximum and minimum bed elevation within a wavelength ( $H_b$ ) and the maximum flow depth within the pools ( $D$ ), both scaled by the uniform flow depth  $D_o^*$  and again averaged over the scanned reach. Notice that the maximum scour contributes to about 3/4 of the total difference between maximum and minimum bed elevation, the ratio  $\eta/H_b$  being fairly constant in the experiments and falling in the range 0.71-0.80.

The output of the scanner device is a large ( $\Delta x^* = 10 \div 20$  cm,  $\Delta y^* = 2$  mm) cartesian arrays of bed elevations with respect to some constant slope level. The data sets were then moved to the  $(s^*, n^*)$  space where a linear interpolation was performed on a regular grid. Back to the  $(x^*, y^*)$  space this means that all nodes now lie on sections normal to the channel axis. In figure 5 the measured bed topography for run W25Q14 is shown. Contours are plotted every 0.5 cm. Thinner lines refer to pools while thicker lines refer to shallow areas. The topography shows an almost regular pattern. Both relative position and amplitude of the scours are fairly constant along the channel.

Table 3: Experimental results.

Run	$\lambda$	$\beta$	$\eta$	$H_b$	D	$\delta$
W15Q07	0.15	19.66	3.34	4.42	5.36	-0.25
W15Q10	0.15	17.33	3.08	4.34	4.97	-0.23
W15Q14	0.15	12.87	2.71	3.59	4.06	-0.09
W15Q16	0.15	11.59	-	-	3.72	-0.08
W20Q07	0.20	19.02	3.66	4.74	5.16	-0.10
W20Q10	0.20	15.49	3.73	4.74	5.00	-0.01
W20Q12	0.20	14.71	3.41	4.40	4.55	0.02
W20Q14	0.20	13.06	3.34	4.33	4.21	0.06
W20Q16	0.20	11.67	2.78	3.72	3.97	0.09
W25Q07	0.25	21.34	4.41	5.49	6.54	0.13
W25Q10	0.25	15.77	3.58	4.54	4.77	0.15
W25Q12	0.25	14.46	3.28	4.26	4.74	0.18
W25Q14	0.25	12.50	2.91	3.90	4.06	0.19
W25Q16	0.25	11.51	2.69	3.61	3.77	0.19
W30Q07	0.30	18.62	3.69	4.71	5.32	0.14
W30Q10	0.30	16.67	3.77	4.94	5.22	0.24
W30Q12	0.30	14.71	3.16	4.12	4.53	0.23
W30Q14	0.30	12.59	2.96	3.91	4.27	0.25
W30Q16	0.30	11.59	2.61	3.55	3.86	0.27

The results were then averaged superimposing all the bend apexes (mirrored when needed). This procedure leads to a one-meander averaged bed topography in which the small differences between different bends are filtered out together with small-scale disturbances arising from propagating bedforms.

The procedure of interpolation and averaging tends to smooth artificially bed profiles, even though the fine spatial-grid used ensures for small damping. Whenever the measurements were seen to be sensitive to this post processing, like in the determination of the position of the maximum scour hole, a local extra measurement was made to increase accuracy.

In figures 6<sub>a-d</sub> four averaged bed topographies are plotted for the runs W20Q07, W20Q16, W30Q07 and W30Q16. As can be easily recognized, the scour hole moves downstream for increasing discharges (Q07  $\rightarrow$  Q10) and increasing  $\lambda$  (W20  $\rightarrow$  W30). The scour always extends on a smaller area than deposition does, being, on the other hand, of larger amplitude.

Figure 7 shows the same plot for the run W15Q10 which exhibits a double scour hole, along the outer bank, a typical feature of all runs at the smallest wavenumber (i.e. longest wavelength and amplitude of the channel axis).

The last operation performed on the bottom data was a 2D Fourier analysis that allowed us to extract some information on the structure of the topography in the Fourier space, to identify the most relevant harmonics and their relative importance. To perform the Fourier analysis data were mirrored along one of the banks because the fundamental harmonic in the transverse direction is twice the width of the channel.

In figure 8 a spectrum of the amplitudes of bed harmonics as a percentage of the total is shown. Not surprisingly the spectrum exhibits a peak on the 1-1 harmonic which is by far the most important and, together with 2-2 and 0-2 harmonics, gains one half of the total "energy". The first index refers to the harmonics in the  $s$  direction (1 means the fundamental, 2 the harmonic with half the wavelength of the fundamental and so on) while the second

index refers to the  $n$  direction so that, for example, the 0-2 harmonic is constant along the longitudinal direction and has a wavelength in the transverse direction equal to the width of the channel.

In figure 9 the behaviour of the fundamental harmonic  $\eta_{11}$  as a function of  $\lambda$  is shown with  $\beta$  as a parameter. As the width ratio increases the role of the fundamental becomes less important, this effect being more evident at lower values of channel wavenumber.

## 5 - CONCLUDING REMARKS

Experimental data have been obtained through detailed investigations of bar topography in sinuous channels characterized by different wavelengths, for given flow conditions. The steady topography obtained at the end of experiments shows a fairly regular pattern along the channel in all runs except for those run with maximum wavelength ( $\lambda = 0.15$ ) where detection of steady topography has been somewhat complicated by the presence of propagating bars superimposed on steady point bars.

However, within the range of values of channel wavelength examined in the experiments, both the intensity of maximum scour and the position of scour holes with respect to bend apex appear to follow a consistent trend. The picture that emerges from experimental data allows one to draw some conclusive answers on the suitability of theoretical models which have been employed to predict steady bar topography in meandering channels. In particular, results of experiments strongly support the idea that within the range of wavelength characteristic of natural meanders the prediction of bed topography based on a linear solution does no longer apply since it appears that resonance does not operate in the form predicted by a linear analysis. Rather than exhibiting a sharp peak within the resonant range, the bed response is found to follow a more smoothed trend, which still exhibits a maximum for values of meander wavenumber which are typically larger than those predicted by linear theory. The maximum response shifts towards higher wavenumbers as channel width ratio increases.

A quantitative comparison between theoretical predictions and experimental data is still in progress. However it is of interest to stress here that preliminar theoretical findings derived within the context of a nonlinear resonant solution (Seminara and Tubino, 1990) appear to be qualitatively confirmed by these data. A glance at figure 2 shows that the nonlinear solution seems to pick up at least the overall trend that emerges from laboratory investigations and predicts a maximum response within the range found in the experiments. Moreover downstream shift of scour holes with increasing meander wavenumber and flow discharge is also reproduced by the theoretical solution, which however seems to overestimate experimental findings.

A further point deserves some additional discussion. A bend stability theory predicts maximum bend growth when both  $\beta$  and  $\lambda$  are close to some resonant values. Results of the detailed investigations on free-meandering made by Fujita and Muramoto (1982) indirectly support these theoretical findings since a clear tendency to meandering was detected in the experiments when channel widening has proceeded enough for the width ratio to have reached a nearly constant value falling within the resonant range. Results of present experiments do not allow to ascertain whether the bed response exhibits a maximum as  $\beta$  increases, since in all the experiments different values of width ratio have been examined by varying the average flow depth, thus leading to consequent variations of Shields and roughness parameters. Therefore, a complete answer on the behaviour of bar topography within the resonant range will require a further set of experiments properly designed so as to examine separately the effect of width ratio variations.

This work has been supported by the Italian Ministry of Public Education under grant MPI (40%). Prof. Giovanni Seminara is gratefully acknowledged for his supervision and support. The authors express their gratitude to Paolo Gnocchi for his assistance in the experiments.

## 6 - REFERENCES

- Blondeaux, P. and Seminara, G. (1985). 'A unified bar-bend theory of river meanders', *J. Fluid Mech.*, 157, 449-470.
- Bridge, J.S. and Jarvis, J. (1982). 'The dynamics of a river bend; a study on flow and sedimentary processes', *Sedimentology*, 29, 499-541.
- Dietrich, W.E. and Smith, J.D. (1983). 'Influence of the point bar on flow through curved channels', *Water Resour. Res.*, 19(5), 1173-1192.
- Dietrich, W.E. and Smith, J.D. (1984). 'Bedload transport in a river meander', *Water Resour. Res.*, 20(10), 1355-1380.
- Engelund, F. (1974). 'Flow and bed topography in channel bends', *J. Hydraul. Div., ASCE*, 100(HY11), 1631-1648.
- Friedkin, J.F. (1945). 'A laboratory study of the meandering of alluvial rivers', Report, 44 pp., *U.S. Waterways Exp. Stn.*, Vicksburg, Miss..
- Fujita, Y. and Muramoto, Y. (1982). 'Experimental study on stream channel processes in alluvial rivers', *D.P.R.I. Bull.* 32, Kyoto University, Japan, 46-96.
- Gottlieb, L. (1976). 'Three-dimensional flow pattern and bed topography in meandering channels', *Tech. Univ. Denmark ISVA Series*, paper 11.
- Hooke, J.M. (1975). 'Distribution of sediment transport and shear stress in a meandering bend', *J. Geol.*, 83, 543-565.
- Ikeda, S. and Nishimura, T. (1986). 'Flow and bed profile in meandering sand-silt rivers', *J. Hydraul. Engng., ASCE*, 112(7), 562-579.
- Ikeda, S., Parker, G. and Sawai K. (1981). 'Bend theory of river meanders. Part 1 - Linear development', *J. Fluid Mech.*, 112, 363-377.
- Johannesson, H. and Parker, G. (1989). 'Linear theory of river meanders', in *River Meandering*, edited by S.Ikeda and G.Parker, Water Res. Monogr., 12, AGU, Washington, D.C., 181-213.
- Kinoshita, R. and Miwa, H. (1974). 'River channel formation which prevents downstream translation of transverse bars', *Shinsabo*, 94, 12-17 (in Japanese), 1974.
- Kitanidis, P.K. and Kennedy, J.F. (1984). 'Secondary current and river-meander formation', *J. Fluid Mech.* 144, 217-229.
- Langbein, W.B. and Leopold, L.B. (1966). 'River meanders-theory of minimum variance', *U.S.G.S. Professional Paper* 422H, 1-15.
- Odgaard, J.A. (1986). 'Meander flow model I: Development', *J. Hydraul. Div., ASCE*, 112(12), 1117-1136.
- Parker, G., and Johannesson, H. (1989). 'Observations on several recent theories of resonance and overdeepening in meandering channels', in *River Meandering*, edited by S.Ikeda and G.Parker, Water Res. Monogr., 12, AGU, Washington, D.C., 379-415.
- Seminara, G. (1989). 'River bars and nonlinear dynamics', Proceedings, *International Workshop on Fluvial Hydraulics of Mountain Regions*, Trent, October 3-6, A125.
- Seminara, G. and Tubino, M. (1985)a. 'Effect of transport in suspension on flow in weakly meandering channels', Proceedings, *Euromech 192*, Munich, FR Germany.

- Seminara, G. and Tubino, M. (1985)b. 'Further results on the effect of transport in suspension on flow in weakly meandering channels', Colloquium on *The Dynamics of Alluvial Rivers*, Genova, Italy.
- Seminara, G. and Tubino, M. (1989). 'Alternate bars and meandering: free, forced and mixed interactions', in *River Meandering*, edited by S. Ikeda and G. Parker, Water Res. Monogr., 12, AGU, Washington, D.C., 267-320.
- Seminara, G. and Tubino, M. (1990). 'Nonlinear resonance in large amplitude meanders', XXII Convegno di Idraulica e Costruzioni Idrauliche, Cosenza, Italy, (in Italian).
- Smith, J.D. and McLean, S.R. (1984). 'A model for flow in meandering streams', *Water Resour. Res.*, 20(9), 1301-1315.
- Thorne, C.R., Zevenbergen, L.W., Pitlick, J.C., Rais, S., Bradley, J.B. and Julien, P.Y. (1985). 'Direct measurements of secondary currents in a meandering sand-bed river', *Nature*, 316, 746-747.
- Tubino, M. (1990). 'Linear and non linear theory of river meanders', *Excerpta*, In press.
- Tubino, M. and Seminara, G. (1990). 'Free-forced interactions in developing meanders and suppression of free bars', *J. Fluid Mech.*, 214, 131-159.

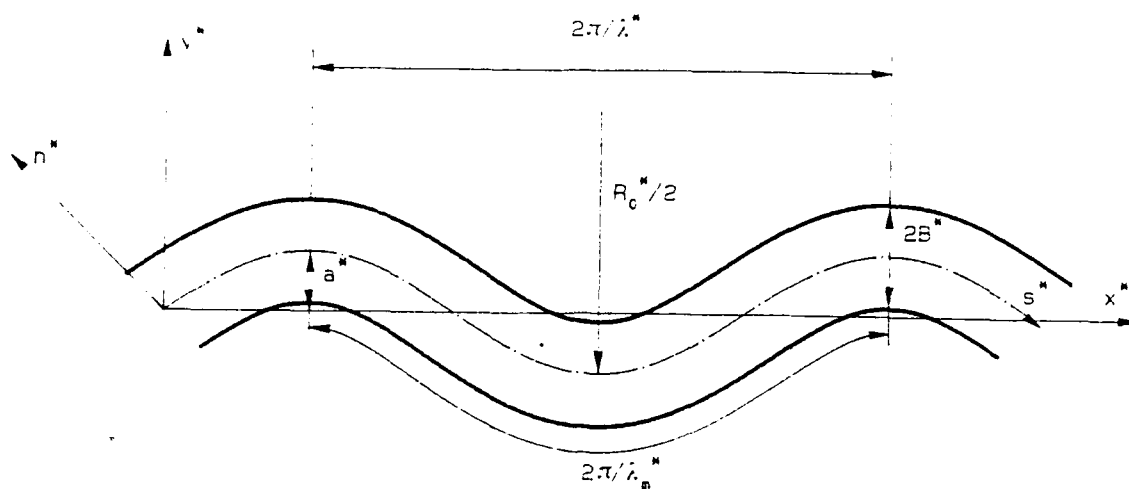


Figure 1 - Geometrical sketch and notation.

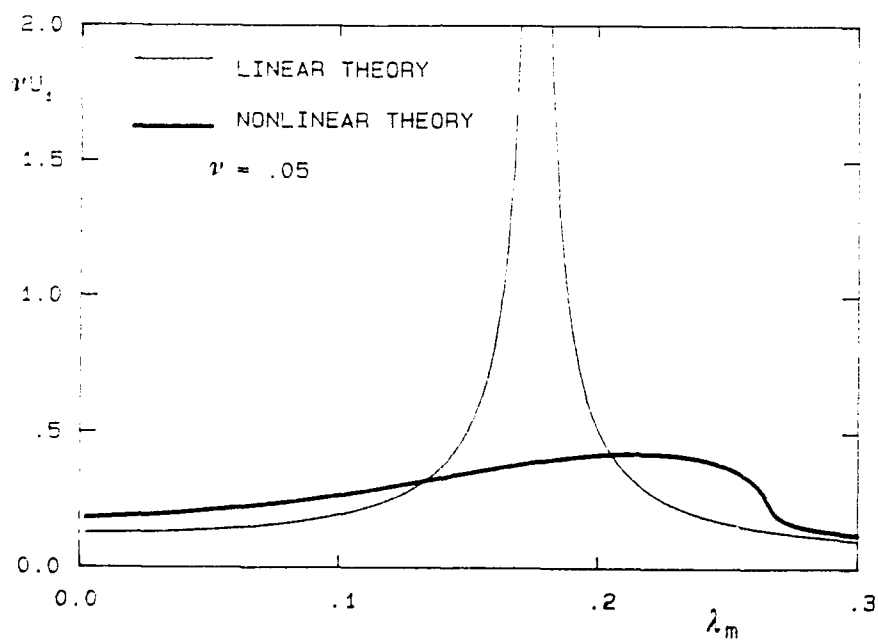
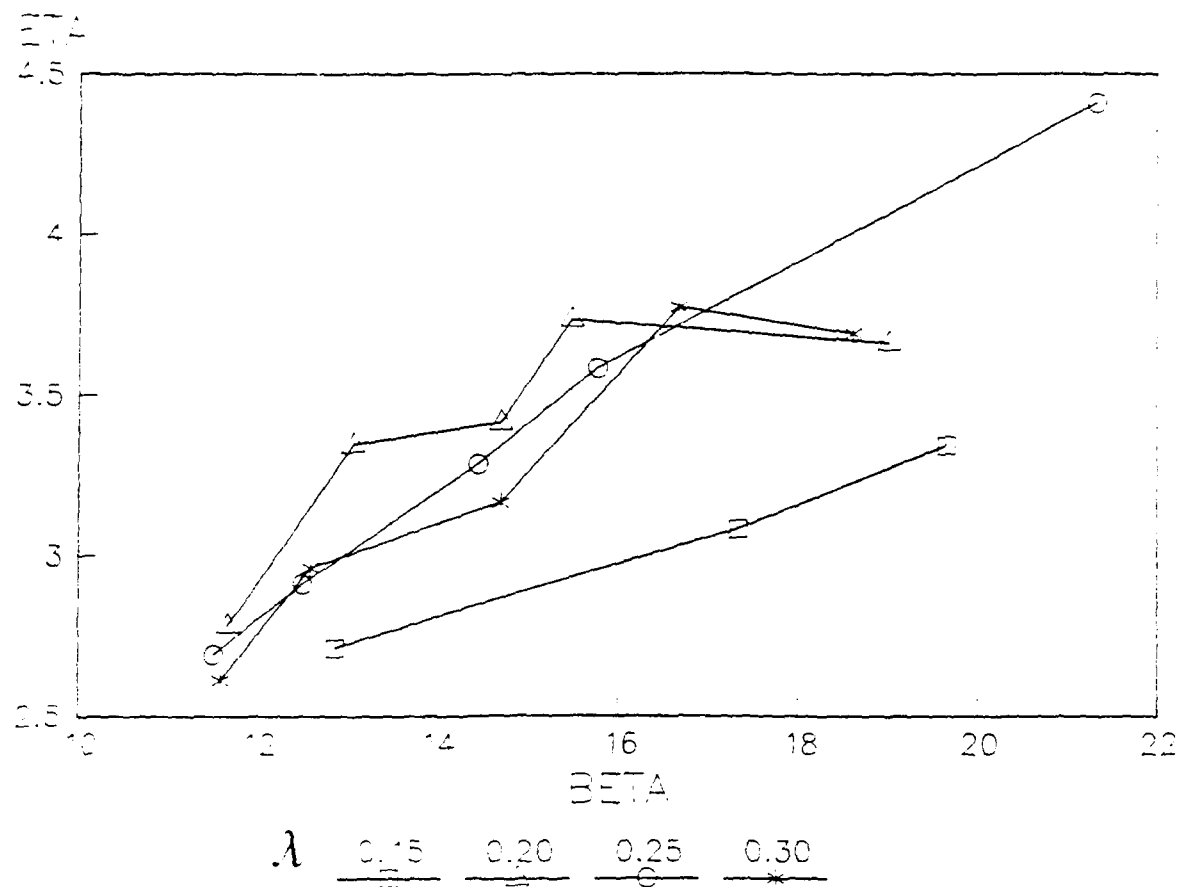
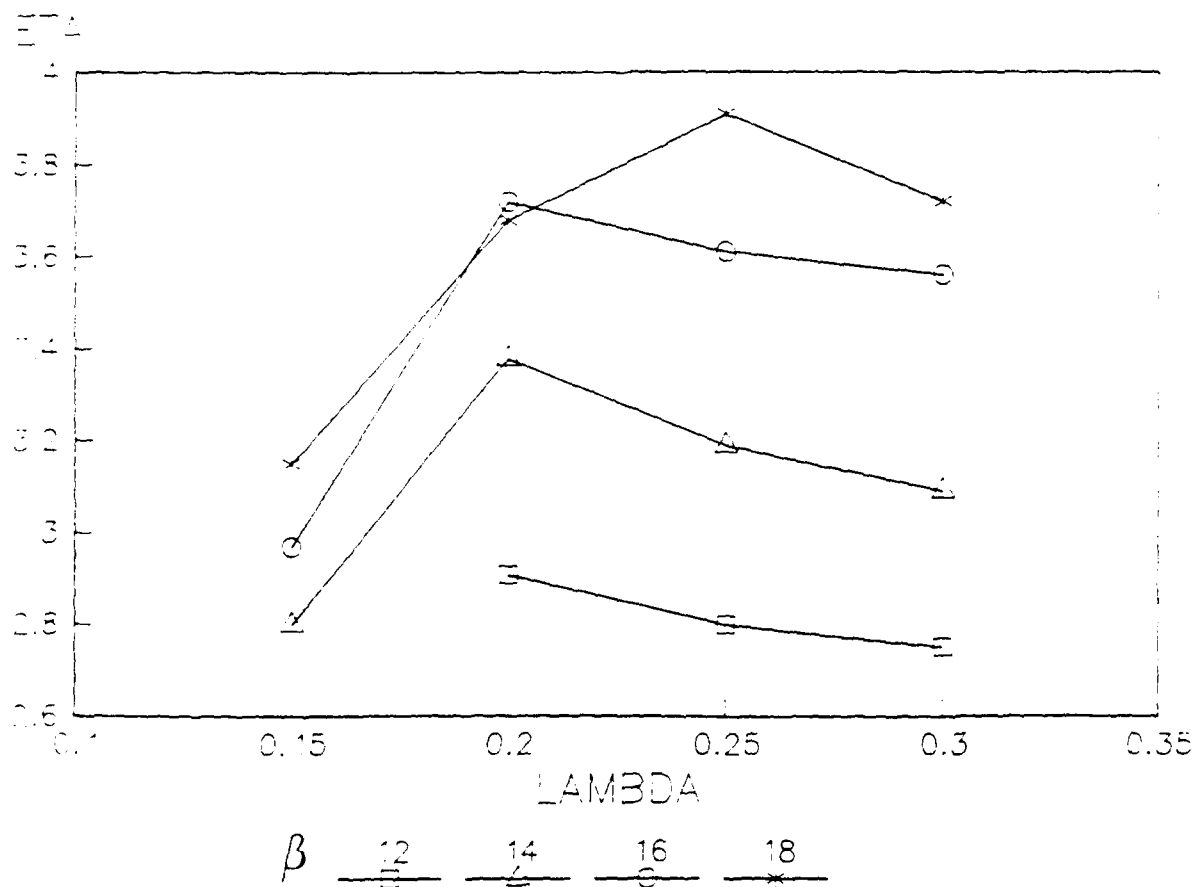


Figure 2 - The amplitude of the linear perturbation of longitudinal velocity ( $\nu U_1$ ) is plotted versus the intrinsic meander wavenumber  $\lambda_m$  and compared with theoretical findings derived within the context of a weakly nonlinear analysis ( $\theta = 0.06$ ,  $d_s = 0.06$ ,  $\beta = 13$ ).



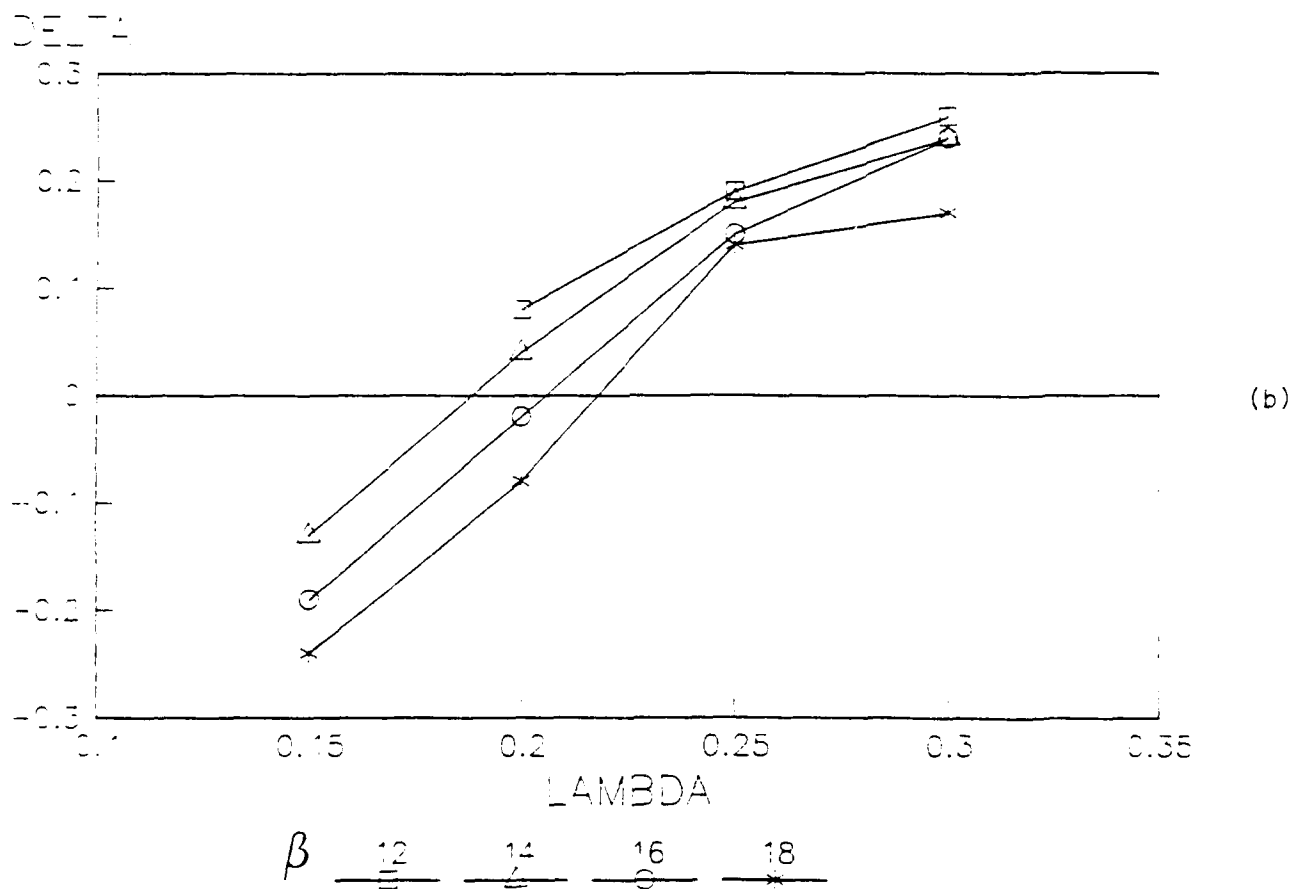
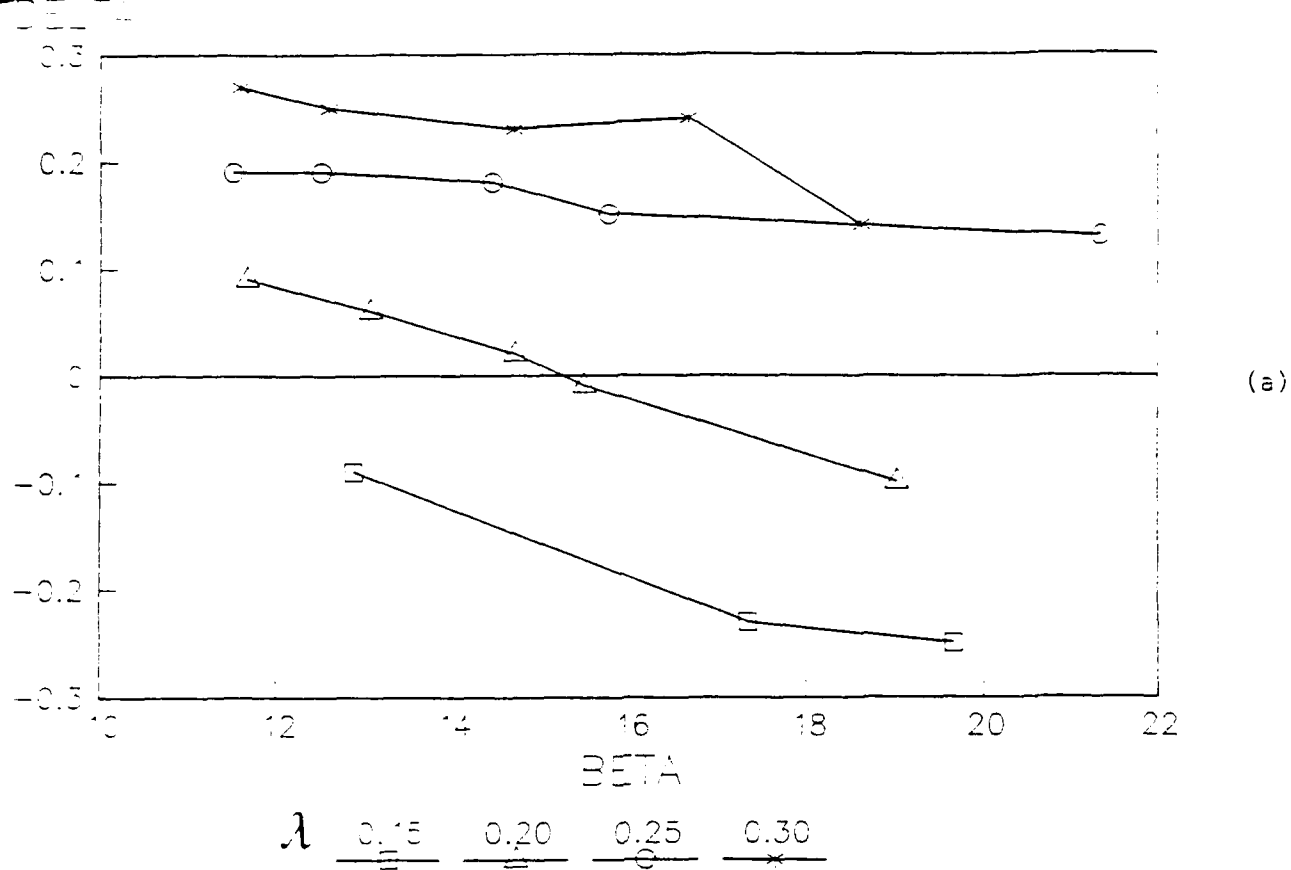


(a)



(b)

Figures 3 (a-b) - Dimensionless maximum scour  $\eta$  as a function of channel width ratio  $\beta$  (a) and wavenumber  $\lambda$  (b).



Figures 4 (a-b) - Phase-lag of scour hole with respect to bend apex as a function of channel width ratio  $\beta$  (a) and wavenumber  $\lambda$  (b).

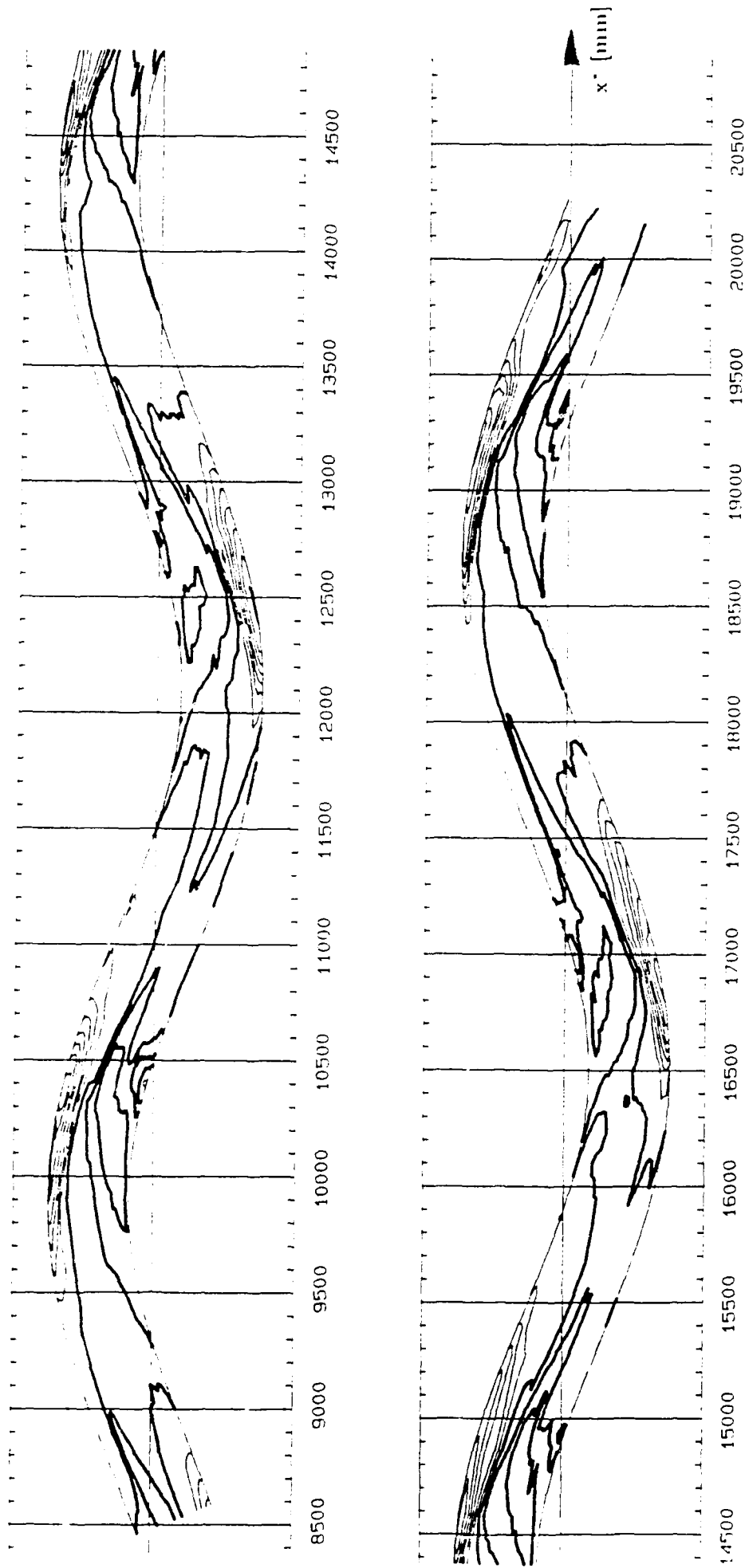


Figure 5 - Measured bed topography for run W25Q14. Contour intervals 0.5 cm. Thicker and thinner lines refer to deposition and scouring areas respectively.



Figures 6 (a-d) - Averaged bed topographies for runs W20Q07 (a), W20Q16 (b), W30Q07 (c), W30Q16 (d). (Contour lines as in figure 5).

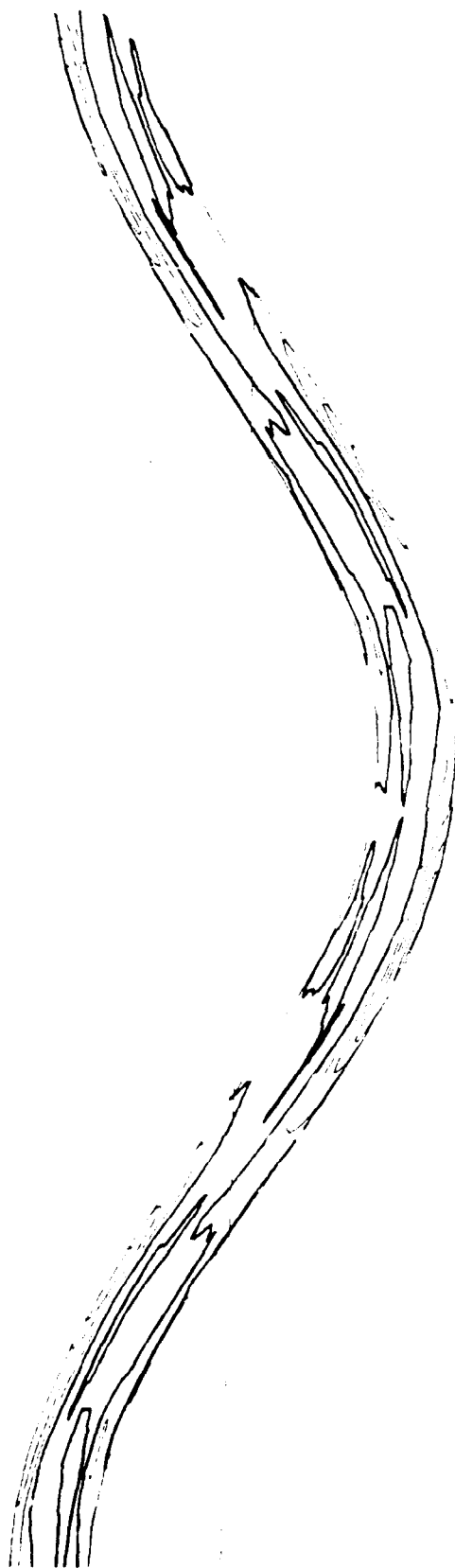


Figure 7 - Average bed topography for run W15Q10. (Contour lines as in figure 5).

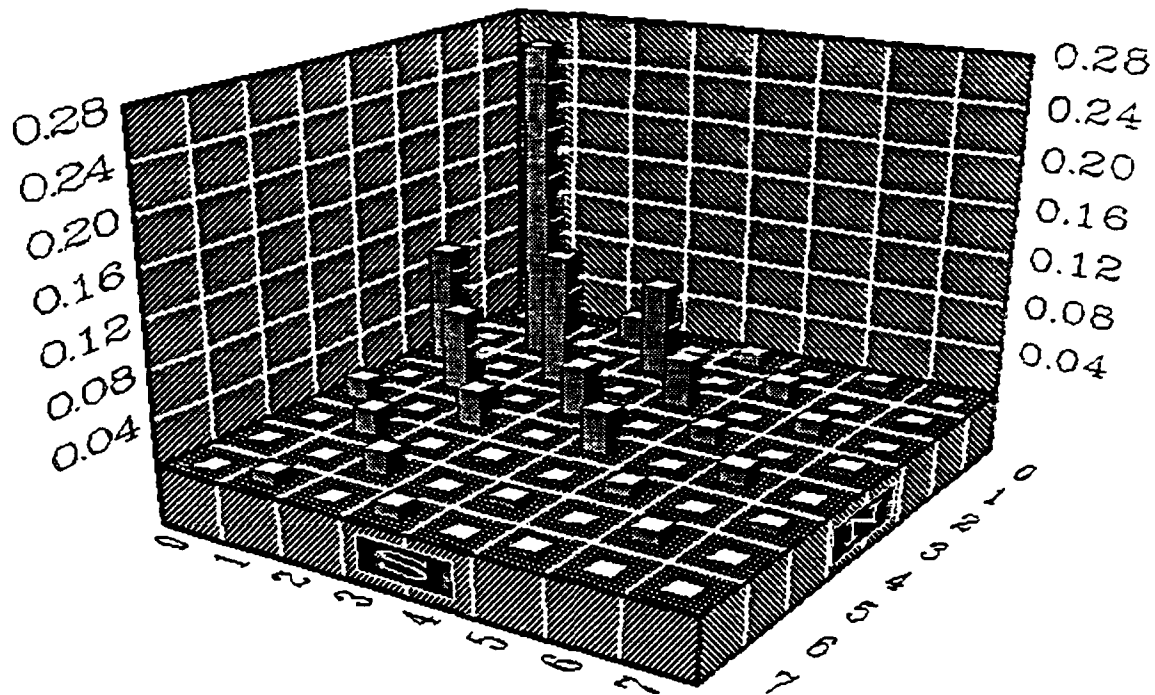


Figure 8 - 2D Fourier spectrum of bed elevation for run W25Q14.

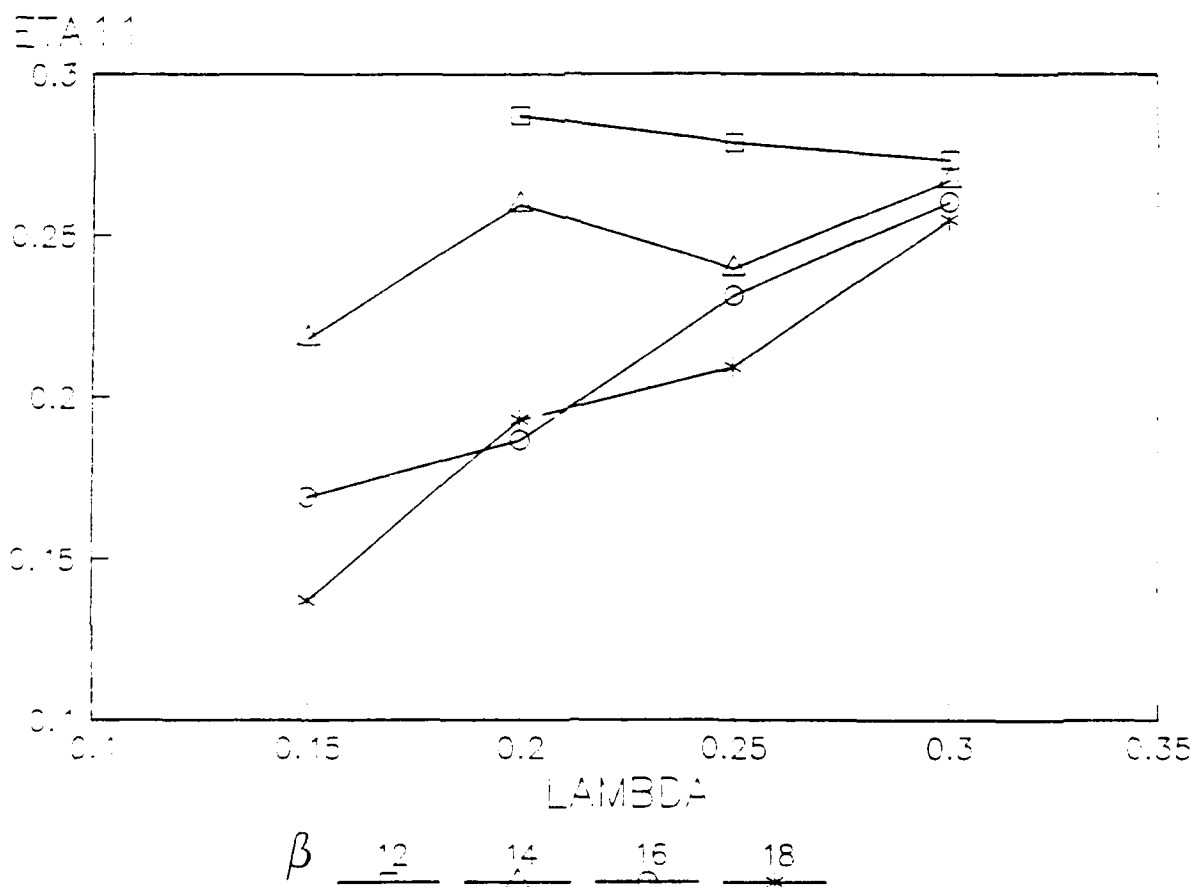


Figure 9 - The 1-1 harmonic of bed elevation ( $\eta_{11}$ ) as a function of wavenumber  $\lambda$  for given values of channel width ratio  $\beta$ .

## **The Sediment Size That Determines Channel Morphology**

Luna B. Leopold  
Department of Geology and Geophysics  
University of California  
Berkeley, California

### **Abstract**

Studies of twelve gravel-bar streams in the mountains of Colorado and Wyoming show that the bulk or largest volume of bedload is in the sand size, much smaller than the size seen in the bed material and on the bars. The coarse fraction, though small in volume of annual transport, determines and comprises the major features of the channel morphology. High discharges carry bedload only slightly more coarse than do low discharges, though the transport rate of high discharge is very much larger than that at low flow.

In gravel-bed streams the bed material is much coarser than the sediment that is largest in amount over a period of time. The coarsest few percent of the total volume make up the bars, the riffles, and the surface material on the bed. The largest clasts as well as the largest volume of the annual bedload are carried at discharges near the bankfull stage.

## **The Sediment Size That Determines Channel Morphology**

Luna B. Leopold  
Department of Geology and Geophysics  
University of California  
Berkeley, California

A growing interest in gravel-bed streams has led to an expanded data base involving bedload transport rates determined by Helley-Smith sampler and associated sediment size distribution. There are also a few data sets in which the total bedload was caught in a settling basin or trap. The latter data include a measure of the large mobile clasts that exceed the size of the mouth of a sampler.

In the snow runoff seasons of 1988 and 1989 detailed measurements were made in several gravel streams in the mountains of Colorado. This unusually complete set of data on bedload and sediment size distribution allows several questions of interest to be discussed. Some characteristics of the streams studied are listed in Table 1.

### Size Distribution of Bed Material and Trapped Sediment

The East Fork River near Boulder, Wyoming in the vicinity of the bedload trap is a few miles downstream from the place where the river leaves the mountains, flows through moraines, and thence meanders in a valley between terraces of glacial outwash. But soon after entering this valley zone, it is joined by a tributary, Muddy Creek, that is contributing sand washed out of glacial material. The sediment load from Muddy Creek is enhanced in recent times by irrigation return flow. The bedload trap and studies of the data have been published (Leopold and Emmett, 1976 and 1977; Emmett, 1980).



**Table 1**  
Channel Characteristics at Locations Where  
Sediment Samples Were Taken

Stream	Elevation (m)	Drainage Area (km <sup>2</sup> )	Bankfull Discharge (m <sup>3</sup> /s)	Channel Width (m)	Slope	D <sub>84</sub> of Bed Material (mm)
East Fork near Boulder, WY	2,200	466	20	15	0.0007	20
Poudre Pass Creek near Chambers Lake, CO	3,050		9.6	20	0.0062	150
Lower Trap Creek, near Chambers Lake	3,000	12.2	4.5	5	0.018	70
Upper Trap Creek, CO near Chambers Lake	3,050	9.8	4.5	9	0.060	152
SFK Cache La Poudre near Nederland, CO	2,340	228	11.3	14	0.008	147
Little Beaver Creek near Pingree Park	2,426	32	1.8	7	0.026	158
Left Hand Creek near Lyons, CO	2,288	134	5.9	9	0.035	120
Middle Boulder Creek near Nederland, CO	2,560	76	11	14	0.015	90
Goose Creek #1 near Cheesman, CO	2,304	209	3.8	7	0.015	120
East Fork Encampment Creek, WY	2,921	9.1		3.3	0.027	170
Coon Creek, WY	2,906	16.8		5.1	0.023	220

The sediment derived from the basin upstream of Muddy Creek is primarily gravel, which is prominently displayed in the riffles. The streambed in pools is generally covered with sand, derived for the most part from Muddy Creek. The bedload, then, consists principally of sand, but the gravel of the riffles also is moved. Painted rocks of gravel size placed on gravel riffles were carried away.

The major morphological features, riffles, central and point bars are composed of and formed by the coarse part of the total bedload. The bulk of the bedload is of finer material, principally sand.

The bedload trap on the East Fork River consisting of an open slot across the full width of the channel, 14.6 m, caught all the bedload. The size distribution of the trapped bedload is shown in Figure 1. Data for Figure 1 are in Emmett's Table 2 (1980). The data represent a composite of samples taken during 31 days in 1976. A single sample representing a given discharge was then the composite of about 40 scoops taken during a period of five to eight hours, or 80 kg of sediment.

The 31 days of sampling in 1976 extended through a whole snow-melt season beginning on May 18, when the discharge was  $9.87 \text{ m}^3/\text{s}$ , and ending June 21, when the discharge was  $9.53 \text{ m}^3/\text{s}$ . The peak discharge in this season was on June 5, when the discharge was  $22.4 \text{ m}^3/\text{s}$ . The bankfull discharge is about  $20 \text{ m}^3/\text{s}$  which in the annual flood series has a recurrence interval of 1.5 years. This snow-melt period of measurement in 1976 included discharges from 0.47 to 1.12 times the bankfull, a typical range in normal runoff years that includes the bulk of the sediment transport during a year.

Note in Figure 1 that the  $D_{50}$  caught in the conveyor-belt trap was 1.13 mm, and that 60 percent of the total weight caught in the trap was a size between 0.5 and 2.5 mm.

The bed material of the East Fork River is described by a composite of 232 individual samples collected at 29 cross sections in a 200-m reach near the bedload trap. The median particle size of each cross section varied from 0.6 mm to 25.4 mm. The largest median values occurred at the two riffles included in the sampled reach. A map showing the cross sections and the bed-material size in each is shown in Figure 5 of Emmett (1980).

The size distribution of the bed material is plotted in Figure 1 so that the bed material may be compared with the sediment caught in the conveyor-belt trap. The  $D_{50}$  of the bed material is 1.25 mm. Sixty percent of the total weight is made up of sizes between 0.5 and 12 mm.

The difference between the trapped sediment and the bed material is in the size classes larger than the median. The distribution of the finer 50 percent by weight is nearly the same for the trapped sediment and the bed material, as can be seen in the near coincidence of the two curves of Figure 1 in the range of 0 to 50 percent by weight.

Another installation where the total bedload was trapped is constructed on two gravel-bed streams in the Medicine Bow area of Wyoming, and measured by the U.S. Forest Service (Wilcox, memorandum of 1989).

On each of Coon Creek and East Fork Encampment Creek (see Table 1), a large wooden box or enclosure was constructed to trap all incoming bedload. Each year, the sediment was excavated by machine and the volume and size distribution measured. Transport rate of bedload was measured during storm periods with a Helley-Smith sampler.

In the years 1986—1988, the sediment removed was 5.5 tons, 9.2 tons, and 12.8 tons, respectively, at Encampment Creek. In the years 1983—1986 and 1988, the totals were 220, 75, 60, 150, and 50 tons, respectively, at Coon Creek. This amounted to an annual yield of 0.92 tonnes/km<sup>2</sup>/year from Encampment Creek and 6.0 tonnes/km<sup>2</sup>/year from Coon Creek.

These unique measurement data are summarized in Figures 2 and 3. In these graphs the size distribution of four materials is plotted, (1) the bulk of the sediment excavated from the box trap labelled "pond," (2) bedload samples taken during storm events with a Helley-Smith sampler, (3) bulk sample of bed material, and (4) bed material measured by pebble count sampling.

Both Encampment Creek and Coon Creek data are similar in certain respects despite the difference in annual sediment yield. The size distribution of the bulk material collected in the box traps was nearly identical to that obtained in the Helley-Smith sampler.

In the largest particle size, above 64 mm, the sampler under-represented the actual load. In the box trap, the sediment caught included a few percent by weight of sizes of 128, 256, and 512 mm that clearly could not go into the 10 cm mouth of the sampler.

In all three of these installations where the total bedload was trapped, the bulk of the load was of sand size despite the fact that the bed material was of much larger size. In the East Fork the riffles are gravel, not sand.  $D_{84}$  of the bed material, 20 mm, is typical of what one sees on the riffles and bars.

In Coon Creek and Encampment Creek the bed material is gravel having a  $D_{84}$  of 220 and 120 mm, respectively. Yet, 70 percent of the material caught in the box trap was less than 6 mm. The  $D_{50}$  of the trapped material was between 1.5 and 2 mm. Thus, the bulk of bedload in these gravel streams is sand yet the streambed is obviously gravel and cobbles.

This conclusion applies not only to the three streams where a trap caught all of the bedload, but also to the other gravel rivers discussed. Table 2 shows the sediment size category comparing the largest percentage by weight of the bedload sampled in the eight mountain streams studied. Note that in all these gravel streams, the size category of either 1 or 2 mm comprised from 15 to 33 percent of the weight of bedload caught during the runoff season. The Colorado streams are gravel bed with  $D_{84}$  of bed material from 150 to 200 mm.

All the streams listed in Table 2 can be classified as gravel-bed channels in that the bars, the riffles, and the point bars are predominantly composed of gravel. In all of these the bed material or surface layer of clasts is somewhat coarser than clasts immediately below the surface. The ubiquitous condition of gravel-bed channels has unfortunately been called armoring or paved, implying the presence of a pavement. Such terms suggest that the surface layer or bed material does not move. Measurements show that even the  $D_{84}$  of the bed

Table 2

Season Totals of Bedload Samples  
Caught in Helley-Smith Sampler, 1989

Stream	Number of Days	Total Weight Caught (g)	Total Weight Per Day of Sampling (g)	Largest Rock Caught (mm)	Size Category * <u>Largest</u> mm	With <u>% of Weight</u> % of Total Weight in Category
Goose Creek #1	17	40,319	2,371	30	1.0	31
Goose Creek #2	10	3,348	334	64	1.0	23
Goose Creek #4	16	8,578	536	41	1.0	23
Left Hand	56	211,297	3,773	113	1.0	33
Middle Boulder	20	32,792	1,639	98	2.0	15
SFK Cache La Poudre	40	11,196	279	43	1.0	27
Little Beaver	40	10,389	259	45	1.0	30
Upper Trap	22	13,841	629	136	2.0	19

\*Sizes listed are passing through, not held on.

Sieve sizes were 0.5, 1, 2, 4, 5, 6, 8, 11.2, 16, 22, 32, and 45 mm.

Size category of 1 mm is from .5 to 1 mm.

material moves in discharges below or at bankfull, but in small quantities. Thus, the occurrence of large clasts larger than 100 mm in the material caught in the box traps or ponds confirms the mobility of bed material.

#### Size Distribution of the Bed Material

In both the Encampment and Coon Creeks bed material was measured in two ways, by a volume taken to the laboratory for drying, sieving and weighing, and by pebble counting.

In both these streams there is a marked difference in sorting of the bulk of the load, mostly sand, and the gravel material. Note in Figures 2 and 3 that the box trap material labeled "pond" is poorly sorted in that there are equal percentages by weight in categories of size from 0.5 mm to 10 mm. In contrast, bed material gravel has a sharp maximum of about 100 mm with smaller percentages by weight of both smaller and larger sizes.

This difference in sorting appears to be general. Figure 4 presents the size distribution of bed material and that caught in the Helley-Smith sampler for three of the mountain gravel bed streams in Colorado. In these data, the same finding is seen for a rather straight cumulative curve describing the bedload caught and the markedly S-shaped curve for bed material. Such curves are available for most of the streams listed in Table 1 and they show similar tendencies.

For many of these streams, size distributions of gravel on channel bars and in the subarmor or subpavement are available. The subarmor nearly always has a curve that lies between the bed material and the bedload caught in the sampler, that is finer than bed material but coarser than the caught bedload.

### Implications for Channel Morphology

The largest portion of the bedload in these gravel bed channels is not in the gravel size but in the sand size. Yet the visual impression of the channels is formed by the coarser fraction that makes up not only the bed, but also the point bars and the pool-riffle sequence. Thus, the principal morphologic features of the channel are made of material representing only a few percent of the total annual bedload. The median size of the bed material in these data is equalled or exceeded in only about three percent of the total bedload moved.

### Discharges that Move the Bulk of the Bedload

The measurement points of streams in Table 1 are all located in proximity to a gaging station for which a flow duration curve was plotted. A bedload rating curve constructed from Helley-Smith sampling is also available. Applying the percentage of time various discharges were experienced to the associated bedload transport rate, the total bedload carried by each discharge category was computed. This computation was carried out for each bedload sampling point.

A typical relation obtained is shown in Figure 5 for Left Hand Creek, drainage area 134 km<sup>2</sup>, D<sub>84</sub> of bed material 120 mm. The upper graph shows the percentage of time various discharges occur. The data are shown in the form of a cumulative curve typically used for a flow duration curve, but also as a histogram of non-cumulated percentages. The most common category was about 0.1 m<sup>3</sup>/s that occurred 24 percent of the time. The average discharge was equalled or exceeded 20 percent of the time, a common characteristic for many rivers.



The bottom graph in Figure 5 shows the percentage of the annual or long term volume of both water and bedload carried by various categories of discharge. The largest volume of water is carried in the category of discharge 2.8-4.5 m<sup>3</sup>/s, or 0.47—0.76 times bankfull discharge.

The maximum bedload is carried in the discharge category 4.5-7.3 m<sup>3</sup>/s or 0.76—1.2 times bankfull. At discharges both smaller and larger, less bedload is transported. The discharge carrying the maximum sediment load has been called the effective discharge. In a study of some gravel-bed streams in Colorado, Andrews (1984) found that the effective discharge was approximately equal to the bankfull discharge. The example above is in agreement with Andrews' findings.

#### Sediment Size Distribution As Discharge Changes

One might expect the size of bedload moved to increase proportionally with increase in discharge. The data show that such increase does occur, but its magnitude is rather small. Two examples are given in Figures 6 and 7. In these figures the size distribution of bedload caught in a Helley-Smith sampler is shown for a large and a small discharge. In Figure 6, at the East Fork in Wyoming, the five-fold increase in discharge resulted in a change of D<sub>50</sub> from 0.7 to 1.4 mm or a two-fold increase. In Figure 7, at Goose Creek #1, a change in discharge from 0.76 to 4.1 m<sup>3</sup>/s resulted in a change of D<sub>50</sub> from 0.55 to 0.75 mm. In all cases studied, low and high discharges both had a wide distribution of bedload size from sand to small gravel, but the increase in size with discharge was not very large.

### Concluding Discussion

Gravel-bed streams have a bedload smaller in grain size than what is seen on the channel bed. Sand is the size of the major volume of bedload in gravel-bed streams. However, the major morphologic features of gravel-bed streams are composed of gravel, not the sand that makes up the bulk of bedload. Channel bed material, point bars, and riffles to the pool-riffle sequence, are made up of gravel that moves at low transport rate, the clasts of which move only occasionally, and for short distances.

Size distribution is characterized by better sorting in the coarse bed material than is the sandy bulk of the bedload. Size in any category is only slightly larger in high than in low discharges. Thus, it appears that the gravel-bed channels, the coarse fraction, moved only occasionally and moved only short distances in any one season, makes up the principal morphologic features of the channel.

## REFERENCES

- Andrews, E. D., 1983, Entrainment of Gravel from Naturally Sorted Riverbed Material, *Geological Society of American Bulletin*, **94**, 1225-1229.
- Andrews, E. D., 1984, Bed Material Entrainment and Hydraulic Geometry of Gravel-Bed Rivers in Colorado, *Geological Society of America Bulletin*, **95**, 371-378.
- Emmett, W. W., 1980, A Field Calibration of the Sediment-Trapping Characteristics of the Helley-Smith Bedload Sampler, *U.S. Geological Survey Professional Paper*, **1139**, 44 p.
- Leopold, L. B. and W. W. Emmett, 1976, Bedload Measurements, East Fork River, Wyoming, *Proc. Natl. Acad. Sci.*, **73**:4, 1000-1004.
- Leopold, L. B. and W. W. Emmett, 1977, 1976 Bedload Measurements, East Fork River, Wyoming, *Proc. Natl. Acad. Sci.*, **74**:7, 2644-2648.
- Wilcox, Marc, Coon Creek Data Report, U.S. Forest Service, Medicine Bow National Forest, *internal memo*, dated October 13, 1989.

## FIGURE CAPTIONS

- Figure 1. Size distribution of bed material and of sediment caught in the bedload trap, East Fork River, Wyoming. The bed material data are the average of 232 samples. Sediment caught in the conveyor-belt trap, transport weighted, is an average of 52 samples caught in 31 days during 1976 (Emmett, 1980, Table 2). Upper diagram, percent by weight of sediment of different size classes, not cumulated. Lower diagram, same as upper diagram, but cumulated; the ordinate is percent by weight equal to or less than each size class.
- Figure 2. Size distribution of bedload in Coon Creek, Medicine Bow National Forest, Wyoming, showing four types of measurements. Bedload in box-pond is nearly identical to that caught in Helley-Smith sampler, but the latter did not catch the clasts greater than 64 mm. Bed material in bulk sample is nearly the same as size determined by pebble count.
- Figure 3. Size distribution of bedload in E. Fork Encampment Creek, Medicine Bow National Forest, Wyoming, showing four types of measurements. As in Coon Creek, sediment caught in box-pond is nearly the same as that in Helley-Smith sampler except for large clasts. Bed material and pebble count data are nearly the same.
- Figure 4. Size distribution of bedload in three mountain streams in Colorado. Bedload caught in Helley-Smith sampler is compared with bed material of the channel.
- Figure 5. Relation of discharge to the percent of time and percent of volume of water in a Colorado mountain stream. The relation of discharge to volume of sediment is shown for bedload. For both relations, data are expressed as a histogram, and the same data is expressed as cumulated values, equal to or more than...
- Figure 6. Bedload size distribution during the day of lowest and highest discharge in the year 1975 at the bedload trap, East Fork, Wyoming.
- Figure 7. Bedload size distribution determined by Helley-Smith sampler at the time of lowest and highest discharge in 1989, Goose Creek #1, Pike National Forest, Colorado.

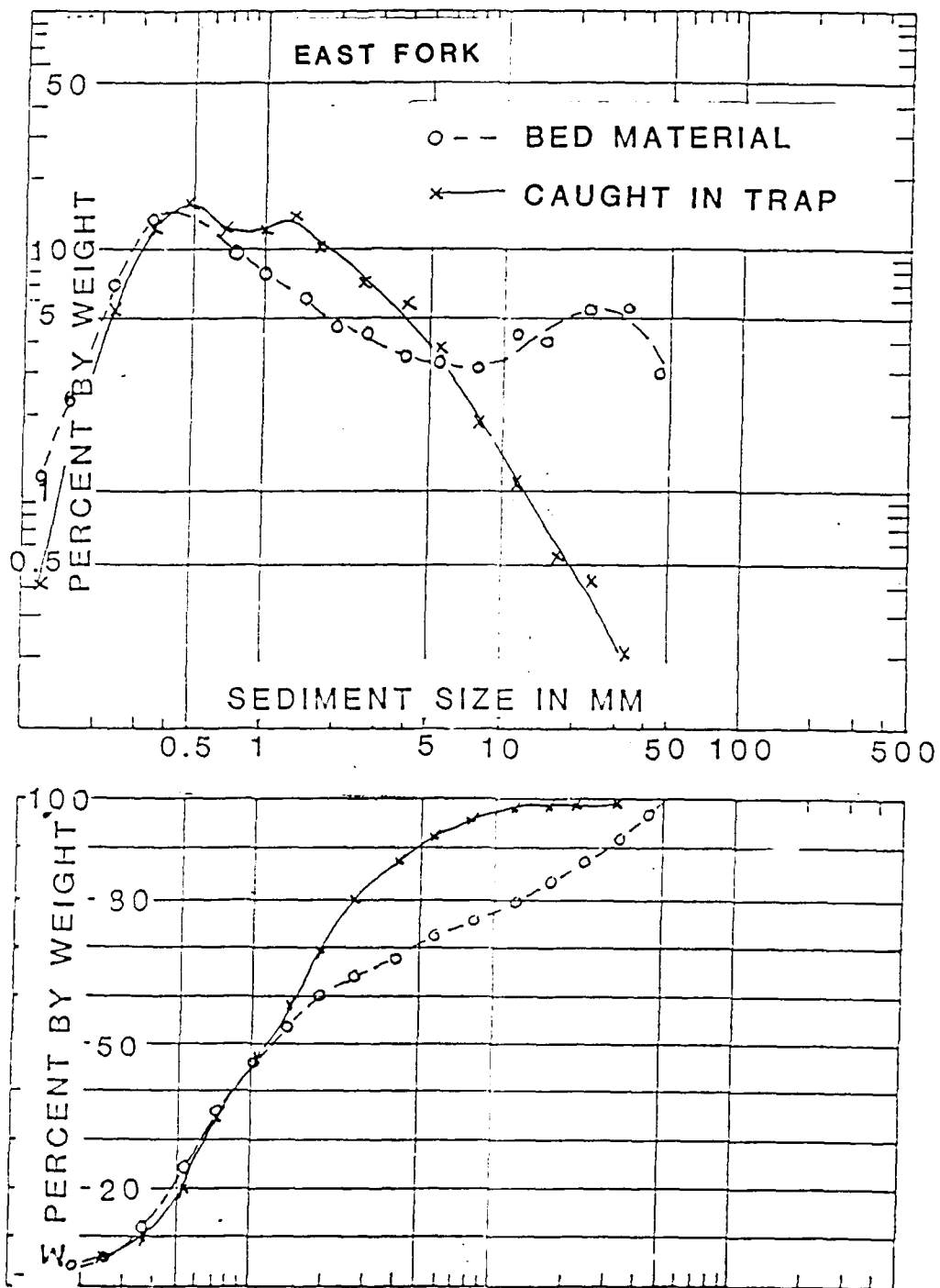


FIG. 1

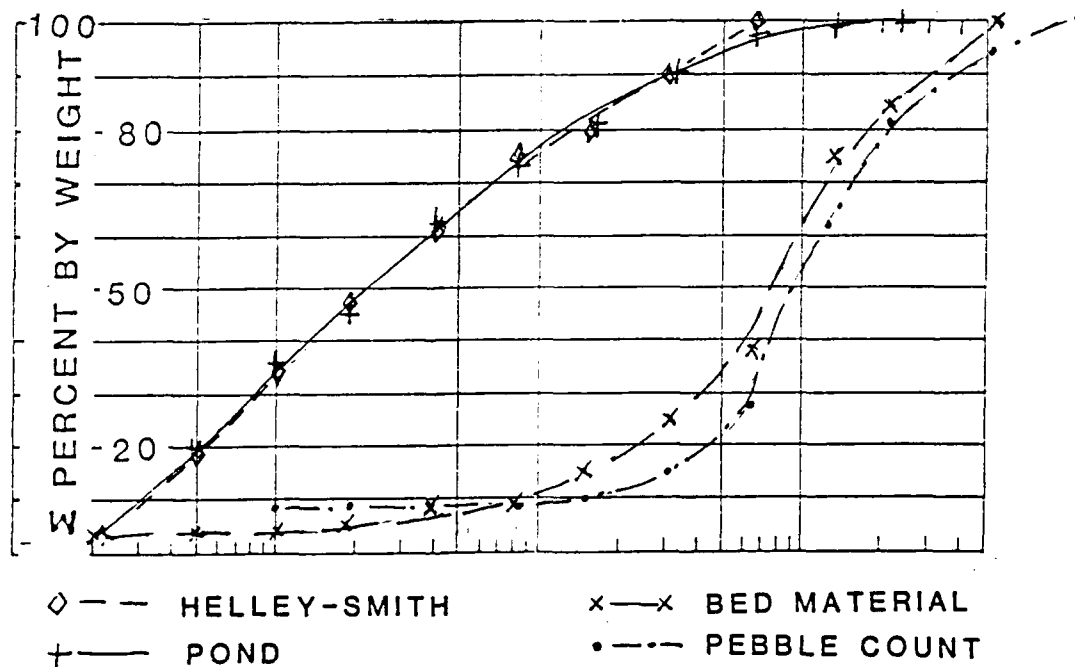
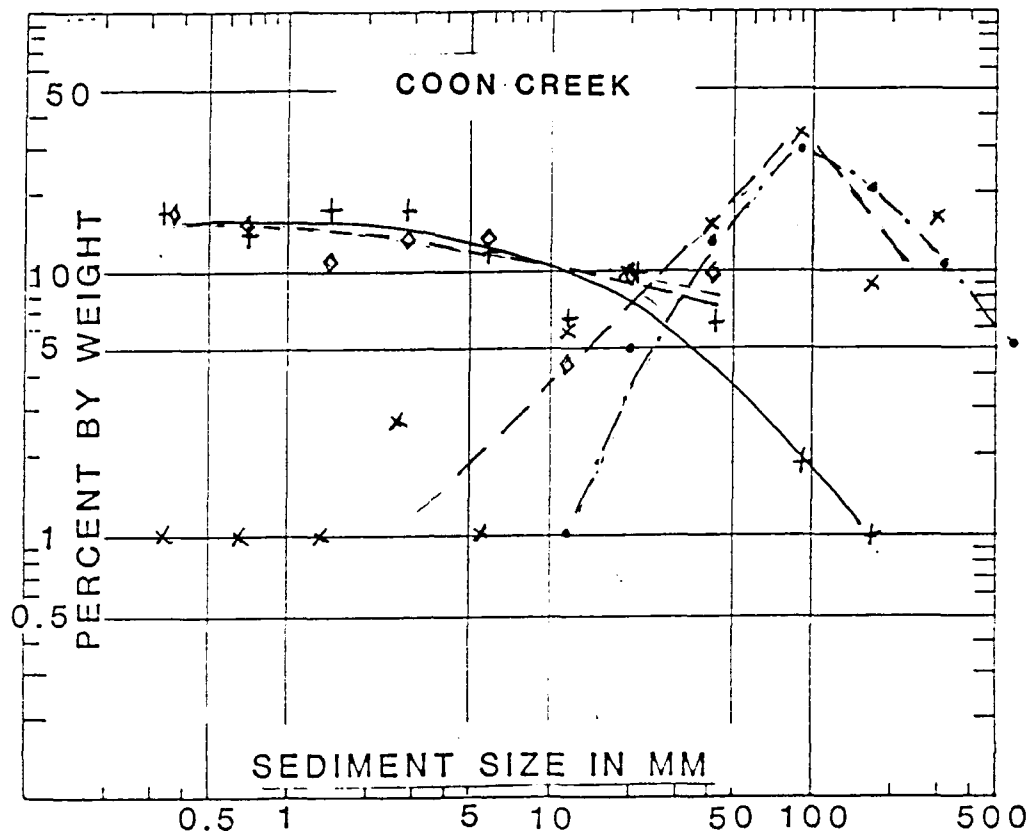


FIG. 2

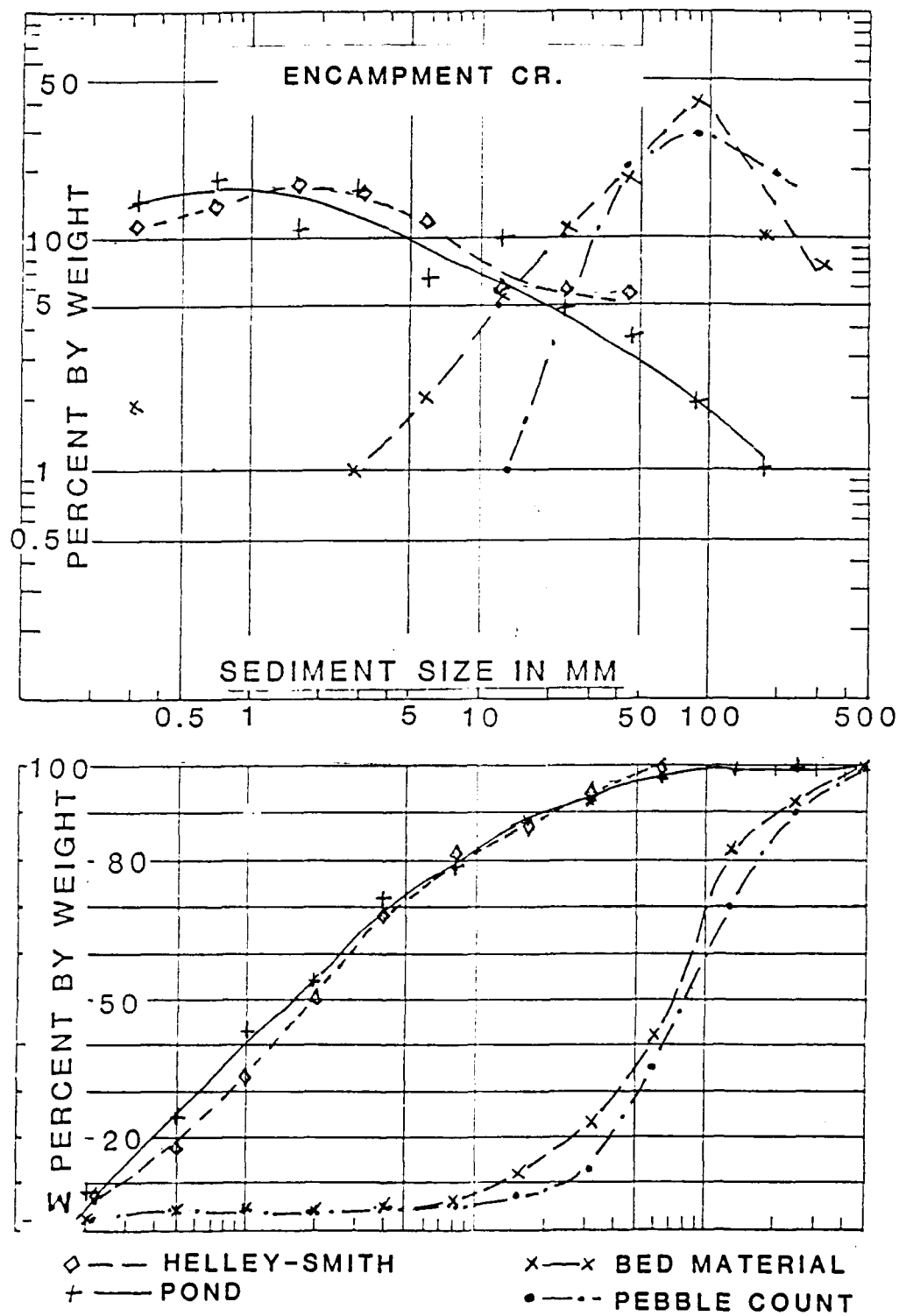


FIG. 3

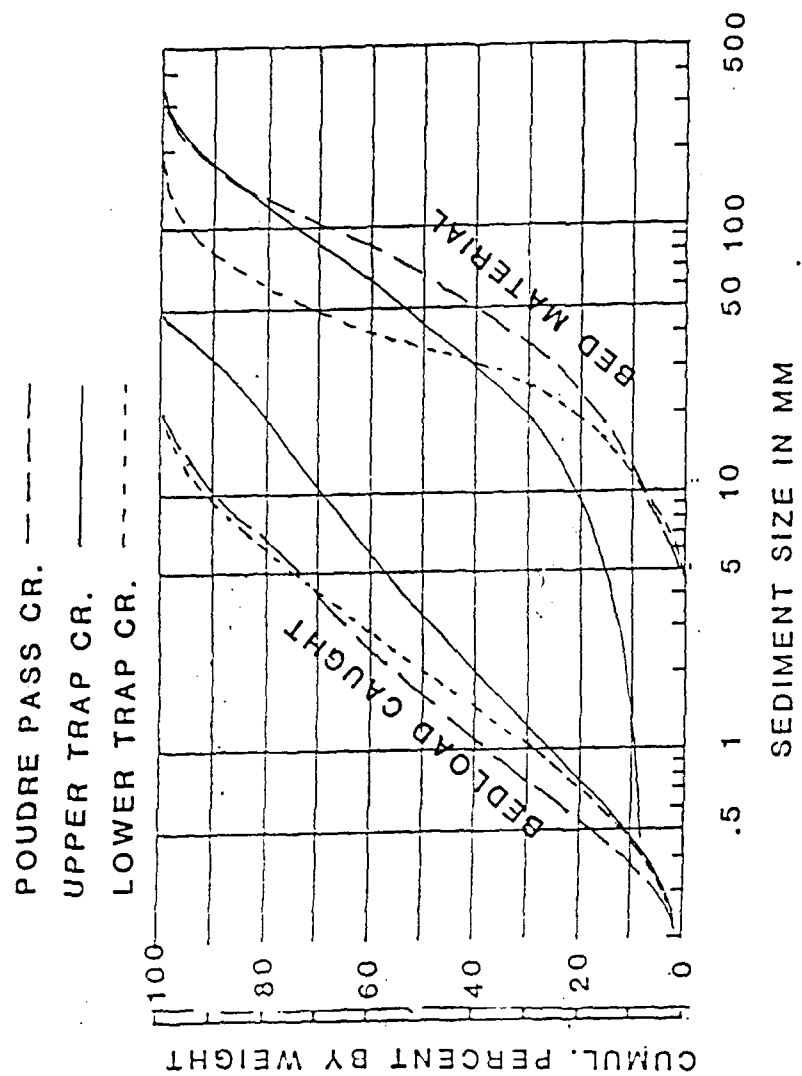


FIG. 4



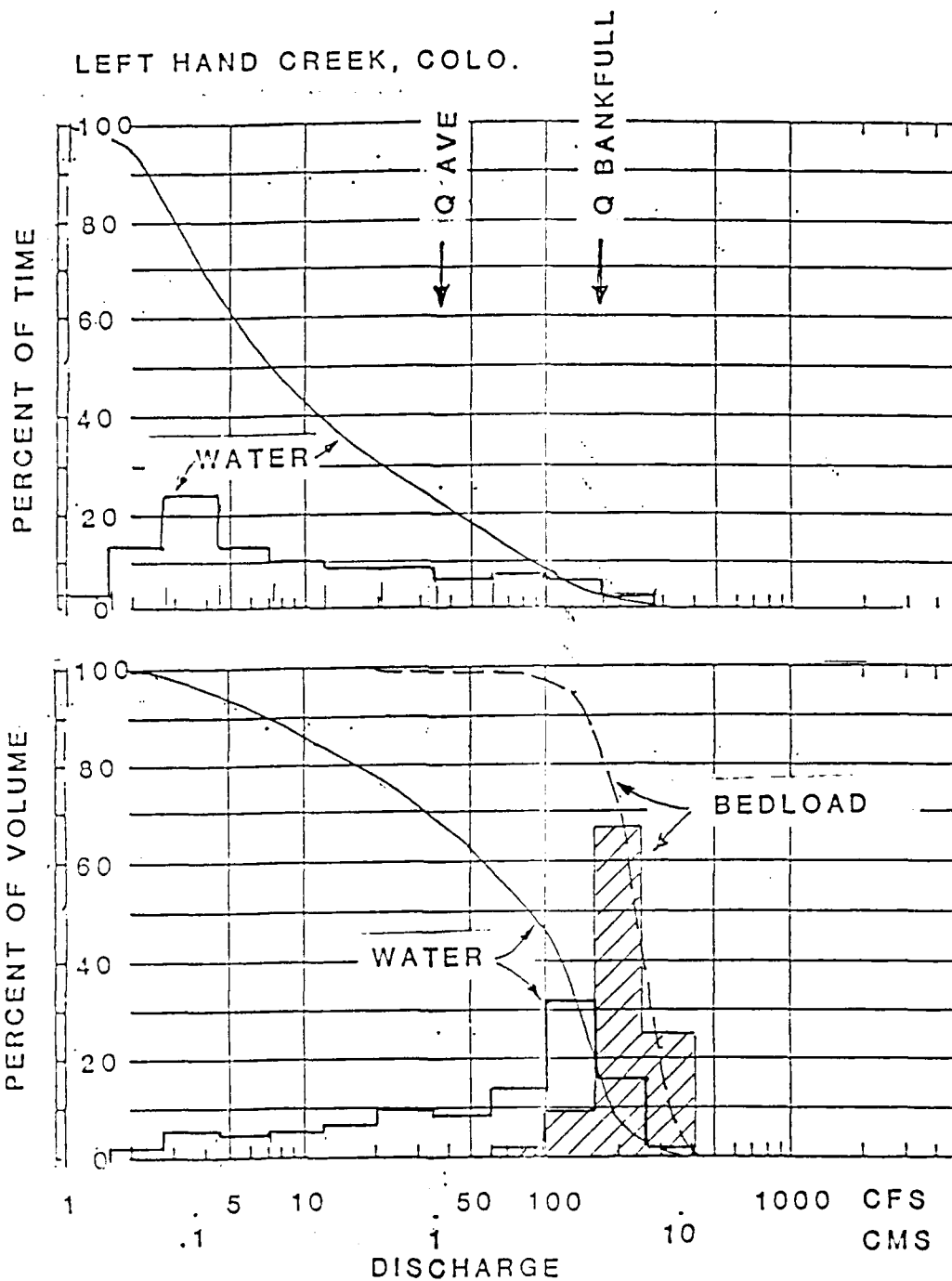


FIG 5

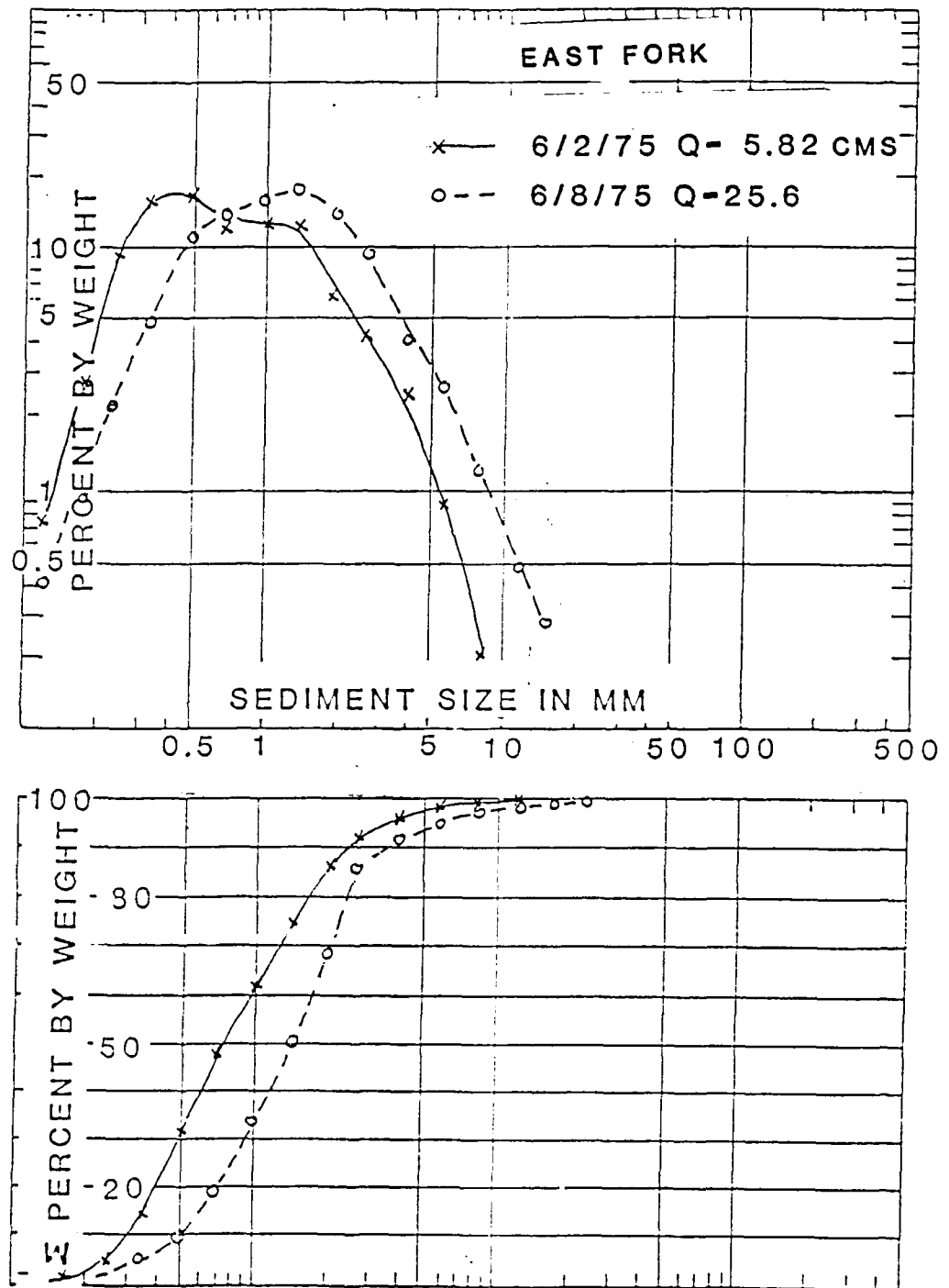


FIG. 6

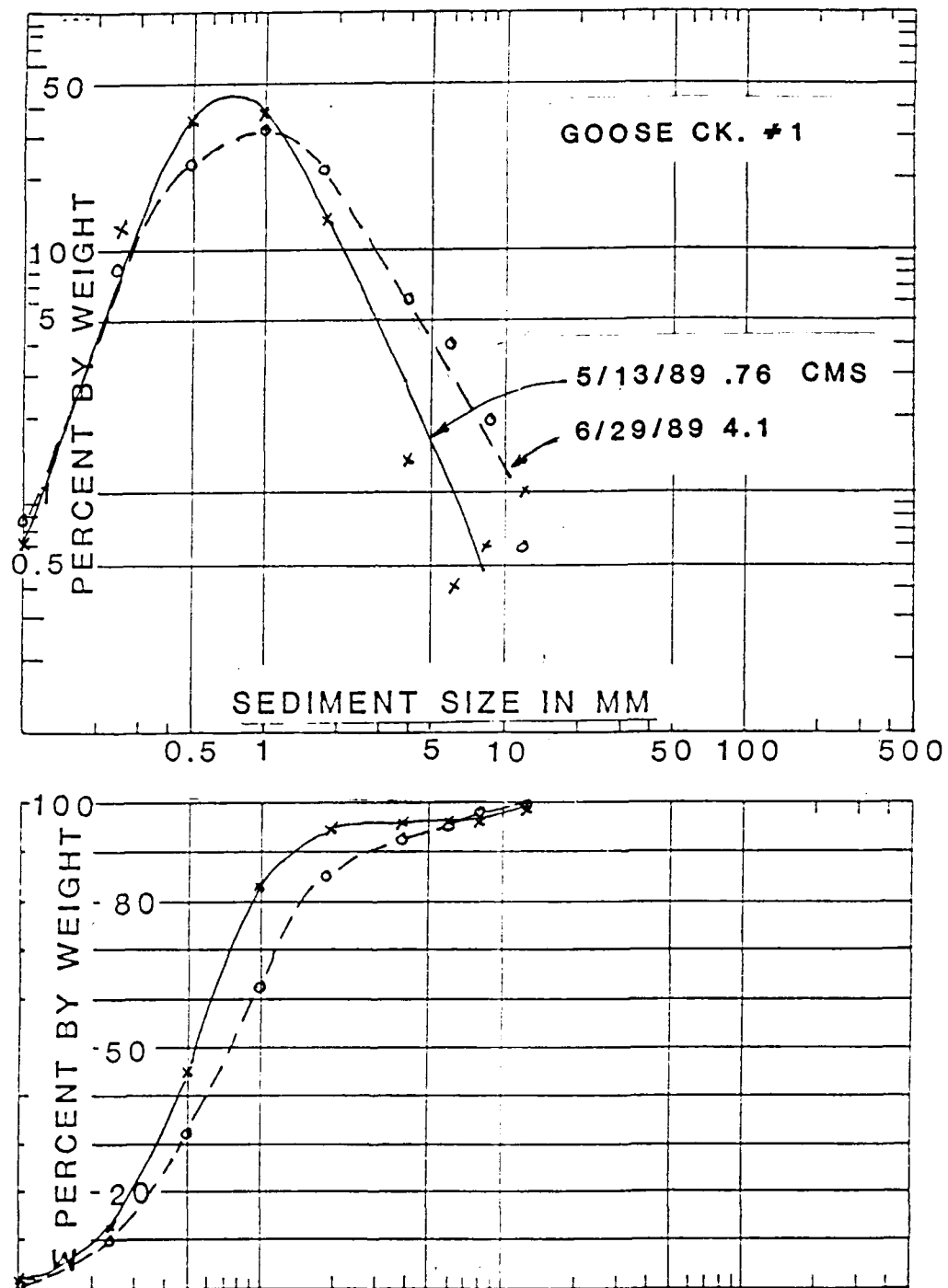


FIG. 7

# SPATIAL PATTERNS OF BEDLOAD TRANSPORT AND CHANNEL CHANGE IN BRAIDED AND NEAR-BRAIDED RIVERS

## ABSTRACT

## 1 INTRODUCTION

The difficulty in applying at the *reach* scale new understanding of hydraulics and gravel transport at the *point* scale lies in the nonuniformity of flow over lengths greater than a few channel widths. Allied to this are lateral and longitudinal variations in bed texture and bedload transport, leading to the possibility that erosion may occur in one part of a reach at the same time as deposition elsewhere. These different aspects of nonuniformity are of course interrelated in a feedback system (Figure 1). The existing irregular channel configuration (three-dimensional form together with bed roughness)

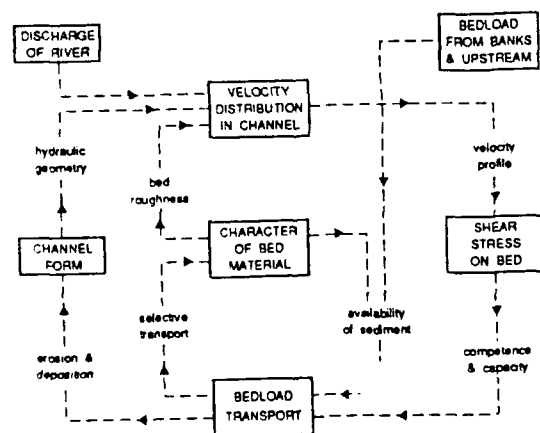


**Figure 1:** System diagram of the interrelationship of channel configuration, flow, and bedload transport in gravel-bed rivers (modified from Ashworth & Ferguson 1986).

controls the nonuniform pattern of flow through the reach at any given discharge. Since discharge is variable the flow is unsteady as well as nonuniform, and its pattern of nonuniformity may vary with stage. The spatially and temporally variable stresses exerted on the bed combine with the availability of sediment, whether in the bed or supplied from local bank erosion or upstream, to determine the rates of transport of different sizes of bedload at different places and times. Since this transport is nonuniform and unsteady, erosion and deposition alter the initial channel geometry, and selective entrainment or deposition may alter the texture of the bed. In braided rivers, channel change may also alter the proportions of total discharge flowing through individual channels. The general character of the river may remain similar in the absence of environmental change or human intervention, but the details of individual reaches are liable to change during competent flows.

To geomorphologists and sedimentologists the challenge is to explain how channel configurations develop through channel change, and how channel change relates to nonuniform processes. Such an understanding also promises better engineering predictions of channel change in specific circumstances. For meandering rivers, there has long been a qualitative understanding and quantitative theory has now been developed to the point that predictions can be made of facies patterns and planform evolution (e.g. Parker & Andrews 1985, 1986). But for braided rivers there are no standard quantitative models for predicting flow patterns or rates of channel change, and even the mode of channel change may be hard to foresee (e.g. Mosley 1987, p.823-4). The few field observations that have been published suggest that similar-looking initial configurations can evolve in different manners (e.g. Church & Jones 1982 Figure 4), and that the same reach can change in essentially opposite ways on different days according to peak flow levels (Ashworth & Ferguson 1986).

In principle it should be possible to model numerically the short-term development of a braided reach. This would involve iterating around the feedback system of Figure 1, using a 2-D finite representation of the vertically-averaged flow to drive a sediment transport and budget model, as proposed by Nelson & Smith (1989) for meandering channels. However, published numerical models for nonuniform stream flow cannot cope with rapid streamwise changes in width, nor with bifurcations and confluences of flow. There are also differences of opinion on the parameterisation of the transport threshold, the transport function, and the lateral and vertical sorting of bed material.

Once the modelling approach is extended to braided channels it will be necessary to validate it by observations. An empirical approach may also give direct insight into how braided rivers work. We have been attempting this for several years. It requires process measurements as well as observations of channel change during periods of competent flow, and the measurements must be spatially distributed. Many practical problems must be overcome to achieve this. This workshop contribution summarises some of our findings, but our main intention is to pass on our experience in making measurements in active gravel-bed rivers and relating process measurements to channel change.

## 2 PROBLEMS IN OBTAINING SPATIALLY DISTRIBUTED MEASUREMENTS

### 2.1 Choice of study area

We argued earlier that most gravel-bed rivers are nonuniform and undergo channel change, but it does not follow that one river is as good as another for an observational study. The need for spatially distributed measurements creates serious practical problems which constrain which rivers can usefully be studied.

The first problem is scale. Froude-scaled laboratory channels give insight into typical modes of behaviour and whole-river sediment transport (e.g. Ashmore 1982), but are so shallow and rapidly changing that spatially distributed measurements are hard to make. Prototype braided rivers, in contrast, tend to be too big and fast for easy or safe measurement by wading, and too rapidly shifting for footbridges to survive long. Davoran & Mosley (1986) have shown the potential of jetboats as measurement platforms, but the necessary equipment and expertise are rarely available. In our field research we have opted for wading (using a wetsuit when necessary) as the simplest and most versatile means of repeating measurements at many points within a reach, and have therefore restricted our studies to small rivers, with discharges of about  $5\text{--}20\text{ m}^3\text{s}^{-1}$  in marginally active conditions.

A second problem relates to hydrological regime. Making measurements at enough points within a reach to gain an idea of spatial patterns of hydraulics and sediment transport can take several hours, over which there must not be significant change in discharge. This rules out floods caused by rainfall events in small catchments. We have worked instead in rivers with partly or wholly nival or glacial regimes in order to take advantage of gradually varying high flows at predictable times of day and year. The rivers concerned are the Lyngsdalselva, a proglacial braided stream in arctic Norway; the Feshie, a near-braided channel in the Scottish Highlands; the White River, a locally braided glacier-fed stream in the northwest US; and the Sunwapta, a proglacial braided river in the Canadian Rocky Mountains.

In each case we selected short study reaches with well developed examples of what we and others regard as key morphological elements of the prevailing channel pattern: a pair of alternate bars and associated pools and riffles in the Feshie, and an X- or Y-shaped braid confluence and bifurcation in the three braided rivers. Simple examples of these basic elements, fairly symmetric and without complications, are even harder to find than simple, regular meander loops; they are therefore characteristic rather than typical, but if we cannot understand how they work, there is little hope of understanding more complicated situations.

## 2.2 Quantifying channel configuration and change

Channel plan form in braided rivers is highly stage dependent, as well as altering over time through erosion and deposition. Mapping water lines on different dates, whether from aerial photos or by ground survey, is not a good guide to channel changes because it confounds stage effects with erosion and deposition. Moreover, mapping cannot reveal scour or fill within the wetted perimeter of any channel. It is therefore essential to make repeated surveys of cross sections, in our case by levelling during the morning/midday low of the diurnal flow cycle. Echo sounding should be possible in larger rivers. The attainable accuracy is limited by the irregular roughness of the bed, but inferred depths of erosion or deposition between surveys should be accurate to within one bed particle diameter. The endpoints of each cross section are marked by wooden posts or metal rods between which can be stretched a tape measure, and all surveys are tied in to the same benchmark. Graphical presentation of channel changes is easier if the sections form a simple rectangular grid, but this may be inappropriate in curved or bifurcating channels.

The other aspect of the channel configuration that must be quantified is the texture of the bed, since this influences both the flow resistance and the availability of different size fractions of bedload. Flow resistance in gravel-bed rivers is best quantified from a size-by-number (i.e. pebble count) grain-size distribution, either using some multiple of the  $D_{50}$ ,  $D_{84}$ , or  $D_{90}$  percentile (e.g. Bray 1980) or using the full distribution (Wiberg & Smith 1987). Sediment availability is normally quantified by a size-by-weight (i.e. bulk sieving) distribution, and is commonly complicated by a difference between relatively coarse surface layer and relatively finer subsurface sediment. Bulk sieving to the standards proposed by Church et al. (1987) is time consuming even for a single site, and much more so when spatial patterns and temporal changes are of interest. We have tended therefore to use the quicker pebble counting approach to quantify spatial and temporal variations in surface texture, and collect and sieve large bulk samples of surface and subsurface sediment only at the start, end, or both of a study and from a few locations within a reach. Size distributions obtained in these different ways are intercomparable to some extent so long as they are truncated at common endpoints.

## 2.3 Flow measurements

In a braided river a knowledge of total discharge, e.g. from a gauging station at an undivided section upstream or downstream, is of limited value for a reach study because the split of total discharge between individual channels can alter considerably from day to day. A manual or automated record of flow stage within the study reach gives a better guide to day-to-day variations, and can be supplemented by velocity-area or salt-dilution gauging if discharge values really are required.

The surface streamline pattern within a reach can be visualised by observing the paths of floats introduced at different lateral positions, and quantified by compass bearings of surface flow direction at different stations along cross sections. Flow direction near the bed may differ from surface direction, especially in confluences where a twin-cell secondary circulation is thought to exist

(Ashmore 1982). It can be measured in clear water by attaching a streamer to a mechanical current meter, or in turbid water by using a two-component electromagnetic current meter.

In our studies we have regarded bed shear stress,  $\tau$ , as the key flow variable for comparison with bedload transport rates. The local value of the main alternative (specific stream power) is most easily estimated as the product of shear stress and mean velocity, so poses the same measurement problems. The formula

$$\tau = \rho g r s \quad (1)$$

(where  $\rho$  is water density,  $g$  the gravity acceleration,  $r$  the hydraulic radius of the channel and  $s$  the water surface slope) is often used for estimating shear stress in gravel-bed rivers but can be inappropriate for several reasons.

(1) It gives only the mean stress averaged over the wetted perimeter, whereas the local stress will tend to increase from banks to talweg. Some workers (e.g. Davoran & Mosley 1986) have therefore replaced  $r$  by the local flow depth  $d$  in equation (1).

(2) Shear stress is only proportional to the width-averaged or local depth-slope product in *uniform* flow. In channels with streamwise variation in depth and/or width, and therefore convective acceleration and deceleration of flow, the momentum equation contains extra terms which do not necessarily cancel out (Dietrich & Whiting 1989).

(3) The shear stress estimated from the energy gradient is the total stress balancing both skin and form resistance to flow, whereas the effective stress for bedload transport is generally regarded as the skin-drag component alone. In gravel-bed rivers with high relative roughness (ratio of characteristic grain size to flow depth) as much as half the total stress may be associated with the form drag of large protruding clasts (Wiberg & Smith 1987).

(4) At a practical level, accurate measurement of water surface slope can be difficult in steep shallow rivers with lateral slopes over bars, hydraulic jumps in the lee of the largest clasts, standing waves around survey staffs and wading rods, and temporal variations as pools and riffles are drowned out.

Our preferred alternative to the depth-slope method is to measure local velocity profiles and estimate the bed shear stress by fitting the logarithmic "law of the wall". In 1984-7 (Lyngsdalselva, Feshie, and White River) we used an array of current meters on a single wading rod in order to measure a four-point velocity profile in 30 seconds. In practice, replication was often necessary because in glacial rivers the bearings of some makes of current meter are intermittently clogged by suspended sediment. In 1989 (Sunwapta River) we therefore switched to using a single current meter on a topsetting rod which allowed the height to be altered without removing and replacing the wading rod, and thus without any change in the precise location and zero height of the velocity profile. This is slower than using an array of meters, but by assembling a larger team of fieldworkers we were able to measure as many profiles per hour.

The "law of the wall" for a turbulent boundary layer states that velocity  $u$  varies with height  $z$  as

$$u/u^* = (1/\kappa) \ln(z/z_0) \quad (2)$$

where  $\kappa = 0.4$  is Von Karman's constant,  $u^* = (\tau/\rho)^{0.5}$  is the shear velocity, and  $z_0$  is the roughness height of the bed. If  $z$  is accurately determined, as in the field procedures we have used (but not when a wading rod is removed and replaced each time  $z$  is altered), ordinary least squares regression of  $u$  on  $\ln(z)$  can be used to fit equation (2). This can be done in the field with a good calculator. If the best fit intercept and slope are  $a$  and  $b$ , and  $\rho$  is taken as  $1000 \text{ kg m}^{-3}$ , the shear stress  $\tau$  and roughness height  $z_0$  are given by

$$\tau = 160b^2 \quad (3)$$

$$z_0 = \exp(-a/b) \quad (4)$$

Integration of the logarithmic profile over the full flow depth  $d$  shows that the mean velocity  $\langle u \rangle$  occurs at height  $d/e$  and can thus be estimated as

$$\langle u \rangle = a - b + b \ln(d) \quad (5)$$

The standard errors  $s_a$ ,  $s_b$  of the regression coefficients  $a$ ,  $b$  can be used to calculate standard errors and confidence intervals for the estimated shear stress and roughness height (Wilkinson 1984). In particular, it is obvious from (3) that

$$s_\tau / \tau = 2 s_b / b \quad (6)$$

Others things being equal, a greater number and range of measurement heights will yield a lower value of  $s_b$  and a more precise estimate of the shear stress. In 1989, with 6-10 points per profile, our shear stress estimates had standard errors averaging about 10%, compared to upwards of 20% for our earlier 3- or 4-point profiles. There are, however, problems in extending the measurements throughout the flow depth. Measurements very close to the bed are very sensitive to the zero height used, i.e. the positioning of the wading rod on the rough bed. In our experience it is impossible to apply zero plane displacements in an objective way to overcome this problem, even though it is often easy to see from curvature in the logarithmic plot (or abnormally low or high estimated roughness heights) that a problem exists. Zero plane error in  $z$  decreases in relative terms as  $z$  increases, so measurements above the height of the largest clasts are not significantly affected; they are also far less vulnerable to distortion by local jet or wake effects near large clasts, and to physical blocking of the current meter by bedload.

Measurements far from the bed may also be misleading. It is known that velocity profiles can be distorted by secondary circulation, convective acceleration, and streamwise changes in bed roughness. Many authors assume that, even without these complications, velocity profiles in open channels are logarithmic only in the bottom 10% or 20% of the depth (e.g. Bathurst 1982). However, other authorities dispute this (e.g. Yalin 1977 p.30-33) and some detailed flume studies (e.g. Cardoso et al. 1989) have found minimal deviation from a logarithmic profile almost to the surface. We have generally found little departure except in confluences (presumably affected by secondary currents or underflow/overflow), though fitting the log law to shallow bar-head profiles can give surprisingly high estimates of shear stress, perhaps because of acceleration or roughness effects.

A more general problem with using the full profile is that a logarithmic outer profile may be distorted near the bed by the form drag of protruding clasts, as noted in a flume study by Nowell & Church (1979) and quantified theoretically by Wiberg & Smith (1987). Heathershaw & Langhorne (1988) appealed to this effect to explain dog-leg logarithmic plots for profiles in tidal currents over an irregular gravel bed. Using only the outer profile in this situation gives a total stress that is relevant to the entrainment of the largest clasts but will overestimate the effective stress on smaller particles; retaining the near-bed points will give a compromise estimate.

Weighing up these conflicting problems, we consider it best to measure at as many heights as conveniently possible up to at least half depth, but look critically at the logarithmic plot and be prepared to omit suspect points especially near the bed. The estimated roughness height can be a useful guide: a value much higher or lower than at adjacent locations may reflect a zero plane displacement or other problem in the measurements, and will tend to be associated with over- or under-estimation respectively of the shear stress since both  $\tau$  and  $z_0$  increase with the regression coefficient  $b$  (in contrast, the mean velocity  $\langle u \rangle$  is much less sensitive to errors in the velocity profile). A typical value of  $z_0$  for a poorly sorted gravel bed is around  $0.1 D_{84}$  or  $0.2 D_{50}$  (e.g. Bray 1980, Heathershaw & Langhorne 1988, Ferguson et al. 1989); we regard values of  $z_0/D_{50}$  outside the range 0.1-0.5 as suspicious.



If one is prepared to accept an empirical or theoretical scaling of  $z_0$  in terms of the bed grain size distribution, a rapid estimate of shear stress is possible using a single velocity measurement (Dietrich & Whiting 1989). This does however require the assumption of a simple logarithmic velocity profile at least up to the height of the single measurement. Another alternative which we are investigating is to measure the turbulent Reynolds stress close to the bed using a two-component electromagnetic current meter.

## 2.4 Bedload transport measurements

In the last gravel-bed rivers workshop Davies (1987) expressed the view that "present methods are unable to obtain accurate and comprehensive bed load data by point sampling or sediment budgeting". Little has happened since then to alter this pessimistic view, though as discussed below we see more merit in sediment budgeting than Davies did.

The best-known problem with direct point sampling of bedload is the short-term variability in transport rates. Some of the evidence for this variability (e.g. Hubbell 1987) relates to flume experiments at high transport rates with migrating bedforms that are not always present in rivers, but the situation is no better at lower transport rates when entrainment clearly has a strong stochastic element. Einstein's model for this allows estimation of confidence intervals (McLean & Tassone 1987), but only in terms of the mean hop length and mean particle rest time, neither of which is likely to be known with any accuracy, especially in a spatial study involving single samples at different locations where the underlying mean transport rates are assumed to differ. Sampling for longer at each location evidently reduces the likely error, but means that fewer sites can be sampled within a given period of steady flow. Empirical investigations of the sampling variability of bedload transport under different conditions may provide useful guidelines (K. Prestegard, pers. comm. 1990).

There are also some more practical, and soluble, problems in bedload sampling. In proglacial rivers with high loads of suspended sediment, the standard 0.25 mm mesh Helley-Smith sampler bag is apt to fill with fines before much gravel has been collected. If the suspended load is not of interest, the standard mesh should be replaced by a coarser one; we use 2 mm woven nylon. A double-size (152 mm) sampler improves the trap efficiency for coarse fractions, but in looking at spatial patterns the sampler must remain easily portable and not require any preparation of the bed at each measurement point. Samplers with tailfins are harder to handle because of the extra drag, and in some patterns the support frame for the tailfin tends to perch on protruding clasts allowing bedload to pass beneath the orifice.

If only the total bedload transport rate is of interest, not its grain size distribution, samples can be weighed while still damp (with subsequent correction to dry weight) and returned immediately to the river; it is usually possible also to extract and measure the coarsest particle as an index of flow competence. If fractional transport rates and/or percentiles of the size distribution are required, it is necessary to bag and label the samples immediately for subsequent drying, sieving and weighing. In our work in meltwater rivers we have generally been able to do this the morning after sampling, drying samples in the sun and using a battery-powered top pan balance for weighing. If dimensionless transport rates or shear stresses are to be calculated a value will be needed for sediment density, so this should be determined, e.g. by weighing a selection of pebbles and the water they displace. In this paper we refer mainly to mass transport rates, denoted by  $q_s$  and measured in units such as  $\text{kg m}^{-1}\text{s}^{-1}$ .

There are of course several other ways of investigating bedload movement. Traps and tracers of various kinds are good choices for some purposes, but appear less useful than portable samplers if the aim is to map spatial patterns of bedload. Indirect estimation of bedload transport from channel change is discussed later.

### 3 METHODS FOR ANALYSING SPATIAL PATTERNS

Once spatially-distributed measurements of flow strength, bedload transport, and channel configuration and change have been made in a particular study reach it is necessary to interrelate the spatial patterns of each component of the system. Perhaps the most obvious way to do this is to plot the flow and transport measurements on maps, or against distance downstream if measurements have been restricted to just one or two transverse positions at each cross section. In Ashworth & Ferguson (1986) we used maps and verbal descriptions of the streamwise trends in shear stress and bedload transport rate to explain observed channel changes in the Lyngsdalselva, but on the basis of very limited data along the talweg only. We present below some new examples with fuller data, and discuss problems with this approach.

#### 3.1 River Feshie, 1986

This study was made on a single day (2 May 1986) of diurnally varying snowmelt flow, with a peak discharge just greater than bankfull in the alternate-bar reach concerned. The general character of the river has been described before (Ferguson & Werritty 1983) and the process measurements were amongst those analysed by Ashworth & Ferguson (1989). They were made by two people over three hours, using tension from a rope to support the person wading since flow depth and mean velocity were relatively high (up to 0.8 m and  $2.4 \text{ m s}^{-1}$ ). Measurements were made at one or two lateral positions on each of six cross sections about 15 m apart along the reach, and were repeated at two different flow stages.

The patterns of  $\langle u \rangle$ ,  $\tau$ , and  $q_s$  are represented by numbers at appropriate locations on a map of the reach in Figure 2a. This form of mapping retains the maximum amount of information but does not give an immediate visual impression of the spatial patterns of the variables. On close inspection it can be seen that velocity and shear stress are high in the left-bank pool head, decrease down the pool along this bank towards the next bar front, but increase again towards the next pool head diagonally rightwards. The 40% increase in discharge during the afternoon was accompanied by an increase in velocity and stress at most locations, but no clear change in their spatial pattern. The plots of velocity and stress against distance along the reach in Figure 2b show this more clearly, and emphasise the out-of-phase pattern on opposite sides of the channel in this alternate-bar morphology.

Bedload transport was restricted to the points of higher velocity and stress, indicating that within-bank flows in this river are only just competent. This being so, the relatively small increase in velocity and shear stress as the discharge rose during the day led to a bigger relative increase in bedload transport, and a more pronounced spatial pattern: increasing (implying erosion) along the uppermost part of the pool, but thereafter decreasing (implying deposition) towards the bar front. This indicates a transfer of sediment from the poolhead to the pooltail and bar front. Figure 2c shows that this is just what happened in this reach over the melt season as a whole, and pebble-tracing studies also showed an accumulation of sediment towards the bar front. The process measurements are therefore consistent with observed channel change, and support the suggestions by Ferguson & Werritty (1983) about mechanisms of bar growth in this type of channel.

#### 3.2 White River, 1986

This study involved intensive measurements by three people in this glacier-fed river over two weeks in late July and early August. As in our earlier Norwegian study an X-pattern (confluence and bifurcation) reach was selected, but in this case all parts of the reach were wadable for most or all of the time. Unfortunately the simple appearance of the reach was misleading, for a ribbon of mobile sand ran along the left side of the talweg and had a considerable effect on shear stress, roughness height, and gravel transport. We have discussed elsewhere (Ferguson et al. 1989) these effects and the statistical relationship between shear stress and bedload transport, but not the spatial patterns.

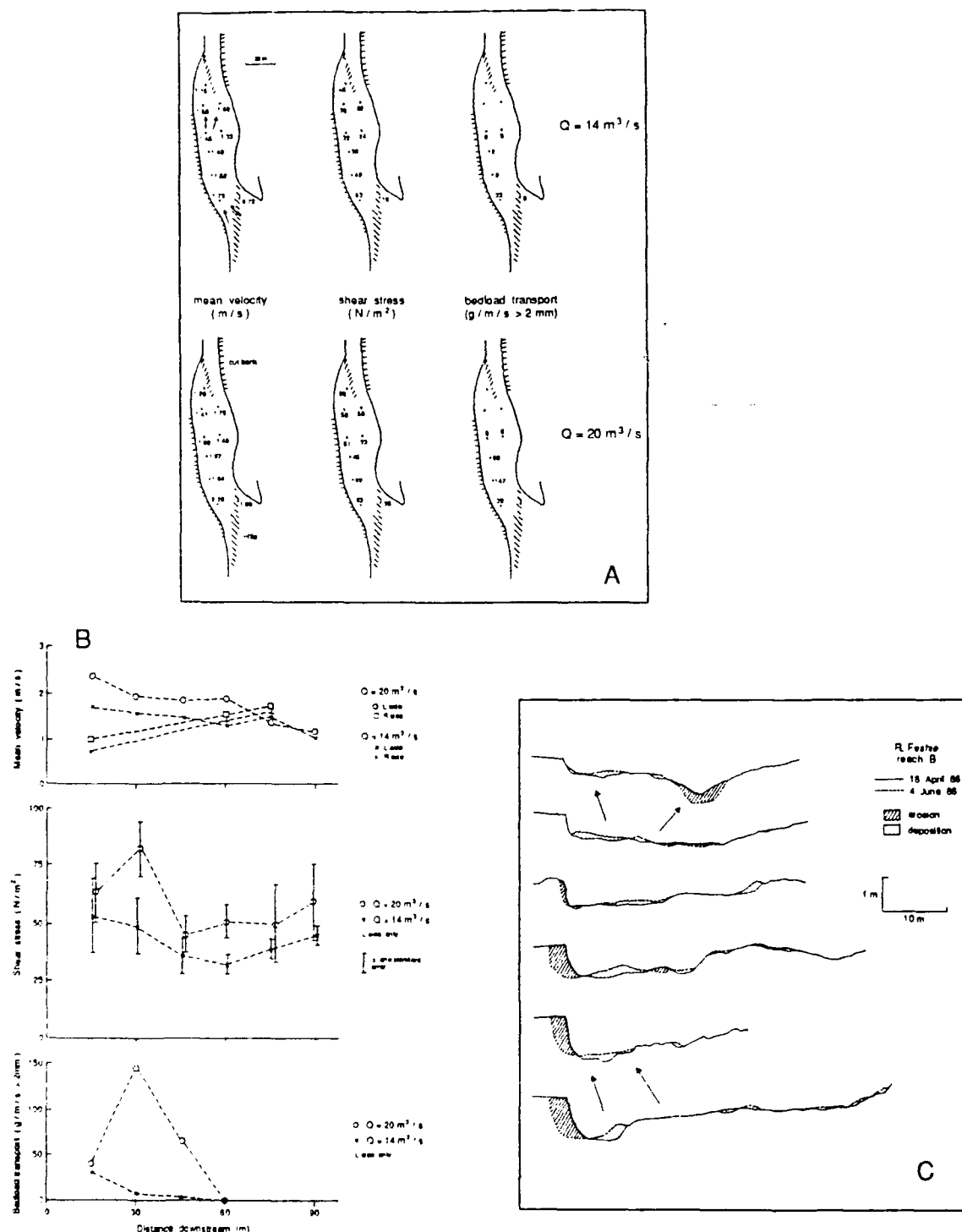


**Figure 2:** Measured mean velocity, shear stress, and bedload transport rate in an alternate-bar reach of the River Feshie, Scotland, at two discharge levels ( $Q$ ) on 2 May 1986. In (a), dots mark locations of measurements, numbers by them indicate values, and no number indicates missing value. In (b) the data are plotted against distance down reach, with points close to the left bank distinguished from those further right. Channel change at the same cross-sections is shown in (c) for a six week period within which the highest discharge was on the day of the process measurements.

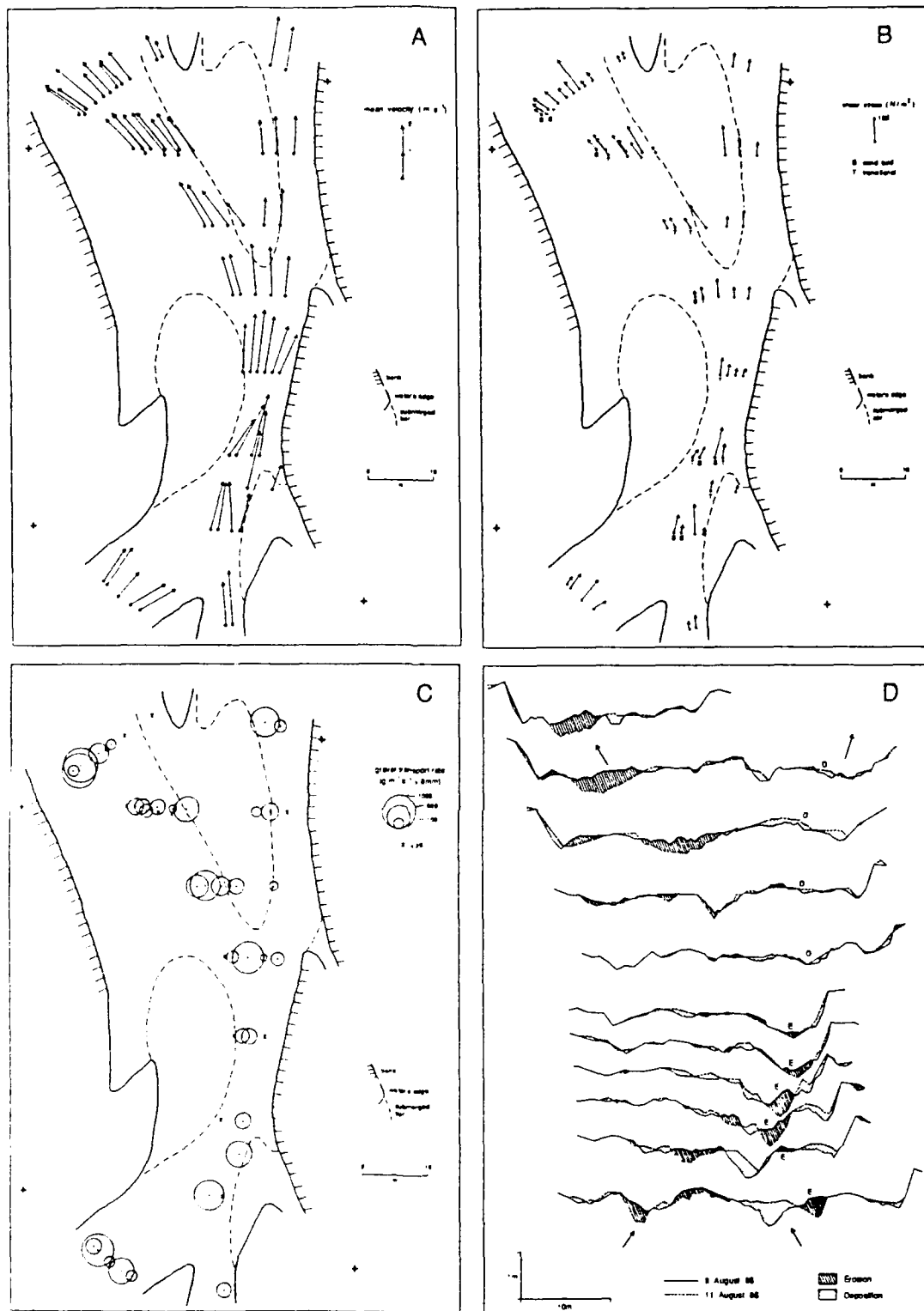


**Figure 3:** Spatial patterns in a braided reach of the White River, northwest US, during high meltwater flows. Measurements on evenings of 8/9 August 1986 are mapped as follows: (a) magnitude of mean velocity, plotted in direction of surface velocity; (b) shear stress, plotted in direction of surface velocity, with non-gravel bed types indicated and dashed arrow where standard error of stress estimate is large; (c) gravel transport rate. Channel change over 8-11 August is shown in (d), with the main cell of erosion and deposition labelled by E and D.

Figure 3 illustrates the patterns of mean velocity, shear stress, bedload transport rate, and channel change in the last few days of the study, when discharge and activity were greatest. Maps with vector arrows or proportional circles for measured quantities are used for maximum visual impression of spatial patterns. The convergence and acceleration into

and past the confluence, and divergence and deceleration in the ensuing bifurcation zone, are apparent in the velocity map but not clearly reflected in the maps of shear stress or transport rate. This is partly because of the complication introduced by the sand ribbon, but no doubt also because sampling and measurement errors in bedload and shear stress are higher than those in mean velocity. We discuss later some ways of dealing with this noise in the spatial patterns.

The channel change diagram (Figure 3d) is also complicated, but less so if changes originating upstream of the study reach are ignored. The main changes that can be compared with our process measurements are erosion in the confluence (zone E in the diagram) with deposition further downstream on the medial bar and right distributary (zone D), and erosion in the left distributary, presumably with deposition further downstream. Both erosion zones approximately coincide with zones of flow acceleration, as in the marginally-competent meltwater flows of the Norwegian and Scottish case studies.

### 3.3 Sunwapta River, 1989

This study involved a bigger team than the previous ones, with up to three current meters and three bedload samplers simultaneously in use in an attempt to obtain detailed and reliable spatial patterns. Velocity profiles were measured at up to 11 heights, and bedload was sampled for at least 5 minutes, to reduce sampling error. The reach was a simple chute and bifurcation, with finer gravel (surface  $D_{50}$  of 20-30 mm) than in the other rivers studied, and measurements were made over a week of high meltwater flows in July-August. The results will be described more fully elsewhere but an example is given in Figure 4. The divergence of bedload transport and the general pattern of erosion in the constriction, deposition downstream of it, are clearly revealed. But is such a map reliable, even when based on such labour-intensive methods? It undoubtedly contains substantial noise as a result of sampling error. In the final sections of this contribution we therefore attempt to assess this error and compare locally-averaged or totalled rates with independent estimates based on observed channel change.

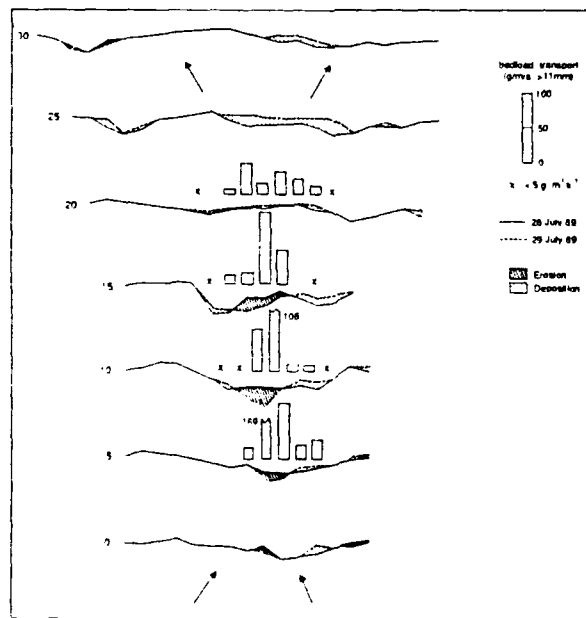


**Figure 4:** Channel changes during 28-29 July 1989 in a reach of the braided Sunwapta River, Canada, and bedload transport rates sampled during high meltwater flow on the evening of 28 July 1989.

### 3.4 Local averaging of measurements

A standard way of dealing with sampling error in independent measurements is to average them, since the sampling variance of their mean is less than that of the individual values. In looking at nonuniform patterns of shear stress or bedload transport in gravel-bed rivers we are naturally keen to retain as much spatial detail as possible, but if the sampling noise overwhelms the spatial trend it may be advantageous to do some averaging of the raw measurements.

If measurements have been made at several locations along each cross section of a reach, one possibility is to calculate a mean value for each section. In the case of bedload transport, a total value for the section ( $Q_s$  as opposed to  $q_s$ ) also has physical meaning. Either  $Q_s$  or a width-averaged  $q_s$  will have greater precision (in percentage terms) than the individual  $q_s$  measurements; totals or means can then be plotted against distance downstream in the hope that streamwise trends emerge more reliably than from the raw data.

This is illustrated in Figure 5 using data from two of the case studies discussed above. In Figure 5a the White River bedload measurements of Figure 3c are averaged over zones of one to three adjacent cross sections, the zone size being varied to achieve a minimum of  $n = 5$  samples in each zone. Standard errors of the mean transport rates are estimated in the ordinary way from the sample size and standard deviation. They are not exact, because we are dealing with small and skewed samples from what is likely to be a non-homogeneous population. In this example the spread of individual transport rates is very high and the sample sizes are low, so the zonal means still have standard errors too large for differences between zones to be significant. The averaging thus fails to define an unambiguous spatial pattern.

In Figure 5b the cross-section totals of bedload in the Sunwapta River on four different days, including the data mapped in Figure 4, are plotted against distance downstream. The standard errors are omitted for clarity but are again high, in the range 30%-60% of the estimated totals. Many of the apparent increases or decreases in transport from one section to the next could therefore be artefacts of sampling error, though the differences between dates are more convincing.

We discuss later how the spatially-averaged bedload measurements illustrated in Figure 5 compare with inferences from observed channel changes in the same reaches.

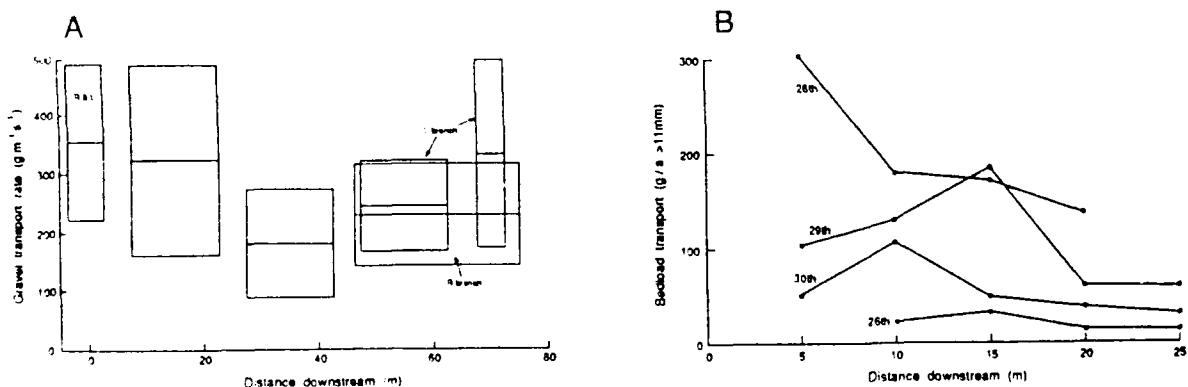


**Figure 5:** Examples of downstream patterns of local averages and lateral totals of sampled bedload transport rates: (a) White River, 8/9 August 1986, (b) Sunwapta River, 28 July 1989. In (a), each box extends one standard error above and below the mean transport rate for the cross-sections concerned.

### 3.5 Inferring bedload transport rates from channel change

The possibility of estimating a spatially and temporally averaged mean sediment transport rate from observed channel changes over a period has been applied many times to bedform migration. Neill (1987) extended it to meander migration over several years, and Church *et al.* (1987) and McLean (1990) have used it in multi-year comparisons of long reaches of large, low-sinuosity rivers. Our application is at far shorter time and space scales but uses the same principle. The general idea is that the volume  $V$  of sediment removed, divided by the average distance  $L$  that it travels before being deposited on the next point bar and by the time interval  $T$  over which  $V$  is measured, gives the mean volumetric flux through the reach. This method will underestimate the true mean transport rate if alternate scour and fill cause net channel change between surveys to fall short of gross change. Our White River and Sunwapta investigations show that channel change at a point can reverse within a few days, and this is supported by Laronne & Duncan's (1989) work using scour chains in a New Zealand river. Underestimation for this reason is likely to increase with the time interval  $T$  between surveys. Another source of underestimation is that some bedload may travel nonstop through the reach; this is decreasingly likely as reach length  $L$  increases, and the available evidence from pebble tracing studies by several researchers is that few pebbles travel further than the next riffle during one period of competent flow.

In braided channels the loci of erosion and deposition are less predictable than in meandering streams, and even over quite short timespans (e.g. 3 days in Figure 3d) there may be a complicated mosaic of net erosion and net deposition through the combined effects of channel scour, fill, migration and avulsion. Resurveys over short periods may however reveal distinct zones of erosion and deposition which can be matched up as transport cells in the same way as in a meander bend. As already illustrated by our case studies, just-competent flows tend to move sediment from pools and confluences to bars and bifurcations. If in such a situation the volumes of erosion and deposition are similar, so that sediment can be inferred to move from one to the other with a well defined mean travel distance, a reasonable estimate of the mean transport rate should be possible.

It is necessary first to compute volumes of erosion or deposition between successive surveys. This is done by superimposing the plotted surveys at times  $t_1$  and  $t_2$  for cross-sections  $i = 1, 2, \dots$  at distances  $x_i$  along the channel, delineating the zone of (say) erosion (as labelled by E in Figure 3d), and determining the width  $w_i$  and mean depth  $d_i$  of erosion at each cross-section. The total volume of erosion within the zone is then obtained by summing increments between adjacent sections, calculated as follows on the assumption that  $w$  and  $d$  vary linearly with distance:

$$V_i = (x_i - x_{i-1})(2w_i d_i + w_i d_{i-1} + w_{i-1} d_i + 2w_{i-1} d_{i-1})/6 \quad (7)$$

Deposition volumes are quantified in the same way. Equation (7) simplifies if either  $w$  or  $w/d$  is constant between adjacent sections. If the sections are not parallel, appropriate corrections can be made to  $x$  and  $w$ . A degree of subjectivity is involved in deciding at just what distance  $w$  and  $d$  go to zero at the ends of a zone, but the volume increments here are small.

Once a volume  $V_e$  of erosion over a time interval  $T$  has been matched up with a similar volume  $V_d$  of deposition a short way downstream, the mean transport rate  $q_s$  in  $\text{m}^3 \text{m}^{-1} \text{day}^{-1}$  or similar units can be estimated as

$$q_s = (V_e/A_e).(L/T) \quad (8)$$

where  $A_e$  is the plan area of erosion and  $L$  is the mean travel distance of particles moving from the erosion zone to the deposition zone.  $L$  can be estimated as the difference in position along the channel of the centroids of  $V_e$  and  $V_d$ , calculated as  $\sum_i (x_i w_i d_i) / \sum_i (w_i d_i)$ . Conversion of the transport rate estimated using equation (8) to mass units such as  $\text{kg m}^{-1} \text{s}^{-1}$ , as for point samples, requires multiplication by an assumed bulk density and by the fraction of the interval  $T$  between surveys during which active transport is thought to have occurred.

We have applied this method to the main erosion/deposition cell in our White River study reach (Figure 3d, zones E and D). Surveyed changes over 3 days amounted to  $19.6 \text{ m}^3$  of erosion from an

area of  $131 \text{ m}^2$ , and  $18.3 \text{ m}^3$  of deposition at a centroid-to-centroid distance of 49 m downstream. Substitution of these values in equation (8) gives a mean transport rate of  $2.4 \text{ m}^3 \text{ m}^{-1} \text{ day}^{-1}$ , or about  $0.18 \text{ kg m}^{-1} \text{ s}^{-1}$  assuming a bulk density of  $1600 \text{ kg m}^{-3}$  and 6 hours per day of active transport. This agrees well with the mean of  $0.17 \pm 0.06 \text{ kg m}^{-1} \text{ s}^{-1}$  ( $> 2 \text{ mm}$ ) for 12 Helley-Smith samples within the erosion/deposition cell in the relevant period. A similar calculation from the  $4.0 \text{ m}^3$  of erosion and  $4.1 \text{ m}^3$  of deposition during the day of maximum change in the Sunwapta River (Figure 4) gives an estimated mean transport rate of  $1.5 \text{ m}^3 \text{ m}^{-1} \text{ day}^{-1}$  or  $0.11 \text{ kg m}^{-1} \text{ s}^{-1}$ . This is in reasonable agreement with the mean of  $0.08 \pm 0.03 \text{ kg m}^{-1} \text{ s}^{-1}$  ( $> 2 \text{ mm}$ ) based on Helley-Smith sampling. On the evidence of these comparisons, it appears that space-time averages of bedload transport can be estimated from channel change at least as reliably as by direct sampling.

### 3.6 Within-reach sediment budgeting

Whether or not clear erosion/deposition cells can be identified, surveyed channel changes at a series of cross-sections within a reach can be used to infer the rate of change of bedload transport along the channel by using the sediment continuity equation. In finite difference form this is

$$\Delta q_s / \Delta x = -V / (w \cdot \Delta x \cdot T) \quad (9a)$$

or

$$\Delta Q_s / \Delta x = -V / (\Delta x \cdot T) \quad (9b)$$

where  $V$  is volume of erosion (negative) or deposition (positive) over channel length  $\Delta x$  and time  $T$ ,  $w$  is width of erosion or deposition,  $q_s$  is volumetric transport rate per unit width and time and  $Q_s$  is totalled over  $w$  and averaged over  $T$ . If  $V$  and  $w$  are known for each of a series of cross-sections, the transport rate need only be known at one section for equation (9) to define its value at all other sections in the reach. If no direct measurements of bedload transport are available all that can be done is to set a lower bound by the requirement of non-negative transport at all sections, as done by Griffiths, (1979) in a pioneering application of this approach to surveyed changes over many km and years in a New Zealand river. In some circumstances a downstream boundary condition of zero gravel transport can be assumed, as in McLean's (1990) budget for the lowermost gravel-bed reach of the Fraser River, Canada, using surveyed changes over 32 years at sections 2 km apart.

Our application of the sediment budget approach is at a quite different scale (steps of 1-3 days and 5-10 m) and the nearest we have to a boundary condition is the mean transport rate in our spatially-distributed Helley-Smith samples. We turn again to the White River and Sunwapta case studies to illustrate the method. Changes over 3 days in the long profile of a 5 m wide talweg strip in the White River are shown in Figure 6a. The pattern of channel change implies a downstream decrease in transport rate into the aggrading head of the confluence zone, an increase past sections 20 and 25 which scoured during this period, then a decrease along the aggrading right distributary but an increase along the degrading left distributary. The volumes of erosion or deposition between successive pairs of sections were estimated using equation (8) and converted using equation (9) to changes in mean transport rate along the channel. The inferred downstream variation in mean transport rate is plotted in Figure 6b, with the general level of transport matched to the  $0.27 \text{ kg m}^{-1} \text{ s}^{-1}$  mean of the 47 Helley-Smith samples collected from various points along this strip on the evenings of 8 and 9 August. As already noted the means of directly-sampled transport rates in the six zones distinguished in Figures 5a and 6b have large standard errors, so that downstream changes are not defined unambiguously. They can best be described as not inconsistent with the predictions from channel change. The predicted curve in Figure 6b lies within one standard error of each of the six zone means, and the locations of the highest predicted and measured mean transport rates (at either end of the reach) agree, but the lowest measured mean transport rate is not at the predicted location.

A similar comparison of cross-section total transport rates ( $Q_s$ ) in the Sunwapta, as estimated from point sampling (Figures 4 and 5b) and from channel change in a 7 m wide central strip, is illustrated in Figures 6c and 6d. The channel aggraded throughout the reach during 22-28 July, implying a downstream decrease in transport rate, but during 28-29 July and 29-30 July there was proximal erosion and distal deposition, which implies a maximum transport rate in mid-reach. The direct samples agree with these qualitative patterns on the 26th and 29th, but not on the 28th. The quantitative agreement is good on the 26th, and fair on the 28th and 29th taking into account the large standard errors of the Helley-Smith estimates of  $Q_s$ .



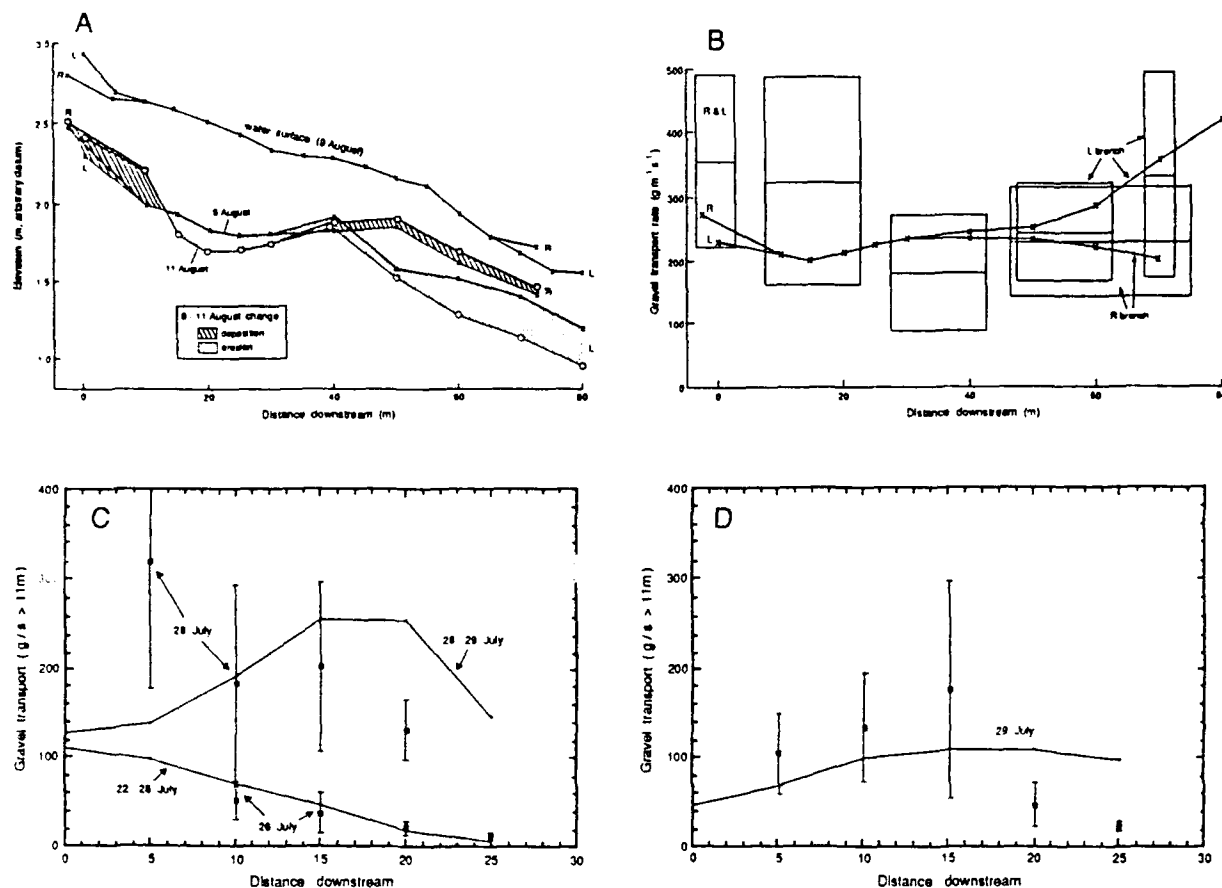


**Figure 6:** Comparisons of downstream variation in mean bedload transport rate as estimated by point sampling and from channel change: (a) aggradation and degradation of 5 m wide talweg strip of the White River; (b) mean transport rates inferred from (a) (continuous lines) compared with those measured directly (boxes as in Figure 5a); (c and d) width-integrated transport rates in the Sunwapta River as inferred from aggradation or degradation of 7 m wide central strip (continuous lines) and from point sampling (symbols with standard error bars).

We feel that these comparisons cast further doubt on the reliability of Helley-Smith sampling of bedload, rather than invalidating the idea of inferring downstream changes in bedload transport from intensive surveys of channel change. A further possibility in future studies would be to estimate  $Q_s$  at a baseline cross section by intensive Helley-Smith sampling across the active width, then use frequent resurveys and equation (9) to calculate transport rates progressively further upstream and downstream. This should give more reliable estimates of cross-section average transport rates along the reach than would be obtained by the same total sampling effort distributed between all the sections, but at the expense of losing information on lateral variations in transport and on grainsize distributions of transport away from the baseline section.

#### 4 CONCLUSIONS

We have described some of the measurement techniques and methods of data presentation and analysis that we have used in the last few years in an attempt to understand channel change in braided rivers in terms of nonuniform processes. Our experience and results show that spatially distributed measurement is feasible, but not easy, and that gaining accurate and reliable measurements is even more difficult. The weakest link is sampling of bedload. The numerical examples discussed here suggest that the relatively easy and accurate measurement of channel change provides a partial alternative, since local mean values of bedload transport can be inferred from volumes of erosion or deposition. However, this is at the price of losing detail of spatial patterns in bedload transport.

## 5 ACKNOWLEDGEMENTS

The field measurements discussed in this paper could not have been collected without support from numerous agencies and individuals. Much of the research was done during Ashworth's tenure of a UK NERC studentship and fellowship, and with equipment and other support provided by Stirling University. Feshie fieldwork was done in collaboration with Alan Werritty and with partial support from NERC grant GR3/5602. White River fieldwork was done in collaboration with Karen Prestegaard and funded by NATO grant 86/310. Sunwapta fieldwork was again funded by NATO and done in collaboration with Peter Ashmore, Chris Paola and Karen Prestegaard, with assistance also from Dave Harrison, Sean Moran, Mark Powell, Christine Snow, and Steve Wiele.

## 6 REFERENCES

- Ashmore, P.E. (1982). 'Laboratory modelling of gravel braided stream morphology', *Earth Surf. Proc. Landf.* 7, 201-225.
- Ashworth, P.J. and Ferguson, R.I. (1986). 'Interrelationships of channel processes, changes and sediments in a proglacial river', *Geogr. Annaler* 68A, 361-371.
- Ashworth, P.J. and Ferguson, R.I. (1989). 'Size-selective entrainment of bed load in gravel bed streams', *Water Resour. Res.* 25, 627-634.
- Bathurst, J.C. (1982). 'Theoretical aspects of flow resistance', in Hey, R.D., Bathurst, J.C. and Thorne, C.R. (eds.) *Gravel-bed rivers*, Wiley: Chichester, 83-105.
- Bray, D.I. (1980). 'Evaluation of effective boundary roughness for gravel-bed streams', *Can. J. Civ. Eng.* 7, 392-7.
- Cardoso, A.H., Graf, W.H. and Gust, G. (1989) 'Uniform flow in a smooth open channel', *J. Hydr. Res.* 27, 603-.
- Church, M. and Jones, D. (1982). 'Channel bars in gravel-bed rivers', in Hey, R.D., Bathurst, J.C. and Thorne, C.R. (eds.) *Gravel-bed rivers*, Wiley: Chichester, 291-324.
- Church, M.A., McLean, D.G. and Wolcott, J.F. (1987). 'River bed gravels: sampling and analysis', in Thorne, C.R., Bathurst, J.C. and Hey, R.D. (eds.) *Sediment transport in gravel-bed rivers*, Wiley: Chichester, 43-79.
- Church, M., Miles, M.J., and Rood, K.M. (1987). '*Sediment transfer along Mackenzie River: a Feasibility Study*', Environment Canada, Inland Waters Directorate, Sediment Survey Report.
- Davies, T.R.H. (1987). 'Problems of bed load transport in braided gravel-bed rivers', in Thorne, C.R., Bathurst, J.C. and Hey, R.D. (eds.) *Sediment transport in gravel-bed rivers*, Wiley: Chichester, 793-811.
- Davran, A. and Mosley, M.P. (1986). 'Observations of bedload movement, bar development and sediment supply in the braided Ohau River', *Earth Surf. Proc. Landf.* 11, 643-652.
- Dietrich, W.F. and Whiting, P. (1989). 'Boundary shear stress and sediment transport in river meanders of sand and gravel', in Ikeda, S. and Parker, G. (eds) *River meandering*, Amer. Geophys. U. Water Resour. Monog. 12, 1-50.
- Ferguson, R.I. and Werritty, A. (1983). 'Bar development and channel change in the gravelly River Feshie, Scotland', *Int. Assoc. Sedim. Sp. Pub.* 6, 181-193.
- Ferguson, R.I., Ashworth, P.J. and Prestegaard, K.L. (1989). 'Influence of sand on hydraulics and gravel transport in a braided gravel bed river', *Water Resour. Res.* 25, 635-643.
- Griffiths, G.A. (1979). 'Recent sedimentation history of the Waimakariri River, New Zealand', *J. Hydrol. N.Z.* 18, 6-28.
- Heathershaw, A.D. and Langhorne, D.N. (1988). 'Observations of near-bed velocity profiles and seabed roughness in tidal currents flowing over sandy gravels', *Est. Coast. Shelf Sci.* 26, 459-482.
- Hubbell, D.W. (1987) 'Bed load sampling and analysis', in Thorne, C.R., Bathurst, J.C. and Hey, R.D. (eds.) *Sediment transport in gravel-bed rivers*, Wiley: Chichester, 89-106.
- Laranne, J.B. and Duncan, M.J. (1989). 'Constraints on the duration of sediment storage in a wide, gravel-bed river, New Zealand', *Int. Assoc. Hydrol. Sci. Pub.* 184, 165-172.
- McLean, D.G., (1990) *The relation between channel instability and sediment transport on Lower Fraser River*, unpubl. Ph.D. thesis, Univ. of British Columbia.
- McLean, D.G. and Tassone, B. (1987). Discussion of Hubbell, op.cit., *ibid.* p.109-113.
- Mosley, M.P. (1987). Discussion of Davies, op.cit., *ibid.* p.821-4.

- Neill, C.R. (1987). 'Sediment balance considerations linking long-term transport and channel processes', in Thorne, C.R., Bathurst, J.C. and Hey, R.D. (eds.) *Sediment transport in gravel-bed rivers*, Wiley: Chichester, 225-.
- Nelson, J.M. and Smith, J.D. (1989). 'Evolution and stability of erodible channel beds', in Ikeda, S. and Parker, G. (eds) *River meandering*, Amer. Geophys. U. Water Resour. Monog. 12, 321-377.
- Nowell, A.R.M. and Church, M. (1979). 'Turbulent flow in a depth-limited boundary layer', *J. Geophys. Res.* 84, 4816-24.
- Parker, G. and Andrews, E.D. (1985). 'Sorting of bed load sediment by flow in meander bends', *Water Resour. Res.* 21, 1361-73.
- Parker, G. and Andrews, E.D. (1986). 'On the time development of meander bends', *J. Fluid Mech.* 162, 139-156.
- Wiberg, P.L. and Smith, J.D. (1987). 'Initial motion of coarse sediment in streams of high gradient', *Int. Assoc. Hydrol. Sci. Pub.* 165, 299-308.
- Wilkinson, R.H. (1984). 'A method for evaluating statistical errors associated with logarithmic velocity profiles', *Geo-Marine Letters* 3, 49-52.
- Yalin, M.S. (1977). *Mechanics of sediment transport* (2nd ed), Pergamon:Oxford.

## BEDLOAD TRANSPORT PATH AND GRAVEL BAR FORMATION

Jonathan B. Laronne

Dept. of Geography, Ben Gurion Univ., Beer Sheva, 84105, Israel

Maurice J. Duncan

Hydrology Centre, DSIR, Box 22-037, Christchurch, New Zealand

### Gravel Bar Formation and Reworking

New, central bars are formed when bed areas are inundated and, with few exceptions (Hein 1974; Smith, 1974), cannot be observed in the field due to the turbidity of the flow. Bar reworking also occurs at flow stages below bankful, when the river bed can be seen, and because the changes are often sufficiently slow to clarify the mechanisms of reworking. Accordingly, most of our understanding concerning bar formation derives from flume studies where suspended sediment has been excluded (Leopold and Wolman, 1957; Ashmore, 1982; 1985; 1987; Hoey, 1989), whereas most of the observations on bar reworking are based on field studies (Fahnestock, 1963; Hitchcock, 1977; Werritty and Ferguson, 1980; Ferguson and Werritty, 1983; Ashworth and Ferguson, 1986; Ashworth, 1987). The difficulty of observing the formation of prototype bars explains why some hypotheses concerning their formation have been highly speculative (Rundle, 1985).

Central bars may be formed by deposition at sites of flow divergence. These may be a new 'nucleus' of coarser gravel (Leopold and Wolman, 1957) or an advancing single or multiple sediment lobes (Ashmore, 1982). Such depositional units have been coined a variety of terms (Smith, 1978; Church and Jones, 1982), but are now often termed 'unit bars' (Smith, 1974). Central bars may also appear due to erosion of existing bed areas. Three erosional mechanisms have been proposed (Ashmore, 1985). Central bars may be formed during high stages of flow due to meander cutoff (Lewin, 1976; Werritty and Ferguson, 1980; Ferguson and Werritty, 1983) and due to alternate bar cutoff (Ashmore, 1982). A second erosional mechanism is dissection of gravel sheets at falling stage (Hein, 1974), and a third mechanism is the formation of miniature 'protochannels', which have been observed to develop on a steep, plane bed (Moss, Walker and Hutka, 1980; Moss, Green and Hutka, 1982).

The conditions favouring one or more of the above mentioned mechanisms of central bar formation have not been determined. The 'nucleus' bar can be formed due to the initial deposition of coarser bed-material, favouring it for gravel rather than sand bed streams. Its preferred formation downstream of a confluence has been observed in a model (Ashmore, 1982) and it is suggested from painted gravel transport paths in two Scottish wandering, gravel bed rivers (Ashworth, 1987). Recent field documentation demonstrates that flow divergence, lower flow velocities and lower shear stresses indeed occur simultaneously downstream of confluences (Ashworth, 1987). Although advancing sediment lobes or gravel sheets have been observed in the field and laboratory, it is yet to be demonstrated whether they are as common in a wide, gravel bed rivers as they are in some flume models (including 1:20 scale models, Ashmore, 1982; Davies and Lee, 1988).

Reworking of gravel bars involves primarily bank erosion resulting in a single, supposedly more sinuous pattern (Werritty and Ferguson, 1987; Ashworth, 1987). This erosion occurs with concomitant deposition of similar quantities of bed material in the opposite bank of wandering gravel bed rivers, an observation particularly well documented in reach D of the Dubhaig (Ashworth, 1987). Reworking also includes channel 'switching' and resultant infilling of previous anabranches as well as the deposition of new gravel sheets (Werritty and Ferguson, 1980).

Gravel tracers may be used to infer modes of bar formation. For instance, Brewster (1986, in Ashworth, 1987) showed that a bar head of the River Feshie may develop by receiving sediment derived far upstream, rather than from the immediate surroundings. Bed material appears to be preferentially deposited on the stoss of point bars (reaches A and C of the Dubhaig) and of longitudinal (compound?) bars (reaches B of the Dubhaig and Feshie; see, Ashworth, 1987). The use of painted gravel is, however, difficult in very active braided rivers due to burial of most of the tracers (Ferguson and Ashworth, 1986).

Additional prototype observations are required to evaluate the relative roles of these mechanisms of bar formation and reworking. The purpose of this study is to determine modes of bar reworking and formation in a wide, braided river, and to compare them to those in a lower, narrower alternate bar reach. Specifically, we assume that bed material transport paths should be strongly controlled by flow divergence and increased friction around an emerging nucleus or a point bar, whereas paths would in large part be parallel to flow direction if sediment accumulation occurs around advancing lobes or sheets.

### Study Area

The North Branch Ashburton River drains 300 km<sup>2</sup> of steep greywacke terrain in the Southern Alps, South Island of New Zealand. The lower catchment, from the gorge to the confluence with the South Branch, is an 80 km<sup>2</sup> segment of the Canterbury Plains, comprising a sequence of Pleistocene and recent alluvial lobes or fans and terraces of gravel and sand (Mabin, 1980). Mean annual precipitation in the North Branch Catchment is 1400 mm. Estimated mean annual and 50 yr flood peaks at the gorge are 180 and 570 m<sup>3</sup> s<sup>-1</sup>.

There are three types of channels in the North Branch: a mostly rock-confined, shallow alluvial channel upstream of the gorge, a wide, braided channel between the gorge and Thompson's Track Bridge and a narrower, alternate bar channel extending 21 km to the confluence with the South Branch.

An upper, braided reach and a lower, alternate bar reach were selected (Fig. 1). The upper reach is located between the Rangitata Diversion Race (RDR) and Thompson's Track Bridge. It is about 220m wide, wider than most other reaches of the river. Based on older aerial photographs we have determined that willow planting has confined it from an earlier width of about 500 m. Mapping based on more recent aerial photographs shows that this reach has well developed longitudinal, medial bars, often with merely 2 primary anabraches that are completely detached from the banks during low flow conditions (Fig. 2a). The river bed comprises active bed areas and a series of sequentially higher and older surfaces or bar complexes covered by dense grass and shrub colonies (Laronne and Duncan, 1989a). These surfaces are dissected by a series of tributary channels that are dry during base flow conditions. The length of reach surveyed was 700 m with an average bed slope of 1.15 percent.

The lower, narrower study reach lies between Thompson's Track Bridge and Shearer's crossing, within Bland's Reach, which has been aggrading since 1937. A wedge of bed material 4 m thick has been accumulating in this reach at an average rate of 5.8 cm yr<sup>-1</sup> and as much as 11.4 cm yr<sup>-1</sup>. The river bed is comprised of alternate bars, it is about 85 m wide, straight, and is confined by willows and high banks for floodplain protection (Fig. 2b). In relation to their original widths, the lower reach has been confined slightly less than the upper reach. The length of reach surveyed for this study was 750 m with an average bed slope of 0.73 percent.

### Methods

The South Canterbury Catchment Board's Old Weir recording site at the gorge provided continuous water level and discharge data. In addition, three temporary installations of 3 m Foxboros supplied gauge records at the Rangitata Diversion Race above the upper reach, at Thompson's Track Bridge below it and at Digby's Bridge further down river (Fig. 1). Several stage staffs were also used. Flow velocity was measured using Gurley current meters at 0.6 flow depth by wading or jet boating. The location along the cross section was measured using a

tight tag line or by surveying. Water surface elevation was determined while measuring flow velocity during two instances using a tachometer or an electronic distance meter (EDM).

The morphological characteristics and bed changes from the gorge to the confluence with the South Branch were documented along 40 km in 7 aerial photography strips taken between 9 November, 1985 to 3 April, 1986. Photographs were taken from a light aircraft at ca. 1500 m above sea level using 35 mm cameras with a focal length of 55 mm (35 mm in one instance). Photographs were near vertical with 5-70 percent overlap. Average scale, calculated from distances between benchmarks, is accurate to  $\pm 5$  percent. The enlarged photographs were used to prepare 1:1000 maps of the study reaches.

Altogether 17 cross sections in the upper reach and 24 in the lower reach were surveyed with a tachometer or EDM before event 1, as well as after events 1,2,3 and 6. The survey parties paid particular attention to significant breaks in slope, to channel banks, to the average bed elevation between or on top of bed particles and to survey all the minor channels. The survey data was transferred either manually or else directly from the EDM electronic field 'notebook' to a programme that allows drawing the cross sections as well as calculation of volume changes between sections (Ibbitt and Duncan, 1985).

Surface texture was determined using a number by number method (Wolman, 1954) described by Mosley (1982), also identifying particles in ranges 2-8 mm and  $< 2$  mm. Surface samples consisted of 100 particles, except bar transects which involved a double sample size. In addition, 200 samples of subsurface bed material were taken from scour chain holes (see below). Each sample weighed about 40 kg and was taken from a depth of 0.2-0.8 m. Boulders (perhaps  $> D_{95}$ ) were unfortunately discarded in the upper reach because they were dangerously large to deal with during the operation with the excavator. Samples from the upper and lower reaches were separately combined in two ca. 4 T heaps, mixed, sampled as required for such coarse material (Church, et al., 1987) and sieved separately.

Magnetic tracer particles, approximately in the  $D_{50}$ - $D_{95}$  size range of the subsurface, were used to evaluate the direction and quantity of bedload (Laronne et al., 1986) and its relationship to bedform development. The original method (Hassan, et al., 1985) was slightly changed to enable detection to a depth of 0.9 m below the surface. This was accomplished by inserting two magnets into every particle. The tracers were sprayed with abrasion resistant yellow paint, numbered on both sides, weighed and their size was measured. Particles were randomly chosen and placed at scour chain positions 30 cm below the surface as well as several on the surface. A total of 534 tracers were placed in the upper reach and 436 in the lower reach.

On location, the depth of burial was measured from the surface to the top of the tracer and location was determined by surveying or tape. Following recovery, the particles were placed in the position where they had been found.

#### Bed material size.

Spatial variations in the texture of surface material are inherent to gravel beds (e.g., Laronne and Carson, 1976; Mosley and Tindale, 1985; Church et al., 1987). We identified five large, distinct textural assemblages: the surface of main anabranches, the average bar surface or bar transect, patches of coarser and finer sediment on bar surfaces and the subsurface (Table 1).

The median particle size on bars ( $D_{50}$ ) is 25 percent smaller in the narrow reach, or 30.6 percent smaller when comparing the median from a distribution that excludes sand.  $D_{84}$  and  $D_{95}$  decrease even more between the reaches, implying selective deposition and some wear downstream. The surface of all the active channels (i.e., excluding the plugged and infilled ones) is coarser than that of adjacent bar areas as it is defined by the median size of the surface material. The surface of the lower reach is coarser than 70 mm in the upper reach. This conforms to many observations of coarse surface layers termed pavement or armour (e.g., Church, 1972; Profitt, 1980; Parker and Klingeman, 1982; Gomez, 1984). The banks of anabranches are often as coarse or coarser than the respective armoured beds. The average texture of the bar surface is similar to that of the subsurface. The median of the subsurface appears to be similar in both reaches, but this is misleading because excluded boulders were only present in the subsurface of the upper reach.

Table 1. Bed material size statistics (mm) from different bed areas.

	Including sand upper reach	Including sand lower reach	Excluding sand upper reach	Excluding sand lower reach
<b>Bar traverse</b>				
D50	28	21	34.3	23.8
D84	74	52	93.7	49.9
D95	137	74	142	81.6
<b>Coarser patches</b>				
D50	34	39	36.8	38.3
D84	82	69	78.8	71.5
D95	128	95	128	104
<b>Main channel</b>				
D50	65	39	64.9	54.9
D84	119	74	119	68.6
D95	181	99	181	99
<b>Finer patches</b>				
D50	23	17	23.4	17.1
D84	47	37	47.8	35.0
D95	74	56	76.1	49.5
<b>Subsurface</b>				
D50	21*	21	25*	25
D84	64*	64	75*	69
D95	147*	112	181*	~104

\*Had boulders been included, the entire distribution would have shifted considerably; D95 (incl. sand) of the subsurface may have been ~250 mm.

#### Flow events and hydraulics

Table 2 summarises characteristics of flow events 1-6. Flow event 2 consisted of a discharge of  $6.5 \text{ m}^3 \text{ s}^{-1}$  plus a  $24 \text{ m}^3 \text{ s}^{-1}$  constant inflow from the RDR, which discharges into the river below the Old Weir site. The RDR discharged water into the N. Branch about weekly, usually less than  $10 \text{ m}^3 \text{ s}^{-1}$ . There was a 24 percent transmission loss between the study reaches during the first, smallest event but the losses were insignificant in all succeeding events (Laronne and Duncan, 1990). The first three events were relatively minor, event 3 being a compound hydrograph comprised of two individual, almost equal rises within three days. Based on the flood frequency curve of the river (Laronne and Duncan, 1990), events 1, 2 and 3 recur on average more than five times per year, and the recurrence intervals of events 4-6 are 6 months, 4 months and 3 years, respectively.

The hydraulic character of flow in the study reaches, as well as in an intermediate reach at Thompson's Track Bridge, are presented in Table 3. Additional hydraulic measurements are presented elsewhere (Laronne and Duncan, 1990). Flow direction is not listed in the table, but critical observation of flow direction at the water surface and 0.6 depth by the gauging parties showed that in all instances except event 1, flow direction in the lower reach was essentially

downchannel, parallel to the general alignment of the reach, and it was parallel to anabranch alignments in the upper reach. The upper reach contained many areas that were neither boatable (too shallow) nor wadeable (too fast) during event 5, an experience shared by Davoren and Mosley (1986), so that additional attempts to gauge it were relinquished. We attempted to gauge the lower reach also during the larger event 6, but standing waves 0.9 m high and shallow depth on bars allowed only partial gauging.

Table 2. *Hydrograph characteristics of North Branch Ashburton River at Old Weir.*

Flow event	Date	Peak discharge ( $\text{m}^3 \text{s}^{-1}$ )	Time to peak (hr)	Bedload Duration <sup>c</sup> (hr)
1	2.12.85	18	16	37
2	11-12.12.85 <sup>a</sup>	31	1	14
3	22.12.85	25	13	14
	25-26.12.85	23	38	74
4	16-17.02.86	58	14	47
5	25.02.86	47	15	66
6	13-14.03.86	173 <sup>b</sup>	32	155

<sup>a</sup> At the upper study reach, flow due to release from RDR.

<sup>b</sup> At least  $207 \text{ m}^3 \text{s}^{-1}$  at Thompson's Track Bridge.

<sup>c</sup> Duration of flow above  $12 \text{ m}^3 \text{s}^{-1}$ , which is the estimated threshold discharge for bedload transport in the lower reach; see Laronne and Duncan (1990) for details.

The water width in the upper reach included many small channels, which complicates analysis of average hydraulic values. It demonstrates the inapplicability of using average sectional values to multiple thread rivers, where only part of a section may be actively transporting sediment (Carson, 1986). For instance, in the upper reach during event 1 the hydraulic radius, computed for all the channels, increased only slightly from the bar head and bar centre (U1 and U4) to the bar tail (U6), where a deep confluence scour pool contained most of the discharge. The depth at the confluence pool was 2.3 times larger than that at the anabrach thalwegs further upstream and flow velocity was also considerably larger, differences masked in average sectional values. Self evidently, the average unit power and shear stress in the pool were considerably larger than the values in Table 3. A similar situation occurred during event 2, at which time the scour pool had undergone incipient filling.

The number of channels conveying water did not alter appreciably as long as bars were not submerged. Because both reaches have been confined, the number of channels decreased to a single, submerged bed during small events (such as event 3) in the lower reach and during larger ones in the upper reach. Hence, the extent of braiding is not constant in confined reaches as it is in natural, braided ones (Mosley, 1982). Average and maximum hydraulic values during events 1, 2 and 5 increased with increase in discharge at both reaches. These responded in a different manner: depth increased much more in the narrow reach whereas velocity increased more in the upper reach. At Thompsons Track Bridge the response was intermediate, noting that the data for the bridge derives from the large event. A marked decrease occurred in the spatial gradients of maximum depth, velocity and Fr within the upper reach as discharge increased. These gradients were attenuated in the lower reach during event 1 due to transmission losses.



Table 2. Hydraulic character of selected North Branch Ashburton River measured cross sections at the stud reaches and Thompson's Truck bridge.

section # of active channels	level	Q (m <sup>3</sup> /s)	w (m)	R (m)	d <sub>max</sub> (m)	d <sub>umax</sub> (m)	u (m/s)	u <sub>max</sub> (m/s)	Fr	Fr <sub>umax</sub> (-)	Fr <sub>umax</sub> (-)	Fr <sub>umax</sub> (-)	Ω (W/m)	Ω <sub>w</sub> (W/m <sup>2</sup> )	ω (cm/s)	τ (N/m <sup>2</sup> )
U1	4	1	18.3	77.0	0.25	0.65	0.5	0.93	1.6	0.59	0.81	0.81	2050	26.8	1.09	28.2
U4	3	1	19.0	76.1	0.25	0.64	0.5	1.11	1.8	0.71	0.81	0.81	2110	28.2	1.15	28.2
U6	4	1	17.8	43.9*	0.31	1.50	1.5	1.29	2.6	0.74	0.68	1.00	2040	45.7	1.50	35.0
U2	2*	2	31.7	35.0*	0.52	1.00	1.0	1.72	2.6	0.76	0.88	0.88	3510	102	2.00	58.6
U4	3	2	31.4	77.9	0.32	0.67	0.6	1.25	2.4	0.71	0.88	0.88	3510	45.5	1.45	36.1
U6	6	2	30.1	86.7	0.25	1.30	1.3	1.38	2.9	0.88	0.81	0.86	3310	39.2	1.60	28.2
U2	3	5	51.0	71.4	0.37	1.17	0.7	1.94	1.7	1.02	1.41	1.41	5710	80.6	2.22	41.7
TT1	1	6	207	99.5	0.72	1.48	0.6	2.86	1.4	1.08	1.18	1.90	18010	182	2.51	62.8
TT3	2	6	40.7	65.6	0.46	0.80	0.7	1.33	1.2	0.38	0.84	1.01	3510	54.2	1.20	40.2
L2	3	1	12.1	34.1	0.29	0.70	0.7	1.20	1.8	0.71	0.69	0.69	817	25.4	0.89	20.8
L4	1	1	14.1	16.4	0.54	0.70	0.7	1.57	1.1	0.73	0.71	0.77	1010	61.6	1.16	38.7
L6	1	1	14.3	40.5	0.43	0.75	0.5	0.82	1.7	0.65	0.70	0.70	1010	25.3	0.60	30.8
L2	2	2	30.1	37.2	0.41	0.76	0.7	0.85	1.3	0.42	0.88	0.91	2110	24.7	0.62	29.4
L4	3	2	30.0	50.5	0.37	0.85	0.8	1.33	1.0	0.70	0.76	0.99	2110	35.5	0.98	26.5
L6	1	2	34.2	36.0	0.32	1.60	1.6	1.22	1.1	0.69	0.81	1.14	2410	28.5	0.91	22.9
L6	1	5	16.9p	10.8+	0.30	0.75+		1.37		0.80			1210	29.7	1.01	21.5
L6	1	6	45.6p	16.0+	0.81	1.20	1.2	1.49	1.7	0.53	0.50	0.51	3210	90.7	1.14	58.0

The symbols at the head of the table denote the following hydraulic parameters:

\* excluding LB minor channels; Q = water discharge; p denotes partial cross section; w = water surface width R = hydraulic radius averaged for all channels in section; d<sub>max</sub> = maximum depth; d<sub>umax</sub> = depth of maximum velocity; u = average flow velocity; u<sub>max</sub> = maximum flow velocity; Fr = u/(gd)<sup>0.5</sup> cross sectional averaged Froude number; Fr<sub>umax</sub> = Froude number at vertical where average velocity is highest; Fr<sub>max</sub> = cross sectional maximum Froude number; Ω = γQS power per unit length ω<sub>w</sub> = γQS/w power per unit width or bed area; ω = Ω/γRv = uS unit power; τ = γRS average shear stress at section; S = average longitudinal bed slope (see Ironne and Duncan (1990) for comparison of S with the local water surface, energy and bed slopes).

### River bed changes

#### The upper reach

Fig. 3 incorporates a series of 7 maps of the upper reach. The discharge at the Old Weir is noted in each map in order to evaluate the extent of braiding without reference to base flow conditions. During event 1 only small changes occurred: the RB channel between U2 and U3 slightly eroded its right bank, erosion which persisted during event 2, continued in event 3 and was the causal mechanism for the partial avulsion; the formation of the channel in the far RB during event 4. This secondary anabranch deepened in event 5. The small channel realignment at U2-U3 during event 1 brought forth a slight left hand course of the RB main channel at U3-U4 during event 2, ultimately causing RB erosion at U4-U5 and the cutoff at U6 during event 3. The LB main anabranch was slightly plugged at U2 after event 2, and remained fossilised thereafter until it was almost completely plugged at U1-U2 during event 5 and infilled during event 6.

The previous sequence of events shows that small amounts of bed reworking and channel adjustment may ultimately cause major changes in location of braids and extent of braiding. Comparing Fig. 3a,b,f and g (note that flow discharge was similar in Fig. 3b and 3f) demonstrates what appear to be two general changes of the braided bed. Some anabranches are abandoned, at times they are plugged at their upper or lower edge, but they are not infilled as additional, rather small events (1-5) recur. It follows that the bed becomes more braided (by adding new anabranches which cut across bars of various sizes and heights) as long as massive overbank flow does not take place. During smaller events channels are realigned and appear to retain the general low sinuosity of 1.1. Overbank flow during a major event and rapid avulsion of the main channel brought about activation of most of the bed, infilling of previous anabranches and the formation of new ones (Fig. 3g-f).

The succession of events leading to bar reworking is also depicted in repeat cross sectional views (Fig. 4a-c) of U2, U4 and U6. At U2 the LB main anabranch remained essentially unchanged while the RB anabranch actively eroded its banks during events 1-3, with total reworking of the river bed, including massive scour and till during events 4-6, essentially event 6 (Fig. 4a). A similar succession of events occurs at U4 (Fig. 4b). The confluence scour hole at the bar tail was still present after event 1 (Fig. 4c), but the cutoff had begun by eroding the slight protrusion to the right hand of the hole. Most of the hole has filled by the end of event 2 while a similar volume of reworked bank had been eroded in the new channel after event 3. Erosion of high, protruding bar tops and massive deposition was also prevalent at this site during event 6. In summary, it appears that reworking occurred during all the events but new bars were formed only during the large event, when flow occurred on bar tops rather than in anabranches with armoured beds and banks.

The preferred location of deposition sites is demonstrated by areas of fill in plan and sectional views, but also from tracer transport. Tracer location in the upper reach is depicted after each event in Fig. 5. Almost all tracers had not moved during events 1-5 on the higher bar platforms. Some particles were transported considerable distances in the LB channel during event 1 (Fig. 5a). They were apparently unstable originally because of protrusion and lack of interlocking (Laronne and Carson, 1976; Fenton and Abbott, 1977; Brayshaw et al., 1983). The RB anabranch could not be searched due to relatively deep flow and the short interval between events 1 and 2. The lines shown in Fig. 5b are not tracer trajectories but simply connect tracer location sites before and after event 2. In fact, the central bar was not overtopped at all during events 1-5, so that it is evident that tracer trajectories must be parallel to and within the anabranches. In the LB branch tracers moved 50-100 m, and most of them remained immobile during events 3-4 and moved an additional distance of 50-100 m during event 5. In the RB branch distances of transport were much larger and, in fact, no tracers were found between sections 1-4 because all had moved in the channel to the stoss, tail of the bar. They were preferentially deposited at the bar head located downstream from U6. During event 3 some of the tracers at the bar head moved slightly to form a bulge or plug at the upstream end of the LB channel. Insufficient evidence is available on transport during event 4 and 5, but it is apparent

that flow velocities were sufficient to remold the protected, LB side of the river bed which had been inactive hitherto. This conclusion is derived from the fact that the tracers were lost downstream or under a fill exceeding 1 m. It is apparent, though, that the previous longitudinal bar had been eroded, and bed material from the bar platform had been moved downstream more than twice the length of the large, longitudinal bars. The shorter distances of tracer transport near the outside banks demonstrate a parallel downriver movement.

### The lower reach

Fig. 6 incorporates a series of 7 maps of the lower reach. Although event 1 had a low peak discharge, the hydrograph rise and fall were prolonged, allowing considerable change to take place in the lower reach (Fig. 6a and b). The main channel at L1-L2 upstream of the RB alternate bar became plugged at this location, a process which culminated in channel infilling during events 2 and 3 (Fig. 6c and d). The main body of the alternate bar was only slightly molded because flow depth was minimal on the bar platform. Nevertheless, the platform was mobilised during the succeeding, artificial event because peak flow was greater even though the time base for bedload transport was short (see Table 2). During event 3 both channels were filled at L1-L4 (Fig. 6d) and two new alternate bar, significantly longer than the previous ones, were formed during event 4. The entire bed was remolded creating brand new bars not only during the largest event but also during event 5 (Fig 6f-g).

The sectional views of the lower reach offer just as convincing evidence (Fig. 7 a-c). At L2, the alternate bar head, the channels filled as much as 1 m and some reworking also occurred on the bar tops (Fig. 7a). Event 2 was capable of remolding the entire bed, with massive erosion and deposition of 0.5 thick sediment wedges during event 3, and total channel change during the succeeding events. Minor changes took place during the first event at the centre of the alternate bar platform due to some bank protection and low peak discharge, more during the second when a central channel had incised into the bar, considerably in the outer bar areas during event 3 and totally during the next events (Fig 7b). The bar unit (section L6, Fig. 7c) behaved in a manner similar to the bar head but bed activity was mirrored to the opposite bank.

Tracer location after events 2, 3, and 6 are depicted in Fig. 8a-c. Only few tracers were found after event 4, so these locations were omitted herein. The short interval of time between events 1 and 2 precluded locating tracers in this reach. Although the lines in Fig. 8a are not all transport trajectories, the shorter ones at L1 and downstream of L6 are assumed to be trajectories on bar platforms. Particles originating at the RB of L2 and L3 appear to have moved along the curved channel and deposited at the top and centre of the next alternate bar. After event 3 many tracers were located. The lines depicted in Fig. 8b involve transport during events 1-3. It is evident that many particles were transported along lines approximately parallel with the general alignment of the river, crossing a part or all the upper alternate bar to be deposited anywhere along the route. The data from event 4-6 is very meagre, but shows that distances of bedload transport were considerable.

### Summary

The evidence presented in this paper reinforces previous suggestions that small events rework bars but may also bring about large changes such as cutoffs, avulsion of the main anabranch and channel switching (Werritty and Ferguson, 1980; Ferguson and Werritty, 1983; Ashworth and Ferguson, 1986; Ashworth, 1987). Additionally, it is apparent that new bars may be formed and that the entire bed may be molded by events of small magnitude provided that bar platforms are sufficiently submerged to allow higher velocities to develop on the platforms. It does not, though, point towards decreased aggradation within such confined reaches (Carson and Griffiths, 1987; Davies and Lee, 1988; Laronne and Duncan, 1990). Flow direction is not listed in the table, but critical observation of flow direction at the water surface and 0.6 depth by the gauging parties shows that in all instances except event 1, flow direction in the lower reach was essentially downchannel, parallel to the general alignment of the reach, and it was parallel to anabranch alignments in the upper reach. The upper reach contained many areas that were neither

boatable (too shallow) nor wadeable (too fast) during event 5, so that additional attempts to gauge it were relinquished. We attempted to gauge the lower reach also during the larger event 6, but standing waves 0.9 m high and shallow depth on bars allowed only partial gauging.. 1987; Laronne and Duncan, 1990). It is also apparent that the lack of a very coarse armour in the bed and banks of the inner channels enables large channel changes to occur during small events.

Bedload moves totally within anabranches and may diverge on bar heads during smaller events. It appears that most bed material is transported on top of bar platforms parallel to the river banks during formation of new bars. This favours a mechanism of bar (both alternate, point-type and medial bar) formation during high stages of flow due to advance of sheets or lobes. The occurrence of some gravel sheets a-la-Hein (1974) in the upper reach after event 6 and the particular character of massive deposition of wide, tabular matrix and somewhat clast supported sheets in the lower reach (Laronne and Duncan, 1989b) also lend support to the notion of sheet or lobe advance.

Self evidently, the formation of bars is directly interrelated with hydraulics and sediment transport. The actual changes in bed elevation derived from scour chains, the sedimentology of the deposited bed material as well as bedload sampling undertaken in this project will be presented elsewhere.

**ACKNOWLEDGEMENTS** We thank Paul Mosley for his invaluable assistance at various stages. Heather Pearce, Richard Roberts and particularly Paul Rodley carried out the bulk of the field work and data collation. We are indebted to a large number of individuals, too many to name individually, who helped in this project. Special thanks are extended to Michael Leehee and the South Canterbury Catchment Board for assistance and to the Department of Geography, University of Canterbury, for the hospitality to LBJ. This project was funded by the Ministry of Works and Development, New Zealand.

#### REFERENCES

- Ashmore, P.E. (1982). 'Laboratory modelling of gravel braided stream morphology.' *Earth Surf. Proc. and Landforms*, 7, 201-225.
- Ashmore, P.E. (1985). 'Process and form in gravel braided streams: Laboratory modelling and field observations.' *Unpubl. Ph.D. dissertation*, Dept. of Geogr., Univ. of Alberta, Edmonton, 414 pp.
- Ashmore, P.E. (1987). 'Bedload transfer and channel morphology in braided streams. Erosion and Sedimentation in the Pacific Rim. Proc. Corvallis Symp., *Int'l Assoc. Hydrol. Sci.*, Publ.165, 333-341.
- Ashworth, P.J. (1987). 'Bedload transport and channel change in gravel-bed rivers.' *Unpubl. Ph.D. dissertation*, Env. Sci. Dept., Univ. of Stirling, Stirling, 352 pp.
- Ashworth, P.J. and Ferguson, R.B. (1986). 'Interrelationships of channel processes, changes and sediments on a proglacial river.' *Geogr. Annlr*, 68, 361-371.
- Brayshaw, A.C., Frostick, L.E. and Reid, I. (1983). 'The hydrodynamics of particle clusters and sediment entrainment in coarse alluvial channels.' *Sedimentol.*, 30, 137-143.
- Carson, M.A. (1986). Transport of gravel in alluvial channels. A review with special reference to the Canterbury Plains, New Zealand.' *N. Canterbury Catchment Board and Reg. Water Board*, Christchurch, 299pp.
- Carson, M.A. and Griffiths, G.A. (1987). 'Influence of channel width on bed load transport capacity.' *Jour. of Hydraul. Eng.*, 113(12), 1489-1509.
- Church, M.A., McLean, D.G. and Wolcott, J.F. (1987). 'River bed gravels: sampling and analysis.' p. in Thorne, C.R., Bathurst, J.C. and Hey, R.D. (eds.): *Sediment Transport in Gravel Bed Rivers*, Wiley, Chichester, 880p.
- Church, M. and Jones, D. (1982). 'Channel bars in gravel bed rivers.' p. 291-338 (incl. discussions) in Hey, R.D., Bathurst, J.C. and Thorne, C.R. (eds.): *Gravel Bed Rivers*, Wiley, Chichester, 857pp.

- Davies, T.R.H. and Lee, A.L., (1988) 'Physical hydraulic modelling of width reduction and bed level change in braided rivers. *Jour. of Hydrol. (NZ)*, 27, 113-127.
- Davoren, A. and Mosley, M.P. (1986). 'Observations of bedload movement, bar development and sediment supply in the braided Ohau River.' *Earth Surf. Proc. and Landforms*, 11, 643-652.
- Fahnestock, R.K. (1963). 'Morphology and hydrology of a glacial stream, White River, Mount Rainier, Washington. *U.S. Geol. Surv. Prof. Paper*, 422-A, 70 pp.
- Ferguson, R.I. and Werritty, A. (1983). 'Bar development and channel changes in the gravelly River Feshie, Scotland.' p. 181-193 in Collinson, C.D. and Lewin, J. (eds.): *Modern and Ancient Fluvial Systems*, *Int'l Assoc. Sedimentol.*, Publ. 6, Blackwell, Oxford.
- Fenton, J.D., and Abbott, J.E. (1977) 'Initial movement of grains on a stream bed: the effect of relative protrusion.' *Proc. Roy. Soc. London, Ser. A*, 352, 523-537.
- Gomez, B. (1980). 'Typology of segregated (armoured/paved) surfaces: some comments.' *Earth Surf. Proc. and Landf.*, 9, 19-24.
- Hitchcock, D. (1977). 'Channel pattern changes in divided reaches: an example in the coarse bed material of the Forest of Bowland. p. 207-220 in Gregory, K.J. (ed.): *River Channel Changes*, Wiley, London, 448pp.
- Hassan, M.A., Schick, A.P. and Laronne, J.B. (1984). 'The recovery of flood dispersed coarse sediment particles. A three-dimensional magnetic tracing method.' *Catena*, Suppl. 5, 153-162.
- Hein, F.J. (1974). 'Gravel transport and stratification origins. Kicking Horse River, British Columbia.', *unpubl. M.Sc. thesis*, Geol. Dept., McMaster Univ., Hamilton, 135pp.
- Hein, F.J. and Walker, R.G. (1977). 'Bar evolution and development of stratification in the gravelly braided Kicking Horse River, British Columbia.' *Can. Jour. Earth Sci.*, 14, 562-570.
- Hoe, T.B. (1989). An examination of the forms and processes associated with bed waves in gravel-bed rivers with special reference to the braided river type. Unpubl. Ph.D. dissertation, Geogr. Dept., Univ. of Canterbury, Christchurch, 287pp.
- Ibbitt, R.P. and Duncan, M.J. (1985). 'RHAP user's guide.' *N.Z. Ministry of Works and Development Soil Science Centre*, Christchurch, Rpt. WS 1013.
- Laronne, J.B. and Carson (1976). 'Interrelationships between bed morphology and bed material transport in a small gravel bed channel'. *Sedimentol.*, 23, 67-85.
- Laronne, J.B. and Duncan, M.J. (1989a). 'Constraints on duration of sediment storage in a wide, gravel bed river, New Zealand.' p. 165-172 in *Sediment and the Environment*, Proc. Baltimore Symp., *Int'l Assoc. Hydrol. Sci.*, Publ. 184.
- Laronne, J.B. and Duncan, M.J. (1989b). 'Formation of clast with overlying matrix supported couplets in gravel bed river deposits.' *Proc. British Sedimentol. Res. Group*, Leeds Mtg., Abstract volume.
- Laronne, J.B. and Duncan, M.J. (1990). 'Dynamics and Morphology of the N. Branch Ashburton River.' *D.S.I.R. Hydrol. Centre*, Publ., Christchurch, forthcoming.
- Laronne, J.B., Duncan, M.J. and Rodley, P.A. (1986). 'Bar dynamics in the North Branch Ashburton River.' p. 230-239 in Smart, S.M. and Thompson, S.M. (eds.): *Ideas on the Control of Gravel Bed Rivers*, *N.Z. Ministry of Works and Develop. Hydrol. Centre*, Pub. 9, Christchurch.
- Leopold, L.B. and Wolman, M.G. (1957). River channel patterns: braided, meandering and straight. *U.S. Geol. Surv. Prof. Paper*, 282-B, 39-85.
- Lewin, J. (1976). Initiation of bed forms and meanders in coarse-grained sediment. *Geol. Soc. Am. Bull.*, 87, 281-285.
- Mahin, M.C.G. (1980). The glacial sequences in the Rangitikei and Ashburton Valleys, South Island, New Zealand. *unpubl. Ph.D. dissertation*, Geogr. Dept., Univ. of Canterbury, Christchurch, 238pp.
- Mosley, M.P. (1982). 'Analysis of the effects of changing discharge on channel morphology and instream uses in a braided river, Ohau River, New Zealand.' *Water Resources Res.*, 128, 800-812.

- Mosley, M.P. and Tindale, D.S. (1985). 'Sediment variability and bed material sampling in gravel-bed rivers.' *Earth Surf. Proc. and Landforms*, **10**, 465-482.
- Moss, A.J., Walker, P.H., and Hutka, J. (1980). 'Movement of loose, sandy detritus by shallow water flows: an experimental study.' *Sediment. Geol.*, **25**, 43-66.
- Moss, A.J., Green P. and Hutka, J. (1982). 'Small channels: their experimental formation, nature and significance.' *Earth Surf. Proc and Landf.*, **7**, 401-415.
- Parker, G., Klingeman, P.C. and McLean, D.G. (1982) 'Bedload and size distribution in paved gravel-bed streams. Jour. Hydraul. Div., Am. Soc. Civ. Eng., 108(JY4), 544-571.
- Profitt, G.T. (1980). 'Selective transport and armouring of non-uniform alluvial sediments.' *Unpubl. Ph.D. dissertation*, Dept. Civ. Eng., Univ. of Canterbury, Christchurch, 203 pp.
- Rundle, A. (1985). 'The mechanism of braiding.' *Zeit. Geomorph., Suppl. Bd. 55*, 1-13.
- Smith, N.D. (1974). 'Sedimentology and bar formation in the Upper Kicking Horse River, a braided outwash stream.' *Jour. of Geol.*, **82**, 205-223.
- Smith, N.D. (1978). 'Some comments for terminology of bars in shallow rivers.' p. 85-88 in Miall, A.D. (ed.): *Fluvial Sedimentology. Can. Soc. Petrol. Geol., Mem. 5*.
- Werritty, A. and Ferguson, R.B. (1980). 'Pattern changes in a Scottish braided river over 1, 30, and 200 years.' p. 53-68 in Cullingford, R., Davidson, D.A. and Lewin, J. (eds.): *Timescales in Geomorphology*, Wiley, London.
- Wolman (1954). 'A method for sampling coarse river-bed material.' *Trans. Am. Geoph. Union*, **35**, 951-956.

### Figure Captions

- Fig. 1 The North Branch Ashburton River Basin, showing the location of the study reaches and gauging locations.
- Fig. 2 Near vertical aerial photographs of the upper study reach (a) and the lower study reach (b).
- Fig. 3 Maps of the upper, wide study reach pre events 1-7 (a-g). The symbols denote identical features in all maps. Observe the location of cross section U1-U6. Map 3a corresponds to Fig. 2a.
- Fig. 4 Resurveys of cross sections at the head of a longitudinal bar at U2 (a), at its centre at U4 (b) and at the downstream end at U6 (c), upper study reach. Vertical exaggeration is 55. Black areas represent scour; dotted ones represent net fill.
- Fig. 5 Tracer locations in the upper reach after events 1-6 (a-f).
- Fig. 6 Maps of the lower, narrow study reach pre events 1-7 (a-g). The symbols denote identical features in all maps. Observe the location of cross sections L1-L2. Map 5a corresponds to Fig. 2b.
- Fig. 7 Resurveys of cross sections at the head of an alternate bar at L2 (a), at its centre at L3 (b) and at the downstream end at L6 (c), lower study reach. Vertical exaggeration is 26.5. Black areas represent scour; dotted ones represent net fill.
- Fig. 8 Tracer locations in the lower reach after events 2,3 and 6 (a-c).

Fig. 1

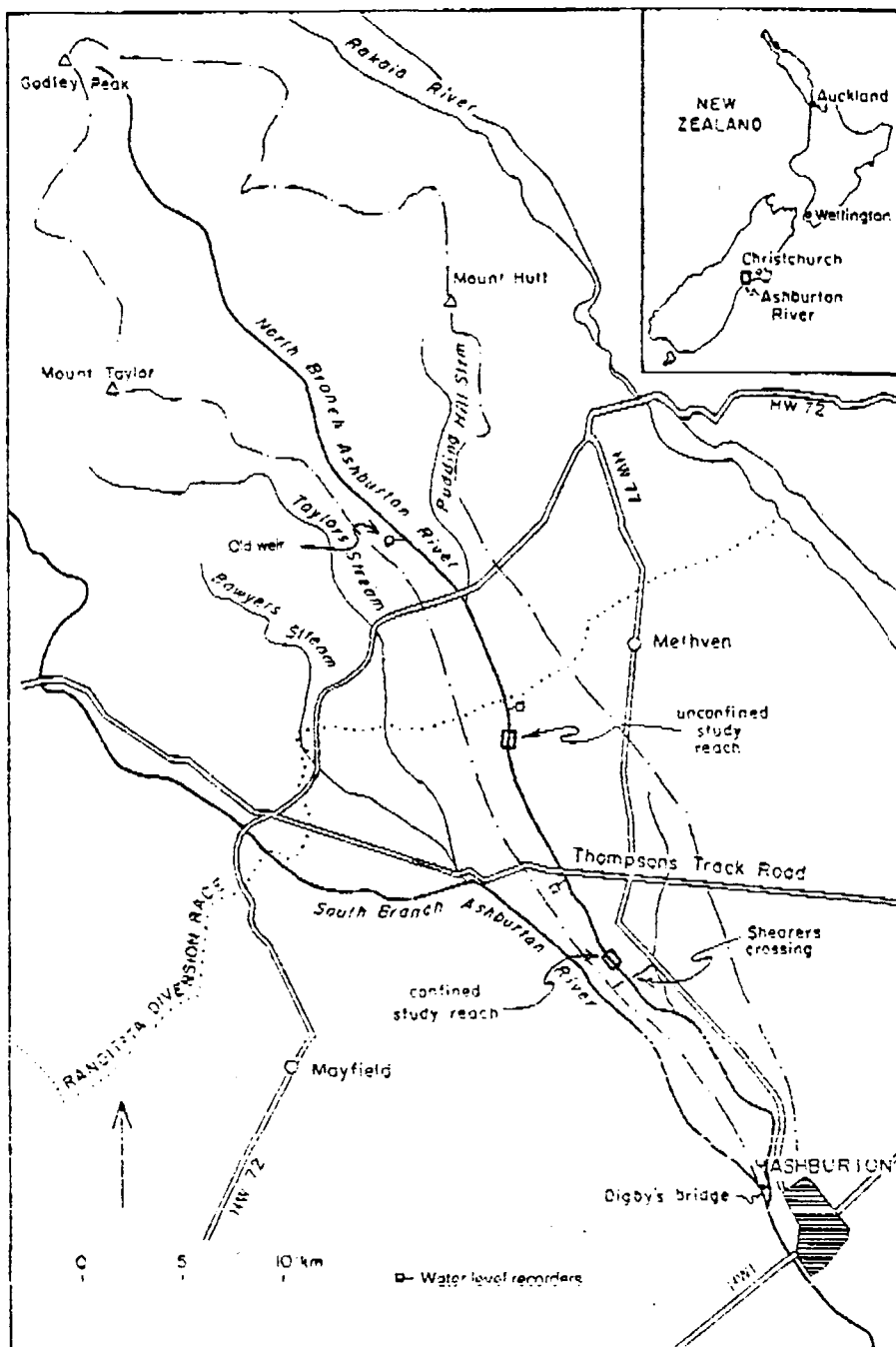
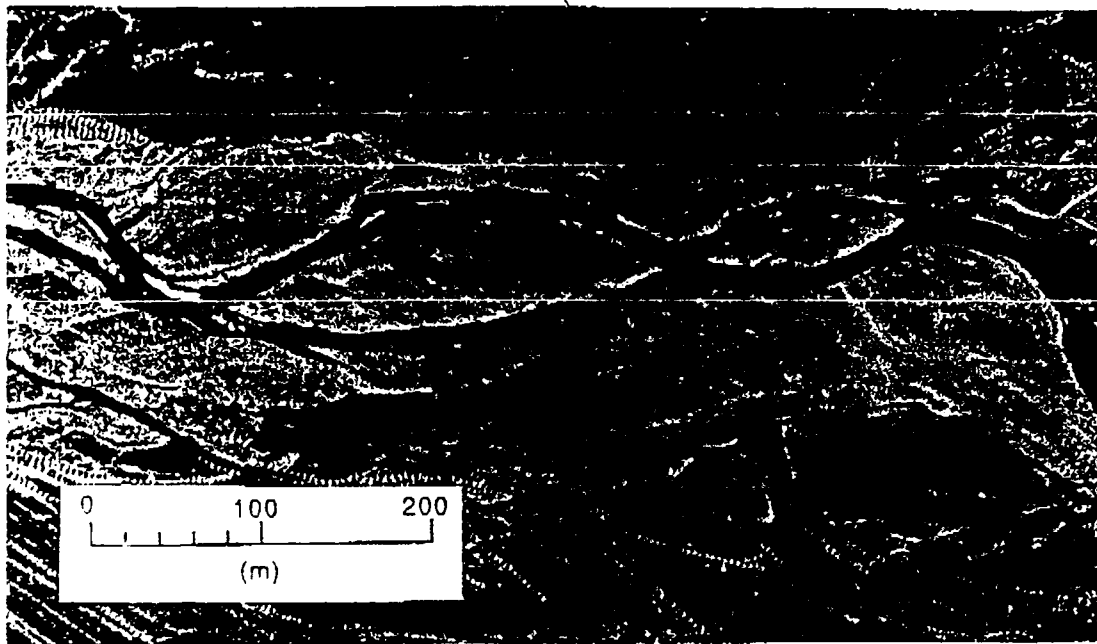


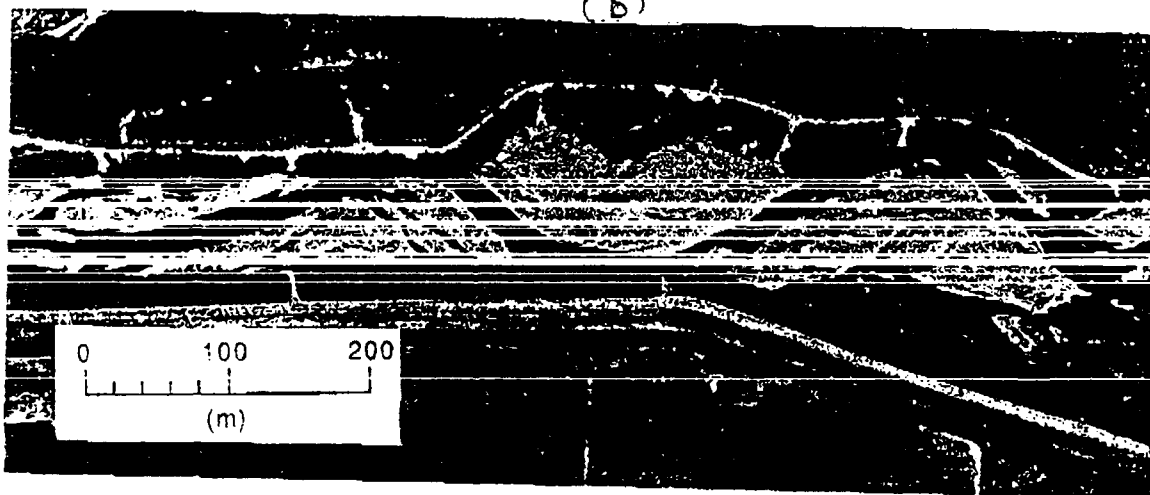
Fig 2

(a)



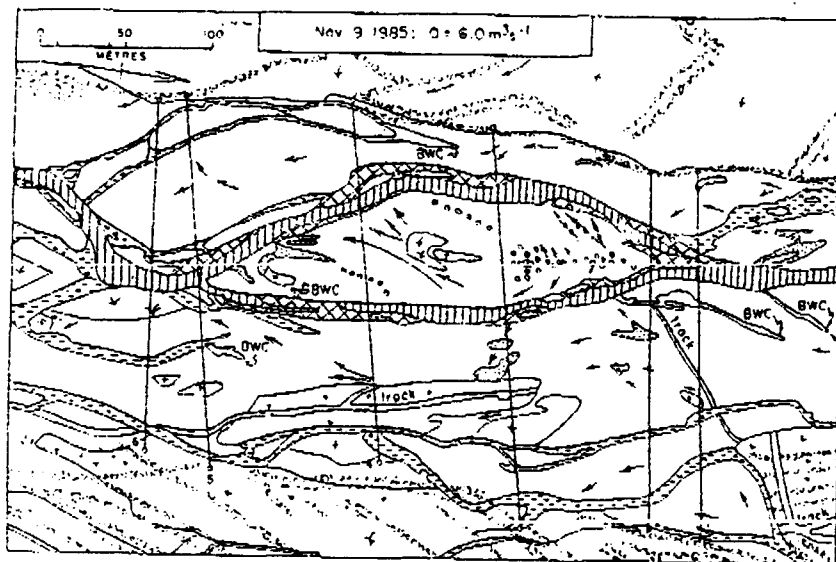
← FLOW

(b)



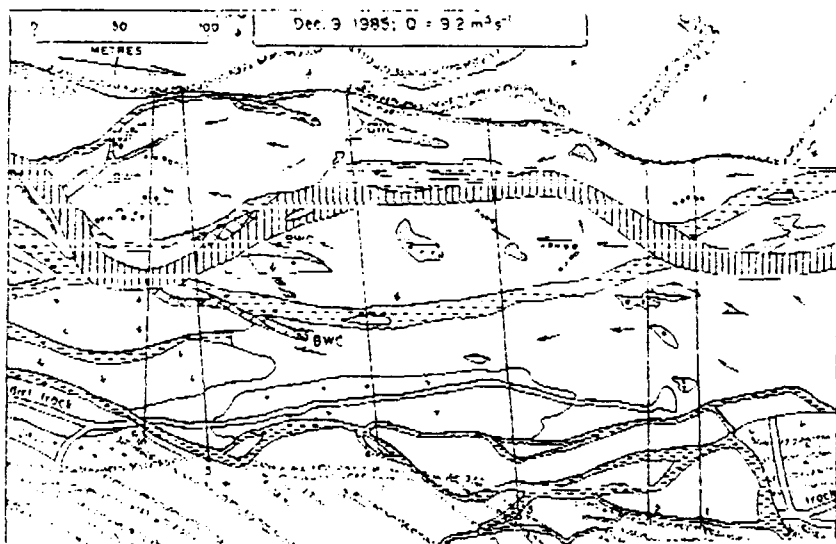
← FLOW



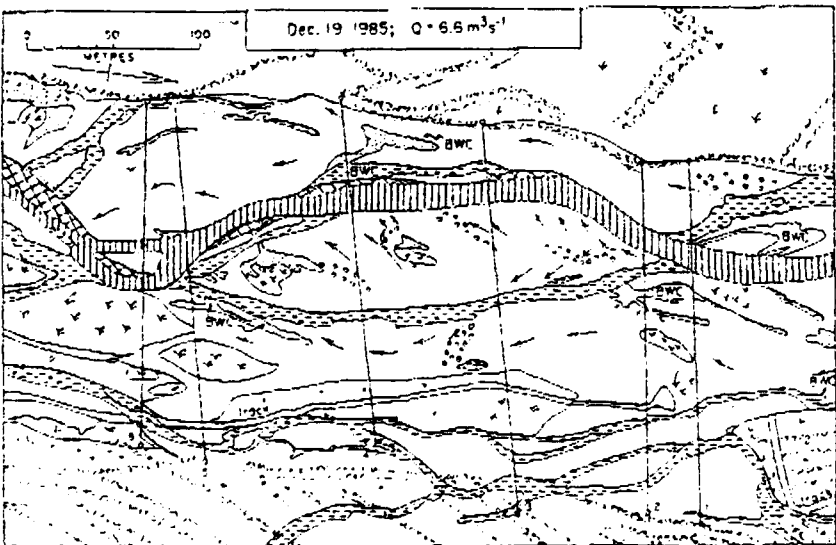


(a)

Fig 3



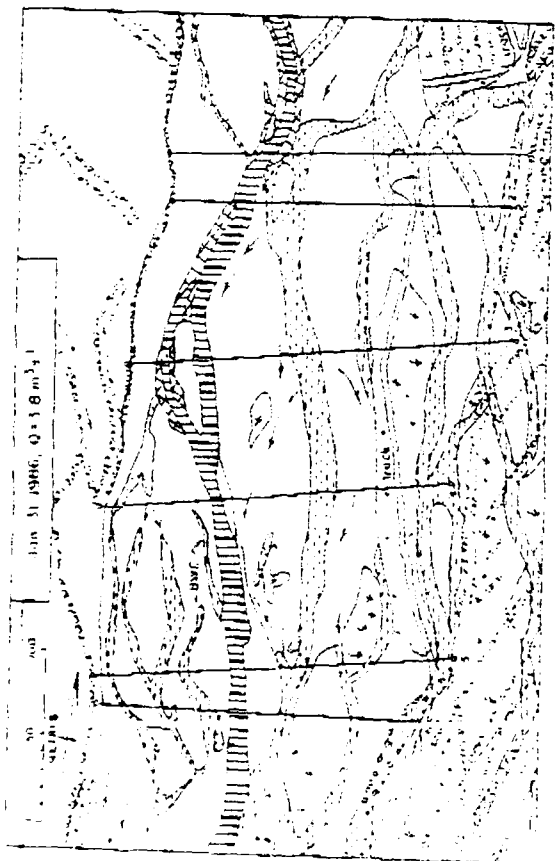
(b)



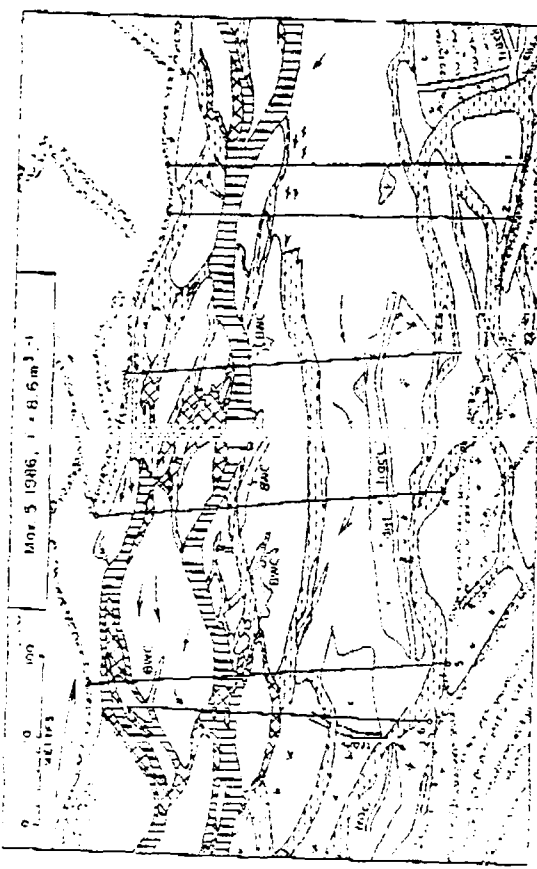
(c)

KEY

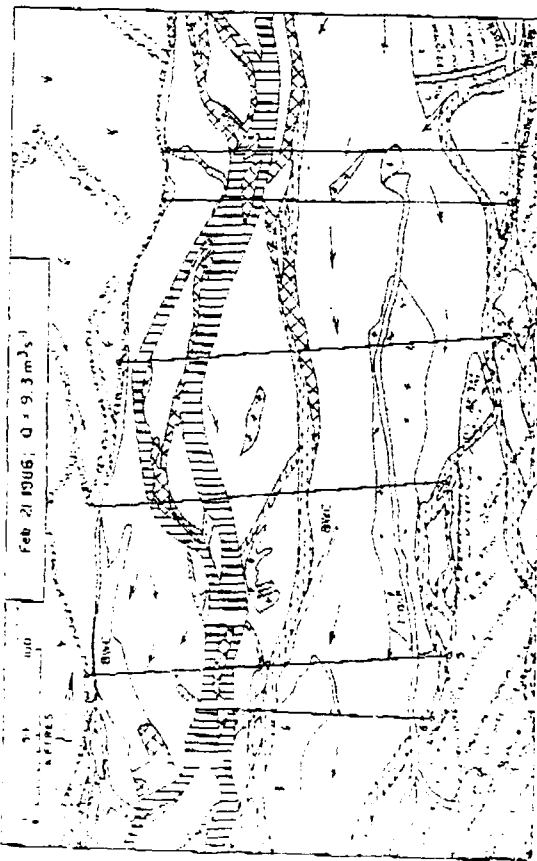
	main channel
	minor channel
	shallow water
	box water channel
	sand
	coarser gravel
	flow direction
	steep bank
	granule-pebble delta
	scour hole
	scour trench
	ground truth marks
	scrub



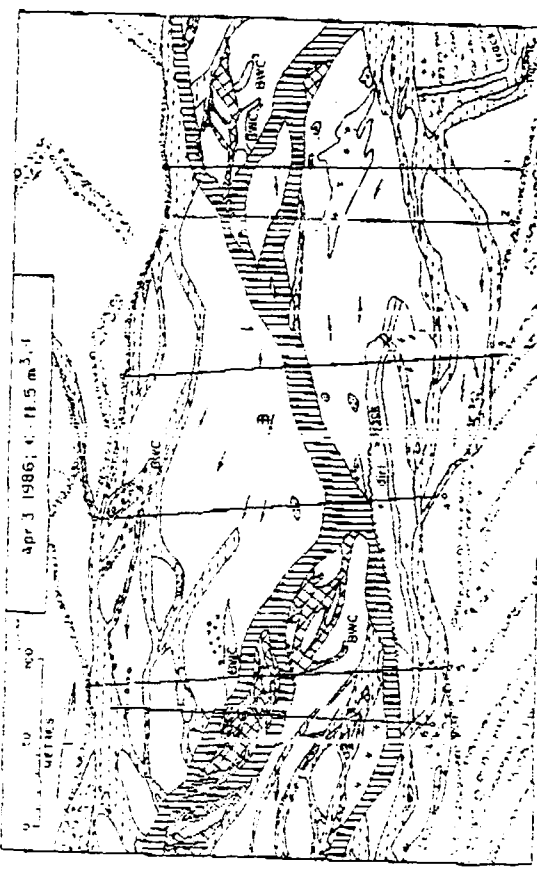
(d)



(c)



(f)



(g)

Fig 3

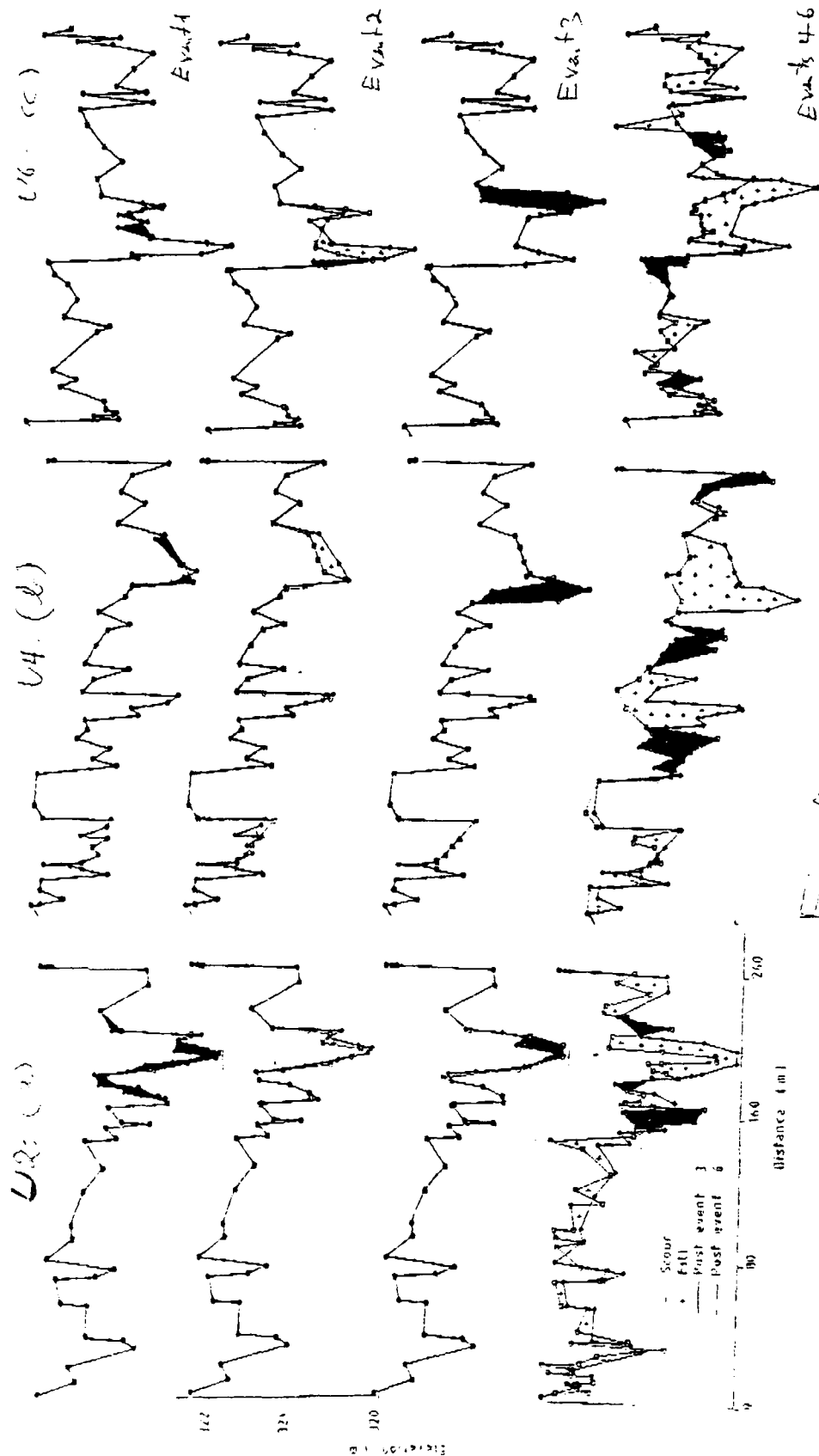


Fig 4

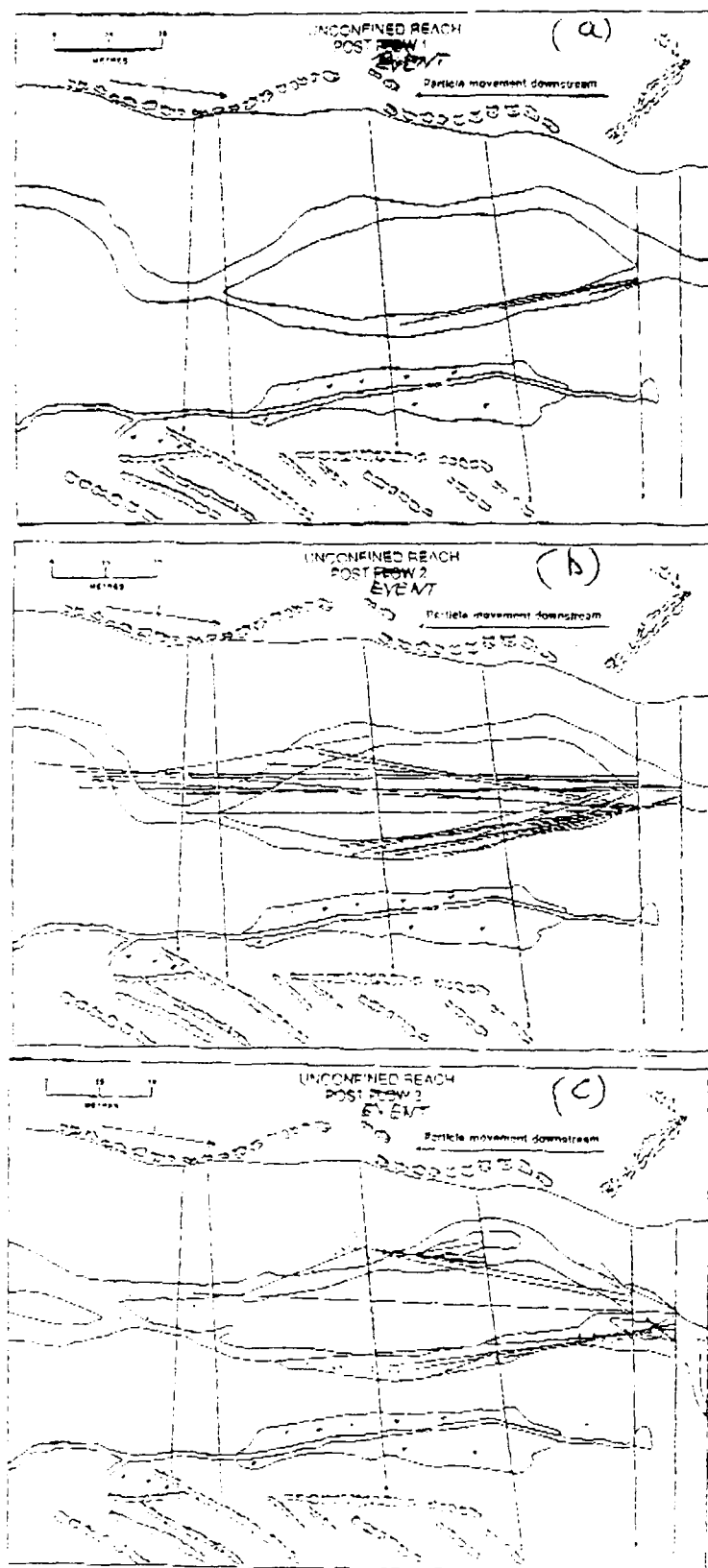


Fig 5

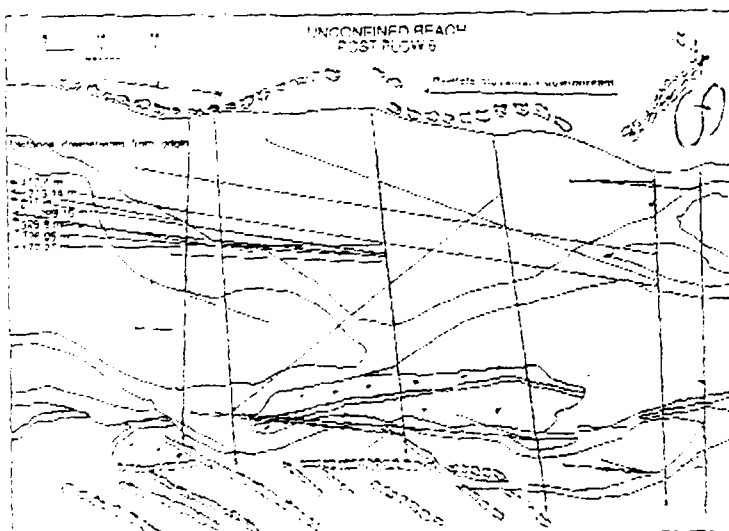
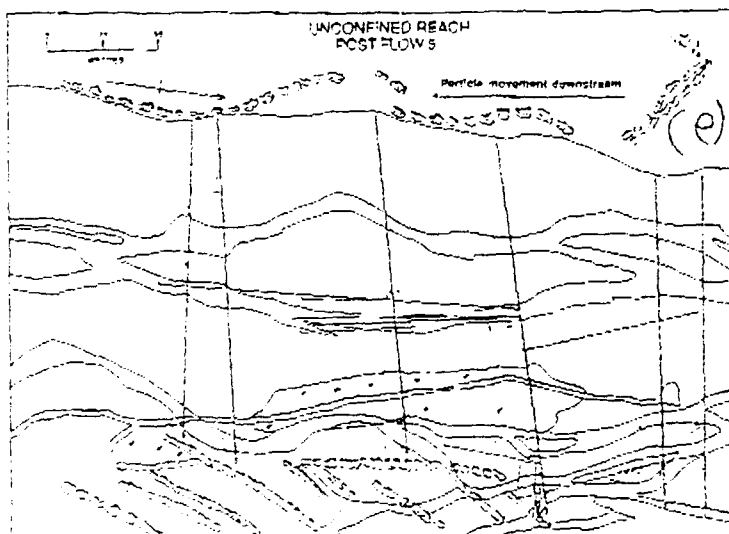
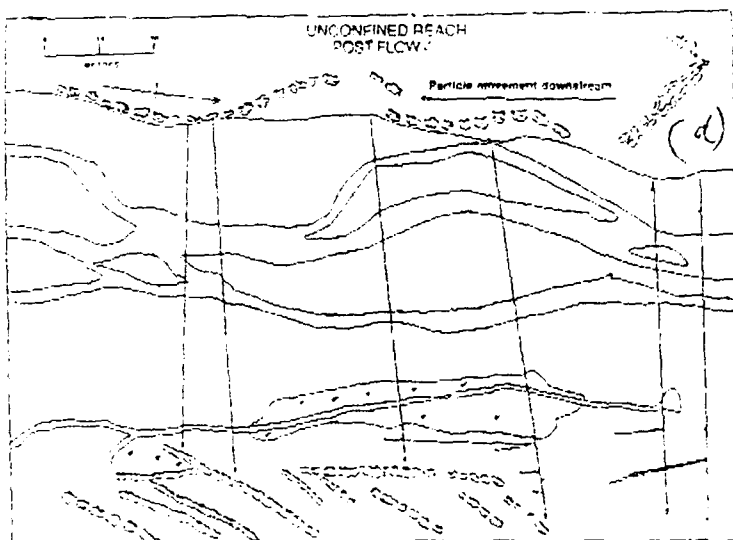


Fig 5

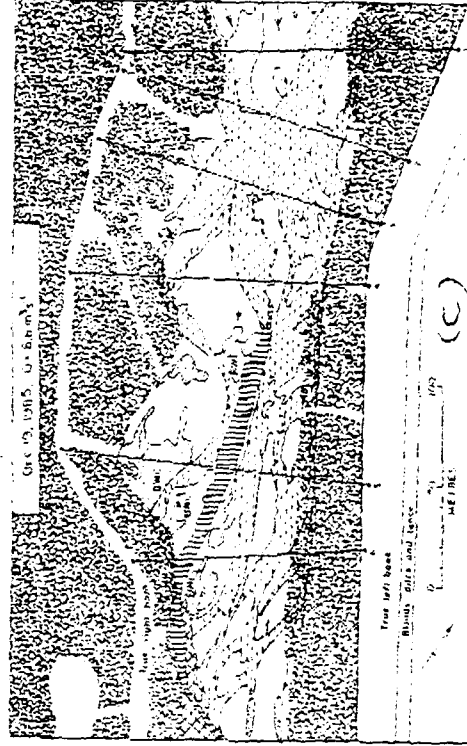
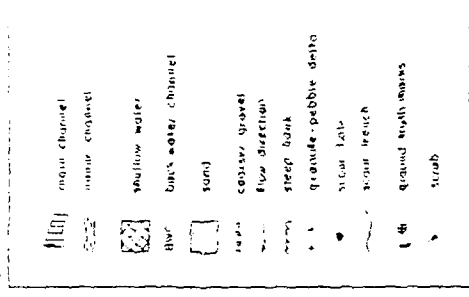
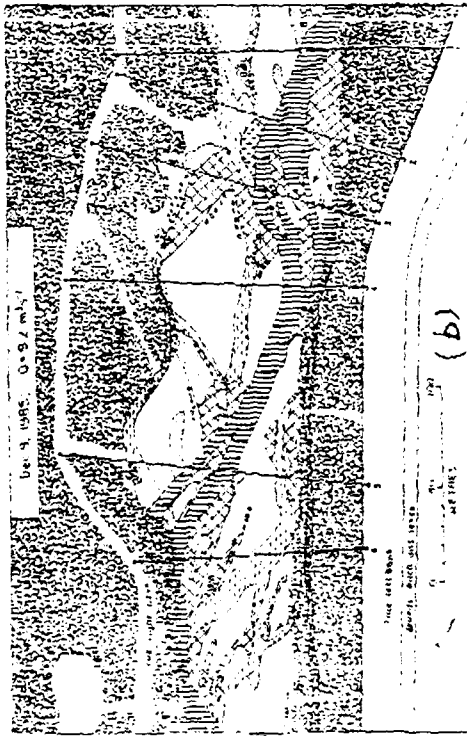
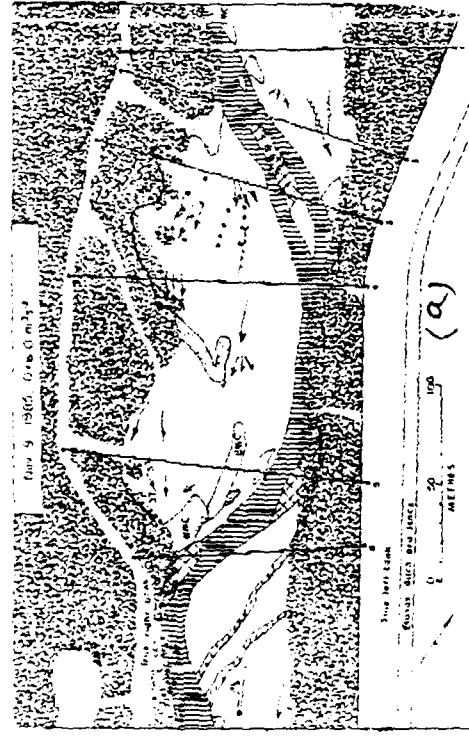


Fig 6

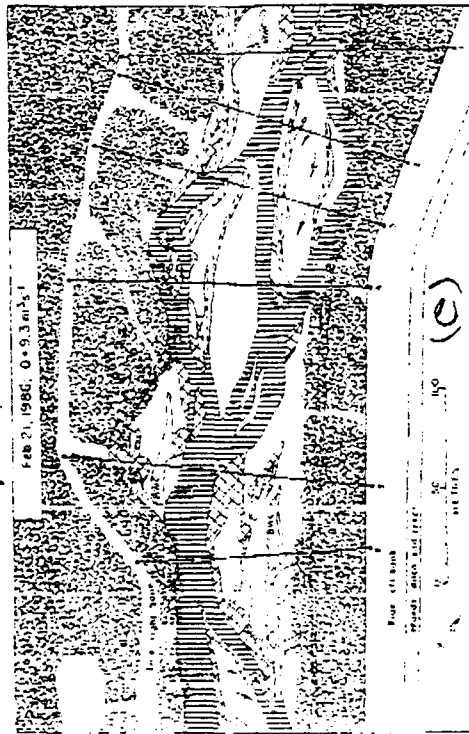
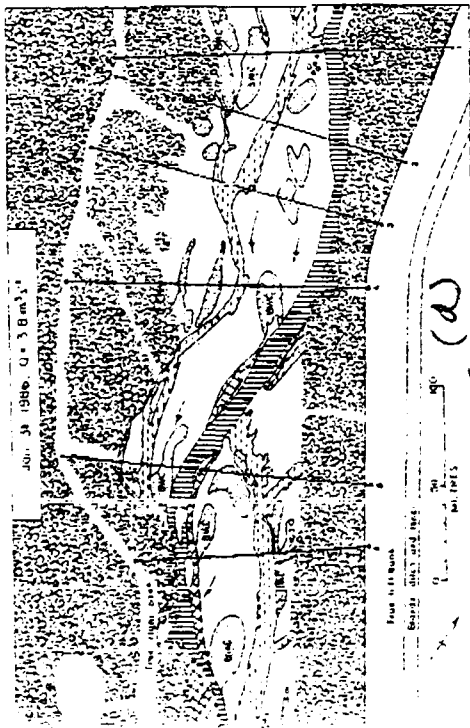
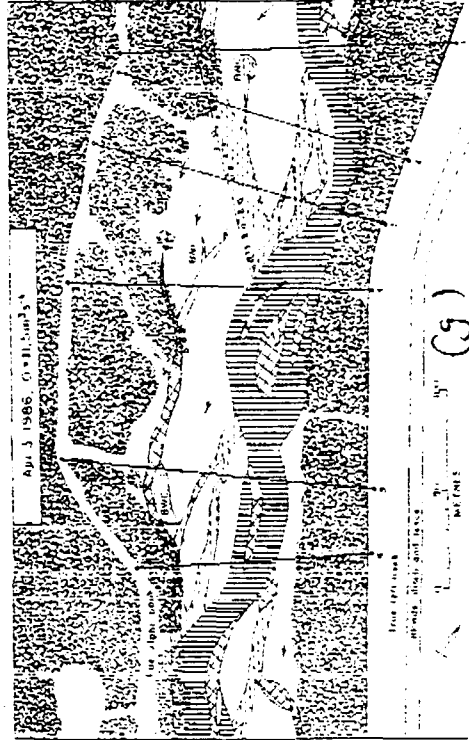
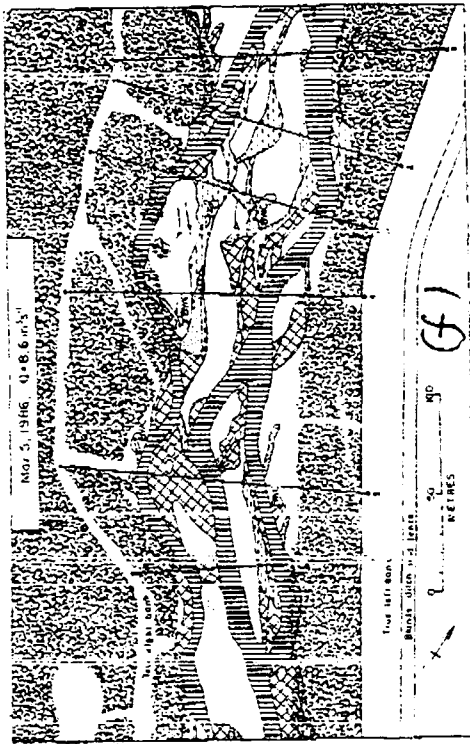


FIG. 6

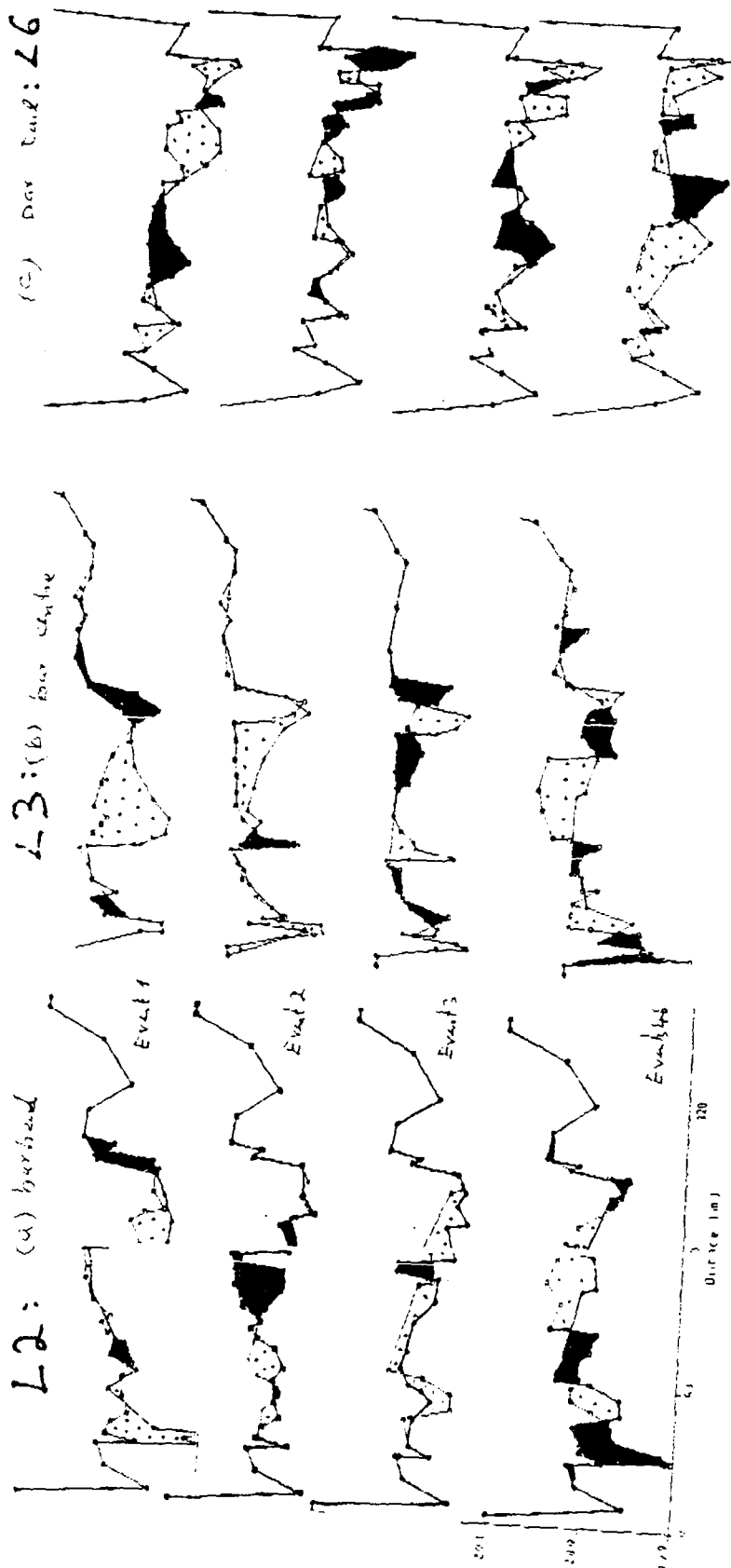


Fig. 7



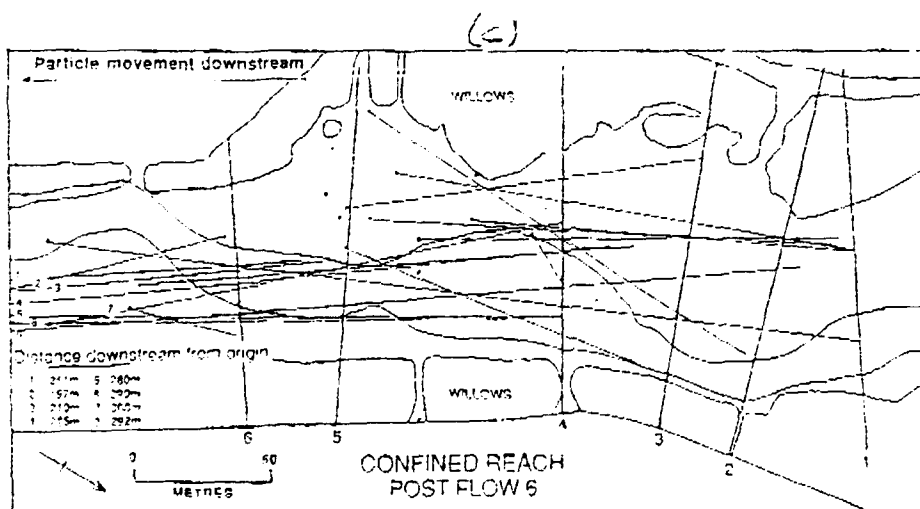
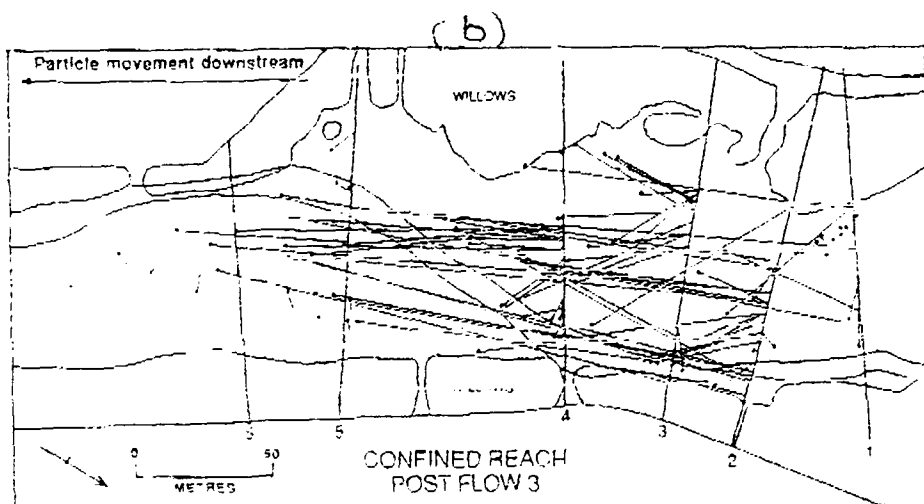
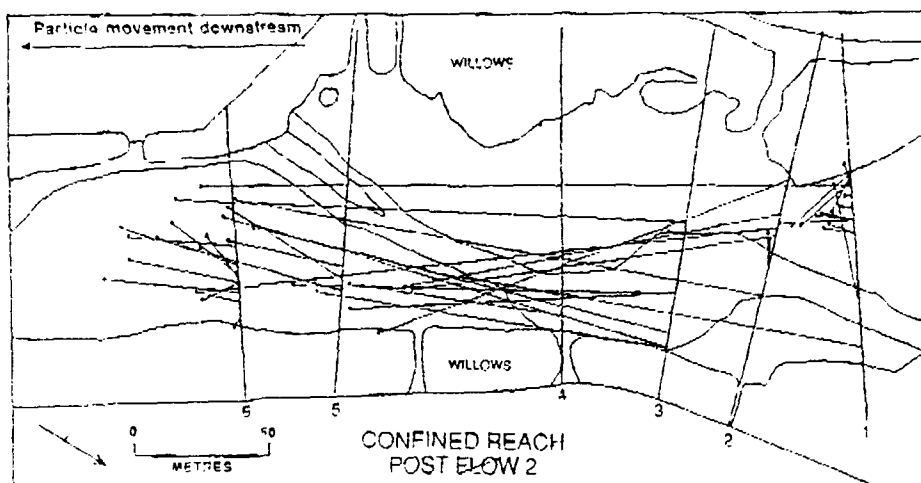


Fig 8

# DOWNSTREAM FINING IN A GRAVEL-BED RIVER IN S. POLAND: LITHOLOGIC CONTROLS AND THE ROLE OF ABRASION

Alan Werritty

Department of Geography and Geology  
University of St. Andrews  
St. Andrews, Fife, Scotland  
U.K. KY16 9S

Draft paper for the 3rd International Workshop on Gravel-bed Rivers  
Florence, September 1990

## INTRODUCTION

It has been known for over a century that the bed material of rivers generally becomes finer in a downstream direction. Explanations for this phenomenon have focussed on abrasion and selective transport as the processes causing this pattern, but their relative importance in different field situations has been the subject of considerable debate amongst geomorphologists.

One of the first analyses of downstream fining was that on the Rhine by Sternberg (1875) who observed that grain size changes in bed material followed an exponential pattern of the general form:

$$W / W_0 = e^{-as}$$

where  $W_0$  is the initial weight of a characteristic particle at distance zero, and  $W$  is the characteristic weight at a distance  $s$  downstream; 'a' being a coefficient of weight reduction. This result was attributed to the process of abrasion as the bed material is transported downstream, a conclusion further confirmed experimentally by tumbling mill experiments by Daubree (1879), Schoklitch (1933) and Krumbein (1941). Kuenen (1956), however, observing that tumbling mills did not adequately reproduce the abrasion processes operating in rivers, developed a circular flume in which the flow was driven by paddles. He identified a number of discrete processes involved in size reduction (splitting, crushing, chipping, cracking and grinding) and generally confirmed an exponential decrease in size. The impact of experimental conditions was also clearly demonstrated by Kuenen's results in which much lower abrasion coefficients were obtained on a concrete bed than on a pebble bed. But the overall pattern of results from a variety of experiments with the circular flume demonstrated that the rates of size reduction observed in natural rivers were much greater than could be attributed solely to abrasion effects.

As a result of these findings, selective transport, or hydraulic sorting, began to be accorded the dominant role in determining the rate at which downstream fining of bed material occurs. Thus Bradley *et al* (1972) claimed that approximately 90% of the size reduction in Knik River gravels in Alaska could be attributed to selective transport and only 10% directly to abrasion. Other field-based studies by Plumley (1948) on terrace gravels in the Black Hills and Unrug (1957) working on the bed material of the River Dunajec in southern Poland have also identified rates of downstream fining which are not in accord with Sternberg's abrasion-based exponential "law". However, further complexities in the processes which determine downstream fining have also been recorded and these have accorded a greater significance to abrasion processes. For example, Bradley (1970) noted an order of magnitude difference in the attrition coefficients for fresh and

weathered granite when subjected to laboratory abrasion tests. Schumm and Stevens (1973) have also argued that even Kuenen's work may underestimate the role of abrasion because of attrition that occurs as stones vibrate at flow velocities below the entrainment threshold. Shaw and Keliarhals are prepared to go even further and tentatively claim for rivers in North Saskatchewan that "no contribution to downstream change in grain size is made by differential transport" (1982, p. 39).

It is clear from the above that the relative roles of abrasion and selective transport in determining the downstream fining of bed material in rivers are still imperfectly understood. One of the major problems has been the failure to identify of a field situations where the two processes can unambiguously be separated from each other. This study, based on a river in Southern Poland, attempts seeks to achieve this separation and thereby assess the role of abrasion on contrasting lithologies quite independently of the effects of selective transport.

## STUDY AREA

The study area comprises a reach of c.20km along the Czarny Dunajec and its tributaries in S. Poland. The River Dunajec rises in a series of headwaters which drain north from the Tatras Mountains (fig. 1). Each of these tributaries successively drains the crystalline basement (mainly granites, schists and quartzites) and then successively Mesozoic limestones and dolomites and Tertiary flysch (shales locally interbedded with massive sandstones). In the case of the Czarny Dunajec the two main tributaries (Chocholowska Dolina and Koscieliska Dolina) rise in the crystalline basement and flow almost due north successively incised into the Mesozoic limestones and dolomites before they join to form the Czarny Dunajec at Roztoki by which time they have emerged from the Tatra massif into the basin of the Podhale flysch.

There are two striking consequences of this sequence of lithologic units which make it ideally suited for this investigation. Firstly, with the minor exception of the sandstone members of the flysch series, no lithologic unit is repeated within the sequence and thus an unambiguous final downstream input of a given lithology can be identified from the geological map. Secondly, the actual sequence of lithologic units is ideal for this study in that the initial inputs of bed material into the headwaters are the most resistant rocks types (quartzites and granites), followed by limestone and dolomite (less resistant) and the sandstones and shales (least resistant). Since the most resistant rock type (quartzite) is one of the first to cease having a direct input into the system, it can be used to provide a 'reference curve' for lithologies which enter later in the sequence.

A second crucial control favouring the selection of this particular reach of the Czarny Dunajec is the recent Quaternary history of the area. During the last glaciation (of Vistulian age), the Tatra massif underwent valley glaciation, but none of the individual icestreams extended beyond the central part of the Tatras. Thus in Chocholowska Dolina and Koscieliska Dolina the maximum extent of the Vistulian ice is recorded by terminal moraines which are located within 1km of the boundary between the crystallines and the Mesozoic sedimentaries (fig. 1). This limit provides a common datum from which the downstream fining of the granites and quartzites can be determined since any crystalline bed material found north of this limit can only have been transported to its current position by fluvial processes. A similar statement can be made for the limestone bed material found north of Kiry on Koscieliska Dolina and north of Siwa Polana on Chocholowska Dolina (fig. 1). Thus for all three lithologies (granite, quartzite and limestone) the last possible input or point source into the Czarny Dunajec system can be determined quite unambiguously. In the case of the massive sandstone units within the flysch sediments the situation is more complex since there are numerous sandstone members within the Podhale flysch series. Nevertheless, it is possible to identify two particularly massive sandstone members: one 500m south of Kojsowka and the other directly west of the village of Chocholowska (fig. 1). The sandstones from both these sources breakdown very rapidly and thus there is no danger of large material derived from

these two sources being confused with each other or with other sandstone members.

Another possible complication which could in part vitiate the underlying rationale behind this project would be the large-scale reworking of coarse older Pleistocene covers. Field checking along the whole 20km reach demonstrated that this problem does not occur. Until the 19th century the Czarny Dunajec was an active, braided gravel-bed river (Krzemien 1981). Since then it has undergone localised river training such that the modern channel is generally undivided. However, where it is not bedrock controlled it is reworking floodplain deposits of very recent origin and not the older Pleistocene covers which are now at some distance from the active channel. When the river ultimately emerges from the Podhale flysch into the Nowy Targ basin it becomes less confined and its tendency to braid substantially increases. This has necessitated extensive river engineering in the form of large concrete drop structures at a spacing of every few hundred metres northwards from the settlement of Koniowka (fig. 1). These act as large scale sediment traps for the coarsest bedload fractions and for this reason the downstream termination of this investigation occurs just upstream of where these drop structures commence.

The long profile of the Czarny Dunajec (fig. 2) reveals an overall gradient of 0.0175 which increases to 0.0208 for the first 5km. Throughout the whole of this long profile the river bed is intermittently in contact with the bedrock and, particularly in the flysch zone, bed material is directly incorporated into the bedload by hydraulic action during floods. Discharge data are available for two sites within the study reach: Koniowka (drainage area 120km<sup>2</sup>) at the end of the reach has recorded a maximum daily flow of 66.4m<sup>3</sup>s<sup>-1</sup> over the period 1976-86, whilst Kojsozka (drainage area 94km<sup>2</sup>) has recorded a maximum of 50.2m<sup>3</sup>s<sup>-1</sup> during the same period.

## DATA COLLECTION

In any study concerned with the size of bed material the sampling strategy and measurement technique require careful selection and justification (Church *et al.* 1987). In this instance, given the number of sites to be investigated plus the particular problem being addressed, it was decided to concentrate on the largest fraction of each lithology present at individual sites. This decision can be justified on the grounds that not only is a consistent measurement required for each site, but also a method needs to be selected which will permit direct comparison between the different lithologies present. As far as possible lateral or mid channel bars were selected, typically up to 80m in length. At each of these 33 sites a systematic search was undertaken to locate the largest sizes present for each of the available lithologies, generally these were to be found either at the head of the bar or close to the active channel. For the most upstream sites only quartzite and granite were available, but as the survey progressed downstream limestone and eventually sandstone became incorporated into the search procedure. For each individual lithology a minimum of the 10 largest clasts was identified, the size of each clast being determined by measuring the B-axis. In the majority of searches substantially more than the 10 largest clasts were measured (in order to be quite certain that the sample did indeed include all the largest clasts present). Later these samples were 'censored' by ranking the data and only including the 10 largest values in the final analysis.

In terms of distribution of sites both headwater tributaries (Chocholowska Dolina and Koscieliska Dolina) were sampled separately and, given the rapid decrease in grain-size, initially the sites were very closely spaced (within a few hundred metres). Thereafter, downstream of the confluence of these tributaries at Roztoki, the sites became more widely spaced. This was partly a reflection of the absence of suitable bars to sample and partly because of the local removal of coarse bed material from the river bed for local construction purposes. Fortunately, this only affected the granite (the most highly prized lithology for building decoration) and was restricted to a specific size range (300mm to 440mm). Only in one instance has this resulted in the granite sample for a particular site being discarded.

## LITHOLOGIC CONTROLS ON DOWNSTREAM FINING

The results are presented in a series of diagrams demonstrating different patterns of downstream fining in each of the headwater tributaries and then in the main channel of the Czarny Dunajec. Taking all the data together for Koscieliska Dolina and its downstream continuation as the Czarny Dunajec, a rather confusing pattern emerges although, as expected, in general the granites and the quartzites both fine much more slowly than the limestones and the sandstones (fig. 3). In addition to the pattern of downstream fining from the last possible input of a given lithology the magnitude of coarse inputs for limestone (A) and sandstone (B, C, and D) are also shown.

Each lithology will now be analysed individually to determine the optimum empirical fit in terms of either exponential or log-linear regression equations. Taking the quartzite curves for Chocholowska Dolina first, a rapid decrease in maximum clasts size from approximately 950mm just beyond the terminal moraine down to 450mm within 5km is recorded in fig. 4. A similar pattern emerges for Koscieliska Dolina although the rate of fining is less with the value after 5km of 593mm. For both tributaries the goodness of fit as measured by the coefficient of determination is high with that for Koscieliska being somewhat better than that for Chocholowska. Thereafter, working downstream along Koscieliska Dolina and into the main stem of Czarny Dunajec, further diminution in size is very small, such that even after 20km quartzite boulders >550mm can still be found in within the river bed. The log-linear model best describes the pattern of downstream fining with higher reduction coefficients (-0.162 and -0.116) for the first 8km of Chocholowska and Koscieliska respectively. These coefficients are both higher than the -0.0875 for the 20km reach of Koscieliska Dolina and the Czarny Dunajec. In no instance did the exponential regression model provide a better fit than log-linear model. For quartzite bed material the very rapid initial decline in maximum clast size favours the log-linear rather than the exponential model (Table 1)

The pattern for fining of the largest granite boulders is broadly similar to that for the quartzites (fig. 5). Again a very rapid reduction from 950mm to 467mm within the first 5km is recorded for Chocholowska Dolina, although the comparable value for Koscieliska Dolina after 5km is higher (581mm). Again log-linear functions best describe the pattern of downstream fining for Koscieliska Dolina with a reduction coefficients of -0.165 being recorded. However, for Chocholowska Dolina the exponential model provides a better fit (R squared of 0.908) and so the reduction coefficient is not directly comparable. Extending the results for Koscieliska Dolina downstream to include the Czarny Dunajec, the size of the largest granite bed material continues to decline only slowly towards 434mm at a distance of 20km from its origin at the terminal moraine. The resulting pattern conforms extremely well to a log-linear curve (coefficient of determination of 0.922 which is strikingly better than the alternative exponential model (Table 1)). The only major anomaly over this 20km reach is at a distance of 7.1km where a value of 625mm is recorded rather than the 526mm predicted by the regression equation. As for the quartzites the log-linear model generally provides a better fit to the granite data than the exponential model.

The pattern of downstream fining for the limestone and dolomite bed material is quite different from that of the crystallines. As can be seen from fig. 6, although the initial values are larger than those for the granites and quartzites (since they include direct input into the river by rockfall) they rapidly decline from values >1000mm to <400mm within 5km. Thereafter, at 8km downstream from the terminal moraines (and approximately at the transition from limestone/dolomite to flysch) the largest limestone bed material is 180mm (Koscieliska) and 260mm (Chocholowska). This pattern of downstream fining continues such that 20km from the origin the largest limestone clasts are only 105mm in size. Given this pattern of results the reduction coefficients of -0.326 to -1.1068 record much more rapid fining than was found for the granites and quartzites. With the exception of Koscieliska Dolina, the log-linear model is generally favoured over the exponential model (Table 1).

The flysch sandstones behave quite differently to the crystallines and the limestones, and provide two major inputs of coarse sandstone blocks within the Czarny Dunajec study reach. The first (just upstream of Kojasowka, site A in fig. 7) comprises a 5m high vertical cliff of massive, well-jointed sandstones which are currently being undercut by the river. Within 300m the largest blocks have been halved in size from 1213mm (at A) to 645mm (at B). Within a further 2.2km they are further reduced to 300mm. An even higher rate of fining occurs at a second site, just west of the village of Chocholowska (fig. 7), where inputs from a bedrock source within the present channel and derived from the local Chocholowska sandstone is reduced from 713mm (D) to 413mm (E) within 400m. It is clear that the rate of reduction for the sandstones is far greater than that for any of the other lithologies. Taking the two very rapid fining cycles starting with coarse inputs at A and D the estimated reduction coefficients are -5.7 and -17.5 respectively. As anticipated, these are an order of magnitude greater than those reported for the limestones and over two orders of magnitude greater than comparable values for the crystallines. As was apparent from field evidence large sandstone blocks are broken up within a few hundred metres of their source.

A final, but rather ambivalent, piece of field evidence supporting the claim that abrasion is a substantial part of the overall pattern of downstream fining is shown by the steady increase in Krumbein sphericity recorded for the quartzites within Koscieliska Dolina as the bed material is transported downstream (fig. 8). The increase of sphericity from 0.66 to 0.73 over 8km is strongly suggestive of abrasion taking place. However, similar investigations of quartzite sphericity downstream in Chocholowska Dolina and the main stem of the Czarny Dunajec fail to reveal a similar pattern. There is thus no strong evidence over the whole study reach linking abrasion with an increase in quartzite sphericity.

On returning to Britain samples of the quartzite, limestone and sandstone were submitted to Lewin and Brewer for abrasion tests in their laboratory at University College Aberystwyth. Full discussion of the findings will be published elsewhere, but it was noteworthy that cubes of quartzite underwent a weight loss over 1-2% during simulated transport of 20km, the limestone recorded a loss of 12% by weight, whereas the sandstone samples suffered losses of 25% by weight and became very well rounded. Only the sandstone appeared to undergo reduction which might conform to an exponential model. The limestone sample underwent major weight loss by breakage. These preliminary experimental findings are completely in accord with the overall pattern of field-based results itemised above.

## DISCUSSION AND CONCLUSIONS

Returning to the initial question, it is clear that the lithologic controls on the downstream fining of the coarsest fractions found with the upper reaches of the Czarny Dunajec drainage basin are very powerful. For quartzites, granites and limestones extremely well-defined fining cycles have been identified downstream of the last possible input of a given lithology. Comparison of the relative merits of exponential and log-linear models to characterise these fining cycles generally favours the latter over the former - in 7 out of 9 analyses the log-linear model provides a better fit. This largely arises because of poor fits for the exponential models in the uppermost reaches, especially when combined with a rapid reduction to quasi asymptotic values by 8km. Such failures to conform to Sternberg's "law" has already been noted in a number of other studies which have investigated channel reaches very close to sediment sources. Thus both Bradley (1970) and Adams (1979) report very rapid declines in particle size at sites immediately downstream of a major sediment source. Similar observations have been made in proglacial and braided outwash environments (Boothroyd and Nummedal 1978, and Brierley and Hickin 1985). The implication of these findings is either that the Sternberg reduction coefficient is not consistent (a view favoured by Shulits (1941) or hydraulic sorting plays a major role (see Brierley and Hickin 1985). However, our concern in this paper is rather different since we have an opportunity to measure the

role of abrasion independently of selective transport.

Inspection of fig. 4 demonstrates that quartzite is the most resistant lithology contributed within this drainage basin. Once the largest quartzite clasts have reached c. 600mm they undergo very little further reduction. Although further abrasion does not occur, they still undergo transport throughout the study reach, and since there are no other sources of quartzitic boulders, one is forced to conclude that occasionally the Czarny Dunajec is competent to transport bed material of this size. Thus the curve in fig. 4 for quartzites in Koscieliska Dolina and Czarny Dunajec can be regarded as a 'reference curve' against which other lithologies can be compared. This curve defines the competence of the river throughout its 20km reach, the fact that the granites fail to retain a largest fraction comparable to that of the quartzites (especially at distances > 8km) arises not because of selective transport but rather because granites of this size are not available beyond 8km. The reason why they are not available is that they have undergone more abrasion. Typically the granites have undergone between 1.13 and 2.13 times more abrasion than the quartzites despite the fact that they share a common source in the two terminal moraines (Table 2). Similarly, the limestone reduction coefficients can be directly compared with those for the quartzites and their much greater susceptibility to abrasion (up to 9.54 times can be measured, Table 2). The sandstone data are difficult to interpret in a quantitative manner since the rate of breakdown is so rapid. A reasonable estimate of their behaviour is to characterise their size reduction as occurring at a rate at least 100 times more rapidly than that for the quartzites.

At this point a cautionary note needs to be added in terms of terminology, since the term 'abrasion' implies the style of wear of sedimentary particles recorded in the tumbling mills and recirculating flumes of Krumbein (1941) and Keunen (1956). It is now realised that size reduction independent of selective transport involves a number of processes including 'abrasion in place' (see Schumm and Stevens' 1973 and referred to as "vibration abrasion" by Shaw and Kellerhals 1982). There is also the role of physical and chemical weathering on clasts exposed on bars surfaces for considerable periods in between competent floods, and for limestone the role of solution when the clasts are buried beneath the local groundwater table. All these processes collectively contribute to size reduction which is independent of hydraulic sorting.

This study has served to demonstrate that for the largest fraction transported by a gravel-bed river, the role of abrasion and other related physical and chemical processes which can reduce the size of large clasts *in situ* is highly significant. In this particular study it has been possible to express the resistance of granites, limestones and sandstones in a quantitative manner relative to that of quartzite. This has a number of implications that warrant further investigation, not least being that of the relative resistance of the modal parts of grain size curves rather than examining the behaviour of the coarsest fraction present. The sampling problems inherent in such an investigation would, however, be very severe. More promising in the short term would be similar analyses involving controlled comparisons for other lithologies than those reported in this study. Since the processes described in this paper determine the shape of the upper tails in grain-size curves for fluvially-derived sediments, further investigations to validate or falsify the above conclusions are clearly needed.

## ACKNOWLEDGMENTS

This project was undertaken with financial support from the British Council, the Jagiellonian University in Krakow and the Carnegie Trust. Whilst in the field I was invaluablely assisted by Ludwik Kaszowski, Wojciech Chelmicki, Kazimierz Krzemien and Piotr Libelt. John Lewin and Paul Brewer kindly undertook laboratory abrasion tests.

## REFERENCES

- Adams, J. (1979) Wear of unsound pebbles in river headwaters. **Science**, 203, 171-172.
- Brierley, G. J. and Hicken, E. J. (1985) The downstream gradation of particles sizes in the Squamish River, British Columbia. **Earth Surface Processes and Landforms**, 10, 597-606.
- Boothroyd, J. C. and Nummedal, D. (1978) Proglacial braided outwash: a model for humid alluvial-fan deposits, in **Fluvial sedimentology**. Canadian Society of Petroleum Geologists Memoir 5, 641-668.
- Bradley, W. C. (1970) Effects of weathering on abrasion of gravel, Colorado Texas. **Bulletin of the Geological Society of America**, 81, 61-80.
- Bradley, W. C. Fahnestock, R. K. and Rowekamp, E. T. (1972) Coarse sediment transport by flood flows on the Knik River, Alaska. **Bulletin of the Geological Society of America**, 83, 1261-1284.
- Church, M., McLean D. G. and Wolcott, J. F. (1987) River bed gravels: sampling and analysis in **Sediment transport in gravel-bed rivers**, ed. Hey., R. D. Bathurst, J. C. and Thorne, C. R. pp. 291-338.
- Daubree, A. (1879) **Etudes synthetiques de geologie experimentale**, Dunod, Paris, 2 Volumes.
- Krumbein, W. C. (1941) The effects of abrasion on the size, shape and roundness of rock fragments, **Journal of Geology**, 49, 482-520.
- Krzemien, K. (1981) Zmienność systemu korytowego Czarnego Dunajca. **Prace Geograficzne Zeszyt**, 53, 123-137.
- Kuenen, Ph. H. (1956) Experimental abrasion by pebbles. 2: Rolling by current, **Journal of Geology**, 64, 336-368.
- Nawara, K. (1960) Skład litologiczny zwirow Białki i Czarnego Dunajca w zależności od frakcji. **Acta Geologica Polonica**, 10, 455-474.
- Plumley, W. J. (1948) Black Hills terrace gravels: a study in sediment transport, **Journal of Geology**, 56, 526-577.
- Schoklitsch, A. (1933) Über die Verkleinerung der Geschiebe in Flussläufen. **Sitzungsbericht der Akademie der**



- Wissenschaft, Vienna. 142, Part 2A, 343-366.
- Schulits, S. (1941) Rational equation of river bed profile, **Transactions of the American Geophysical Union**, 222, 622-631.
- Schumm, S. A. and Stevens, M. A. (1973) Abrasion in place: a mechanism for rounding and size reduction of coarse sediment in rivers, **Geology**, 1, 37-40.
- Shaw, J. and Kellerhals, R. (1982) The composition of recent alluvial gravels in Alberta river beds, **Bulletin of the Alberta Geological Survey**, 41, 151pp.
- Sternberg, H. (1875) Untersuchungen über Längen und Querprofil geschiebeführende Flüsse, **Zeitschrift für Bauwesen**, 25, 483-506.
- Unrug, R. (1957) Recent transport and sedimentation of gravels in the Dunajec valley (Western Carpathians), **Acta Geologica Polonica**, 2, 252-257

Table 1      **Regression equations for downstream fining patterns**

	Reduction coefficient	Coefficient of determination (log-linear)	Coefficient of determination (exponential)
(a) <u>Quartzite</u> :			
Chocholowska	-0.162	0.656	0.240
Koscielika	-0.1159	0.785	0.470
Czarny Dunajec	-0.0875	0.661	0.356
(b) <u>Granite</u> :			
Chocholowska	-0.183	0.732	0.908 *
Koscielika	-0.1652	0.881	0.669
Czarny Dunajec	-0.1864	0.922	0.751
(c) <u>Limestone</u> :			
Chocholowska	-0.326	0.865	0.684
Koscielika	-1.1068	0.980	0.992 *
Czarny Dunajec	-0.7894	0.888	0.715

\* exponential model better fit than log-linear model

Table 2      **Comparative reduction coefficients from log-linear models**

	Chocholowska	Koscieliska	Czarny Dunajec
Quartzite	-0.162	-0.1159	-0.0875
Granite	-0.183	-0.1652	-0.1864
Limestone	-0.326	-1.1068	-0.7894
Granite/quartzite	1.13	1.43	2.13
Limestone/quartzite	2.01	9.54	9.02
Limestone/granite	1.78	6.70	4.23

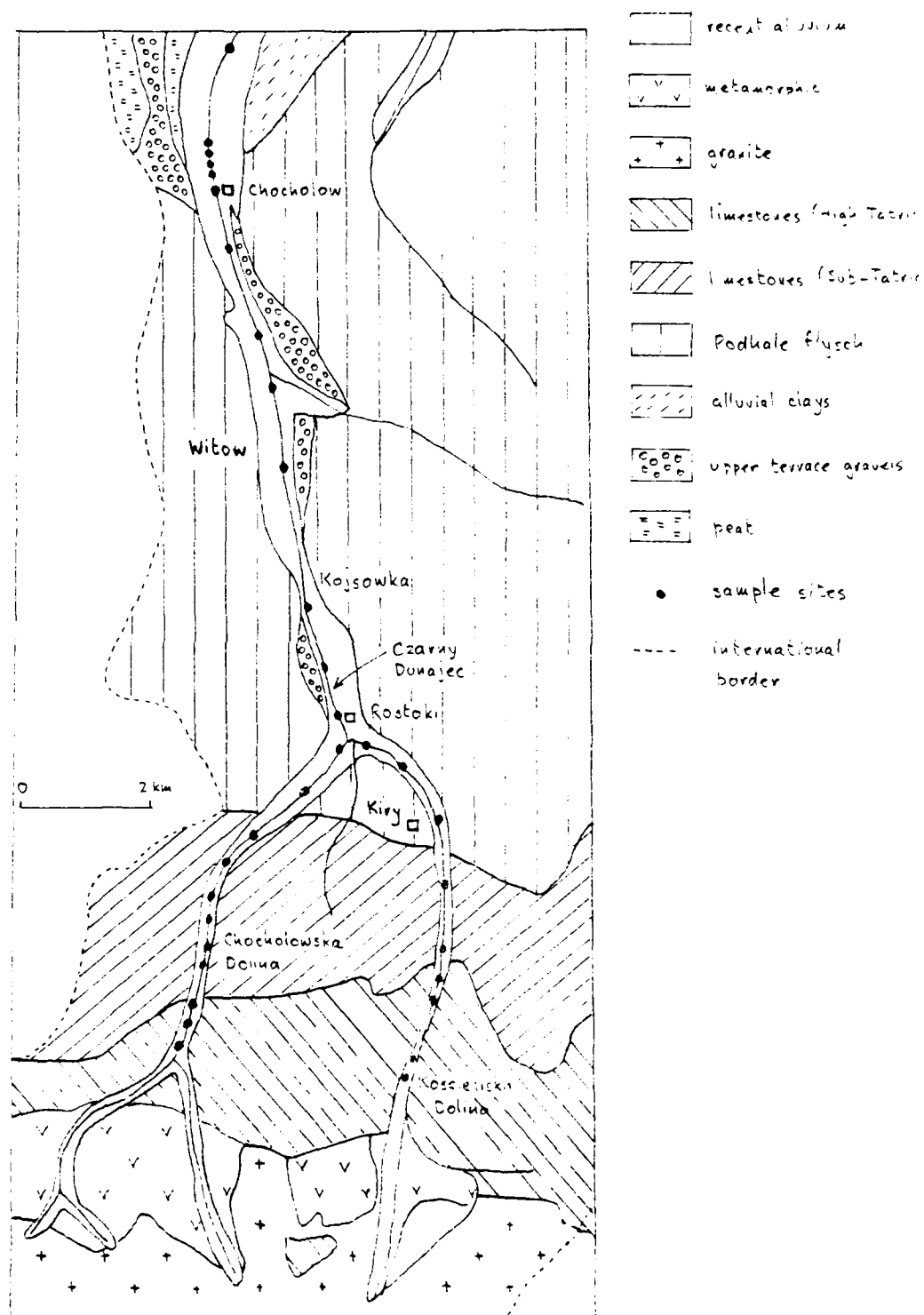


Figure 1 Sketch map of Czarny Dunajec drainage basin showing bedrock geology, stream network and sampling locations.

### Long profile of Koscieliska Dolina - Czarny Dunajec

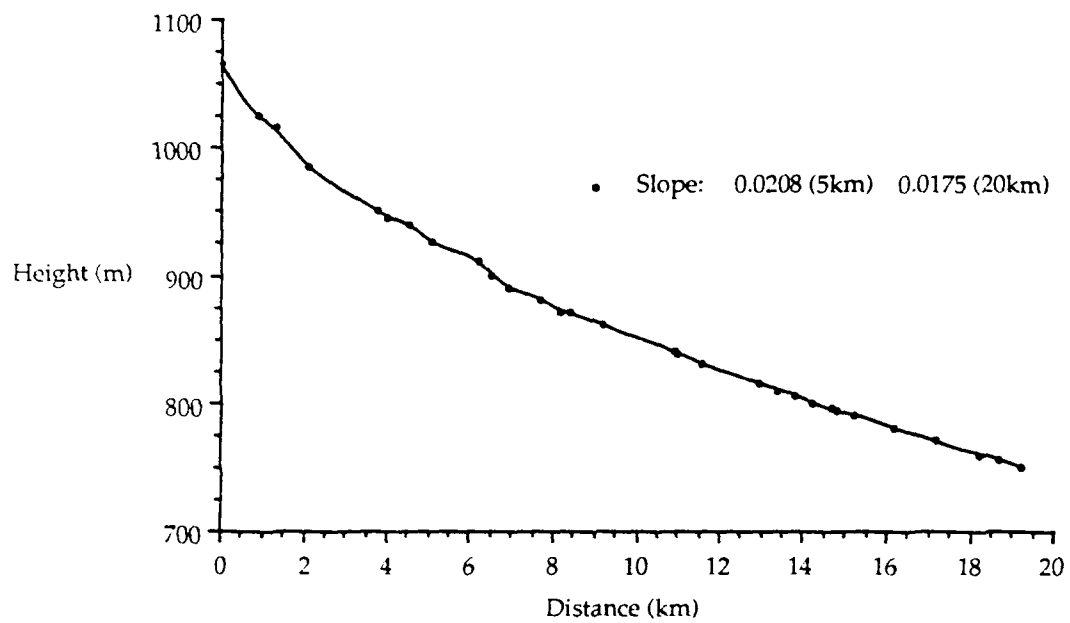


Figure 2 Long profile of Koscieliska Dolina - Czarny Dunajec

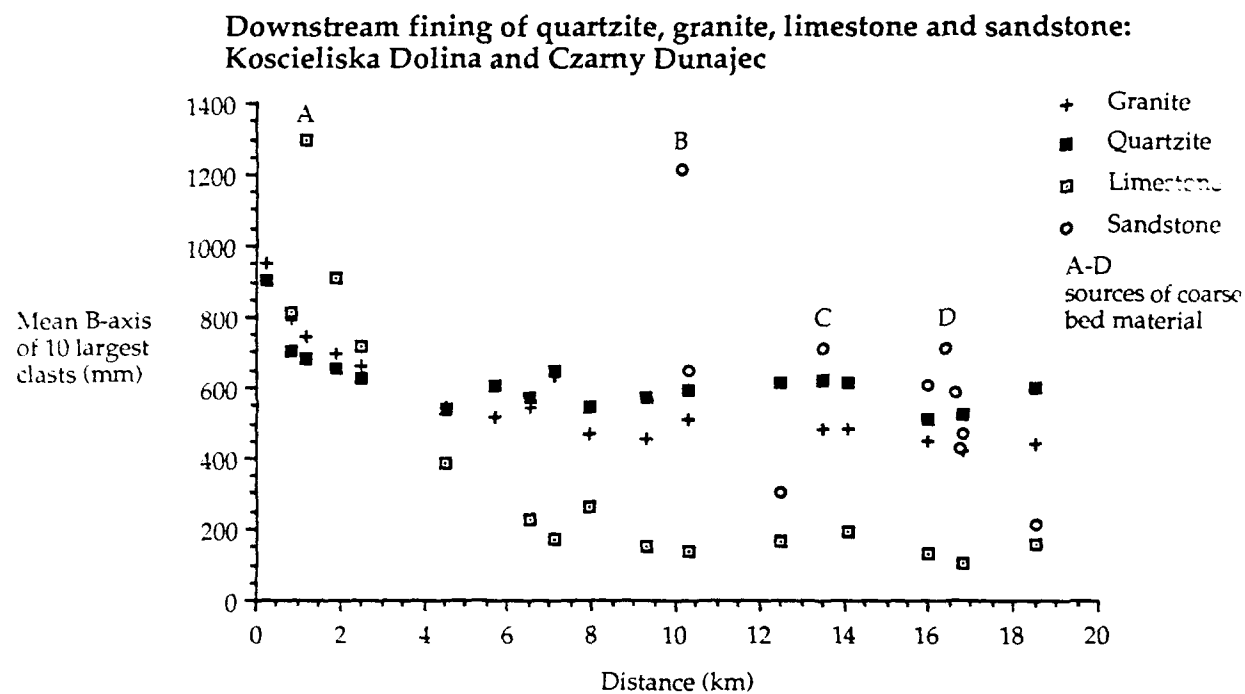


Figure 3 Downstream fining of all four lithologies for Koscieliska Dolina - Czarny Dunajec

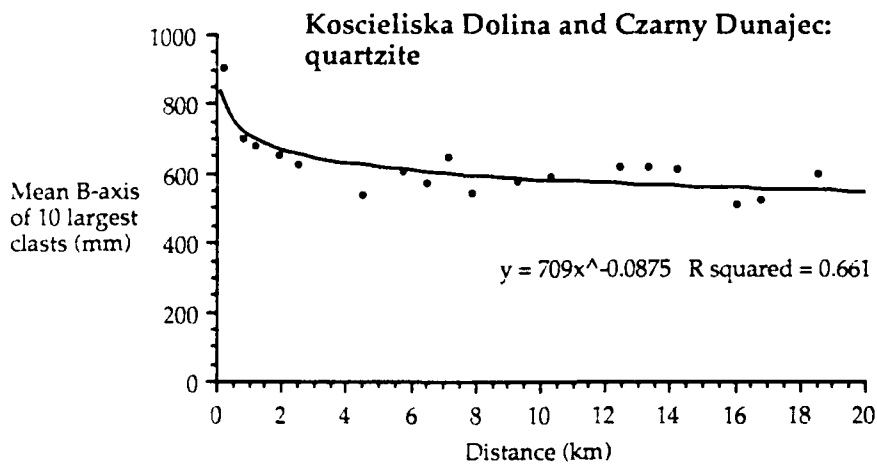
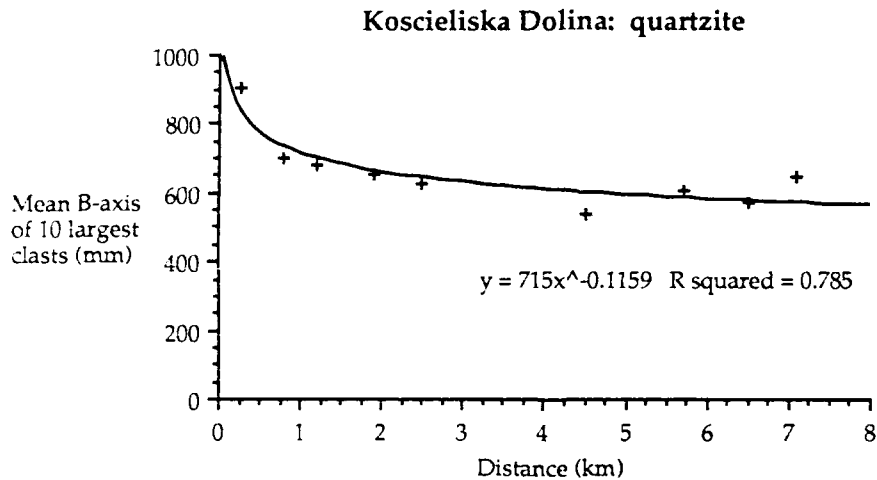
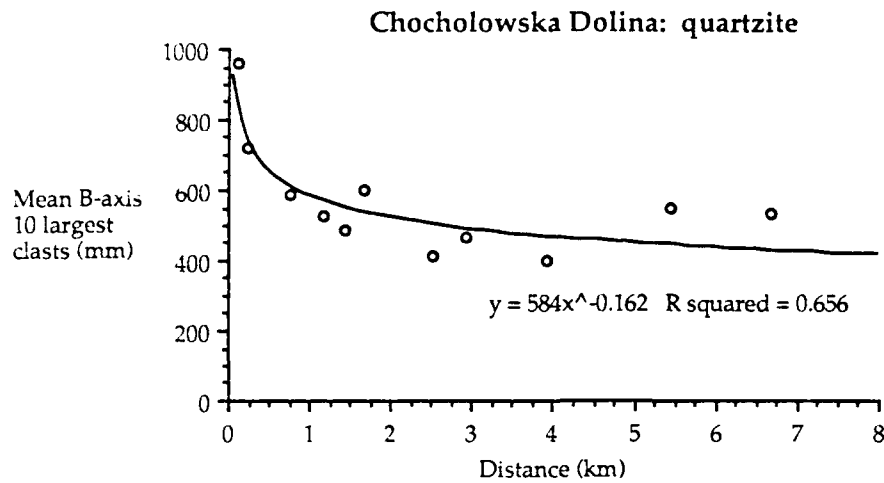


Figure 4 Downstream fining of quartzite

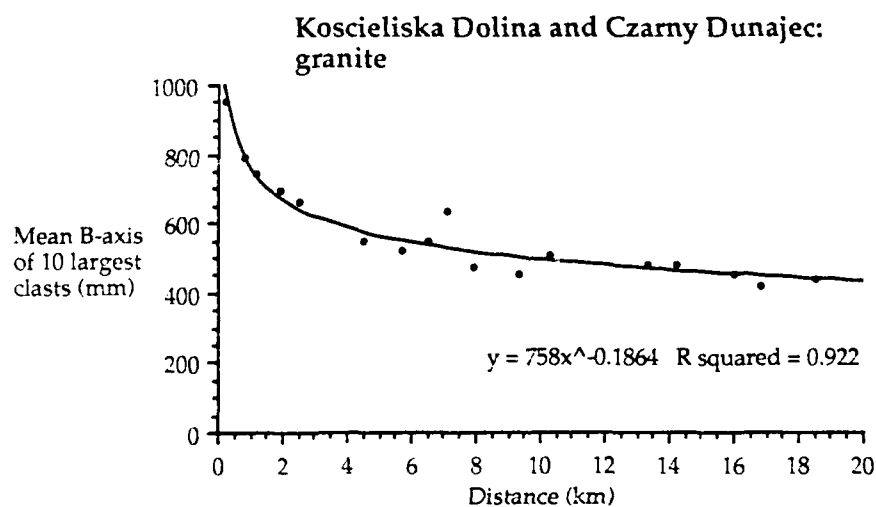
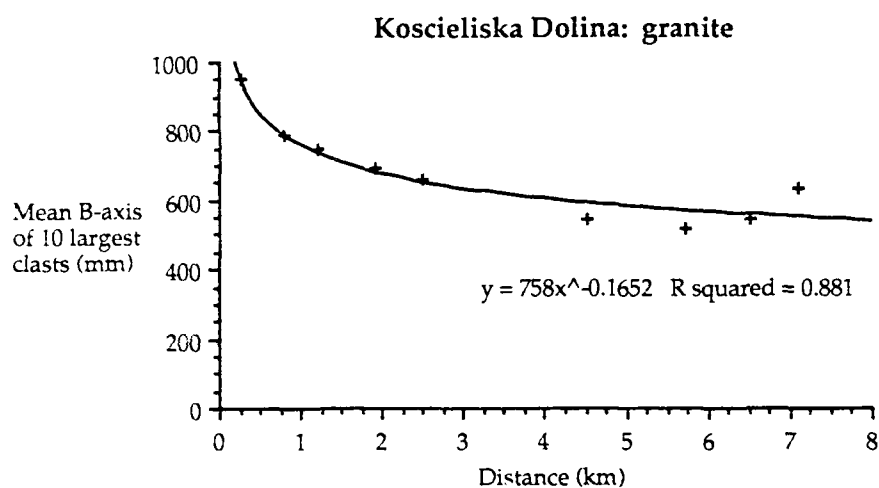
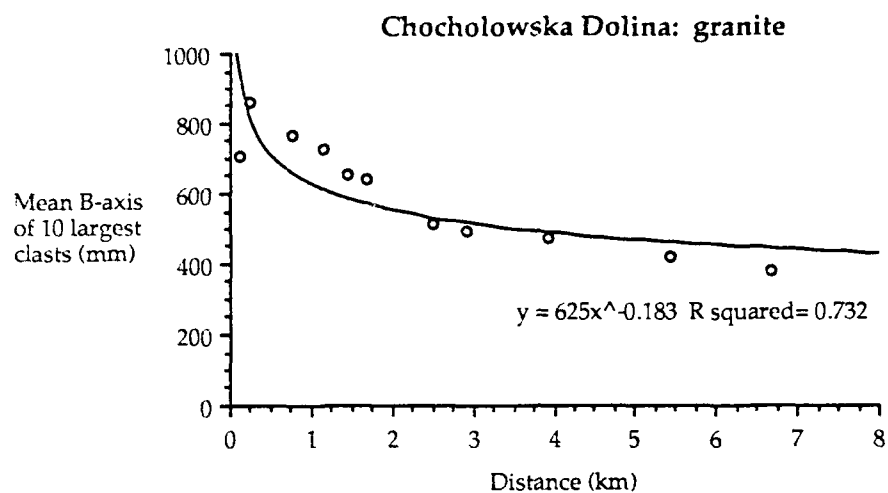


Figure 5 Downstream fining of granite

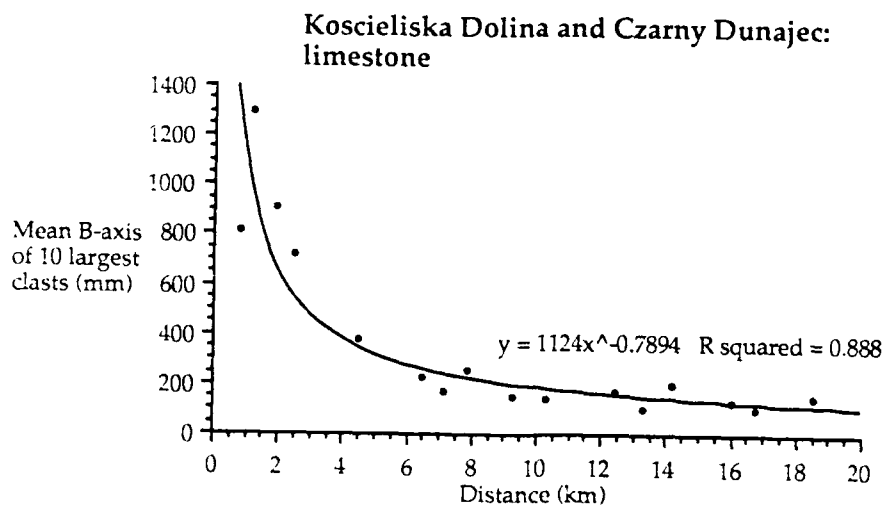
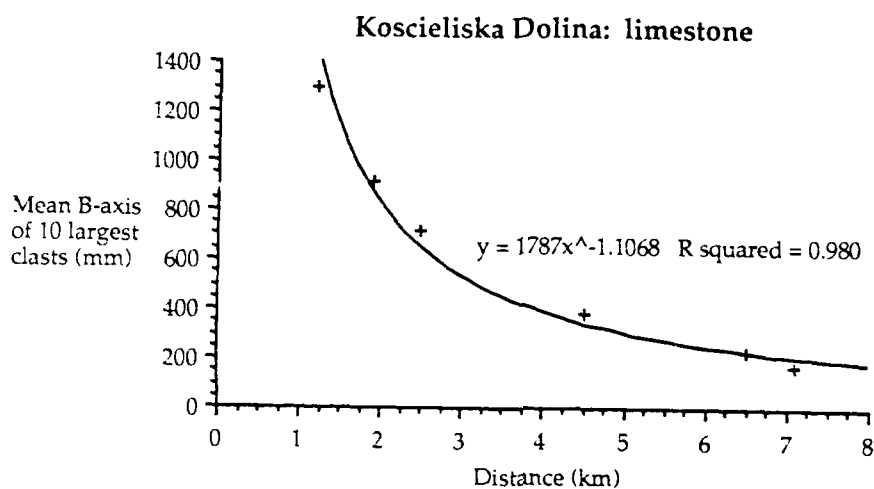
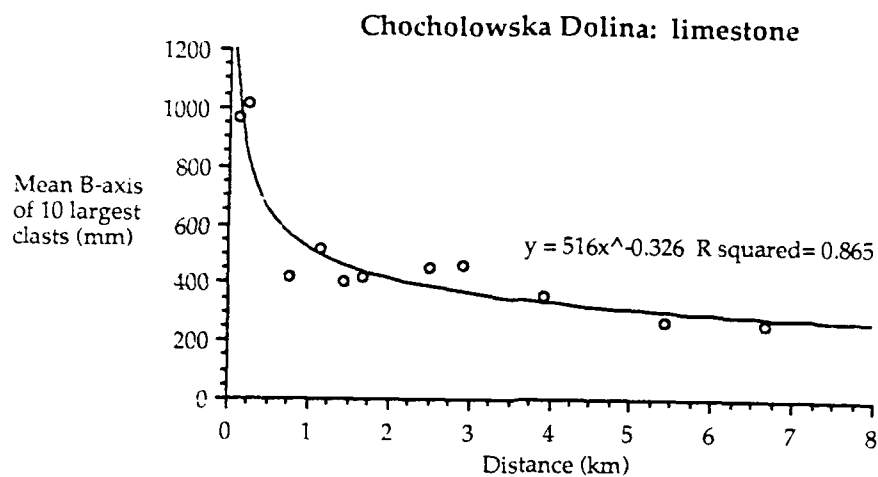


Figure 6 Downstream fining of limestone



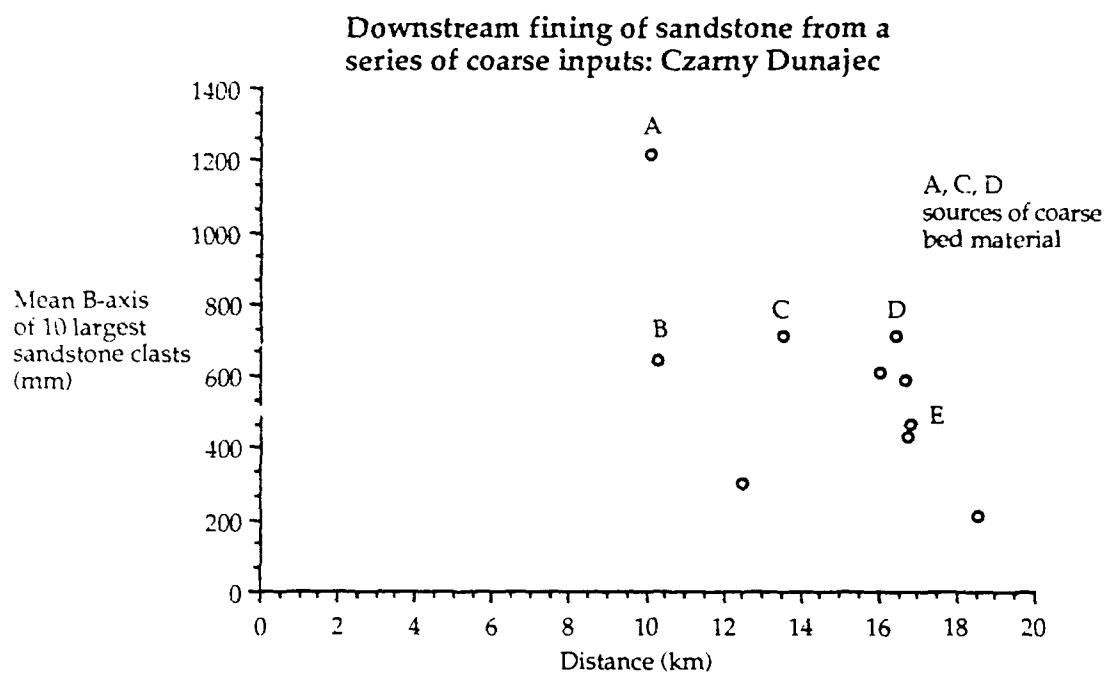


Figure 7 Downstream fining of sandstones from a series of coarse inputs

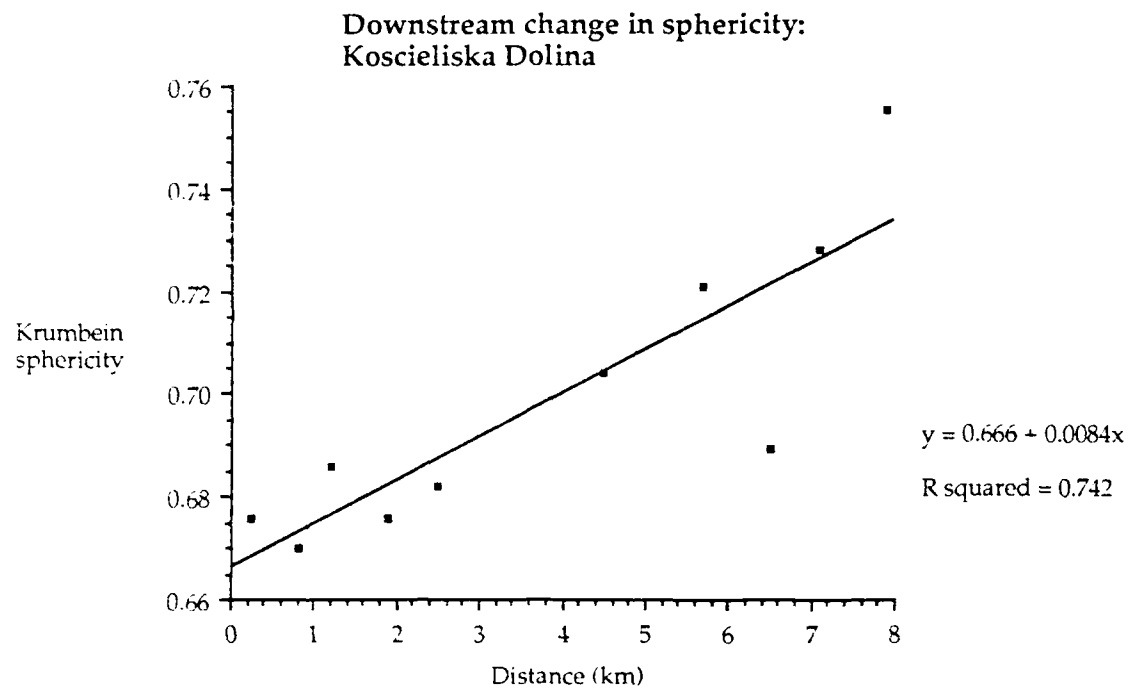


Figure 8 Downstream changes in sphericity: Koscieliska Dolina

INTERNATIONAL WORKSHOP ON GRAVEL-BED RIVERS  
Florence, 25-29 September 1990

VARIATION OF BED AND TRANSPORT MEAN DIAMETERS  
IN EROSION-DEPOSITION PROCESSES

Aronne Armanini  
University of Trent-Trent Italy

**ABSTRACT**

The paper presents a mathematical scheme able to model the evolution of deposition-erosion processes in a one-dimensional stream, also taking account of non uniform grain size mixtures and possibly non-equilibrium of sediment transport rate.

Instead of describing the sediment transport for fractions, that is, each fraction by means of its continuity equation, the model uses mean diameter and second-order (and possibly third-) moment of grain size distribution. As a consequence the number of equations and variables is reduced.

**INTRODUCTION**

The problem of aggrading and degrading of rivers has been strongly emphasized in the recent years. The interest in solving this problem is related not only to a certain unresolved problems in the field of the research, but also to a better insight of long and short time consequences of river training engineering.

A number of numerical models has been proposed in the literature in order to describe the sediment transport of non uniform grain size material, some of them even able to account for non-equilibrium transport rate (Ashida and Michiue, 1971) (Karim and Kennedy, 1982) (Armanini and Di Silvio 1982 and 1988) (Rahuel and Holly, 1989) (Andrews and Parker 1987).

The general approach adopted in order to consider the different behavior of different grain-size materials is based on the idea of dividing the grain-size distribution curve into a discrete number of classes and describe the behavior of each class by means of separate mass- or volume- balances.

Following the procedure adopted by Einstein(1950), the actual transport rate of each class is related to the percentage present in the bed sediment transport.

Aim of this paper is to approach the problem in terms of first-, second- and possibly third-order moments of the grain-size distribution.

## GENERAL FORMULATION OF THE PROBLEM

The continuity equation for sediment transport in a quasi one-dimensional stream is given by :

$$\frac{\partial T}{\partial x} + \frac{\partial Ch}{\partial t} = -\frac{\partial Z}{\partial t} \quad (1)$$

where  $h$  and  $Z$  are water depth and bottom elevation;  $T = \int ucdy$  is the actual transport rate and  $C = \int cdy$  is the depth-averaged concentration of sediments.

In natural rivers, but also in many laboratory settings, the bed material is far different from uniform.

In this case the transport rate of each individual grain fraction depends on its size. Nevertheless the continuity within each grain size class must be established.

Following Einstein, the ratio between the actual transport rate  $T_j$  for each grain size fraction  $j$ , and its transport capacity  $T_{c_j}$  (that is the transport rate in case of steady flow and uniform grain size material) is equal to the percentage  $\beta_j$  of the same class present in the bed. That is :

$$T_j = \beta_j T_{c_j} \quad (2)$$

This assumption, referred as *similarity hypothesis*, exhibits at least two limitations. The first one is that it refers to (local) equilibrium condition; that is, it does not account for different adaptation processes due to unsteadiness of sediment transport. The second limitation lies in the fact that it does not account for hiding effect, that is the sheltering exerted by the coarser materials over the finer fraction.

As far as the sediment transport is concerned, a linear adaptation model can generally describe the process (Armanini and Di Silvio 1988) as in the following eq.(3):

$$T_j = \beta_j T_{c_j} - L_j^* \frac{\partial}{\partial x} T_j - \tau_j^* \frac{\partial}{\partial t} T_j \quad (3)$$

$L_j^*$  and  $\tau_j^*$  represent, respectively, the adaptation length and the adaptation time for the same class.

$L_j^*$  accounts for the space lag between the actual transport rate  $T_j$  and the transport capacity  $\beta_j T_{c_j}$ ; this effect is more pronounced the smaller the grain size of the class. For suspended load the following expression has been proposed by Armanini and Di Silvio (1988).

$$\frac{L^* w}{hU} = \frac{a}{h} + (1 - \frac{a}{h}) \exp[-1.5(\frac{a}{h})^{-1/6} \frac{w}{u_*}] \quad (4)$$

where  $w$  is the particles falling velocity,  $a$  is the thickness of the bottom layer,  $h$  and  $U$  water depth and mean velocity.

In eq.3)  $\tau_j^*$  accounts for time lag between the same quantities as above. For suspended load one can assume:

$$\tau^* = \frac{L^*}{U} \quad (5)$$

For bed load, adaptation length and adaptation time are small (e.g. of order of magnitude of bed forms), so in general it is possible to assume immediate adaptation of bed load to equilibrium condition.

This assumption is generally accepted in case of gravel bed rivers where the bed load prevails over suspended load. That is:

$$L^* \sim \tau^* \sim 0 \quad (6)$$

It should be remarked that  $\beta_j$  is the percentage of  $j$  class present on the bed surface. Experimental evidence in fact shows, under the layer where sediment transport occurs, the existence of a *surface layer*, where the longitudinal transport is negligible, but where the vertical exchange of sediments with the

transport layer is determinant. This exchange is in fact responsible for the sorting process of the bed material.

The thickness of such a mixing layer (or surface layer)  $\delta$  is order of magnitude of roughness elements. In duned beds it can be assumed as half the dune height  $\Delta$ :

$$\delta = \frac{1}{2}\Delta \quad (7)$$

As far as hiding effect concerns, it is possible to account for this effect by introducing a proper hiding factor. This factor reduces the transport capacity of finer fraction of the mixture and increases the transport capacity of the coarser fraction. Different expression for the hiding factor have been proposed in the literature, suitable to be applied to different kind of sediment transport formulas (Eghiazaroff 1965), (Einstein 1950), (Day 1980), (Ranga Raju 1985), (Andrews and Parker 1987). In general the hiding factor is a function of the ratio between the diameter  $d_j$  of  $j$  class and the mean diameter  $\bar{D}$  of the mixture:

$$\xi_j = \xi_j \left( \frac{D_j}{\bar{D}} \right)^m$$

The mixing process among the classes constituting the bed material may be described by means of the continuity equation inside the mixing bed layer  $\delta$  (where just mixing but not longitudinal transport takes place), as described by the following eq.8).

$$\frac{\partial}{\partial t} \delta \beta_j = \beta_j^* \frac{\partial(\delta - Z)}{\partial t} - \left( \frac{\partial T_j}{\partial x} + \frac{\partial}{\partial t} C_j h \right) \quad (8)$$

In the erosion processes,  $\beta_j^*$  represents the percentage in the subsurface layer, (the volume below the mixing layer) of the material that belongs to the  $j$ -th class; while during the deposition phase  $\beta_j^* = \beta_j$ .

Finally the total transport  $T$  is the summation of the transport rates of each class  $j$ , that is:

$$T = \sum_{j=1}^m T_j \quad (9)$$

If  $m$  is the number of classes, the set formed by eqs. 1), and 9), and  $n$  eqs.2) (or eqs.3) and 8), in the  $2(n+m+2)$  unknowns:  $Z, T, m, T_j, m, \beta_j$ , (coupled with the appropriate hydrodynamics equations), are sufficient to describe the behavior of each class of sediments.

The relationship between  $C_j$  and  $T_j$  is given by the transport formula and concentration distribution; it is generally possible to put:

$$C_j = \frac{T_j}{U_j}$$

being  $U_j$  the celerity of the  $j$ -th class of the grain size distribution.

The set of equation can be numerically solved for a discrete number of classes. Many numerical models have been recently proposed in literature (Andrews and Parker 1987), (Armanini and Di Silvio 1988), (Rahuel and Holly 1989), (Bouchard et alii. 1989). The models differ for the sediment transport formula, for the expression of adaptation quantities  $L_j^*$  and  $\tau_j^*$ , for the definition of the mixing layer, as well as for numerical scheme and number of classes. Since now the number of classes adopted in literature ranges from 2 to 5. From a numerical point of view the models are quite complex owing to the number of (non linear) equations: one possibility to simplify the problem is to write the equations in terms of mean values instead of single grain-size quantities.

## EQUATIONS IN TERMS OF MEAN DIAMETERS

Adding up to  $n$  classes all the terms in eq.2, one obtains:

$$T = \sum_{j=1}^m \beta_j T_{c_j} \quad (10)$$

Given that  $\beta_j$  is a distribution function, it vanishes as when the diameter tends to zero and infinity and the summation in eq.10) can be calculated expanding in Taylor series  $T_{c_j}$ .

If transport capacity for each class  $j$  is expressed by a formula linking it to the power of respective diameter  $D_j$ , one obtains:

$$T_{c_j} = A D_j^{-n} \quad (11)$$

Expanding 11) in Taylor series, the second term of eq. 10) can be written as:

$$\sum_{j=1}^m \beta_j T_{c_j} = T_{c_b} [1 + c_2 \sigma_b + c_3 \gamma_b + O(\kappa_b)] \quad (12)$$

where  $T_{c_b}$  is the transport capacity related of the mean diameter of the bed material :

$$D_b = \sum_{j=1}^m \beta_j D_j \quad (13.a)$$

$\sigma_b$ ,  $\gamma_b$  and  $\kappa_b$  are second-, third- and fourth-order dimensionless moments of the  $\beta_j$  distribution (variance, skewness and kurtosis)

$$\sigma_b = \sum_{j=1}^m \frac{\beta_j (D_j - D_b)^2}{D_b^2} ; \quad \gamma_b = \sum_{j=1}^m \frac{\beta_j (D_j - D_b)^3}{D_b^3} ; \quad \kappa_b = \sum_{j=1}^m \frac{\beta_j (D_j - D_b)^4}{D_b^4} \quad (13.b)$$

The coefficients  $c_2$  and  $c_3$  are, respectively:

$$c_2 = \frac{n(n+1)}{2!} \quad (14.a)$$

$$c_3 = \frac{-n(n+1)(n+2)}{3!} \quad (14.b)$$

After substitution of eqs. 12) into eq.10), one obtains:

$$T = T_{c_b} [1 + c_2 \sigma_b + c_3 \gamma_b + \dots] \quad (15)$$

The terms in eq.2) are now multiplied by the respective diameter  $D_j$ , and summed up to the  $n$  classes, so that:

$$\sum_{j=1}^m T_j D_j = \sum_{j=1}^m \beta_j D_j T_j \quad (16)$$

Introducing a mean transport diameter  $D_t$ , defined as follows:

$$D_t = \sum_{j=1}^m \alpha_j D_j \quad (17)$$

where  $\alpha_j$  is the percentage of the class  $j$  present in the transport layer: by definition it is:

$$T_j = \alpha_j T \quad (18)$$

For the first term of eq.16), one has :

$$\sum_{j=1}^m T_j D_j = T \sum_{j=1}^m \alpha_j D_j = T D_t \quad (19)$$

Following a procedure similar to that used in eq. 12), one obtains for the right hand side term of eq. 16):

$$\sum_{j=1}^m \beta_j D_j T_j = D_b T_{cb} [1 + c_1 \sigma_b + c_2 \gamma_b + \dots] \quad (20)$$

where :

$$c_1 = \frac{n(n-1)}{2!} \quad (21)$$

After substitution of eqs. 19) and 20) into eq. 16), one has:

$$T D_t = D_b T_{cb} [1 + c_1 \sigma_b + c_2 \gamma_b + \dots] \quad (22)$$

Finally multiplying eq. 8) by the respective diameter  $D_j$  and summing up the  $n$  classes, gives:

$$\frac{\partial}{\partial t} \delta D_b = D_b^* \frac{\partial}{\partial t} \delta - Z - \frac{\partial}{\partial x} T D_t - \frac{\partial}{\partial t} \frac{T D_t}{U_t} \quad (23)$$

Assuming that the variance and the skewness  $\gamma_b$  of  $\beta_j$  remains unchanged, the set formed by eqs. 1), 15), 22) and 23), in the unknowns  $T$ ,  $Z$ ,  $D_t$ ,  $D_b$  is complete and can be solved numerically or, in some simplified cases, analytically. If the latter hypothesis proves unsatisfactory, an equation for the second moment can be obtained just multiplying each term of eq. 10) by  $D_j^2$  and repeating the same procedure as above.

When the bed load prevails over suspended load, as in gravel bed rivers, it is reasonable to assume:

$$\frac{\partial}{\partial x} T D_t \gg \frac{\partial}{\partial t} \frac{T D_t}{U_t} \quad (24)$$

The complete set of equations in this case will be the following:

$$\frac{\partial T}{\partial x} = - \frac{\partial Z}{\partial t} \quad (25.a)$$

$$T = T_{cb} [1 + c_2 \sigma_b + c_3 \gamma_b \dots] \quad (25.b)$$

$$T D_t = D_b T_{cb} [1 + c_1 \sigma_b + c_2 \gamma_b + \dots] \quad (25.c)$$

$$\frac{\partial}{\partial t} \delta D_b = D_b^* \frac{\partial}{\partial t} (\delta - Z) - \frac{\partial}{\partial x} T D_t \quad (25.d)$$

It should be noted that a similar procedure can also account for the adaptation process (see eq.3). In this case an adaptation length and time relevant to mean transport diameter will appear (Armanini, 1989).

Combining eqs. 25.b and 25.c) one has:

$$\frac{D_t}{D_b} = \frac{1 + c_1 \sigma_b + c_2 \gamma_b + \dots}{1 + c_2 \sigma_b + c_3 \gamma_b + \dots} \quad (26)$$

Eq. 26) states that the ratio between the mean diameter of the transport load and mean diameter of the surface bed material, is function of the moments of the bed load distribution and of the transport formula, (through the coefficients c).

If transport formula can be expressed as a power law (see eq. 11), the above ratio depends just on the exponent  $n$ . In fact substituting eqs. 14) and 21) into eq. 26) (neglecting  $O(\gamma_b)$  terms) gives:

$$\frac{D_t}{D_b} = \frac{2 + c_1 \sigma_b n(1 - n)}{2 + \sigma_b n(1 + n)} \quad (27)$$

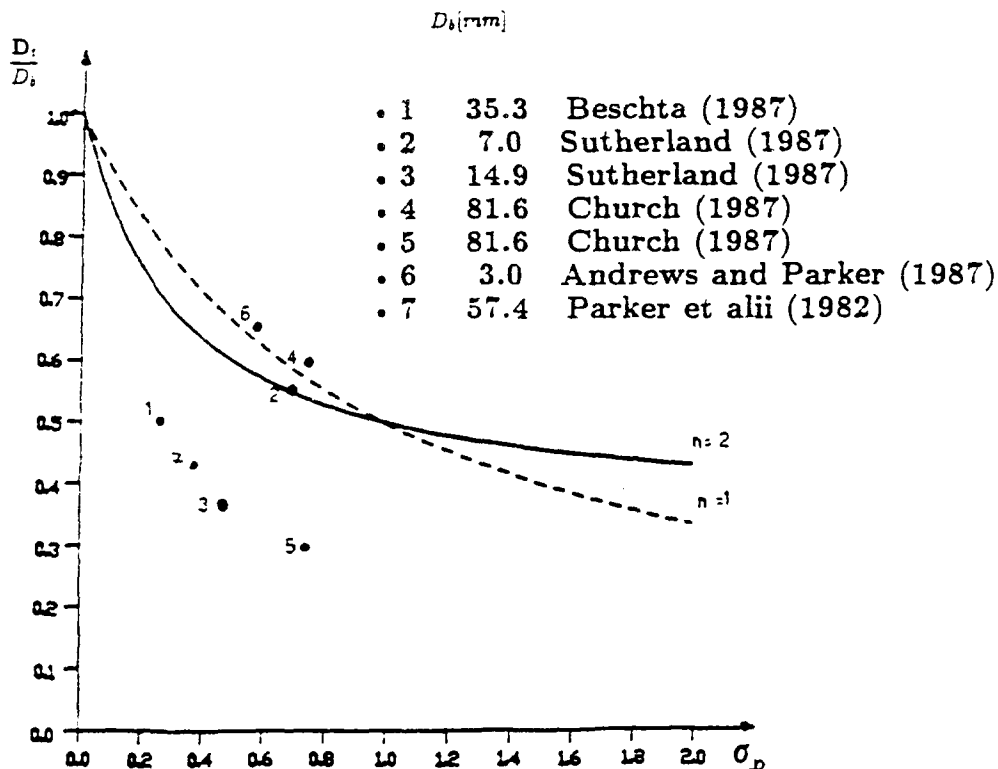


Fig.1 The ratio between mean diameters of bed-load and surface bed material are compared to eq.27)



In fig. 1, eq. 27) is compared to some experimental data.

The value  $n = 0$  corresponds to equal mobility condition; in this case, infact,  $D_t/D_b \rightarrow 1$ ; the same result is obtained when  $n \rightarrow \infty$  (absence of sediment transport).

The value  $n = 1$  for the exponent in eq. 11) is a reliable value accounting for hiding effect.

The two curves in Fig.1 correspond respectively to  $n = 1$  and  $n = 2$ ; for small values of  $\sigma_b$ , the difference between the two curves is not striking. In the same figure almost 3 points lie definitely above the curves. All these points correspond to a static armouring situation.

From eq. 27) one has that no real values for exponent  $n$  can match these experimental points. On the other hand, it must be remarked that the power law (eq. 11) for sediment transport formula can be used if the gradation curve is not very wide, and, above all, if sediment transport is far from incipient motion condition.

Instead of eq.11, it is possible to use a binomial expression (e.g. Mayer-Peter Mueller type equation):

$$T_{c_j} = \text{const}_1 \sqrt{g} D_j^{1.5} \left( \frac{u_*^2}{g D_j} - \xi_j \cdot \text{const}_2 \right)^{1.5} \quad (28.a)$$

Eq. 28 can be generalized in the following form:

$$T_{c_j} = (B_2 - A_2 D_j^{n_1})^s \quad (28.b)$$

where  $B_2$  and  $A_2$  depend on hydrodynamic conditions, but not on  $D_j$ . In this case the coefficients  $c_1$  and  $c_2$  will be:

$$c_1 = - \frac{ns.A_2(1-n)D_b^n}{2!(B_2 - A_2 D_b^n)^2} (-B_2(1+n) + A_2(1+ns)) \quad (29)$$

$$c_2 = c_1 - \frac{ns.A_2}{B_2 D_b^n - A_2} \quad (30)$$

Eqs. 29) and 30), inserted in eq. 26), allow for any solution for  $D_t/D_b < 1$ , provided that the correct sediment transport formula is given.

Unfortunately eqs. 29) and 30) are more difficult to be used, because they require the knowledge of the sediment transport formula (this quantity does not appear in eq. 27). Comparison between theory and literature experiments is under way.

Eqs.29) and 30) must be used instead of eq. 14.a) where the gradation curve is wide.

When  $n \rightarrow 0$  in eqs. 29) and 30) (equal mobility),  $D_t/D_b \rightarrow 0$ . The same results when transport rate tends to zero.

Similar conclusions can be drawn for the coefficient  $c_3$ . More in general  $c_1$ ,  $c_2$  and  $c_3$  are function of  $D_b$ .

From eqs. 25.a) - 25.d), algebraic manipulation (and neglecting skewness terms) yields:

$$\delta \frac{\partial}{\partial t} D_b = D_b^* \frac{\partial}{\partial x} T_{cb} [1 + c_2 \sigma_b] - \frac{\partial}{\partial x} D_b T_{cb} [1 + c_1 \sigma_b] + (D_b^* - D_b) \frac{\partial \delta}{\partial t} \quad (31)$$

In aggrading processes, (deposition)  $D_b^*$  is equal to  $D_b$ , and eq.31) leads to:

$$\frac{\partial}{\partial t} \delta D_b + T_{cb} [1 + c_1 \sigma_b] \frac{\partial D_b}{\partial x} = D_b \frac{\partial}{\partial x} T_{cb} \sigma_b [c_2 - c_1] \quad (32)$$

and:

$$\frac{\partial}{\partial t} \delta D_b + [T_{cb} (1 + c_1 \sigma_b) - n D_b \sigma_b \frac{\partial T_{cb}}{\partial D_b}] \frac{\partial D_b}{\partial x} = n D_b \sigma_b \frac{\partial U}{\partial x} \frac{\partial T_{cb}}{\partial U} \quad (33)$$

Eq.33) gives the following celerity, for the propagation for the mean diameter:

$$\bar{c}_{D_b} = \frac{[T_{cb} (1 + c_1 \sigma_b) - n D_b \sigma_b \frac{\partial T_{cb}}{\partial D_b}]}{\delta} = \frac{T_{cb}}{\delta} [1 + \sigma_b (c_1 + n^2)] \quad (34)$$

In nonuniform flow, the celerity is obviously non constant, and increases with increasing velocity. The thickness  $\delta$  of the mixing layer reduces then the celerity.

## CONCLUSIONS

This mathematical model can describe the behavior, in one-dimensional channels, of a mixture of materials having non uniform grain size distribution.

Compared to complete schemes, where each fraction of the gradation curve is described by one (or two) partial differential equation(s), the model is based on mean diameters and variance of grain size distribution (and if necessary, of the other moments of the distribution).

From a numerical point of view the model, reducing the number of variables, represents a relevant simplification.

some questions are still open in particular concerning:

- the role of the hiding factor (this is a open point also for the other models);
- the possibility of describing the armouring processes (static armouring);
- the legitimacy of keeping variance (and other moments) constant in space and time;
- the legitimacy of neglecting higher order moments.

Comparison between the proposed scheme and literature experiments, as well as comparison with complete models, are under way.

Finally an improvement in the model can be obtained, writing the moments in terms of logarithm of the particles diameter instead of the diameter itself.

## NOTATIONS

The following symbols have been used in this paper:.

$A_2, B_2$	parameters of sediment transport formula
$C$	concentration
$c_1, c_2, c_3$	coefficients
$\bar{c}_{D_b}$	celerity of transported mean diameter
$D_j$	mean diameter of class j-th
$D_b$	mean diameter in the mixing layer
$D_t$	mean diameter of the transported material
$h$	water depth
$L^*$	adaptation length
$m$	number of grain size classes
$n$	exponent
$x$	longitudinal coordinate
$t$	time
$T_j$	transport rate of j-th grain size class
$T_c$	transport capacity of the j-th grain size class
$U$	depth averaged velocity
$U_j = \frac{T_j}{C_j}$	
$u_*$	friction velocity
$w$	particle fall velocity
$Z$	bed elevation
$\alpha_j$	percentage of the j-th class inside the transport layer
$\beta_j$	percentage of the j-th class into the exchange layer
$\delta$	exchange layer thickness
$\Delta$	height of the dunes
$\sigma_b, \gamma_b$	second and third moments of grain size distribution inside the mixing layer
$\sigma_t, \gamma_t$	second and third moments of grain size distribution of transported material
$\tau^*$	adaptation time
$\xi_j$	hiding factor for j-th grain size class

## REFERENCES

- Andrews, E.D., Parker, G. (1987). Formation of Coarse Surface Layer as the Response to Gravel Mobility. *Sediment Transport in Gravel-bed Rivers*, John Wiley & S. Ltd., p.269-300.
- Armanini, A. (1989). Variation of bed and Transport Mean Diameter in non-equilibrium condition, Proc. of Int. Workshop on Fluv. Hydr. of Mount. Regions, Trent, Italy.
- Armanini, A., Di Silvio, G. (1982). Sudden Morphological Modifications along Mountain River Simulated by Mathematical Model. 3rd Congress of the APD of IAHR, Bandung, Indonesia.
- Armanini, A., Di Silvio, G. (1988). A One-dimensional Model for the Transport of Sediment Mixture in Non-equilibrium Condition, *Juorn. of IAHR*, vol26, n.3.

- Ashida,K.,Michiue,M.(1971),An Investigation of River Bed Degradation of Dam, Proc. 14th IAHR Congr., vol.3. pp 247-255,1971.
- Beschta,R.L.(1987). Conceptual Models of Sediment Transport in Streams. *Sediment Transport in Gravel-bed Rivers*, John Wiley & S. Ltd.,p.387-420.
- Bouchard,J-P.,Cordelle,M.,Labadie,g.,Lorin,J.(1989) Numerical Simulation of Mud Erosion in reservoirs by Floods Application to Reservoir of the Durance River. Proc. of XXIII IAHR Congr., Vol.B,Ottawa.pp. 575-581.
- Church,M.A.(1987) Discussion,*Sediment Transport in Gravel-bed Rivers*, John Wiley & S. Ltd.,p.314-322.
- Day,T.J.(1980). A Study of the Transport of Graded Sediments. HRS Wallingford Rep. No.IT 190,April.
- DiSilvio,G.,Peviani,A.(1989),Modelling Short and long term Evolution of Mountain river: an Application to Torrent Mallero Italy, Proc. of Int. Workshop on Fluv. Hydr. of Mount. Regions, Trent, Italy
- Eghiazaroff,I.V.(1965). Calculation of Non-Uniform Sediment Concentrations. Proc.A.S.C.E. J.Hydr.Div., 91(HY4)
- Einstein,H.A.(1950). The Bed-Load Function for Sediment Transport in Open Channel Flows. Tech. Bull. No.1026, U.S.Dept. of Agr., Soil Cons.Serv., Sept.
- Karim,M.F.,and Kennedy,J.F.(1982).Computer Based Predictors for Dediment Discharge and Friction Factor of Alluvial Streams. IIHR report no.242,The University of Iowa.USA.
- Parker,G.,Klingeman,P.C. and McLean,D.G.(1982), Bedload and size distribution in paved gravel- bed stream. Proc. A.S.C.E., J. Hydr. Div.,HY4,108,544-571
- Ranga Raju,K.G.(1985). Transport of Sediment Mixture, Ippen Lecture, XXI IAHR Congr., Melbourne, Australia.
- Rahuel,J.,Holly,F.M.(1989), Numerical Simulation of Sediment Mixture Dynamics. Proc. XXIII-IAHR Congr., vol.B, Ottawa, pp.315-320.
- Sutherland,A J.(1987). Static Armour Layers by Selective Erosion, *Sediment Transport in Gravel-bed River*, John Wiley & S. Ltd.,p.243-267.

# THE MYSTERY OF BIMODALITY: FALSIFICATION OF CURRENT CONCEPTS, PROPOSAL OF A NEW ONE

Hillert Ibbeken  
Institut für Geologie  
Freie Universität Berlin  
Germany

## Preface

This paper is part of an extensive study of provenance in Calabria, South Italy (Fig. 1). Bimodality is only one of many aspects treated in this context. However, the broad background of quantitative information in Calabria makes it possible to check elements of bimodality against most of the variables assumed to be relevant for this problem.

The study area: The Ionian slope of the Calabrian Massif is an active plate margin, 19 basins drain the 1850 km<sup>2</sup> research area (area 16-160 km<sup>2</sup>, maximum length 20 km, maximum elevation 2000 m). Four of these 19 braided rivers reach the seventh order, the other 15 rivers are of the sixth order. Drainage density ranges from 5.1 l/km to 10.36 l/km, bifurcation ratios vary between 3.8 and 5.8. The relief (altitude standard deviation) ranges between 213 and 481 m, the slopes of the main trunks vary between 1:30 and 1:110. Mean annual precipitation is between <600 mm and >2000 mm, rainstorms with precipitations of more than 400 mm a day are the most striking climatic events of the area.

The hinterland comprises granite (24 % area), gneiss (7 %), schist (30 %), limestone (1 %), conglomerate (9 %), sandstone (9 %), siltstone (12 %) and argillite (8 %). Mean longterm (1 Ma) erosion rate is 206 mm/ka, mean shortterm rates (50 a) are 1700 mm/ka, calculated over landslide activity, geodetic survey of long profiles and the refill of a landslide-created lake.

## Summary

Calabrian river-mouth sediments are both bimodal and unimodal. The gravel mode of the bimodal distributions, mostly Rosin-distributed, is interpreted as a first order element, a primary feature inherited from the jointed and weathered source rocks whereas the sand mode can be seen as a second order element acquired during fluvial attrition and transportation.

If the percentage of the fraction 1-20 mm exceeds about 35 % the distributions became unimodal. So this fraction is crucial for modality and it is called, consequently, a third order element.

All single factors assumed to control modality such as relief, basin shape, source rock-petrography, the petrographical composition of the river-sediment itself or postdepositional refill of interstices fail to exert a significant or mono-causal influence on modality. In addition, no hydrodynamic conditions are known which specifically select, as a rule and within the grain-size range of gravel and sand, this fraction of 1-20 mm. Thus, other possibilities having excluded, only availability

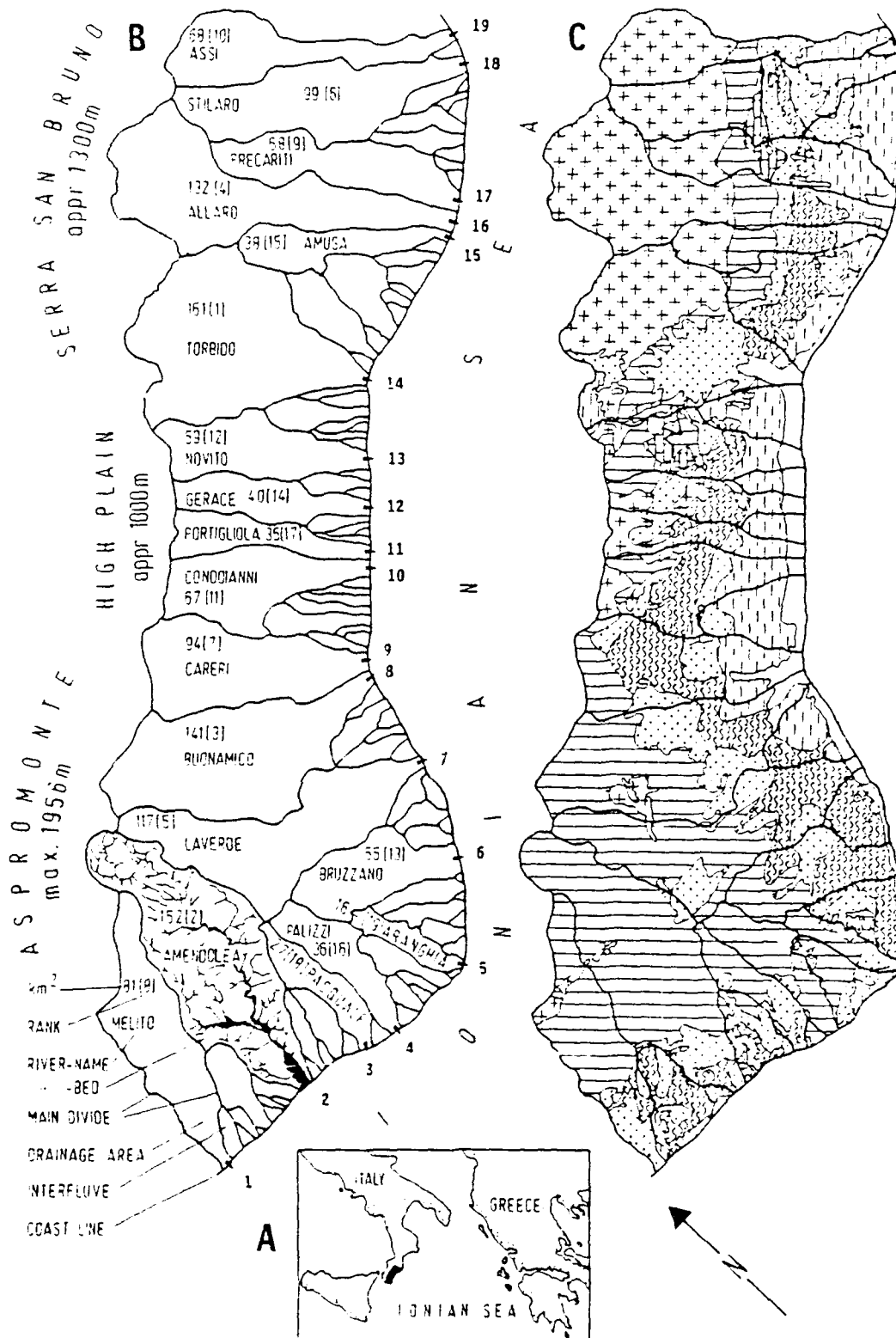


Figure 1. **A:** Position of the study area. **B:** The 103 basins and interfluves and some data of the 19 rivers studied in more detail. **C:** Regional distribution of the most important rock-families: Granite (++++); metamorphic rocks (—); limestone (||||); sandstone and conglomerate (::::); siltstone (~~~~) and argillite (---)

remains, but not in the sense of source-area related sediment production. It is assumed that different floods drive the "sedimentary mill" of these mountain rivers differently and that the formation of the fraction 1-20 mm is sensitive to these differences.

**Data base:** 133 samples, jointed and weathered source rocks (in situ, 25 samples), transition (regolith, talus debris, alluvial cone, 22), river-course (downstream of the fall line, 17), river-mouth (35) and beach (shoreface, 34)

**Method:** The mean sample size is 270 kg, the maximum grain-size 256 mm. The samples were taken as channel samples by means of a crowbar (handspike) or motor hammer. The fraction >16mm was sieved in the field by means of a transportable sieving and splitting machine in 1/3 phi steps (Ibbeken 1974), the fraction <16 mm was split and taken to the lab. The results of the sieve analyses are stored in a data bank, like all other data, i.e. digitized maps and analyses of the river-mouth sediments.

### **Unimodal and bimodal distributions**

The problem of bimodality or, more generally, of deficiencies of certain grain-size classes within grain-size distributions of terrigenous sediments, expressed by "kinks" of the cumulative frequency distribution, finds much interest among sedimentologists. We refer exclusively to the deficiencies of sandy gravel deposits somewhere in the range of 1 to 20 mm. Shea (1974) gives an overview of the problem. He states that most contributions to the deficiency complex are not accompanied by statistically rigorous techniques and that many theories are simply contradictory. Shea presents a histogram of an overall weighed average of 11,212 analyses, which shows no deficiencies. However, many of our modern Calabrian deposits display both evidently bimodal and unimodal distributions and our knowledge of the source area conditions should lead us to a better understanding of the problem. This is of special interest, because some authors believe bimodality to be a provenance factor. But this can be only partly true. As pointed out by Ibbeken, 1983, only the shape of the gravel mode has to be seen as an inherited element, whereas the sand mode represents an acquired one, created mainly during fluvial transportation. However, bimodal or unimodal, in Calabria this depends mainly on whether the amount of the fraction 1-20 mm exceeds 35 % or not.

### **The gravel mode (first order element)**

Gravel modes of bimodal distributions in Calabria are mostly Rosin- instead of lognormally distributed (Ibbeken 1983). The "RG-ratio", the Rosin/Gauss ratio, stands for the quotient of the number of Rosin- to Gauss- distributed samples of an environment. In Calabria, the jointed and weathered source rocks yield a "RG-ratio" of 4, transition (3.6), river-course (5),

river-mouth (8) and beach (0.65). This means that the Rosin-tendency increases towards the river-mouth and it is only the beach environment which creates a symmetrization.

#### **The sand mode (second order element)**

The sand budget of both bimodal and unimodal river-mouth sediments is exactly balanced, the average sand content is 24.95 % (bimodal sediments) and 25.19 % (unimodal sediments), 60 % of the bimodal and 61.9 % of unimodal river-mouth sediments have sand contents under 25 %. In single cases the sand content varies considerably, between about 10 % and 50 %. Thus, compared to the never missing gravel mode, the Calabrian sand modes are a relatively unstable feature.

The mean sand content increases continuously from the jointed and weathered source rocks (4.6 %) over the transitional stage (13.6 %) and the river-course (16.5 %) to the river-mouth (28 %).

Calabrian sand modes are almost exclusively lognormally distributed. Ibbeken (1983) interpreted this as a transport-specific, acquired property. This implies that the sand comes from rock disintegration and soil formation. Geochemical evidence makes this argument refutable: Constant oxide- and gain and loss calculations of the geochemical composition of the source rocks, source soils and river-mouth sediment, comparing the 63-500  $\mu\text{m}$  fraction, demonstrate that the river-mouth sediment resembles the fresh source rock rather than the soils. It is probable, from this, that attrition during bankfull stages of these powerful, high gradient mountain rivers is the most important process of sand formation in Calabria.

#### **The 1-20 mm fraction (third order element)**

Figure 2A shows the average of 51 bimodal distributions. The gravel modes (A1) shift from 12.5-128 mm, the sand modes (A2) vary between 0.135 and 1.6 mm, but the position of the "valley" in between (A3), much more stable, ranges only between 1.25 and 4 mm. The "kink" of the 1.6-2 mm class stems from sample splitting at 2 mm.

Figure 2B displays the average of 22 unimodal distributions, the much less peaked modes vary between 8 and 80 mm.

As pointed out, the sand content of both bi- and unimodal distributions is well balanced, ranging from about 10 to 50 % with an average of 25 %, regardless of bi- or unimodal distributions. Thus it is not the amount of sand which is responsible for modality. This is demonstrated by Figure 2C. Here the difference between the two types of distribution is calculated simply by subtracting the mean unimodal from the mean bimodal distribution. It turns out that the fraction 1-20 mm is the essential one which makes the difference between bi- and unimodal distributions. It is called, consequently, a third order element (Ibbeken 1983, p.1230). Figure 5A shows that most unimodal rivers contain more than 35 % of this fraction, the Bruzzano [06] excepted. Ibbeken (op.cit., Fig. 8C) demonstrated that it is possible to split the average Calabrian unimodal distribution into a Rosin-distributed gravel mode (first order), a log-



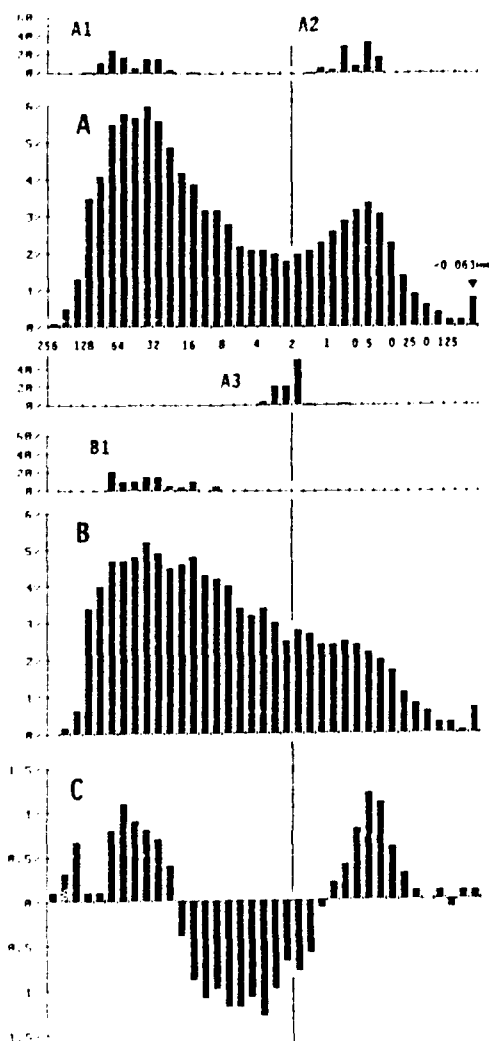


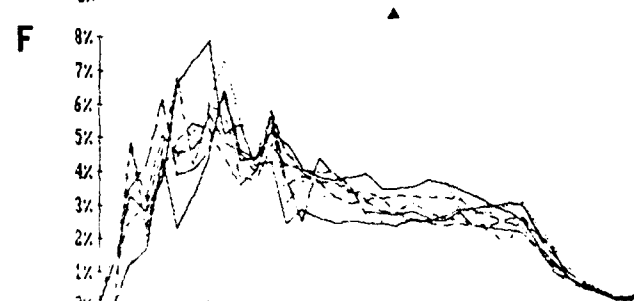
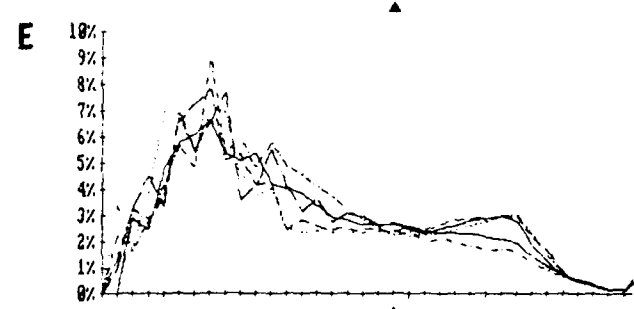
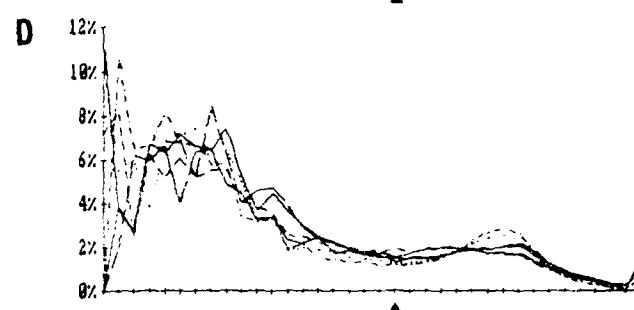
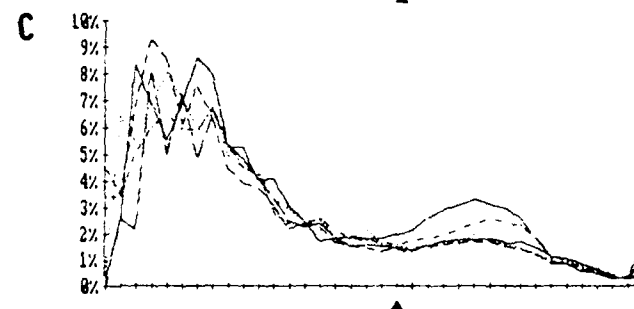
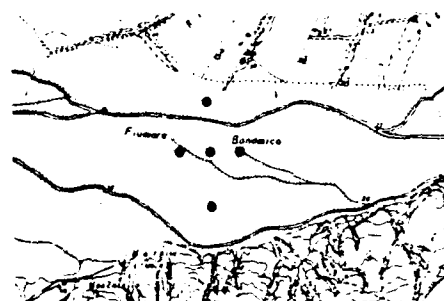
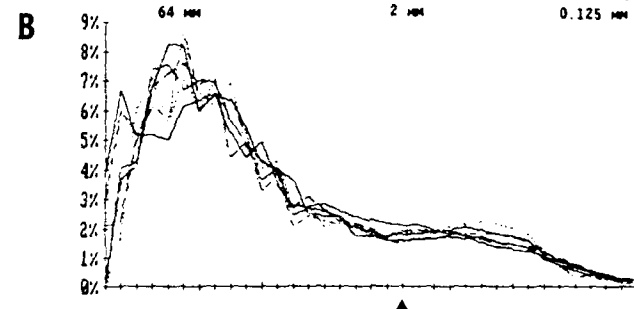
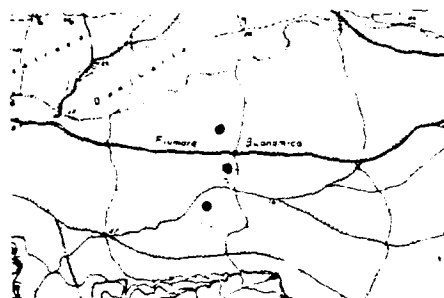
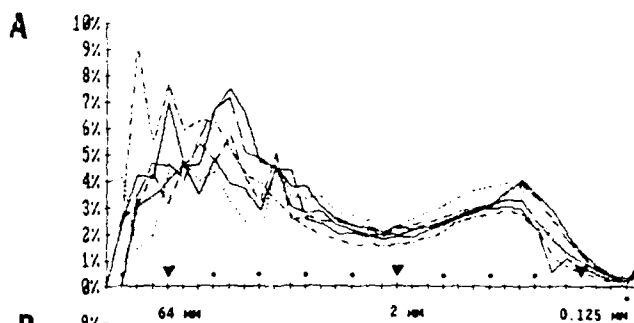
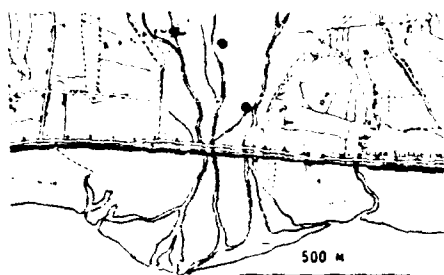
Figure 2. **A:** Average of 52 bi-modal distributions;  
**A1:** Distribution of the gravel modes;  
**A2:** Distribution of the sand modes;  
**A3:** Distribution of the "valleys" (lowest percentage) in between;  
**B:** Average of 22 unimodal distributions;  
**B1:** Distribution of the gravel modes;  
**C:** Average bimodal distribution (A) minus average unimodal distribution (B). The presence or absence of the fraction 1-20 mm decides on uni- or bimodality. There is no correlation either between the position of the modes and the "valleys" or between the respective percentages, all these features vary independently from each other.

normal distributed sand mode (second order), and a remainder which comprises the fraction 1.6-12.5 mm, corresponding almost perfectly to the 1-20 mm interval which makes the difference between the average bimodal and unimodal distribution. This third order element, crucial for modality, is believed to be more dependent on availability than on hydrodynamics and this problem will be resumed in the conclusion section after more data have been presented.

### Test sampling

The objective of the test-sampling campaigns was to find out whether modality depends on the following circumstances:





occurs. Consequently, an operator error can be excluded. The Amendolea [02], 152 km<sup>2</sup>, is one of the largest rivers of the area. The source area is dominated by metamorphic rocks, and conglomerates feed recycled granitic gravels into the river-mouth sediments. The twin samples, at distances of several 100 m, taken within some days under constant conditions, show surprisingly uniform sand modes, less stable gravel modes and an obviously stable bimodality (Fig. 3A). From this one is tempted to speak of evidently bimodal river-mouth sediments of this river. Two other samples taken in other years (Fig. 4) disturb this picture, because one of these samples display only a very weak sand mode close to unimodality.

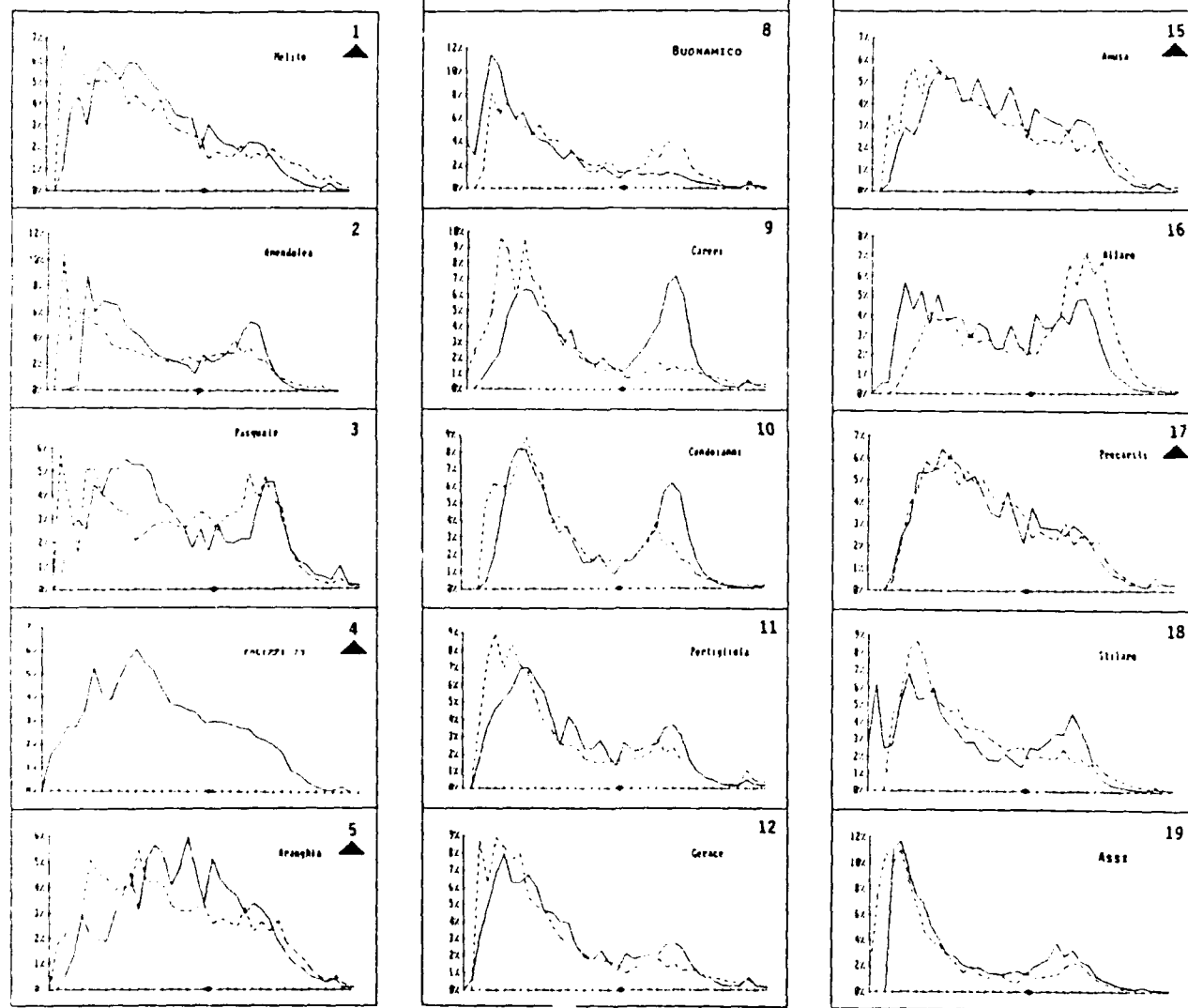
The Buonamico [08], 139 km<sup>2</sup>, one of the largest and most characteristic Calabrian Fiumaras with a mostly metamorphic source area was chosen to investigate a possible downstream development of modality. The three twin samples from upstream, 10 km from the coast (Fig. 3B), display nearly unimodal distributions with relatively stable gravel modes. The midstream section, 3.6 km from the coast, shows a bimodal and a nearly unimodal distribution close to the banks as well as the same ambiguous situation in a triple sample sequence in between (Fig. 3C). The same picture is yielded by the river-mouth sediments (Fig. 3D). Thus, in this campaign, the Buonamico appears as an producer of very slightly bimodal sediments. But only during this campaign. Additional sampling in other years (Fig. 4) in the river-mouth area presents both a strictly unimodal and, one year later, a strictly bimodal Buonamico.

The Torbido [14], 160 km<sup>2</sup>, is the largest river under investigation, the source area is granite- and sediment-dominated. A river of this type is commonly expected to be a powerful producer of sand. But again, the sand modes are very modest or lacking (Fig. 3E). The modality of these river-mouth sediments depends on where these bulk samples are taken. Additional sampling in different years makes this even more evident (Fig. 4). Here, we obtained a weakly bimodal sample as during the test-sampling and a year later a strongly bimodal one.

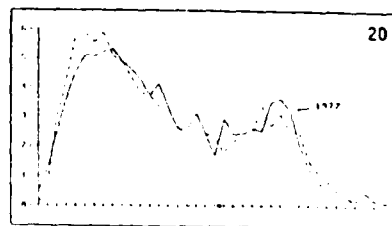
The Amusa [15], 38 km<sup>2</sup>, is a very small river with a predominantly granitic source area, followed by metamorphic rocks. This river displays a strong unimodal tendency over all samples (Fig. 3F), one of the SW-bank excepted. The same is true for the additional samples (Fig. 4).

The results of the sampling-test campaign demonstrate that none of the criteria listed displays a significant and mono-causal influence on bi- or unimodality. Both types of distributions may occur more or less irregularly under all circumstances. This becomes even more striking if we compare the overall grain-size distributions of the river-mouth sediments of the 1972 and 1973 campaigns, before and after the disastrous January flooding (Fig. 4). Strong differences in modality from year to year signalize that nearly all rivers are able to produce both types of distribution, uni- and bimodal. From this it becomes evident that modality is not a given characteristic of a given river in space and time and it may appear useless to look at possible links between modality and source-area conditions

Figure 4. Grain-size frequency distributions of the 19 river-mouth sediments, 1-19: 1972 and 1973 campaign, the Palizzi [04] was only sampled once. 20: average 72 and 73. The Careri [09] is the most striking example for changing modality conditions within one and the same river.



Abscissa in 1/3 phi steps, dots indicate the 1.6-2 mm interval. Triangles (▲) refer to the predominantly unimodal distributions which are used for possible source area correlations (Fig. 5).



or other properties which have to be assumed as constant in space and time. However, the phenomenon of modality exists as such and our understanding of it may be improved by narrowing down possible solutions at the expense of falsificated ones.

### Modality and the source-area variables

Looking for explanations for bi- or unimodal river sediments we will ignore the possible longterm changes in modality of a given river and trust the results of the two-year campaigns plotted in Figure 4. Here the river-mouth sediments of 7 rivers display at least a certain unimodal tendency and an acceptable similarity between the two campaigns:

Melito	[01]	Novito	[13]
Palizzi	[04]	Amusa	[15]
Aranghia	[05]	Precariti	[17]
Bruzzano	[06]		

The Palizzi, however, was only sampled once. Suppose these 7 rivers produce predominantly unimodal sediments and the other 12 rivers favour bimodal ones, we are now able, in the case of Calabria, to check most arguments for or against bimodality cited in the literature. These are geomorphology, petrography and primary grain-size distributions of the source areas, the petrography of the river-mouth sediments itself, packing and the refill of interstices and, only indirectly interpretable, runoff- and hydrodynamic conditions.

### Source area morphology and modality

If runoff- and hydrodynamic conditions characteristic of high-gradient mountain rivers were be responsible for the uni- or bimodality of fluvial sediments, and if these runoff- and hydrodynamic conditions were be relatable to morphological features of the source area such as relief, dissection, basin shape or the gradient of the trunk slope - then these features, in turn, should correlate with the modality of the river-mouth sediments. Strahler (1964, p.4-45), for example, expects low but extended peak flows from elongated basins and sharp peaks from rotund basins. High relief rivers should create river-mouth sediments different from low relief rivers. Furthermore, current velocities of a river with a steep trunk slope should be higher than those of rivers with lower gradients. However, the Calabrian data do not reveal the slightest relationship between the morphology of the source area and the modality of river-mouth sediments. Figure 5B shows the relief of the 19 basins in terms of the altitude standard deviation, Figure 5C presents the hypsometric integral or dissection in terms of the altitude skewness and Figure 5D displays the basin shapes according to Horton's formula (Horton 1932): On all plots the rivers with predominantly unimodal river-mouth sediments are marked. There are certain tendencies, but they are never exclusive of one modality alone. For example, all unimodal river-mouth sediments belong to elongated basins characterized by low Horton ratios. But Laverde [07], Portigliola [11] and Assi [19],

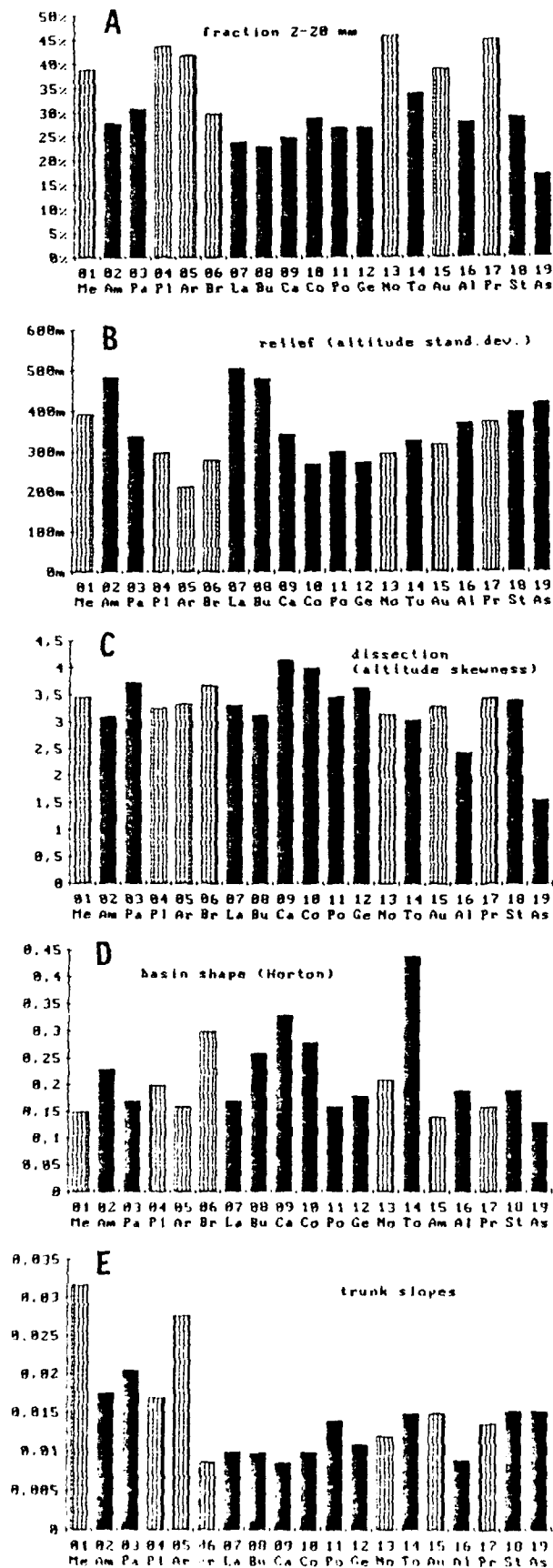


Figure 5. Uni- and bi-modality of the river-mouth sediments of the 19 basins versus sediment- and source-area variables. River-mouth sediments with predominantly unimodal distributions are hatched, bimodal ones are marked black.

A: Percentage of the fraction 2-20 mm. Rivers with more than about 35 % of this fraction are unimodal, the Bruzzano [06] excepted (Fig. 4/6). So this fraction is crucial for modality.

B: Relief (altitude standard deviation) does not correlate with modality.

C: Dissection (altitude skewness) does not correlate with modality.

D: Basin shape  $R_f$  (Horton 1932) does not correlate with modality.

E: Slope of the trunk (river segment of the highest order) does not correlate with modality.

with partly even lower Horton ratios, produce predominantly bimodal river-mouth sediments. Figure 5E shows the trunk slopes of the 19 rivers, the gradients of the main channel of highest order: These gradients vary noticeably between about 0.03 and 0.01, this is, by factor 3, but unimodality is combined with both lowest and highest gradients.

#### **Source area petrography and modality**

Source rock petrography is probably the most popular argument to account for bimodality. The missing grain sizes - mostly granules - are said to be less frequently produced by certain rock types. There is no support for this in Calabria.

The area percentage and the erosional budget of the 19 basins in terms of granitic, sedimentary- and metamorphic rocks demonstrate some combinations of unimodality and granite-poor source areas, but not exclusively. Five "bimodal rivers" fall into this category, too. The test was repeated using various combinations of metamorphic- and sedimentary rocks, but no preferred correlation occurred. Finally a combination of granite, sandstone and conglomerate of the source areas versus the modality was plotted in order to find out whether these predominantly sand producing units correlate with the modality of the river-mouth sediments - again without success. In Calabria the modality of river-mouth sediments is definitely not controlled by source rock petrography, as supposed and proposed in other regions by Hough (1942), Yatsu (1955) or Rogers et al. (1963).

#### **Source area grain-size distributions and modality**

Wolcott (1988) proposed the size distribution of the input material as being largely responsible for the size distribution of channel deposits. Apart from the fact that it is hard to explain how such a hydrodynamically delicate structure like bimodality is maintained during fluvial transport over several kilometers - in the case of Calabria it has been known for years that most jointed and weathered source rocks are extremely unimodal and most river-mouth sediments are strikingly bimodal. So the bimodality of river-mouth sediments in Calabria is definitely not controlled directly by the granulometric properties of the source rocks.

#### **Petrography of river-mouth sediments and modality**

Very little attention has been paid to the petrography of the sediments itself as a possible reason for modality (Davies et al., 1978). However, in Calabria this question leads into a blind alley, too. The petrographic composition of the gravel fractions 16-80 mm and 1-20 mm of the 19 river-mouths was determined. There is definitely no correlation between the character of modality and any petrographic composition of the two gravel fractions. This is especially important in the case of the range of 1-20 mm, the third order element, because this fraction constitutes the main part of the mysterious "gap"



which defines modality. The same is true for the petrographic composition of the sand mode. The light mineral indices of all 19 river-mouth sediments are analysed. The content of rock fragments or the quartz/feldspar ratio may account for the breakdown of certain fractions and may be responsible, in this way, for modality - but there is not the slightest correlation between these or other compositional parameters and modality. So even the petrographic composition of the river-mouth sediments itself can definitely be excluded as a possible factor controlling modality - in the case of Calabria.

#### **Packing and refill of interstices and modality**

In 1935 an important statement concerning our topic was made by Fraser, barely cited thereafter (Plumley 1948, p.542, Pettijohn 1957, p.45). Fraser (1935, p.987) says: "... it is difficult to understand how a river capable of carrying all sizes up to large boulders can deposit them at the same time. At any instant, the largest particle that may be moved varies at the sixth power of the current velocity". Fraser calculates that the velocity of a stream capable of carrying 250 mm pebbles has to decrease 60 % before 1 mm sand could be deposited. "Hence it seems improbable that large pebbles and fine sand are necessarily deposited simultaneously", and "The periods during which river gravels may be moved, sized and sorted are usually brief and are followed by much longer quiescent periods during which infiltration and arrangement of the finer sizes may be accomplished" (op.cit., p.984). Fraser calculates the effects of various gravel grain-sizes enabling finer fractions to enter the framework after deposition and defines a "critical ratio of entrance" (op.cit., p.919). Plumley (1948, p. 544) agrees with Fraser and finds, by theoretical considerations, ratios between 22 % and 32 % for the sand content of gravels. Plumley finds this confirmed by his samples and states that the weight ratios of the infilling fractions increase with decreasing mean size of the sediment.

As pointed out, this and all other features of the grain-size distributions were checked, but no correlation was found: the grain-size classes of both the gravel and the sand modes, the "valley" in between, the sand content and finally the percentage of the third order element, the fraction 1-20 mm - all vary independently among themselves.

Only the mean sand content of 25 % corresponds nicely to the sand contents claimed for filling interstices, but this, unfortunately, is irrelevant for uni- or bimodality.

#### **Hydrodynamic conditions and modality**

Many authors believe that selective transportation due to different hydrodynamic behavior of different grain sizes is a main factor controlling modality. These arguments are largely refuted by Shea (1974, p.1000). The most cited authors in this context are Sundborg (1956) and especially Russel (1968), who argues "that the fractions 1-6 mm are more readily entrained and more rapidly transported than grains of larger or smaller size. Currents, mainly of wave origin, concentrate these grains in

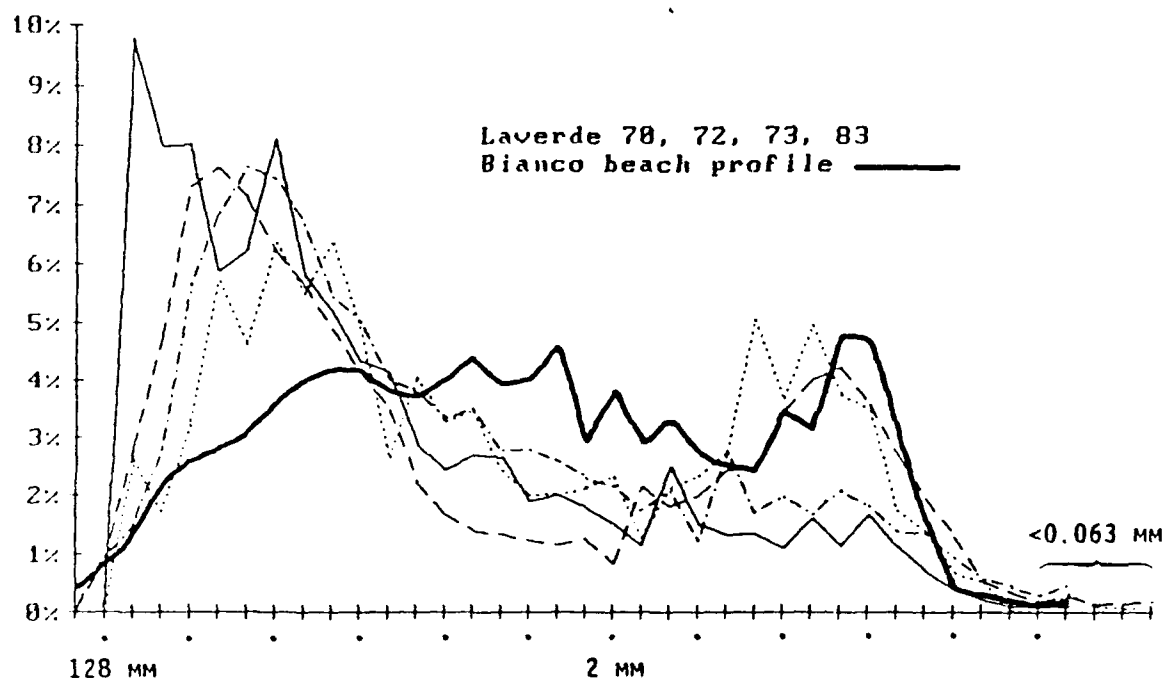


Figure 6. Comparison of fluvial and coastal grain-size distributions, Laverde [07] and Bianco Beach. The Laverde is the main feeder of the Bianco Beach. The four Laverde samples stem from the 1970, 1972, 1973 and 1983 campaigns. The heavy line refers to the "Strand Profil", a continuously sampled beach-normal profile 70 m long, from 2 m above to 4 m below sea level, comprising a total of 7 t. The profile tries to bridge the entire beach in motion.

beaches, where they are present in more-than-ordinary abundance" (op.cit.p.31). The first problem which arises with regard to Russel's idea is that the Calabrian grain-size gap is much larger than from 1-6 mm. As pointed out by Shea (1974, p.1000) no hydrodynamic mechanism is known which favours continuously the entrainment and transportation of grain-sizes between 1 and 20 mm. It was not possible to check the hydrodynamic qualities of this argument, but the bulk grain-size distribution of the beach was calculated to check the consequences claimed by Russel. This sample (Fig. 6) represents the average of 32 excavator samples, 7 tons as a whole, of a 70 m profile of the entire beach in motion, normal to the coast from the backshore 2 m above sea level to the offshore strip 4 m below sea level. From the Laverde river-mouth [07], which feeds this beach there are 4 samples, from 1970, 72, 73 and 83. The single fluvial distributions vary between nearly unimodal and strongly bimodal. The coastal distribution admittedly fills the fluvial gap (Fig. 6) if referred to the bimodal distributions. However, the coastal sand mode slightly exceeds the gravel mode, and there is a deficiency, too, somewhat shifted towards the fines. Thus from the merely descriptive point of view Russel is not

wrong, but the question remains whether the fill of the gap in the coastal realm stems from increased fluvial input or simply from attrition of the coarse mode during longshore transportation.

As a result, none of the reasons assumed to be responsible for uni- or bimodality can be accepted in Calabria. The interpretation given in this paper focuses attention on attrition and selective transport or deposition as already supposed by Shea (1974, p.1001).

## Conclusion

To return to the synoptical comparison of the river-mouth sediment's grain-size distributions of the 1972 and 1973 campaign (Fig. 3, 01-20). The basic or first order feature present in all samples is the positively skewed gravel mode. This Rosin distributed gravel mode is interpreted as an inherited, primary source rock element (Ibbeken 1983, p.1227), which is maintained during fluvial attrition and selection until the river-mouth areas are reached. It goes without saying that during this development the gravel mode is modified shifting towards the fines and flattening. Thus the gravel mode carries both a compositional and a textural provenance signal.

The other important, second order feature is the sand mode of the bimodal distributions, usually lognormally or Gauss-distributed. This mode may be very pronounced (Careri [09] and Condoianni [10]) or nearly absent (Melito [01], Palizzi [04] and Precariti [17]). The geochemical evidence makes it a reasonable assumption that the overwhelming portion of fluvial sand does not come from the jointed and weathered source rocks or soils, nor from disintegration or decomposition (Pettijohn et al. 1987, p.252) but from attrition mainly during the floods of the high-gradient mountain rivers. This is the only way to create sand whose geochemical composition is fresher and more original than that of the debris of slopes and soils. It is not clear why the sand modes of the bimodal distributions almost exclusively display lognormal instead of Rosin distributions, as expected from the process of sand formation by attrition. Lognormality is usually seen as a transport-specific feature. Obviously the movement of sand, much more frequent than that of gravels, is sufficient to cause a Rosin/Gauss transformation. Thus the sand mode carries only a compositional or petrographic provenance signal, but not a textural one.

Bimodality, in Calabria, may be simply explained as the result of mixing between these different modes, gravel and sand. Ibbeken (1983, Fig. 10) mixed an ideal, coarse grained Rosin-distribution and an ideal fine grained lognormal distribution in accordance with the grain-sizes and parameters of the average Calabrian river-mouth sediment, 70 % and 30 %, and obtained a bimodal distribution which corresponds nearly perfectly to that of the mean bimodal river-mouth sediment in Calabria. It may be reasonable to infer that the bimodal Calabrian river deposits originate from gravel modes with a long fine tail, superimposed by a sand mode.

This picture is seriously disturbed by the presence of unimodal distributions. These are characterized by amounts of more than about 35 % of the fraction 1-20 mm, the third order element. The crucial question is what controls the appearance or non-appearance of this grain-size interval. All source area variables and all variables of the sediment itself, as petrographic composition or grain-size parameters were falsificated and excluded. So the only remaining variables not directly tested are hydrodynamics and availability. Obviously hydrodynamics can be excluded, too. As pointed out, there is no reason why the fraction 1-20 mm should somehow be selected by hydrodynamics. On the other hand, the complex process of attrition during bank-full stages of mountainous rivers is not accessible as yet. Consequently the following can only be a matter of belief: The process of crushing during floods differs, in space and time, between bed load, transitional stages and suspended load. The suspended load, at any given time, is largely protected against further crushing, the bed load itself is not. Thus floods of varying intensity may produce varying grain-sizes, and the third order element, the fraction 1-20 mm, may be especially susceptible for these differences, being destroyed or not, so that bi- or unimodal lag sediments result. It is necessary to speculate on this topic alone, availability via attrition, in order to explain the confusing variability of modality in space and time: all other variables cited can definitely be ruled out, in the case of Calabria.

## References

- Davies, D.K., Vessell, R.K., Miles, R.C., Foley, M.G. and Bonnis, S.F., 1978, Fluvial transport and downstream modifications in an active volcanic region: In Miall, A.D. (Ed.): Fluvial sedimentology. Canadian Soc. Petroleum Geologists Mem. 5, 61-84.
- Fraser, H.J., 1935, Experimental study of the porosity and permeability of clastic sediments: The Journal of Geology, 48, 912-1009.
- Horton, R.E., 1932, Drainage basin characteristics, Trans. Am. Geophys. Union, 13, 351-361.
- Hough, J.L., 1942, Sediments of Cape Code Bay, Massachusetts: Jour. Sed. Petrology, 12, 10-30.
- Ibbeken, H., 1974, A simple sieving and splitting device for field analysis of coarse grained sediments: Jour. Sed. Petrology, 44, 939-946.
- Ibbeken, H., 1983, Jointed source rock and fluvial gravels controlled by Rosin's law: A grain-size study in Calabria, South Italy: Jour. Sed. Petrology, 53, 1213-1231.
- Pettijohn, F.J., 1957, Sedimentary Rocks: Harper & Brothers, New York, 718 p.
- Pettijohn, F.J., Potter, P.E. and Siever, R., 1987, Sand and sandstone, 2<sup>nd</sup> ed.: Springer Verlag, 553 p..
- Plumley, W., 1948, Black Hills terrace gravels: A study in sediment transport: The Journal of Geology, 56, 526-577.
- Rogers, J.W., Krueger, W.C. and Krog, M., Sizes of naturally abraded materials: Jour. Sed. Petrology, 33, 628-632.
- Russel, R.J., 1968, Where most grains of very coarse sand and fine gravel are deposited: Sedimentology, 11, 31-38.

- Shea, J.H., 1974, Deficiencies of clastic particles of certain sizes: Jour.Sed.Petrology, 33, 180-190.
- Strahler, A.N., 1964, Quantitative geomorphology of drainage basins and channel networks, in: Ven te Chow, PH.D. (ed.): Handbook of applied hydrology, McGraw-Hill, 4/39-4/76.
- Sundborg, A., 1956, The river Klaralven, a study in fluvial processes, Geogr. Annaler, Ser.A, 11, 127-316.
- Yatsu, E., 1955, On the longitudinal profile of the graded river: Transactions, American Geophysical Union, 36, 655-663.

# COUNTING INSTEAD OF WEIGHING: GRAIN-SIZE COMPOSITION OF COARSE MATERIAL BEDLOAD IN A MOUNTAIN STREAM EXPRESSED IN PARTICLE NUMBER TRANSPORT RATES

KRISTIN BUNTE

Institut fuer Physische Geographie, Grunewaldstr. 35  
1000 Berlin 41, Federal Republic of Germany

## INTRODUCTION

Coarse material bedload transport processes are not fully understood. In particular the interpretation of fluctuations in bedload transport needs clarification. The processes on the river bottom require closer attention. However, direct observations and measurements of processes on the river bottom during transport events under natural conditions are difficult.

Statistical methods should be developed that yield more information about processes during bedload transport events based on novel analyses of coarse material bedload. At Squaw Creek improved methods of bedload sampling and a special data analysis were developed.

## HYDROLOGICAL AND SEDIMENTOLOGICAL CONDITIONS AT SQUAW CREEK

The Squaw Creek is a mountain river draining parts of the Gallatin Range in Montana, USA. Coarse bedload is exclusively transported during spring snow-melt. The average discharge during spring high-flow is 4 - 6 m<sup>3</sup>/s with diurnal fluctuations of flow. Conditions at Squaw Creek are described in several papers (ERGENZINGER & CUSTER, 1983; BUNTE et al., 1987; CUSTER et al., 1987; BUGOSH & CUSTER, 1989). The coarse material on the river bottom (> 11.2 mm) has a D<sub>50</sub> of 150 mm and is coarser than the average bedload.

## METHODS OF BEDLOAD TRANSPORT MEASUREMENTS, BEDLOAD SAMPLING AND DATA ANALYSES

### Magnetic tracer technique

Bedload transport was measured continuously at Squaw Creek using the magnetic tracer technique. (This method makes use of the naturally magnetic pebbles and cobbles of the river bed. When a pebble crosses a detector log extending over the whole river width a voltage peak is induced according to the Faraday inductive principle. The voltage peaks are amplified and recorded.) This real-time record of bedload transport shows various patterns of a fluctuating wave-like transport. During the daily rising flow bedload transport increases fluctuating only moderately, whereas immediately after peak flow the transport decreases to a minimum and continues with several large waves of transport superimposed by smaller bedload waves during the falling limb of daily flow. In between bedload waves transport often occurs randomly. The relation of voltage peak rates (BUNTE et al., 1987) or bedload transport rates with discharge shows a variation of more than one order of magnitude (BUNTE, 1990). A further step of analysis was to determine the grain-size distribution of these bedload transport waves in order to investigate the processes on the river bottom which might be responsible for the bedload fluctuations.

### Large frame-net bedload sampler

A large sampler is desirable because small devices exclude large heavy clasts which are detected by the real-time bedload transport magnetic tracer technique. During the snow-melt high-flow in spring of 1988 a large frame-net bedload sampler was used for bedload sampling. The frame has an opening of 1.6 m x 0.3 m and did not truncate the coarse tail of the bedload grain-size distribution, but the mesh width of the net allowed all particles smaller than 10 mm to pass through. Compared to standard Helley - Smith bedload samplers the large frame-net bedload sampler collects all the large particles representatively because the opening is much wider. Due to its construction the large frame bedload sampler can be operated in fast flows with flow velocities of 2 m/s in which a 6 x 6 inch hand - held Helley - Smith sampler is unmanageable. However, it takes three persons to maneuver the large frame bedload sampler and requires some

knowledge about the river's transport rates to determine a satisfactory sampling duration. Samples should be as large as possible without overloading the sampler. The sampling device is described in BUNTE (1990).

#### Grain-size distributions of coarse river sediments and their standard grain-size analysis

A standard grain-size analysis is based on the weight of the particles in the various grain-size classes. Plotting the weight or the weight percentages of each grain-size fraction in consecutive order yields in its simplest form a unimodal distribution curve resembling a Gaussian distribution. The statistical methods available to analyze these distributions (descriptive measures such as the mode, mean, variance and standard deviation) are only suitable if the distribution is a Gaussian distribution or at least approximates such a distribution. However, many grain-size distributions of non-cohesive river sediments are not Gaussian. Focussing on coarse material bedload samples in this paper, their grain-size distributions deviate from Gaussian distributions by being truncated on their tails and by showing internal irregular weight percentages in consecutive grain - size classes.

#### Truncation

The truncation on the lower end of a coarse material bedload sample is a sampling artifact owing to the smallest sieve used. The truncation of the upper end of a coarse material grain-size distribution can be a sampling artifact due to small samplers, the great mass needed to collect a statistically representative sample or by natural processes related to an insufficient sediment availability or an incompetent stream power. Facing these natural and practical restrictions, the coarse part of bedload is rarely sampled in a statistical representative way unless the sampling time is extended over a long time. Long sampling periods cause unmanageably large samples and prevent an investigation of short-term temporal variation of bedload transport rates.

#### Irregular grain-size distribution

Short-term coarse material bedload samples are often irregular distributed. Individual grain-size classes are over- or underrepresented and their weight or weight percentage deviates considerably from a smooth Gaussian distribution. This abundance or dearth of particles in individual grain-size classes, however, should be



taken into account in the data analysis because these irregularities might yield some valuable information on the processes on the river bed.

#### Deficiencies of standard grain-size analyses

The results of a standard grain-size distribution analysis following FOLK & WARD (1957) and the "moment" method used by SCHLEYER (1957) is described in BUNTE (1990). Applying a FOLK & WARD analysis to truncated grain-size distributions is problematic because any extrapolation to obtain a value for the distal percentiles is an interpretation of the "missing" part of the grain-size distribution. The "moment" method is slightly better suited for the analysis of truncated coarse material bedload samples as it does not depend on distal extrapolated percentiles. Nevertheless, neither the FOLK & WARD analysis nor the descriptive grain-size parameters obtained by the "moment" method (the "moments" similar to the parameters such as mean, sorting, skewness and kurtosis) are suitable to analyze any irregularities in the sample distribution. By solely describing a sample distribution as a whole, these parameters do not allow an analysis of the number of particles in the individual grain-size classes. Nevertheless, the abundance or dearth of particles in an individual grain-size class in a bedload sample might give insights into processes on the river bottom. Trying to study river processes this valuable information should not be omitted by using an unsuitable method of grain-size distribution analysis.

#### Grain-size distribution analysis: particle number transport rates

Although particles interact in all size levels, in sand individual particle interaction is difficult to study. In previous studies on (river) sediments, especially on sand material, the sediment size distribution was analyzed by the particles' weight percentage because sand grains are very small and the number of grains is uncountable. It had to be assumed that the weight percentage was related to the percentage of the number of particles in a grain-size class. As particle size increases, individual particles can more easily be seen. In future studies it might prove to be a better approach to analyze a grain - size distribution by the particle number. Since individual particles are interacting (hiding, exposure, ...) on the river bed during a bedload transport event individual particle interaction is important to be understood. Using the number frequency of a grain-size class leads itself to a statistical analysis.

For coarse grained sediments with countable specimens present it seems to be a better way to quantify the particles by their number per sieve class than using the particles weight in a sieve class. The bedload samples collected at Squaw Creek did not reach the sample weights which IBBEKEN (1974) and CHURCH et al. (1967) recommended for a statistical grain-size analysis. However, the counting method for grain-size analysis can be effectively applied to truncated or irregular grain-size distribution which are common for short-term coarse material bedload samples in order to analyze particle dynamics.

The grain-size analysis depicted here examines the particle transport rate for each grain-size class present. Sieving was done in 0.5 phi units for particles in the range of 11.2 mm to 180 mm. The particle transport rate for a given grain-size class was calculated by counting the number of particles in each grain-size class per meter width and minute. A time unit of minutes was chosen to reduce the number of decimals to make the data more legible. Counting the particles in consecutive sieve classes gives the advantage of obtaining a grain-size distribution that can be described by a simple monotonic function (linear, exponential or power function) if the number of particles transported in consecutively increasing grain-size classes decreases regularly. The particle transport rate is plotted for all samples (s.fig.1)

Further calculations with these simple monotonic functions are more sensible and graphic than calculations with Gaussian style functions that are equivocal. As the number of particles transported in consecutive, increasing grain-size classes decreases as a monotonic function, the regression lines of particle transport rates of given grain-size classes versus discharge (s.fig.2) or versus total bedload transport rates (s.fig.4) plot in consecutive order. Plotting weight percentages of given grain-size classes versus discharge or total bedload transport rates would yield regression lines that one by one moved upward on a plot until the grain-size class with the largest weight percentage is reached. For the following grain-size classes with decreasing weight percentages the regression lines would move down on that plot, leaving a bundle of lines that is difficult to interpret.

## DATA ANALYSIS

### Comparison of the three sedimentary units: gravel bar, channel surface and bedload

The first step of analysis compares the gravel bar, channel surface and bedload distribution to assess of how these sedimentary units relate to each other. In a bulk sample from the gravel bar the number of particles per grain-size class decreases very regularly (exponentially) with an increase in grain-size. The channel surface sample shows the same regular decrease in the amount of particles for the gravel and pebble sizes but an abundance of cobbles (SUTHERLAND, 1967) which stabilize the river bed as a pavement. The number of cobbles is roughly the same for each size class in the cobble section and decreases only towards the very large cobbles. The bedload samples show a less regular decrease in the number of particles for consecutive grain-size classes. Compared to the grain-size distribution of the gravel bar the bedload samples consist of less gravels and more pebbles suggesting that pebbles are transported preferentially. This patterns can not be found in samples taken at very small rates of bedload transport which have a random grain-size distribution (samples #20, #21 (not shown in fig.1 but similar to sample # 22), #22, #24, #25.).

### Comparison of consecutively taken samples

Two series of samples were taken consecutively in 1 - 2 hour intervals at normal high-flow discharges between 5 and 6 m<sup>3</sup>/s. Focussing on these serial samples of bedload provides an opportunity to investigate the particle size class responsible for rapidly fluctuating transport rates (bedload waves).

### Particle number transport rates versus discharge

The particle transport rates (particles / m - min) of all bedload samples were plotted versus discharge (fig.2). The data show that for a given discharge the number of particles transported per minute in each grain-size class can vary by two orders of magnitude. To better analyze these data, exponential functions were fitted through the particle transport rates of each particle size class with discharge (s. last plot of fig.2). The correlation coefficient  $r^2$  is generally low and still best for the smallest grain-size

class (11.2 - 16 mm) (fig.3).

The regression lines group into two sets of lines: lines 1 - 4 representing the grain-size classes 1 - 4 (11.2 - 45 mm) and lines 5 - 7 representing the grain-size classes 5 - 7 (64 - 125 mm). With the exception of line 1, both sets of regressions are each parallel to each other. Particles smaller 45 mm (line 1 - 4) have a common threshold of motion at around 3.5 m<sup>3</sup>/s and their transport rates increase with discharge exponentially. (As in log - linear plot there is no zero line the threshold for particle motion is set at a transport rate of 0.01 particles per meter per minute which equals a transport rate of 1 particle per meter width per 100 minutes). Particles larger than 45 mm do not start to move unless the discharge exceeds 4.5 m<sup>3</sup>/s and their contribution to the sample increases at a faster rate as discharges increase than the contribution of smaller particles. At higher discharge rates of over 5.5 m<sup>3</sup>/s the differences in the particle transport rates of individual size classes become less distinct which could suggest the possibility of an equal mobility transport at high discharge rates. More data might also bring the regression lines into parallelism, but this possibility can not be definitely confirmed or denied.

In order to examine the causes of the scatter in the data the particle transport rates of consecutive samples were marked. The first serial sample (sample # 5 - 9 marked by large dots in fig. 2) was taken at relatively low discharges on the rising limb of one night's high flow with discharges ranging from 5.0 to 5.26 m<sup>3</sup>/s and shows a basically regular increase of particle transport rates for the various grain-size classes up to the pebble range (64 mm). The second set of serial bedload samples (sample # 10 - 16) was taken at higher discharges (5.58 to 5.73 m<sup>3</sup>/s) during the next night's high-flow from waxing to waning flow. On the falling limb of the hydrograph the total bedload transport rates fluctuate considerably (BUNTE, 1990). Marked by squares and triangles to distinguish between large and small total bedload transport rates this second set of serial samples shows much variation in the transport rates of the small and medium sized particles (gravels and pebbles). To further investigate this variation the particle transport rates for all grain-size classes were plotted versus the total bedload transport rate of each sample (fig. 4).

#### Particle number transport rates versus total bedload transport rates

In each grain-size class the number of particles transported per meter and minute increases very regularly with the total bedload transport rate in grams per meter and second. The power functions that were fitted through the data (s. last plot of fig. 4) yield high correlation coefficients (fig. 3) which are best for the particle number transport rates in the range of pebbles (22.4 - 64 mm). This shows that the number of pebbles increases rather regularly with the total amount of bedload while smaller as well as bigger particles are variable in their contribution to a sample's total bedload rate.

The parallelity of the regression functions suggest that with an increasing total bedload transport rate the number of particles transported in each size class increases regularly. The regression lines group into two sets again. Lines 1 - 3 (or 4) representing the namely grain-size classes are closer to each other than the regression lines 5 - 7. This indicates that the transport rates for smaller particles are similar to each other while the transport rates of bigger particles are distinctly different in each size class. Considering a particle number transport rate of 0.01 particles per meter per minute as a threshold for particle motion a total bedload transport rate of 2 grams per meter per second has to be exceeded before the a cobble of 90 - 125 mm can be moved.

For total bedload transport rates larger than 2 grams per meter per second the number of particles per size class increases regularly. This result could confirm the ANDREWS & PARKER (1967) theory on equal mobility of all particles present for larger transport rates.

Closer examination of the two serial samples described above shows a regular tendency for all of the first set of serial samples (large dots) that were taken during rising flow: the number of particles in consecutive grain-size classes increase regularly with the total bedload transport rate. Conversely, the second set of serial samples taken from rising to waning flow can be clearly divided into samples with large total bedload transport rates ranging from 42 - 72 g/m·s ( sample # 11,12,14 and 16 (see the squares)) and small total bedload transport rates of 3 -12 g/m·s (sample # 10, 13 and 15 (note the triangles)). While at large bedload transport events (squares) the particle number transport rate in each size class follows the general trend in the plots the particle number transport rates cause some scatter in the plot during smaller

transport rates (triangles). The deviation from the regression lines is strongest for small gravel particles which are either over- or underrepresented and for cobbles which are mostly absent. However, the medium particle range (pebbles) adjusts best to all bedload transport rates.

## DISCUSSION

Coarse material bedload transport rates are poorly related to discharge (BUNTE et al., 1987 and BUNTE, 1990). Bedload transport rates often fluctuate and their fluctuation has been attributed to a number of processes by various authors (GOMEZ, NAFF & HUBBLE 1989).

Investigating the grain-size composition of bedload samples provides insight into the processes on the river bottom. The method suggested in this paper offers a relatively easy tool to analyze the grain-size distribution of coarse material bedload samples.

Various patterns of bedload transport have been detected at Squaw Creek during the daily high-flows (BUNTE et al., 1987). Statistical representative bedload samples were taken during different transport patterns and their grain-size distribution was analyzed. Different transport patterns revealed different grain-size distributions.

A series of bedload samples collected during rising flow with only moderately fluctuating transport rates show grain-size distribution in which the number of particles of consecutive grain-size classes decreases rather regularly with discharge and with total bedload transport rate, suggesting that bedload transport in this transport phase is mainly hydraulically controlled.

During the passage of a crest of a bedload pulse the grain-size distribution also follows regular pattern. The number of particles per each grain-size class decreases regularly with increasing grain-size class. All or almost all the grain-sizes present are transported. In this phase of transport the ANDREWS & PARKER (1987) theory on equal mobility of all grain-size classes present on the river bottom seems to be applicable.

During the passage of a trough of a bedload transport wave the grain-size distribution

of the bedload deviates from the regular patterns described above. These small bedload transport rates do still consist of an appropriate number of pebbles compared to the small amount of bedload, but the number of gravel and cobble particles is less predictable. The gravels and cobbles seem to be subject to selective transport during phases of the passage of troughs in wavy transport. A possible reason for this selective transport is that gravels and cobbles are most strongly influenced by the effects of hiding and exposure. While cobbles are only transported after being fully exposed to flow gravels are abundantly transported when being winnowed out and are rarely transported when trapped in between cobbles. The pebbles are evenly transported as they are too big for excessive hiding and are not easily trapped. Pebbles can be transported when the shear stress is large enough for motion during high-flow's bankfull stage. Gravels and cobbles strongly interact on the river bottom, hindering or favoring each other's transport while pebbles are effected by the roughness of the river bottom to a much lesser extent and smoothly move through.

The temporal variation of coarse material bedload transport rates at Squaw Creek can be explained by a switching of transport modes which alternate between equal mobility and selective transport owing to the changes in roughness of the river bottom and the resulting effects of hiding and exposure of particles. The equal mobility transport mode causes high bedload transport rates, the selective transport reduces bedload transport rates. An alternation between the two transport modes leads to a fluctuation in bedload transport rates.

Though the fluctuation in bedload transport rates occur at a much faster rate (hourly intervals) than variations in discharge (daily intervals) it remains to be clarified whether the temporal and spacial variation in the hydraulic conditions of a diurnally changing flow during a snow-melt run-off contribute to the rapid temporal variation of bedload transport rates.

#### ACKNOWLEDGEMENTS

I would like to thank Prof. Steve Custer from the Montana State University and Prof. Peter Ergenzinger from the Freie Universitaet Berlin for the inspiring discussions. Prof. Steve Custer contributed much to this paper by a critical review. I am very grateful to the Big Timberworks Inc. in Gallatin Gateway, Montana who gave me access to their

computer and Ulli Achter who helped with some of the graphs.

## LITERATURE

- ANDREWS, E.D. & PARKER, G. (1967): Formation of a coarse surface layer as a response to gravel mobility. - Sediment Transport in Gravel Bed Rivers. C.R.Thorne, J.C. Bathurst & R.D.Hey (eds.). John Wiley & Sons, New York.
- BUGOSH, N. & CUSTER, S.G. (1999): The effect of a log-jam burst on bedload transport and channel characteristics in a headwater stream. - Proceedings of the Symposium on Headwater Hydrology, held at Missoula, Mt., W.W.Woessner & D.F.Potts (eds.).
- BUNTE, K.; CUSTER, S.G.; ERGENZINGER, P. & SPIEKER, R. (1987): Messung des Grobgeschiebetransportes mit der Magnettracertechnik. - Gewaesserkundliche Mitteilungen, 31,2/3: 60-67.
- BUNTE, K. (1990): Experiences and results from using a big-frame bed load sampler for coarse material bed load. - (to appear in the proceedings of the IAHS meeting in Lausanne, August 1990).
- CHURCH, M.A.; McLEAN, D.G. & WALLCOTT, J.F. (1987): Bed load sampling and analysis. - Sediment Transport in Gravel Bed Rivers. C.R.Thorne, J.C.Bathurst & R.D.Hey (eds.). John Wiley & Sons, New York.
- CUSTER, S.G.; ERGENZINGER, P.E.; BUGOSH, N. & ANDERSON, B.C. (1967): Electromagnetic detection of pebble transport in streams: A method for measurements of sediment transport waves. - Recent Developments in Fluvial Sedimentology. F.Ethridge & R.Flores (eds.) Society of Paleontologists and Mineralogists, Special Publication, 39: 21-26.
- ERGENZINGER, P. & CUSTER, S.G. (1983): Determination of bedload transport using naturally magnetic tracers: First experiences at Squaw Creek, Gallatin County, Montana. - Water Resources Research 19,1: 187-193.
- FOLK, R.L. & WARD, W.C. (1957): Brazos River Bar: A study in the significance of grain size parameters. - Journal of Sedimentary Petrology, 27,13-26.
- GOMEZ, B.; NAFF, R.L. & HUBBLE, D.W. (1989): Temporal variation in bed-load transport rates associated with the migration of bed-forms. - Earth Surface Processes and Landforms, 14: 135-156.
- IBBEKEN, H. (1974): A simple sieving and splitting device for field analysis of coarse grained sediment. - Journal of Sedimentary Petrology, 44,3: 939-946.
- SCHLEYER, R. (1957): The goodness-of-fit to ideal Gaus and Rosin distribution: A



new grain size parameter. - Journal of Sedimentary Petrology 57.5 671-880.  
SUTHERLAND, A.J. (1967): Static armour layers by selective erosion. - Sediment  
Transport in Gravel Bed Rivers. C.R.Thorne; J.C.Bathurst & R.D.Hey (eds.).  
John Wiley & Sons. New York.

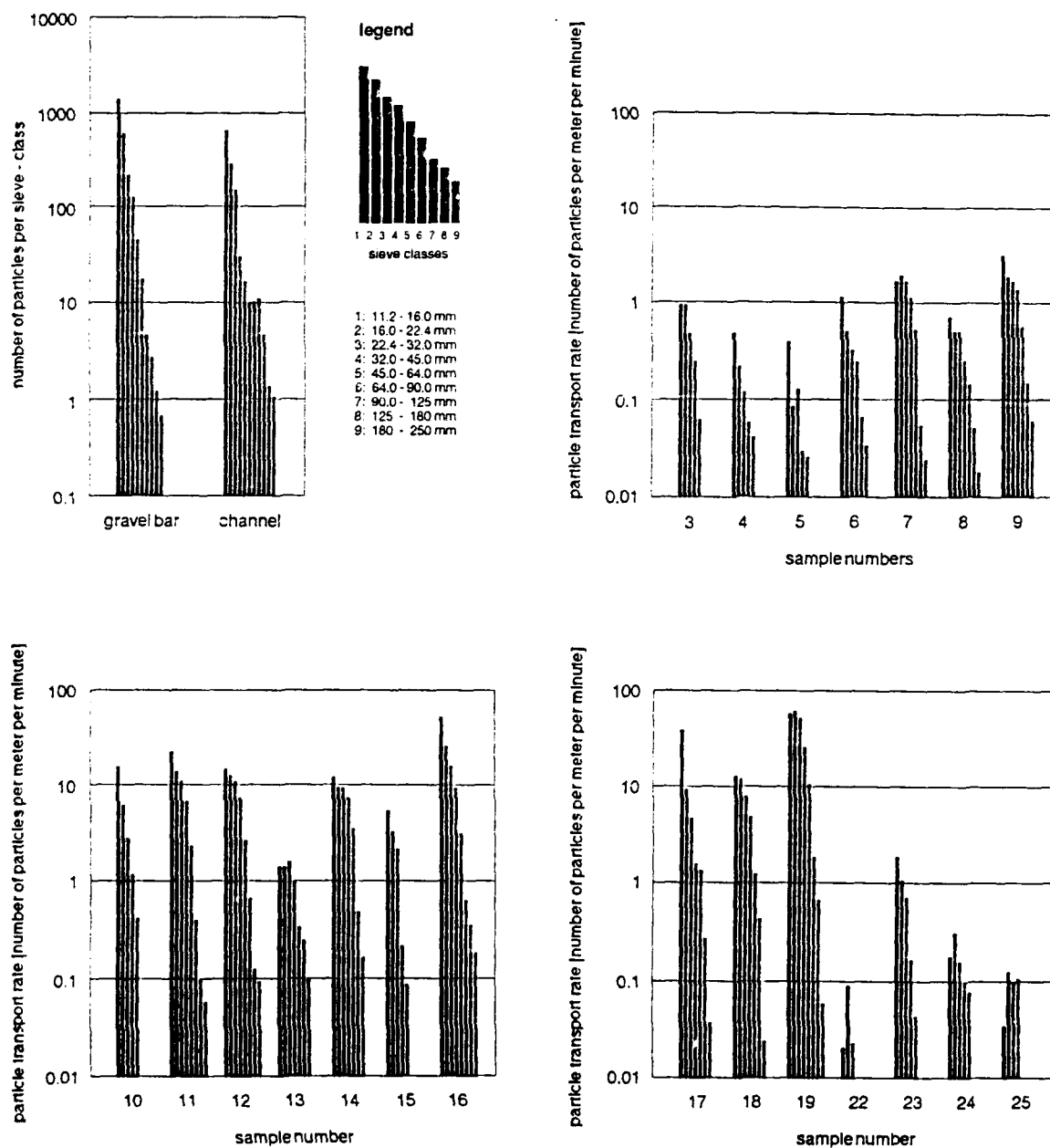
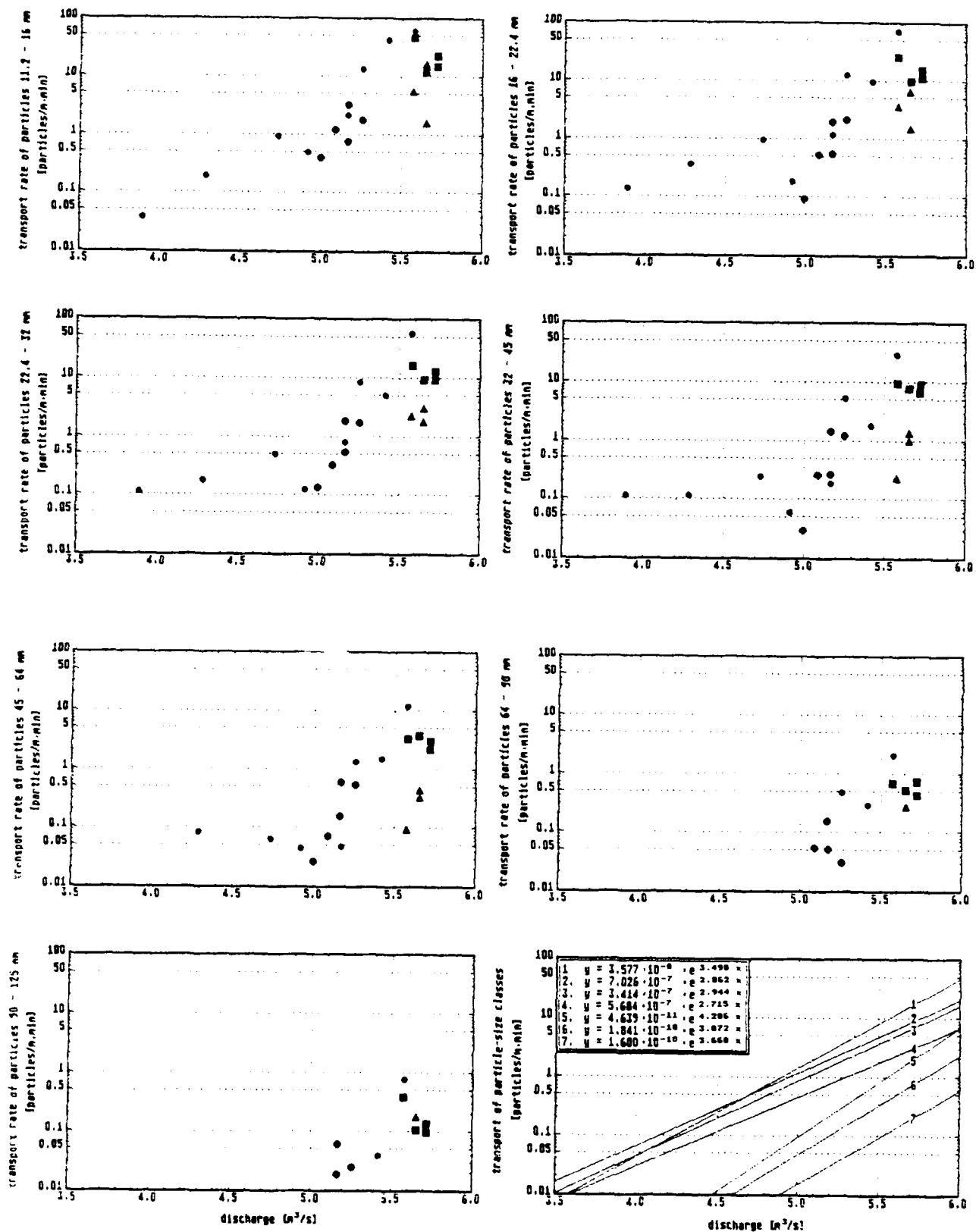


Fig. 1: Particles and particle transport rates: number of particles in consecutive grain-size class per meter per minute.



- May 23 - 24, 1988,  $Q: 5.0 - 5.3 \text{ m}^3/\text{s}$ ,  $q: 0.3 - 9.3 \text{ g/m} \cdot \text{s}$
- May 24 - 25, 1988,  $Q: 5.3 - 5.8 \text{ m}^3/\text{s}$ ,  $q: 3 - 12 \text{ g/m} \cdot \text{s}$
- May 24 - 25, 1988,  $Q: 5.3 - 5.8 \text{ m}^3/\text{s}$ ,  $q: 21 - 73 \text{ g/m} \cdot \text{s}$
- May 20 - June 6, 1988,  $Q: 3.9 - 5.8 \text{ m}^3/\text{s}$ ,  $q: 0.1 - 187 \text{ g/m} \cdot \text{s}$

Fig 2: Particle transport rates versus discharge.

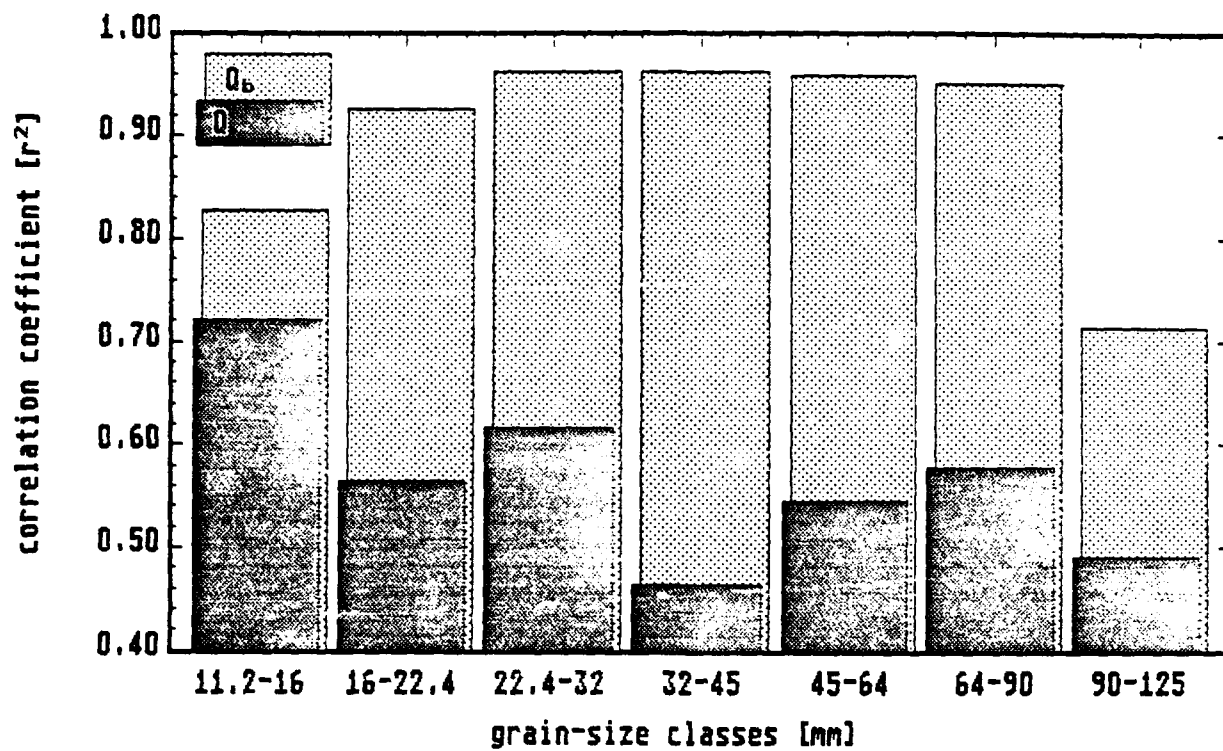
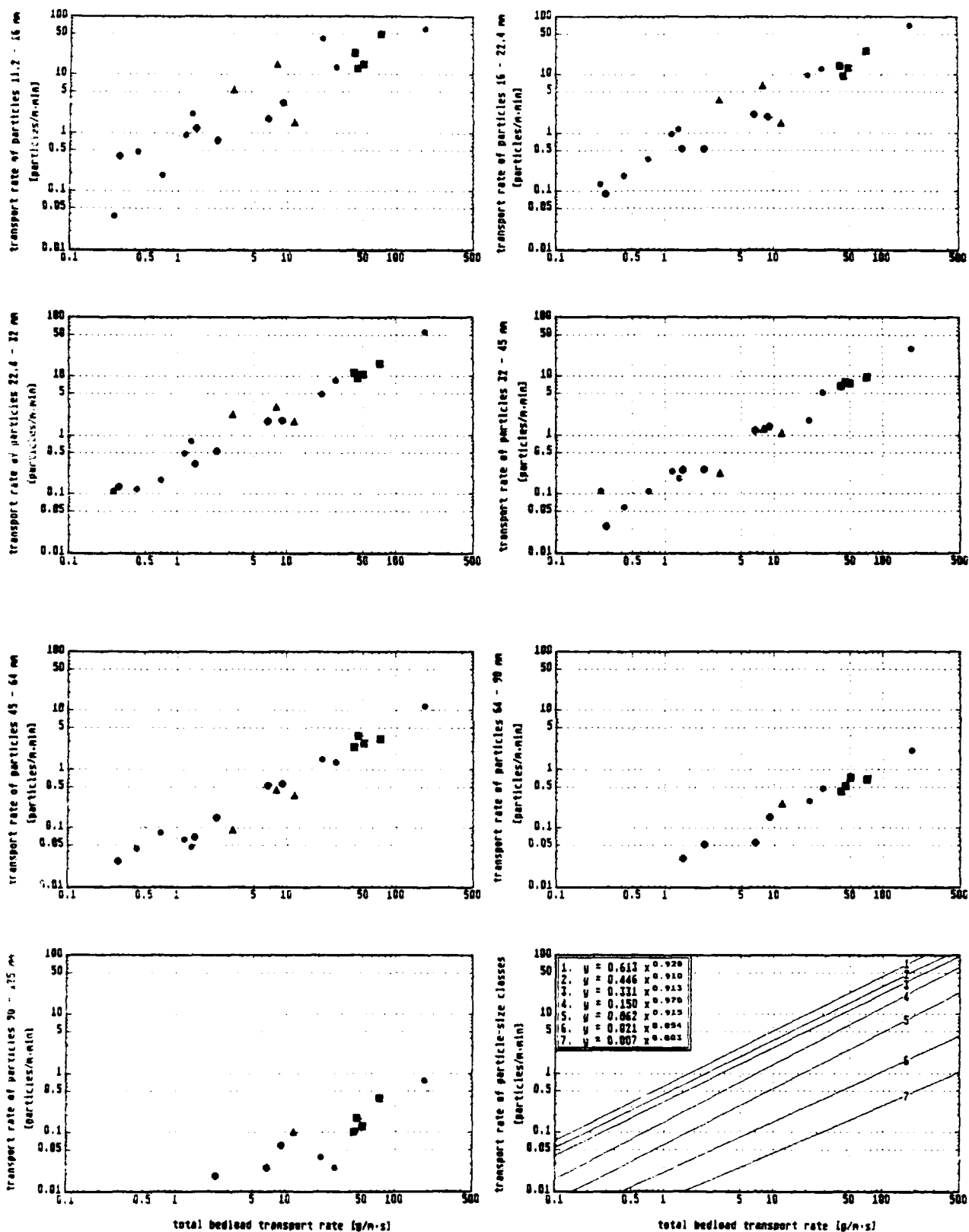


Fig. 3: Correlation coefficients of regressions of particle transport rates versus discharge and versus total bedload transport rates.



- May 23 - 24, 1988,  $Q: 5.0 - 5.3 \text{ m}^3/\text{s}$ ,  $q_b: 0.3 - 3.3 \text{ g/m-s}$
- May 24 - 25, 1988,  $Q: 5.2 - 5.8 \text{ m}^3/\text{s}$ ,  $q_b: 1 - 12 \text{ g/m-s}$
- May 24 - 25, 1988,  $Q: 5.1 - 5.8 \text{ m}^3/\text{s}$ ,  $q_b: 21 - 73 \text{ g/m-s}$
- May 28 - June 6, 1988,  $Q: 1.5 - 5.8 \text{ m}^3/\text{s}$ ,  $q_b: 0.1 - 187 \text{ g/m-s}$

Fig. 4: Particle transport rates versus total bedload transport rates.

## **Deposition and Removal of Fines in Gravel-Bed Streams**

by

Panayiotis Diplas<sup>1</sup> and Gary Parker<sup>2</sup>

### **ABSTRACT**

Laboratory experiments, which model gravel-bed streams with poorly sorted bed material, were conducted to examine the deposition of fines into and their release from a channel bed. Two flumes were used. The first one was long and narrow and operated as a recirculating system. The second flume was shorter and wider and operated as a feed system. Several features of gravel-bed streams, such as the existence of a pavement and a pool-and-riffle structure were reproduced in the laboratory. As it has been indicated from several field studies, these features play an important role in the infiltration and removal of fines in the bed of gravel-bed streams.

The fines initially introduced into the flume tend to collect in the immediate substrate, where they create a seal that restricts any deeper penetration within the bed material. As more fines are added, they saturate the subpavement and start appearing in the surface layer. The amount of fines in the pavement depends on the mean flow concentration of fines and other flow parameters. Higher amounts tend to deposit at the bar tail and the pool areas.

In the absence of bed load motion fines are released only from the surface bed layer. Particle entrainment allows for the removal of fines from the subpavement. Infrequent floods, that mobilize the whole pavement, tend to obliterate the pool-and-riffle structure and clean the channel bed from fines up to the bottom layer.

---

1 Assistant Professor, Department of Civil Engineering, Virginia Polytechnic Institute and State University, Blacksburg, VA 24061, USA

2 Professor, St. Anthony Falls Hydraulic Laboratory, University of Minnesota, Minneapolis, MN 55414, USA

## INTRODUCTION

As an ecological phenomenon, the process of fines input to and accumulation in gravel bed streams falls in the category of non-point source pollution, and is considered to be one of the most significant pollution problems in this category. As indicated by a voluminous body of research, the presence of excessive amount of fines in the stream bed is one of the most important factors that could adversely affect the spawning success of salmon and other species of fish (Shea and Mathers, 1978; Koski, 1966).

The pool and riffle structure, which is characteristic of gravel bed streams, provides considerable variation in flow depth and velocity as a function of location that can in turn result in areas suitable for spawning activities for a variety of fish. The intergravel stage of life of the fish, as incubating egg first and as alevin later, represents a period they may be most susceptible to damages from high levels of fines. Increased amounts of fines may injure the ova, (Gibbons and Salo, 1973), reduce the intergravel flow which is necessary for the removal of the toxic metabolic wastes produced by the eggs, (Iwamoto et al., 1978), and lower the levels of dissolved oxygen supplied to the incubating eggs and alevins which is necessary for their adequate survival and growth (Phillips and Campbell, 1961). In addition, increased amounts of fines reduce the population and diversity of the benthic community which is the main food resource for the fish emerging from the intergravel environment (Gibbons and Salo, 1973). The reason for the paramount importance of fines is that, of all factors deleterious to spawning likely to be exacerbated by the activities of man, it is one of the most prevalent. This can be caused by human activities such as clear-cutting, road building and agriculture, which result to inputs of fine material into streams that are well above the inputs due to natural erosion processes. Furthermore, stream regulation tends to eliminate the annual peak discharges which are capable of activating the bed and thus releasing the fines that accumulate during low flows.

It is therefore evident that stream sedimentation is a serious source of stream pollution. In order to keep the pollution of a stream below dangerous levels, management criteria for the land use in the corresponding watershed should be developed. This requires the knowledge of the following three general relations:

1. A relation predicting the quantity and type of fines flowing into streams as a function of specific watershed activity, basin geological and vegetal structure, and hydrological regime.
2. A relation predicting the characteristics of deposition of fines in and their release from the stream bed as a function of fines input, flow discharge and other factors.
3. A relation indicating the effect of fines in the substrate on spawning success.

The purpose of the present study is to examine the second relation, the deposition and removal of fines in gravel-bed streams. The available literature on the subject is reviewed first. Subsequently, the results of laboratory experiments simulating the process of fines accumulation and retention in gravel beds, and their effect in the stream behavior are examined.

## PREVIOUS RESEARCH

While the detrimental effects of fines on the survival and emergency of salmonid fry were recognized quite early (Harrison, 1923), most of the research on the mechanisms of deposition and erosion of fines in gravel matrices has been conducted during the last two decades. Both field studies and laboratory experiments have been performed.

Various aspects of the mechanics of fines retention in gravel-bed streams have been examined in field studies carried out with adequate instrumentation by Milhous (1973) on Oak Creek, Adams and Beschta (1980) on five small streams located in the Oregon Coast Range, Frostick, Lukas and Reid (1984) on Turkey Brook tributary, Lisle (1989) on three streams located in the Coast Range of northern California, and by Alonso et al. (1988) on Tucannon River.

Milhous (1973) verified the existence of a surface bed layer, called pavement, that is coarser than the subsurface material. He also observed that the role of the pavement on the deposition and retention of fines is quite important. At low flows the immobile pavement layer acts as a sink of the suspended sediment, which tends to deposit in the interface between the bottom of the pavement and the top of the subsurface, called the "silt reservoir". At higher stages, when the pavement is set in motion, the bed acts as a source by supplying fines for suspension, at rates determined by the pavement. The sand ( $< 2$  mm) fraction in the Oak Creek substrate takes a value near 12 percent. This value has been maintained over more than ten years, suggesting that it is in some sense in balance with the stream and watershed on a long-term basis.

In their study of five streams, Adams and Beschta (1980) found that the percentage of fines ( $< 1$  mm) within the stream bed varied between streams, between riffle areas in the same stream, and within the same riffle. It is also mentioned that the variation across the channel is typically more pronounced than it is along the channel. In addition to spatial variability, temporal variability of the fines in the substrate was observed. They attributed the spatial variation to differences in the size of the gravel substrate and fines, the supply of fines, and the hydraulic condition of the flow. For a single stream the amount of fine sediment in the bed was correlated to the stream sinuosity and bankfull stage; an equivalent set of flow parameters will be depth and velocity of flow. The temporal variability of the fines is attributed to the flushing of fines, which takes place mainly during high flows when the bed is set in motion. Furthermore, an extensive sampling program undertaken by Adams and Beschta (1980) on twenty one Coast Range streams during summer low flows indicated an average amount of fines content within the channel bed of 19.4 percent; for the streams on undisturbed watersheds the level of fines ranged from 10.6 to 29.4 percent, while for the streams on disturbed watersheds it reached a high value of 49.3 percent. The fines content was stratified with depth; an average value of 17.4 percent was measured for a 10-cm surface bed layer, while the corresponding value for a 30-cm subsurface bed layer was 22.3%.

Frostick et al. (1984) monitored the amount and type of fines infiltrating the pavement of Turkey Brook by installing six traps at its bed. Each trap had an opening of  $0.5\text{m}^2$  and was 0.33 m deep, and was divided into sixteen removable compartments, that were filled with different size of substrate material. A lid of pebbles, having the size distribution of the pavement layer at Turkey Brook, covered each trap rendering its surface flush with the surrounding bed. Their results indicate that the presence of a coarser surface bed layer and bed load motion are the dominant parameters influencing the amount and size of the infiltrating fines. The coarse surface layer superimposed on a finer substrate, which is typical of gravel bed rivers, was found to encourage the clogging of the near-surface pores



with matrix fines. Flow events that caused bed activation resulted in higher amounts and larger size of ingressed fines. The intruding fines exhibited spatial variation, with higher amounts in pools compared to bars, while for the same cross-section the area of highest fines content coincided with the area of highest velocity. During high flows, that were capable of mobilizing the channel bed, fines were flashed from the bed up to a depth of 8 cm at the thalweg. This depth is approximately equal to  $2 D_{p90}$ , where  $D_{p90}$  is the sieve diameter of the grain that is coarser than ninety percent of the pavement material.

Lisle (1989) studied the sedimentation of spawning gravel beds in three streams of north coastal California. He buried a number of cans, 17 cm in diameter and 22 cm deep, filled with well sorted subrounded gravel, below the pavement, in areas likely to be used by anadromous fish for spawning. He measured the amounts of fines deposited into the cans as well as the depth of their infiltration. Lisle's observations are similar to those of Frostick et al. (1984). He found that silts and very fine sands were concentrated at the bottom of the cans, while sand and granules were caught in interstices near the top forming a seal. This seal penetrated deeper in areas of higher energy. The average depth of the infiltration of fines was  $2.6 D_{90}$ , where  $D_{90}$  is the 90th grain size percentile of the subsurface material. The suspended sediment comprised the bulk of the total sediment transport, but it constituted only one-fifth of the infiltrated material found in the cans. This is attributed to the better access that the finer bed load particles have to the pores of the pavement, being continuously in contact with the bed. The fine sediment ( $0.25 < D < 2$  mm) that accumulated in the subsurface, averaged overall the cans of a stream, correlated well with the total amount of bedload in the same size range, transported during storms. Furthermore, Lisle observed that scour of stream beds during floods and subsequent fill may deposit at least as much and as deep fine sediment in clear gravel beds as infiltration. With parts of the stream bed being scoured during individual storms to depths of 0.1 m, incubating eggs could be crushed. Therefore, scour and fill could be equally crucial to the survival of eggs and embryo, as is the infiltration of fines.

The purpose of the Alonso et al. (1988) field study was to calibrate a computer program that simulates the deposition of fines in coarse gravel matrices and its effect on the quality of aquatic habitat. They also reported that scour at some locations of the Tucannon River was severe enough to affect salmonid eggs. Contrary to the account given by others (e.g. Lisle, 1989), however, Alonso et al. observed that the infiltrating fines did not create a seal within the bed subsurface, and that their amount was directly related to the suspended load. The different depositional behavior of the fines infiltrating the Tucannon River substrate is mainly due to the large difference in size between the framework gravel and the matrix material, a situation that is not commonly encountered in natural streams.

Laboratory experiments on the characteristics of fines intrusion and retention into gravel beds have been carried out by Einstein (1968), Beschta and Jackson (1977), Dhamotharan et al. (1980), Carling (1984), and O'Brien (1987).

In his pioneering work, Einstein studied the intrusion of silica flour (3.5 to 30 microns) into a gravel bed. He used two flumes with gravel mixtures as bed material, and water with fines were recirculated at flows not large enough to move the gravel. He noted that the fines settled into the gravel reaching the bottom of the flume and gradually filled the pores from the bottom up. Einstein's experiments represent an important contribution in the siltation of gravel matrices when almost all the sediment moves in suspension, and the bed material is considerably coarser and immovable. They give, however, a simplistic and probably misleading description of the phenomenon in the light of field data. The main deficiencies of these experiments are the lack of pavement, the absence of bed load motion and pool-and-riffle structure, and the great size difference between the coarse and fine sediment phases. The last factor, which is probably the most significant, dictated the mode

of fines deposition. The first factor may also be crucial in the creation of a seal within the substrate. The second and third factors may provide important cleaning mechanisms of the gravel bed from the fines (Vaux, 1968; Alonso et al. 1988; Lisle, 1989).

In their experiments, Beschta and Jackson (1979) used well-sorted gravel with  $D_{50} = 15$  mm as bed material, and two uniform sands with  $D_{50} = 0.5$  mm and 0.2 mm as fines. Water and fine sediment were fed at the upstream end of the flume, and gravel bed load, except for a jiggling motion, was essentially absent. When the fines with 0.2 mm median size were fed into the channel, the gravel pores filled from the bottom up in the Einsteinian mode. The use of the coarser fines, however, resulted in a sand seal. Increasing Froude numbers forced the seal deeper into the gravel substrate.

Dhamotharan et al. (1980) conducted a physical model study of Oak Creek to examine whether phenomena characteristic of natural gravel bed streams can be reproduced in a laboratory flume. The flow rate in the experiments was capable of entraining even the coarser grains of the bed material. The resulting transported material was recirculated with the water through the flume. A pavement and a weak pool-and-riffle structure, similar to those observed in the field, were developed in the flume. After the equilibrium stage was reached, some preliminary experiments were carried out with fines feeding. It was found that the fines collect predominantly between the subpavement and pavement, and that the accumulation of fines resulted in a reduction of the bed load transport rate when compared with the same experiment but in the absence of fines.

The purpose of Carling's (1984) flume experiments was to determine the role of gross flow parameters on the siltation rate of sand into a gravel bed. He used well sorted gravel, with median size of 15.6 mm, as bed material and three different grades of sand ( $D_{50} = 0.15$  mm, 0.19 mm, 1.4 mm) as fines. The flow was not capable of entraining the gravel, so no self-formed pavement was present. The coarsest sand was the only one to form a seal. He concluded that the initial flow concentration of sand was the only mean flow parameter that correlated well with the siltation rate. He observed that the siltation rate was high even at low flow concentrations, and that the surface bed layer remained free of sand.

O'Brien (1987) carried out field work in Yampa River and subsequently a full scale physical model study of the same river. His emphasis was on determining minimum streamflow requirements necessary for the maintenance of fishery habitat. In agreement with other researchers, he observed that in the absence of gravel mobilization the bed could be cleaned from the fines to a depth close to the median size below the bed surface.

In addition to the above mentioned field and laboratory studies, several researchers have suggested methodologies for flushing gravel matrices from fines that would result in acceptable quality of aquatic habitat. Most of these methodologies are purely empirical in nature and have been reviewed by others (Reiser et al., 1985; Milhous, 1986).

## PRESENT EXPERIMENTS

The purpose of the present study was to study the process of deposition and removal of fines in a gravel-bed stream under conditions encountered in natural streams. Two flumes were used to meet this objective. The first flume was 16.75 m long, 0.3 m wide, and 0.61 m deep, and the second one was a tilting flume 12 m long, 0.91 m wide, and 0.38 m deep. They will be referred to as the long and the tilting flume, respectively.

Most of the experimental work was carried out in the long flume, which recirculated both sediment and water. The major advantages of this flume are its length and its transparent glass walls. The bed load motion, and the infiltration of fines into the bed can be observed closely through the walls. The narrow width of the channel, which suppressed any tendencies for the formation of bars, is its major disadvantage.

The tilting flume facility operated as a feed system in both water and sediment. Two sediment feeders are used at the upstream end of the channel; one is introducing into the flume material identical to the original bed mixture, and the other feeds the flume with fines. The important feature of the tilting flume is its width, which was sufficient to allow for bars to develop. The short length of the channel and its opaque walls are its major drawbacks.

The mixture used as bed material was poorly sorted, with median grain size of 2.44 mm and standard deviation of 2.75. Two sizes of silica flour were used as fines, one with  $D_{50} = 0.08$  mm and the other with  $D_{50} = 0.11$  mm, both being well sorted. The white color of the fines was very helpful for observation purposes.

Six series of experiments were conducted in the long flume and a single series in the tilting flume. The initial bed slope for the long flume ranged from 0.003 to 0.008, while for the tilting flume it was 0.012. The dimensionless design Shields stress varied from 0.10 to 0.15, based on the mean size of the original mixture. On the average, six experiments were conducted for each series.

Before the beginning of each series a fresh mixture of bed material was introduced into the channel and was screeded with a template to the desired initial slope. The first experiment of each series in the long flume was performed in the absence of fines. During the rest of the experiments in each series, fines were introduced into the flume, with their amount being progressively increased with each experiment.

Seven experiments were performed in the tilting flume. No fines were fed during the first experiment. During the rest of the experiments, the impregnation of fines into the gravel bed was examined, as well as the ability of the flume to purge itself of the fines accumulated in the bed.

Each experiment was assigned a symbol, e.g. S2:E3, where S stands for series and E for experiment. The above symbol thus refers to the third experiment of the second series. The tilting flume experiments belong to the seventh series.

## RESULTS

The field studies reviewed earlier indicated that gravel bed streams are typically characterized by the presence of a pavement, bed material that is poorly sorted, bed shear stress that moderately exceeds the critical value for particle entrainment, and by frequent bed activation. In addition the size of the finer matrix material overlapped, at least partially, with the size of the coarser framework particles. The same studies demonstrated the importance of these factors in the process of fines infiltration into and their removal from a gravel bed. Nevertheless, most of the laboratory studies did not simulate several of these features in the experiments of the deposition of fines in gravel matrices.

The purpose of the first experiment of each series was to allow for a self-formed pavement layer to develop from the original bed material. In the tilting flume case a pool-and-riffle structure was also present at the end of the first experiment. The time required for the channel to reach equilibrium ranged from 30 to 54 hours. During this period a significant part of the finer material ( $D < 0.5$  mm) infiltrated below the surface layer and collected within the subpavement. At the completion of the experiment the bed material was sampled by removing three consecutive layers. Wet clay was forced against the bed surface to remove the top layer, or pavement, whose thickness was about 0.65 cm ( $\approx D_{90}$ ). The subsequent two layers, called subpavement and bottom layer, were extracted with a spoon, both being about 1.5 cm ( $\approx 2.3 D_{90}$ ) thick. The top sample is close to an areal while the other two are close to a volumetric (Diplas and Fripp, 1990). The size distribution of these three layers and that of the bed load material obtained during the fourth series are shown in Fig. 1. Although areal samples cannot be compared directly with volumetric samples, Fig. 1 indicates that the pavement is coarser than the subpavement (Diplas and Sutherland, 1988). The latter was also evident from side by side visual comparison of these two layers. Typical relations among subpavement median size,  $D_{50}$ , bottom layer median size,  $D_{b50}$ , and bedload median size,  $D_{l50}$ , are  $D_{50} \approx D_{b50}$  and  $D_{l50} \approx 1.14 D_{50}$ . In addition, the subpavement contains considerably higher amounts of finer particles ( $D < 1.0$  mm). At the end of the first experiment in the tilting flume, a well developed pool-and-riffle sequence in conjunction with three bars, that were alternatively attached to the channel side walls, had formed. Detailed sampling of the bed material composing the surface of a bar revealed a gradual decrease in grain size in the downstream direction. The resulting bed configuration and variation of the grain size along a bar are in good agreement with field observations (Lewin, 1976; Bluck, 1982).

The characteristics of the subpavement material for both the tilting and long flume experiments were essentially identical. The same holds true for the material of the corresponding bottom layers. Thus, the only difference, in terms of bed material, between the experiments without fines in the two flumes was restricted to the surface layer.

### Experiments with Fines in the Long Flume

Starting from the second experiment of each series, fine material was introduced into the flume. The following program of incremental increase of fines supply was used for the experiments of series two to five. The amount of fines introduced into the flume during the second experiment accounted for a system concentration of  $2,000 \text{ mgL}^{-1}$ , where the system concentration is defined as the ratio of the mass of fines and the total volume of water in the system (flume and pipes). The fines added during the third, fourth, fifth and sixth experiments corresponded to system concentrations of  $3,000 \text{ mgL}^{-1}$ ,  $5,000 \text{ mgL}^{-1}$ ,  $10,000$

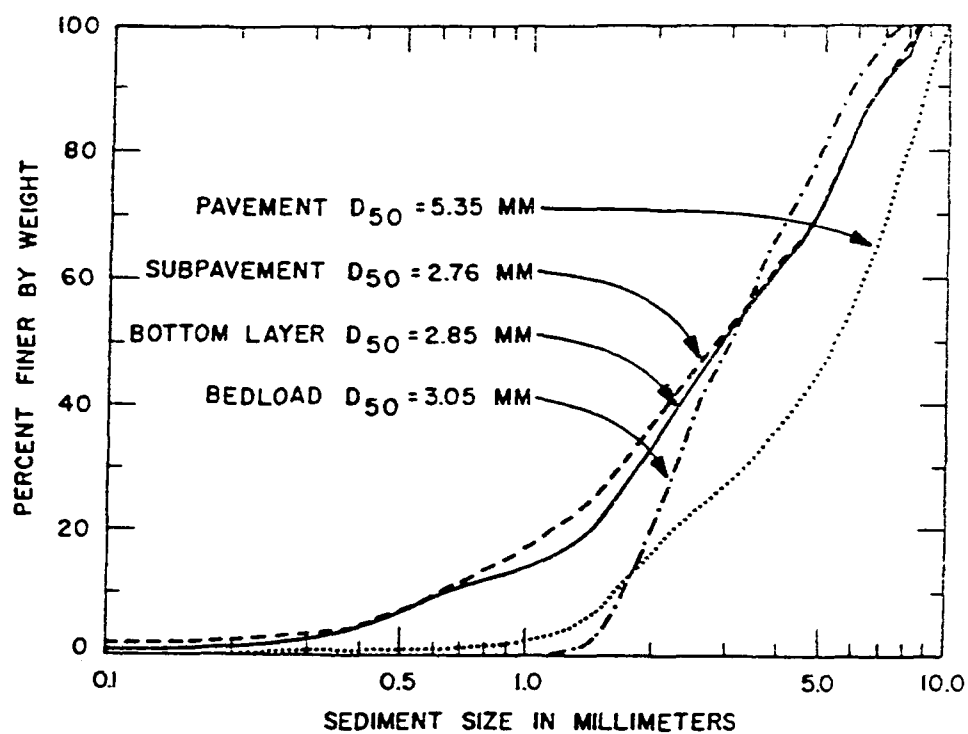


Fig. 1. Pavement, subpavement, bottom layer, and bed load size distributions for the experiment S4:E3.

$\text{mgL}^{-1}$ , and  $10,000 \text{ mgL}^{-1}$  respectively. The total amount of fines introduced into the long flume during a single series of experiments ranged from 19.5 to 27 kgr. During series four and five, fines with 0.11 mm median diameter were used. For the rest of the series (one, two, three and six), fines with a median diameter of 0.08 mm were used.

Fines have been observed to infiltrate into gravel beds in two different ways. The first one is characterized by unobstructed settling through the voids of the framework material. In the second way the fines are inhibited from settling freely, and instead they bridge the gaps among particles of the gravel bed, thus creating a seal that limits any deeper penetration of fines. The mode of deposition is mainly controlled by the relative size of the settling fines and the voids of the framework gravel (Sakthivadivel and Einstein, 1970; Sowers and Sowers, 1970). The presence of a coarser surface bed layer promotes the latter mode of deposition (Frostick et al., 1984) with clogging taking place close to the bed surface. When the subpavement material is poorly sorted, the possibility of a seal forming near the bed surface is further enhanced.

To demonstrate visually the infiltration of fines into the channel bed, approximately six bed layers were cleaned of their finer particles over a segment of the channel bed during the first series. Figures 2 and 3 show two views of the channel bed from the side wall at the end of the sixth and seventh experiments. In Figure 2, the white contour identifies the maximum depth of infiltration of the silica flour. As shown in Figure 3, fines subsequently added to the flow deposit at all levels above the white contour, with the bulk of the filling progressing from this contour upwards to the gravel surface. Furthermore, these two figures show that the difference in size between the depositing fines and the coarse framework material dictates the depth of deposition of the fines.

Prediction of the seal thickness would be important for determining the effects of fines on spawning grounds and the possibility for their flushing. During the present experiments the added fines never infiltrated deeper than the bottom layer of the channel bed in any appreciable amounts. Most of the times the top of the bottom layer corresponded to the deepest penetration of the fines. This depth was about 2.1 cm from the bed surface or in terms of size of bed material  $\approx 3D_{90}$ . For a more conservative estimate it is considered that the maximum infiltration depth is  $\approx 5D_{90}$ , which corresponds to the bottom of the bottom layer. From his field study, Lisle (1989) found an average value of  $2.6D_{90}$  for the thickness of the seal, while Beschta and Jackson (1979) suggest values ranging from 2.5 to  $5.0 D_{90}$  based on their laboratory experiments. Figure 4 shows the pavement, subpavement and bottom layers for the experiment S5:E6.

The sixth series was designed to examine the influence of the added fines on the bed load transport rate. During this series considerable variation in the bed load transport rate was observed. The water surface slope and the velocity profile, however, did not exhibit any noticeable changes during this series. It is therefore suggested that the factor likely to be responsible for the otherwise unexplained bed load variation is the accumulation of fines in the channel bed.

The grains that participate in the bed load transport are typically entrained from the surface layer of the bed material. Small amounts of added fines normally settle in the subpavement and are not expected to interfere with the bed load motion. As more fines accumulate in the bed, they start impregnating the pores of the surface layer and thus increasing the stability of surface grains, resulting in a gradual reduction of the bed load transport rate. As even more fines deposit into the channel bed, the subpavement gradually becomes saturated with them, and the interstices between the grains of the



Fig. 2 A view of the fines infiltrating into the channel bed from the sidewall of the long flume for S1:E6. The bed material has been locally cleaned of its finer grains for a few coarse layers.

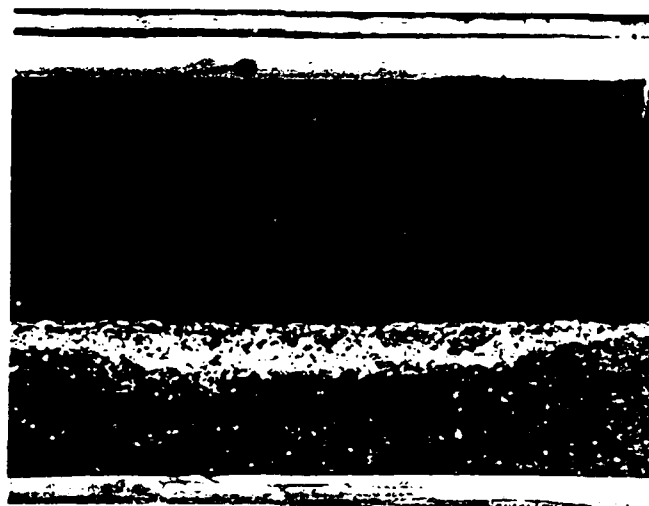


Fig. 3 A view of the fines infiltration from the sidewall, of the flume site shown in Figure 2, at the end of run S1:E7.



(a)



(b)

Fig. 4 Photographs of (a) the pavement and subpavement layers and  
(b) the pavement and bottom layers, from S5:E6.



pavement start to fill. During this process the mobility of the pavement particles is further reduced, while the bed surface becomes smoother, thus increasing the mobility of the grains moving on top of it. Eventually these opposing tendencies balance each other and the bed load rate stops declining. A further increase of the amount of fines in the pavement enhances the mobility of the moving grains resulting in an increase of the bed load transport rate. In this state, the number of moving grains has been significantly reduced, but the rest periods between motions are much shorter compared to grains moving on a pavement in the absence of fines. By adding even more fines, the bed gradually changes from gravel to sand as the gravel is buried. At this state ripples, bed forms characteristic of sandy streams, appear on the bed of the channel (Figure 5).

From the present experiments it was roughly estimated that when the amount of the deposited fines comprised about five percent of the subpavement material, the bed load transport rate started to decline. The lowest bed load transport rate observed represents a 57 percent reduction in the bed load value in the absence of fines. Dhamotharan et al. (1980) observed a 30 percent reduction under similar conditions. When the deposited fines comprised about five percent of the pavement material the bed load rate started to increase.

#### Experiments with Fines in the Tilting Flume

Fines, with a median size of 0.11 mm, were fed into the tilting flume during the second experiment at a rate of 2.0 gr/sec, which corresponds to a feed rate concentration of  $156 \text{ mgL}^{-1}$ . The feed rate concentration is defined as the ratio of the fines feed rate and the water volume discharge. The water discharge and coarse sediment feed rate of the second experiment were identical to those of the first experiments. The only thing that changed during the third experiment was the fines feed rate concentration, which became  $350 \text{ mgL}^{-1}$ . The coarse sediment feed rate was interrupted during the fourth experiment, the flow rate was decreased to the point that bedload transport become negligible, and the feed rate concentration of fines was adjusted to  $430 \text{ mgL}^{-1}$ . No fines were fed into the flume during the fifth experiment, keeping everything else the same as for the previous experiment. The sixth experiment was identical to the first one. In the seventh experiment the flow rate and coarse sediment feed rate were considerably increased, while no fines were fed into the flume.

The purpose of the second, third and fourth experiments was to examine the despoitional pattern of fines in a stream with pool-and-riffle structure, under various flow conditions. The ability and extent to which the stream could purge itself of the fines was tested during the last three experiments.

At the end of the second and third experiments samples obtained from the channel bed indicated that higher amounts of fines were deposited at the bar tail (downstream end of the bar) and in the pool area, or in those parts of the channel bed where the flow is fairly tranquil. Reflecting the higher feeding rate of fines during the third experiment an increase in the deposited fines was observed in this experiment. Further increase in the deposited fines occurred during the fourth experiment in the absence of bed load motion. Fine material was present in the pavement layer, with larger quantities in the bar tail and pool areas. Frostick et al. (1984) also found larger quantities of fines being deposited in the pool compared to the deposition in the bar head during their field tests.



Fig. 5 View of the channel bed at the end of run S6:E7. A rather well developed ripple configuration is present on the channel bed. The flow direction is from the top to the bottom of the photograph.

The ability and extent to which the channel was able to clean its bed of fines, in the absence of bedload motion, was examined in the fifth experiment. The fines that were deposited in the subpavement and bottom layers remained intact. The pavement was partially cleaned. In agreement with observations from the previous experiments, areas of swift flow, such as the bar head, experienced more thorough cleaning of the pavement.

Other researchers (Milhous, 1973; O'Brien, 1984) have also emphasized the necessity of pavement mobilization for removing fines below the pavement layer.

The cleaning process under conditions of broken pavement was examined during the sixth experiment. Both the pavement and subpavement layers were effectively purged from the fines during this experiment, while the fines in the bottom layer were not affected.

The last experiment was designed to simulate a rather infrequent flood, and examine the effectiveness of such a flood in the process of cleaning the bed from fine material. The bed load transport rate in this experiment was about two and one half times the bed load transport of the sixth experiment. The pool-and-riffle structure was obliterated during the seventh experiment, rendering the channel bed flat. It is believed that this experiment modeled the scour and fill process of streambeds that is encountered in natural streams (Alonso et al. 1988; Lisle, 1989). Samples of the channel bed material revealed the removal of fines from the pavement, subpavement, and bottom layers.

Finally, it was observed that the behavior of the added fines ( $D_{50} = 0.11$  mm) was different from the behavior of the finer particles ( $0.177 \text{ mm} < D < 0.42 \text{ mm}$ ) of the original bed material. While the amount of fines in the channel bed increased during the first four experiments and decreased during the last three, the percentage of the finer portion of the bed material remained roughly constant throughout the series. In addition, the added fines can be transported in suspension by the channel flow while the finer bed material grains are too heavy to be suspended in significant quantities. It is therefore suggested here that the grains that are likely to be removed by the flow from the subsurface bed material are only those that can be suspended by the flow.

## SUMMARY AND CONCLUSIONS

The results of the present experiments and those of earlier studies provide a good description of the process of fines settling to and removal from coarse bed material. As soon as fines are introduced into the channel, they start depositing on the bed, infiltrating below its surface. The depth of infiltration depends on the difference in size between the penetrating grains and the coarser bed material, and the boundary shields stress. Both types of fines used during the present experiments created a seal within the substrate. This seal was deeper into the substrate for the fines with median size of 0.08 mm, and it never exceeded a depth of  $5 D_{90}$ . The seal is pushed deeper in areas of higher shields stress. The amount of fines than can ultimately deposit within the subpavement layer is independent of the boundary shear stress or other flow parameter. As long as there are fines in the channel flow moving in suspension or as bed load, they will keep infiltrating in the bed until they have saturated the subpavement layer. The fines that settle in the surface bed layer do interact with the flow. It is suggested that their amount depends on the boundary shields stress, the fall velocity of fines, the particle Reynolds number, and the mean flow concentration of fines (Diplas and Parker, 1985).

In the presence of an alternate bar structure on the bed, and when the flowing water covers these bars over their entire length, then the fines first removed from the flow are most likely to be deposited in the subpavement of the bar tail and the pool. As more fines deposit into the bed, they progressively infiltrate the subpavement throughout the channel bed, while fine grains start appearing in the pavement of the pool and the bar tail. With additional fines being introduced into the flume, the subpavement eventually becomes saturated, and the fines content in the surface layer increases considerably. The maximum mean flow concentration of  $3,000 \text{ mgL}^{-1}$  in the tilting flume experiments exceeds the fines concentration typically encountered in natural streams during peak discharges (Walling and Webb, 1987; Lisle, 1989).

The bed load transport varied as a result of the fines that accumulated in the channel bed. This bed load variation correlates well with the amount of fines in the subpavement and pavement.

In the absence of bed load motion, a channel flow without any suspended material can at most remove the fines from the surface layer of the bed. Conditions of mobilized pavement are required if layers below the surface are to be purged of the fines. Sporadic bed load motion does not affect the bed configuration and removes the fines to the bottom of the subpavement ( $\approx 3D_{90}$ ). During the cleaning of the bed, fines are first removed from the bar head and subsequently from the pool and bar tail. General bed load motion, which occurs during major floods, tends to efface the pool-and-riffle structure and removes the fines from up to the bottom layer of the channel bed.

## REFERENCES

- Adams, J. N. and Beschta, R. L. (1980), "Gravel Bed Composition in Oregon Coastal Streams", *Can. J. Fish. Aquat. Sci.*, 37(10), pp. 1514-1521.
- Alonso, C. V., Theurer, F. D. and Zachmann, D. W. (1988), "Tucannon River Offsite Study: Sediment Intrusion and Dissolved-Oxygen Transport Model", U.S. Dept. of Agriculture, Agricultural Research Service, Hydro-Ecosystems Research Group, Fort Collins, Colorado, U.S.A.
- Beschta, R. L. and Jackson, W. L. (1979), "The Intrusion of Fine Sediments into a Stable Gravel Bed", *J. Fish Res. Board Can.*, 36, pp. 204-210.
- Bluck, B. J. (1982), "Texture of Gravel Bars in Braided Streams", in *Gravel-Bed Rivers*, Hey, R.D., Bathurst, J.C. and Thorne, C. R. (eds.). Wiley, London, pp. 339-355.
- Carling, D. A. (1984), "Deposition of Fine and Coarse Sand in an Open-work Gravel Bed", *Can. J. Fish. Aquat. Sci.*, 41, pp. 263-270.
- Dhamotharan, S., Wood, A., Parker, G. and Stefan, H. (1980), "Bedload Transport in a Model Gravel Stream", Proj. Rep. No. 190, St. Anthony Falls Hydraulic Laboratory, University of Minnesota, Minneapolis, MI., U.S.A.
- Diplas, P. and Parker, G. (1985), "Pollution of Gravel Spawning Grounds Due to Fine Sediment", Proj. Rep. No. 240, St. Anthony Falls Hydraulic Laboratory, University of Minnesota, Minneapolis, MI., U.S.A.
- Diplas, P. and Sutherland, A. J. (1988), "Sampling Techniques for Gravel Sized Sediments", *J. Hydraul. Eng., Am. Soc. Civ. Eng.*, 114(5), pp. 484-501.
- Diplas, P. and Fripp, J. (1990), "Properties of Areal and Volumetric Samples", Manuscript in preparation for submission for publication.
- Einstein, H. A. (1968), "Deposition of Suspended Particles in a Gravel Bed", *J. Hydraul. Div., Am. Soc. Civ. Eng.*, 94(5), pp. 1197-1205.
- Frostick, L. E., Lucas, P. M. and Reid, I. (1984), "The Infiltration of Fine Matrices into Coarse-grained Alluvial Sediments and Its Implications for Stratigraphical Interpretation", *J. Geol. Soc. London*, 141(6), pp. 955-965.
- Gibbons, D. R. and Salo, E. O. (1973), "Annotated Bibliography of the Effects of Logging on Fish of the Western United States and Canada", USDA For. Serv., Gen. Tech. Rep., PNW-10, pp. 145.
- Harrison, C. W. (1923), "Planting Eyed Salmon and Trout Eggs", *Trans. Am. Fish. Soc.*, 53, pp. 191-200.
- Iwamoto, R. N., Salo, E. O., Madej, M. A. and McComas, R. L. (1978), "Sediment and Water Quality: A Review of the Literature Including a Suggested Approach for Water Quality Criteria", Report, U.S. Environmental Protection Agency Region X, Seattle, WA.
- Koski, K. V. (1966), "The Survival of Coho Salmon Egg Deposition to Emergence in Three Oregon Coastal Streams", M.S. Thesis, Oregon State University, Corvallis, OR, U.S.A.
- Lewin, J. (1976), "Initiation of Bed Forms and Meanders in Coarse-grained Sediment", *Geol. Soc. of America Bulletin*, 87, pp. 281-285.
- Lisle, T. E. (1989), "Sediment Transport and Resulting Deposition in Spawning Gravels, North Coastal California", *Water Resour. Res.*, 25(6), pp. 1303-1319.
- Milhou, R. T. (1973), "Sediment Transport in a Gravel Bottomed Stream", Ph.D. Thesis, Oregon State University, Corvallis, OR, U.S.A.
- Milhou, R. T. (1982), "Effect of Sediment Transport and Flow Regulation on the Ecology of Gravel-bed Rivers", in *Gravel-Bed Rivers*, Hey, R.D., Bathurst, T.C. and Thorne, C.R. (eds.). Wiley, London, pp. 819-841.

- Milhous, R. T. (1986), "Determining Instream Flows for Flushing Fines and Channel Maintenance--a Review", Proceedings: 1986 Front Range Hydrology Days Conference, Colorado State University, Fort Collins, CO, U.S.A.
- O'Brien, J. S. (1987), "A Case Study of Minimum Streamflow for Fishery Habitat in the Yampa River", in *Sediment Transport in Gravel-Bed Rivers*, Thorne, C.R., Bathurst, J.C. and Hey, R.D., Wiley, New York.
- Phillips, R.W. and Campbell, H.J. (1961), "The Embryonic Survival of Coho Salmon and Steelhead Trout as Influenced by Some Environmental Conditions in Gravel Beds", *Pac. Marine Fish. Comm.*, 14th Annual Report, pp. 60-73.
- Reiser, D. W., Ramey, M. P. and Lambert, T. R. (1985), "Review of Flushing Flow Requirements in Regulated Streams", Dept. of Engineering Research, Pacific Gas and Electric Co., California, U.S.A.
- Shea, M. and Mathers, J. S. (1978), "An Annotated Bibliography on the Effects of Roads on Aquatic Systems", Report, Ontario Ministry of Natural Resources, Canada.
- Sakthivadivel, R. and Einstein, H.A. (1970), "Clogging of Porous Column of Spheres of Sediment", *J. Hydraul. Div., Am. Soc. Civ. Eng.*, 96(2), pp. 461-472.
- Sowers, G. B. and Sowers G. F. (1970), "Introductory Soil Mechanics and Foundations", Macmillan, 3rd. Ed., London.
- Vaux, W. G. (1968), "Intragravel Flow and Interchange of Water in a Stream Bed", *Bulletin, U.S. Fisheries and Wildlife Service*, 66(3), pp. 479-489.
- Walling, D. E. and Webb, B. M. (1987), "Suspended Load in Gravel-bed Rivers: UK Experience", in *Sediment Transport in Gravel-Bed Rivers*, Thorne, C.R., Bathurst, J.C. and Hey, R.D., Wiley, New York.

THE SIZE DISTRIBUTION OF SALMONID SPAWNING GRAVELS

G. Mathias Kondolf  
University of California, Berkeley, USA

for presentation at the  
Third International Workshop on Gravel-Bed Rivers  
Firenze, 24-28 September 1990

## THE SIZE DISTRIBUTION OF SALMONID SPAWNING GRAVELS

G. Mathias Kondolf  
University of California, Berkeley USA

## ABSTRACT

Salmonids (salmon and trout) require freshwater stream gravels for spawning. Spawning gravels have been identified by biologists as limiting salmonid populations in many settings, either because of a shortage of gravels with suitable framework sizes or because of a large proportion of interstitial fine sediment. As a result, many studies have been conducted on spawning gravels since the 1950's, mostly by fisheries biologists, and mostly appearing only in the grey literature. Unfortunately, results have been inconsistently reported in many cases, with many studies reporting only one summary statistic (different for each study) from the gravels, rendering comparisons among studies difficult. This study compiled data from many previous studies and from original field work to determine what the distinguishing characteristics of spawning gravels might be, how they vary with the size of the spawning fish, and whether they differ in sedimentologic characteristics from fluvial gravels reported in the geologic literature.

A total of 135 spawning gravel size distributions were compiled by species. Most of these distributions represent the average or composite of numerous individual samples. The median grain sizes of these distributions ranged from 5.4 (for coho salmon redds in Flynn Creek, Oregon) to 78 mm (for chinook salmon in the Columbia River near Vantage, Washington, with a grand median of 22 mm. Values of geometric standard deviation range from 1.6 to 21, with half the values between 3.3 and 5.2. Nearly all of the distributions are negatively skewed, with half of the skewness coefficients falling between 0.24 and -0.39.

These spawning gravels appear to be somewhat coarser than most gravel size distributions reported in the geologic literature, but they do not differ in sorting or skewness. Contrary to Pettijohn's (1975) suggestion that most gravels are bimodal, very few of the spawning gravel size distributions analyzed here were bimodal.

The results also confirm the widely held assumption among fisheries biologists that bigger fish can spawn in bigger gravels. However, although these larger fish are capable of using larger gravels, they are not obligated to do so and often spawn in smaller gravels. The relation between fish size and spawning gravel size is thus described by an envelope curve, which can be used as a general guide to the likely gravel requirements of various fish. Fish 30-cm long can use gravels up to about 30 mm in size, while 90-cm-long fish can use gravels up to 80 mm in size.



## PROBLEM STATEMENT

The availability of gravels of sizes suitable for spawning has been recognized as a factor limiting salmonid populations (Allen 1969, Reiser and Bjornn 1979). Although experienced field biologists can usually identify a suitable spawning gravel when they see one, prior to this study, there has been no systematic attempt to compile a wide range of gravel size distributions from the literature for purposes of comparison, to determine what their distinguishing characteristics might be, how they vary with the size of the spawning fish, and whether they differ in sedimentologic characteristics from fluvial gravels reported in the geologic literature.

A great deal of information on spawning gravel sizes has appeared in the fisheries literature since the 1950's, but it has been inconsistently reported. Most publications have not reported the same measures, nor included the complete size distributions (from which other descriptors could be computed), so comparisons are difficult. A number of papers have been occupied in a quest for a single variable descriptor (one statistic drawn from a gravel size distribution) for use as an index of gravel quality, and following these leads, some authors have reported only one statistic from their gravel samples (as reviewed by Kondolf 1988). This trend has been unfortunate, because the gravel size requirements of spawning fish vary with life stage, and the appropriate measures will vary accordingly. Thus, no single statistic is perfectly suited as an index of gravel quality, and the failure to report the entire size distribution makes comparisons difficult among studies.

It is widely acknowledged among field biologists that big fish can spawn in bigger gravels. This is due not only to the greater upward pull that larger fish can exert on the stream bed, but also to their ability to hold in faster currents, which assist them in moving larger particles. Larger gravels also tend to be associated with higher velocities, so these variables are not independent. Behavioral patterns also confound the relation between fish size and gravel size. For example, pink salmon typically spawn in low-gradient reaches of coastal rivers, where gravels are small and contain abundant fine-grained sediment. In contrast, silver and chinook salmon may ascend rivers to headwater reaches, where gradients are high and bed material is larger.

This study examined the range of size distributions reported in the literature from spawning gravels and other gravels in the geologic record. The literature-derived data were augmented by original field work.

## METHODS

### Compilation of Size Distributions and Redd Characteristics

At the outset of this study, there appeared to be relatively few published spawning gravel size distributions in existence, so their compilation promised to be a relatively simple task. As the literature search and train of telephone contacts and correspondence proceeded, however, the existence of more and more gravel size distributions came to light. Most of these have appeared in the "grey" literature, in such outlets as state and federal fish and game agency reports, theses, and consultant reports; others exist only as unpublished data. The data presented here were drawn from size distributions of spawning gravel samples collected for this study and from 22 other sources. Of these other sources, only four in the open literature; 18 were in the grey literature or unpublished, and many were obtained only by direct request of authors or originating agencies. Besides those mentioned above, many other reports were obtained and examined, but were not included in these tables, either because full size distributions were not presented in them or because too few sieves were used to adequately characterize the size distribution.

In many sources, the size distributions presented were averages or composites of many samples collected in the study area. This was a constraint that dictated, in large measure, the approach used here. Because only average values were available from many studies, for purposes of comparison, average values were computed from studies in which individual size distributions were reported. Individual size distributions were utilized in other analyses (Kondolf 1988).

Some published gravel size distributions are for samples obtained in redds, others from potential spawning gravels. The latter are unspawned gravels known to be representative of those used for spawning either because of historical observations of spawning at the site or because they were collected adjacent to redds. The spawning female can effect a change in the size distribution of gravel, so the two populations (redds and unspawned) are not strictly comparable. Curiously, many published studies refer only to "spawning gravels" without explicitly stating whether the samples were obtained from redds or from potential spawning gravels. In this study, potential spawning gravels and gravels in redds were treated as two distinct populations. Data collected for this study included samples of both redds and adjacent, unspawned gravels (Kondolf 1988).

To analyze the size distributions, the general procedure was to plot the cumulative size distribution curve and to read off percentile values needed to calculate size descriptors for

comparison. Size descriptors compiled from all sources were the median, D50, geometric mean, dg, sorting index, sg, skewness, sk (Inman 1952, Vanoni 1975), and graphic mean, mg (Folk 1980). These are computed as:

$$\begin{aligned} dg &= [(D84)(D16)]^{0.5} \\ mg &= [(D84)(D50)(D16)]^{0.333} \\ sg &= (D84/D16)^{0.5} \\ sk &= \log(dg/D50)/\log(sg) \end{aligned}$$

In some cases, cumulative size distributions were presented in the source; in others they were computed from the presented values of weight or percent retained on each sieve. Only histograms or plotted cumulative curves were presented in some sources, so values were read from the graphs, and two sources presented values of D50, dg, or sg, which were directly incorporated in Tables 1-3. Length data for the spawning fish obtained from published sources or by contacting the authors or other experts familiar with the species in the region (Kondolf 1988).

Sorting and skewness for averaged and individual cumulative frequency distributions were plotted against mean size to ascertain if they varied systematically with grain size. Redd characteristics (mean grain size, redd area, and velocity and depth at the redd site) were plotted against fish length to define envelope curves of these redd characteristics as functions of fish size (Kondolf 1988). The degree to which the gravels are bimodal, as suggested by Pettijohn (1975) was assessed by inspection of cumulative size distribution curves. The degree to which gravels are lognormally distributed was assessed by plotting selected curves on log-probability paper and by comparing attributes of the sample distribution with values of the attributes expected for a normal distribution (Kondolf 1988).

## LIMITATIONS OF THE DATA

### Definition of Tails

In many studies, size distribution curves were not well defined at the tails because only a small number of sieves were used. In fact, data from a number of sources could not be used in this study for that reason (e.g., McNeil and Ahnell 1964, Burns 1970, Peterson 1978, and many samples of Platts et al. 1979). Other studies did not define the upper limit of the largest size class, denoting the largest class only as "larger than" some size. Inadequate definition of the fine tails of distributions was encountered in fewer studies (e.g., Chambers et al. 1953, 1954), probably because assessment of fine sediment has been an objective of most recent studies.

Failure to define the upper limit of the largest class produces

a problem when plotting the cumulative curve because one doesn't know what size should correspond to "100 percent finer than." In compiling data for this study, the observed progressions of sieve sizes were generally extrapolated to set the maximum size, but this often required some judgement. For example, if 1-inch (25 mm) and 2-inch (50 mm) sieves were used, is the next logical step 3 inches (75 mm) or 4 inches (100 mm)? (Smaller sieves often followed neither an arithmetic nor geometric progression, so could not be used as a basis for making the judgement). Depending on the percentage caught in the coarsest sieve, the choice could influence the value of D95 and perhaps D90. If the coarsest sieve contains more than 16 percent of the sample, the value of D84 will also be influenced.

The problems of inadequate definition of the distribution (because of too few sieves) and failure to define the upper limit of the largest size class are compounded by the potential errors introduced by the small sizes of many samples of coarse gravels, which may lead to substantial errors, especially in calculation of the D95, D90, and D84 (Church et al. 1987). It is often not possible to obtain a rigorously large sample of coarse gravel in a redd, because the redd itself may not contain enough gravel.

A number of authors have reported that they discarded large rocks from their samples. Of the data sets used in Tables 1-3, the only authors who reported excluding large rocks were Chambers et al. (1954,1955), who excluded rocks larger than 152 mm, Helle (1970), who excluded rocks larger than 100 mm, and Hobbs (1937), who excluded rocks larger than 76 mm. It is possible that other workers also excluded large rocks, but made no statement to that effect in their description of methods. Exclusion or inclusion of large rocks in samples is a potentially large source of variability among studies because exclusion of large rocks affects the percentages assigned to all other size classes.

D95, D90, D10, and D05 values were read from cumulative curves and kurtosis values were computed by Kondolf (1988). However, these percentile values were frequently poorly defined, so kurtosis values may not be meaningful and are not presented here.

#### Spatial and Temporal Variability

Most entries in Tables 1-3 represent averages or composites for a number of samples collected in one river or stream. The number of samples represented by the entries ranged from 1 to 310. While the average values are probably most representative of typical conditions at the site, they may mask substantial variability among individual samples arising from differences in microenvironment of deposition among sample sites.

In addition to this spatial variability, temporal variability in gravel size at one site may be pronounced. Variations over

time in fine sediment content have been documented by Cederholm and Salo (1979), Adams and Beschta (1980), and Scrivener and Brownlee (1982). These temporal variations presumably result from seasonal variations in sediment transport and may reflect, to a large extent, changes in the population of mobile fine sediment in comparatively stable gravel beds. However, gravel deposits themselves may be subject to wholesale replacement at some sites in some years. Kondolf et al. (in press) painted potential spawning gravels at seven sites in four streams in eastern California and documented that all particles had been scoured and washed downstream during the high flows of 1986 (recurrence interval about 7 years). At three of the nine sites, new gravel of size suitable for spawning had moved in to replace the washed-out gravel, but at the other sites, the suitably-sized gravel had been replaced by cobble and coarse gravel, which was probably too coarse for spawning by resident brown trout. This wholesale gravel washout does not occur every year; a new set of tracer gravels emplaced at the same sites were undisturbed over the 1987 season (recurrence interval < 1 year).

Thus, the gravel size descriptors shown in Tables 1-3 (except for samples from stable terraces) reflect conditions at the time of measurement. In another year or season, bed material composition might differ.

#### Influence of Study Site Selection

Finally, it should be recognized that the gravels sampled and the observed hydraulic conditions at sample sites (reported in Kondolf 1988) also reflect the choice of study areas by investigators and the limitations imposed by working conditions. Observations made in typical chinook salmon stream in the Pacific Northwest can be reliably accepted to reflect typical conditions for many populations. However, fish may adapt to different environments and use very different hydrologic conditions. For example, the large chinook salmon of the Kenai River, Alaska, utilize velocities and depths far greater than recorded elsewhere (entry 28, Table 1). Similarly, chum salmon of the Susitna River utilize sites with extremely fine-grained surface material but which are characterized by upwelling groundwater (entry 131, Table 2). If criteria developed from observations elsewhere were applied to these sites, they would be deemed unsuitable for spawning, but both these populations reproduce very successfully. The conditions most commonly studied are likely to be those most commonly encountered by fishermen and fishery biologists. Sites with difficult access may be avoided for logistical reasons, and sites with unusual conditions may be avoided simply because they are not "representative" of most spawning by the species. Thus, the unusual circumstances in which the adaptability of the fish

is displayed will be less often studied. Finally, field studies in fisheries research may follow the same patterns as field studies in geomorphology, which tend to concentrate in areas near major research universities or field research centers (Graf 1984).

In addition to the potential bias introduced in the choice of study area, the limitations of working conditions may impose a further bias. In streams and rivers whose range of available habitat includes deep and swift sections, the maximum depth recorded at redds is typically just under the height of the observer's chest waders. Redds in deeper parts of the channel may not be visible, or, if they are, it may be impossible to make measurements there by wading. Similarly, samples may be unobtainable with conventional bulk core or freeze core samplers.

Burger et al. (1983) radiotagged chinook salmon in the Kenai River and used boats to measure velocity and depth over redds in deep waters; to collect gravel samples, they returned during lower flows. Without the technical advance of radiotagging, biologists might still not know that fish could spawn in such deep waters.

To measure particle size in deep water, divers have been used to collect samples (Klingeman and Emmett 1982) or to take scaled photographs (Chapman et al. 1983). Clearly, these techniques require a substantial investment of time, effort, and equipment. Little wonder that most studies are conducted on sites with good access and shallow flows.

An illustration can be drawn from field work conducted for this study in the Grand Canyon, where portability was an important consideration because access to sites was by river raft with limited cargo space. Samples of rainbow trout spawning gravels were collected with a portable core sampler that cannot operate in water deeper than about 50 cm. At one site (Tapeats Creek), redds in deeper water could not be included in the sample population.

## RESULTS AND DISCUSSION

### Presentation of Data

Background information (reference, location, number of samples, species and fish length) and size descriptors (D50, dg, mg, sg, and sk) for studies of redd gravels is presented in Table 1. (Redd length, width, and area; and mean velocity and depth at the redd site are presented in Kondolf 1988). The entries are grouped by species; the species code used in these tables is explained in Table 4. Comparable data for samples of potential spawning gravels are presented in Table 2, and Table 3 presents

background data and size descriptors for fluvial gravels reported in the geologic literature.

Because most entries in Tables 1-3 represent average or composite values for a number of samples collected in a river or stream, it is probably not appropriate to compute grand means of these entries. However, one objective of this study was to examine general trends in these data. If the entries are assumed to reflect typical conditions at the sampled sites, it is appropriate to examine the spread of these entries as indicative of the range of spawning gravel sizes encountered in the field.

Size distributions for selected entries of trout and salmon redds are presented in Figures 1 and 2 using box-and-whisker plots modified after Tukey (1977). For each entry, the rectangle (box) encompasses the middle 50% of the distribution, from the D25 to D75 values, termed the "hinges". The median size, D50, is represented by a horizontal line through the box. Above and below the box are lines (whiskers) extending to the D90 and D10 values. Unlike conventional box-and-whisker plots, the ordinate in Figures 1 and 2 utilizes a logarithmic scale, reflecting the similarity between these distributions and the lognormal distribution. Also, in standard box-and-whisker plots, the whiskers extend to the extreme values, or extreme values are plotted and identified and the whisker extends to the innermost identified value. Because of the wide range of grain sizes in natural gravels and the poor definition of tails in many studies, it would be impossible to extend the whiskers to the absolute extremes. Even if all distributions were completely defined, it can be imagined that there is some small amount of clay present in almost any gravel, and it would be impractical to extend whiskers into the clay range.

These plots provide an easily comprehended depiction of the range and central tendency of sediment size distributions and permit the reader to compare multiple samples graphically. This mode of presentation solves a problem encountered when one attempts to present multiple cumulative size distribution curves in the conventional format, namely that the lines overlap and become indistinguishable unless the distributions are all very different.

#### General Properties of Spawning Gravel Size Distributions

Taken as a whole, median diameters for all 135 spawning gravel entries in these tables have a median value of 22 mm. The range is quite large, from 5.4 mm for coho salmon redds in Flynn Creek, Oregon (Koski 1966), to 78 mm for potential chinook salmon spawning gravels in the Columbia River near Vantage, Washington, a site now inundated by Priest Rapids Dam (Chambers et al. 1954).

This range is even greater if the 0.1 mm value from unspawned,

silty substrates adjacent to chum salmon redds in sloughs of the Susitna River, Alaska (entry 131), are included. As documented by Vining et al. (1985), chum salmon utilize sites of upwelling groundwater in the side sloughs of the river, often excavating 30 cm of this fine sediment before encountering gravel in which to deposit their eggs. Thus, the 0.1 mm value is an outlier that accurately represents the surficial substrate where chum salmon excavate redds but not the particle size in egg pockets.

Of the median grain sizes presented for entries in Tables 1-3, 50 percent lie between 14.5 and 35 mm. Similarly, half of the entries for graphic mean diameter fall between 10 and 27 mm, for geometric mean, between 8.7 to 24 mm (Table 5). Values of geometric standard deviation range from 1.6 in chinook salmon spawning gravels of the Yuba River, California, to 21 in poorly-sorted chum salmon spawning gravels of Susitna River Slough 10. However, half the entries lie between 3.3 and 5.2, with a median sg of 4.0 mm (Table 5). The vertical spread of the box-and-whisker plots (Figures 1 and 2) provides an indication of the sorting of the plotted entry. (The spread of these box-and-whisker plots is from the 10th to 90th percentiles, whereas the sorting index using the 16th and 84th percentiles, so the two are not ex comparable.)

Nearly all of the average spawning gravel size distributions in Tables 1-2 are negatively skewed, with half of the skewness coefficients falling between -0.24 and -0.39 (Table 5). Only 3 entries did not show any negative skewness: chinook spawning gravels in Benjamin Creek, Alaska (sk = 0.06), pink salmon spawning gravels in Little Creek, Alaska (sk = 0.0), and the silt deposits of the Susitna River sloughs (sk = 0.10). Negative skewness can be detected in the box-and-whisker plots by longer whiskers below the box, reflecting extended fine sediment tails. The negative skewness is characteristic of these distributions on a log-transformed basis; if the distributions were considered without transformation, they would be positively skewed.

Differences in gravel sizes used by different species are indicated in Table 6, which presents the spread (median, lower and upper extremes) of entries by species. For median grain size, the median value of entries ranges from 8.5 mm for brook trout to 34.5 mm for chinook salmon. For geometric mean, median value of entries ranges from 4.2 mm for brook trout to 24.5 mm for chinook salmon. These interspecific differences are also visible in the box-and-whisker plots presented in Figures 1 and 2.

#### Comparison of Spawning Gravels with Fluvial Gravels in the Geologic Literature

Because of the intense interest in spawning gravels, it is of



some interest to ask whether spawning gravels are distinctive from fluvial gravels studied by geologists and engineers. Results of this study indicate that spawning gravels tend to be coarser than most gravels reported by geologists, but no different in sorting and skewness. When the 135 entries for spawning gravels are considered, the median values of D50, mg, and dg are all higher than median values for these descriptors drawn from the eleven entries for fluvial ("other") gravels drawn from the geologic literature (Table 5). Median values of sg and sk, however, are virtually identical for the two populations. (Differences in extreme values of sg and sk can be attributed to the different number of entries of the groups.)

The size distributions presented by Morris and Johnson (1967) as "typical" for "water-laid gravel" (entries 143-145) are smaller still than the average size of spawning gravels, but are less negatively skewed ( $-0.02$ ,  $0.08$ , and  $0.02$ ) than the other fluvial gravels or the spawning gravels.

Thus, it appears that the natural gravels used by spawning fish are not distinctive from other fluvial gravels in sorting or skewness, but they tend to be coarser than many of the gravels that have been sampled by geologists.

#### Modality of Gravels

Pettijohn (1975) reviewed the studies of Conkling et al. (1934), Krumbein (1940, 1942), and Plumley (1948), and concluded that most gravels are bimodal, distinct from sands, which tend to be unimodal. The cumulative frequency distributions of bimodal gravels should have a steep fine sediment tail, a flatter middle portion, and another steep leg in the gravel range. Distributions that define a smoothly concave-upward curve are not bimodal. Inspection of numerous cumulative frequency curves by Kondolf (1988) indicated that most were not obviously bimodal. The curves that best displayed bimodality were the fluvial gravels cited by Pettijohn (1975), although the secondary mode (in the sand range) is often not pronounced. Most spawning gravel curves are not bimodal. Many have extended fine tails, but there is no indication of a secondary peak in the sand range in most. Less than one fourth of the size curves examined by Kondolf (1988) could be considered bimodal.

Thus, bimodal curves occur, but are not the rule, among spawning gravels. Many more of the fluvial gravels reported in the geologic literature appear to be bimodal, but, again, this characteristic is not universal.

#### Influence of Mean Size on Other Properties

Church et al. (1987, p.51-52) noted that "mixtures of clastic material frequently display variance proportional to the mean

size, which is not surprising since all sizes may be present up to some cutoff point." To determine if sorting and skewness were related to grain size, the values of these descriptors in Tables 1-3 were plotted as functions of graphic mean diameter. Values of sg have a smaller spread and tend to be lower for larger gravels (Figure 3), indicating the sorting is less variable and somewhat better for larger gravels. (The outlier is the value for silt deposits used by chum salmon in the Susitna River sloughs.) Skewness and graphic mean (of the entries in Tables 1-3) appear to be unrelated (Figure 4).

An inverse relationship (albeit weak) between sg and mean size is inconsistent with the finding of Church et al. (1987) that standard deviation increased with mean grain size in 78 surface samples from one river. The data set used here is not really comparable to that of Church et al. (1987) because it comprises samples from a wide range of environments, which can be expected to differ in many respects besides mean grain size. If the only independent variable were framework grain size, then sg (which is defined as geometric standard deviation) could be expected to increase with increasing grain size. The (weak) opposite trend may reflect the influence of fine sediment content on both the graphic mean and sorting: if framework gravel size is held constant, higher percentages of matrix sediment should decrease mean grain size and increase the standard deviation. Such a relation is suggested for the entries in Tables 1-3 by the relation between sorting index and D16 shown in Figure 5. The sorting index shows no relation to the value of D84 (Figure 6), indicating that the variations in sorting index are controlled primarily by the amount of fine sediment rather than the presence of large particles. In large part, this could be due to the practice of many investigators to exclude large particles, variously defined as particles larger than 51 to 152 mm, from the sample (e.g., Helle 1970, Chambers et al. 1954, 1955).

The dependence of sorting and skewness on mean size was also examined for individual size distributions by Kondolf (1988) and found to be weak or absent.

The observed relationships between sorting and skewness, and mean size can be summarized as follows: larger gravels may be better sorted and more negatively skewed, but the relation is weak.

#### Influence of Fish Size on Redd Characteristics

Numerous conversations with fishery biologists have indicated a widespread recognition that gravel size, water depth and velocity, and redd size vary with the size of the spawning fish. Despite its widespread recognition, little has been published that describes this relation, and many studies of spawning

preferences do not include information on size of the spawning fish. Differences in gravel size used by various species have been described and attributed (explicitly or implicitly) to differences in size of the species (e.g., Burner 1951; Chambers et al. 1954, 1955). Hunter (1973, p.26) recommended that the size of the spawning fish be recorded whenever spawning habitat investigations were conducted, noting that, "Interspecies spawning preferences for salmonids of the same size will be closer than intraspecies requirements for fish of varying size." Van den Berghe and Gross (1984) measured depth of egg burial in a population of coho salmon and found that depth of burial was strongly correlated with size of the spawning female.

A relation between fish size and gravel size is intuitively satisfying because larger fish are capable of moving larger gravels by virtue of the greater upward pull they can exert on the stream bed, and by virtue of their ability to maintain themselves in deeper and swifter flow, where the greater force of the current assists in entrainment of particles. However, while a large chinook salmon may be capable of spawning in a steep, swift stream with a coarse gravel bed, she is not obligated to do so. She may just as easily utilize smaller gravels in lower gradient streams. Thus, the ability of larger fish to utilize larger gravels can be viewed as determining an envelope curve rather than a linear relation between fish size and gravel size. The actual gravel sizes used by fish will be determined in large measure by the sizes available in the channel at any given site. The same principle should apply to other redd characteristics such as redd size, and the depth and velocity at the redd site. Vronskiy (1972) found no relation between the size of individual chinook salmon and the size of their redds in the Kamchatka River.

The data in Tables 1 and 2 were used to construct Figures 7 and 8, in which gravel size is plotted as a function of size of the spawning fish. The maximum gravel size and the range of gravel sizes used for spawning increase with fish size, but larger fish use smaller gravels as well as larger gravels. Envelope curves have been drawn through the maximum gravel sizes utilized by different size fish, but excluding some outlying points. The envelope curve in Figure 7 shows that 30 cm fish can generally use gravels up to about 30 mm in median size, while 90 cm fish can use gravels up to 80 mm in median size. Similarly, the envelope curve in Figure 8 shows that 30 cm fish can use gravels up to about 28 mm in graphic mean diameter, while 90 cm fish can use gravels about 50 mm in graphic mean.

Kondolf (1988) compiled data on redd area and velocities and depths at the redd sites. In general, larger fish construct larger redds, but the relation is poorly defined. Fish 30 cm

long can spawn in water velocities of up to 0.5 m/s and depths as great as 0.25 m, while 100 cm fish can spawn in velocities up to 1.25 m/s and depths as great as 2.0 m.

These results indicate that the maximum values of the redd attributes of gravel size, depth, and velocity are related to fish size. However, confounding factors exist. These factors include variability in the sizes of fish in a spawning run, differences in the availability of different sizes of gravel from site to site, and the presence of upwelling or downwelling currents that may make a given site attractive to spawners.

There can be wide variations in fish size within a given spawning population, as illustrated in tributaries to the Owens River, California, where a single stream may have spawning brown trout ranging in size from 20 to 45 cm (D. Wong, Calif. Dept. Fish and Game, Bishop, personal communication 1987). If the gravel sizes available for spawning in such a stream were limited, it would mean that fish of very different size were utilizing gravel of the same size. The size of spawning fish in a given stream may fluctuate from year to year reflecting variations in the age structure of the spawning population, or there may be a long term secular change in the age structure of the spawning run. For example, in the Upper Sacramento River system, the spawning run of chinook salmon had a ratio of ocean age 3:4 year fish of about 50:50 in the early 1960's, when the spawning gravel samples of Van Woert and Smith (1962) were collected. However, increased harvesting of the run by commercial fishing interests offshore has resulted in a change in the composition of the run, so that it now has a ratio of about 65:35. The ocean age 3 year fish average 73 cm in size, while the ocean age 4 year fish average 95 cm in size, so the average size of spawning chinook salmon in the upper Sacramento system has decreased (Fred Meyer and John Hayes, Calif. Dept. Fish and Game, Sacramento, personal communication 1987). Thus, the size of spawning fish in a given stream may vary substantially over time.

It is now widely recognized that utilization of habitat components is influenced by their availability (Baldrige and Amos, 1981), and the size of gravels available to spawning fish can vary substantially from site to site. The range of gravel sizes available in a stream is a function of geomorphic variables such a climate, drainage area, basin lithology, structure, and of the local channel slope that results from the interaction of the other variables. The gravel sizes selected by one species in one region may show a wide variation because of gravel availability. For example, individual samples of rainbow trout spawning gravels in the Colorado River and tributaries ranged widely in size, from 7 to 48 mm in graphic mean diameter, but showed no

systematic increase in gravel size with fish length. The smallest fish occurred in small tributary streams with relatively limited habitat and low nutrient levels; these small streams are also steep and have coarse bed material. In contrast, the largest fish occurred in the mainstem where the gradient is lower and bars are composed of finer gravel (Kondolf et al. 1989).

Fish select spawning sites based not only on gravel size, but on other factors as well, such as water depth and velocity, cover, and the presence of upwelling or downwelling currents. Higher velocities would tend to be associated with coarser gravels, but the other variables should, for the most part, be independent of substrate size. Thus, a fish may select a spawning site with gravels much finer than the maximum size she can move as indicated on the envelope curve in Figures 7 and 8. For example, chum salmon in sloughs of the Susitna River select sites based primarily on the presence of upwelling currents, and spawn in extremely fine-grained substrates if upwelling currents are present (Vining et al. 1985).

In summary, there are physical reasons to expect that larger fish cause larger gravels for spawning, and such a pattern is widely recognized by fisheries biologists. The data presented here show that the maximum size utilized by a given size fish is related to fish length, but fish commonly spawn in gravels smaller than they are capable of using. Thus, the relation between fish size and gravel size is an envelope curve defining the minimum size movable as a function of fish size. Similarly, water depth and velocity are related to fish size by an envelope curve (Kondolf 1988).

#### REFERENCES CITED

- Adams, J.N., and R.L. Beschta. 1980. Gravel bed composition in Oregon coastal streams. *Can. J. Fish. and Aquatic Sci.* 37:1514-1521.
- Allen, K.R. 1969. Limitations on production in salmonid populations in streams. in T.G. Northcote, ed., *Symposium on salmon and trout in streams*. Univ. of British Columbia, Vancouver. p.3-18.
- Baldrige, J.E., and D. Amos. 1981. A technique for determining fish habitat suitability criteria: a comparison between habitat utilization and availability. in *Proceedings of the Symposium on Acquisition and Utilization of Aquatic Habitat Inventory Information*, October 1981. American Fisheries Society, Portland OR. p. 251-258.
- Burger, C.V., D.B. Wangaard, R.L. Wilmont, and A.N. Palmisano. 1983. Salmon investigations in the Kenai River, Alaska, 1979-1981. U.S. Fish and Wildlife Serv., Nat. Fish. Res. Center, Alaska Field Sta., Anchorage. 139 pp.
- Burner, C.J. 1951. Characteristics of spawning nests of Columbia River salmon. U.S. Fish and Wildlife Service Bulletin, 61:97-110.
- Burns, J.W. 1970. Spawning bed sedimentation studies in northern California streams. *Calif. Fish and Game*. 56:253-270.
- Cederholm, C.J., and E.O. Salo. 1979. The effects of logging road landslide siltation on the salmon and trout spawning gravels of Stequaleho Creek and the Clearwater River Basin, Jefferson County, Washington, 1972-1978. Fisheries Research Institute, University of Washington, Report No. FRI-UW-7915.
- Chambers, J.S., G.H. Allen, and R.T. Pressey. 1955. Research relating to study of spawning grounds in natural areas. Annual rept. to U.S. Army Corps of Eng., Contr. no. DA.35026-Eng-20572. Avail. from Washington State Dept. Fisheries, Olympia.
- Chambers, J.S., R.T. Pressey, J.R. Donaldson, and W.R. McKinley. 1954. Research relating to study of spawning grounds in natural areas. Ann. rept. to US Army Corps of Eng., Contract no. DA 35026-Eng-20572. Avail. from State of Washington, Dept. of Fisheries, Olympia.

- Chapman, D.W., D.E. Weitkamp, T.L. Welsh and T.H. Schadt.  
1984. Effects of minimum flow regimes on fall chinook spawning at Vernita Bar, 1978-82. Don Chapman Consultants and Parametrix, Rept. to Grant County Public Util. Dist., Ephrata, Washington.
- Church, M.A., D.G. McLean, and J.F. Wolcott. 1987. River bed gravels: sampling and analysis. in C.R. Thorne, J.C. Bathurst, and R.D. Hey, eds. Sediment Transport in Gravel-bed Rivers. John Wiley & Sons, Chichester, England. p.43-79.
- Conkling, H., R. Eckis, and P.L.K. Gross. 1934. Groundwater storage capacity of valley fill. Calif. Div. of Water Resources Bull. 45. 279 pp.
- Folk, R.L. 1980. Petrology of Sedimentary Rocks. Hemphill Publishing Co., Austin. 182pp.
- Graf, W. 1984. The geography of field geomorphology. The Professional Geographer 36:78-82.
- Hartman, G.F., and D.M. Galbraith. 1970. The reproductive environment of the Gerrard stock rainbow trout. Fisheries Management Publication No.15. Department of Recreation and Conservation, Fisheries Research Section, Victoria, BC. 51pp.
- Helle, J.H. 1970. Biological characteristics of intertidal and freshwater spawning of pink salmon at Olsen Creek, Prince William Sound, Alaska, 1962-63. US Fish and Wildlife Serv. Spec. Sci. Rept. Fish. No.602, 19 pp.
- Hobbs, D.F. 1937. Natural reproduction of quinnat salmon, brown and rainbow trout in certain New Zealand waters. New Zealand Marine Department Fisheries Bulletin 6, 104 pp.
- Hunter, J.W. 1973. A discussion of game fish in the state of Washington as related to water requirements. unpub. rept. avail. from Fishery Management Div., Wash. State Dept. of Game. 66 pp.
- Inman, D.L. 1952. Measures for describing the size distribution of sediments. Journal of Sedimentary Petrology 22:125-145.
- Klingeman, P.C., and W.W. Emmett. 1982. Gravel bedload transport processes. in Hey et al. (eds.) Gravel Bed Rivers. John Wiley and Sons, Chichester. p.141-179.

- Knott, J.M., and S.W. Lipscomb. 1983. Sediment discharge a for selected sites in the Susitna River basin, Alaska, 1-82. US Geol. Survey Open File Rept.83-870.
- Kondolf, G.M., G.F. Cada, and M.J. Sale. 1987. Assessing flushing-flow requirements for brown trout spawning gras in steep streams. Water Resources Bull. 23:927-935.
- Kondolf, G.M. 1988. Salmonid spawning gravels: a geomorp! perspective on the size distribution, modification by spawning fish, and criteria for gravel quality. PhD Dissertatio the Johns Hopkins University, Baltimore, Maryland, USA.
- Kondolf, G.M., S.S. Cook, H.R. Maddux, and W.R. Persons. 1989. Spawning gravels of rainbow trout in Glen and Grd Canyons, Arizona. Journal of the Arizona-Nevada Acadenof Sciences. v. p.
- Kondolf, G. M., G. F. Cada, M. J. Sale, and T. Felando. Distribution and mobility of potential salmonid spawning gravels in steep boulder-bed streams of the eastern Sierra Nevada. Trans. Am. Fish. Soc. (in press)
- Koski, K. V. 1966. The survival of coho salmon (Oncorhynchus kisutch) from egg deposition to emergere in three Oregon coastal streams. MS thesis, Oregon Stat University, Corvallis. 84 pp.
- Krumbein, W.C. 1940. Flood gravel of San Gabriel Canyo, California. Geol. Soc. Am. Bull. 51:636-676.
- Krumbein, W.C. 1942. Flood deposits of Arroyo Seco, Los Angeles County, California. Geol. Soc. AM. Bull. 53:1355-1402.
- Maddux, H.R., D.M. Kulby, J.C. deVos, Jr., W.R. Persons, R. Staedicke, and R.L. Wright. 1987. Effects of varied flow regimes on aquatic resources of Glen and Grand Canyons. Final report prepared for US Department of Interior, Bureau of Reclamation under contract No.4-AG-40-01810. 291pp.
- McNeil, W. J., and W. H. Ahnell. 1964. Success of pink salmon spawning rclative to size of spawning bed materials. U.S. Fish and Wildlife Service Special Scientific Report Fisheries No. 469. 15 pp.
- Morris, D.A , and A.I. Johnson 1967 Summary of hydrological



- physical properties of rock and soil materials as analyzed  
in the hydrological laboratory of the US Geological Survey  
-1960. US Geological Survey Wat. Supply Paper 1839-D.
- Ogden, D.R., B.R. Pulliam, and A. Arp. 1968. Characteristics  
of steelhead trout redds in Idaho streams. Trans. Am. Fish.  
Soc. 97:42-45.
- Pohn, R.H. 1978. Physical characteristics of Atlantic  
salmon spawning gravels in some New Brunswick streams. Fish.  
Res. Serv. Tech. Rept. 785, 28pp.
- Pohn, F.J. 1975. Sedimentary Rocks, Third Edition.  
John Wiley and Sons, New York. 628 pp.
- Plafin, W.S., M.A. Shirazi, and D.H. Lewis. 1979. Sediment  
gravel sizes used by salmon for spawning with methods for  
determination. US EPA Rept. no. EPA 600/3-79-043.
- Plafin, W.J. 1948. Back Hills terrace gravels: a study in  
sediment transport. J. Geology 56:526-577.
- Reid, D.W., and T.C. Bjornn. 1979. Habitat requirements of  
anadromous salmonids. USDA For. Serv. Gen. Tech. Rept. PNW-96.
- Reid, D.W., and T.A. Wesche. 1977. Determination of  
physical and hydraulic preferences of brown and brook trout in  
the selection of spawning locations. Water Resources Series  
No. 10. Wyoming Water Resources Research Institute, University  
of Wyoming, Laramie.
- Schick, J. 1957. Upland gravels of southern Maryland. Geol.  
Soc. Am. Bull. 68:1371-1410.
- Scribner, J.C., and M.J. Brownlee. 1982. Analysis of  
Carnation Creek gravel quality data 1973 to 1981. in G.F.  
Hartman (ed.), Proc. of the Carnation Creek Workshop, a 10-year  
review. Pacific Biological Station, Nanaimo BC p.154-173.
- Shirazi, M.A., W.K. Seim, and D.H. Lewis. 1981.  
Characterization of spawning gravel and stream system  
evaluation. in Salmon-Spawning Gravel: A Renewal Resource in  
the Pacific Northwest? State of Washington Water Research  
Center, Washington State Univ., Pullman WA. Rept. no. 39. p.  
227-273.
- Spoon, P.L., 1985. Reproductive biology of brown and rainbow

trout below Hauser Dam, Missouri River, with reference to proposed hydroelectric peaking. MS thesis, Montana State University, Bozeman. 144 pp.

Tukey, J.W. 1977. Exploratory Data Analysis. Addison-Wesley Publishing Company, Reading, MA. 688pp.

Van den Berge, E.P., and M.R. Gross. 1984. Female size and nest depth in coho salmon (Oncorhynchus kisutch) Can. J. Fish. Aquat. Sci. 41:204-206.

Van Woert, W.F., and E.J. Smith, Jr. 1962. Upper Sacramento River tributary study: Relationship between stream flow and usable spawning gravel, Cottonwood and Cow Creek, Tehama and Shasta Counties. Calif. Dept. Fish and Game, Redding, unpubl. office rept..

Vining, L.J., J.S. Blakely, and B.M. Freeman. 1985. An evaluation of the incubation life-phase of chum salmon in the Middle Susitna River, Alaska. Alaska Dept. of Fish and Game Winter Habitat Investigations (September 1983 -May 1984) Rept. no. 5, Vol. 1.

Vronskiy, B.B. 1972. Reproductive biology of the Kamchatka River chinook salmon [Oncorhynchus tshawytscha (Walbaum)]. J. Ichthyology 12:259-273.

Warner, K. 1963. Natural spawning success of land-locked salmon (Salmo salar). Trans. Am. Fish. Soc. 92:161-164.

Witzel, L.D. 1980. Relation of gravel size to spawning site selection and alevin production by Salvelinus fontinalis and Salmo trutta. MS thesis, Univ. of Guelph.

## Fish

Entry	Reference	Species	Location	Fish Length (cm)	n	D50	mg	dg	vg	sk
1	Hitzel 1980	BK	Sheldon Ck, Ontario	18	32	8.9	5.7	4.6	5.5	-0.39
2		BK	Skunk Ck, Ontario	18	6	8.2	4.9	3.8	5.7	-0.44
3		BK	Galt Ck, Ontario	18	3	7.2	4.8	3.9	4.7	-0.4
4		BK	Conger's Ck, Ontario	18	16	10.7	6.3	4.8	5.5	-0.47
5	Warner 1963	AS	Cross Lake Thoroughfare, ME	49	23	16.5	9.5	7.2	4.8	-0.52
6		AS	Long Lake Thoroughfare, ME	53	10	15.0	9.1	7.0	4.7	-0.49
7	Hobbs 1937	BT	Various rivers, New Zealand	43	5	18.5	16.0	14.8	3.5	-0.17
8	Reiser and Wesche 1977	BT	Douglas Ck abv Cheyn Dv, NY	31	20	24.0	18.0	15.5	4.4	-0.29
9		BT	Douglas Ck bel Cheyn Dv, NY	31	53	28.0	22.1	19.7	2.7	-0.36
10		BT	Lake Ck, NY	31	16	11.0	9.0	8.1	5.8	-0.17
11		BT	Pioneer Canal, NY	31	6	17.0	11.6	9.6	3.5	-0.45
12		BT	Laramie R at EP site, NY	31	60	32.0	15.8	11.1	7.9	-0.51
13		BT	Laramie R bel Pionr Cnl, NY	31	7	18.0	12.4	10.2	4.1	-0.40
14		BT	Hog Park Ck, NY	31	8	17.0	11.4	9.3	5.2	-0.37
15	Hitzel 1980	BT	Skunk Ck, Ontario	32	4	9.2	6.0	4.8	5.0	-0.4
16		BT	Salt Ck, Ontario	32	2	5.8	4.8	4.4	5.6	-0.16
17		BT	Beatty Sauguen R, Ontario	32	5	14.5	10.3	8.7	4.2	-0.36
18		BT	Syndenham R (1), Ontario	32	6	8.4	6.1	5.2	5.2	-0.29
19		BT	Syndenham R (2), Ontario	32	30	9.9	6.6	5.4	5.0	-0.38
20	Carling (unpub)	BT	Carl Beck, England	29	22	50.0	28.0	21.0	5.2	-0.52
21		BT	Eggeshope Beck, England	29	35	19.0	12.6	10.3	8.6	-0.29
22	Maddux et al 1987	RBT	Colorado R, AZ	45	2	10.5	6.9	5.6	5.3	-0.37
23	This study	RBT	Colorado R tributaries, AZ	40	10	32.0	26.7	24.3	2.9	-0.26
24	Orcutt et al 1968	SH	N.Fk Clearwater R tribs, ID	76	60	42.0	30.3	25.7	4.3	-0.34
25		SH	Salmon R tribs, ID	76	8	46.0	25.6	19.1	5.8	-0.50
26	Chambers et al 1954-5	SH	Kalama R, WA	75	3	31.0	25.8	23.5	3.9	-0.20
27	Hobbs 1937	CH	Hindling R, New Zealand	81	2	16.5	15.6	15.2	3.3	-0.07
28	Burger et al. 1983	CH	Kenai R, AK	101	4	31.8	29.0	27.8	2.7	-0.14
29		CH	Benjamin Ck, AK	94	4	22.0	22.8	23.2	2.7	0.06
30	Uronskiy 1972	CH	Kanchatka R, mainstem	90	2	47.0	34.9	30.0	3.7	-0.34
31		CH	Siberia: arm 1	90	2	26.0	23.3	22.0	3.9	-0.12
32		CH	Siberia: arm 2	90	2	16.0	13.7	12.7	3.8	-0.17
33	This study	CH	Crooked Ck, AK	90	4	36.0	29.7	27.0	2.3	-0.34
34		CH	Yuba R, CA	81	1	34.0	28.3	25.8	2.2	-0.34
35	Chambers et al.	CH	Kalama R, WA	86	13	54.0	43.8	39.5	3.0	-0.28
36	1954, 1955	CH	Snake R, ID	86	8	21.0	18.4	17.2	3.4	-0.16
37		CH	Cispus R, WA	82	7	50.0	39.5	35.1	3.2	-0.30
38		CH	Imnaha R, OR	82	4	41.0	36.8	34.8	2.9	-0.15
39		CH	American R, WA	82	5	35.0	28.4	25.6	3.0	-0.28
40		CH	Cowlitz R, WA	82	8	51.0	35.0	29.0	3.9	-0.42
41		CO	Spring Ck, WA	65	4	35.0	24.4	20.3	3.4	-0.44
42		CO	Toutle R, WA	65	4	16.5	15.6	15.2	3.2	-0.07
43		CO	Burns Ck, WA (1953)	65	7	29.0	23.4	21.0	3.3	-0.27
44		CO	Burns Ck, WA (1954)	65	4	33.0	25.3	22.1	3.1	-0.36
45	Koski 1966	CO	Deer Ck, OR	67	nr	12.0	5.4	3.6	10.6	-0.51
46		CO	Needle Branch, OR	67	nr	6.3	3.6	2.7	9.6	-0.37
47		CO	Flynn Ck, OR	67	nr	5.4	3.4	2.7	9.1	-0.31
48	Helle 1970	PN	Olsen Ck, upper intdl	43	12	8.8	8.0	7.6	4.2	-0.10
49		PN	AK low grad	43	10	11.0	8.0	6.8	5.1	-0.29
50		PN	AK mid intdl	43	43	10.0	8.2	7.5	4.7	-0.19
51		PN	AK lower intdl	43	29	8.0	6.3	5.6	5.3	-0.21
52	Chambers et al	SO	Okanagan R, BC	65	12	25.0	20.1	18.0	3.3	-0.27
53	1954, 1955	SO	Little Wenatchee R, WA	50	4	17.8	14.7	13.4	2.7	-0.29
54	This study	SO	Quartz Ck, AK	35	3	19.0	18.6	18.4	3.5	-0.03

1. Most entries are averages of more than one sample, as indicated by n.

2. See Table 4 for explanation of species code

Table 2

Fish  
Length  
(cm)

Entry	Reference	Species	Location	Length (cm)	n	DSO	mg	dg	sg	sk
55	Spoon 1985	BT	Missouri R, MT	50	11	22.5	18.9	17.4	3.0	-0.24
56		BT	Beaver Ck, MT	23	15	13.0	9.0	7.4	6.2	-0.31
57	This study	BT	Queens R tributaries, CA	29	12	18.0	14.7	13.3	3.2	-0.26
58	Hartman AGalb 1970	RBT	Lardeau R, BC	75	6	23.5	17.2	14.7	3.6	-0.37
59	Platts et al. 1979	RBT	N Fk Boise R, ID	30	45	20.0	14.5	12.4	6.5	-0.25
60	Spoon 1985	RBT	Missouri R, MT	44	7	12.5	9.5	8.3	4.6	-0.27
61		RBT	Beaver Ck, MT	44	19	15.0	10.9	9.3	4.9	-0.30
62	Maddux et al 1987	RBT	Colorado R, AZ	45	1	16.0	7.6	5.2	10.5	-0.47
63	This study	RBT	Colorado R tributaries, AZ	40	8	21.9	17.4	15.5	3.8	-0.26
64		RBT	Montezuma R, NC (<90mm)	21	14	24.5	18.8	16.5	3.8	-0.30
65	Chamberlain 1954-5	RBT	Montezuma R, NC (<90mm)	21	14	46.3	32.0	26.6	4.0	-0.40
66	Chamberlain 1954-5	SH	Montezuma R, NC (<90mm)	75	2	40.0	31.6	28.1	4.3	-0.24
67	Bjornn unpub	SH	Kalana R, WA	66	2	12.4	9.4	8.2	2.9	-0.38
68		SH	Tucannon R, OR: mouth	66	4	25.4	18.8	16.2	3.7	-0.34
69	Cederholm and	SH	Staqualeho Ck, WA: site 1	65	34	19.5	13.2	10.9	5.4	-0.35
70	Sato 1979	SH	Staqualeho Ck, WA: site 2	65	43	22.0	14.5	11.7	5.1	-0.38
71		SH	Staqualeho Ck, WA: site 3	65	38	22.0	14.7	12.0	4.8	-0.38
72		SH	Clearwater R, WA: site 1	70	27	10.4	9.6	9.3	4.8	-0.07
73		SH	Clearwater R, WA: site 2	70	22	13.5	10.5	9.3	4.8	-0.24
74		SH	Clearwater R, WA: site 3	70	25	18.0	11.8	9.6	5.6	-0.36
75		SH	Clearwater R, WA: site 4	70	39	19.0	12.2	9.8	6.5	-0.35
76		SH	Clearwater R, WA: site 5	70	73	23.0	14.3	11.2	5.3	-0.43
77		SH	Clearwater R, WA: site 6	70	61	15.0	12.0	10.8	4.0	-0.24
78		SH	Clearwater R, WA: site 7	70	17	22.0	10.2	6.9	8.4	-0.54
79	Shirazi et al 1981	SH	Beaver Ck, OR	68	3	26.5	20.4	17.9	3.3	-0.39
80		SH	Three Rivers, OR	68	3	32.4	23.2	19.6	3.8	-0.38
81		SH	Gopher Ck, OR	68	3	33.7	26.7	23.8	2.7	-0.35
82		SH	Rock Ck, OR	68	3	36.7	32.9	31.1	2.7	-0.17
83	Chambers et al.	CH	Columbia R, WA	96	4	78.0	51.2	41.4	3.2	-0.55
84	1954, 1955	CH	Snake R, ID	96	10	21.0	16.4	14.5	4.1	-0.26
85		CH	Kalana R, WA	86	7	49.0	35.8	30.6	4.0	-0.34
86		CH	Coulitz R, WA	82	14	42.0	30.1	25.5	4.9	-0.31
87		CH	Imanah R, OR	82	3	52.0	37.4	31.7	3.8	-0.37
88		CH	Cispus R, WA	82	10	37.0	27.1	23.2	4.7	-0.30
89		CH	American R, WA	82	8	34.0	27.2	24.3	3.2	-0.28
90	Van Hoert and	CH	Sacramento R, CA	84	3	44.0	29.9	24.7	4.7	-0.38
91	Smith 1962	CH	Cottonwood Ck, CA	84	12	31.0	22.1	18.6	4.8	-0.33
92		CH	Cow Ck, CA	84	3	52.0	37.7	32.1	3.2	-0.41
93		CH	Battle Ck, CA	84	3	66.0	44.8	36.9	3.5	-0.46
94	Platts et al	CH	S Fk Salmon R, ID: Stolle Me	86	145	22.0	11.7	8.5	7.1	-0.49
95	1979	CH	S Fk Salmon R, ID: Poverty R	86	310	11.2	8.0	6.8	7.5	-0.25
96		CH	S Fk Salmon R, ID: Poverty R	86	80	16.5	10.8	8.7	6.4	-0.34
97		CH	Johnson Ck, ID	86	100	24.5	14.9	11.6	5.8	-0.43
98		CH	Bear Valley Ck, ID	86	20	10.8	8.0	6.9	6.0	-0.25
99		CH	Elk Ck, ID	86	20	15.2	10.7	9.0	3.9	-0.39
100		CH	Loon Ck, ID	86	20	21.5	14.4	11.7	5.1	-0.37
101		CH	Salmon R, ID: Lower Decker	86	5	27.0	18.5	15.3	5.1	-0.35
102		CH	Salmon R, ID: Upper Decker	86	5	13.2	11.4	10.6	4.6	-0.14
103		CH	Alturas Ck, ID	86	20	14.5	11.9	10.7	4.3	-0.21
104	Shirazi et al 1981	CH	Grant Ck, OR	82	4	30.0	22.8	19.9	3.6	-0.32
105		CH	Rogue R, OR: Old Bridge	82	4	37.8	35.9	35.1	2.1	-0.1
106		CH	Rogue R, OR: Hatchery	82	3	39.7	32.2	29.9	4.4	-0.2
107		CH	Rogue R, OR: Sand Hole	82	3	69.3	64.6	62.4	1.6	-0.3
108		CH	Rogue R, OR: Dam Site	82	1	59.0	42.0	35.5	2.4	-0.59
109		CH	Rogue R, OR: Big Butte Ck	82	3	35.0	25.5	21.7	3.3	-0.40
110	Chapman et al 1983	CH	Columbia R (Vernita), WA	86	2	43.0	37.6	35.1	2.9	-0.19
111	This study	CH	Crooked Ck, WA	90	4	41.3	30.3	25.9	2.3	-0.58
112		CH	Yuba R, CA	81	1	35.0	28.1	25.1	2.2	-0.42
113		CH	Spring Ck, WA	65	2	13.0	11.2	10.4	1.5	-0.18
114	Chambers et al.	CO	Toutle R, WA	65	2	10.0	9.2	8.8	3.7	-0.10
115	1954, 1955	CO	Burns Ck, WA (1953)	65	1	29.0	25.5	24.0	2.9	-0.18
116		CO	Burns Ck, WA (1954)	65	4	33.0	27.6	25.3	2.5	-0.29
117	Helle 1970	PN	Olsen Ck, AK: upper Intdl	43	22	9.2	7.5	6.8	5.4	-0.16
118		PN	Olsen Ck, AK: Middle Slough	43	25	6.5	5.2	4.6	5.0	-0.21
119		PN	Little Ck, AK	43	25	9.6	7.5	6.6	3.3	-0.00
120	Shirazi et al 1981	CH	Porcupine Ck, AK: mainstem	65	2	9.6	7.5	6.6	1.9	-0.57

Table 2 (cont)

Entry	Reference	Species	Location	Length (cm)	n	D50	mg	dg	sg	sk
125	Vining et al	CH	Susitna R, AK: mainstem	65	2	62.0	36.6	28.1	5.5	-0.46
126	1985	CH	Susitna R, AK: Side chl 10	65	4	21.8	10.6	7.4	9.7	-0.48
127		CH	Susitna R, AK: Side chl 21	65	5	36.4	22.8	18.1	6.6	-0.37
128		CH	Susitna R, AK: Slough 10	65	3	42.3	10.2	5.0	21.1	-0.70
129		CH	Susitna R, AK: Slough 11	65	6	20.5	16.9	15.3	4.9	-0.19
130		CH	Susitna R, AK: Slough 21	65	3	42.7	25.4	19.6	6.4	-0.42
131		CH	Susitna R, AK: silt	65	4	0.1	0.1	0.1	2.2	0.10
132		CH	Fourth of July Ck, AK	65	4	25.7	21.7	19.9	4.2	-0.18
133	Chambers et al.	SO	Okanagan R, BC	65	5	48.0	37.1	32.7	2.7	-0.38
134	1954, 1955	SO	L. Henatchee R, WA	50	4	14.5	11.2	9.9	3.5	-0.30
135	This study	SO	Quartz Ck, AK	35	3	22.9	18.5	16.6	3.3	-0.27

Table 3 Size Descriptors (mm) for Samples of Fluvial Gravels in the Geologic Literature \*

Entry	Reference	Location	n	D50	mg	dg	sg	sk
136	Conkling 1934	alluvial fans, CA	33	28.3	20.1	17.6	3.8	-0.30
137	Kruebein 1940	San Gabriel Dym, CA	15	9.35	6.4	5.3	6.4	-0.30
138	Kruebein 1942	Arroyo Seco, CA	20	4.98	4.2	3.8	6.8	-0.14
139	Plumley 1948	Rapid Ck terraces, SD	10	23.0	15.1	12.2	5.1	-0.39
140		Bear Butte Ck terraces, SD	7	29.6	22.3	19.3	3.9	-0.31
141		Battle Ck terraces, SD	6	21.3	12.9	10.0	7.1	-0.39
142	Schnee 1957	upland gravels, MO	72	5.2	3.0	2.2	11.2	-0.35
143	Morris and	Arapahoe County, CO	1	2.7	2.7	2.7	1.5	-0.02
144	Johnson 1967	Douglas County, CO	1	4.1	4.2	4.3	1.6	0.08
145		Arkansas R Valley, AR	1	8.3	8.3	8.4	1.5	0.02
146	Knott and Lipscomb 1983	Chulitna R, AK	10	20.2	18.8	18.3	3.1	-0.05

\* All values are in mm except n, sg, and sk, which are dimensionless.

Table 4. Species code used in Tables 1-3

Code	Common Name	Scientific name
AS	Atlantic salmon	Salmo salar
BK	Brook trout	Salvelinus fontinalis
BT	Brown trout	Salmo trutta
CH	Chinook salmon	Oncorhynchus tshawytscha
CM	Chum salmon	O. keta
CO	Coho salmon	O. kisutch
PN	Pink salmon	O. gorbuscha
RBT	Rainbowtrout	O. mykiss
SH	Steelhead	O. mykiss
SO	Sockeye	O. nerka

Att: Dr Paolo Billi  
 Università di Firenze  
 Dipartimento di Ingegneria Civile

From: Matthias Konradt  
 Landscape Architect  
 Berkeley

Table 4 of manuscript to be received  
 via Federal Express

Table 5. Spread of Size Descriptors for Entries in Tables 1-3. \*

Size Descriptor	Spawning Gravels			Other Gravels		
	Extr	P75	P50	P25	Extr	Extr
D50	78	35	22	14.5	0.13	29.6
mg	64.6	27.2	16	10.2	0.1	22.3
dg	62.4	24	14.8	0.7	0.1	19.3
sg	21.1	5.2	4	3.3	1.6	11.2
sk	0.1	-0.24	-0.31	-0.39	-0.7	0.08
						-0.3
						-0.39

\* All 135 entries for redd gravels and potential spawning gravels are presented together under "spawning gravels." Extremes are listed in columns labelled "Extr", and P75, P50, and P25 designate first quartile, median, and third quartile, respectively.

Table 6. Spread of Entries in Tables by Species

Species	number of entries	Median Diameter (mm)			Geometric Mean Diameter (mm)		
		Extr	Median	Extr	Extr	Median	Extr
Brook trout	4	7.2	8.5	10.7	3.8	4.2	4.8
Atlantic salmon	2	15	15.8	16.5	7	7.1	7.3
Brown trout	18	5.8	17.5	50	4.4	9.9	21
Rainbow trout	10	10.5	21	46.3	5.2	12.4	26.7
Steelhead	20	10.4	22.5	46	6.9	11.9	31.1
Chinook salmon	42	10.8	34.5	78	6.8	24.4	62.4
Coho salmon	11	5.4	16.5	35	2.7	15.2	25.3
Chum salmon	13	0.13	25.7	62	0.1	15.3	31
Pink salmon	7	6.5	9.2	11	4.6	6.8	9.6
Sockeye salmon	6	14.5	22	48	9.9	17.3	32.7

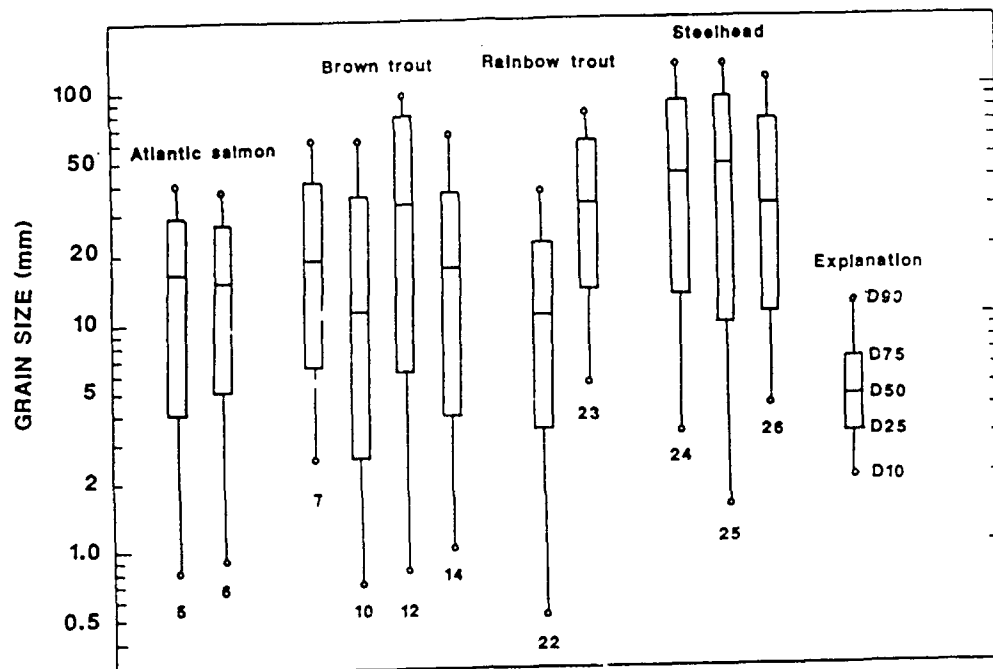


Figure 1. Box-and-whisker plots of size distributions of gravels from trout redds. Each plot is labeled with the number corresponding to its entry in Table 1. Box encompasses the middle 50 percent of the distribution, with the median indicated by horizontal line. Whiskers extend to D90 and D10.

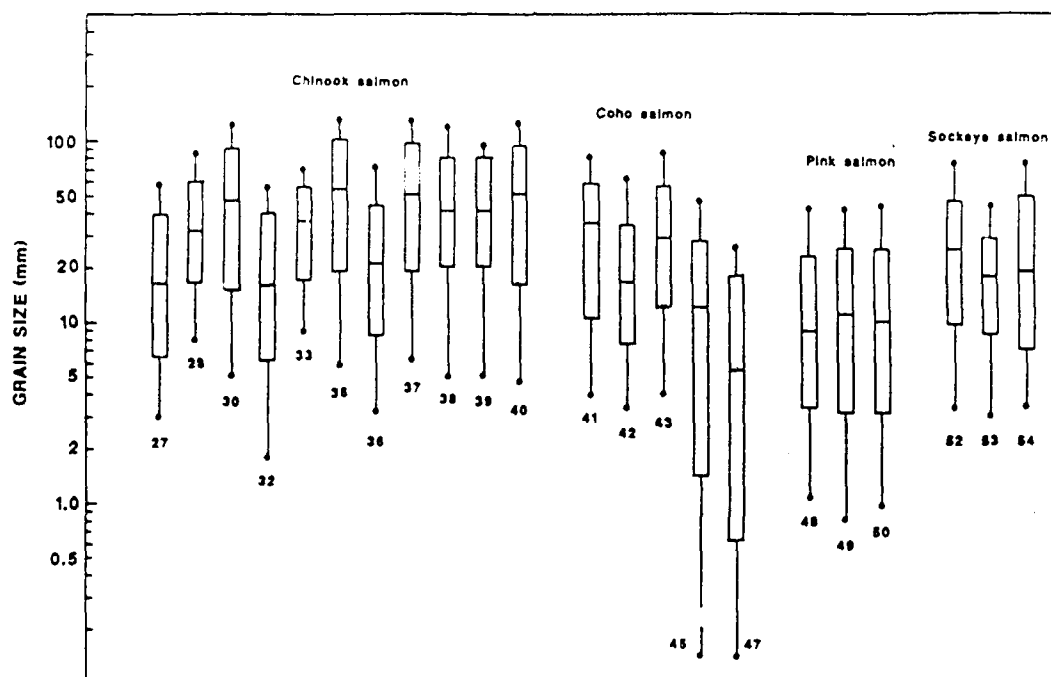
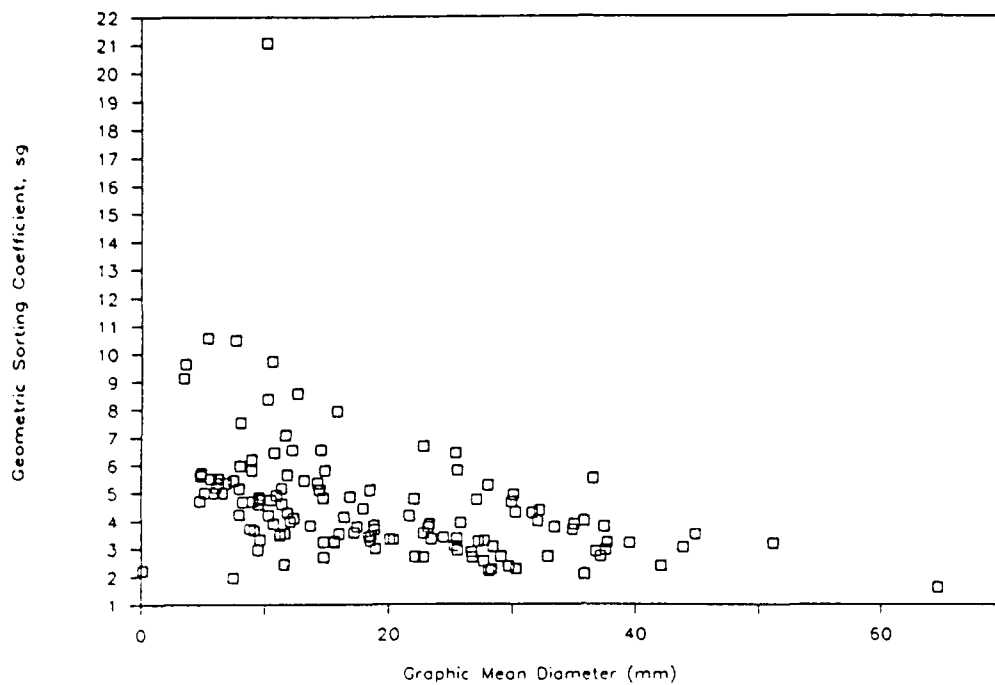


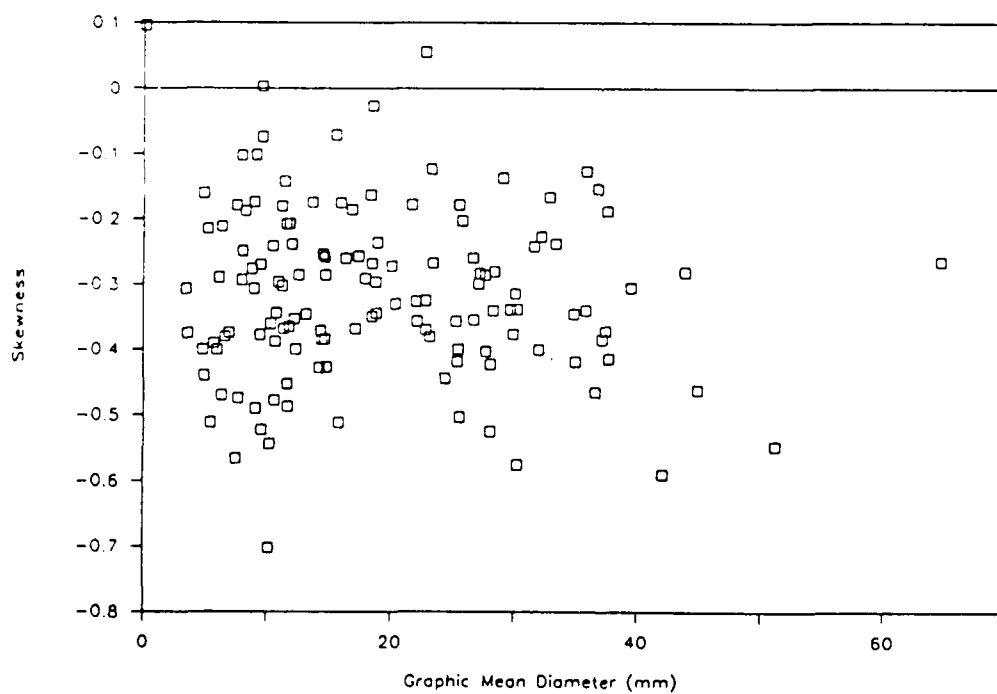
Figure 2. Box-and-whisker plots of size distributions of gravels from salmon redds. Each plot is labeled with the number corresponding to its entry in Table 1. Box encompasses the middle 50 percent of the distribution, with the median indicated by horizontal line. Whiskers extend to D90 and D10.





3

Figure 2. Sorting coefficient vs graphic mean diameter for entries in Tables ~~6.1-6.7~~ 1-3.



4

Figure 2. Skewness vs graphic mean diameter for entries in Tables ~~6.1-6.7~~ 1-3.

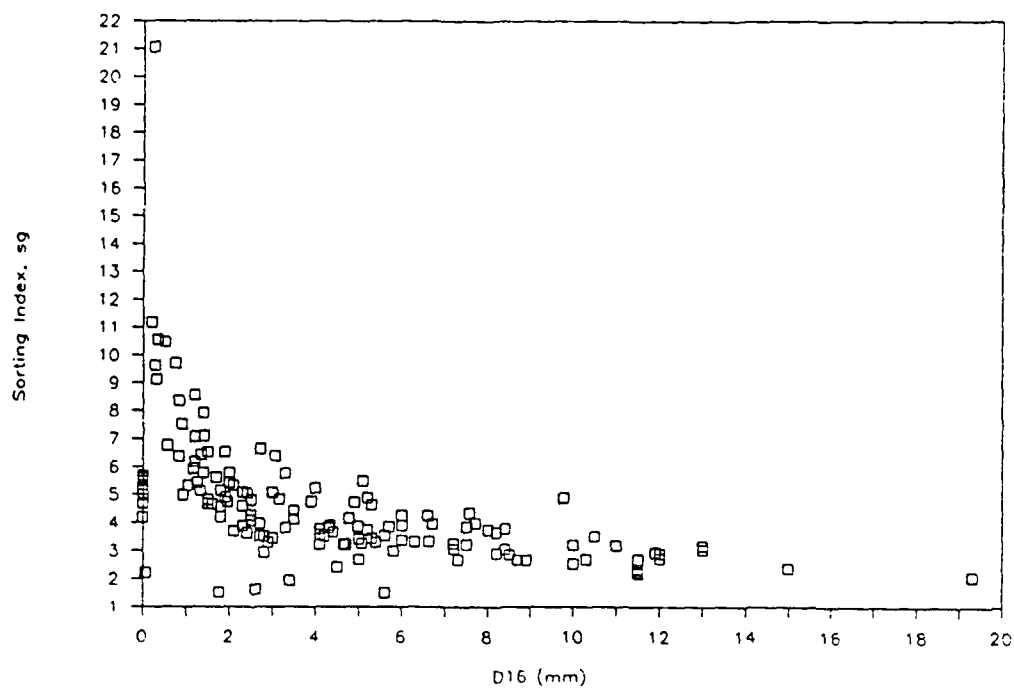


Figure <sup>5</sup> ~~5~~. Sorting coefficient vs D16 for entries in Tables ~~5-1-6-7~~ <sup>1-3</sup>.

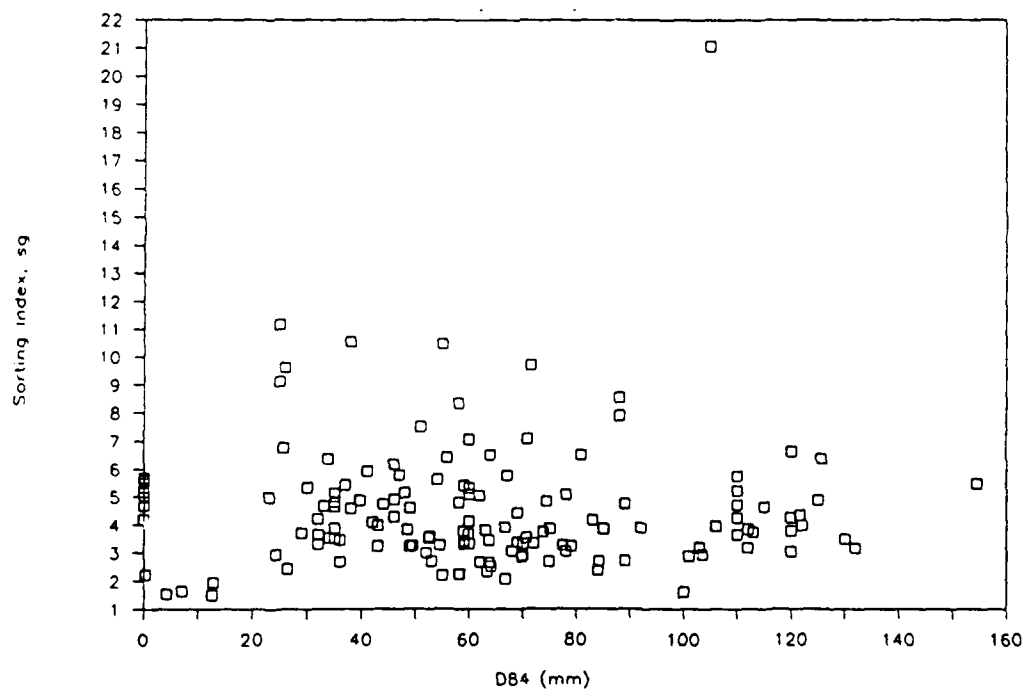


Figure <sup>6</sup> ~~6~~. Sorting coefficient vs DB4 for entries in Tables ~~5-1-6-7~~ <sup>1-3</sup>.

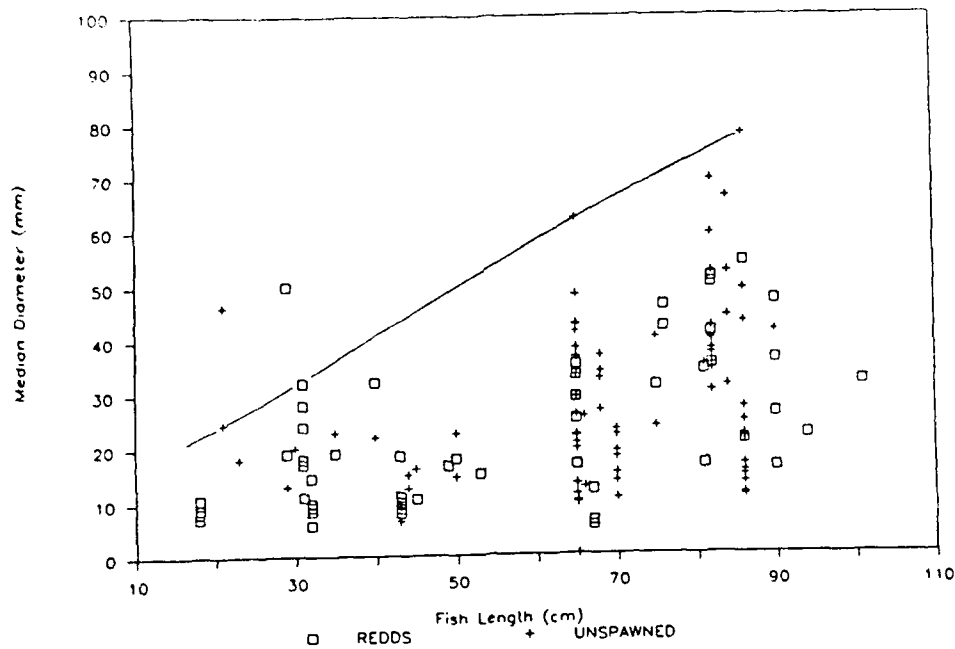


Figure 7. Relation between fish size (total length) and median size of spawning gravel for entries in Tables 1-2. The envelope curve defines the probable upper limit of acceptable gravel size for most conditions, but excludes two outlying points (entry 65 for rainbow trout in the Nantahala River, and entry 20 for brown trout in Carl Beck) so that the range of most entries is better defined.

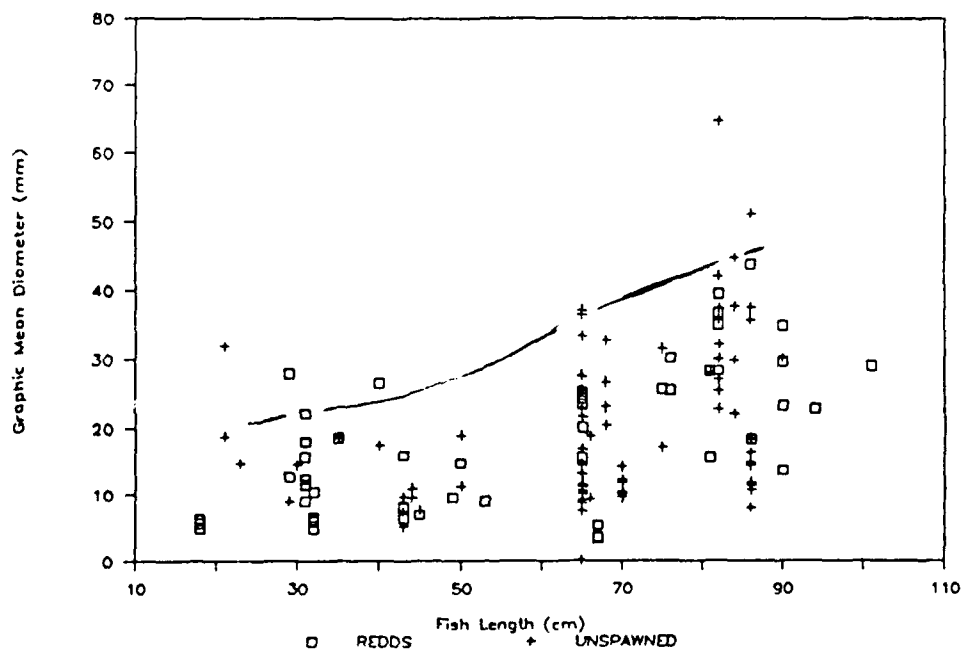


Figure 8. Relation between fish size (total length) and graphic mean diameter of spawning gravel for entries in Tables 1-2. The envelope curve defines the probable upper limit of acceptable gravel size for most conditions, but excludes entry 65 and entry 107 (for chinook salmon in the Rogue River) to better define the range of most points.

LABORATORY OBSERVATIONS OF BED ARMOURING  
AND CHANGES IN BED LOAD COMPOSITION

B.B. Willetts,\* S.J. Tait\* and J.K. Maizels<sup>+</sup>

\* Department of Engineering       )  
  ) University of Aberdeen, U.K.  
+ Department of Geography        )

Summary

A series of three laboratory experiments was carried out at a constant flow and initial bed slope. Continuous observations were made of the bed surface composition, of the bed load transport rate and of bed load composition. The bed load transport rate was found to diminish progressively after an initial period in which it varied slightly. Its size distribution was found to change in a broadly systematic fashion with time. Although observation of the bed surface was difficult, a tentative link was established between the characteristics of the bed load and of the bed surface.

## 1. INTRODUCTION

Most of the published sediment transport rate prediction methods have been developed using a "uniform" size of sediment. This was done so that the effect of sediment size on transport rates could be determined. However in the natural environment, river bed composition is rarely uniform. Non-uniform beds exhibit very different behaviour from that of simple sizebeds. If no sediment is introduced, the bed degrades and coarse material accumulates on the surface reducing the rate of transport significantly (Harrison, 1950). In some circumstances the transport rate is reduced to zero, and then the bed is said to be armoured.

Some of the single size prediction formulae have been amended to take account of mixed grain size (e.g. Bettés and White 1981). Empirical adjustments, determined from large sets of both laboratory and field data, have been proposed to reflect the interaction between grain sizes has occurred (Ranga Raju 1984). These methods frequently refer to a steady state equilibrium transport rate and are therefore unsuitable when considering the development of an armour layer as may occur during a flood.

It has been observed that the armour is a surface layer one grain diameter thick (Harrison 1950, Sutherland 1985). It is also generally accepted that all size fractions present in the original material are present in the armour layer.

It is clear that to understand the phenomenon of bed armouring detailed knowledge must be obtained of the processes which occur in the armour layer. These processes involve the entrainment of grains, sorting of size fractions and interaction between grain sizes. Observations of systematic changes in the composition of the armour layer could indicate the different processes present as the transport rate changes. Once this understanding has been acquired, reliable numerical models can be produced which will attempt to model actual physical processes and not just 'fit' known data sets. Therefore the ability to make observations of the changes in sediment composition of the armour layer is important. However there is considerable difficulty even in the laboratory in making sound observations of either the sorting of the armour layer or the composition of the bed load.

In this investigation periodic observations were made of both the bedload and the armouring bed. Observations of bedload were made using a sediment trap developed from a prototype used by Hardwick and Willetts (1989). The surface composition of the surface layer was studied by an "aerial" photography procedure (Bettés 1982). This paper reports experiments during which the bedload composition and transport rate and the bed surface layer were monitored during the development of a bed armour layer.

## 2. EXPERIMENTAL WORK

### 2.1 Apparatus

The experiments were carried out in a recirculating, tilting, glass-sided flume which was 12.5 metres long and 0.3 metres wide. The slope of the flume was adjusted to 0.001 for all the experiments. All water and bed level measurements were made relative to a datum plane, set by two parallel rails running along either side of the

flume. The distances from the datum plane to the bed and water surfaces were measured using a point depth guage with an accuracy of  $\pm 0.1\text{mm}$ . The water depth was controlled by an adjustable sharp edged weir at the downstream end of the flume. This was adjusted so as to minimise the drawdown effects and give as large as possible a reach of flow at a uniform depth.

The bedload sediment trap consisted of an opening in the base of the flume, a valve and several interchangeable sediment collection boxes. ( figs 1,2). The trap was installed 10.5 metres downstream from the flume inlet ( Fig. 3). The opening in the base of the flume was 200mm x 9mm, the larger dimension being perpendicular to the direction of flow. These dimensions allowed the trap to collect the bedload across the whole width of the flume because even though the dimension of the opening in the flume base (200mm) is smaller than the overall width of the flume (300mm) the bed material lay around the trap at an angle of repose which funnelled the grains moving beside the flume walls down into the trap. The minimum opening dimension (9mm) restricted the maximum size of grain which could be trapped. This was accepted as 6mm and was the overriding limit as regards the maximum size fraction present in any of the bed mixtures used.

The bedload collection boxes were split into three sections laterally. Sediment was thus collected from three separate zones across the width of the flume, each 100mm wide. This was done after it was discovered that at the flow depth used, four secondary flow cells were set up dividing the flow into a central zone and two sidewall zones each 100mm wide.

The important feature of this bedload trap is that the collected bedload can be recovered easily and frequently without disruption to the flow or the gravel bed. This enables the amount and composition of the bedload to be monitored virtually continuously.

A camera was mounted on a carriage which moved along the rails. This was used to take photographs in plan view of the gravel bed surface at intervals of approximately 2 hours and at three points along the flume. Thus indicating changes in the bed surface were recorded at 3 metres, 6 metres and 9 metres from the flume inlet as the bed armour develop with time.

Flow was measured by integrating a velocity profile obtained at a particular cross-section using a Laser Doppler Anemometry system. Flow was held constant throughout each experiment by controlling the height of water above the downstream weir.

## 2.2 Procedure

Three experiments were carried out, keeping the hydraulic influences as constant as possible so that any reduction in sediment transport was attributable to bed sediment composition changes and not to changes in the flow environment. The object of each experiment was to obtain a stable armoured sediment bed by parallel degrading. Flow was monitored and any necessary valve adjustments made to keep it constant. Bed slope and water depth were also monitored in order to discover if they and the average bed shear stress calculated from these parameters remained sensibly constant throughout.

The base of the laboratory flume was covered to a depth of 100mm with a thoroughly mixed sediment mixture. The sediment was then slowly flooded for its whole depth and then drained to aid settlement. It was then scraped level using a scraper which ran on the datum rails. The excess material was discarded.

This gave a level sediment bed of a constant slope equal to 0.001. The surface contained all the sizes in the parent material. The only blemishes were a small number of drag marks, caused by dragging by the scraper of larger grains. However these were small in number and considered insignificant. The bed was then exposed to a low flow (below the estimated threshold of motion) to remove any unnaturally exposed grains arising from the bed-laying operations. The bed was then ready for the experiment to start. Photographs were taken and bed samples noted so that the initial state of the sediment bed was recorded.

A constant flow was now introduced and the weir adjusted to extend the uniform depth of flow. The flow in each of the three experiments was large enough to move the finest grains, but not to move every grain size. Selective erosion therefore occurred and the bed began to armour. Two experiments had a duration of 100 hours and the third of 50 hours. Experiments were stopped when either the sediment transport rate had declined to approximately 10% of its original value or 100 hours had elapsed.

During the experiments the flow was kept constant and the bedload, the surface of the bed and the flow parameters were sampled at intervals

#### 2.2.1 Sampling Techniques

##### Flow Conditions

The water and the bed levels were recorded every 60mm across the width of the flume and at 1 metre intervals along the working length from 3 metres to 9 metres measured from the flume inlet - (fig. 3). The readings at each cross-section were averaged from seven measurements. From these measurements accepted values of bed depth, water depth and bed shear stress were calculated. The shear stress calculation employed a sidewall correction (Einstein 1942).

##### Bedload Sampling

Sediment transport rate measurements were made, every 30 minutes for approximately the first 6 hours. Then the time interval and the sampling period were increased gradually to hourly, then every 2 hours, every 4 hours and eventually before and after overnight runs. The elapsed time of the transport rate measurement was taken as the time to the middle of the sample period.

From the bedload recovered, the sediment transport rate, and the composition of the bedload were determined at intervals throughout the experiment. The bedload samples were dried, weighed and then sieved. All the sediment samples were analysed using a series of sieves at 40 intervals. A mechanical shaker with a shaking time of 10 minutes was used. Weights were determined to an accuracy of 0.01 grams.

#### Bed Armour Sampling

In order to record the development of the bed armour, non-destructive sampling was required at different positions along the flume and at different times. For this reason aerial photography was used. The information contained in these photographs enabled a bulk mass-size distribution of the armour to be determined.

At intervals throughout the experiment the flow was stopped, the water surface fell to a level dictated by the setting of the adjustable tail weir. Photographs were then taken with the camera over the centreline of the flume at three positions, 3m, 6m, and 9m downstream of the flume inlet. For analysis these photographs were enlarged to approximately four times the actual size - a square grid of one hundred points was superimposed on the photographs and the size of each stone under each point was measured. Sediment grains below 0.125mm in diameter could not be measured. The grain sizes were analysed on a size to number basis, this should give the same grading curve as a bulk mass-size distribution according to Hey (1983).

### 3. RESULTS AND DISCUSSION

Three experiments were concluded. It was intended to use the same mixture for each experiment. However the first mixture differed from the mixture used in the last two experiments because of unforeseen variations in a commercially supplied ingredient (Fig. 4). The experimental conditions are summarised in table 1.

Experiment No.	Flow L/s	Original Bedslope	Original Flow Depth mm	Average Shear Velocity m/s
1	7.5	0.001	65.7	0.0221
2	6.0	0.001	57.8	0.0205
3	9.0	0.001	72.8	0.0247

Table 1 Summary of experimental conditions



### 3.1 Bedload Results

#### Sediment Transport Rate

The rate of bedload transport decreased with time, (fig. 5,6,7) as it had in the previous work of Harrison (1950) and Proffitt (1960). For an initial period the sediment transport rate remained approximately constant or declined very gradually. The initial value of sediment transport rate must be interpreted with caution as the area around the trap stabilised, resulting in some initial disruption of the natural flow of sediment. There then occurred a period of rapid decline in sediment transport, clearly visible in fig. 5,6,7.

Comparison of fig. 6 and 7 suggest that the duration of the nearly constant transport rate is a function of bed shear stress (or shear velocity). These two graphs represent experiments with almost identical initial grain mixtures, yet in experiment 3 the onset of rapid decline of transport rate occurs much sooner than in experiment 2. It is clear that this factor also depends on the composition of the original bed. The duration of nearly constant transport rate observed in experiment 1 was much larger than in experiments 2 and 3. It was concluded that the longer fine tails of the size distribution of bed material in experiment 1 (fig. 4) resulted in more grains being available for transport, thus prolonging the zone of small change in the sediment transport rate.

#### Bedload Mass-size Distributions

The size distribution of the bedload also changed systematically with time. It was decided to fit hyperbolic curves to logarithmic plots of the sieve data (Barndorff-Neilsen 1980). This method was used as it can more adequately describe the distribution of grain sizes than the traditional log-normal distribution.

Figures 8,9,10,11 show the size distribution at various sampling periods during experiment 3 and fits a hyperbola to each set of points. It has been found that the selective transport which causes bed armouring involves a systematic change in the bedload which is shown by the changing characteristics of the hyperbolic distribution (Barndorff-Neilsen, Christiansen 1986).

As the sediment transport rate declined it was noted that the modal grain size of the transported material changed dramatically (fig. 12). This plot indicates that the modal grain size of the bed load remained reasonably constant, fluctuating about a value of approximately 0.75mm. After about 600 minutes the modal grain size started to decrease until it reached a value of 0.425mm. The value of the modal grain size then fluctuated wildly from a maximum of 0.875mm to a minimum of 0.425mm. It seems that waves of coarse material are released at intervals which appear to increase with time. This can only be interpreted tentatively because of the small number of sample points in the later stages of the experiment.

It has been found that sediment transport processes which involve systematic change can be clearly shown on a plot of the domain of  $\xi$  and  $\eta$ .  $\xi$  and  $\eta$  give indications of the peakiness and skewness of the hyperbolic distributions respectively. Figures 13, 14 show the trend discovered in experiment 3.

The points in this plot are grouped in three areas. In area I the skewness of the distributions were small indicating symmetrical distributions which had a modal grain size of approximately 0.75mm.  $\xi$  indicates that the distributions were neither excessively peaked nor flat. In area II the distributions have skewed towards the smaller size fraction and a lower value of  $\xi$  suggests that the distributions were less well sorted about the mean grain size than before. The bedload samples now jumped from area II to area III, indicating that the bedload had skewed to the larger fractions - the modal grain size was approximately 0.85mm and the sample was better sorted, i.e. a more "peaked" shape.

These plots (fig. 13,14) indicate that several processes were involved in a systematic fashion in the creation of an armoured bed. The results show that rather coarse material was transported initially. After depletion of this fraction in the bed, smaller material was transported in greater quantities. When enough material was thus removed the sediment transport rate declined because of the non-availability of suitable sediment and the sheltering effect of the larger more resistant grains. The fluctuations in modal grain size, skewness and kurtosis occurred when these larger grains lost their stability because of the winnowing of fine sediment from around them. The larger grains were then transported away, leaving unprotected fines to be entrained as bedload, resulting in another fluctuation in the bedload characteristics. These fluctuations continue for a considerable time. As the transport rate decreases, the fluctuation sequences involve a progressively smaller proportion of the original size fractions. Thus a comparatively small number of coarse grain dislodgements are required to sustain transport rate fluctuations in the later stages of armouring.

### 3.2 Composition of the Surface Layer

It was clear from the photographs taken of the bed surface (Figs. 15, 16, 17, 18, 19, 20) that, as the sediment mix coarsened, the flow boundary got progressively rougher. This roughening began at the upstream end of the flume and progressed slowly downstream. Consequently the uniform depth increased at constant flow as the experiment progressed.

The experiments produced a substantial collection of plan view photographs of the changes occurring in the sediment bed. It is intended to analyse them using the technique outlined above, in order to discover the link between the changes in the grain population of bedload with the changes in the grain population on the sediment bed. The changes in the sediment transport rate and the bedload composition need to be related to the changes in the composition of the bed in a synchronised manner.

#### 4. CONCLUSIONS

This series of experiments though limited in number has produced evidence from which useful and reliable conclusions were reached.

There is confirmation again that sediment transport rate declines with time and that this decline may be split into two zones (Proffitt 1980), one of small change in the sediment transport rate and one of rapid decline. The pattern of decline in sediment transport is a function not only of flow vigour but also of the original bed composition.

Continuous sampling of the bed load enabled us to observe the composition of the bedload as it changed with time. When the mass-size distributions were plotted in a logarithmic plot fitted with hyperbolic curves it was revealed that the characteristics of these plots behaved in a systematic fashion dependent on the processes present. This information is important, as bedload sampling is not encumbered with the great difficulties associated with the sampling of the bed surface composition.

As the sediment transport rate dropped the bed progressively coarsened due to the loss of fines. The rate of coarsening declined markedly as the sediment transport rate declined and the composition of the bedload fluctuated. These bed surface observations are generally compatible with the bed load measurements. Although it is clear that there is a relationship between the compositions of the bed and of the bedload, further work still needs to be done to match with respect to time the characteristics of the bed with the known characteristics of the bedload.

## Schedule of Figures and Tables

### Figures

Figure 1	Side View of Bedload Sediment Trap Attached to Flume
Figure 2	Photograph of Bedload Sediment Trap
Figure 3	Sketch of Flume and Experimental Setup
Figure 4	Size Distribution of Original Bed Mixtures
Figure 5	Decline in Sediment Transport with Time : Experiment 1
Figure 6	Decline in Sediment Transport with Time : Experiment 2
Figure 7	Decline in Sediment Transport with Time : Experiment 3
Figure 8	Size Distribution Bedload Sample: Experiment 3 Elapsed Time 70 mins.
Figure 9	Size Distribution Bedload Sample: Experiment 3 Elapsed Time 755 mins.
Figure 10	Size Distribution Bedload Sample: Experiment 3 Elapsed Time 1136 mins.
Figure 11	Size Distribution Bedload Sample: Experiment 3 Elapsed Time 4318 mins.
Figure 12	Modal Grain Size with Time: Experiment 3
Figure 13	Plot of the domain of $\xi$ and $\chi$
Figure 14	Plot of the domain of $\xi$ and $\chi$ outlining areas I, II, and III: Experiment 3
Figure 15	Plan View Photograph of Bed at 3m Time Elapsed 20 mins: Experiment 3
Figure 16	Plan View Photograph of Bed at 3m Time Elapsed 4157 mins: Experiment 3
Figure 17	Plan View Photograph of Bed at 6m Time Elapsed 120 mins: Experiment 3
Figure 18	Plan View Photograph of Bed at 6m Time Elapsed 4157 mins: Experiment 3
Figure 19	Plan View Photograph of Bed at 9m Time Elapsed 120 mins: Experiment 3
Figure 20	Plan View Photograph of Bed at 9m Time Elapsed 4157 mins: Experiment 3

### Tables

Table 1	Summary of Experimental Conditions
---------	------------------------------------

## References

1. Bagnold, R.A., Barndorff-Nielsen, O. : (1980) The Pattern of Natural Size Distributions, *Sedimentology*, 27, p 199-207.
2. Barndorff-Nielsen, O., Christiansen, C. : (1986) Erosion Deposition and Size Distributions of Sand, Research Report No. 149, Dept. of Theoretical Statistics, Univ. of Aarhus.
3. Bettess, R. and White, W.R.: (1981) Mathematical Simulation of Sediment Movement in Streams. *Proc. Inst. Civil Eng. Part 2*, 71, p. 879-892.
4. Bettess, R.: (1982) Degradation of River Beds and Associated Changes in the Composition of Sediments. *Euromech 156, Mechanics of Sediment Transport*, Istanbul, p. 237-242.
5. Einstein, H.A.: (1942) Formulas For The Transportation of Bed Load, *Trans. ASCE*, 107, p.575-577.
6. Harrison, A.S.: (1960) Report on Special Investigations of Bed Sediment Segregation in a Degrading Bed., Report Series No. 33 University of California Inst. of Eng. Research, Berkley, California.
7. Hardwick, R.I., Willetts: (1969) Changes with Time of the Transport Rate of Sediment Mixtures, Seminar 4, 23rd Congress, I.A.H.R., Ottawa.
8. Hey, R.D., Thorne, C.R.: (1983) Accuracy of Surface Samples from Gravel Bed Material. *Proc. A.S.C.E. Jour. of Hyd. Eng.* 109, p.642-651.
9. Proffitt, G.T.: (1980) Selective Transport and Armouring of Non-Uniform Alluvial Sediments. Report No. 80/22 Dept. of Civil Eng., Univ. of Canterbury.
10. Ranga Raju, K.G.: (1985) Transport of Sediment Mixtures, *Proc. 21st Congress I.A.H.R., Melbourne*, 6, p.35-46.
11. Sutherland, A.J.: (1987) Static Armour Layers by Selective Erosion. *Sediment Transport in Gravel Bed Rivers*, eds. Thorne, C.R., Balhoist, J.C., Hey, R.D. P.243-267.

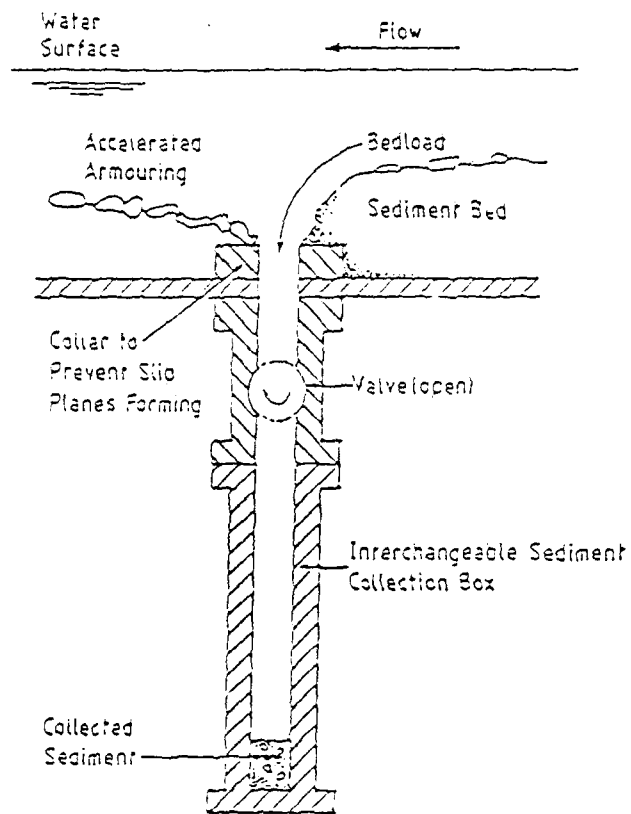


Figure 1 Side View of Bedload Sediment Trap Attached to Flume

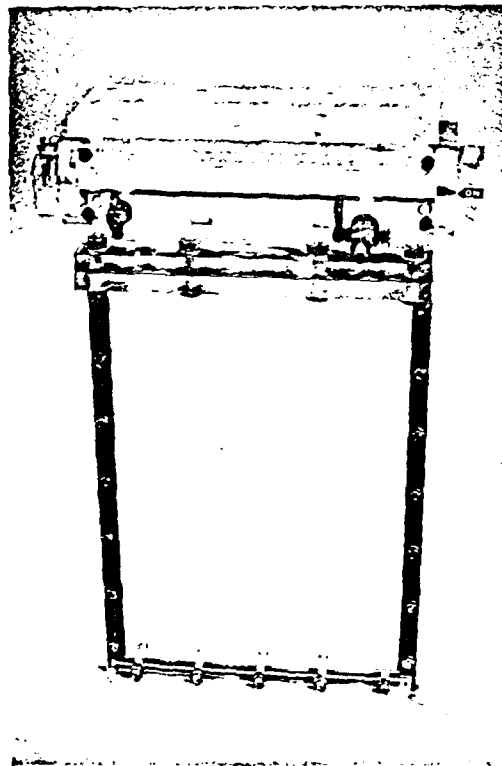


Figure 2 Photograph of Bedload Sediment Trap

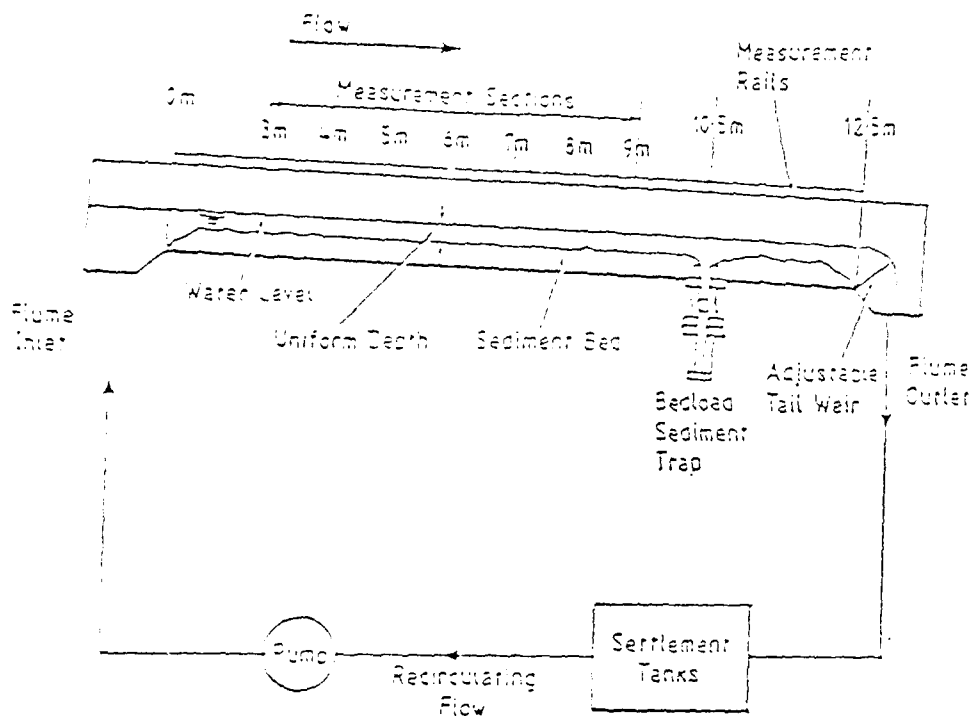


Figure 3 Sketch of Flume and Experimental Setup.

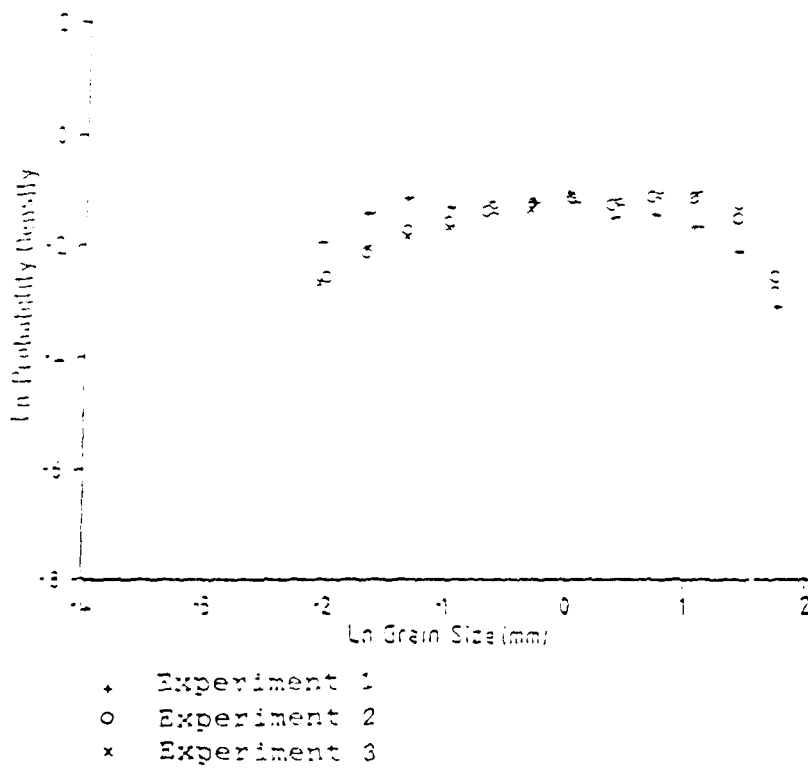


Figure 4 Size Distribution of Original Sed Mixtures

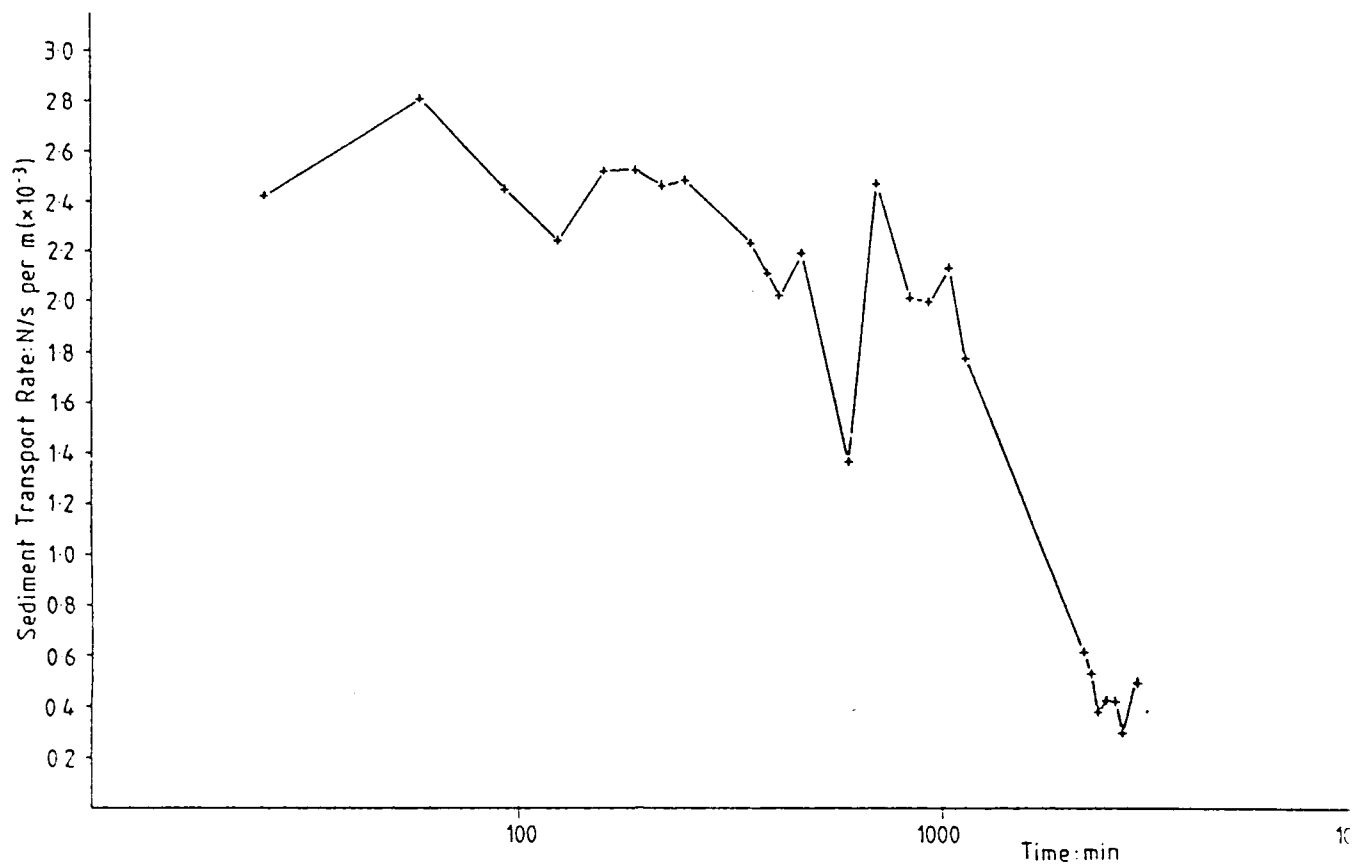


Figure 5 Decline in Sediment Transport with Time: Experiment 1

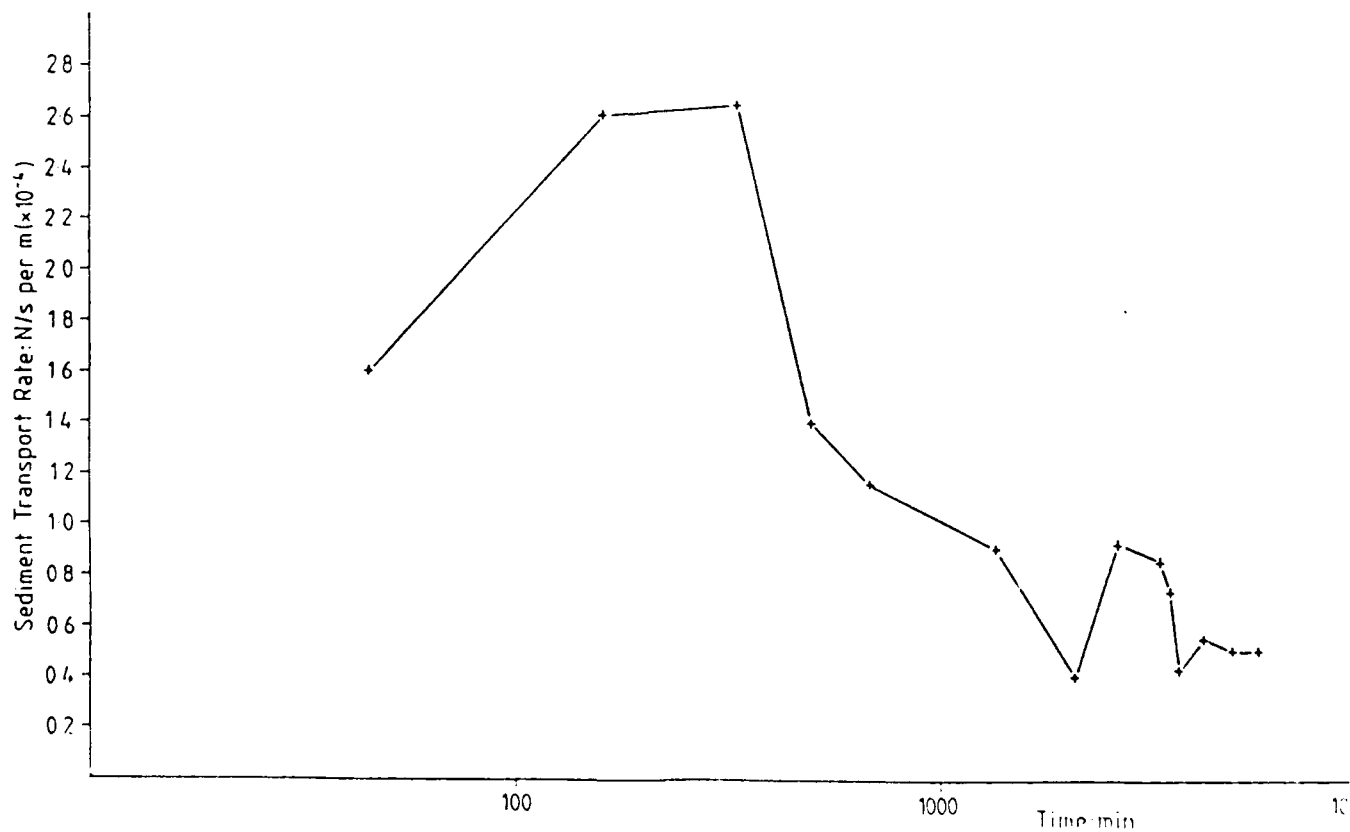






Figure 1 Decline in Sediment Transport with Time: Experiment 3

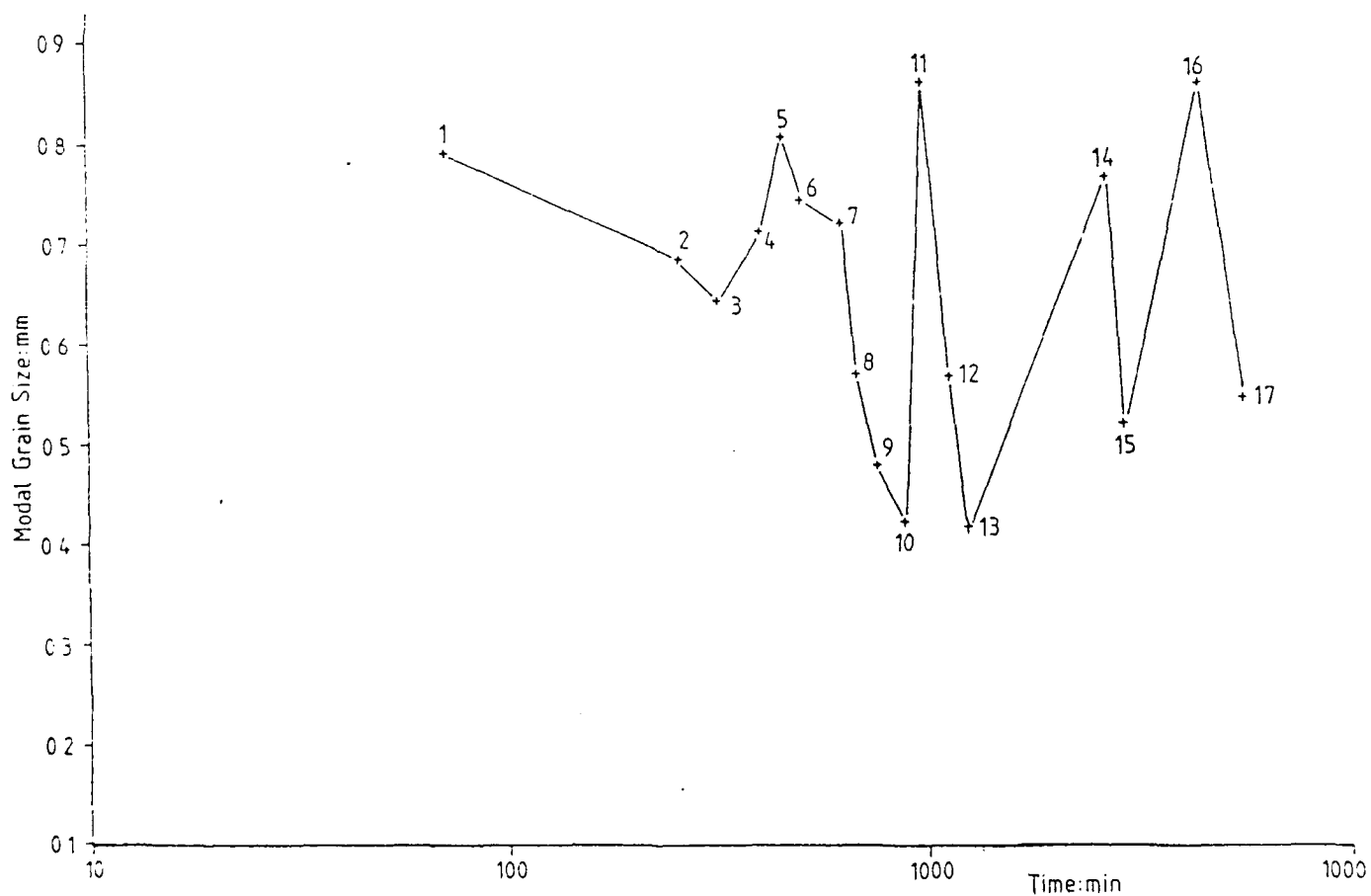


Figure 2 Modal Grain Size with Time: Experiment 3

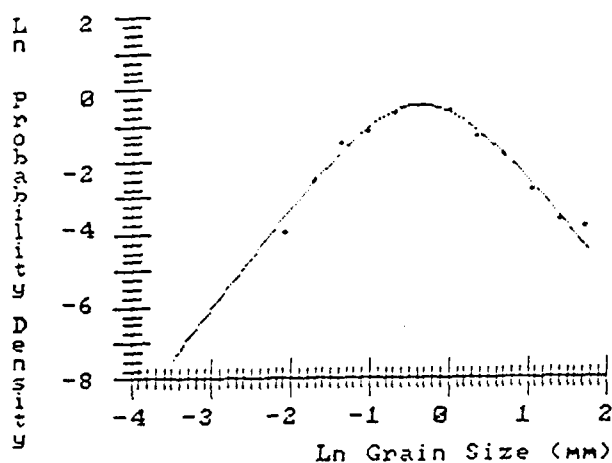


Figure 9  
Size Distribution Bedload Sample  
Experiment 3 Elapsed Time 70 mins.

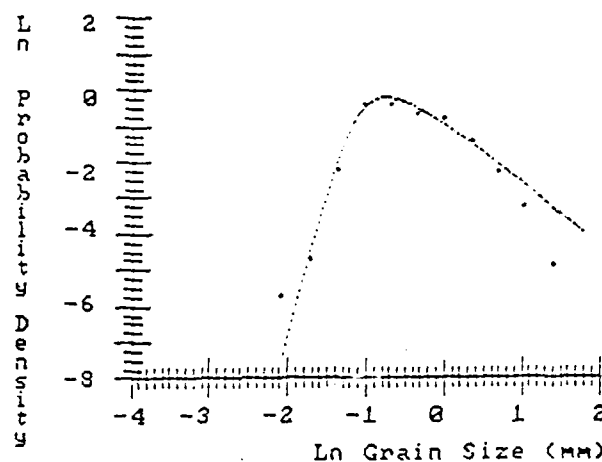


Figure 10  
Size Distribution Bedload Sample  
Experiment 3 Elapsed Time 755 min.

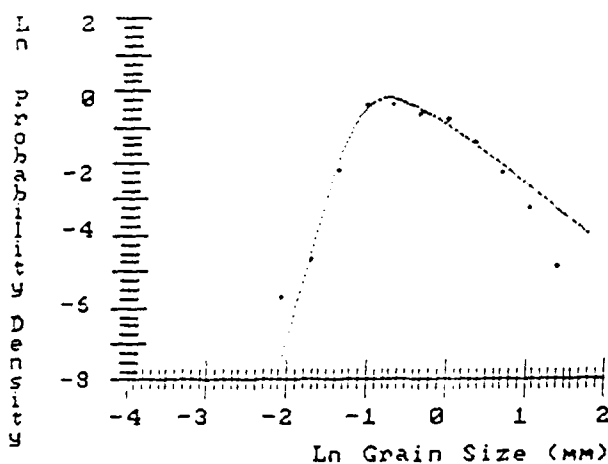


Figure 11  
Size Distribution Bedload Sample  
Experiment 3 Elapsed Time 1136 min.

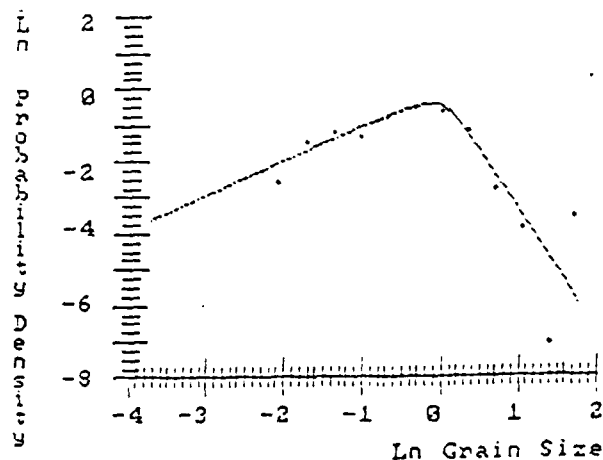


Figure 12  
Size Distribution Bedload Sample  
Experiment 3 Elapsed Time 4318 min.

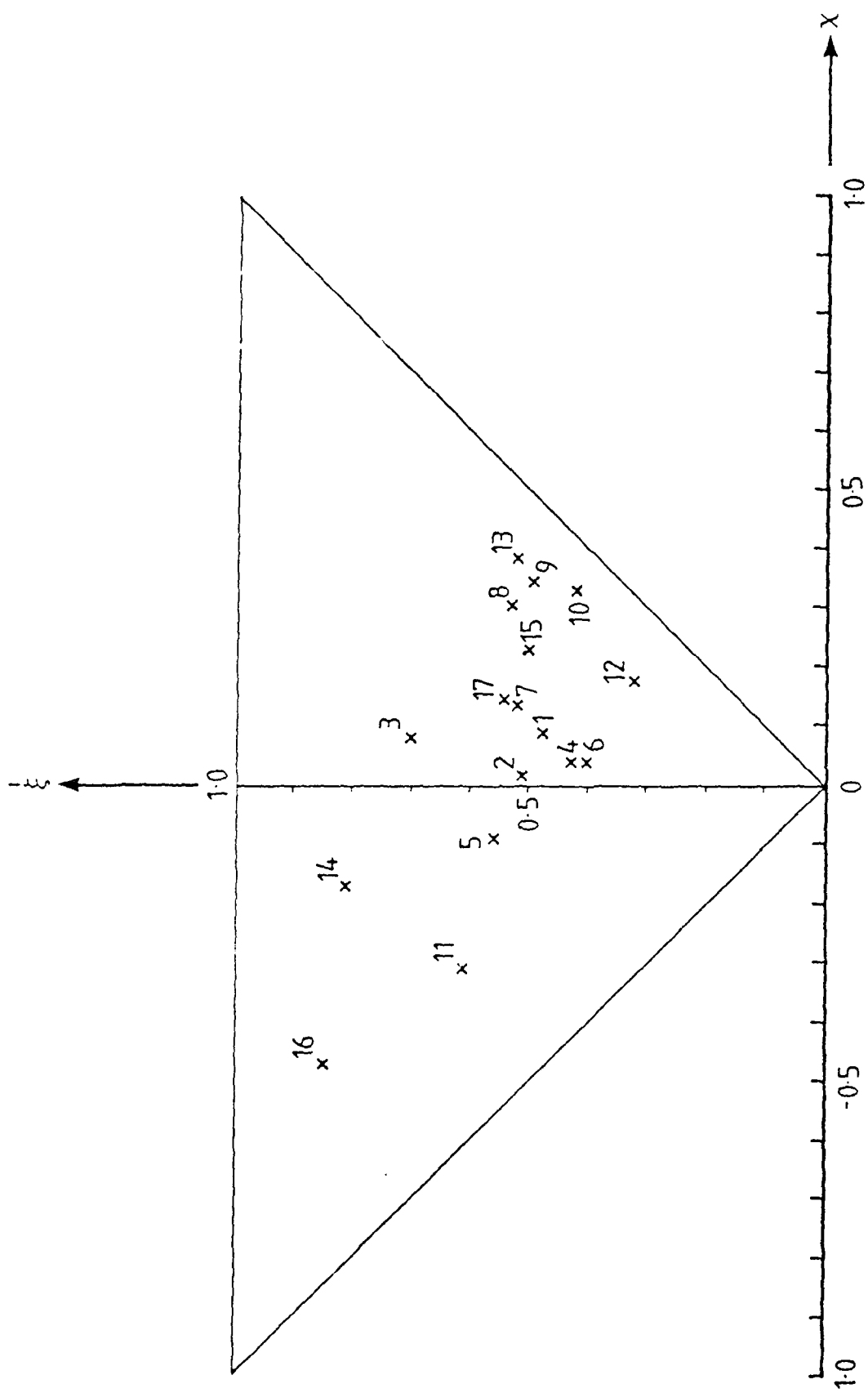


Figure 13 Plot of the domain of  $\xi$  and  $x$

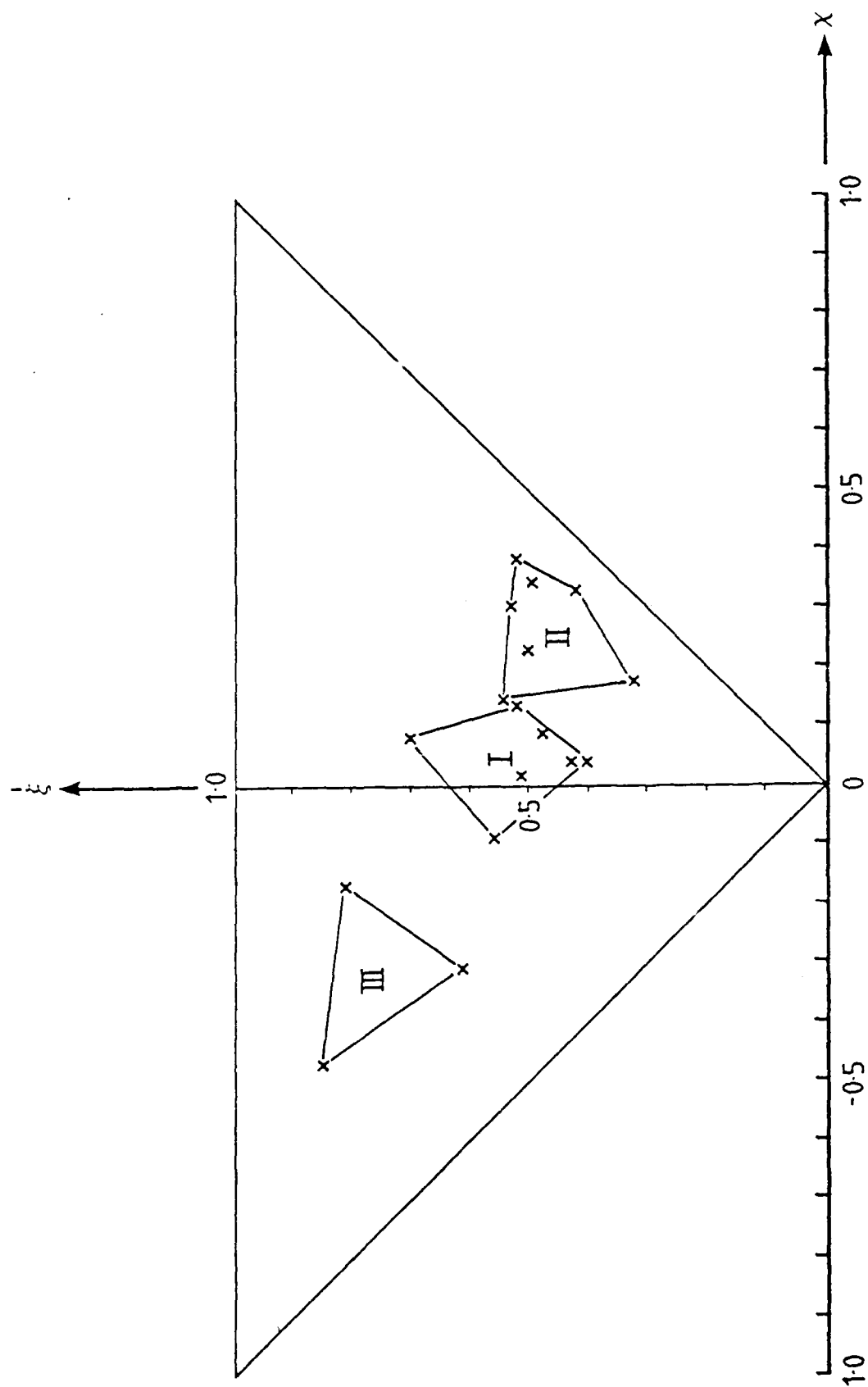


Figure 14 Plot of the domain of I, II, and III: Experiment 3.

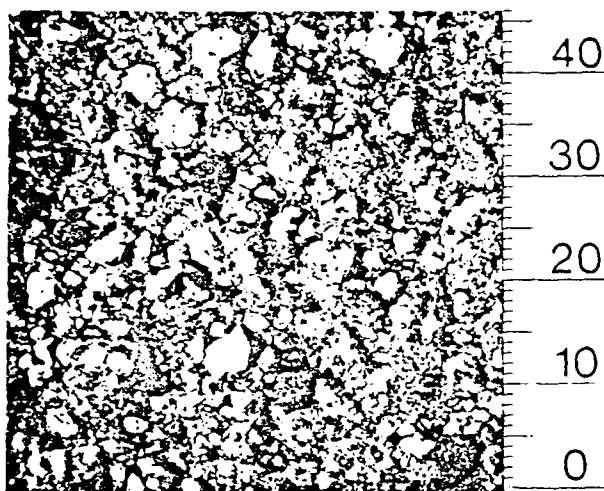


Fig. 15 Plan View Photograph of Bed at 3 m  
Time Elapsed 120 mins ; Experiment 3

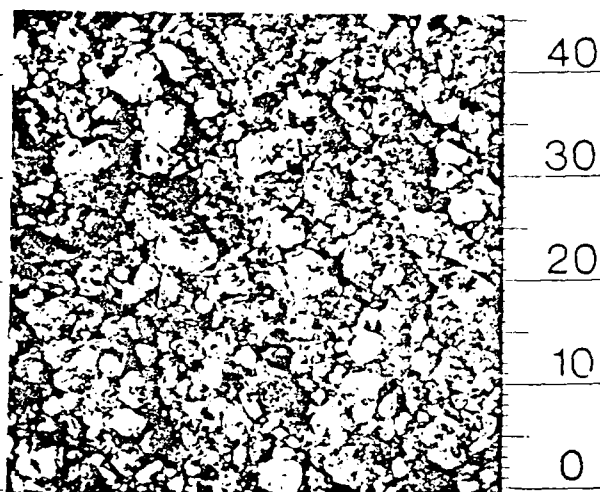


Figure 16 Plan View Photograph of Bed at 3 m  
Time Elapsed 4157 mins ; Experiment 3

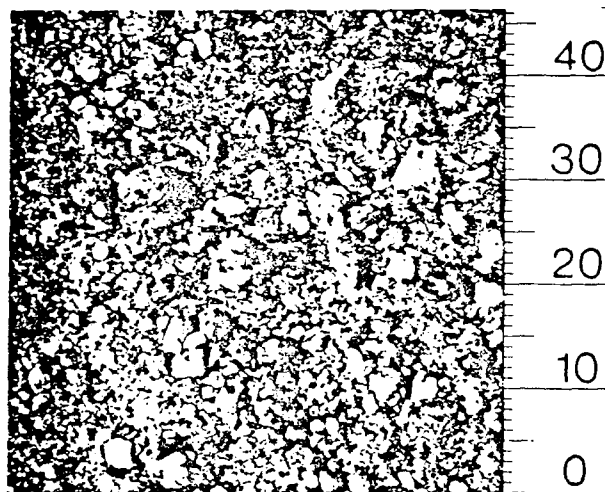


Figure 17 Plan View Photograph of Bed at 6 m  
Time Elapsed 120 min. ; Experiment 3

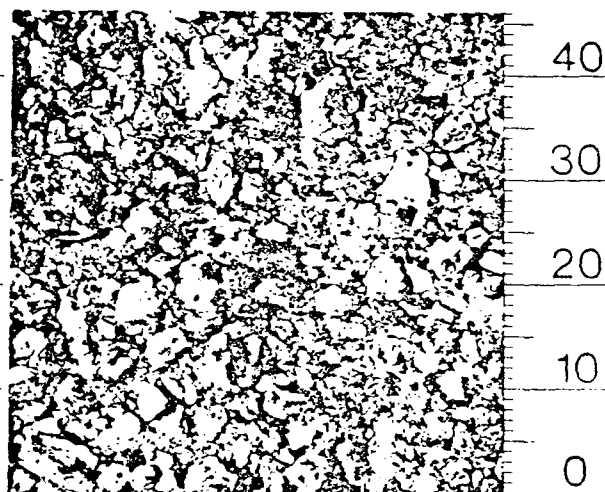


Figure 18 Plan View Photograph of Bed at 6 m  
Time Elapsed 4157 min. ; Experiment 3

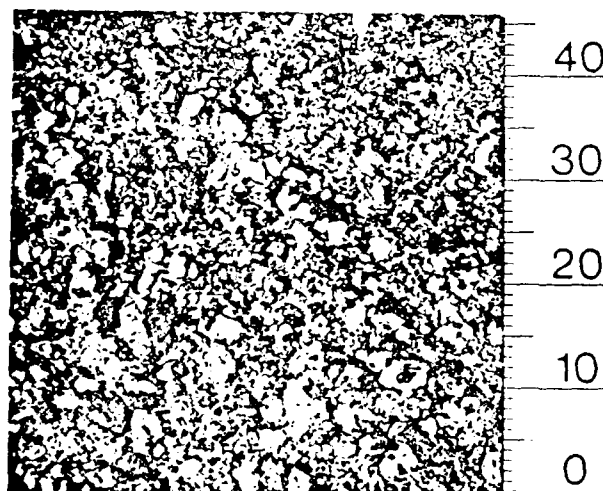


Figure 19 Plan View Photograph of Bed at 9 m  
Time Elapsed 120 min. ; Experiment 3

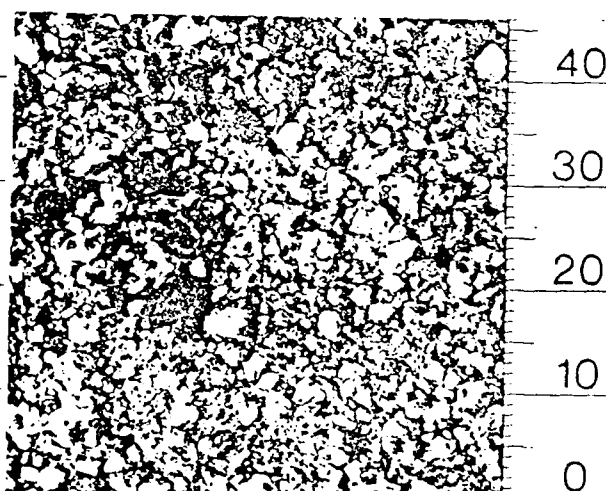


Figure 20 Plan View Photograph of Bed at 9 m  
Time Elapsed 4157 min. ; Experiment 3

Flow Direction top to bottom of page

All scales in mm.

# 3rd INTERNATIONAL WORKSHOP ON GRAVEL-BED RIVERS

Firenze, 24-28 September 1990

## ANALYSIS OF ARMOURING PROCESSES THROUGH LABORATORY EXPERIMENTS

Alberto LAMBERTI (\*), Enio PARIS (\*\*)

(\*) Istituto di Idraulica, Universita' di Bologna  
Viale del Risorgimento, 2 - 40136 Bologna (ITALY)

(\*\*) Dipartimento Ingegneria Civile, Universita' di Firenze  
Via di S. Marta, 3 - 50139 Firenze (ITALY)

### SUMMARY

The process of formation of the armour layer has been experimentally investigated. Eleven runs have been carried out using three different bed sediment mixtures combined with different hydraulic conditions. The characteristics of the armour layer are discussed through the analysis of the temporal evolution of bed surface composition and its effects on sediment transport process.

## 1 - INTRODUCTION

Sediment transport in alluvial rivers originates from the mutual interaction between hydraulic and sediment characteristics; under certain circumstances the sediment transport process may lead to the formation of a protective cover generally consisting of a layer of grains on the bed surface (here called armour layer) which are coarser than the subsurface material.

This phenomenon has been investigated in several aspects:

- the sediment and hydraulic conditions under which the coarse layer develops (Lane & Carlson, Garde & Hasan, Little & Mayer, Knoroz, Proffitt, Sutherland);

- the effects on incipient motion and on sediment transport induced by the non uniformity of grains (Harrison, Einstein & Chien, Egiazaroff, Gessler '65, Day, Ashida & Michiue '73, Misri et Al., Proffitt & Sutherland, Samaga et Al., Falcon, Ribberink, Andrews & Parker);

- the relation between the final grain-size distribution of the coarse layer and the characteristics of the subsurface material (Gessler '65, Ashida & Michiue '71, Little & Mayer '72, Proffitt & Sutherland, Saad)

- the erosion associated to the coarse layer development (Little & Mayer, Proffitt, Saad);

- the temporal evolution of the surface layer and/or transport rate during the formation process (Little & Mayer, Proffitt, Mosconi).

Mathematical simulation of the armouring processes has been also proposed by Hirano, Bayazit, Deigaard & Fredsoe, Borah et al., Shen & Lu, Karim & Kolly, Falcon, Ribberink, Lee & Odgaard, Willers et al., Palaniappan & Godbole, Arnanini & Di Silvio.

In order to have a better understanding of the armour process, three set of experimental investigations has been carried out at the laboratory of "Istituto di Idraulica" of the University of Bologna (Italy). Preliminary results obtained by the first set of experimental data have been already presented (Lamberti & Paris). Here, the total amount of experimental data are presented and discussed.

## 2 EXPERIMENTAL APPARATUS AND PROCEDURES

The experimental equipment has been already described in a previous paper (Lamberti & Paris); therefore only a brief description is given here.

A recirculating and tilting flume, 12 m long, 0.30 m wide and 0.50 m deep has been used to run sediment-free water over an initial flat bed made by non-cohesive sediment; the characteristics of the three sediment mixtures used in the experiments are summarized in table 1.

*table 1. Sediment characteristics*

Type of sediment	D <sub>16</sub> mm	D <sub>50</sub> mm	D <sub>84</sub> mm	$\sigma$	Sg	$\epsilon$
1	1.45	2.69	5.27	0.90	2.58	0.35
2	1.00	3.68	7.73	1.38	2.59	0.34
3	1.10	2.36	6.54	1.13	2.58	0.35

In each run, the formation of the armour layer was obtained under practically uniform flow conditions, during which measurements of liquid discharge, water temperature, piezometric and total head, velocity profiles, solid discharge, bed level variations and bed surface grain sizes have been carried out.

The runs were prolonged until a small fraction of the initial sediment transport (generally less than 5%) was collected in the sediment trap located at the downstream end of the flume; to this point the bed was considered to be armoured. Then, a sudden increase of discharge was



imposed until the armoured layer appeared completely removed.

Three series of runs have been carried out, one for each type of bed material, for a total number of 11 runs. The characteristics of each runs are summarized in tables 2-12 where symbols are:  $S_b$ , initial bed slope,  $t$ , run time (hours),  $Q$ , liquid discharge (l/s),  $T$ , water temperature ( $^{\circ}C$ ),  $h$ , water depth (cm),  $S_f$ , energy slope,  $U_v$ , mean velocity derived from velocity profiles (cm/s),  $U_p$ , mean velocity derived from Pitot measurements (cm/s),  $v_{svp}$ , bed shear velocity obtained from velocity profile (cm/s),  $v_{swc}$ , bed shear velocity obtained from side wall correction (cm/s),  $R_b$ , bed hydraulic radius (cm),  $Q_s$ , sediment discharge (kg/h),  $D_{84}$ ,  $D_{50}$ ,  $D_{16}$ , grain sizes for which the 84%, 50% , 16% of bed material is finer, while subscripts  $e$  and  $a$  refer to the eroded material (collected in the sediment trap) and the material of the armour layer surface, respectively.

## 2.1 BED SURFACE SAMPLING

One of the major problem to investigate the evolution of bed surface during an armouring process is the sampling technique; in order to preserve the integrity of the armour layer throughout the experiments , the size frequency distribution has been obtained by analyzing photographs of the bed surface according to the grid sampling method (Adams).

To this aim, photographs of the surface layer at the upstream, the middle and the downstream end of the testing reach have been taken at the beginning of the run, at the end of the armoured layer development and after its destruction.

Figure 1 shows a comparison between sediment diameters estimated from photograph analysis of bed surface and the sediment diameters obtained from sieve analysis, for the initial bed conditions. As it can be seen, there is a satisfactory agreement between the two set of diameters. Therefore, the same technique has been extended to survey the bed surface during the experiments.

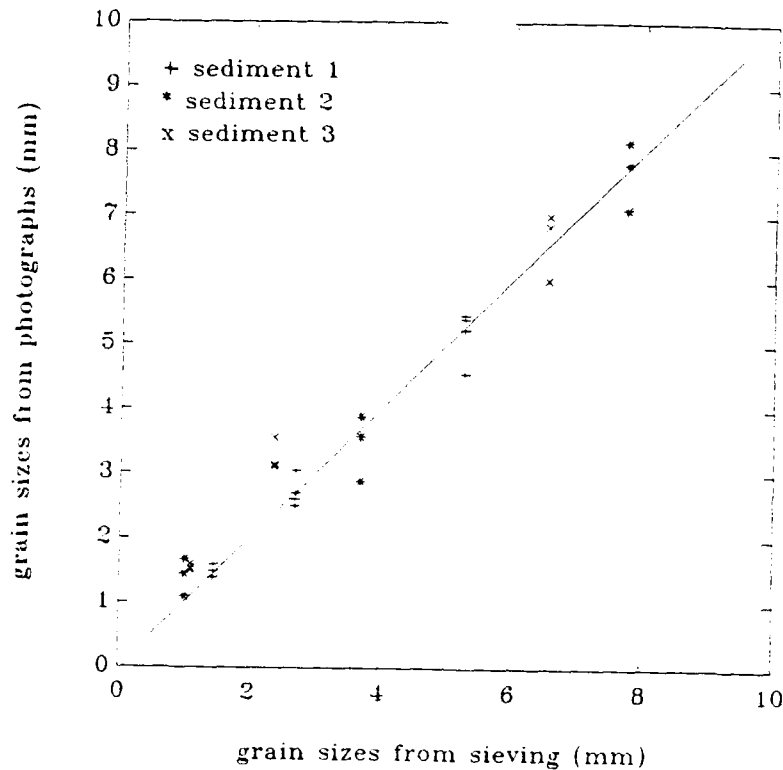


Fig. 1 - Sediment sizes estimated from photographs compared with sieve diameters.

## 2.2 SIDE WALL EFFECTS

During the experiments, runs have been conducted under a wide range of the width to depth ratio (from 1:1 up to 6:1); therefore, the side wall effects have been taken into account according to the procedure described in the previous paper (Lamberti & Paris). The reliability of the side wall correction has been verified by comparing the values of bed shear velocity  $v_{*wc} = \sqrt{gR_b S_f}$  with the values of shear velocity obtained from analysis of velocity profiles,  $V_{*pv}$ . Results are listed in tables 2 - 12.

Table 2 - sediment 1

**RUN 1**
 $D_{84} = 4.80 \text{ mm}$      $D_{50} = 2.82 \text{ mm}$      $D_{16} = 1.51 \text{ mm}$      $S_b = 0.002$ 

t	Q	T	h	Sf	U <sub>p</sub>	U <sub>v</sub>	v <sub>pv</sub>	v <sub>wc</sub>
hrs	l/s	°C	cm	× 1000	cm/s	cm/s	cm/s	cm/s
0.00	40.8	18.8	18.8	2.45	-	-	-	5.4
2.00	"	"	18.9	2.40	-	-	-	5.3
5.00	"	18.9	19.1	2.25	-	-	-	5.2
11.00	"	19.4	19.4	2.15	-	-	-	5.1
13.00	"	19.3	"	2.10	-	-	-	5.1
18.50	"	19.6	19.8	2.08	-	-	-	5.1
21.50	"	19.9	20.0	2.01	-	-	-	5.1
28.50	"	20.0	20.0	2.00	-	-	-	5.1
43.50	"	20.4	20.2	1.95	-	-	-	5.0
59.50	"	20.8	20.3	1.85	-	-	-	5.0
84.50	"	21.1	20.3	1.95	-	-	-	5.0
85.50	68.7	20.2	30.0	1.45	-	-	-	4.5
86.00	"	20.3	-	-	-	-	-	-
87.00	"	20.2	-	-	-	-	-	-

	Rb	Qs	d84e	d50e	d16e	d84a	d50a	d16a
hrs	cm	kg/h	mm	mm	mm	mm	mm	mm
1.00	12.5	0.75	5.28	3.40	2.13	4.81	2.80	1.46
2.00	12.5	2.38	4.75	2.94	1.82	4.18	2.66	1.33
7.00	12.6	2.12	4.51	2.60	1.55	6.34	3.00	1.30
12.00	12.7	1.22	4.59	2.54	1.49	6.80	3.30	1.21
19.50	13.0	0.67	4.28	2.60	1.55	7.25	3.50	1.11
28.50	13.0	0.40	4.20	2.55	1.57	6.98	3.63	1.07
43.50	13.0	0.41	4.63	2.58	1.48	7.45	3.73	1.05
63.50	13.0	0.64	4.35	2.21	1.25	7.78	4.10	1.52
85.50	14.1	0.12	3.94	2.39	1.48	7.87	4.20	1.54
86.00	-	2.98	-	-	-	-	-	-
87.00	-	1.81	5.24	2.77	1.39	-	-	-

Table 3 - sediment 1

**RUN 2**
 $D_{84} = 4.80 \text{ mm}$      $D_{50} = 2.82 \text{ mm}$      $D_{16} = 1.51 \text{ mm}$      $S_b = 0.002$ 

t	Q	T	h	Sf	U <sub>p</sub>	U <sub>v</sub>	v <sub>wpv</sub>	v <sub>wc</sub>
hrs	l/s	C	cm	$\times 1000$	cm/s	cm/s	cm/s	cm/s
0.00	40.8	15.2	19.0	2.40	-	-	-	-
1.00	"	"	19.0	2.38	-	-	-	4.8
3.50	"	"	19.5	2.36	68	66	5.0	5.0
4.00	"	16.1	19.4	2.37	-	-	-	4.9
20.00	"	17.4	"	2.29	-	-	-	5.2
43.00	"	17.5	19.8	2.22	68	-	-	5.2
47.00	"	19.2	19.8	2.10	67	-	-	5.3
54.00	"	18.5	19.5	2.00	65	67	5.0	5.3
65.50	"	20.1	21.3	1.70	65	66	5.3	5.3
68.50	68.0	20.0	31.1	1.65	-	-	-	6.0
69.00	"	20.0	31.2	1.65	72	-	-	6.0
69.50	"	19.0	31.1	1.65	-	-	-	6.1
71.50	"	19.0	31.1	1.65	-	-	-	6.1

t	Rb	Qs	d84e	d50e	d16e	d84a	d50a	d16a
hrs	cm	kg/h	mm	mm	mm	mm	mm	mm
1.00	12.0	2.56	4.59	2.88	1.71	5.35	2.77	1.39
4.00	12.4	2.28	4.59	2.52	1.51	6.11	3.01	1.32
20.00	13.8	1.41	4.92	2.57	1.51	7.70	3.73	1.16
43.00	14.0	0.04	4.90	2.41	1.46	7.70	3.77	1.16
47.00	14.0	0.34	4.36	2.46	1.43	7.60	3.81	1.16
54.00	14.2	0.49	6.64	3.20	1.52	7.50	3.61	1.16
68.50	14.4	0.17	4.23	2.43	1.43	7.14	3.73	1.16
69.00	18.8	1.16	4.85	3.01	1.48	-	-	-
69.50	19.1	1.38	4.92	2.75	1.45	-	-	-
71.50	19.1	3.48	4.53	2.57	1.47	-	-	-

Table 4 - sediment 1

**RUN 3** $D_{34} = 4.80 \text{ mm}$  $D_{50} = 2.82 \text{ mm}$  $D_{16} = 1.51 \text{ mm}$  $S_b = 0.005$ 

t	Q	T	h	Sf	U <sub>p</sub>	U <sub>v</sub>	v <sub>pv</sub>	v <sub>wc</sub>
<u>h<sub>s</sub></u>	<u>l/s</u>	<u>C</u>	<u>cm</u>	<u>× 1000</u>	<u>cm/s</u>	<u>cm/s</u>	<u>cm/s</u>	<u>cm/s</u>
1.00	11.9	18.5	6.20	7.00	53	54	-	6.1
2.00	"	"	6.40	6.90	53	52	-	-
3.00	"	-	6.40	6.75	-	-	-	6.1
4.00	"	-	6.40	6.50	53	-	-	6.0
5.00	"	-	-	-	-	-	-	-
7.00	"	-	-	-	-	-	-	-
8.00	"	18.7	-	-	-	-	6.5	-
9.50	"	18.8	6.60	6.30	53	-	-	6.0
11.00	"	18.9	-	-	-	-	-	-
13.00	"	19.2	6.60	6.30	53	-	-	-
15.00	"	19.3	6.60	6.30	53	-	-	-
18.00	"	19.4	6.60	6.30	53	-	6.7	6.0
18.50	15.6	19.5	8.00	6.00	55	-	-	-
19.00	"	19.0	-	5.50	-	-	-	-
19.50	19.6	19.7	9.40	5.00	64	-	-	6.3
20.00	"	-	-	-	-	-	-	-
20.50	"	19.7	9.60	-	-	-	-	-

t	Rb	Qs	d84e	d50e	d16e	d84a	d50a	d16a
<u>h<sub>s</sub></u>	<u>cm</u>	<u>kg/h</u>	<u>mm</u>	<u>mm</u>	<u>mm</u>	<u>mm</u>	<u>mm</u>	<u>mm</u>
1.00	5.40	17.56	4.96	2.93	1.74	6.16	2.40	1.08
2.00	-	18.16	3.83	2.23	1.41	7.75	3.78	1.04
3.00	5.70	13.00	4.22	2.44	1.46	7.83	4.24	1.02
4.00	5.70	4.66	4.00	2.34	1.38	7.94	4.19	1.08
5.00	-	2.21	4.31	2.63	1.52	8.01	4.63	1.03
7.00	-	2.21	4.03	2.30	1.32	8.18	4.86	1.19
9.50	5.80	1.71	4.20	2.30	1.30	8.13	4.93	1.35
11.00	-	1.25	4.16	2.58	1.69	8.17	4.98	1.19
13.00	-	2.71	4.53	2.49	1.47	8.20	5.02	1.02
15.00	-	1.30	4.69	2.75	1.58	8.38	5.02	1.01
18.00	5.80	0.54	4.25	2.41	1.44	8.22	5.07	1.00
18.50	-	0.56	5.65	2.77	1.29	-	-	-
19.00	-	5.24	5.20	2.77	1.47	-	-	-
19.50	8.0	4.03	5.24	2.43	1.26	-	-	-
20.00	-	23.98	4.56	2.51	1.39	-	-	-
20.50	8.1	30.61	4.44	2.39	1.36	-	-	-

Table 5 - sediment 1

**RUN 4**
 $D_{84} = 4.80 \text{ mm}$      $D_{50} = 2.82 \text{ mm}$      $D_{16} = 1.51 \text{ mm}$      $S_b = 0.005$ 

t	Q	T	h	Sf	U <sub>p</sub>	U <sub>v</sub>	v <sub>pv</sub>	v <sub>wc</sub>
<u>h-s</u>	<u>l/s</u>	<u>°C</u>	<u>cm</u>	<u>x 1000</u>	<u>cm/s</u>	<u>cm/s</u>	<u>cm/s</u>	<u>cm/s</u>
1.00	11.9	17.6	6.00	5.30	56	57	5.8	5.2
2.00	-	17.8	6.50	5.30	56	57	-	5.4
3.00	-	-	-	-	-	-	-	-
7.00	-	18.0	6.50	5.00	57	-	-	5.3
10.00	-	18.2	6.50	-	-	-	-	-
22.50	-	18.1	6.50	-	-	-	-	-
23.50	-	17.9	6.50	5.00	-	-	-	-
24.00	19.7	18.4	8.80	4.80	-	-	-	5.8
24.50	-	18.5	-	4.60	-	-	-	-
26.00	-	-	9.50	4.50	66	65	6.7	5.8

t	Rb	Qs	d84e	d50e	d16e	d84a	d50a	d16a
<u>h-s</u>	<u>cm</u>	<u>kg/h</u>	<u>mm</u>	<u>mm</u>	<u>mm</u>	<u>mm</u>	<u>mm</u>	<u>mm</u>
1.00	5.20	12.44	4.96	2.91	1.63	5.67	2.65	1.35
2.00	5.70	-	-	-	-	-	-	-
3.00	-	4.13	4.22	2.53	1.54	6.87	2.99	1.17
7.00	5.70	1.33	3.94	2.43	1.48	7.00	3.48	1.12
10.00	-	0.60	3.92	2.31	1.40	7.20	3.63	1.11
22.50	-	0.31	4.35	2.53	1.47	7.63	3.76	1.10
23.50	-	0.28	3.81	2.26	1.44	7.65	3.78	1.10
24.00	7.20	15.88	5.24	2.67	1.37	-	-	-
24.50	-	13.24	4.95	2.69	1.49	-	-	-
26.00	7.70	6.74	4.72	2.58	1.46	-	-	-

Table 6 - sediment 1

**RUN 5** $D_{84}=7.73\text{mm}$  $D_{50}=3.68\text{mm}$  $D_{16}=1.00\text{mm}$  $S_b=0.01$ 

t	Q	T	h	Sf	U <sub>p</sub>	U <sub>v</sub>	v*
<u>h<sub>rs</sub></u>	<u>l/s</u>	<u>°C</u>	<u>cm</u>	<u>× 1000</u>	<u>cm/s</u>	<u>cm/s</u>	<u>cm/s</u>
1.00	6.4	17.4	4.0	10.30	44	45	6.3
3.00	"	"	-	-	-	-	-
7.00	"	17.5	4.0	9.80	43	43	6.2
10.00	"	"	"	"	-	-	-
22.00	"	-	-	-	-	-	-
24.00	"	17.5	4.0	9.20	44	45	6.0
24.50	11.3	"	5.2	8.20	68	69	6.3
25.00	"	"	"	"	-	-	-
26.00	"	"	-	-	-	-	-

t	Q <sub>s</sub>	d <sub>84e</sub>	d <sub>50e</sub>	d <sub>16e</sub>	d <sub>84a</sub>	d <sub>50a</sub>	d <sub>16a</sub>
<u>h<sub>rs</sub></u>	<u>kg/h</u>	<u>mm</u>	<u>mm</u>	<u>mm</u>	<u>mm</u>	<u>mm</u>	<u>mm</u>
1.00	10.82	4.86	2.93	1.71	5.94	2.61	1.33
3.00	4.77	4.35	2.60	1.57	7.04	2.91	1.11
7.00	1.57	4.16	2.48	1.45	7.19	3.42	1.05
10.00	0.65	4.08	2.31	1.41	7.32	3.55	1.05
22.00	0.50	4.22	2.34	1.39	7.84	3.84	1.07
24.00	0.39	4.08	2.38	1.43	7.86	3.86	1.07
24.50	22.26	5.31	2.96	1.61	-	-	-
25.00	21.72	4.72	2.54	1.41	-	-	-
26.00	12.17	4.82	2.54	1.40	-	-	-

Table 7-sediment 2

**RUN 6** $D_{84}=7.73 \text{ mm}$  $D_{50}=3.68 \text{ mm}$  $D_{16}=1.00 \text{ mm}$  $S_b=0.01$ 

t	Q	T	h	Sf	U <sub>p</sub>	U <sub>v</sub>	v*
<u>h<sub>rs</sub></u>	<u>l/s</u>	<u>°C</u>	<u>cm</u>	<u>× 1000</u>	<u>cm/s</u>	<u>cm/s</u>	<u>cm/s</u>
0.50	6.4	16.7	3.8	-	-	-	-
1.50	"	"	"	-	-	48	-
2.50	"	16.7	"	10.50	52	-	6.0
3.50	"	-	-	-	-	-	-
7.00	"	16.8	3.8	10.50	50	-	6.0
7.50	11.2	17.0	5.2	-	-	-	6.6
8.00	"	17.0	4.8	-	-	-	-
9.00	"	-	"	9.00	68	69	6.1
10.50	"	-	"	8.50	72	-	-
11.00	"	17.2	-	-	-	-	-
14.50	"	17.4	4.9	8.50	76	-	5.9
15.00	16.9	"	5.2	-	-	-	6.3
15.50	"	"	6.0	-	-	-	-
16.50	"	"	6.3	-	76	77	-
17.00	"	"	6.4	7.50	-	-	6.2
18.50	"	"	6.5	-	-	-	-
21.00	"	"	6.7	7.00	76	-	-
21.50	"	"	-	-	-	-	6.2

t	Q <sub>s</sub>	d <sub>84e</sub>	d <sub>50e</sub>	d <sub>16e</sub>	d <sub>84a</sub>	d <sub>50a</sub>	d <sub>16a</sub>
<u>h<sub>rs</sub></u>	<u>kg/h</u>	<u>mm</u>	<u>mm</u>	<u>mm</u>	<u>mm</u>	<u>mm</u>	<u>mm</u>
00.50	11.72	5.78	1.57	1.03	7.98	4.85	0.99
01.50	01.78	1.88	1.23	0.85	8.18	5.58	1.01
03.50	00.47	1.68	1.17	0.80	8.28	5.72	1.03
07.50	00.19	1.65	1.16	0.79	8.36	5.81	1.05
08.00	30.28	6.80	1.82	0.96	9.08	6.33	1.27
09.00	10.13	5.93	1.38	0.85	9.44	6.81	1.27
11.00	01.41	5.10	1.26	0.79	9.52	6.94	1.28
15.00	00.42	4.48	1.22	0.77	9.58	7.01	1.28
15.50	35.56	7.34	4.62	1.01	9.65	7.05	1.17
16.50	19.30	7.05	1.84	0.90	9.74	7.12	1.23
18.50	02.26	6.03	1.29	0.77	9.79	7.26	1.33
21.50	00.47	5.98	1.27	0.78	9.84	7.28	1.37



Table 8 - sediment 2

**RUN 7**
 $D_{84} = 7.73 \text{ mm}$      $D_{50} = 3.68 \text{ mm}$      $D_{16} = 1.00 \text{ mm}$      $S_b = 0.005$ 

t	Q	T	h	Sf	Up	Uv	v <sub>spv</sub>	v <sub>swc</sub>
<u>h<sub>rs</sub></u>	<u>l/s</u>	<u>°C</u>	<u>cm</u>	<u>× 1000</u>	<u>cm/s</u>	<u>cm/s</u>	<u>cm/s</u>	<u>cm/s</u>
1.50	12.6	17.5	6.50	6.70	56	54	6.5	-
2.00	"	-	6.50	6.70	54	-	-	6.2
3.50	"	17.6	-	-	-	-	-	-
7.50	23.7	17.8	10.10	6.70	57	-	-	6.0
8.00	"	17.9	10.20	-	55	63	8.2	-
9.00	"	18.0	10.40	4.50	-	-	-	-
10.00	"	"	-	-	-	-	-	-

t	Rb	Qs	d84e	d50e	d16e	d84a	d50a	d16a
<u>h<sub>rs</sub></u>	<u>cm</u>	<u>kg/h</u>	<u>mm</u>	<u>mm</u>	<u>mm</u>	<u>mm</u>	<u>mm</u>	<u>mm</u>
0.50	5.70	7.75	6.81	1.93	1.08	7.87	2.66	0.98
1.50	5.70	2.37	5.68	1.34	0.92	7.97	4.41	0.99
3.50	-	0.76	1.99	1.26	0.87	8.13	4.93	1.00
7.50	-	0.27	1.88	1.21	0.82	8.24	5.33	1.02
8.00	5.70	55.63	7.22	2.79	0.99	9.14	5.77	1.01
9.00	8.00	12.65	6.54	1.53	0.89	9.32	5.95	1.08
10.00	-	1.44	5.85	1.32	0.89	9.43	6.45	1.09

Table 9 - sediment 2

**RUN 8**
 $D_{84} = 7.73 \text{ mm}$      $D_{50} = 3.68 \text{ mm}$      $D_{16} = 1.00 \text{ mm}$      $S_b = 0.002$ 

t	Q	T	h	Sf	U <sub>p</sub>	U <sub>v</sub>	v <sub>apv</sub>	v <sub>wc</sub>
<u>h<sub>rs</sub></u>	<u>l/s</u>	<u>°C</u>	<u>cm</u>	<u>× 1000</u>	<u>cm/s</u>	<u>cm/s</u>	<u>cm/s</u>	<u>cm/s</u>
1.00	47.4	18.3	22.3	-	56	-	-	-
2.00	52.9	"	24.8	-	-	-	-	-
3.00	"	"	"	2.04	-	64	7.0	5.6
4.00	"	18.7	"	-	65	-	-	-
7.50	"	-	-	2.00	65	-	-	-
8.00	"	19.1	24.8	-	-	-	-	-
11.50	"	-	"	2.00	65	-	-	5.6
15.00	"	19.0	-	-	-	-	-	-
28.50	"	-	24.9	2.00	65	-	-	5.6
29.00	67.5	19.5	26.2	-	-	-	-	-
29.50	"	18.8	-	-	-	-	-	-
30.50	"	19.0	26.8	2.50	72	78	8.5	6.3
31.00	"	19.2	-	-	-	-	-	-

t	Rb	Qs	d84e	d50e	d16e	d84a	d50a	d16a
<u>h<sub>rs</sub></u>	<u>cm</u>	<u>kg/h</u>	<u>mm</u>	<u>mm</u>	<u>mm</u>	<u>mm</u>	<u>mm</u>	<u>mm</u>
1.00	15.5	1.34	4.89	1.44	1.03	7.39	3.69	1.00
2.00	"	0.97	4.10	1.34	0.98	7.79	4.24	1.00
3.00	"	-	-	-	-	-	-	-
4.00	-	0.47	2.34	1.30	0.94	7.87	4.55	1.00
7.50	15.5	-	-	-	-	-	-	-
8.00	-	0.23	1.91	1.25	0.88	7.79	4.88	1.01
15.00	-	0.11	6.43	1.50	0.95	7.85	5.00	1.01
29.00	16.0	0.06	6.63	1.38	0.91	7.91	5.15	1.02
29.50	16.3	16.40	6.44	1.50	0.87	8.56	5.89	1.08
30.50	16.3	15.93	6.78	1.69	0.90	9.02	6.34	1.13
31.00	-	5.36	7.01	1.73	0.93	9.12	6.38	1.14

Table 10 - sediment 3

**RUN 9**
 $D_{84} = 6.54 \text{ mm}$      $D_{50} = 2.36 \text{ mm}$      $D_{16} = 1.10 \text{ mm}$      $S_b = 0.002$ 

t	Q	T	h	Sf	U <sub>p</sub>	U <sub>v</sub>	v <sub>spv</sub>	v <sub>wc</sub>
hrs	l/s	°C	cm	× 1000	cm/s	cm/s	cm/s	cm/s
1.00	47.3	17.9	20.5	-	65	67	-	-
3.00	"	18.3	"	2.10	64	-	7.1	5.2
16.00	"	18.5	20.7	2.30	64	-	-	-
18.00	"	19.2	"	-	-	-	-	-
25.00	"	19.4	-	-	-	-	-	-
27.00	"	19.7	20.8	-	-	-	6.9	-
40.50	"	-	"	2.40	65	-	-	5.4
41.00	67.3	20.1	26.5	-	-	79	7.7	5.8
42.00	"	-	26.9	3.00	-	-	-	-
43.00	"	-	27.7	-	67	-	-	-

t	Rb	Qs	d84e	d50e	d16e	d84a	d50a	d16a
hrs	cm	kg/h	mm	mm	mm	mm	mm	mm
0.50	-	2.63	5.67	2.76	1.36	6.85	2.38	1.11
1.50	-	1.30	4.66	2.43	1.43	7.07	2.37	1.10
3.00	13.1	-	-	-	-	-	-	-
3.50	-	2.01	5.39	2.32	1.27	7.67	2.39	1.07
16.00	13.1	0.62	5.36	2.07	1.73	8.49	2.78	0.94
18.00	-	0.21	4.38	2.05	1.29	8.54	2.83	0.93
25.00	-	0.24	3.71	1.78	1.23	8.73	3.48	0.92
27.00	-	0.18	3.82	1.74	1.07	8.77	3.56	0.92
40.50	13.2	-	-	-	-	-	-	-
41.00	-	0.10	4.42	1.84	1.08	8.88	3.94	0.93
41.50	16.7	37.25	6.58	2.52	1.08	9.42	2.45	1.06
42.50	-	29.09	6.10	2.48	1.20	9.51	2.70	0.97

Table 11 - sediment ?

**RUN 10**
 $D_{84} = 6.54 \text{ mm}$      $D_{50} = 2.36 \text{ mm}$      $D_{16} = 1.10 \text{ mm}$      $S_b = 0.005$ 

t	Q	T	h	Sf	Up	Uv	v <sub>pv</sub>	v <sub>wc</sub>
<u>hrs</u>	<u>l/s</u>	<u>C</u>	<u>cm</u>	<u>x 1000</u>	<u>cm/s</u>	<u>cm/s</u>	<u>cm/s</u>	<u>cm/s</u>
1.50	12.2	19.2	6.10	-	-	-	-	-
2.00	"	19.4	"	5.30	58	62	6.8	5.2
5.50	"	-	"	5.50	57	-	"	-
7.50	"	19.6	"	-	-	-	-	-
9.50	"	19.7	"	-	-	-	-	-
22.50	"	-	6.20	5.10	59	-	-	-
23.50	21.1	20.0	8.90	5.10	-	64	8.8	-
24.00	"	-	"	-	-	-	-	-
24.50	"	18.5	-	4.60	-	-	-	-

t	Rb	Qs	d84e	d50e	d16e	d84a	d50a	d16a
<u>hrs</u>	<u>cm</u>	<u>kg/h</u>	<u>mm</u>	<u>mm</u>	<u>mm</u>	<u>mm</u>	<u>mm</u>	<u>mm</u>
0.50	-	12.06	5.52	2.34	1.27	7.33	2.31	1.05
1.50	-	2.82	4.78	1.86	1.08	7.59	2.51	1.06
2.00	5.1	-	-	-	-	-	-	-
3.50	-	0.96	1.96	1.98	1.14	7.74	2.61	1.05
5.50	5.1	-	-	-	-	-	-	-
7.50	-	0.46	5.00	1.89	1.14	7.85	2.75	1.04
9.50	-	0.20	3.73	1.75	1.08	7.88	2.80	1.05
22.50	5.1	0.12	4.48	1.87	1.10	7.99	3.06	1.05
23.50	-	0.12	3.78	1.81	1.12	8.00	3.08	1.05
24.00	-	25.57	6.73	3.05	1.26	8.49	2.25	0.97
24.50	7.0	-	-	-	-	-	-	-
25.00	-	13.40	6.61	2.90	1.22	8.97	2.26	0.94

Table 12- sediment 3

**RUN 11**

$D_{84} = 6.54 \text{ mm}$      $D_{50} = 2.36 \text{ mm}$      $D_{16} = 1.10 \text{ mm}$      $S_b = 0.01$

t	Q	T	h	Sf	U <sub>p</sub>	U <sub>v</sub>	v*
<u>h<sub>zs</sub></u>	<u>l/s</u>	<u>°C</u>	<u>cm</u>	<u>× 1000</u>	<u>cm/s</u>	<u>cm/s</u>	<u>cm/s</u>
0.50	6.5	18.7	3.5	-	-	-	-
1.00	"	-	"	-	-	58	-
1.50	"	-	"	10.00	56	-	5.9
3.50	"	19.2	-	-	-	-	-
7.50	"	19.4	-	-	-	-	-
9.50	"	-	3.4	10.50	57	-	5.9
10.50	"	19.4	-	-	-	-	-
22.50	"	19.5	"	-	58	-	-
23.50	13.0	"	4.9	10.00	-	-	6.9
24.50	"	-	6.7	8.50	76	-	7.4

t	Qs	d84e	d50e	d16e	d84a	d50a	d16a
<u>h<sub>zs</sub></u>	<u>kg/h</u>	<u>mm</u>	<u>mm</u>	<u>mm</u>	<u>mm</u>	<u>mm</u>	<u>mm</u>
00.50	20.93	5.72	2.46	1.26	7.31	2.65	1.05
01.50	5.90	4.93	1.99	1.15	7.82	3.22	1.03
03.50	1.15	4.19	1.73	1.04	7.99	3.64	1.05
07.50	0.41	4.08	1.82	1.12	8.17	3.93	1.05
10.50	0.25	3.73	1.68	1.03	8.25	4.07	1.05
22.50	0.10	3.84	1.74	1.07	8.37	4.28	1.06
23.50	0.07	3.06	1.63	1.00	8.38	4.30	1.06
24.00	66.00	7.23	4.14	1.45	8.54	1.67	0.92
25.00	22.38	6.23	2.34	1.12	8.95	1.68	0.93

## 3 FRAMEWORK OF ANALYSIS

Let us assume the simple Bayazit scheme to describe the exchange of grains between the surface and the subsurface layer of bed sediment; if the approaching flow is sediment depleted, grains will be picked up from the mixing layer and replaced in the same quantity by the parent bed material entering the moving control volume from the layer below the mixing layer (Fig. 2).

We denote with:  $m_i$ , the fraction of grains in class interval  $i$  for the mixing layer;  $p_i$ , the fraction of grains in class interval  $i$  in the parent bed;  $t_i$ , the fraction of grains in class interval  $i$  for the transported material;  $M$  and  $P$ , the mass of sediment per unit area, in the mixing layer and in the parent bed, respectively; assuming constant the apparent density on bed material,  $P$  and  $M$  may also be interpreted as the elevation of the top of the parent bed and as the thickness of the mixing layer, respectively;  $T$ , the mass sediment transport rate per unit width. The equation for the conservation of mass applied to the moving control volume for each size fraction yields:

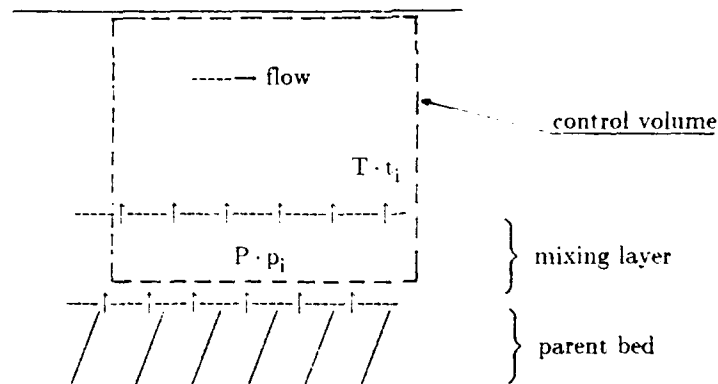


Fig. 2 - Definition sketch of the of the mixing layer.

$$1) \quad \frac{\partial(M m_i)}{\partial t} + p_i(P) \frac{\partial(P)}{\partial t} + \frac{\partial(T t_i)}{\partial x} = 0$$

(the mass of the sediment in motion is neglected).

Summing over all the size classes and considering that:

$$\sum_i m_i = \sum_i p_i = \sum_i t_i = 1$$

we obtain:

$$2) \quad \frac{\partial(M + P)}{\partial t} + \frac{\partial T}{\partial x} = 0$$

Denoting with E the eroded mass rate:

$$3) \quad E = - \frac{\partial(M + P)}{\partial t} = \frac{\partial T}{\partial x}$$

Under the assumptions that during the armouring process the thickness of mixing layer is constant with time, and the composition of eroded material is approximately constant along the channel length, that is:

$$\frac{\partial M}{M \partial t} \ll \frac{\partial m_i}{m_i \partial t} \quad \frac{\partial T}{T \partial x} \ll \frac{\partial t_i}{t_i \partial x}$$

the equation of mass conservation gives:

$$4) \quad M \frac{\partial m_i}{\partial t} + p_i \frac{\partial P}{\partial t} + t_i \frac{\partial T}{\partial x} = 0$$

In the same order of approximation, eq. 4 can be written as:

$$5) \quad M \frac{\partial m_i}{\partial t} + E (t_i - p_i) = 0$$

## 4 ANALYSIS OF EXPERIMENTAL DATA

### 4.1 TEMPORAL VARIATION OF BED SURFACE GRAIN SIZES

Changes in grain size distribution occurring at the bed surface during the armouring process can be evaluated through the continuity equation for each size fraction, eq. 5, applied to an appropriate control volume. In particular, by integrating eq. 5 over the finite interval  $\Delta t$ , we obtain:

$$7) \quad M \Delta m_i = \Delta E (p_i - t_i)$$

where  $\Delta m_i$  is the variation of the fraction  $i$  in the mixing layer during the time interval  $\Delta t$ , and  $\Delta E$  is the mass of sediment which is removed from the bed during the same interval  $\Delta t$ .

The value of the thickness of the mixing layer has been found by comparing the results obtained by eq. 7 with those obtained by the analysis of photographs. The value which provides the best



fitting with experimental data has been found to be equal to the  $D_{50}$  of the armoured layer during its formation, while for the calculation of the bed surface grain size evolution during the destruction process the best results were obtained with the thickness of the mixing layer equal to  $2 \cdot D_{50}$ .

In figures 3 and 4 are plotted the sediment diameters of bed surface obtained from photographs against the corresponding values calculated through eq. 7, for armoured conditions and after destruction of the armoured layer, respectively.

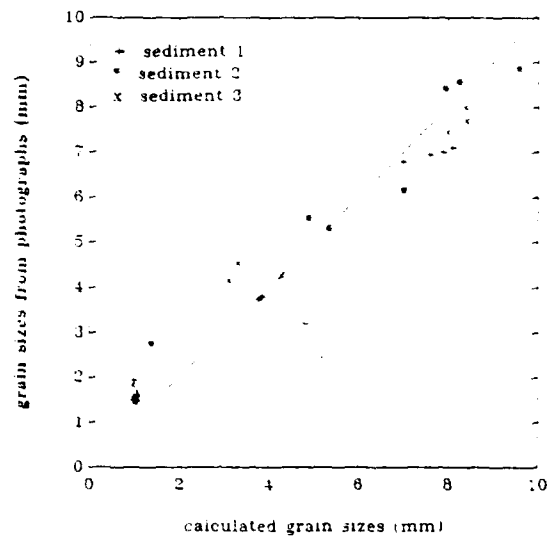


Fig. 3 - Calculated and observed sediment sizes of the surface layer for armour conditions.

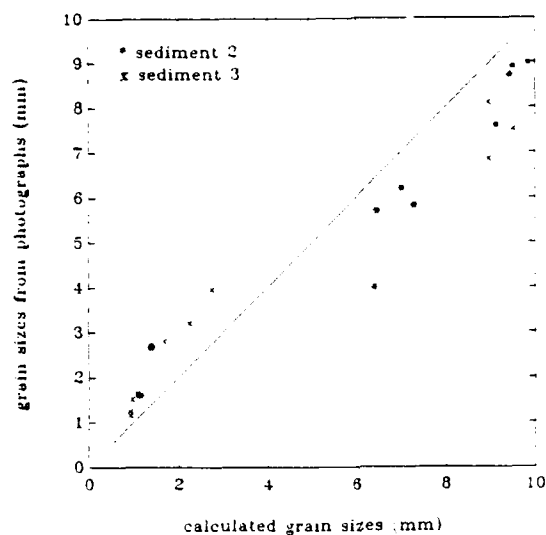


Fig. 4 - Calculated and observed surface sediment sizes after destruction of the armour layer.

#### 4.2 FORMATION OF THE ARMOUR LAYER

Let  $v_i$  be any variable associated to the size class  $i$  (e.g., the central diameter of size fraction  $i$ ,  $D_i$ , or the square  $D_i^2$ ), and  $v_m$  the mean value of  $v_i$  according to the frequency distribution curve  $m_i$  (i.e.,  $\sum_i v_i m_i$ ); hence,  $v_m$  represents the mean value of a generic variables for the mixing layer:

Similarly, extending the same definition to the parent bed and the eroded material, we obtain the mean values  $v_p$  and  $v_t$  respectively.

Multiplying equation 5 by  $v_i$  and summing over all classes, we obtain:

$$6) \quad M \frac{\partial v_m}{\partial t} + E (v_t - v_p) = 0$$

The choice of characterization of the distribution and of the associated form of the mass balance, eqs. 5 or 6, depends on the shape of the size distribution: equation 5 is more appropriate when the bed material is obtained by mixing few classes of monogranular sediments, while equation 6 appears more convenient when, for instance, the size distribution is lognormal.

Analysis of eq. 5 and 6 leads to the conclusions that, in a erosive process of armour layer formation, as in the present case (  $E > 0$  ), the progressive coarsening of the mixing layer (i.e.,  $\frac{\partial D_m}{\partial t} > 0$  ) is associated to the condition:

$$D_t < D_p$$

and viceversa for the destruction process.

In the initial stage of armour process (i.e., when  $D_m = D_p$  ), the development of armouring is automatically controlled by the selectivity of transport: consequently,  $D_t < D_m$ ; as the armour condition develops,  $D_m$  becomes coarser than  $D_p$  until new equilibrium conditions are reached.

The following equilibrium conditions can be identified:

- STATIC ARMOUR, if  $T = E = 0$ ;
- DYNAMIC ARMOUR, if  $t_i = p_i$  and  $E > 0$  ( pavement according to Parker);
- SEMI-STATIC ARMOUR, if  $E = 0$  and  $T > 0$ , that is, the coarser fractions are not mobile and the finer fractions, coming from the upstream reaches, are in motion: in other words, static armour for the coarser fractions coexisting with a dynamic armour of the finer fractions.

The case  $E = 0$  with all classes in motion (  $T \neq 0$ ;  $t_i = p_i$  ) eliminates any dynamical connection between the surface processes ( sediment transport and mixing layer dynamics) and the subsurface layer. It can be considered a particular condition of a dynamic armour (pavement) without any interaction with the sub-layer.

Following these considerations, the analysis of the formation of the armour layer has been made on the basis of the experimental data. Eq. 6 allows the analysis by assuming just one representative parameter,  $\alpha$ , of the grain size distribution: for sediment 1, which is

approximately lognormally distributed, the mean diameter has been assumed as significative parameter: for sediment 2 (bimodal frequency distribution), the percentage of finer material (less than 2.8 mm) was considered while for sediment 3, showing a quite flat frequency distribution, the mean diameter plus the percentage of fine has been assumed.

In figures 5, 7, and 9 the temporal evolution of the representative parameters is shown for sediment 1, 2 and 3 respectively.

Figures 6, 8 and 10 show the behaviour of sediment transport rate, referred to the maximum value,  $q_{smax}$ , obtained in each run, as function of time referred to the armouring time,  $t_d$ . run 3 has not been represented because it was partially fed with sediment material from upstream during the experiment.

Sediment 1: from figures 5, 6 it can be seen that the condition for a static armour, i.e.,  $E \rightarrow 0$ ,  $T \rightarrow 0$ , and  $v_t < v_p$  is practically satisfied for all runs. It is worth to note that, at the very initial stage of armour formation, where  $E > 0$ , figure 3 shows that  $v_t > v_p$ ; according to eq. 6 this should imply  $\frac{\partial v_m}{\partial t} < 0$ ; results obtained from eq. 7 for run 1, where this phenomenon is more pronounced, seem to confirm the initial trend of the surface layer to become finer and this is probably due to the "artificial disposition" of bed material surface when it is initially placed in the flume at the beginning of each run.

Sediment 2: with reference to figures 7, 8, a trend toward a regime of static armour can be observed in runs 6, 7, and 8; particularly, run 6 was prolonged after the first armour destruction occurred 8 hours later the beginning of run; the process of armour formation was activated again generating a new static equilibrium; after 8 hours, a second destruction was imposed to the bed; again, the armour layer start to develop, until the end of the run.

Sediment 3: for this type of material, the pattern shown in figure 9, 10 is similar to the one obtained for sediment 1. In this case, the initial artificial sorting of the bed surface was less marked than sediment 1, while the temporal evolution appeared practically similar.

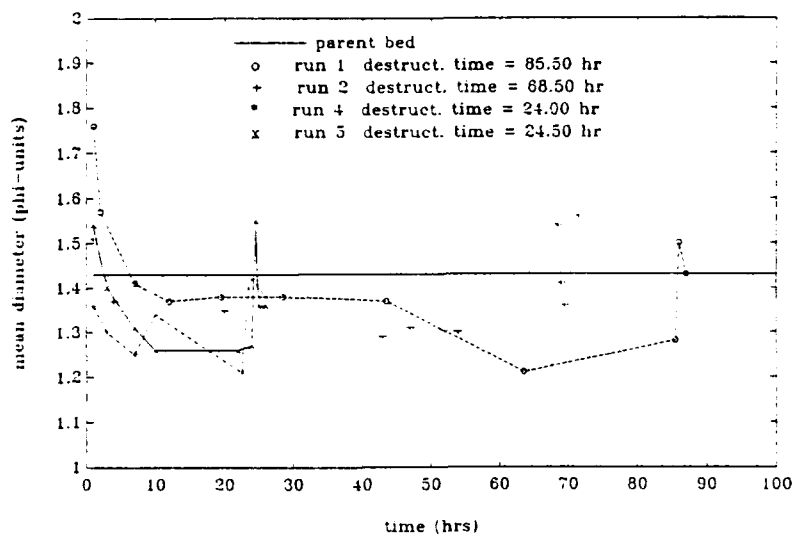


Fig 5 - Temporal evolution of the mean diameter for runs 1, 2, 4, 5.

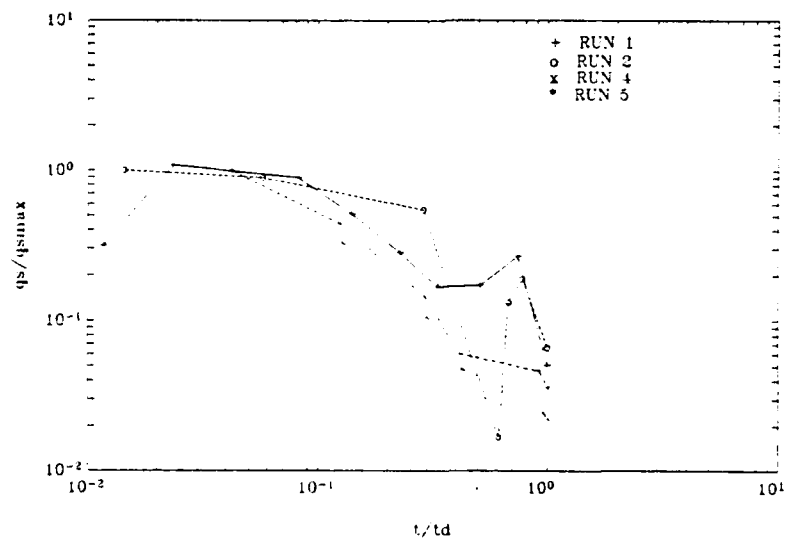


Fig. 6 - Sediment transport rate as a function of time for runs 1, 2, 4, 5 (sediment 1).

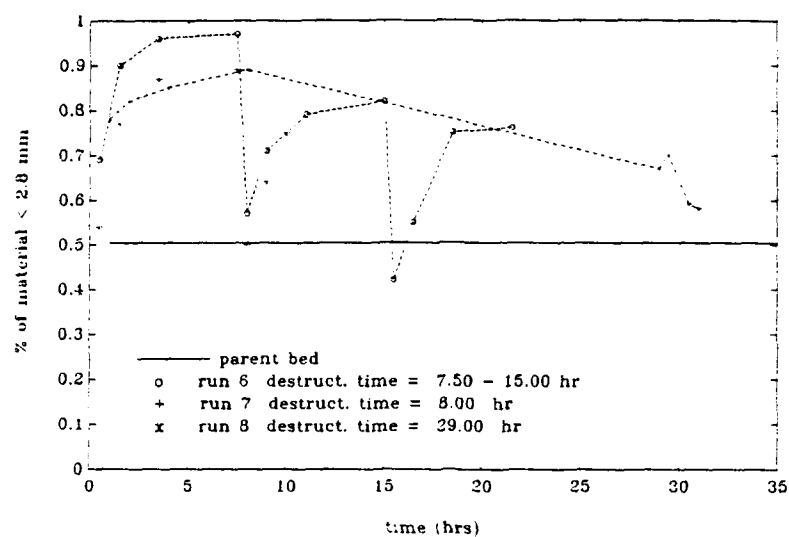


Fig. 7 - Percentage of fine material as a function of time for sediment 2.

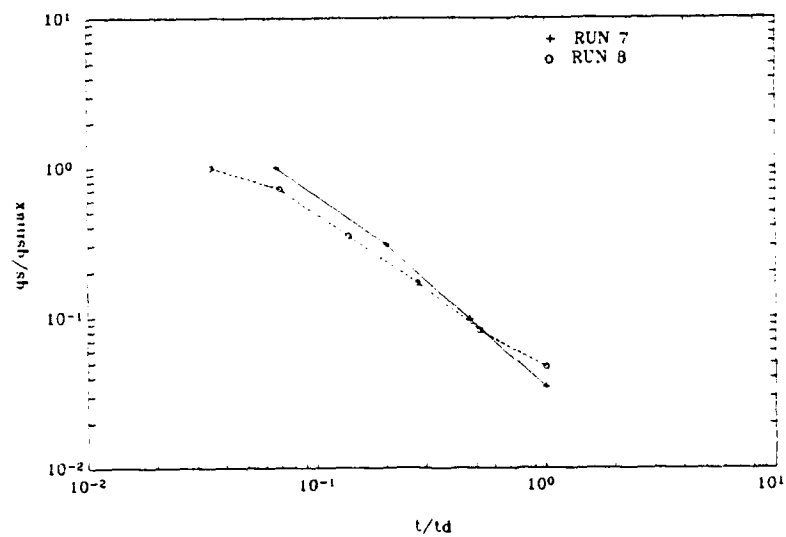


Fig. 8 - Sediment transport rate as a function of time for runs 7, 8 (sediment 2).

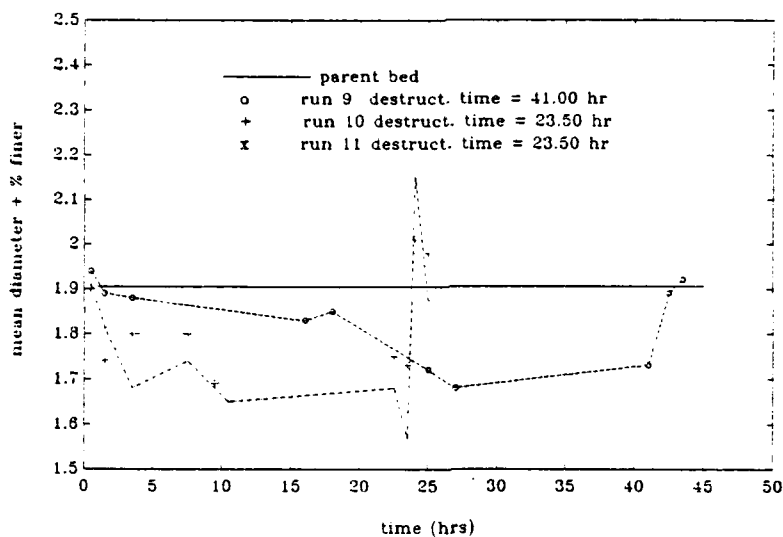


Fig. 9 - Temporal evolution of the representative parameter for sediment 3.

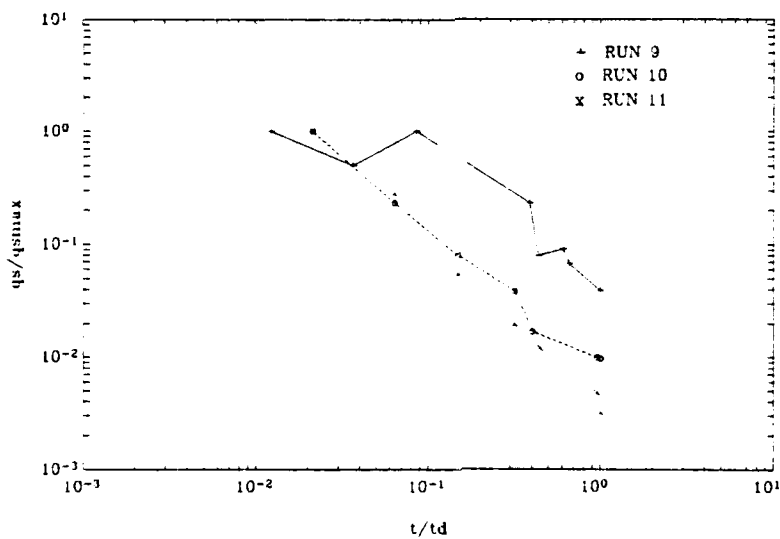


Fig. 10 - Sediment transport rate as a function of time for runs 9, 10, 11 (sediment 3).

## 5 CONCLUSIONS

Experimental results obtained by a laboratory investigation on armour processes have been presented . The following conclusions can be drawn:

- analysis of the continuity equation applied to the mixing layer shows that the coarsening of the surface layer may be consequent either to a progressive reduction of the sediment transport rate reaching practically zero ( static armour) or to a progressive equalization of the size fractions transported with fractions present in the parent bed material ( dynamic armour); intermediate levels of the armour process may occur when some coarse fractions are immobile and the finer are in motion (semi-static armour). According to these definitions, the present experimental investigation has been carried out to analyze static armour conditions.
- the experimental results seem to confirm that the equilibrium condition of the armour layer is essentially controlled by the mechanism of sediment sorting which practically vanishes as the sediment transport tends to zero. However, an increase of the bed shear stress may reactivate the sediment transport and its selectivity and the process of the armour layer formation starts again to generate a new equilibrium condition. On the other hand, if the increase of bed shear stress is able to reduce considerably the selectivity of the transport, all the fractions would be in motion, leading to the general destruction of the armour layer.
- in the case of a dynamic armour, an increase of bed shear stress inevitably induces a reduction of the grain size distribution difference between parent bed material and surface layer leading at least to a partial destruction of the armour coat, as a consequence of the more marked reduction of the flow selective capacity with increasing shear stress. The selective capacity is here assumed to be the ratio of the transport capacity of the finer fraction to the coarser ones.
- the experimental data have confirmed the validity of assuming a constant thickness of mixing layer during the armouring process equal to the  $D_{50}$  of the armour layer in representing the temporal evolution of bed surface grain sizes.



- photograph technique has been proved to be a reliable method to sample bed surface composition without altering bed structure during the experimental run.

#### BIBLIOGRAPHY

**Adams J.**, "Gravel size analysis from photographs", ASCE J. Hydraulics Div., 105 HY10, oct 1979.

**Andrews E.D., Parker G.**, " Formation of a coarse surface layer as the response to gravel mobility". Sediment Transport in Gravel-bed Rivers. C.R. Thorne, J.C. Bathurst and R.D.Hey. John Wiley & Sons Ltd., 1987.

**Armanini A., Di Silvio G.**, "A one-dimensional model for the transport of a sediment mixture in non-equilibrium conditions", J. Hydraulic Res., vol.26 no.3, 1988.

**Ashida K., Michiue M.**, "Studies on bedload transport rate in open channel flows", Proc. Int. Symposium on River Mechanics, Bangkok, Vol. 1, pp.407-418, 1973.

**Ashida K., Michiue M.**, "An investigation of river bed degradation downstream of a dam", Proc. 11th IAHR Congress, vol.3, pp.247-256, 1971

**Bayazit M.**, "Simulation of armor coat formation and destruction", Proc. 16th IAHR Congress , Sao Paulo, Brazil, paper B10, pp.73-80, 1975.

**Borah D.K., Alonso C.V., Prasad S.N.**, " Routing graded sediments in streams: formulations" , " Routing graded sediments in streams: applications", ASCE J. Hydraulics Div., 108 HY12, pp. 1486-1517, dec 1982.

**Day T.J.**, "A study of the transport of graded sediments", HRS Wallingford, rep. IT 190, apr

1980.

**Egiazaroff P.I.**, "Calculation of non-uniform sediment concentrations", ASCE J. Hydraulic Div., 91 HY4, jul 1965.

**Einstein H.A., Chien N.**, "Transport of sediment mixture with large range of grain sizes". MRD Sediment Series No. 2, U.S. Army Eng. Div., Missouri River, Corps of Engineers, Omaha, Neb., 1953.

**Ettema R.**, "Sampling armor-layer sediments", ASCE J. Hydraulics Div., 110 HY7, pp. 992-996, jul 1984.

**Falcon M.**, "Interaction between bedload and armoring", Proc. 3rd Int. Symposium on River Sedimentation, Jackson, Mississippi, U.S.A., 1986.

**Garde R.J., Hasan S.M.**, "an experimental investigation on degradation in channels", Proc. 12th Congress of International Association of Hydraulic Research, 3, 1967.

**Gessler J.**, "The beginning of bedload movement of mixtures investigated as natural armoring in channels", rep.no. 69 Lab. Hydraulic Research and Soil Mechanics, Swiss Fed. Inst. of Technology, Zurich, 1965.

**Gessler J.**, "Self-stabilizing tendencies of alluvial channels", ASCE J. Waterways Harbors Div., 96 WW2, pp.235-249, may 1970.

**Harrison A.S.**, "Report on special investigation of bed bed sediment segregation in a degrading bed", U.S Army Corps of Engineers, Missouri River Div., Sediment Series No. 30.

**Iirano M.**, "On phenomena of river bed lowering and armouring below reservoirs" 14th Proc. of

A.Lamberti E.Paris

Hydr. Lect. Meeting, Hatsumei, Kaikan, 1970

**Hirano M.**, "River bed degradation with armouring" Trans. of JSCE vol.3 part 2, 1971.

**Hirano M.**, "Studies on variation and equilibrium state of a river bed composed of non-uniform material" Trans. of JSCE vol.4, 1972.

**Holly F.M., Karim M.F.**, "Simulation of Missouri river bed degradation", ASCE J. Hydraulic Eng., 112 HY6, pp.497-517, jun 1986

**Karim M.F., Holly F.M.**, "Armoring and sorting simulation in alluvial rivers", ASCE J. Hydraulic Div., 112 HY8, pp.705-715, aug 1986.

**Knoroz V.S.**, "Natural armouring and its effect on deformation of channel beds formed by materials non-uniform in size", Proc. 14th Cong. Int. Assoc. Hydr. Res., 3, 1971.

**Lamberti A, Paris E.**, "Experimental analysis of armouring process", Proc. of Int. Workshop on Fluvial Hydraulics of Mountain Regions, University of Trento, Italy, 1989.

**Lane E. W., Carlson E. J.**, "Some factors affecting the stability of canals constructed in coarse granular material", Proc. Int. Assoc. Hydraul. Res., Int. Hyd. Conv., Minneapolis, 1, 1953.

**Lee H.Y., Odgaard J.A.**, "Simulation of bed armoring in alluvial channels", ASCE J. Hydraulic Div., 112 HY9, pp.794-801, sep 1986.

**Little W.C., Mayer P.G.**, "The role of sediment gradation on channel armouring", publ. no. ERC-0672, Georgia Institute of Technology, Atlanta, 1972.

**Little W.C. , Mayer P.G.**, "Stability of channel beds by armouring", ASCE J. Hydraulics Div.,

102 HY11, pp.1647-61, nov 1976.

**Mosconi C.E.**, "River bed variations and evolution of armor layers". Thesis submitted in partial fulfillment of the requirements for the Degree of Doctor of Philosophy, Graduate College, University of Iowa, may 1988.

**Misri R.L., Garde R.J., Ranga Raju K.G.**, "Bedload transport of coarse non-uniform sediments". ASCE J. Hydraulics Div., 110 HY3, pp.312-28, mar 1984.

**Odgaard A.J.**, "Grain-size distribution of river-bed armor layers". ASCE J. Hydraulics Div., 110 HY10, pp.1479-84, oct 1984.

**Palaniappan A.B., Godbole P.N.**, "Modeling of armouring process in alluvial streams". Proc. 3rd International Workshop on Alluvial River Problems, TIWARP-89, pp.63-72, Roorkee, India, 1989.

**Parker G., Klingeman P.C., McLean D.G.**, "Bedload and size distribution in paved gravel-bed streams". ASCE J. Hydraulics Div., 108 HY1, pp.544-571, apr 1982.

**Proffitt G.T.**, "Selective transport and armouring of non uniform alluvial sediments". Dept. Civil Eng. Univ. of Canterbury N.Z., Res. Rept. 80/22, pp.1-203, 1980.

**Proffitt G.T., Sutherland A.J.**, "Transport of non-uniform sediment", IAHR J. Hydraulic Res., 21-1, pp.33-43, 1983.

**Raudkivi A.J., Ettema R.**, "Stability of armour layers in rivers". ASCE J. Hydraulics Div., 108 HY9, pp.1047-57, sep 1982.

**Ribberink J.S.**, "Mathematical modelling of one-dimensional morphological changes in rivers with

A.Lamberti E.Paris

non-uniform sediments". Rep. no. 87-2. Delft Univ. of Technology, 1987.

**Saad M.B.**, "Armouring of alluvial channel beds". Proc. IARR Int. Conf. Fluvial Hydraulics, pp.52-57, Budapest, 1988.

**Samaga B.R., Ranga Raju K.G., Garde R.J.**, "Bedload transport of sediment mixtures", ASCE J. Hydraulics Div., 112 HY11, pp.1003-18, nov 1986.

**Shen W.H., Lu J.Y.**, "Development and prediction of bed armorings", ASCE J. Hydraulic Div., 109 HY4, apr 1983.

**Sutherland A.J.**, "Static armour layers by selective erosion", Sediment Transport in Gravel-bed Rivers, C.R. Thorne, J.C. Bathurst and R.D.Hey, John Wiley & Sons Ltd., 1987.

**Willetts B.B., Maizels J.K., Florence J.**, "The simulation of stream bed armouring and its consequences", Proc. Instn Civ. Engrs, Part 1, 82, pp.799-814, aug 1987.

## SPATIAL VARIATION IN ARMOURING IN A CHANNEL WITH HIGH SEDIMENT SUPPLY

Thomas E. Lisle: Pacific Southwest Research Station, Forest Service,  
U.S. Department of Agriculture, Arcata, California, USA

Mary Ann Madej: Redwood National Park, Arcata, California, USA

**ABSTRACT:** Recent advances in the understanding of the origin and function of armouring of gravel-bed rivers have not addressed the role of nonuniformity and unsteadiness of flow. These leave a strong imprint on both surface and subsurface bed material sizes observed at low flow, from which we draw interpretations of bedload transport at high flow.

Mean bed armouring, measured as the difference in grain size of surface and subsurface bed material, is low in a channel in which recent and ongoing bed aggradation indicates that sediment supply has exceeded transport capacity. Alternate bar topography induces strong variations in boundary shear stress especially at low flow. Resulting winnowing of fine sediment from zones of high stress and deposition in zones of low stress produce wide variations in armouring. Bed areas with coarse surfaces are strongly armoured; fine areas are unarmoured and commonly consist of a thin layer of fine sediment overlying coarser material.

Spatial variation in armouring and boundary shear stress can lead to apparent size-selectivity in bedload transport in subsequent rising stages. The relatively fine bedload transported during early rising stages can originate from unarmoured deposits of fines, where all particle sizes present on the bed surface may be nearly equally mobile. These surfaces are devoid of larger particles, however, that appear in bedload only when coarser armoured surfaces become more widely entrained.

### INTRODUCTION

In recent years there have been considerable progress and some controversy over the origin and function of armouring of gravel riverbeds. Parker and Klingeman (1982) and Andrews (1983) stimulated new attention on the problem by advancing the hypothesis of approximate equal mobility of bed particles represented on the surface of a heterogeneous gravel bed. Accordingly, a coarse surface layer is a necessary condition of equilibrium transport of heterogeneous sediment under moderate excess boundary shear stress. Large particles, which inherently resist entrainment as uniform bed material more than small particles, are overrepresented on the bed surface, so that the mobility of all grain sizes tends to be equal. Debate continues on whether or not the degree of size selection observed in sediments entrained from mixed-size bed material justifies an approximation of equal mobility (Komar and Li, 1988). Nevertheless, experiments (Kuhnle and Southard, 1988), field data (Milhous, 1973; Andrews and Erman, 1986) and theory (Wiberg and Smith, 1987) indicate that the mobility of particles of different size on a coarse surface layer are much closer in mobility than they would be if each size composed a uniform bed, and that the equal mobility approximation is reasonably accurate in many cases.

The bed surface layer ceases to be coarser than the subsurface when the transport of all sizes present is intensive. Parker and Klingeman (1982) predicted that surface coarsening would disappear at boundary shear stresses

greatly exceeding the entrainment threshold of the median particle size, or specifically, at a value of  $\tau^* = \tau / g(\rho_s - \rho) D_{50} = 0.26$ . Wilcock and Southard (1989) found it to occur at  $\tau^* = 0.07$  in a flume experiment employing a recirculating sediment system (transport rate dependent on flow).

Dietrich et al (1989) demonstrate that intensive bedload transport can also diminish surface coarsening under moderate stresses when a high sediment load is imposed. In their experiment, mixed-size sediment was fed at a high rate into a flume containing the same size mixture as the feed. At a value of  $\tau^*$  of only 0.087, which is well exceeded at bankfull stage in many gravel-bed rivers, bed armouring disappeared. But as the feed rate was reduced in two steps to one-tenth the original while boundary shear stress was held approximately constant, the surface coarsened until nearly the entire bed was armoured. At equilibrium, the size mixture of bedload necessarily equalled that of the feed at all feed rates. Dietrich et al (1989) quantify the adjustment of surface coarseness to load as  $q^*$ , the ratio of bedload transport computed from a predictive equation using bed surface particle size to that computed using bedload or subsurface particle size. Qualitative correlations of  $q^*$  with sediment load in six stream channels in California (Kinerson and Dietrich, 1989) support this hypothesis.

The interpretation of the role of the coarse surface layer in sediment transport of Dietrich et al (1989) is somewhat different than that of Parker and his associates. The coarseness of the surface of a streambed offers resistance to the entrainment of bed material. If transport capacity exceeds the sediment load supplied from upstream, the bed surface coarsens, thereby increasing resistance to sediment transport. This interpretation is not in conflict with the equal mobility approximation.

The interpretation of armouring processes observed in flumes to that occurring in rivers is limited by necessarily choosing between sediment systems that impose either complete independence or dependence of transport rates. If transport rate is considered a dependent variable (mimicking sediment recirculation), then degree of surface coarsening in nature becomes a function of boundary shear stress and so varies little between gravel-bed rivers; if transport rate is an independent variable (mimicking sediment feed), coarsening is independent of stresses exceeding the entrainment threshold of the bed.

Bedload transport in natural channels can be either more nearly independent or dependent on hydraulic forces, depending on scales of time and space considered (Wilcock and Southard, 1989). Over a period of decades or centuries, a river conveys the sediment load imposed by its basin and adjusts accordingly. Most bedload is typically stored in the bed itself, however, which thus constitutes the supply, and so sediment transport through a reach of river over a period of hours or days depends more closely on hydraulic forces than on supply. That sediment supply still affects armouring at this scale is suggested by Kinerson and Dietrich's correlation of armouring with supply in rivers. At still shorter spatial scales, sediment supply to a local area of bed may be augmented or depleted by changes in sediment transport direction or by bed scour or fill occurring upstream under different hydraulic or sedimentological conditions, and therefore appear independent of local conditions.

Before controversies over the applications of various models for the causes and functions of bed surface armouring can be resolved, the effects of nonuniform and varied flow, which are definitive aspects of natural channels, must be determined. We usually observe the texture of channel beds when much of the surface is out of water or at least visible, and do not understand very well how waning flows have modified the bed since significant transport took place. As the flow varies over a channel with nonuniform topography, such as that typically produced by bars, changes occur locally in sediment transport direction and the magnitude of boundary shear stress relative to that over other areas of the channel. Some parts of the channel continue to supply sediment to transport while others become sites of deposition. All of these changes must bear on the process of armouring and add complexity to bed surface texture. The degree of armouring, for example, has been shown to vary widely between local areas of a streambed (Mosley and Tindale, 1985; Maloy, 1988; Church et al, 1989).

The purpose of the study described below was to investigate spatial variations in degree of armouring and their relation to the distribution of boundary shear stress. We selected a channel with a large in-channel supply of bedload because we expected variations in armouring to be high and most of the bed surface to have been active during recent high flows.

#### REDWOOD CREEK

Redwood Creek drains a 720 km<sup>2</sup> basin in north coastal California, USA (Fig. 1). Streamflow, sediment supply and transport rate, channel change, and land use history are well documented (Janda, 1978). The basin receives an average of 2000 mm of precipitation annually, most of which falls as rain between October and March. Total basin relief is 1615 m; average hillslope gradient is 26 percent. For much of its 108-km length Redwood Creek flows along the trace of the Grogan Fault, which juxtaposes two distinct bedrock types. The east side of the basin is generally underlain by unmetamorphosed sandstones and siltstones of Mesozoic Franciscan Assemblage, whereas the western side is predominantly underlain by a quartz-mica schist. Both rock units are deformed by numerous fractures and shear zones. The rock incompetence due to this deformation coupled with high rainfall and steep terrain contribute to the high erodibility of the watershed.

Water discharge records (since 1955) and sediment discharge records (since 1970) are available for five U.S. Geological Survey (USGS) gaging stations in Redwood Creek (Fig. 1). Sediment discharge is strongly flow-dependent; a large proportion of the annual sediment load is transported in infrequent, high magnitude flows. The estimated long-term sediment yield (suspended sediment and bedload) from 1954-1980 was 2480 t/km<sup>2</sup>/yr at South Park Boundary and 2100 t/km<sup>2</sup>/yr at Orick (USGS, written communication, 1981). Bedload constitutes 10-30% of the clastic load. Since 1980 sediment loads have decreased to 1190 and 920 t/km<sup>2</sup>/yr at the two stations respectively, primarily due to mild winter storm seasons during the last decade. These sediment yield rates are still higher than those from other rivers in the U.S that do not drain active volcanoes or glaciers.

Early aerial photographs taken in 1936 and 1947 show that the basin was covered with old-growth redwood and Douglas fir forests and a few areas of grassland. Redwood Creek was narrow and sinuous in most reaches, and bordered



by a thick canopy of trees over much of its length. Very little logging or road construction had occurred by 1947.

Timber harvest in the Redwood Creek basin began in earnest in the early-1950's, and by 1978 81 percent of the old-growth coniferous forest had been logged (Best, 1984), and thousands of kilometers of logging roads had been built. Erosion rates during the period of accelerated timber harvest (Janda (1978) were about 7.5 times greater than the natural rate estimated by Anderson (1979).

#### Channel-bed aggradation and degradation

Widespread channel changes have occurred since 1964 in response to large floods and a destabilized landscape. Large floods occurred in the Redwood Creek basin in 1861, 1890, 1953, 1955, 1964, 1972, and 1975, but accelerated erosion and channel response was not substantial before the flood of 1964. From 1954 to 1980, a total of  $30.5 \times 10^6$  tonnes entered Redwood Creek mostly from streamside landslides (debris slides, streambank failures, forested block slides, and earthflows), and fluvial erosion originating on unpaved logging roads (gullies, stream diversions, failed stream crossings) (Kelsey et al, 1981; Weaver et al, in press). Most of the sediment was input during the floods of 1964, 1972, and 1975. The 1964 flood was especially damaging and caused streamside landsliding, widespread aggradation (up to 7 m) and channel widening in Redwood Creek (Madej, in press), even though the peak flow was not unusually high (recurrence interval of 50 years; Coghlan, 1984). Floods of 1972 and 1975 resulted in additional aggradation in the downstream third of Redwood Creek.

Of the total sediment input during this period, 31% was deposited on floodplains and in the Redwood Creek channel; little sediment was stored on the steep hillslopes of the basin. Channel-stored sediment has become an on-going source of sediment to downstream reaches. For example, from 1964 to 1980,  $1.8 \times 10^6$  t of sediment was eroded from the channel bed in the upstream two-thirds of Redwood Creek, and much of that sediment was redeposited in the downstream lower gradient reaches of Redwood Creek (Madej, in press). Annual surveys since 1973 of 60 channel cross profiles show that the 1975 flood (recurrence interval = 25 years) caused the upstream third of the channel to degrade as much as 1.3 m while the downstream-most 25 km aggraded as much as 1.5 m (Varnum and Ozaki, 1986). Since 1980, surveys show that in Upper Redwood Creek the stream bed has stabilized at its pre-1964 level, the channel bed in the middle reach continues to erode, and the downstream 16 km of Redwood Creek either continues to aggrade or remains at an elevated level. Thus effects of high sediment input upstream will have been felt downstream for decades.

#### Study reaches

We selected two study reaches, one showing recent degradation (Fig. 2a), and the other, 12 km farther downstream, showing recent aggradation (Fig. 2b). Although the upstream reach is actively degrading, it still carries a high sediment load and may not yet have scoured down to its pre-1964 level. Both study sites are straight alluvial reaches at least 15 channel-widths in length and have similar channel characteristics (Table 1). Each study reach begins

and ends at riffle crests, and has well developed alternate bars and pool-riffle sequences.

Table 1. Characteristics of Study Reaches

Reach:	Degraded	Aggraded
Drainage area (km <sup>2</sup> )	523	605
Bankfull discharge (cms)	370	430
Bankfull width	60	110
Bankfull depth (m)	2.2	1.9
Channel gradient (m/m)	0.0026	0.0014
Length (m)	1284	1670
Sinuosity	1.09	1.03
D50-bed surface (mm)	22	15

Gaging stations lie in or near each study reach. The Wier Creek gaging station is located in the middle of the upstream study reach. The Elam Creek (aggraded) reach lies between two gaging stations (Miller Creek station 5 km upstream and the Orick station 4 km downstream). The Miller Creek gaging station is at a transition point between degrading reaches upstream and aggrading reaches downstream. From 1973-1983, the U. S. Geological Survey periodically collected bedload samples at the Miller and Wier Creek gaging stations with a Helley-Smith bedload sampler. Flows up to a recurrence interval of five years were sampled.

Field work commenced in 1988 in the aggraded reach and in 1989 in the degraded reach. Peak flows measured in Redwood Creek at Orick for 1988 and 1989 were 431 and 606 cms, respectively (recurrence intervals of 1.3 and 1.7 years). These moderate flows caused minor channel modifications, but were still capable of transporting considerable bedload. Bedload measured at the Orick gaging station was similar in the two years, 56,500 t in 1988 and 55,300 t in 1989.

#### METHODS

##### Mapping of surface grain size and channel topography

The channel bed in both study reaches showed distinct spatial variation in bed surface texture. In order to map the spatial distribution of bed surface grain size and to efficiently sample bed material, we stratified the bed into recognizable areas whose bed-surface grain size composition fell into certain predetermined grain-size ranges, which were arbitrarily chosen to represent common grain size ranges observed on the bed surface of each reach. Individual mapped areas are referred to as facies; each facies represents one of three or four facies types defined by a range of grain size. We delineated facies boundaries based on a visual estimate of the D75 of the surface particles, and then stratified individual facies by facies type for sampling purposes. In the aggraded reach the definitions of facies types were:

- D75 < 22mm = fine pebble facies
- 22 mm < D75 < 64 mm = coarse pebble facies
- D75 > 64 mm = cobble facies

In the degraded reach, the same definitions were used with the addition of a fourth facies type -- bimodal sand -- whose bed surface was covered with >25% sand intermixed with coarse pebbles or cobbles.

Facies were mapped over each reach by staking out and surveying boundaries between facies. In most cases the boundaries between facies were distinct, and mappers independently delineated the same boundaries. Topographic maps were constructed by using elevation data from facies boundaries and surveying miscellaneous elevations (aggraded reach) or by surveying a series of cross sections spaced at intervals of one- to two-thirds channel width (degraded reach). Surveys encompassed the channel banks to at least bankfull height, and covered all significant topographic features of the channel bed.

We selected individual facies to sample by probability proportional to size (in this case, facies area) without replacement. The number of facies sampled was proportional to the total area of the facies type relative to the total channel area (Table 2). We gave slightly more weight to sampling the cobble facies type because its size distribution was more variable than the other types. Total areas of each facies type were similar between the two reaches. The coarse pebble facies, which differed most in area, would have been more similar if bimodal facies in the aggraded reach had been classified separately instead of, in most cases, included in coarse pebble facies. Facies types were well represented in both reaches. The bimodal facies type in the degraded reach had the smallest proportion of bed area (9.3%); the coarse pebble type in the aggraded reach had the largest (52.9%).

Table 2. Number of sampling units in study reaches

Reach:	Degraded		Aggraded	
Facies type	# of units	% of total area	# of units	% of total area
Fine pebble	6	27.5	16	30.7
Coarse pebble	13	43.4	19	52.9
Cobble	8	19.8	15	16.5
Bimodal sand	5	9.3	-	-
Total	32		50	

#### Measurements of particle size

Surface and subsurface bed material in each selected facies were sampled systematically. Over each facies, we selected 100 to 150 particles from paced grids (Wolman, 1954), and determined the sieve size range of each particle by passing it through a template with square holes whose sizes ranged at half-phi intervals down to 4 mm. The size distribution of material <4mm on the bed surface material was estimated using the size distribution <4mm of sampled subsurface material (described below).

Samples of subsurface material from each sample facies were compiled from nine to twelve subsamples taken from points on rectangular grids set up using random starts. Subsamples were taken instead of single large samples because a pilot study had shown that the median grain size of one large sample had a higher variance than that of several smaller samples of equal total weight

taken from the same facies (Lisle, Madej, Hilton in preparation). Each compiled subsurface sample totalled about 100 kg. This sample volume was deemed adequate to give reproducible results based on the criteria of Church et al (1987) that the largest particle, which usually did not exceed 90 mm in this case, would comprise about 1% of the sample weight.

At each subsample location, we removed the surface layer with a flat-bottomed shovel to a depth equal to the D90 size of the surface, although for fine pebble facies we removed about 2 cm regardless of surface grain size. We then collected a subsample of about 10 kg of subsurface material from a layer about twice as thick as that removed from the bed surface. Subsamples from areas under water were collected from inside a 30-cm-diameter cylinder that had been worked vertically into the bed (McNeil and Ahnell, 1964). Approximately 20% of all subsamples were taken under water.

Samples were dried on tarps and field sieved into size classes at half-phi intervals down to 11 mm, and weighed. The fraction <11 mm was split, and a 6-8 kg subsample was brought back to a laboratory to be sieved at half-phi size intervals down to 1 mm. The fraction <1 mm was disregarded because suspended sediment samples (U.S. Geological Survey, 1970-88) indicated that 1 mm was the approximate upper size limit of suspended sediment, which we assumed did not play a role in armouring processes. Samples taken under water were wet sieved in the field down to 11 mm, the finer fraction was split and retained for dry sieving in the laboratory, and wash water containing suspended material was discarded.

#### Data Analysis

Particle size distributions of surface and subsurface material, expressed as the percentage by weight falling within each size class, were computed for each sampled facies. Sampling of surface and subsurface material by different methods may lead to non-equivalent grain size distributions. Using the formal conversion factors of Kellerhals and Bray (1971), we assumed that grain size distributions from grid-by-number measurements (pebble counts) are equivalent to those from sieve-by-weight measurements (subsurface material). This is supported by an empirical test by Church et al (1987) using a sample of 200 stones.

From these distributions, values of D50 were computed for each sampled facies, then each facies type, and finally for the reach as a whole, weighted by area in each step. Similarly, the distributions for each facies were weighted by area to compute mean percentages of each size class for each type and similarly for each study reach, using a method suggested by Baldwin (U.S. Forest Service, personal communication). Values of D50 for surface and subsurface material and  $D50(\text{surface})/D50(\text{subsurface})$ , hereafter referred to as the D50 ratio, were computed for each facies type and a mean weighted average determined for the study reach.

### RESULTS

#### Spatial distribution of facies types

The coarseness of the bed surface correlated commonly with the qualitative magnitude of boundary shear stress at moderate flow when the bed surface was

last active. This was most apparent in the part of the channel submerged at low flow. Cobble facies commonly occurred in zones of high or downstream-increasing boundary shear stress at low flow, such as over riffles or upstream portions of bar surfaces where streamlines converged toward pools (fig. 3). Fine pebble facies occurred in zones of low or downstream-decreasing shear stress at low flow, such as pools, downstream portions of bars, and along streambanks.

#### Size distributions of facies types

Mean surface and subsurface grain size distributions for the reaches as a whole and for each facies type showed distinct patterns (fig. 4). All grain size distributions (except surface sizes of bimodal facies) were unimodal, spanning sizes from sand to large cobbles. All sizes present in surface material of each facies type were also present in their respective subsurface material. Subsurface grain size distributions were similar between the different facies, particularly near the coarse end of the size spectrum.

Coarser facies were more strongly armoured than finer facies. With increasing coarseness of facies types, subsurface grain size distributions became slightly coarser, but not as much so as the surface grain size distributions. Similar results in another channel are reported by Maloy (1988). As quantified by D50 ratios (Table 3), cobble facies in Redwood Creek were most strongly armoured; coarse pebble facies exhibited an intermediate degree of armouring approximately equal to that of the channel as a whole. Fine pebble facies in both reaches were unarmored as were bimodal facies in the aggraded reach.

Table 3. D50 of surface and subsurface material and D50 ratios and their respective standard errors (s.e.) for study reaches of Redwood Creek.

Reach:	Degraded			Aggraded		
	D50(s.e.)		D50ratio(s.e.)	D50(s.e.)		D50ratio(s.e.)
Facies type	Surface	Subsur.		Surface	Subsur.	
Fine pebble	5.7(1.0)	10.5(1.6)	0.68(0.14)	6.1(0.7)	6.2(0.5)	1.05(0.14)
Coarse pebble	26.2(1.5)	19.2(1.1)	1.44(0.06)	14.9(0.6)	9.7(0.4)	1.60(0.09)
Cobble	38.2(2.6)	24.4(2.6)	1.66(0.19)	30.0(1.3)	13.0(0.6)	2.45(0.16)
Bimodal Sand	18.4(4.1)	22.0(3.1)	0.96(0.19)	--	--	--
Weighted Ave.	22.2(0.9)	18.1(0.9)	1.23(0.06)	14.7(0.4)	9.1(0.3)	1.57(0.07)

Fine pebble facies commonly appeared to be, in fact, "anti-armoured", that is, having a surface layer finer than the subsurface layer. For example, the D50 ratio averaged for the fine pebble facies of the degraded reach (0.68) was well less than unity. In this reach, the thickest and most extensive fine pebble facies consisted of sheets of sand and small pebbles less than 0.5 m thick that mantled the beds of pools (fig. 5). Deep water in much of these areas prevented taking subsurface samples. Downstream, as the water became shallow enough to obtain samples, the fine deposits thinned and graded into bimodal facies, which graded into coarse pebble or cobble facies as large particles underlying fine sediment were increasingly exposed. Subsurface

samples were thus biased toward thin areas of fine pebble facies, which were likely to be anti-armoured.

Fine pebble facies in the aggraded reach were more widely distributed and were commonly associated with unit bars, which will be described later. Fine facies in pools contained abundant pebbles. The thickness of these deposits could not be probed because they were more difficult to penetrate than the sandy deposits in pools of the degraded reach, and any underlying coarser layer could not be detected. Comparison of topographic surveys done one year apart showed that the new deposits were locally as much as 1 m thick.

Anti-armouring is somewhat an artifact of our method to sample the subsurface. In scraping away the surface of fine pebble facies that were thin, we essentially removed those facies -- that is, the bedload material that was last transported in that location -- and sampled coarser, underlying material. Considering difficulties in obtaining subsurface samples unbiased by water depth and uncertainties in interpreting anti-armouring, it is perhaps prudent to assume that fine facies have D50 ratios no less than unity.

#### Comparison between reaches

An unexpected result was that the bed of the aggraded reach, whose transport capacity was demonstrably exceeded, was apparently more strongly armoured on average than that of the degraded reach. A possible explanation is that a greater instability of the aggraded reach apparently led to stronger apparent armouring of its coarsest facies. The greatest difference in D50 ratios of facies types between the two reaches was the greater armouring of the cobble facies of the aggraded reach (D50 ratio of 2.45 vs. 1.66). The difference in D50 ratios arose primarily from the superior coarseness of subsurface material of the cobble facies in the degraded reach (Table 3, fig. 4). Although both surface and subsurface material of cobble facies of the degraded reach were coarser than those of the aggraded reach, subsurface materials showed the greatest contrast, and that of the aggraded reach had a pronounced mode at approximately 64mm.

A possible origin for the difference in D50 ratios is that the subsurface layer of cobble facies in the aggraded reach may have been locally thinner (in particle diameters) than in the degraded reach. If so, there would be a greater likelihood in the aggraded reach that subsurface samples of cobble facies would incorporate underlying material from finer facies. In contrast, cobbles in the degraded reach perhaps accumulated in the subsurface as the buried frameworks of armour layers created under consistent sedimentologic conditions that favored accumulation of the coarsest particles in transport. Coarsening of subsurface bed material in a degrading channel with alternate bars was observed in a laboratory experiment (Iseya et al, 1989), in which a constant, poorly graded size distribution of transported bedload was maintained. Sequential aerial photograph of the degraded reach show that its large-scale alternate bars have been essentially stationary over the last decade and smaller-scale unit bars have not been observed in the field.

In contrast, aggradation and unit bar migration in the aggraded reach apparently often destabilized local sediment transport conditions under which coarse particles could accumulate to any thickness. Resurveying of bed topography of the aggraded reach after one rainy season revealed that

migrating unit bars with average heights of 0.2 m had significantly altered channel morphology (fig. 6). These bars, similar to those described by Bluck (1982) in a braided channel, covered approximately one-fourth of the channel and had accreted onto the larger scale alternate bars. Deposition of unit bars accounted for most of the aggradation at least over that season. Particularly in the portion of the channel submerged at low flow, the new deposits had become so modified after becoming annealed to the major alternate bar topography as to become indistinct as unit bars.

## DISCUSSION AND CONCLUSIONS

### Comparison of armouring with that of other channels

In comparison with other single-thread, gravel-bed rivers, the bed of Redwood Creek is weakly armoured (fig. 7), that is, the bed surface is only slightly coarser than the subsurface. Although data on sediment loads of the other channels is not available, we assume that, per basin area, most are smaller than that of Redwood Creek. Redwood Creek's sediment transport capacity has clearly been equalled or exceeded by the supply of bedload delivered to its channel, as indicated by its aggraded channel. Comparison of armouring must be made with caution because bed samples for the other data sets were fewer and were located nonrandomly. The D50 ratio of most of the other channels exceeds a value of 2; the reach-averaged values for the aggraded and degraded reaches of Redwood Creek are 1.57 and 1.23, respectively. Material less than 1mm in diameter was not included in calculating D50 ratios for Redwood Creek. If all sizes are included in order to more fairly compare with the other channels, D50 ratios for Redwood Creek equal 1.77 and 1.39 for the aggraded and degraded reaches respectively. Thus the conclusion that the bed of Redwood Creek is weakly armoured remains valid.

The fact that the bed is weakly armoured provides further evidence that armouring can adjust to sediment supply and thereby alter bed resistance to sediment transport (Dietrich et al, 1989). This evidence is given additional weight by the intensity of measurement of armouring, which to the best of our knowledge has not been exceeded elsewhere.

We speculate that mean bed armouring in both reaches of Redwood Creek has decreased to a minimum, and that deposition of bedload sediment in the form of unit bars in the aggraded reach manifests a further adjustment to excess sediment load not represented in the degraded reach. The aggraded reach, whose transport capacity was clearly exceeded, was significantly armoured (D50 ratio = 1.6, s.e. = 0.07) and more so than the degraded reach (D50 ratio = 1.2; s.e. = 0.06), which apparently had a smaller relative sediment supply. Mean bed armouring, therefore, is not a simple function of sediment supply. As described earlier, superior channel stability of the degraded reach has allowed coarse particles to accumulate to a greater thickness in cobble facies of that reach than in those of the aggraded reach, resulting in a smaller difference between surface and subsurface material in the cobble facies of the degraded reach and in the bed of the reach overall.

Moreover, the difference in mean bed armouring between study reaches is minor compared to that between Redwood Creek and other channels that presumably have a much smaller relative supply of sediment. Although trends in bed elevation of the aggraded and degraded reaches show categorically different responses to

changing sediment supply, the contrast in supply relative to transport capacity between the two reaches is not strong. The degraded reach remains aggraded after floods of the past decades and is supplied with large volumes of sediment from channel erosion upstream (fig. 8).

#### Importance of winnowing

Winnowing and selective accumulation of coarse particles on the bed surface can both be responsible for armour formation. Grain size distributions of facies types in Redwood Creek give evidence that winnowing leaves a strong imprint on the bed surface when sediment transport has ceased. Differences in bed material indicate some selectivity in sizes deposited. All facies types, however, exhibit similarities between the coarse limb of the frequency distribution of surface and subsurface layers. This suggests that the surface layer of the armoured facies was depleted in fines, not enriched in coarse particles. In contrast, the surface of the bed classified as the finest facies type was enriched in fines and commonly consisted of a veneer of fine material overlying a coarser bed. Together, these suggest that winnowing of fines from coarse facies and deposition downstream to form fine-grained facies was largely responsible for spatial variations in armouring observed at low flow. The coincidence of high boundary shear stress at low flow with coarse (winnowed) facies and low shear stress with fine-enriched facies is consistent with this interpretation.

It is important to distinguish between vertical and downstream winnowing (Parker and Klingeman, 1982). In vertical winnowing, fines are lost to the subsurface layer; in downstream winnowing fines are carried downstream. As Gomez (1984) points out, vertical winnowing requires that the coarse particles in the surface layer be mobile; downstream winnowing requires that they be temporarily immobile. The juxtaposition of coarse and fine facies indicates that downstream winnowing of coarse armour layers in Redwood Creek was prevalent, at least during waning stages.

The size composition and location of different facies in Redwood Creek indicate that a strong imprint on the texture of the surface, including mean bed armouring, has been left by wide spatial variation of sediment sorting processes in response to varying flow. The bed at low flow, when it is practical to observe armouring of the entire channel, is to a large degree the product of waning flows. Although low flows are too feeble to transport important volumes of bedload, spatial variations in shear stress near entrainment thresholds enhance heterogeneity in bed texture through size-selective transport and deposition. As general transport ceases, fine sediment is eroded from vulnerable hiding places among the large particles on the bed surface, especially where shear stress remains relatively high. Fine sediment is thereby winnowed from zones of high shear stress and deposited in zones of low shear stress. Thus some areas of the bed of any channel in which armouring is uniformly weak at important bedload-transporting stages can be expected to exhibit strong armouring at low flow. Coupled winnowing and deposition driven by bar topography may affect observed mean bed armouring. One must therefore use caution in interpreting bedload transport processes at high stages from armouring and apparent bed mobility observed at low stages.

#### Equal mobility vs size-selective entrainment



Spatial distribution of surface particle sizes and boundary shear stress at low flow also has bearing on the relative mobility of different grain sizes represented in the bed of Redwood Creek. At relatively low discharges (no greater than 17 cumecs) we have observed sand and fine gravel transported, commonly as migrating dunes over an armour layer. Bedload samples at high flow (USGS, 1970-88) contain the largest particles that can fit into a Helley-Smith bedload sampler with a 3-inch orifice. Comparisons of the overall grain size distribution of bed material with bedload samples over a range of flows, therefore, would lead one to conclude that there is strong stage-dependent, selective transport by grain size.

Extrapolation of such results to the channel as a whole is erroneous, however. The most mobile sources of bedload at discharges when only sand and granules are transported are fine-grained winnowed sediment deposited in pools during the previous waning stages. These areas are the last to be deposited upon and the first to be entrained. All particle sizes on these areas may be nearly equally mobile; gravel and cobbles are simply not represented on the bed surface. This fine bedload is imposed on intervening coarser areas and overpasses a stable armour layer as streaks of moving material that disappear as stage drops and the bed is winnowed. Thus the degree of size selection in entrainment and transport depends on the part of the bed observed. At rising stages bedload may be first entrained from fine areas that exhibit equal mobility. The apparent size selectivity of entrainment on the bed taken as a whole, in this case, arises not so much from selective entrainment of particles from a mobile armour layer but from areal sorting that is induced by topographically driven variations in boundary shear stress and sediment transport direction.

#### ACKNOWLEDGMENTS

Sue Hilton supervised data collection and calculated grain size parameters. Stephan Stringall prepared final versions of maps. We were assisted in the field by Alice Berg, Scott Bowman, George Cook, Carrie Jones, Mike Napolitano, Vicki Ozaki, Christine Shiveille, Sherry Skillwoman, Stephan Stringall, and Victor Vrell. Bill Dietrich and Jonathan Nelson provided valuable discussions.

#### REFERENCES CITED

- Anderson, H.W., 1979, Sources of sediment-induced reduction in water quality appraised from catchment attributes and land use: Proceedings of Third World Congress on Water Resources, Mexico City, April 23-28, V. 8, p. 3606-3616.
- Andrews, E. D., 1983, Entrainment of gravel from naturally sorted riverbed material, Geological Society of America Bulletin 94, 1225-1231.
- Andrews, E.D., 1984, Bed-material entrainment and hydraulic geometry of gravel-bed rivers in Colorado. Geological Society of America Bulletin 95, 371-378.
- Andrews, E.D and D.C. Erman, 1986, Persistence in the size distribution of surficial bed material during an extreme snowmelt flood. Water Resources Research, Vol. 22, p. 191-197.
- Best, D., 1984, Land use of the Redwood Creek basin, U.S. Dept. of Interior Redwood National Park Technical Report 9, 24 p, 6 maps.
- Bluck, B.J., 1982, Texture of gravel bars in braided streams, in "Gravel-bed

- rivers" ed. by R. D. Hey, J. C. Bathurst, and C. R. Thorne, John Wiley and Sons, p. 339-355.
- Church, M.A., D.G. McLean and J.F. Wolcott, 1987, River bed gravels: Sampling and Analysis, in "Sediment transport in gravel-bed rivers" eds. Thorne, C.R. et al, Wiley, London, p. 43-88.
- Coghlan, M. 1984, A climatologically-based analysis of the storm and flood history of Redwood Creek, U.S. Dept. of Interior Redwood National Park Technical Report 10, 47 p.
- Dietrich, W.E., J. W. Kirchner, H. Ikeda, and F. Iseya, 1989, Sediment supply and the development of the coarse surface layer in gravel-bedded rivers, *Nature*, Vol. 340. p.215-217.
- Gomez, B., 1984, Typology of segregated (armoured)/paved) surfaces: Some comments, *Earth Surface Processes and Landforms* 9, 19-24.
- Iseya, F. and H. Ikeda, 1987, Pulsations in bedload transport induced by a longitudinal sediment sorting: A flume study using sand and gravel mixtures, *Geografiska Annaler* 69A(1), p. 15-27.
- Iseya, F., Ikeda, H. and T.E. Lisle 1989, Fill-top and fill-strath terraces in a mixture-bed flume, 2nd International Conference of Geomorphology, Frankfurt/Main, Sept 3-9.
- Janda, R.J., 1978, Summary of watershed conditions in the vicinity of Redwood National Park, California. U.S. Geological Survey Open File Report 78-25, 82 p.
- Kellerhals, R., and D.I. Bray, 1971, Sampling procedures for coarse fluvial sediments, *Journal of the Hydraulics Division, American Society of Civil Engineers* 97(HY8), 1165-1180.
- Kelsey, H.M., M. Coghlan, J. Pitlick, D. Best. Geomorphic analysis of streamside landsliding in the Redwood Creek basin. in U.S. Geological Survey Professional Paper 1454, in press.
- Kelsey, H. M., Madej, M.A., Pitlick, J., Coghlan, M., Best, D., Belding, R., and Stroud, P., 1981, Sediment sources and sediment transport in the Redwood Creek basin - a progress report. U.S. Dept. of Interior National Park Service Technical Report 3, Arcata, California. 114p.
- Kinerson, D., and W.E. Dietrich, 1989, Bed surface response to sediment supply (abstract), *EOS Transactions. American Geophysical Union* 70(43), p. 1121.
- Komar, P.D. and Li, Z., 1988, Applications of grain-pivoting and sliding analyses to selective entrainment of gravel and to flow-competence evaluations, *Sedimentology*, Vol 35, p. 681-695.
- Kuhnle, R.A. and J.B. Southard, 1988, Bed load transport fluctuations in a gravel bed laboratory channel, *Water Resources Research* Vol 24, No. 2,p. 1137-1151.
- Madej, M.A., in press, Recent changes in channel-stored sediment in Redwood Creek, California, in U.S. Geological Survey Professional Paper 1454.
- Maloy, J.A. 1988, Changes in grain-size distribution in an gravel-bed stream due to a point-source influx of fine sediment, MS thesis, Western Washington University, Bellingham, 50pp.
- McNeil, W.J., and W.H. Ahnell, 1964, Success of pink salmon spawning relative to size of spawning bed materials. Special Science Report 469, US Fish & Wildlife Service, 15p.
- Milhous, R.T.. 1973, Sediment transport in a gravel-bottomed stream, Ph.D. thesis, Oregon State University, Corvallis, 232 pp.
- Mosley, M.P. and D.S. Tindale, 1985, Sediment variability and bed material sampling in gravel-bed rivers. *Earth Surface Processes and Landforms*, Vol. 10, 465-482.

- Parker, G. and P.C. Klingeman, 1982, On why gravel bed streams are paved. Water Resources Research, Vol. 18, No.5 p. 1409-1423.
- Parker, G., Klingeman, P.C., and D.G. McLean, 1982, Bedload and size distribution in paved gravel-bed streams. Journal of the Hydraulics Division, American Society of Civil Engineers 108(HY4), 544-571.
- Parker, G., S. Dharotharan and H. Stefan, 1982, Model experiments on mobile, paved gravel bed streams, Water Resources Research Vol. 18, No.5, p. 1395-1408.
- Thorne, C.R. and R.D. Hey, 1983, Discussion of 'Bedload and size distribution in paved gravel-bed streams' by G. Parker, P.C. Klingeman, and D.G. McLean, Journal of Hydraulic Engineering 109(5), 791-793.
- U.S. Geological Survey, 1970-1988, Water resources data for California: Pacific slope basins from Arroyo Grande to Oregon state line except Central Valley.
- Varnum, N. and V. Ozaki, 1986, Recent channel adjustments in Redwood Creek, California, U.S. Dept. of Interior Redwood National Park Technical Report No. 18, 74 p.
- Weaver, W.E., Hagans, D.K., and J.H. Popenoe, Magnitude and causes of gully erosion in the lower Redwood Creek drainage basin, in U.S. Geological Survey Professional Paper 1454, in press.
- Wiberg, P.L. and J.D. Smith, 1987, Calculations of the critical shear stress for motion of uniform and heterogeneous sediments, Water Resources Research, Vol. 23, No. 8, p. 1471-1480.
- Wilcock, P., 1988, Methods for estimating the critical shear stress of individual fractions in mixed-size sediment, Water Resources Research, Vol. 24, No. 7, p. 1127-1135.
- Wilcock, P.R. and J.B. Southard, 1988, Experimental study of incipient motion in mixed-size sediment, Water Resources Research, Vol. 24, No. 7, p. 1137-1151.
- Wilcock, P.R. and J. B. Southard, 1989, Bed load transport of mixed size sediment: Fractional transport rates, bed forms and the development of a coarse bed surface layer, Water Resources Research 25(7), 1629-1641.
- Wolman, M. G., 1954, A method of sampling coarse river bed material. Transactions of the American Geophysical Union, V. 35 No. 6. p. 951-56.

## Figure Captions

1. Location map showing Redwood Creek, aggraded and degraded study reaches, and five gaging stations.
- 2a. Cross section 20 of Redwood Creek showing a general lowering of the gravel bar surface and thalweg from 1973 to 1989. This scour is typical of the degraded reach.
- 2b. Cross section 6 of Redwood Creek showing both the gravel bar surface and thalweg at higher elevations in 1988 than in 1973. This pattern of elevation channel beds is typical of the aggraded reach.
3. Channel bed topography and facies of the degraded and aggraded study reaches, Redwood Creek. Contour interval is 0.5 m.
4. Grain size distributions for surface and subsurface bed material averaged for facies types and for study reaches, Redwood Creek.
5. Longitudinal profile of the water surface, bed surface, and armour layer buried under fine sediment in a pool of the degraded reach, Redwood Creek. The survey was conducted during low flow (31/8/89).
6. Map of the upstream half of aggraded reach showing channel areas that had aggraded more than 0.2 m from 1988 to 1989. Most of these areas were associated with discernible unit bars superimposed on the existing channel morphology.
7. Median grain size of subsurface bed material vs median grain size of surface bed material for gravel-bed rivers including Redwood Creek. The line demarks a ratio of 2.
8. Cross section 23, located 2 km upstream of the degraded reach, showing extensive erosion of left bank flood deposits from 1973 to 1989. As Redwood Creek erodes channel-stored sediment, the channel bed and banks become an important source of sediment to downstream reaches.

Figure 1

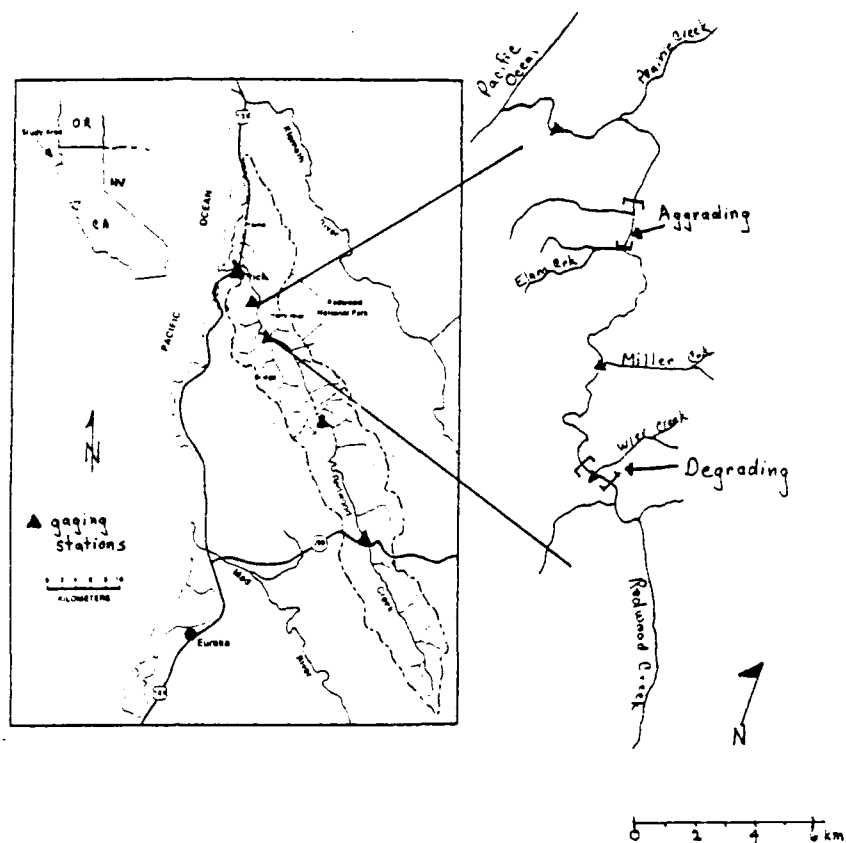


Figure 2a

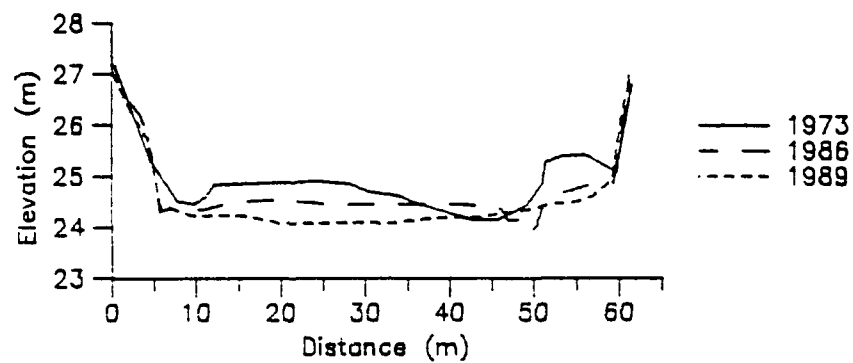
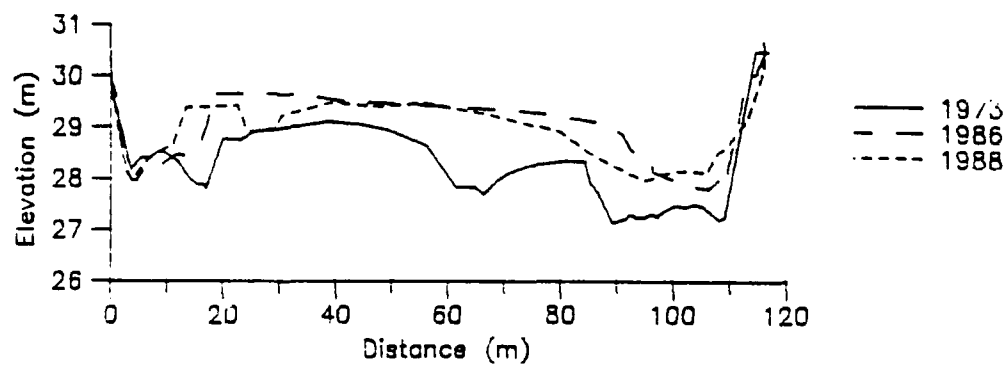
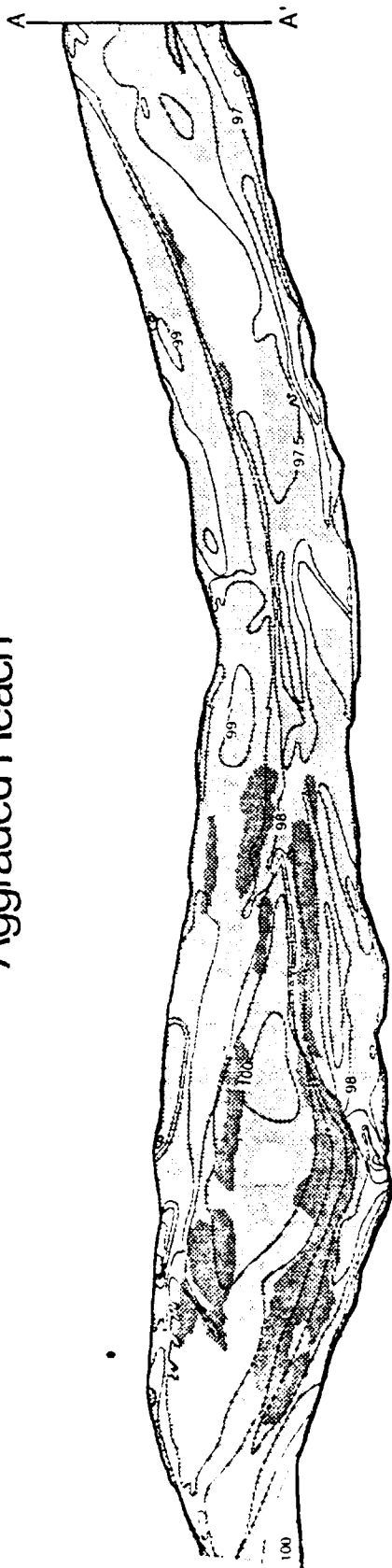








Figure 2b



# Aggraded Reach



-  fine pebble
-  coarse pebble
-  cobble
-  bimodal sand
-  woody debris
-  unclassified

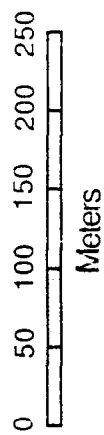
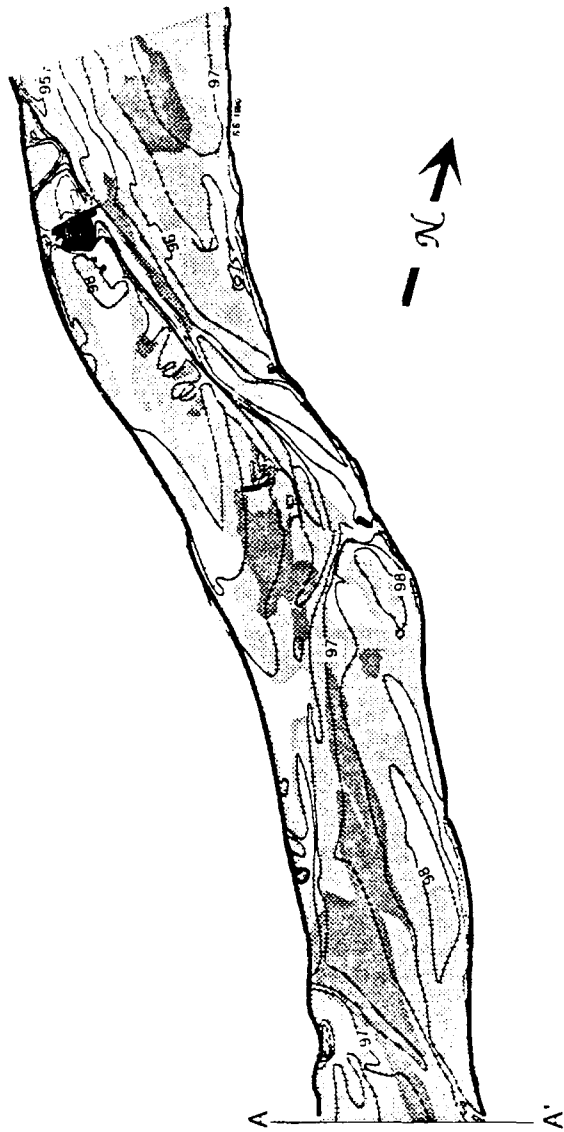
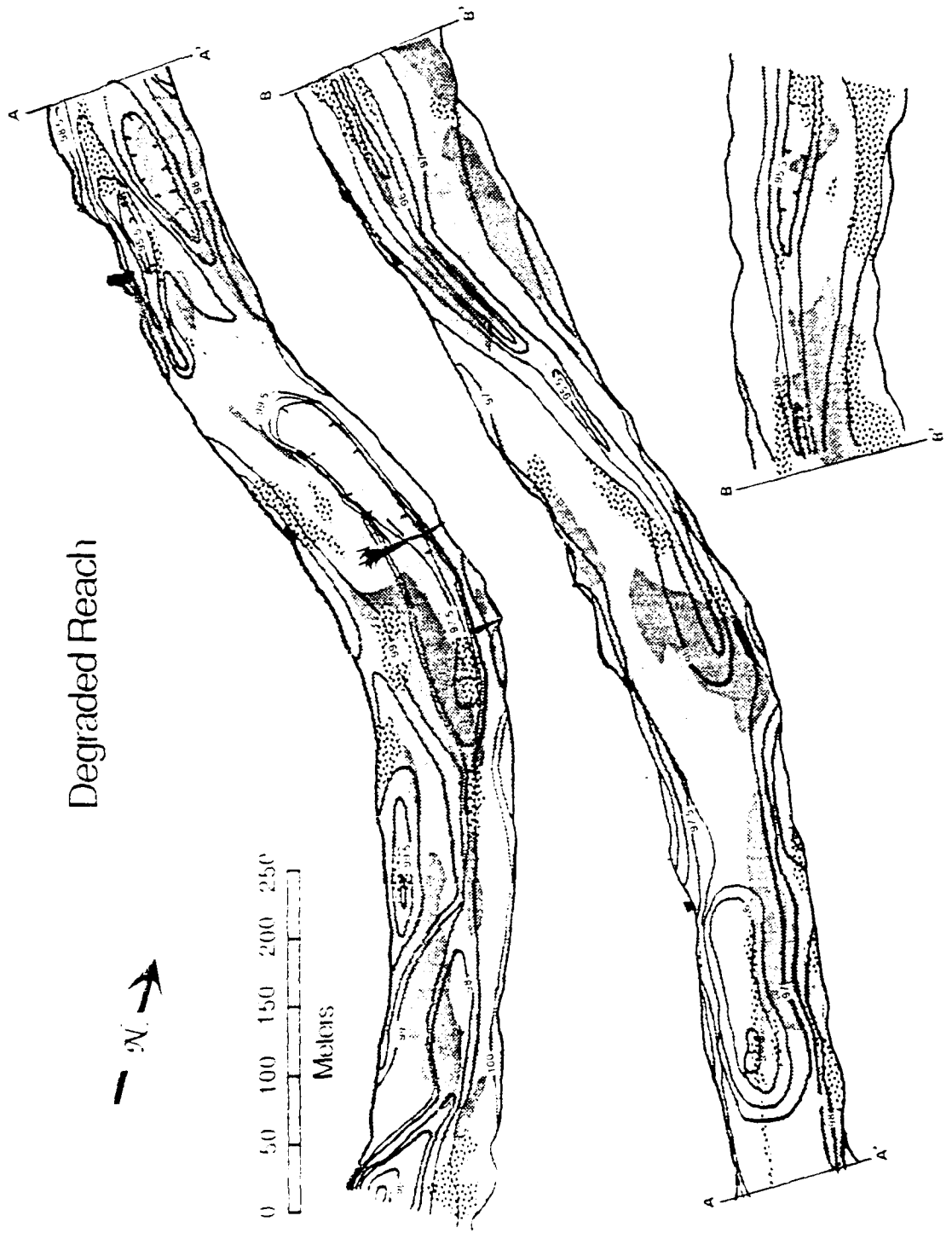
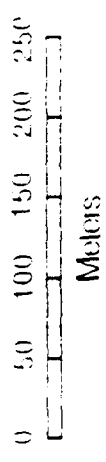
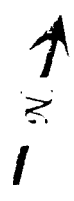


Figure 3

Degraded Reach



# Aggrading reach

# Degrading reach

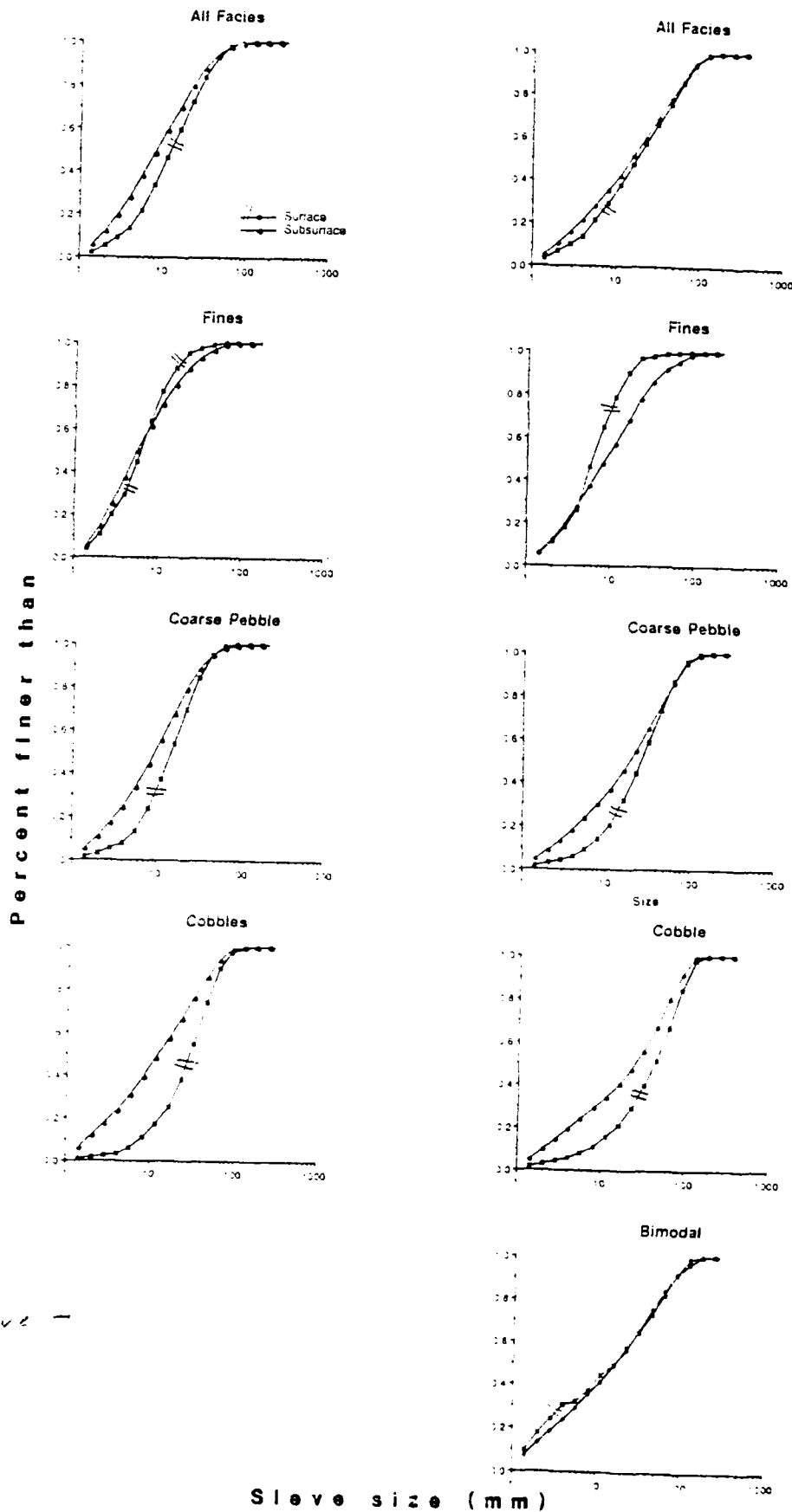


Figure 1



Figure 5

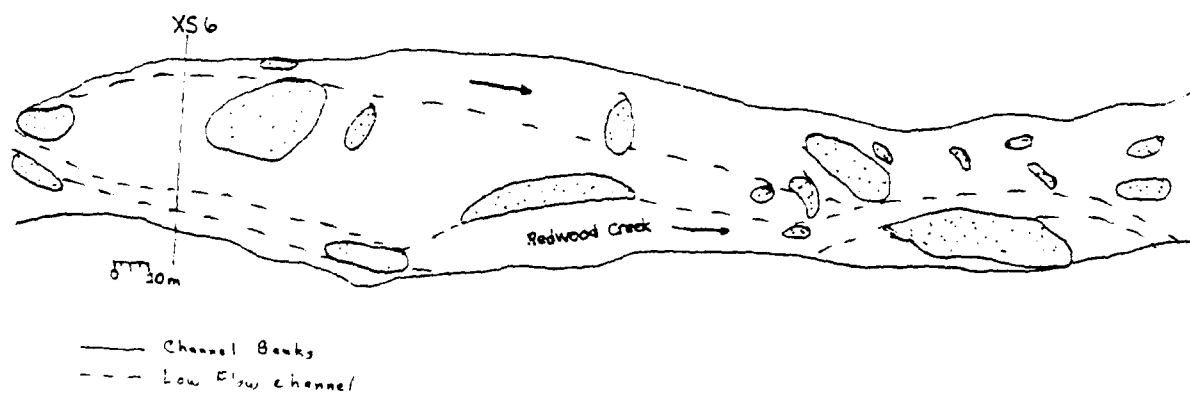
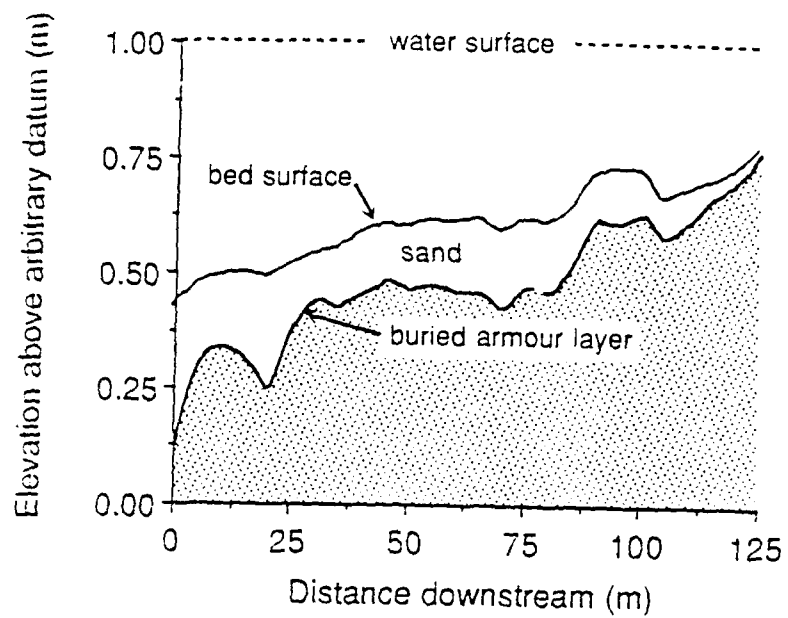


Figure 6

Figure 7

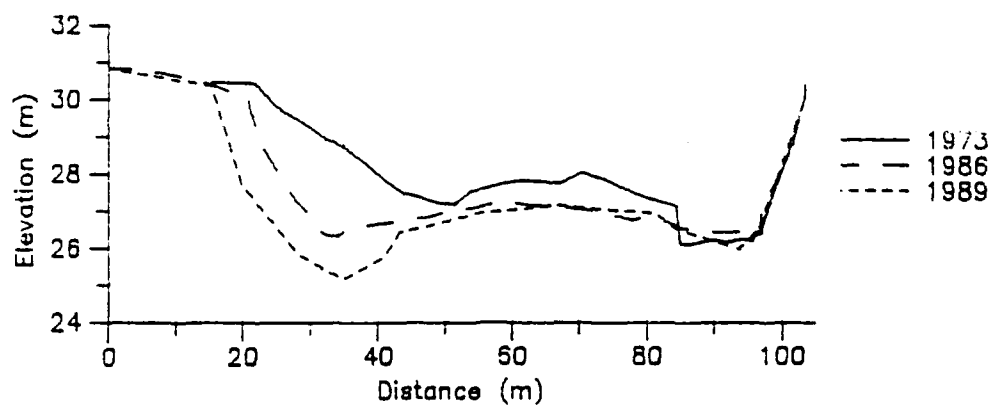
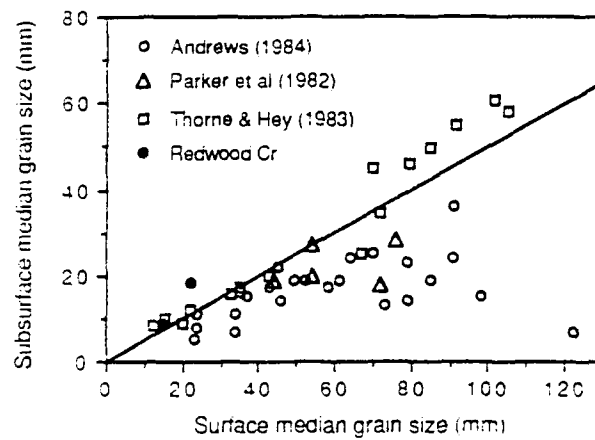


Figure 8

# Equal Grain Mobility Versus Changing Bedload Grain Sizes in Gravel-Bed Streams

Paul D. Komar and Shyuer-Ming Shih

*College of Oceanography, Oregon State University  
Corvallis, Oregon 97331*

## ABSTRACT

Parker et al. (1982) made an assumption of equal-grain mobility as a first-order approximation in developing relationships for evaluating bedload transport rates of grain-size fractions in Oak Creek, a gravel-bed stream. That assumption yielded reasonable results in determinations of gravel transport rates, but did not account for observed variations in bedload grain-size distributions at different flow stages. As discharges and bed stresses increase in Oak Creek, the bedload grain sizes become significantly coarser and their distributions are increasingly skewed as they approach the distribution of the bed material (pavement plus subpavement). These changing bedload grain sizes demonstrate that there is a marked departure from equal grain entrainment and transport in Oak Creek. Higher-order solutions for predicting transport rates, those which do not assume equal mobility, have been developed by Diplas (1987) and Shih and Komar (1990). These advanced analyses provide predictions of changing bedload grain sizes as well as yielding improved calculations of transport rates.

Various lines of evidence have been offered in support of the equal-mobility hypothesis. A series of publications have analyzed the relationship between the largest particles found in bedload samples and flow discharges or bed stresses. Rather than demonstrating that the bedload grain-size distributions are nearly constant at all flow stages, which should prevail during equal mobility, those studies show that there are rapid changes in grain sizes as reflected by the largest particles in the bedload samples. It can be argued that these data represent a transitional stage during which the grain-size distributions of bedload samples are approaching the size distributions of the bed material, and that the faster this transition, the closer the conformity with the equal-mobility hypothesis. This interpretation constitutes a broader view of equal mobility in a stream than the specific conditions to which the bedload transport analyses of Parker et al. (1982) apply. There are problems with this broader interpretation in that comparisons between data from Oak Creek (well-developed pavement) and Great Eggleshope Beck (absence of a pavement) imply that the latter stream comes closer to equal mobility, in spite of the expectation that the pavement in Oak Creek should tend to equalize grain mobility. It is clear from this example that factors other than the presence of a pavement layer are important to sorting processes leading to variations in bedload grain sizes and the relative transport rates of different size fractions.

## INTRODUCTION

Gravel-bed streams characteristically have wide ranges of grain sizes and display size-sorting patterns within their bed deposits. Particularly important is that the surface of the bed layer, its pavement, may be considerably coarser than the subpavement gravel [We are using these terms, as opposed to armor versus subarmor, to denote the frequent mobility of the gravels, corresponding to the use by Parker et al. (1982)]. This vertical sorting into pavement and

subpavement plays an important role in sediment transport in gravel-bed streams. Parker et al. (1982) have hypothesized that the existence of a bed pavement regulates the entrainment of particles by the stream, resulting in their being approximately equal in mobility, that is, all grain sizes are entrained at about the same flow discharge and are transported at rates in proportion to their presence in the bed material. This has come to be known as the equal-mobility hypothesis.

Subsequent studies have supported this hypothesis. Andrews (1983) and Andrews and Erman (1986), utilizing data from several streams, examined variations in the largest particle sizes found in bedload samples at different flow stages. They concluded that the maximum particle size undergoes almost no change over a range of flow discharges or bed stresses. Wilcock and Southard (1988) have undertaken flume experiments involving bed sediments of mixed sizes, and concluded that "all fractions in a size mixture begin moving at close to the same value of bed shear stress during steady-state transport conditions." A theoretical foundation for the hypothesis has been provided by the analysis of Wiberg and Smith (1987). The collective impact of these studies has been to "prove" the equal mobility or near-equal mobility of gravel entrainment and transport in streams.

This strong support for equal mobility appears to go well beyond the original intention of Parker et al. (1982) when they formulated the hypothesis. The objective of their work was to develop a method for calculating transport rates of different size fractions, and an assumption of equal mobility served as a first-order approximation. However, a corollary of perfect equal mobility is that with varying flow discharges, there should be no change in the grain-size distributions of the bedload samples, including no shifts in the maximum particle sizes. Parker et al. based their analysis on the data of Milhous (1973) from Oak Creek, Oregon, and noted that there actually are significant variations in bedload grain sizes with changing flow stage. Parker et al. recognized that such variations in bedload grain sizes represent a departure from their assumption of perfect equal mobility. With that recognition, they were the first to attempt the development of a higher-order analysis that would account for varying bedload grain-size distributions. Their approach was later modified by Diplas (1987).

Our research initially focused on flow-competence techniques, the evaluation of flood hydraulics from the sizes of particles transported (Komar, 1987a, 1987b, 1989; Komar and Li, 1988). Competence evaluations have traditionally depended on observations of the largest particle sizes moved, and assume that the greater the flood discharge the larger the particles in the resulting deposits. This use of variable maximum particle sizes has been interpreted by some as being in conflict with the equal-mobility hypothesis. It does disagree with the results of Andrews (1983) and Andrews and Erman (1986) who, based on analyses on maximum particle sizes in bedload samples, concluded that all sizes are entrained at effectively the same flow stress (a conclusion that would make flow-competence evaluations impossible). On the other hand, Ashworth and Ferguson (1989) found significant variations in bedload medians and maximum particle sizes in three streams, and concluded that there is substantial size-selective transport representing a departure from equal mobility. Our recent work has further established the nature of the shifting size distributions of bedload gravels, and has examined alternatives to maximum particle sizes for flow-competence evaluations (Shih and Komar, 1990a, 1990b; Komar and Carling, in review).

The objective of this paper is to undertake a reexamination of the equal-mobility hypothesis and the various types of data and analyses that have been offered to test the concept. This will begin with a review of the theory itself, as developed by Parker et al. (1982) and modified by Diplas (1987). Particular attention will be given to how the reference transport relates to grain threshold and to reformulations in terms of maximum particle sizes, and thus to variations in

bedload grain-size distributions. The analyses presented here will be based on the Oak Creek measurements of Milhous (1973), a data set of particular relevance to questions of equal mobility in view of its use by Parker et al. (1982) to establish that concept. A general review will be presented of the studies reporting on the movement of maximum particle sizes and changing grain-size distributions in an attempt to discern whether there is a tendency toward equal mobility resulting from the presence of a bed-material pavement.

## THE EQUAL-MOBILITY HYPOTHESIS

### Basic derivation by Parker et al. (1982)

The study of Parker et al. (1982) was based primarily on a reanalysis of the bedload samples collected by Milhous (1973) in Oak Creek, a flume-like gravel-bed stream in western Oregon. Oak Creek has a well-developed pavement, consisting of a narrow range of large grain sizes with a median diameter of 6 cm; the grain-size distribution of the subpavement is broader, with a median of 2 cm. Bedload samples were collected in a vortex trap which insured a high sampling efficiency for all grain sizes within the bedload range. Milhous provides sieve analyses of the bedload samples, which permit evaluations of their individual transport rates.

The approach of Parker et al. (1982) was to analyze ten grain-size ranges, governed by the sieve intervals, and attempt to correlate the bedload transport rates of each range with the flow stresses. They used only those measurements of Milhous (1973) obtained during conditions of broken pavement, that is, when most of the grain sizes in the pavement are represented in the bedload. This limited the analysis to 22 measurement sets collected at discharges in excess of approximately 1 m<sup>3</sup>/sec. The analysis was placed in dimensionless form. If  $q_{si}$  denotes the volumetric bedload transport rate per unit channel width, then the dimensionless Einstein bedload parameter for the  $i$ th grain-size range, represented by a mean  $D_i$  for that sieve fraction, is

$$q_{si}^* = \frac{q_{si}}{f_i [RgD_i]^{1/2} D_i} \quad (1)$$

where  $R = (\rho_s - \rho)/\rho$  and  $\rho_s$  and  $\rho$  are respectively the gravel and water densities [Table 1 defines the symbols used here, together with those employed by Parker et al. (1982)]. In equation (1),  $f_i$  is the frequency of the sieve fraction as found in the size distribution of the subpavement; its inclusion has the effect of normalizing the transport rate of that size fraction to its availability in the stream bed [Parker and Klingeman (1982) provide a similar analysis in terms of the pavement grain-size distribution]. The flow stress  $\tau$  is made dimensionless by its inclusion in the Shields entrainment function

$$\theta_i = \frac{\tau}{(\rho_s - \rho)gD_i} \quad (2)$$

expressed in terms of  $D_i$  for the size fractions. Correlations were developed between  $\theta_i$  and

$$W_i^* = \frac{q_{si}^*}{(\theta_i)^{1.5}} \quad (3)$$

As noted by Parker et al. (1982), there are two advantages in using  $W_i^*$  rather than  $q_{si}^*$  as a

dimensionless sediment transport rate. Plots of  $q_{si}^*$  versus  $\theta_i$  are very steep, whereas the slopes of  $W_i^*$  versus  $\theta_i$  are lower, and this makes the job of determining empirical relationships from the data somewhat easier. In addition,  $W_i^*$  is independent of  $D_i$  (the dependencies of  $q_{si}^*$  and  $\theta_i$  on  $D_i$  cancel in the  $W_i^*$  ratio); in the correlation between  $W_i^*$  and  $\theta_i$ , only the Shields function contains  $D_i$ .

The correlations of Parker et al. (1982) involved log-log plots and least-square regressions for each grain-size range to establish relationships of the form

$$W_i^* = \alpha_i (\theta_i)^{m_i} \quad (4)$$

Each grain-size range formed an individual correlation having different  $\alpha_i$  and  $m_i$  coefficients. These were collapsed into a single relationship by the establishment of a reference bedload transport level. This was set at  $W_r^* = 0.002$ , and the corresponding  $\theta_{ir}$  reference values were obtained from the regressions of equation (4) for the individual size fractions. These  $\theta_{ir}$  values were plotted as a function of  $D_i/D_B$ , where  $D_B$  is the median diameter of the subpavement bed material. The correlation yielded

$$\theta_{ir} = 0.0876(D_i/D_B)^{-0.982} \quad (5)$$

This definition of a  $W_{ir}^*$  reference transport rate, and accompanying reference  $\theta_{ir}$ , enabled Parker et al. to collapse the ten regressions of equation (4) for the individual size fractions into a single curve of  $W_i^*$  versus  $\theta_i/\theta_{ir}$ , given by

$$W_i^* = 0.002 \left( \frac{\theta_i}{\theta_{ir}} \right)^{m_i} \quad (6)$$

Parker et al. selected a weighted-mean value of 13.38 for the  $m_i$  exponent. In doing so, they noted that  $m_i$  actually increases with increasing  $D_i$  size fraction, and that this represents a departure from perfect equal mobility.

The above derivation is the first-order analysis of Parker et al. (1982), that which is based on an assumption of perfect equal mobility of different size fractions within the bedload. As seen in Figure 1A, the analysis provides a reasonable comparison between predicted and measured transport rates of gravel sieve-size fractions in Oak Creek. However, it should be recognized that in sediment transport predictions, an acceptable result is one where the predicted and measured values are within a factor of 5 or less. From that standpoint, this first-order solution would be acceptable in most applications. Therefore, the analysis has been a success in terms of predicting gravel-transport rates.

### The reference transport and grain threshold

Arguments by subsequent investigators in favor of the equal mobility hypothesis have focused mainly on the reference condition of equation (5) for  $\theta_{ir}$ . Most noteworthy is that the exponent is close to -1. From the definition of the Shields entrainment function, equation (2), the relationship of equation (5) is equivalent to

$$\tau_{ir} \propto D_i^{0.018} \quad (7a)$$

which indicates that there is only a very small dependence of the reference stress on  $D_i$ . With an exponent of -1 in equation (5), this becomes

$$\tau_{ir} \propto D_i^0 = \text{constant} \quad (7b)$$

indicating that there is no dependence on  $D_i$ . If the reference transport,  $W_{ir}^*$ , and its derivative  $\theta_{ir}$ , are thought of as a grain-threshold condition, then equation (7b) implies that all grain-size fractions are entrained at the same flow stress – i.e., there is an equal mobility of the several size fractions with respect to their entrainment.

The origin of equation (5) is somewhat circuitous. It begins with a comparison of  $W_i^*$  and  $\theta_i$ , equation (4), which actually involves an *a priori* assumption that the transport rate ( $W_i^*$ ) is inversely proportional to  $D_i$  which is found in the denominator of  $\theta_i$ . That assumption turns out to be incorrect, and this results in the horizontal displacements of the regressions of equation (4) parallel to the  $\theta_i$  axis. The analysis leading to equation (5) has the effect of undoing this initial assumption that  $W_i^* \propto 1/D_i$ . This circularity accounts for the near-perfect correlation found in establishing equation (5), with  $r^2 = 0.9997$  (Parker et al., 1982).

This does not detract from the usefulness of a reference transport rate  $W_r^*$  and equation (5) as employed by Parker et al. (1982) to collapse the regressions for the individual size fractions into a single relationship, equation (6). The reference transport can also be viewed as something of a threshold criterion for the several size fractions. However, equation (5) again obscures this threshold condition which should be thought of as some level of bedload transport which is the same for each size fraction. If we assume that the exponent in equation (5) is -1, then combining that relationship with the  $W_r^* = 0.002$  reference transport level and the  $W_i^*$  definition of equation (3), leads to

$$q_{sir} = 0.0000519 f_i (Rg)^{1/2} D_B^{3/2} \quad (8)$$

for the actual reference transport rate, having eliminated its dimensionless form. It is seen that  $q_{sir}$  lacks any direct dependence on individual  $D_i$  sizes, but is proportional to  $f_i$  of the size fractions as found in the subpavement, and also depends on the  $D_B$  median of the subpavement. Both of these dependencies are reasonable for a threshold condition. The use of a small level of transport as a threshold criterion has been used in previous studies [see review by Miller et al. (1977)]. Those earlier studies involved the entire bedload transport, rather than individual size fractions. In formulating such a threshold criterion for a size fraction within the bedload, it is reasonable to have it proportional to the availability of that size in the stream bed (i.e., to  $f_i$ ), and to the overall grain size as represented by the  $D_B$  median of the bed material. This is in keeping with the quantitative definitions of grain threshold as developed by Neill and Yalin (1969) and extended by Wilcock (1988) in the context of applications to grain-size fractions.

It is of interest to explore just how much bedload transport is involved in the reference level established in the analysis of Parker et al. (1982). This can be calculated directly with equation (8) – the resulting  $q_{sir}$  for the 10 size fractions are given in Figure 2A. As expected from the formulation of equation (8) and its dependence on  $f_i$  of the subpavement, the resulting histogram of the transport rates of size fractions mirrors the grain-size distribution of the subpavement. The

histogram of Figure 2B gives the results expressed in terms of the numbers of particles transported in the size fractions for the reference transport rate. As expected, the reference transport involves thousands of grains in the small to medium-size fractions. There is a rapid decrease in numbers of grains in the coarser fractions. Even with several hours of transport at this low rate, no particles would be captured in the coarsest sieve fractions. The largest particles of the bedload samples, those employed in flow-competence evaluations (Komar, 1987a), are mainly found in still coarser sieve sizes than diagramed in Figure 2 and included in the analysis of Parker et al. (1982). Additional analyses show that the bedload transport contributed by those largest particles in almost all cases falls below the  $W_{r*} = 0.002$  reference level. It is apparent that the reference transport rate defined by Parker et al., which can be viewed as a type of threshold criterion, differs from the initial movement of the largest particles found in the bedload samples. There is no straight-forward way to relate the two approaches, which are conceptually different.

### Higher-order solutions

The first-order solution of Parker et al. (1982), that which assumes equal mobility, does not account for changing grain sizes of the bedload. It always yields the same distribution as the subpavement, just as seen in Figure 2A for the reference transport. As flow discharges or bed stresses increase, the quantities of transport of the size fractions are greater, but remain in the same proportions so that the resulting grain-size distributions are invariant. As noted in the Introduction, Parker et al. were aware that size-distributions of bedload samples from Oak Creek do undergo marked changes, and this induced them to develop a higher-order solution. Their initial attempt has been extended by Diplas (1987), who concentrated on variations in the  $m_i$  exponent of equation (4). Diplas noted that rather than being constant as assumed by Parker et al.,  $m_i$  ranges from 5.49 to 21.41 with increasing grain size, a 290% change. Diplas correlated  $m_i$  and  $D_i$  to obtain

$$m_i = 13.71(D_i/D_B)^{0.3214} \quad (9)$$

Bedload grain-size distributions calculated with this modified approach for a series of flow discharges are shown in Figure 3A. These were obtained by evaluating transport rates of the 10 size fractions, calculating the total bedload for a 1-hour interval, and then converting it to a grain-size distribution. The original 10 size fractions represent irregular sieve intervals, so some have been combined to yield the 8 size fractions given in Figure 3A, representing even  $1-\phi$  intervals. It is seen that this higher-order solution of Diplas (1987) yields a coarsening of the bedload grain sizes as the flow discharge increases, and even displays the development of asymmetry as found in actual bedload samples from Oak Creek (Shih and Komar, 1990a). This represents an obvious improvement over the equal-mobility approximation of Parker et al. (1982). As seen in Figure 1B, there is also a considerable improvement in the calculated transport rates of the size fractions when the Diplas (1987) solution is compared with the equal-mobility results (Figure 1A).

It is of interest that the modification by Diplas (1987) involved changes in the  $m_i$  exponents. It is apparent from the basic dependence of equation (4), that an increase in  $m_i$  for the coarser size fractions will enhance their transport rates relative to the finer fractions; this accounts for the coarsening of the bedload samples at the higher flow stages. In modifying the bedload computations, Diplas obtained nearly the same coefficients as given in equation (5) for the reference transport



condition, those obtained by Parker et al. (1982). The exponent was changed by Diplas to -0.943, and in spite of its still being close to -1, the results now yield realistic variations in grain-size distributions and, therefore, significant departures from equal grain mobility. It is apparent that variations in the  $m_i$  exponents are more important to arguments of equal mobility, or are at least represent a more sensitive test, than examinations of the reference transport and grain threshold conditions.

## ANALYSIS BASED ON GRAIN-SIZE DISTRIBUTIONS

A distinctly different approach has been taken by Shih and Komar (1990a, 1990b) to evaluate transport rates of the grain-size fractions in Oak Creek. It was first established that there is a systematic evolution of the bedload grain-size distributions, demonstrating that the distributions progressively become more skewed with increasing flow stage. Goodness-of-fit comparisons established agreement with the theoretical Rosin distribution at discharges in excess of 1 m<sup>3</sup>/sec, and empirical relationships were established between the peak mode grain size ( $k$ ) and spreading coefficient ( $s$ ) of the Rosin distribution with the flow stress and discharge (Figure 4A). The total gravel transport rate, also a function of the flow stress or discharge, was then apportioned within the frequency distribution of grain sizes to determine the distribution of fractional transport rates (Figures 4B and 4C). Among the advantages of this approach are that it yields smooth frequency curves of both the bedload grain-size distributions and transport rates, rather than being confined to histograms based on the sieve-size intervals that happened to be used in the original data analyses. If desired, the frequency curves can be "degraded" back into sieve-size evaluations of bedload grain sizes and transport rates. A series of calculated bedload grain-size distributions is shown in Figure 3B, both as the original smooth frequency curves as well as the derivative histograms. These provide a closer simulation of the changing bedload distributions in Oak Creek than does the Diplas series in Figure 3A. The analysis procedure yields the predicted versus measured transport comparison shown in Figure 1C – it is apparent from the respective diagrams in Figure 1 that the approach of Shih and Komar provides better predictions than either the equal-mobility approximation of Parker et al. (1982) or the modified analysis of Diplas (1987).

*Note: We are presently using the procedures developed by Shih and Komar to simulate evolving bedload grain-size distributions and fractional transport rates. This simply involves a change in the flow-stress dependencies of  $k$  and  $s$  of the Rosin distributions, and the dependence of the total bedload transport rate on the flow stage. This generates "data" for fractional transport rates of the series of sieve fractions, having manipulated the degree of overall changes in the bedload grain-size distributions and how they might approach the distribution of the bed material. The simulated "data" are being analyzed by the procedures of Parker et al. and Diplas to further establish how the reference equation (5) and the  $m_i$  exponents of equations (4) and (6) depend on varying degrees of evolution of bedload grain-size distributions. We had hoped to be further along so as to provide some discussion of the results here. We would like to add it later.*

## EQUAL MOBILITY AND FLOW COMPETENCE

### Correlations involving maximum-particle diameters

Subsequent investigations to test the relative mobility of gravels in streams have focused primarily on equation (5), rather than on examinations of the actual transport rates of the various size fractions or on the  $m_i$  exponents. As noted above, this is unfortunate in that

variations in  $m_i$  and the accompanying changes in bedload grain-size distributions provide a more sensitive test. The analyses have involved the largest particle sizes ( $D_m$ ) found in bedload samples, so that equation (5) was modified to

$$\theta_m = a(D_m/D_B)^b \quad (10)$$

where  $D_B$  is the median diameter of the bed material. This seemingly straight-forward change has led to confusion with respect to what actually constitutes equal grain mobility. Equation (10) is equivalent to the basic proportionality

$$\tau \propto D_m^{b+1} \quad (11)$$

since the other parameters ( $\rho_s$ ,  $\rho$  and  $D_B$ ) are constants for a given stream reach. It has been assumed by most investigators that a  $b = -1$  exponent provides evidence for equal mobility, just as it did in equation (5). Equation (11) then reduces to

$$\tau \propto D_m^0 = \text{constant} \quad (12)$$

Equations (11) and (12) are basically flow-competence relationships between the flow stresses and the maximum particle diameters entrained from a deposit of mixed sizes. For nearly all data sets of gravel movement in streams, the exponent of equation (11) is greater than 0 (i.e.,  $b > -1$ ), so that  $\tau$  increases with increasing  $D_m$ , the typical flow-competence correlation (Komar, 1987a, 1987b). The zero exponent of equation (12) implies the absence of such a relationship, making flow-competence calculations impossible. However, a more precise meaning of the condition inherent in equation (12) is unclear. It could be obtained, for example, by the collection of repeated samples at a fixed flow stage, so that  $\tau$  is essentially constant while there is a range of  $D_m$  values from the series of samples. With respect to flow-competence considerations, equation (12) denotes an extremely rapid change in  $D_m$  with little or no change in  $\tau$ . However, this is contrary to the basic premise inherent in the equal-mobility assumption for computations of gravel transport rates, that is, the grain-size distributions of the bedload samples (presumably including  $D_m$ ) do not change with the flow stress.

Rather than viewing the variations of maximum particle sizes as an aspect of grain threshold, it is more enlightening to consider the  $D_m$  values as part of the bedload grain-size distributions, and to examine how the total spectrum of sizes varies with the flow stage. This reversal makes the flow stress the independent variable, and  $D_m$  the dependent variable, a more natural consideration of the actual processes. Equation (10) then reduces to

$$D_m \propto \tau^{1/(b+1)} \quad (13)$$

However, now we can generalize to consider any grain-size parameter of the bedload distributions, so that the relationships become

$$\theta_x = a(D_x/D_B)^b \quad (14)$$

and

$$D_x \propto \tau^{1/(b+1)} \quad (15)$$

where  $D_x$  could variously be the medians ( $D_{50}$ ) of the bedload distributions, other percentiles ( $D_{60}$ ,  $D_{70}$ , etc.), as well as  $D_m$ . The condition of equal mobility in terms of there being no changes in bedload grain-size distributions now becomes

$$D_x \propto \tau^0 = \text{constant} \quad (16)$$

that is, all percentiles including  $D_m$  remain invariant, independent of  $\tau$ . From equations (15) and (16) we have  $1/(b+1) = 0$  and therefore  $b = \infty$ . Hence, viewing  $D_m$  as one of several parameters representing the bedload grain sizes yields a much different interpretation of equation (10). Furthermore, it is apparent in equation (15) that as  $b$  approaches -1, the value generally assumed to represent equal mobility, the  $1/(b+1)$  exponent rapidly increases, signifying that there are progressively greater changes in  $D_x$  for a given change in  $\tau$ . When  $b = -1$ , the relationship becomes  $D_x \propto \tau^\infty$ ; in effect, an instantaneous jump in  $D_x$  for an infinitesimal increase in flow stress  $\tau$ .

The measured  $D_m$  maximum diameters,  $D_{50}$  bedload median diameters and  $D_{90}$  percentiles for Oak Creek are plotted in Figure 5 as a function of the flow stress, the dependence indicated by equation (15). This is the data collected by Milhous (1973) at discharges in excess of the critical  $1 \text{ m}^3/\text{sec}$  when the pavement layer is mobilized, the same subset utilized by Parker et al. (1982) to establish the equal-mobility model. The line for  $D_{50}$  versus  $\tau$  is significantly steeper than that for  $D_m$ , establishing that for a give change in  $\tau$ , there is a larger variation in  $D_{50}$  than for  $D_m$ . The respective proportionalities are:

$$D_{50} \propto \tau^{8.9} \quad (17a)$$

$$D_{90} \propto \tau^{3.8} \quad (17b)$$

$$D_m \propto \tau^{2.8} \quad (17c)$$

Comparable relationships have been obtained for the other grain-size percentiles of the bedload distributions ( $D_{60}$ ,  $D_{70}$ , . . .  $D_{95}$ ). The exponents are intermediate between those for  $D_{50}$  and  $D_m$ , forming a continuous trend of decreasing exponents as  $D_x = D_{50}$ ,  $D_{60}$  . . .  $D_m$  shifts to coarser sizes (Komar and Carling, in review). This pattern reflects the development of increasing skewness in the grain-size distributions at higher flow stresses, as shown by Shih and Komar (1990a), with the  $D_{50}$  medians shifting most rapidly and  $D_m$  showing the least response to varying flow stresses. With respect to the equal mobility assumption that there are no variations in bedload grain sizes,  $D_m$  comes closest to that condition while the  $D_{50}$  medians represent the greatest departure. The proportionalities of equation (17) are equivalent to

$$\theta_{50} = \tau/(\rho_s - \rho)g D_{50} \propto (D_{50}/D_B)^{-0.89} \quad (18a)$$

$$\theta_{90} = \tau/(\rho_s - \rho)g D_{90} \propto (D_{90}/D_B)^{-0.74} \quad (18b)$$

$$\theta_m = \tau/(\rho_s - \rho)g D_m \propto (D_m/D_B)^{-0.64} \quad (18c)$$

The exponent of the  $\theta_{50}$  relationship comes closest to the  $b = -1$  value, in spite of the fact that  $D_{50}$  represents the greatest deviation from a condition of equal mobility as an approximation for computations of gravel-transport rates.

Rather than viewing the above results as the actual conditions required for application of the equal-mobility analysis to compute gravel transport rates, as developed by Parker et al. (1982), one can consider them as the transitional phase leading to that condition of equal mobility. This is evident for the Oak Creek data in Figure 5. By this interpretation, the shifts in  $D_{50}$  . . .  $D_m$  with increasing flow stresses represent an evolution in bedload grain-size distributions as they progressively approach the distributions of the bed material. The medians of the pavement and subpavement distributions are marked by arrows in Figure 5, and the line for the  $D_{50}$  medians of the bedload samples has been extrapolated (dashed portion) to illustrate how the transitional stage of increasing  $D_{50}$  might reach the  $D_{50} = \text{constant}$  condition necessary for application of the equal-mobility computations of gravel-transport rates. In our comparisons of the complete grain-size distributions (Shih and Komar, 1990b), we concluded that the bedload samples collected at the highest flow stages were approaching an approximate mixture of 70% subpavement and 30% pavement. That mixture yields the  $D_{50} = 3.5$  cm bedload median for the level "equal mobility" portion of the dashed curve in Figure 5. All of the percentiles, and  $D_m$ , should follow a similar evolution and at some high flow stage reach nearly-constant values determined by the bed material grain-size distribution.

This interpretation that the Milhous (1973) data from Oak Creek represent a transitional phase of rapidly evolving bedload grain-size distributions is certainly valid. It is unfortunate that Milhous did not obtain additional measurements at still higher flow stages in that Figure 5 implies that the change over to the  $D_x = \text{constant}$  equal-mobility condition must take place at only marginally greater flows (discharges on the order of  $5 \text{ m}^3/\text{sec}$ ). Recognition that the Milhous measurements represent a transitional phase explains the inadequacies of the equal-mobility approximation for calculating bedload transport rates. It is apparent that the assumptions made by that analysis, specifically that the bedload grain-size distributions are the same as the bed material and do not vary with flow stage, are not achieved in Oak Creek until discharges exceed about  $5 \text{ m}^3/\text{sec}$ .

A similar interpretation has been made by Ashworth and Ferguson (1989) for their bedload samples collected in three streams. They established that the medians and maximum particle sizes increase with flow stage, and concluded that the data represent selective size-sorting. Their measurements suggest the proportionalities  $D_{50} \propto \tau^{1.1}$  and  $D_m \propto \tau^{3.8}$  (obtained respectively from an approximate fit to their plotted data, and algebraic modification of their  $\theta_m$  versus  $D_m/D_B$  correlation). Their results differ from those obtained here for Oak Creek in that  $D_m$  changes more rapidly than  $D_{50}$ . The implication is that the bedload samples collected by Ashworth and Ferguson shift toward coarser sizes with increasing flow stage, but the distributions do not become progressively skewed as do those in Oak Creek. However, their trends for  $D_{50}$  variations are based mainly on data collected in the Lyngsdalselva, while variations in  $D_m$  are supported mainly by data from the Dubhaig and Feshie. Therefore, conclusions about evolving bedload grain-size distributions (skewness, etc.) are not possible without detailed analyses of the original samples. Their results do clearly establish, however, that the data represent a transitional stage of changing grain sizes, and that if true equal mobility is achieved, it will be at a higher flow stage than represented by their measurements.

### Comparisons of field data for $D_m$ variations

It is probable that most, if not all, of the studies that have examined  $D_m$  variations in streams are for data in the transitional phase with rapidly evolving grain-size distributions. In that case,

the closer the  $b$  exponent of equation (10) is to  $-1$ , the more rapid the transition of bedload grain sizes toward that of the bed material. Accordingly, this can be incorporated into a broader view of what constitutes equal mobility in a stream, one that includes the transitional phase of evolving bedload distributions as well as the final achievement of the true equal-mobility condition when  $D_x = \text{constant}$ . Then, the more rapid the transition (i.e., the closer  $b$  is to  $-1$ ), the sooner the equal-mobility approximation of Parker et al. (1982) could be used in transport calculations.

The results of several studies of  $D_m$  variations are compiled in Table 2, ordered with respect to magnitudes of the  $b$  exponents in equation (10). Oak Creek forms one extreme with  $b = -0.43$  if the total winter-1971 data of Milhous (1973) are used and  $b = -0.64$  if only the subset for  $Q > 1 \text{ m}^3/\text{sec}$  are employed (Komar, 1987a; Komar and Carling, in review). With the assumption that  $b = -1$  constitutes equal mobility, Oak Creek gravel entrainment and transport would represent the greatest departure, in spite of its well-developed pavement which should act to equalize mobility. In contrast, Great Eggleshope Beck yields  $b = -0.82$ , even though it has a minimal development of bed pavement (Carling, 1983; Komar and Carling, in review). This argues against the broad interpretation that for measurements in the transitional phase of changing bedload grain sizes, the stream that comes closest to  $b = -1$  due to regulated entrainment from a pavement layer represents equal mobility.

The listing in Table 2 shows that the studies of Andrews (1983) and Andrews and Erman (1986) obtained exponents closest to  $b = -1$  in equation (10). Andrews (1983) based his analysis on data from the East Fork River, Wyoming, obtained with a total bedload trap (Leopold and Emmett 1976, 1977), and from the Snake and Clearwater Rivers of Idaho, collected with a Helley-Smith portable sampler (Jones and Seitz, 1980). Andrews and Erman (1986) sampled gravel transport in Sagehen Creek, California, also employing a Helley-Smith sampler. The  $-0.87$  exponent obtained by Andrews (1983) is equivalent to the proportionality  $D_m \propto \tau^{7.7}$  so that a 3-fold increase in the flow stress, modest for most streams, results in a 4,700-factor change in  $D_m$ .

In analyzing the East Fork data, Andrews (1983) had to rely on the geometric mean of the coarsest sieve fractions of transported bedload, since the data collections did not include direct measurements of the maximum-size clasts. In order to test whether this procedure can still reflect the changing flow competence, we analysed the Oak Creek data in the same way, that is, by using the coarsest sieve fractions reported by Milhous (1973). The analysis yielded essentially the same empirical exponents as obtained utilizing the largest grain sizes transported. Therefore, it can be concluded that the reliance of Andrews on sieve fractions probably yielded reasonable results and does not account for his obtaining a  $b$  closer to  $-1$  than found in other studies.

The investigations that have obtained exponents closest to  $-1$  in equation (10) relied almost exclusively on portable bedload samplers, whereas the Oak Creek data (Milhous, 1973) and Great Eggleshope measurements (Carling, 1983) were both obtained with total bedload traps. This suggests that the spectrum of  $b$  exponents seen in Table 2 may have resulted in part from differences in sampling techniques. The potential sampling problems in using the Helley-Smith to determine the movement of the coarsest fractions is illustrated by the study of Andrews and Erman (1986) in Sagehen Creek, California. Their results are graphed in Figure 6 in terms of  $\theta_m$  versus  $D_m/D_B$  so as to provide a comparison with equation (10). It is seen that the data do yield an exponent  $b = -1$ . Andrews and Erman report that runoff during the two weeks of their sampling was the longest period of sustained high flows that had occurred in the previous 30 years. The largest particles captured in the Helley-Smith ranged up to a maximum 8.6 cm. However, their experiments at other times with tagged clasts showed that material of 10-cm diameter readily moves, even during flow stages that are significantly lower than when the Helley-Smith

measurements were made. It appears that in this particular study the Helley-Smith was unsuccessful in sampling the larger clast sizes required to evaluate flow competence and to provide an adequate test of equation (10). However, any systematic under-representation of  $D_m$  obtained by Andrews and Erman in their gravel sampling probably does not account for the plotting pattern of their data in Figure 6 and the resulting  $b = -1$  exponent. It would be reasonable to expect that as the flow stress increases in the stream, there would be greater problems in sampling the increasingly larger  $D_m$ . This would have the effect of increasing the slope of a  $\tau$  versus  $D_m$  regression, and a counter-clockwise rotation of the line fit to  $\theta_m$  versus  $D_m/D_B$ , that is, away from the  $b = -1$  condition. Instead, the  $b = -1$  result in Figure 6 for Sagehen Creek probably results from the measurements of  $D_m$  being random rather than representing systematic sampling errors. Further evidence for this is that the data collected by Andrews and Erman were obtained under a small range of flow stresses, the median diameters of the bedload samples showed little change (1.1 to 1.9 cm), while the maximum diameters varied more widely (5.2 to 8.6 cm). Using a random-number generator on a computer, constrained by similar ranges of stresses and  $D_m$  values, we obtained "data" that look very similar and yield  $b = -1$  in equation (10). If the flow stress were absolutely constant, then a plot of stream-derived data as  $\theta_m$  versus  $D_m/D_B$  simply constitutes a graph of  $1/D_m$  versus  $D_m$ , and the scattered  $D_m$  values yield a  $b = -1$  exponent. Thus, the closer the data is to random, the better the fit to equation (10) with  $b = -1$  and  $r^2 = 1$ .

Caution is, therefore, required in interpreting  $\theta_m$  versus  $D_m/D_B$  diagrams, particularly if the exponent is close to  $b = -1$ . This is more generally illustrated in Figure 7, employing the complete set of winter-1971 data from Oak Creek (Milhous, 1973). In Figure 7A the data are plotted as  $\tau$  versus  $D_m$ , a flow-competence comparison, while in Figure 7B the same measurements are presented as  $\theta_m$  versus  $D_m/D_B$ . The solid curve in Figure 7A is based on a fit of  $\tau$  versus  $D_m$ , and yields

$$\tau = 108 D_m^{0.569} \quad (19a)$$

Algebraic manipulation of this, using the constant values  $\rho_s = 2.85$  and  $\rho = 1 \text{ g/cm}^3$  and  $D_B = 2 \text{ cm}$  for the subpavement, yields

$$\theta_m = \tau/(\rho_s - \rho)g D_m = 0.044(D_m/D_B)^{-0.43} \quad (19b)$$

which has been plotted in Figure 7B. The dashed curves have been derived in reverse order, based first on a comparison of  $\theta_m$  versus  $D_m/D_B$ , and then simplified to  $\tau$  versus  $D_m$ . The corresponding relationships are

$$\tau = 125 D_m^{0.35} \quad (20a)$$

and

$$\theta_m = 0.045(D_m/D_B)^{-0.65} \quad (20b)$$

Equation (20b) was obtained by Komar (1987a) for the combined data of Milhous (1973), Carling (1983) and Hammond et al. (1984). It shows best agreement with the latter data sets, but from the  $\theta_m$  versus  $D_m/D_B$  comparison in Figure 7B, it would appear to represent the Oak Creek data as well. However, when the equivalent equation (20a) is plotted as  $\tau$  versus  $D_m$  in Figure 7A, it becomes apparent that the agreement is poor. Three of the data points that appear to substantiate the relationship in Figure 7B are now seen to be outliers. The data collected at low flow stages, particle sizes less than 5 cm, are seen in the  $\tau$  versus  $D_m$  comparison to have little or no trend of their own. However, these data are important in establishing equation (20b) in the  $\theta_m$  versus  $D_m/D_B$  comparison since they are strung out over a  $D_m/D_B$  range 0.4 to 2.3. That subset of

data from low-flow stages is essentially random, and taken alone yields an exponent  $b = -1$ . Therefore, the  $b = -0.65$  exponent in equation (20b) is a combination of the  $-1$  exponent from the random subset of data and the  $-0.43$  exponent which is based mainly on data collected at discharges greater than  $1 \text{ m}^3/\text{sec}$ .

The influence of a subset of random data is still more apparent in analyses of the  $D_{50}$  median diameters from the same Oak Creek bedload samples. The data are presented in Figure 8, again as  $\tau$  versus  $D_{50}$  and  $\theta_{50}$  versus  $D_{50}/D_B$ . There is a very tight correlation at stress levels above the critical stage for breakup of the armor, Figure 8A, which yields the relationship

$$\tau = 339 D_{50}^{0.152} \quad (21a)$$

Algebraic conversion to yield  $\theta_{50} = \tau/(\rho_s - \rho)gD_{50}$  versus  $D_{50}/D_B$  gives

$$\theta_{50} = 0.104(D_{50}/D_B)^{-0.848} \quad (21b)$$

which is seen in Figure 8B to agree with the principal data trend. The dashed line in Figure 8B is fit to the subset of data obtained at low flow stages which are again basically random. It is seen in Figure 8A that for this subset, there are large fluctuations in the measured medians of the bedload samples while the flow stresses have only a very small range of values. When plotted as  $\theta_{50}$  versus  $D_{50}/D_B$  in Figure 8B, this subset taken alone yields a  $b = -1$  exponent.

Some portion of the differences in degrees of sorting found by the various studies, represented by the  $b$  exponents tabulated in Table 2, is undoubtedly a product of contrasting environmental conditions. In the case of the Oak Creek versus Great Eggleshope Beck data, we have concluded that the differences in the  $b$  exponents result mainly from contrasting degrees of skewness of the bed materials in these two streams and how this regulates the evolution of the bedload grain-size distributions (Komar and Carling, in review). It was also shown in that study that the exponents in the competence relationships can be significantly affected by sampling intervals, whether the samples are collected over a relatively short period of constant stage (Oak Creek) or represent integrated samples over a complete flood cycle (Great Eggleshope). It is certain that there will also be systematic differences resulting from the use of total bedload traps, as employed by Milhous (1973) and Carling (1983), versus the use of portable samplers. It might be expected that this would affect  $D_m$  comparisons more than the  $D_{50}$  medians of the bedload distributions. Finally, it has been seen here that the resulting empirical coefficients can be greatly affected by the data analysis, specifically if the comparison is  $\theta_x$  versus  $D_x/D_B$  or  $\tau$  versus  $D_x$ . It is probable that the range of empirical coefficients compiled in Table 2 result mainly from these systematic differences in experimental and analysis techniques, which unfortunately obscure potential environmental factors.

## SUMMARY AND DISCUSSION

An assumption of equal grain mobility by Parker et al. (1982) proved to be a reasonably successful first-order approximation for calculations of bedload transport rates of grain-size fractions in gravel-bed streams. The essence of the equal-mobility analysis is that at some low-flow stage all grain sizes are entrained in their relative proportions found in the bed material, and as the flow increases the transport rates of the size fractions increase but remain in those initial proportions. Therefore, according to the equal-mobility model, the bedload

grain-size distributions are always the same as found in the bed material and do not change with flow stage.

This assumption of constant bedload grain-size distributions constitutes the most obvious failure of the equal-mobility hypothesis. In Oak Creek the bedload distributions become progressively coarser with increasing flow, and become systematically more skewed as they approach the distribution of the bed material. Estimates here indicate that agreement between bedload and bed-material distributions is not achieved in Oak Creek until discharges exceed about 5 m<sup>3</sup>/sec. The data of Milhous, therefore, represent a transitional phase of evolving bedload transport and size distributions rather than a condition of true equal mobility. This requires higher-order transport calculations than provided by the equal-mobility assumption, approaches that have been developed by Diplas (1987) and Shih and Komar (1990b). Diplas modified the basic analysis of Parker et al. (1982), while Shih and Komar developed an approach that more closely follows the evolving bedload grain-size distributions. Both analyses predict changing bedload grain sizes (Fig. 3) as well as yielding improved estimates of transport rates (Fig. 1).

Most subsequent studies designed to test the equal mobility of gravel transport in streams have focused on the reference transport condition, and the derivative equation (5) which has been viewed as a grain-threshold criterion. This is unfortunate in that the analyses by Diplas (1987) demonstrated that variations in the  $m_i$  exponents of equation (4) are more critical to changing grain-size distributions and the departure from equal mobility. The focus, instead, has been mainly on variations in the  $D_m$  maximum particle sizes in bedload samples, fitted to the empirical equation (10) as  $\theta_m$  versus  $D_m/D_B$ . The results have been interpreted in terms of grain threshold, an extension of equation (5) for the series of size fractions. It has been argued here that equation (10) is better viewed as part of the changing bedload grain-size distributions,  $D_m$  being one of several grain-size parameters ( $D_{50}$ ,  $D_{60}$ , ...,  $D_{95}$ ,  $D_m$ ) that would reflect variations in distributions with flow stage. By this interpretation, the closer the exponent is to  $b = -1$  the more rapid the change in bedload grain sizes as they approach the distribution of the bed material. This could constitute a broader view of equal mobility in a stream where the presence of a pavement layer enhances the rate of this evolution (making  $b$  closer to -1). However, this interpretation is not borne out by comparisons of data from various streams. Oak Creek, with a classic development of pavement and subpavement sorting, yields a  $b$  exponent that departs most from -1 of the streams studied. It was concluded that this  $b$  exponent can reflect the development of skewness in the bedload samples as they approach the distribution of the bed material, as well as any influence of a bed pavement in regulating entrainment. In addition to these environmental dependencies,  $b$  can also be affected by sampling techniques and data analysis procedures. Unfortunately, the critical  $b = -1$  condition is most apt to represent random samples, data where the flow stress has a small range of values (typical for most streams) while fluctuations in  $D_m$  are large. This was illustrated with the Oak Creek data (Figs. 7 and 8), where it was seen that even when a small subset of the data is random or where there are outliers, a plot of  $\theta_m$  versus  $D_m/D_B$  tends to yield a steeper slope, one that is closer to  $b = -1$ . It was apparent in the analysis that it is preferable to first directly compare  $\tau$  with  $D_m$ , and then to algebraically derive  $\theta_m$  versus  $D_m/D_B$ .

The existence or degree of departure from equal mobility in a stream is best reflected in grain-size distributions of bedload samples and how they compare with bed-material distributions. There should be greater emphasis on documenting the complete distributions of bedload grain sizes and how they respond to varying flow stresses and discharges, rather than relying solely on the largest transported particles which tend to be affected by sampling techniques. Detailed analyses of bedload grain-size distributions are required if we are to



understand grain-sorting patterns and how they are controlled by environmental factors such as the presence of a bed pavement.

## REFERENCES CITED

- Andrews, E.D. (1983) "Entrainment of gravel from naturally sorted riverbed material", *Geol. Soc. Amer. Bull.*, **94**, 1225-1231.
- Andrews, E.D. and Erman, D.C. (1986) "Persistence in the size distribution of surficial bed material during an extreme snowmelt flood", *Water Resources Research*, **22**, 191-197.
- Andrews, E.D., and Parker, G. (1987) "Formation of a coarse surface layer as the response to gravel mobility", In *Sediment Transport in Gravel-Bed Rivers*, edited by C.R. Thorne, J.C. Bathurst and R.D. Hey, John Wiley & Sons, p. 269-300.
- Ashworth, P.J., and Ferguson, R.I. (1989) "Size-selective entrainment of bed load in gravel bed streams", *Water Resources Research*, **25**, 627-634.
- Carling, P.A. (1983) "Threshold of coarse sediment transport in broad and narrow natural streams", *Earth Surface Processes*, **8**, 1-18.
- Diplas, P. (1987) "Bedload transport in gravel-bed streams", *Jour. of Hydraulic Engineering*, Amer. Soc. Civil Engrs., **113**, 277-292.
- Hammond, F.D.C., Heathershaw, A.D. and Langhorne, D.N. (1984) "A comparison between Shields' threshold criterion and the movement of loosely packed gravel in a tidal channel", *Sedimentology*, **31**, 51-62.
- Jones, M.L., and H.R. Seitz (1980) "Sediment transport in the Snake and Clearwater Rivers in the vicinity of Lewiston, Idaho", U.S. Geological Survey, Water-Resources Investigations, Open-File Report 80-690, 179 pp.
- Komar, P.D. (1987a) "Selective grain entrainment by a current from a bed of mixed sizes: A reanalysis", *Jour. Sedimentary Petrology*, **57**, 203-211.
- Komar, P.D. (1987b) "Selective gravel entrainment and the empirical evaluation of flow competence", *Sedimentology*, **34**, 1165-1176.
- Komar, P.D. (1989) "Flow-competence evaluations of the hydraulic parameters of floods: an assessment of the technique", In *Floods: Hydrological, Sedimentological and Geomorphological Implications*, E. Beven and P. Carling (editors), John Wiley & Sons, p. 107-134.
- Komar, P.D., and Li, Z. (1988) "Applications of grain-pivoting and sliding analyses to selective entrainment of gravel and to flow-competence evaluations", *Sedimentology*, **35**, 681-695.
- Leopold, L.B., and Emmett, W.W. (1976) "Bedload measurements, East Fork River, Wyoming", *Proceedings of the National Academy of Sciences*, **73**, 1000-1004.
- Leopold, L.B., and Emmett, W.W. (1977) "1976 bedload measurements, East Fork River, Wyoming", *Proceedings of the National Academy of Sciences*, **74**, 2644-2648.
- Milhous, R.T. (1973) "Sediment transport in a gravel-bottomed stream", Unpublished Ph.D. thesis, Oregon State Univ., Corvallis, 232 p.
- Miller, M.C., McCave, I.N., and Komar, P.D. (1977) "Threshold of sediment motion in unidirectional currents", *Sedimentology*, **24**, 507-528.
- Neill, C.R., and Yalin, M.S. (1969) "Quantitative definition of beginning of bed movement", *Jour. Hydraulics Div., ASCE*, **95** (HY1), 585-587.
- Parker, G., Klingeman, P.C. and McLean, D.G. (1982) "Bedload and size distribution in paved gravel-bed streams", *Jour. Hydraulics Div., Amer. Soc. Civil Engrs.*, **108** (HY4), 544-571.
- Parker, G., and Klingeman, P.C. (1982) "On why gravel bed streams are paved", *Water Resources Research*, **18**, 1409-1423.
- Shih, S.-M., and Komar, P.D. (1990a) "Hydraulic controls of grain-size distributions of bedload gravels in Oak Creek, Oregon, USA", *Sedimentology*, **37**, 367-376.
- Shih, S.-M., and P.D. Komar (1990b) "Differential bedload transport rates in a gravel-bed stream: A grain-size distribution approach", *Earth Surface Processes and Landforms*.

- Weiberg, P.L., and Smith, J.D. (1987) "Calculations of the critical shear stress for motion of uniform and heterogeneous sediments", *Water Resources Res.*, **23**, 1471-1480.
- Wilcock, P.R. (1988) "Methods for estimating the critical shear stress of individual fractions in mixed-size sediment", *Water Resources Res.*, **24**, 1127-1135.
- Wilcock, P.R., and Southard, J.B. (1988) "Experimental study of incipient motion in mixed-size sediment", *Water Resources Research*, **24**, 1137-1151.
- Yalin, M.S., and Karahan, E. (1979) "Inception of sediment transport", *Jour. Hydraulics Div., Amer. Soc. Civil Engrs.*, **105** (HY11), 1433-1443.

## FIGURE CAPTIONS

Figure 1: Measured versus predicted transport rates of sieve-size fractions in Oak Creek: A. The equal-mobility analysis of Parker et al. (1982). B. The modified higher-order solution of Diplas (1987). C. The grain-size distribution approach of Shih and Komar (1990b). The individual sieve-size fractions are not identified here, but can be seen in the plots as presented in Shih and Komar (1990b).

Figure 2: A. The distribution of the  $q_{sfr}$  bedload transport rates for the individual size fractions, based on equation (3) which is equivalent to combining the  $W_{fr}^* = 0.002$  reference transport of Parker et al. (1982) with the derivative relationship, equation (5). B. The reference transport rate in terms of the numbers of grains found in each size fraction.

Figure 3: A. Grain-size distributions derived from calculated bedload transport rates obtained with the Diplas (1987) analysis approach. B. Frequency curves and derived histograms for bedload grain-size distributions calculated according to the approach of Shih and Komar (1990).

Figure 4: A schematic summary of the procedure of Shih and Komar (1990a, 1990b) for calculating bedload grain-size distributions and fractional transport rates. A. The Rosin distribution, with its mode size  $k$  and spreading coefficient dependent of  $\tau$  for the bedload size distributions in Oak Creek. B. The total bedload transport rate as a function of  $\tau$ . C. Partitioning the total transport into the distribution of sizes, to obtain frequency curves for the fractional transport rate as a function of  $\tau$ .

Figure 5: Changes in the maximum particle sizes ( $D_m$ ), the  $D_{90}$  coarse percentile and the medians ( $D_{50}$ ) of the Oak Creek bedload samples with varying discharges and bed stresses.

Figure 6: The data of Andrews and Erman (1987) from Sagehen Creek, yielding  $b = -1$  in eq.(10).

Figure 7: A. The Oak Creek flow-competence relationship for the flow stresses  $\tau$  versus the maximum particle sizes,  $D_m$ . B. Plotting of the same data in terms of  $\theta_m$  versus  $D_m/D_B$  where  $D_B$  is the median diameter of the subpavement.

Figure 8: A. The Oak Creek flow-competence relationship for the stresses  $\tau$  versus the  $D_{50}$  median diameters of the bedload samples. B. Plotting of the same data in terms of  $\theta_{50}$  versus  $D_{50}/D_B$ .

**Table 1** – List of the symbols used here, compared with those employed by Parker et al. (1982).

Meaning of Symbol	This Paper	Parker et al.
Grain diameter representative of sieve-size fraction:	$D_i$	$D_i$
Median diameter of subpavement bed material:	$D_B$	$D_{50}$
Median diameter of bedload sample:	$D_{50}$	--
Percentile sizes of bedload samples:	$D_{60}$ , etc.	
Largest particle diameter in bedload sample:	$D_m$	--
Frequency of $D_i$ sieve fraction in subpavement:	$f_i$	$f_i$
Exponents in transport relationships [eqs. 4 and 6]	$m_i$	$m_i$
Volumetric bedload transport rate of size fraction:	$q_{si}$	$q_{Bi}$
Dimensionless volumetric transport rate:	$q_{si}^*$	$q_{Bi}^*$
Normalized, dimensionless transport rate:	$W_i^*$	$W_i^*$
Grain density:	$\rho_s$	$\rho_s$
Water density:	$\rho$	$\rho$
Stream flow mean bed stress:	$\tau$	$\tau$
Shields entrainment function:	$\theta$	$\tau^*$

**Table 2** – Exponents in the  $\theta_m = a(D_m/D_B)^b$  empirical relationship obtained by various investigations.

	b	$D_m/D_B$
Oak Creek		
total data set	-0.43	0.4 - 6
$Q > 1 \text{ m}^3/\text{sec}$	-0.64	2 - 6
English Channel (Hammond et al.)	-0.58	0.4 - 5
Lyngsdalselva, Dubhaig and Feshie (Ashworth & Ferguson)	-0.74	0.1 - 2
Great Eggeshope Beck (Carling)	-0.82	1 - 25
East Fork, Snake & Clearwater (Andrews)	-0.87	0.3 - 6
Sagehen Creek (Andrews & Erman)	-1.	1 - 4

Figure 1:

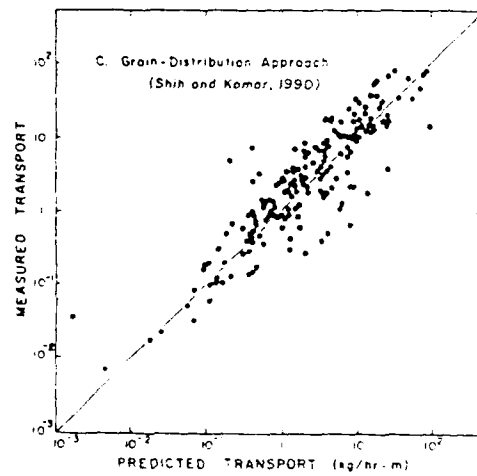
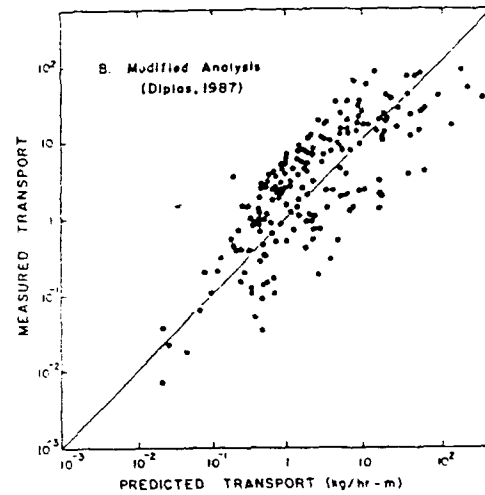
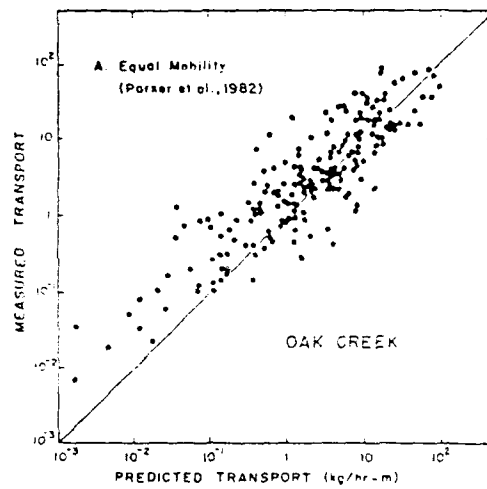
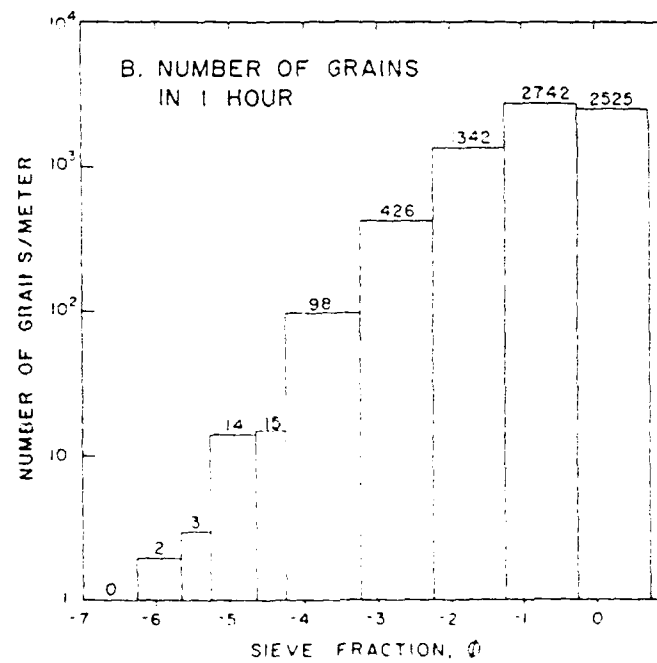
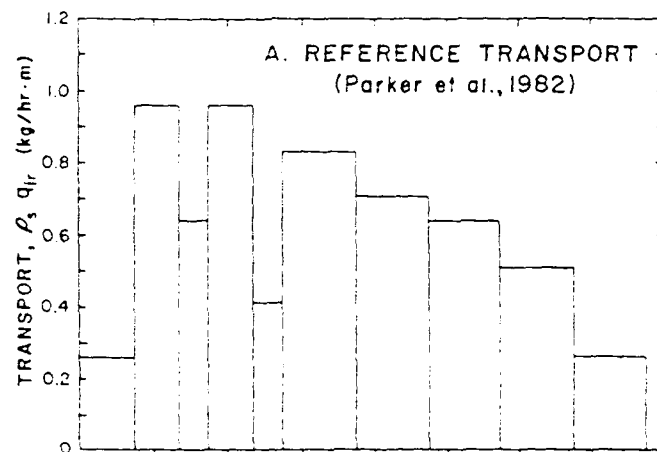
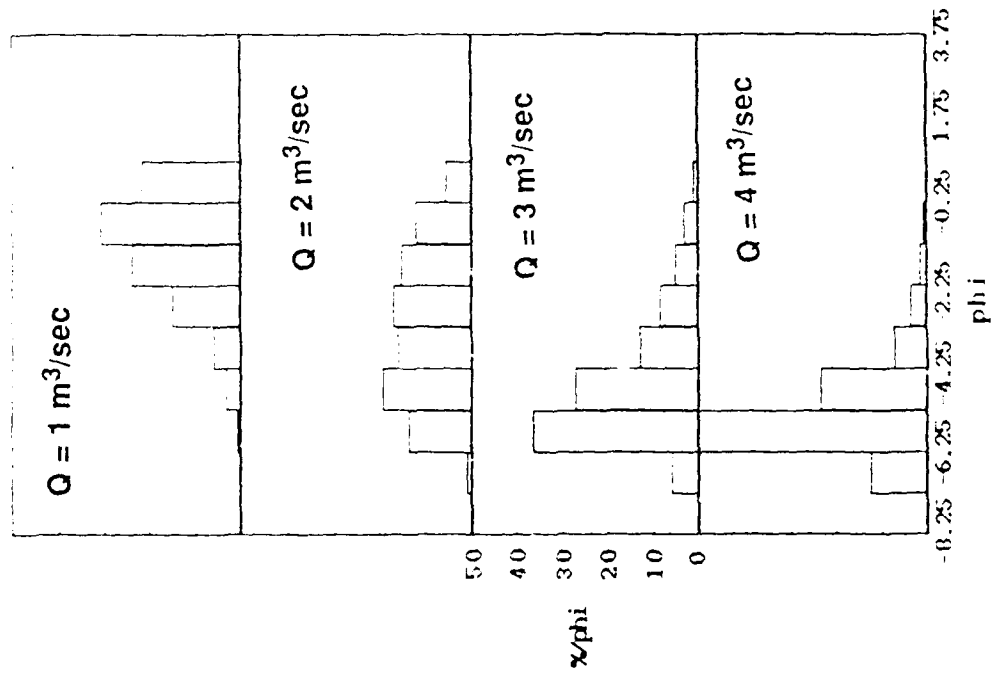


Figure 2:



# Predictions of Bedload Grain-Size Distributions

A. Diplas (1987)



B. Shih and Komar (1990)

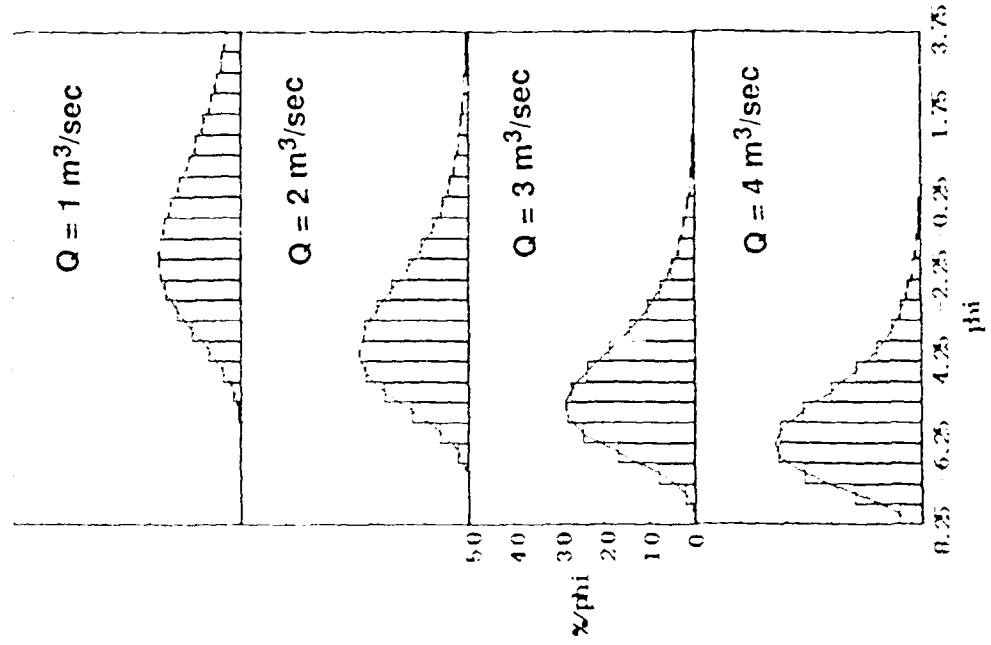


Figure 3:

# BEDLOAD GRAIN-SIZE AND TRANSPORT DISTRIBUTIONS

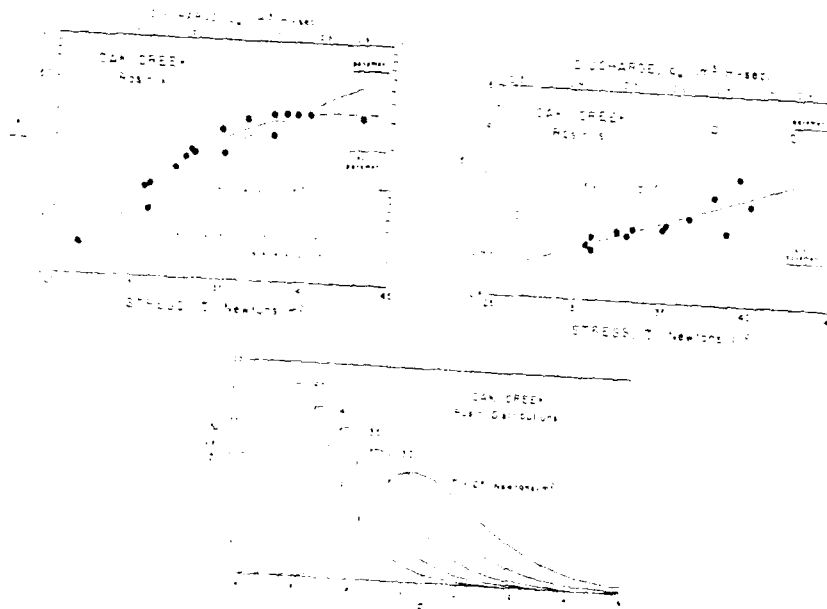
(Shih and Komar, 1990)

Figure 4:

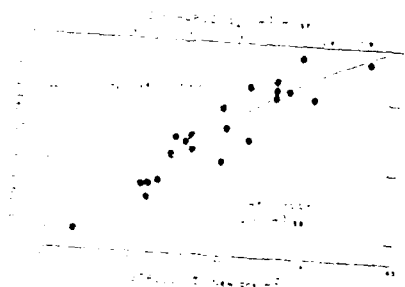
## A. Rosin Grain-Size Distributions

$$f(D_i) = 100 (s/k) (D_i/k)^{s-1} \exp[-(D_i/k)^s]$$

where  $k$  = grain size at peak frequency  
 $s$  = spreading coefficient



## B. Total Bedload Transport Rate, $q_b$



Note:

This figure will be redrafted to simplify the graphs and to make the summary more schematic.

## C. Fractional Transport Distribution

$$q_b(D_i, t) = q_b(t) f(D_i, t)$$

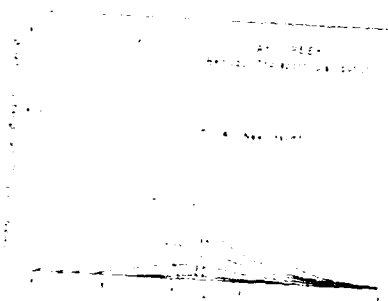


Figure 5:

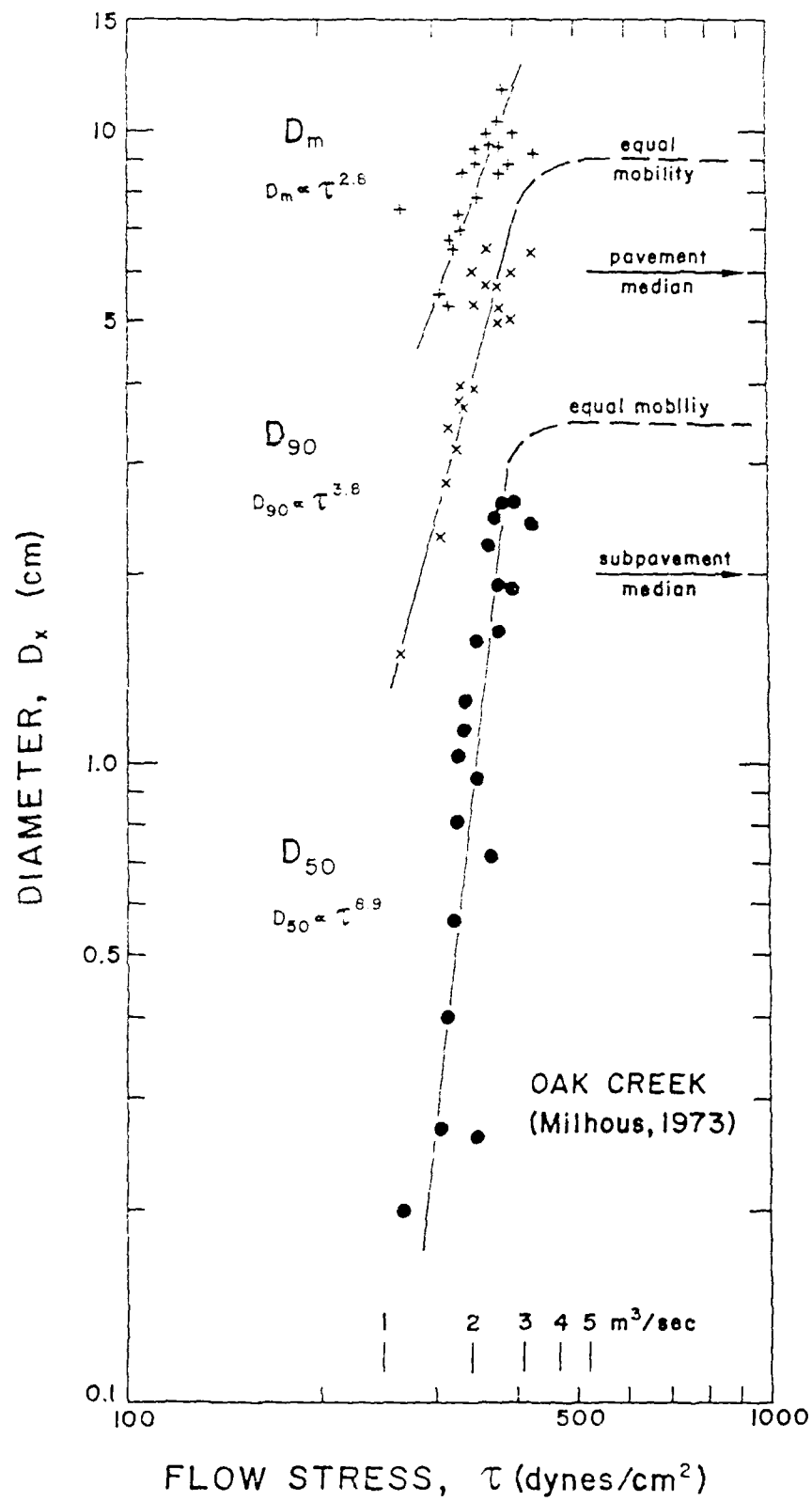




Figure 6:

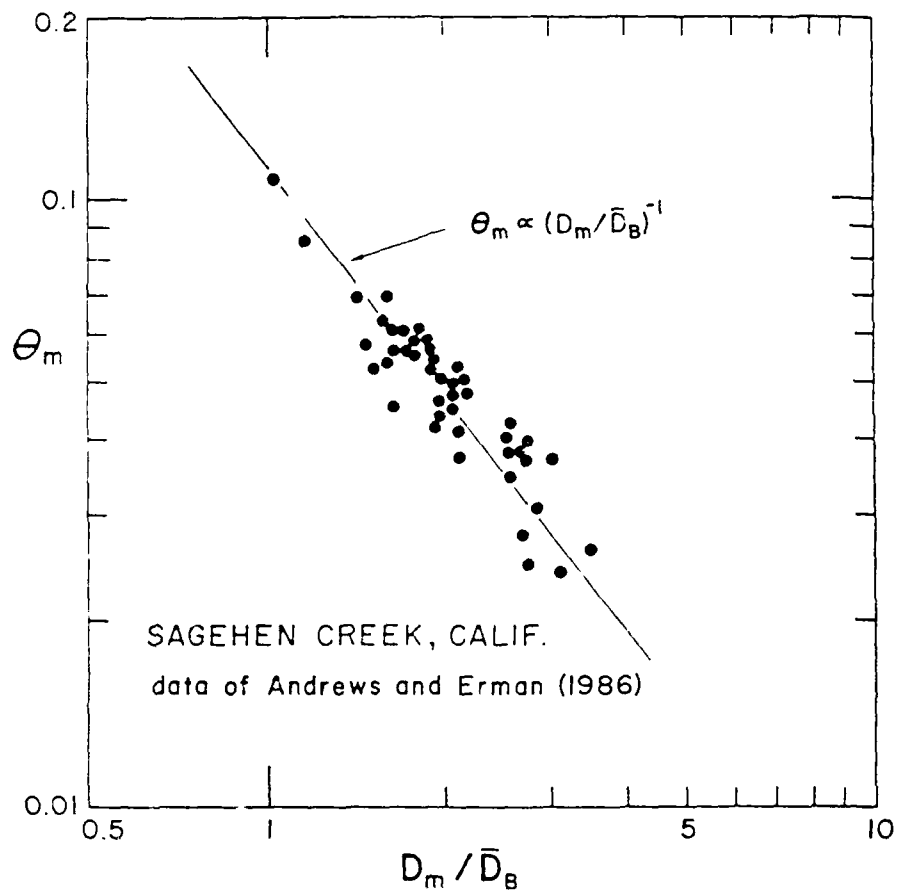


Figure 7:

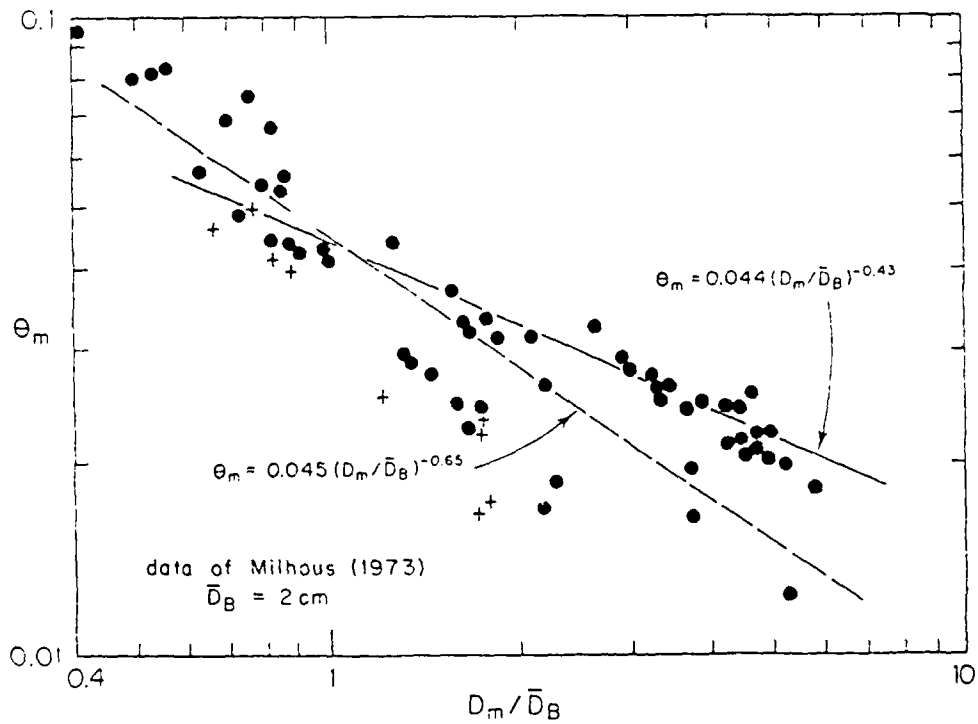
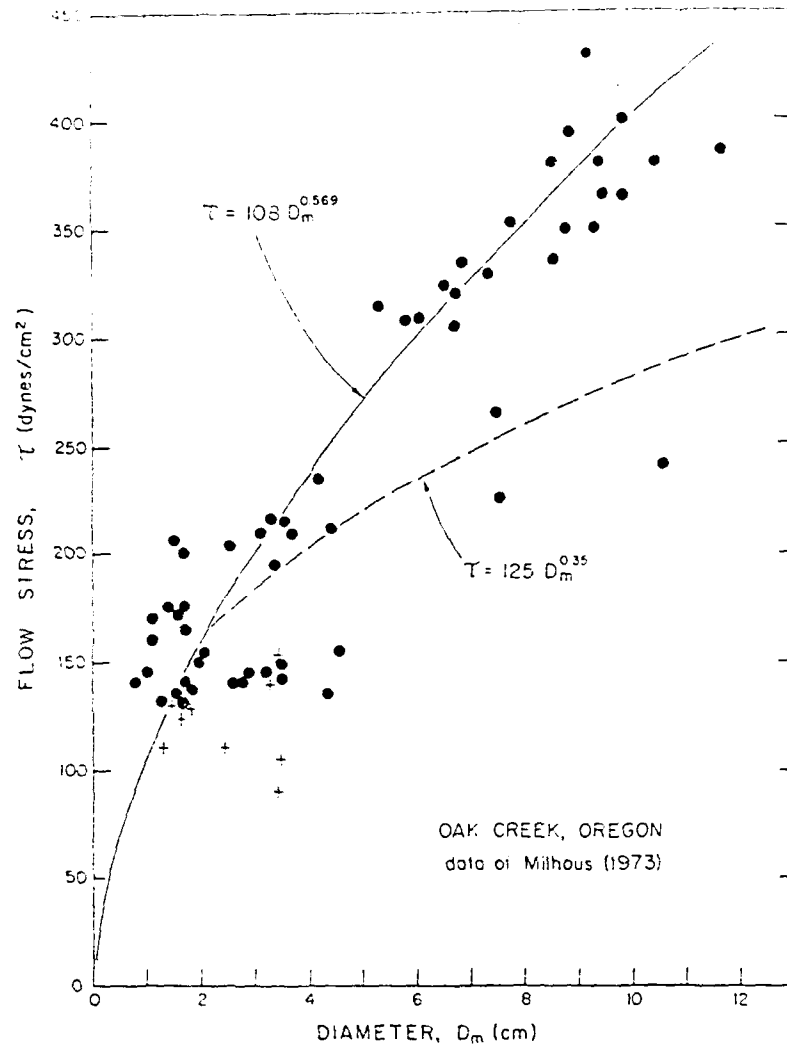
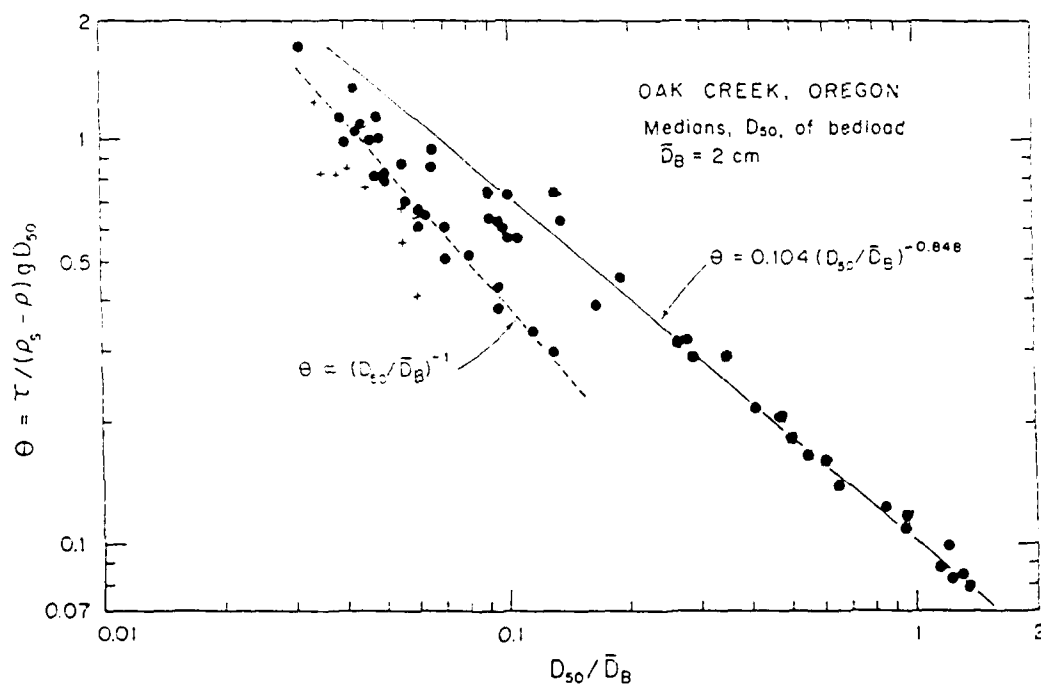
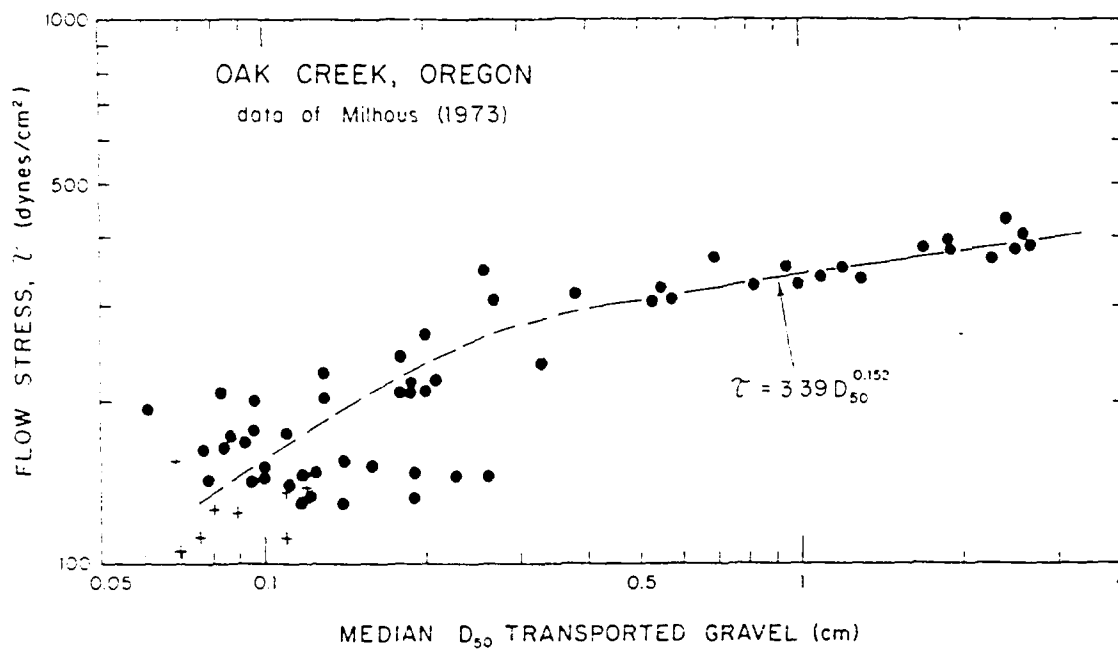


Figure 8:



3rd International Workshop on Gravel-bed Rivers

BED-LOAD TRANSPORT OF MIXED-SIZE SEDIMENT

Peter R. Wilcock

Department of Geography and Environmental Engineering

The Johns Hopkins University

Baltimore, Maryland 21218 USA

INTRODUCTION

In order to predict the response of mixed-size sediment to flow, it is necessary to predict the transport rates of the individual size fractions in the mixture. It has been well demonstrated that fractional transport rates depend strongly on relative grain size, which is most commonly expressed as  $D_i/D_m$ , where  $D_m$  is a central value of the bed grain-size distribution, commonly  $D_{50}$ . But  $D_i/D_{50}$  does not uniquely specify the relative grain size of individual fractions, so it is necessary to ask whether relative grain size effects are well described by  $D_i/D_{50}$  alone. Using a lognormal size distribution as an example, it is not immediately clear that the fractional transport rates for the fraction  $D_i/D_{50} = 2$  will be the same when it is on the coarse fringe of a mixture (98% finer than for  $\sigma_\phi = 0.5$ ) or closer to the center of the mixture (68% finer than for  $\sigma_\phi = 2.0$ ). Can a hiding function based on a single relative grain size parameter (e.g.  $D_i/D_{50}$ ) work for all sediment mixtures? Do fractional transport rates depend on the local bed shear stress  $\tau_o$  and  $D_i/D_{50}$  in the same fashion for all size mixtures?

The goal of this paper is to investigate the effect on fractional transport rates of different sediment mixtures. The results are reported from experimental work in which transport and flow observations were made over a range of flows for eight sediments, including five with a mixture of sizes. In three mixtures, only the mixture sorting was varied while the grain-size distribution shape and mean size of the sediment were held constant. In three other mixtures, the effect of bimodality was examined by using three bimodal sediments in which the proportion in each mode and the spread between modes was varied. Observations of the mixture effect on transport are also extended to other mixtures using field and flume data collected by others.

As in most things, it is true in sediment transport work that one sees only what one looks for. Beyond the basic experimental plan leading to the choice of sediment mixtures used in the experiments, the results reported here depend on the suite of variables measured in the transport experiments. The experiments and measurement program were designed to investigate the mixture effect on:

- (1) Incipient motion of individual size fractions (by clustering flows near initial-motion conditions).
- (2) Established motion of individual size fractions (by varying the flow by a factor of 2.5 or more in  $\tau_o$ )
- (3) The bed surface texture (using magnetic spray paint samples of the bed surface)
- (4) The bed configuration (using longitudinal profiles and bed descriptions)

The last three observations provide the opportunity to investigate the interaction among bed surface texture, bed configuration, and fractional transport rates, particularly as it effects our ability to predict mixed-size sediment transport.

EXPERIMENTAL MATERIALS, APPARATUS, AND METHODS

We report here on 58 experimental runs made with eight different sediments. General hydraulic and transport parameters for each run are given in Table 2. The experiments were conducted so that flow depth was held within a small range about 11cm while  $\tau_o$  varied over a wide range.

### Sediments

The heart of the experimental program is the range of different sediment mixtures used. General properties of these mixtures are shown in Figure 1 and Table 1. Table 1 also includes properties of sediments used by others whose transport results will be discussed in this paper. The effect of mixture sorting alone was examined using three sediments with the same mean size (1.83mm) and grain-size distribution (lognormal), but different values of mixture standard deviation  $\sigma_\phi = 0.2\phi, 0.5\phi, 0.99\phi$  for the mixtures MUNI, 1/2 $\phi$  and 1 $\phi$  respectively, where  $\sigma_\phi$  is the standard deviation of the size distribution when expressed in  $\phi$  units ( $\sigma_g = 2^{(\sigma_\phi)}$ , where  $\sigma_g$  is the geometric standard deviation of the size distribution expressed in mm). To provide comparison with the better understood unisize case, two additional, nearly unisize, sediments ( $\sigma_\phi \approx 0.2\phi$ ) were used. These are named FUNI and CUNI, and fall toward the fine and coarse ends of the 1 $\phi$  mix.

The next set of sediments reported on here were bimodal and incorporated parts of the nearly unisize FUNI, MUNI, and CUNI sediments. In considering additional mixture properties whose effect on transport we wished to examine, bimodal sediments were chosen for several reasons. For the lognormal sediments, we found that mixture sorting by itself had little effect on fractional transport, once  $D_{50}$  and  $D_3/D_{50}$  were accounted for. Therefore, it seemed unlikely that higher orders of the bed sediment grain-size distribution would produce important mixture effects. This conclusion was further supported by the fact that we observed similar and consistent initial-motion conditions for a variety of different sediment mixtures used by others, including rectangular, fine-skewed, and weakly bimodal grain-size distributions. A more likely mixture property that would cause observed mixture effects to break down would be bimodality. How far apart can the modes of a bimodal sediment be separated until the relatively consistent behavior observed for unimodal sediments no longer occurs? Does the proportion in each mode make a difference? Because many gravel-bed rivers have bimodal grain-size distributions (e.g., Shaw and Kellerhals, 1982), an investigation of the effect of bimodality on mixed-size sediment transport is of interest directly, as well as part of a general study of mixture effects on transport. Three bimodal sediments were used, one with equal amounts of MUNI and CUNI (MC50), one with equal amounts of FUNI and CUNI (FC50), and one with 67% FUNI and 33% CUNI (FC70).

### Apparatus

The experiments were conducted in two flumes, one at MIT and the other at the Johns Hopkins University (JHU). Both flumes have clear acrylic channels 0.6m wide and 0.3m deep. Some runs in the JHU flume were conducted with a 0.15m flow width. The MIT flume is considerably longer, with a working length of 22m compared to 11m at JHU. The operation of both flumes is identical. Water and sediment are recirculated separately. The water passes into a tailbox with no overfall and the mean flow depth is set by the volume of water in the flume. Uniform flow is obtained by adjusting the flume slope to match the water surface slope. All of the sediment is caught in a trap at the downstream end of the flume and recirculated with a small amount of water using an air-driven double-diaphragm pump. Sediment transport is sampled by intercepting the sediment/water mixture leaving the trap and passing it through a sieve that removes all of the sediment and allows the water to be recirculated. An open-air, gravity-driven sampling system was chosen to provide maximum flexibility in sampling methods and periods (sample intervals from 10s to 4 hours were used) and to allow convenient removal of samples for size analysis. The capability of sampling the entire transport load and removing samples of this load for size analysis are requirements for accurate mixed-size sediment transport work.

An upstream portion of each flume bed was artificially roughened to allow the boundary layer to become developed before encountering the loose sediment bed. Water discharge was determined using calibrated head-loss

sections in the water return pipe. Mean flow depth and water surface slope were determined using a point gage mounted on a cart that traversed rails parallel to the flume floor.

Samples of bed surface texture were taken by spray-painting an area of the bed 12.7 cm in diameter with a mixture of paint and fine magnetite. Surface grains (defined as those having any paint on them) were removed from the sample with a strong hand magnet. Some additional separation was necessary to remove unpainted grains that had adhered to painted grains during removal of the sample from the bed. This technique (Wilcock and Stull, 1989) was developed because manual removal of painted grains finer than 1 or 2mm was found to be impossibly tedious. We prefer the magnetic-paint technique because it allows direct observation of the sample and thereby provides an accurate check that all grains on the surface have been sampled, and that the sample contains only those grains that were on the bed surface. A considerable controversy exists as to whether areal surface samples, such as those collected by the paint or clay techniques, may be compared with samples taken volumetrically, such as by removing a predetermined volume of sediment from the bed (Church et al., 1987; Diplas and Sutherland, 1988). We have chosen to sidestep this problem by making comparisons only among samples taken with identical techniques. Transport samples are compared only with each other and use the volumetric grain-size distribution of the sediment mixture as a reference. Surface samples are compared only to other surface samples and use as a reference surface samples taken with the same method from the bed at its start-up condition. Although limiting ourselves in this fashion prevents us from making direct comparisons between particular transport and bed-surface grain-size distributions, it does allow us to make unambiguous comparisons of the different transport and bed surface grain-size distributions, which is one of our goals in this paper.

#### Procedure

The sediment was entirely homogenized and screeded to a plane bed before each run. After filling with water, a run was begun by adjusting the flume slope and discharge to a value close to that needed for uniform flow. Flow and transport measurements were made after long-term steady transport became established. In early experiments (Wilcock and Southard, 1988), equilibrium was judged by the absence of long-term variability in the flow properties (related to the development of a stable bed configuration) and in the size distribution of the transported sediment (related to the development of a stable grain-size distribution on the bed surface). To avoid any significant impact on the sediment bed and transport rates during the run, intermediate samples were not taken and final equilibrium was assumed to have been established when the run duration was greater than or equal to sufficient values in previous runs. While the transport sampling was underway, the water-surface elevation was read and the head loss in the return pipe was measured for later conversion to water-surface slope and discharge. After each run, the flume was drained, the bed was described and photographed, a profile of the bed elevation along the flume centerline was made, and bed-surface samples were taken.

#### Estimating Bed Shear Stress

Because bed forms were present in many runs, an estimate of the skin-friction portion  $\tau_o'$  of the total bed shear stress was necessary. Different models were evaluated in an attempt to derive the best estimate of the skin friction. Unfortunately, very limited means exist to evaluate the accuracy of skin-friction estimates. The only sensitive test available to us was to evaluate the degree to which a given skin-friction estimate decreases the observed scatter in the transport rate. In this regard the drag-partition model of Einstein (1950) performed best. This model involves a fictitious flow hydraulic radius  $R'$  that corresponds only to the skin friction and is computed iteratively from a Keulegan-type profile

$$\frac{U}{\sqrt{gR'S}} = \frac{1}{\kappa} \ln \left( \frac{R'}{2.718z_0} \right) \quad (1)$$

where  $U$  is mean channel velocity,  $g$  is the acceleration of gravity,  $S$  is the water slope,  $\kappa$  is von Karman's constant, taken here to be 0.4, and  $z_0$  is roughness length characteristic of the sediment bed. A value of  $z_0 = D_{65}/30$  was found to give a good approximation of the roughness for the unimodal sediment beds for flows with plane beds and little or no transport. For the bimodal beds, the mean grain size of the coarse mode (5.66mm) was used in place of  $D_{65}$  because the coarse grains clearly protruded from the bed at low flows and presumably controlled the bed roughness. Because the primary use of the bed shear stress data in this paper is to determine a critical shear stress, no corrections were made for an increased roughness attributable to moving grains. To provide a good estimate of bed shear stress and transport rates near incipient motion, several runs with each sediment were clustered about initial-motion conditions. The transport rates of these plane-bed runs fell near the reference value used to estimate the critical shear stress of each fraction. At least two runs with a plane bed were conducted for each sediment. For these runs,  $\tau_o' = \tau_b$ , the total bed shear stress, and  $\tau_o'$  can be determined with much better accuracy than for runs with bed forms. For plane-bed runs, values of  $\tau_o'$  were found to be nearly identical to values of  $\tau_b$  given by sidewall correction formulas (Vanoni and Brooks, 1957; Shimizu, 1990). For consistency, (1) was used to compute  $\tau_o'$  for all runs.

## INITIAL MOTION

### Method

The initial-motion conditions, or critical shear stress  $\tau_{ci}$ , of individual fractions in a mixed-size sediment have typically been determined using one of two different classes of methods. The first method involves estimating  $\tau_{ci}$  as a reference bed shear stress  $\tau_{ri}$  that produces a small transport rate for each fraction. Transport rates of individual fractions are measured for a number of flows and the shear stress that corresponds to the reference transport rate is determined from a fitted relation between dimensionless shear stress and dimensionless transport rate for each fraction (Parker et al., 1982; Day, 1980b). The second method involves determining the largest clast in a sediment mixture that is moved by a given bed shear stress. The largest grain displaced may be measured directly using the largest clast found in a transport sample (Andrews, 1983; Carling, 1983) or measured visually by observing the largest grain moving over an area of the bed (Hammond et al., 1984). The largest mobile grain is assumed to represent initial-motion conditions if coarser grains are available in the bed. Wilcock (1988) describes and compares these methods in some detail. In this paper, the reference-transport method is used to estimate  $\tau_{ci}$ . This is because the largest-grain method suffers from serious sample-size effects and because it may not be used to properly scale the estimates of  $\tau_{ci}$  so that they may be compared between fractions (Wilcock, in review). The reference transport method was also used because, for some of the mixtures, all sizes were found to be in transport even at the lowest transport rates. Under these conditions, the largest-grain method provides no information on  $\tau_{ci}$  for any fraction other than the coarsest and may not be used.

The reference transport method used here to estimate  $\tau_{ci}$  is based on that used by Parker et al. (1982) wherein the reference transport rate is defined as a constant value of the fractional-transport parameter  $W_i^*$ ,

$$W_i^* = \frac{(s-1)g q_{bi}}{f_i (\tau_o/\rho)^{3/2}} \quad (2)$$

where  $s$  is the ratio of sediment and water density  $\rho_s/\rho$ ,  $f_i$  is the proportion of fraction  $i$  in the sediment bed,  $q_{bi}$  is the fractional transport rate computed as  $p_i q_b$ ,  $p_i$  is the proportion of fraction  $i$  in the transport, and  $q_b$  is mass

transport rate per unit width. A reference transport method based on the Ackers and White (1973) transport model has also been used by Day (Day, 1980b; White and Day, 1982). A comparison of the two methods is given by Wilcock (1988) and Wilcock and Southard (1988). The Parker et al. method is used here because grain size is not present in  $W_i^*$  and the  $\tau_{ri}$  values are, therefore, undistorted with respect to grain size, a considerable convenience when comparing  $\tau_{ri}$  among different size fractions.

Values of  $\tau_{ri}$  were determined by fitting a transport relation to plots of  $W_i^* - \tau_{ri}^*$  for each fraction, where  $\tau_{ri}^*$  is the Shields parameter  $\tau_o/(s-1)\rho g D_i$  formed using the fraction size. To preserve the grain size independence of the fitting procedure, a single transport curve was fitted to the data for each fraction and this curve was translated only parallel to the  $\tau^*$  axis. Because the transport data show a concave-downward trend, a curved transport relation was used. The relation chosen is a power approximation of the Einstein (1950) bed-load function at low stresses derived by Parker (1979)

$$W_i^* = 11.2 \left( 1 - \frac{0.8531 \tau_{ri}^*}{\tau_i^*} \right)^{4.5} \quad (3)$$

This curve was fitted by eye to the transport data for each fraction. Its position was primarily determined by the position of data points located near the reference transport rate  $W_{ri}^* \approx 0.002$ . The accuracy of the fit is dependent on points found near or below  $W_{ri}^*$ , so some runs with each mixture were clustered at low transport rates. The fit of (3) to the data at higher transport rates was generally good for our data, although this fit was of minor concern because of the presence of data points near  $W_{ri}^*$ . The fit of (3) to the  $W_{ri}^* - \tau_{ri}^*$  data of others was more important, because some of these data did not include transport rates near  $W_{ri}^*$ . Under these conditions, the use of a curved transport relation such as (3) provided a more reasonable estimate than the straight log line used previously (Parker et al., 1982). For each fraction, an estimate of the error in  $\tau_{ri}^*$  was determined by recording values of  $\tau_{ri}^*$  when the transport curve was moved as far as possible to the right and left while still providing some conceivable fit to the fractional transport data. Because of the subjective nature of the process, these error bounds were made as large as possible. The error bounds were typically on the order of 10% and do not affect the conclusions drawn in this paper. For clarity, the error bounds are not shown on the figures presented here.

### Test of Sorting

Figure 2 presents  $\tau_{ri}$  for the two lognormal mixed-size sediments and the three unisize sediments. Comparison of  $\tau_{ri}$  between fractions of the same size (and therefore the same  $D_i/D_{50}$ ) in the  $1/2\phi$  and  $1\phi$  mixtures clearly demonstrates that the relative-size effect on  $\tau_{ri}$  can be well characterized by only one relative-size parameter, in this case  $D_i/D_{50}$ . Even though the sorting differs by a factor of two between the two mixtures and, therefore, the percentile value for a given fraction differs between the two mixtures,  $\tau_{ri}$  is identical for two fractions with the same  $D_i$  (and  $D_i/D_{50}$ ). Beyond showing that mixture sorting does not affect  $\tau_{ri}$  for these mixtures, once  $D_i/D_{50}$  is specified, Figure 2 also shows that for these sediments  $\tau_{ri}$  does not vary with  $D_i$  (or  $D_i/D_{50}$ ). This is part of the equal mobility concept, which will be discussed further below. Because only mixture sorting varies between the  $1/2\phi$  and  $1\phi$  mixtures, Figure 2 clearly demonstrates that mixture sorting does not effect  $\tau_{ri}$ , once the effect of  $D_i/D_{50}$  is taken into account. It also shows that the absence of a sorting effect is evident in sediments that range from poorly sorted to unisize.

Figure 3 presents initial-motion relations in terms of  $\tau_{ri}^*$  against  $S^*$  ( $=[D_i^3(s-1)g]^{1/2}/v$ ), a convenient alternative to the grain Reynolds number found in the classic Shields curve. Shown in this plot are our data, along with our estimate of  $\tau_{ri}^*$  for the other, previous published, data. On this curve, an absence of size dependence in  $\tau_{ri}$



plots as a line with slope of  $-3/2$ . The slopes of all these curves fall within the narrow range of  $-1.31$  to  $-1.59$ , which means that the exponent  $b$  of the relation

$$\tau_{ri} = a \left( \frac{D_i}{D_{50}} \right)^b \quad (4)$$

falls between  $0.19$  and  $-0.09$ . Only one of the values of  $b$  differs from  $0.0$  by more than  $0.1$ . This is the value of  $0.19$  for sediment A of Day (1980), which was the only sediment for which no values of  $W_i^*$  fell close to  $W_r^*$ , making it the least certain of the sets of  $\tau_{ri}$  values. The narrow range in the observed values of  $b$  is striking, because the experimental control behind our data in Figure 2 is not maintained in Figure 3. Even though the mixture sorting of the sediment in Figure 3 varies from  $0.19\phi$  to  $2.1\phi$ , there is no consistent trend between mixture sorting and the  $\tau_{ri}-D_i/D_{50}$  slope. This provides more general empirical support for our controlled experimental result. In addition to the broad variation in mean size and sorting evident in Figure 3, other potentially important independent variables, such as relative depth, grain Reynolds number, and mixture grain-size distribution, vary between the mixtures but do not apparently influence the observed  $\tau_{ri}-D_i/D_{50}$  relations. Also shown on Figure 3 is the Shields curve for incipient motion of unisize sediment. Even though the mixtures examined here are broadly distributed across the plot and extend to varying degrees into the transitionally rough and smooth turbulent ranges of the figure, the form of the  $\tau_{ri}$  plots are remarkably consistent.

Although the relative-size effect is well explained by  $D_i/D_{50}$ , the separation between the various curves on Figure 3 is a result of the absolute size of each mixture. Figure 4 presents a plot of  $\tau_{r50}$  ( $\tau_{ri}$  for  $D_{50}$ ) against  $D_{50}$  for each mixture, which shows that the Shields value for  $D_{50}$  predicts  $\tau_{r50}$  well (a value 88% of the Shields value provides the best prediction of  $\tau_{r50}$ ).

#### Test of Bimodality

Figures 3 and 4 suggest that remarkably consistent incipient-motion relations exist for individual fractions in a wide range of mixtures. One of our goals in performing experiments with bimodal mixtures was to see if these results might hold for a broader range of mixtures. Figure 5 present values of  $\tau_{ri}$  for three bimodal mixtures, along with our unimodal mixtures. For the MC50 mixture, which contains equal parts of two modes separated in size by a factor of 2.8, the results are similar to those for the unimodal sediments.  $\tau_{ri}$  is essentially the same for all sizes, and the critical shear stress for the entire mixture is well represented by the Shields value for  $D_{50}$ . These results are also similar to those we obtained using the fractional transport rates measured with four bimodal mixtures by Misri et al. (1984). In their experiments, the two modes were separated in size by a factor of 2.6. Our estimate of  $\tau_{ri}$  from these data show that all sizes begin moving at a single shear stress that is well represented by the Shields value for  $D_{50}$ .

The mixtures FC50 and FC70, which are composed of the FUNI and CUNI sediments and separated in size by a factor of 8.0, show strikingly different results. The two different modes in each have significantly different values of  $\tau_{ri}$ . For FC50, which has equal proportions of the two modes, the coarse fractions have  $\tau_{ri}$  similar to MC50, but  $\tau_{ri}$  for the fine fractions are smaller by a factor of almost three. The fine fractions begin moving at a much lower shear stress than the coarse fractions. For FC70, in which 67% of the bed sediment is composed of FUNI, values of  $\tau_{ri}$  for both modes are smaller by a factor of about 1.5 relative to FC50.  $\tau_{ri}$  values for the coarse fractions in FC70 are the same as those for identical fractions in the  $1\phi$  mixture, suggesting the existence of a minimum value of  $\tau_{ri}$  for coarse fractions in FC mixtures. It is important to note that the difference in  $\tau_{ri}$  between FC50 and FC70 is due to the proportion in each size fraction only, and, therefore, cannot be accounted for by  $D_i/D_{50}$  alone. For FC50, the critical shear stress of the entire mixture is well represented by the Shields value for  $D_{50}$  (if  $D_{50}$  is approximated as the geometric mean of the two modes, even though no sediment of that size is found in the mixture). This is not

the case for FC70, in which  $D_{50}$  falls within the fine mode and the Shields value for this fraction is too low. Also, the Shields value for the geometric average of the two modes (which equals  $D_{50}$  for FC50, but not FC70) does not provide a good estimate for the critical shear stress of the FC70 mixture. The lower values of  $\tau_{*i}$  for the FC70 mixture are consistent with the concept that a finer sediment bed will decrease the resistance to motion and increase the flow exposure of any given size fraction, but prediction of  $\tau_{*i}$  for strongly bimodal sediments is clearly not as simple as for unisize, unimodal, or weakly bimodal sediments.

### ESTABLISHED MOTION

The effect of relative grain size (and, hence, sediment mixture properties) is not necessarily limited to incipient motion only. Once a sediment is in motion, the transport rate of each fraction may be a function of  $D_i/D_{50}$  and mixture properties, even when size-dependent variation in  $\tau_{*i}$  is accounted for. The degree to which mixture effects on fractional transport rates are evident depend on the manner in which the data are presented. Most commonly used is a dimensionless plot of transport rate versus the fractional Shields parameter  $\tau_{*i}$ . Such a plot, using  $W_i^*$  vs.  $\tau_{*i}$ , is shown in Figure 6a for the 1 $\phi$  mixture. This plot immediately suggests that a simple similarity transformation may be used to collapse the data to a single trend, as has been done by Parker et al. (1982), White and Day (1982), and others. In the case of the 1 $\phi$  mixture, the incipient motion results discussed above suggest that such a collapse may be achieved by simply replacing  $\tau_{*i}$  with  $\tau_{*i}/\tau_{*i}$ . For  $\tau_{*i} = \tau_{*r50}$ , this transformation is equivalent to  $\tau_o/\tau_{50}$ . Unfortunately, this view of the fractional transport rates hides important aspects of the problem which can lead to errors of greater than an order of magnitude when predicting fractional transport rates. The chief problem is that the plot in Figure 6a obscures very large differences in  $q_{bi}$  from fraction to fraction. This problem is illustrated in Figure 6b, which presents the fractional transport rates for the same sediment and flows as Figure 6a, but in this case using a dimensional form of the fractional transport  $q_{bi}/f_i$ , as a function of grain size expressed as  $D_i/D_{50}$ . It is immediately apparent from Figure 6b that  $q_{bi}$  varies by as much as two orders of magnitude over all sizes for a given run.

Figure 6b may be thought of as a plot of the transport grain-size distribution expressed as  $p_i/f_i$  and scaled by  $q_b$ . This figure is well suited for examining the existence of equal mobility in the fractional transport rates. The complete definition of equal mobility is simply  $p_i = f_i$ , that is, the transport grain-size distribution is equivalent to that in the bed. In Figure 6b, equal mobility would appear as a straight line parallel to the abscissa.

A similarity collapse based only on adjusting  $\tau_{*i}$  for size-dependent differences in  $\tau_{*i}$  cannot incorporate size-dependent differences in  $q_{bi}$ . Although Parker et al. (1982) showed that three different fractional transport functions were necessary to fit the fine, middle, and coarse portions of the Oak Creek transport data, the general approach to modeling fractional transport rates has been to assume that relative size effects on fractional transport rates are included only in their effect on  $\tau_{*i}$  (Ashida and Michue, 1972; White and Day, 1982; Parker and Klingeman, 1982; Andrews and Parker, 1987). The goal of this section is to examine relative size and mixture effects on fractional transport rates. To do this, we will use plots like Figure 6b.

### Test of Sorting

Figure 6b and 7 present the fractional transport rates for the 1 $\phi$  and 1/2 $\phi$  mixtures. The legends in these figures use a value of  $\tau_c$  for the entire mixture, which is straightforward in these and other cases where all sizes begin moving at nearly the same value of  $\tau_o$ . At the lowest flow with the 1 $\phi$  mixture ( $\tau/\tau_c = 1.14$ ), the finer fractions show roughly equal mobility, but the coarse fractions do not. At higher flows, but still less than  $\tau/\tau_c = 2$ , both fine and coarse fractions are substantially underrepresented in the transport. Once  $\tau/\tau_c$  exceeds a value somewhere

between 1.7 and 2.4, all size fractions become equally mobile. The results for the  $1/2\phi$  mixture are similar to those for  $1\phi$ , but merely appear stunted because of the smaller grain size range.

Figure 8 presents the fractional transport rates for representative samples of the Oak Creek transport data of Milhous (1973). To provide a clear plot of the 22 samples, the geometric means of several transport samples for each  $\tau/\tau_c$  value are plotted on Figure 8. The trend in these data is similar to that in our data, in that the fine and middle fractions are close to equal mobility at the lowest  $\tau/\tau_c$ , and become less mobile at higher  $\tau/\tau_c$ . The coarse fractions are underrepresented in the transport at all flows, which go to a maximum of  $\tau/\tau_c = 1.43$ .

#### Test of Bimodality

Figure 9 presents the fractional transport rates of the bimodal mixtures. The variation in  $q_{bi}/f_i$  for MC50 in Figure 9a is similar to that of  $1\phi$  and Oak Creek. At low values of  $\tau/\tau_c$ , both fine and coarse fractions are underrepresented. At values of  $\tau/\tau_c$  greater than roughly two,  $q_{bi}/f_i$  values for all sizes fall within a factor of two.

The trend in Figure 9b for FC50 is more complex than those of the better sorted mixtures because  $\tau_{pi}$  varies with grain size in FC50. At  $\tau/\tau_c < 4$ , the finest fraction and all of the coarse fractions are underrepresented in the transport. In the range  $4 < \tau/\tau_c < 6$ , nearly equal mobility appears to hold for all fractions. This value for the transition to equal mobility is twice that observed in MC50 and the unimodal mixtures. However, if  $\tau/\tau_c$  is computed using the value of  $\tau_c$  for the CUNI fractions (which is roughly 2.6 times that of the FUNI fractions and, therefore, the entire mix), the transition to equal mobility occurs at  $1.70 < \tau/\tau_c < 1.95$ . The trend in Figure 9c for FC70 is similar to that of FC50. The finest fraction achieve equal mobility at  $\tau/\tau_c \approx 4$ , whereas the coarsest fraction does not achieve equal mobility at  $\tau/\tau_c$  as high as 5.25 ( $\tau/\tau_c = 2.35$  using  $\tau_c$  for the coarse fractions).

That all sizes should achieve equal mobility at some large value of  $\tau/\tau_c$  has been suggested by Parker and Klingeman (1982), who demonstrated that, if the same exponent in  $q_{bi} \propto (\tau/\tau_c)^\beta$  holds for all fractions at large values of  $\tau/\tau_c$ , the transport rates of each fraction will asymptotically approach the same value at large  $\tau/\tau_c$ . Using the common value of  $\beta = 1.5$ , the value of  $\tau/\tau_{ci}$  at which all sizes would achieve the same transport rate is in the range of 10 and 50, if  $\tau/\tau_{ci}$  is computed using the largest value of  $\tau_{ci}$  for the mixture. That equal mobility is observed in real mixtures at considerably smaller values of  $\tau/\tau_c$  is a result of relative size effects on the fractional transport rates.

#### BED CONFIGURATION

Although much information has been collected on the effect of grain size on bed configuration in unisize beds, little is known about the effect of sediment mixtures on bed configuration.

A consistent sequence of bed forms was observed in runs with the lognormal sediments. At the lowest flows, transport occurred over a plane bed. At higher flows, long low dunes appeared that were regular in appearance with straight, flow-perpendicular crests. The height of these bed forms increased with flow strength to a maximum of several centimeters, and the spacing between bed forms decreased with flow to values on the order of 80 to 120 cm. Taken together, these trends caused the bed forms to steepen with increasing flow (Figure 10). The bed forms also became more irregular in shape at higher flows, becoming quite three-dimensional at the highest flows.

The plane bed—dune sequence in the bed configuration is consistent with that expected for sediments with a mean size of 1.83 mm (Southard and Boguchwal, in press). There is also a sorting effect evident in Figure 10. For the unisize mixture MUNI, the plane-bed to dune transition occurred at a higher flow strength than in the mixed-size sediment, and the MUNI bed forms were shorter and steeper than those in the mixed-size sediments. Bed forms appeared at the weakest flow strength in the poorly sorted  $1\phi$  mixture, and the steepness of the bed forms at strong flows was smaller than in the better sorted sediments. The range of sizes in the mixture (and therefore the sorting)

may play two roles in explaining this trend. The presence in the mixture of fine grains, which tend to form shorter, steeper bed forms at lower flows than coarser grains, may trigger bed-form development at lower flows than would be the case with a better sorted mixture of the same mean size. The presence of coarser grains in the mixture may limit the depth of trough scour and, therefore, bed-form height and steepness at higher flows.

The bed forms found in the bimodal sediments are significantly different and more complex than those found in the lognormal sediments. For the MC50 mixture, a plane bed was observed at the lowest flows. Bed-load sheets were evident over a narrow range of  $\tau$ , followed by dunes at the highest flows we observed. The bed-load sheets were similar to those observed in the field by Whiting et al. (1988). These bed forms are somewhat ephemeral and characterized by a height equal to one or two CUNI grain diameters, a spacing of 1m to 2m, and, most distinctively, a spatial pattern of grain size segregation wherein the leading edge of the bed form is primarily coarse-grained, while the rest of the bed form is either well mixed or primarily fine-grained. Grain paths within these bed forms are distinctive in that many grains, particularly finer ones, often do not travel all the way to the downstream end of the bed form as they would in a dune or ripple, but are continuously deposited and reentrained on the back of the bed form.

At low flows with the FC mixtures, the FUNI fractions were transported over an essentially immobile bed of CUNI. At higher flows, the FUNI became organized into irregular, short, low dunes (typically 0.5cm to 1.5cm high, 15cm to 30 cm long, with a spacing of 30cm to 100cm) migrating over a coarse, planar bed composed of more CUNI than the bulk mix. These isolated FUNI bed forms persisted at the highest flows we used, even in the presence of substantial transport of the CUNI grains. The distinctive feature of these bed forms is that the CUNI grains were typically not deposited within the bed form, but instead traveled quickly over the fine-grained, bed-form surface. The proportion of CUNI grains trapped in the lee of the bed form varied as a function of bed-form size and shape.

The primary distinction between the MC and FC bed forms is the degree to which the different modes interacted in the bed configuration. In the MC runs (modes separated in size by a factor of 2.8), both modes were found within the bed forms. In the FC runs (modes separated in size by a factor of 8.0), sediment from the two modes did not substantially interact within the bed forms, even when the transport rates of the two modes were equivalently large. Instead, the FUNI grains formed well-sorted, short, steep dunes (with a bed-form height similar to that observed with a bed composed entirely of FUNI), while the CUNI grains remained in planar sections of the bed (a plane bed is the equilibrium bed configuration for CUNI at the flows we examined). Because of the more complex and spatially variable bed configurations found with the bimodal sediment, it is not possible to construct a simple quantitative description of the mixture effect on the bed forms, as done with Figure 10.

#### BED SURFACE TEXTURE

Samples of the bed surface texture were taken following each run with the 1 $\phi$  mixture. When bed forms were present, the samples were taken from the bed-form troughs. The troughs form the exposed portion of the surface over which the bed forms move and, therefore, represent the surface on which, or through which, size-dependent exchange of sediment may occur as the bed adjusts towards equilibrium.

Figure 11 presents the variation with  $\tau/\tau_c$  of the bed surface texture for the 1 $\phi$  runs. Plotted on the figure are the percentage of grains on the bed surface finer than 4.0mm and 1.0mm. For reference are two lines that represent the equivalent values for the well mixed bed at the start of each run. The proportions of fine and coarse fractions in the final bed-surface texture increase with flow strength up to roughly  $2\tau_c$ . As  $\tau_c$  increases, the fine fractions increase from a proportion smaller than present in the well mixed bed and approach a proportion equivalent to that of the start-up bed, while the coarse fractions become increasingly overrepresented on the bed surface with increasing

$\tau_0$ . At  $\tau > 2\tau_c$  the coarse surface layer is completely broken up; both fine and coarse fractions are present on the bed surface in a proportion close to that of the well mixed bed.

Previous discussions of the development of an equilibrium coarse surface layer have been criticized because bed-surface samples were compared to the bulk mix, thereby involving a comparison between areal and volumetric bed samples (Parker, 1980; Parker et al., 1982b; Day and Egginton, 1983). Because of this sampling problem, the existence of an equilibrium coarse surface layer was questioned (Day and Egginton, 1983). Because the same sampling method was used for both the start-up and equilibrium samples, Figure 11 clearly shows that the bed-surface layer coarsens during adjustment towards equilibrium.

#### INTERACTION AMONG FRACTIONAL TRANSPORT RATES, BED CONFIGURATION, AND BED SURFACE TEXTURE

Figure 12 shows values of the percentage of the transport finer than 4.00mm and 1.00mm for the 1 $\phi$  mixture at both equilibrium transport conditions and initial transport sampled shortly after each run was started with a completely mixed sediment bed. At values of  $\tau < 2\tau_c$ , when the bed and transport adjust from the well mixed start-up condition toward an equilibrium condition, the mobility of both the fine and coarse fractions consistently decreases with time, moving away from a condition of equal mobility. This process cannot be explained with a conceptual model that states that all size fractions must adjust toward equal mobility for equilibrium transport. However, an equilibrium transport system must operate at equal mobility only in the special case of a perfect feed system in which the material of the sediment bed is used as the feed material. Feed and recirculating flumes can produce very different equilibrium transport conditions, even when the same initial flow and sediment bed are used. In non-feed systems, equilibrium transport may occur at conditions far from equal mobility, as demonstrated in our experiments (Figure 6b, 7, and 9).

A clear interaction among fractional transport rates, bed configuration, and bed surface texture was observed in the 1 $\phi$  runs. Bed forms were present in all but the two samples with the smallest  $\tau/\tau_c$  in Figures 11 and 12. Bed forms and a coarse surface layer can clearly coexist. The bed forms observed in the the highest two runs in Figure 11 were the largest and most irregular in shape. Greater irregularity in the magnitude of the scour in the lee of these bed forms contributed to the break up of the coarse surface layer. Comparison of Figures 11 and 12 shows that the presence of an armor layer coincides with an underrepresentation of the fine and coarse fractions in the transport, and that the break up of the coarse surface layer corresponds to the onset of nearly equal mobility in the fractional transport rates.

#### CONCLUSIONS

##### Incipient motion

Incipient motion occurs at nearly the same shear stress for all size fractions in a wide range of unimodal and weakly bimodal sediments. For these sediments, the critical shear stress for each size fraction is well represented by a value slightly smaller than the Shields value for  $D_{50}$  of the mixture. This observation was made for the Oak Creek data by Parker et al. (1982) and can be extended to a wide range of experimental sediment mixtures. Mixture sorting was demonstrated to have no effect on  $\tau_{ci}$  for two sediments that differed only in their grain-size distribution standard deviation.

For strongly bimodal mixtures, the size independence of the fractional critical shear stress is no longer maintained when the modes are separated in size by a factor between 2.8 and 8.0. For modes separated in size by a factor of 8.0, we observe that the finer fractions begin moving at a shear stress considerably smaller than the coarse

fractions, and that the values of  $\tau_{ci}$  depend on the proportion present in each fraction. These results suggest that incipient motion of individual fractions in bimodal sediments depends on at least four parameters: the absolute size of the sediment (represented, perhaps, by  $D_{50}$ ), the relative size of each fraction ( $D_i/D_{50}$ ), the separation in size between the two modes, and the proportion in each mode.

#### Established Motion

All sediments discussed here showed a similar pattern in fractional transport rates. Over a finite range of  $\tau/\tau_c$ , both fine and coarse fractions are underrepresented with respect to the bed grain-size distribution during equilibrium transport conditions. At higher values of  $\tau/\tau_c$ , all fractions show equal mobility. This consistency in the variation in fractional transport rates with  $\tau_c$  is striking in that it arises from both lab and field data, from bed grain-size distributions covering a wide range of sorting, and for lognormal, fine-skewed, and bimodal grain-size distributions. The occurrence of distinctly non-equal mobility ( $p_i \neq f_i$ ) is also striking for those sediments for which all sizes begin moving at nearly the same shear stress. The variation of  $q_{bi}$  with  $\tau_c$  depends not only on  $\tau_{ci}$ , but on relative grain-size effects controlled by the bed configuration and the presence of a coarse surface layer. Based on our laboratory data, the value of  $\tau/\tau_c$  at which all fractions achieve equal mobility appears to be about 2.0 for the lognormal and more narrow bimodal sediment, and in the range of 1.7 to greater than 2.35 for the more poorly sorted bimodal sediment.

#### Bed Configuration

Mixture sorting was observed to have a clear and measurable effect on the size and shape of bed forms in the unimodal sediments we investigated. Bed-form height was observed to decrease, while bed-form spacing and spacing/height ratio increased with mixture sorting. In the bimodal sediments, a different, more complex, and spatially variable sequence of bed forms was observed. For the sediments whose modes were separated in size by a factor of 8.0, the different modes appeared to act in a relatively independent fashion, with the fine fraction forming starved dunes and the coarse fraction forming a planar surface. For the bimodal sediment whose modes were separated in size by a factor of 2.8, a bed form sequence of plane bed — sheets — dunes was observed and involved both fractions.

#### Bed Surface Texture

A distinct coarse surface layer was unambiguously shown to develop as the 1 $\phi$  unimodal sediment bed adjusted to equilibrium. We observed the coarse surface layer to become better developed as  $\tau$  increases, up to the point where intense flow in the lee of bed forms broke up any surface grain-size sorting. At flows where bed forms and a coarse surface layer coexist, bed forms may contribute to the development of a coarse surface layer by increasing the supply of actively transported coarse grains. The coarse surface layer need not serve as a regulator of the mobility of different size fractions except in the special case of a sediment-feed flume. Its presence in our recirculating flume data is a result of size-dependent variation in grain mobility, development of a partial static armor, and a geometrically necessary vertical sorting process that occurs when at least some grains of all sizes are in motion.

# REFERENCES

- Ackers, P., and W.R. White, 1973. Sediment transport: new approach and analysis, *J. Hydraul. Div., Amer. Soc. Civil Eng.*, 99(HY11), 2041-2060.
- Andrews, E.D., 1983. Entrainment of gravel from naturally sorted riverbed material, *Geol. Soc. Amer. Bul.*, 94, 1225-1231.
- Andrews, E.D., and G. Parker, 1987. Formation of a coarse surface layer as the response to gravel mobility, in Thorne, C.R., J.C. Bathurst, and R.D. Hey (eds.), *Sediment Transport in Gravel-bed Rivers*, John Wiley & Sons.
- Ashida, K., and M. Michiue, 1972. Study on hydraulic resistance and bedload transport rate in alluvial streams, *Trans. Jpn. Soc. Civ. Eng.*, 206, 59-69.
- Carling, P.A., 1983. Threshold of coarse sediment transport in broad and narrow natural streams, *Earth Surface Processes and Landforms*, 8, 1-18.
- Church, M.A., D.G. McLean, and J.F. Wolcott, 1987. River bed gravels: sampling and analysis, in Thorne, C.R., J.C. Bathurst, and R.D. Hey (eds.), *Sediment Transport in Gravel-bed Rivers*, John Wiley & Sons.
- Day, T.J., 1980a. A study of the transport of graded sediments, *Report No. IT 190*, Hydraulics Research Station, Wallingford, England.
- Day, T.J., 1980b. A study of initial motion characteristics of particles in graded bed material, *Geol. Survey of Canada, Current Research, Part A*, Paper 80-1A, 281-286.
- Day, T.J., and P. Egginton, 1983. Particle-size distributions of the surface of alluvial channel beds, *Geol. Survey of Canada, Current Research, Part B*, Paper 83-1B, 299-302.
- Dhamotharan, S., A. Wood, G. Parker, and H. Stefan, 1980. Bedload transport in a model gravel stream, *Proj. Report No. 190*, St. Anthony Falls Hydr. Lab., Univ. Minnesota.
- Diplas, P., and A.J. Sutherland, 1988. Sampling techniques for gravel sized sediments, *J. Hydraulic Eng., Amer. Soc. Civil Eng.*, 114(5), 484-501.
- Einstein, H.A., 1950. The bedload function for sediment transport in open channel flows, *Tech. Bull. 1026*, U.S. Dep. of Agric., Soil Conserv. Serv., Washington, D.C..
- Hammond, F.D.C., A.D. Heathershaw, and D.N. Langhorne, 1984. A comparison between Shields' threshold criterion and the movement of loosely packed gravel in a tidal channel, *Sedimentology*, 31, 51-62.
- Milhous, R.T., 1973. Sediment transport in a gravel-bottomed stream, Ph.D. thesis, Oregon State Univ., Corvallis.
- Misri, R. L., R. J. Garde, and K. G. Ranga Raju, 1984. Bed load transport of coarse nonuniform sediment, *J. Hydr. Eng., Am Soc. Civil Eng.*, 110(3):312-328.
- Parker, G., 1979. Hydraulic geometry of active gravel rivers, *J. Hydraul. Div. Am. Soc. Civ. Eng.*, 105(HY9), 1185-1201.
- Parker, G., 1980. Experiment: on the formation of mobile pavement and static armor, *Tech. Report*, Dept. Civil Eng., Univ. Alberta, Edmonton.
- Parker, G., and P.C. Klingeman, 1982. On why gravel bed streams are paved, *Water Resources Res.*, 18, 1409-1423.
- Parker, G., P.C. Klingeman, and D.L. McLean, 1982. Bedload and size distribution in paved gravel-bed streams, *J. Hydraul. Div., Am. Soc. Civ. Eng.*, 108(HY4), 544-571.
- Shaw, J. and R. Kellerhals, 1982. The composition of Recent alluvial gravels in Alberta river beds, Alberta Research Council *Bulletin* 41, 151 p.
- Shimizu, Y., 1990. Channel flow with lateral stress, *Tech. Report*, Civil Engineering Research Institute, Hokaido Development Bureau, Japan.

- Southard, J.B. and L.A. Boguchwal, in press. Bed configurations in steady, unidirectional water. Part 2. Synthesis of flume data, *J. Sedimentary Petrology*, vol. 60.
- Vanoni, V.A., and N.H. Brooks, 1957. Laboratory studies of the roughness and suspended load of alluvial streams, *Sedimentation Laboratory Report No. E68*, Calif. Inst. Technol., Pasadena, Calif..
- White, W. R., and T. J. Day, 1982. Transport of graded gravel bed material, in *Gravel-bed rivers*, edited by R. D. Hey, J. C. Bathurst, and C. R. Thorne, pp. 181-213, John Wiley, London.
- Whiting, P.J., W.E. Dietrich, L.B. Leopold, T.G. Drake, R.L. Shreve, 1988. Bedload sheets in heterogeneous sediment, *Geology*, 16:105-108.
- Wilcock, P. R., 1987. Bed-load transport of mixed-size sediment, Ph.D. dissertation, 205 pp, Massachusetts Institute of Technology, Cambridge, Mass.
- Wilcock, P.R., 1988. Methods for estimating the critical shear stress of individual fractions in mixed-size sediment, *Water Resour. Res.*, 24(7), 1127-1135.
- Wilcock, P.R. and J.B. Southard, 1988. Experimental study of incipient motion in mixed-size sediment, *Water Resour. Res.*, 24(7), 1137-1151.
- Wilcock, P.R., and J.B. Southard, 1989. Bed-load transport of mixed-size sediment: fractional transport rates, bed forms, and the development of a coarse bed-surface layer, *Water Resources Research*, 25, 1629-1641.
- Wilcock, P.R., and R.S. Stull, 1989. Magnetic paint sampling of the surface and subsurface of clastic sediment beds, *J. Sedimentary Petrology*, 59, 626-627.
- Wilcock, P.R., in review. The poverty of flow competence, submitted to *Geology*, 1990.

TABLE 1  
Properties of Grain Size Distributions

Mixture	Mixture Type	Dm (mm)	D15 (mm)	D50 (mm)	D85 (mm)	Sorting ( $\phi$ )	Sorting (geom.)	Reference
MUNI	=unisize	1.87	1.63	1.86	2.20	0.20	1.15	Wilcock (1987)
1/2 O	lognormal	1.82	1.25	1.83	2.59	0.50	1.41	Wilcock (1987)
O	lognormal	1.85	0.893	1.83	3.88	0.99	1.99	Wilcock (1987)
CUNI	=unisize	5.31	4.68	5.28	6.17	0.18	1.13	Wilcock (1987)
FUNI	=unisize	0.662	0.538	0.670	0.807	0.26	1.20	Wilcock (1987)
MC-50	Strongly bimodal	3.19	1.75	2.55	6.00	0.79	1.73	This Paper
FC-50	Strongly bimodal	1.88	0.600	2.00	5.88	1.51	2.85	This Paper
FC-70	Strongly bimodal	1.30	0.550	0.750	5.54	1.45	2.73	This Paper
DAY A	Weakly bimodal	1.50	0.336	1.82	6.05	1.77	3.41	Day (1980a)
DAY B	Weakly bimodal	1.17	0.318	1.57	3.49	1.45	2.73	Day (1980a)
MISRI N1	=lognormal	2.37	1.15	2.36	4.91	1.00	2.00	Misri et al. (1984)
MISRI N2	Rectangular	3.78	1.21	3.81	11.9	1.44	2.71	Misri et al. (1984)
MISRI N3	=lognormal	4.09	1.70	4.00	10.1	1.18	2.27	Misri et al. (1984)
SAF	Weakly bimodal	2.10	0.828	2.16	6.04	1.29	2.45	Dhamotharan et al. (1980)
OAK CREEK	Long fine tail	13.1	2.37	19.5	56.6	2.10	4.29	Milhous (1973)



Table 2. General Hydraulic Properties of Experimental Runs

Mix	Flume	Run	Water	Flow	Mean	Slope	$\tau_0$	$q_0$	$q_0$	Bed
	Width		Discharge	Depth	Velocity			initial	equil.	Configuration
	(cm)		$\text{cm}^3 \times 10^3$	cm	cm/s	$\times 10^4$	Pa	g/ms	g/ms	
MUNI	60	A2	30.6	11.4	44.8	9.6	0.89	na	1.85E-03	Plane
	60	A3	35.3	11.4	51.8	12.4	1.15	na	3.59E-01	Plane
	60	A4	39.7	11.5	57.6	14.2	1.37	na	3.19E+00	2D dunes
	60	A5	43.6	11.8	61.8	21.5	1.73	na	8.91E+00	2D dunes
	60	A6	48.8	12.0	67.5	24.2	2.08	na	2.30E+01	2D dunes
	60	A7	55.7	12.8	72.4	29.3	2.53	na	4.64E+01	2D-3D dunes
1/2 Ø	60	B1	28.7	11.0	43.6	10.0	0.91	na	1.44E-02	Plane
	60	B2	30.4	11.2	45.3	10.3	0.87	na	3.70E-02	Incipient 2D dunes
	60	B3	35.6	11.2	52.8	12.6	1.17	na	1.12E+00	2D dunes
	60	B4	39.3	11.3	58.0	16.8	1.47	na	5.98E+00	2D dunes
	60	B5	43.4	11.6	62.2	21.4	1.78	na	1.37E+01	2D dunes
	60	B6	47.7	11.7	67.9	33.4	2.38	na	2.58E+01	2D dunes
	60	B7	54.9	11.5	79.4	49.2	3.74	na	9.70E+01	2D-3D dunes
1Ø	60	C1	28.6	11.1	43.1	10.4	0.97	na	2.31E-02	Plane
	60	C2	30.3	10.9	46.5	11.1	1.00	na	3.30E-02	Plane
	60	C3	35.0	11.2	52.4	18.2	1.32	na	2.32E+00	Incipient 2D dunes
	60	C4	39.1	11.2	58.0	21.4	1.63	na	1.07E+01	2D dunes
	60	C5	43.4	11.0	65.5	28.0	2.17	na	2.97E+01	2D dunes
	60	C6	47.8	10.9	72.9	33.0	2.78	na	5.94E+01	2D-3D dunes
	60	87-1	29.4	11.3	43.5	10.9	1.03	1.67E-01	1.59E-02	Plane
	60	87-2	31.5	11.1	47.5	12.5	1.17	3.42E-01	4.68E-01	Plane
	60	87-3	33.7	11.3	49.9	14.4	1.26	2.50E+00	1.96E+00	2D dunes
	60	87-4	35.9	11.2	53.4	18.4	1.36	9.94E+00	4.50E+00	2D dunes
	60	87-5	37.7	11.3	55.9	21.4	1.56	7.88E+00	9.69E+00	2D dunes
CUNI	60	D1	39.2	11.1	59.1	25.5	2.47	na	3.35E-03	Plane
	60	D2	43.2	11.0	65.4	31.0	2.99	na	3.45E-02	Plane
	60	D3	47.7	10.8	73.3	38.2	3.63	na	5.55E-01	Plane
	60	D4	54.8	11.1	82.6	49.1	4.77	na	9.55E+00	Plane
FUNI	60	E1	17.8	10.8	27.5	2.9	0.25	na	2.47E-03	Plane
	60	E2	19.6	10.8	30.2	3.2	0.26	na	2.45E-02	Plane
	60	E3	21.7	10.8	33.4	3.6	0.30	na	1.89E-01	Plane
	60	E4	25.2	11.2	37.7	5.8	0.38	na	1.75E+00	2D dunes
	60	E5	27.7	11.4	40.4	14.1	0.54	na	4.12E+00	3D dunes
	60	E6	30.2	11.2	44.9	17.5	0.72	na	6.31E+00	3D dunes
MC-50	15.6	1	8.9	11.1	51.6	29.8	1.8	na	3.28E-03	Plane
	15.6	2	9.5	11.2	55.2	31.9	2.0	na	2.22E-02	Plane
	15.6	7	10.2	11.4	57.5	29.8	2.1	na	1.12E-00	Plane
	15.6	6	11.8	11.0	69.1	43.0	3.1	na	1.80E+01	Spatial size segregation
	15.6	3	12.9	10.7	77.8	60.5	4.0	na	6.30E+01	Bed-load sheets
	15.6	5	14.2	10.5	86.8	75.7	5.0	na	1.31E+02	Isolated trains of 2D dunes
	15.6	4	15.4	10.6	93.3	99.9	6.0	na	2.23E+02	Isolated trains of 2D dunes
FC-50	60	12	22.3	11.3	33.0	6.8	0.64	na	6.90E-03	Plane
	60	11	25.1	10.9	38.4	8.9	0.85	na	3.47E-02	Plane
	60	10	30.5	11.5	44.3	10.2	1.09	na	2.31E-01	Plane
	15.6	7	6.7	11.1	39.1	16.2	1.04	na	3.17E-01	Plane
	15.6	2	7.4	10.8	44.6	19.6	1.32	na	1.15E+00	Plane
	15.6	1	8.6	11.2	49.7	25.8	1.67	na	2.56E+00	Plane
	15.6	5	9.0	10.8	53.8	26.8	1.89	na	8.00E+00	Incipient FUNI dunes
	15.6	4	10.2	11.1	59.7	30.9	2.28	na	1.33E+01	Isolated FUNI dunes
	15.6	3	11.1	10.8	66.0	42.4	2.89	na	3.88E+01	Isolated FUNI dunes
	15.6	6	12.1	10.7	72.8	42.5	3.32	na	7.95E+01	Isolated FUNI dunes
	15.6	8	13.7	11.0	80.7	46.8	3.95	na	1.32E+02	Isolated FUNI dunes
FC-70	60	1	19.4	11.2	28.8	4.7	0.47	na	1.80E-03	Plane
	60	2	22.7	11.3	33.7	5.3	0.61	na	5.02E-02	Plane
	60	3	24.7	11.2	36.8	6.2	0.73	na	2.40E-01	Plane
	60	4	26.8	11.2	39.8	6.3	0.82	na	5.08E-01	Plane
	60	5	29.2	11.2	43.7	8.1	1.00	na	1.06E+00	Plane
	60	6	32.5	11.2	48.6	9.6	1.23	na	3.67E+00	Isolated FUNI dunes
	60	8	37.9	11.2	56.5	15.2	1.73	na	1.42E+01	Isolated FUNI dunes
	60	7	40.5	11.1	60.6	15.8	1.94	na	2.65E+01	Isolated FUNI dunes
	60	10	45.4	11.1	68.2	20.4	2.47	na	4.91E+01	Isolated FUNI dunes

FIGURE 1. SUMMARY OF EXPERIMENTAL MIXTURES

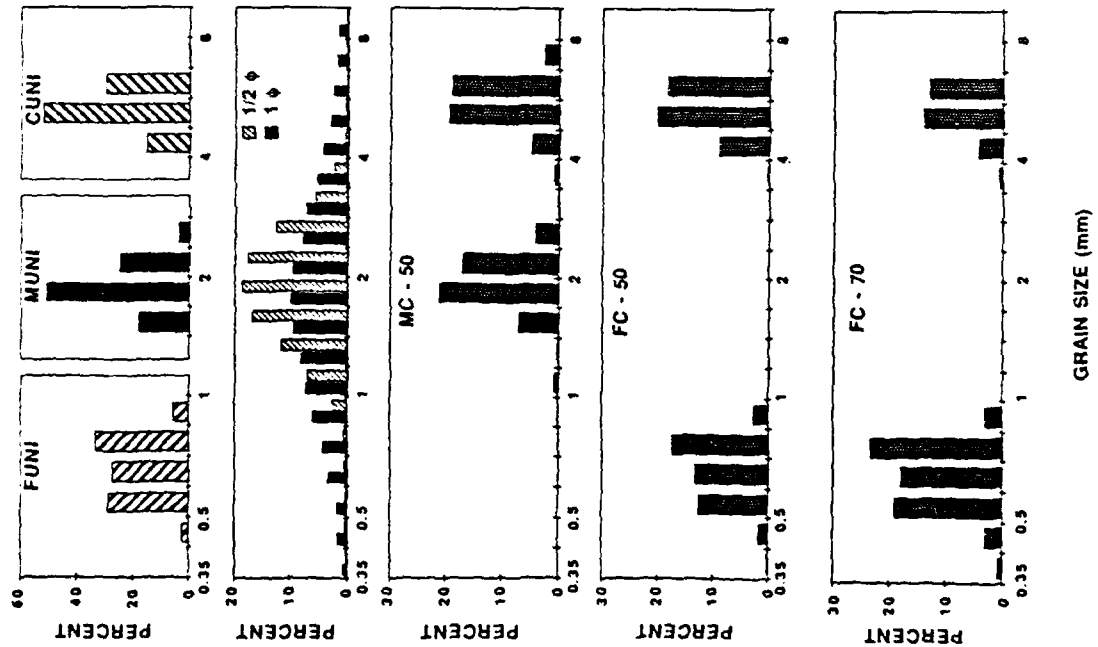


FIGURE 2. Reference shear stress for unimodal sediments

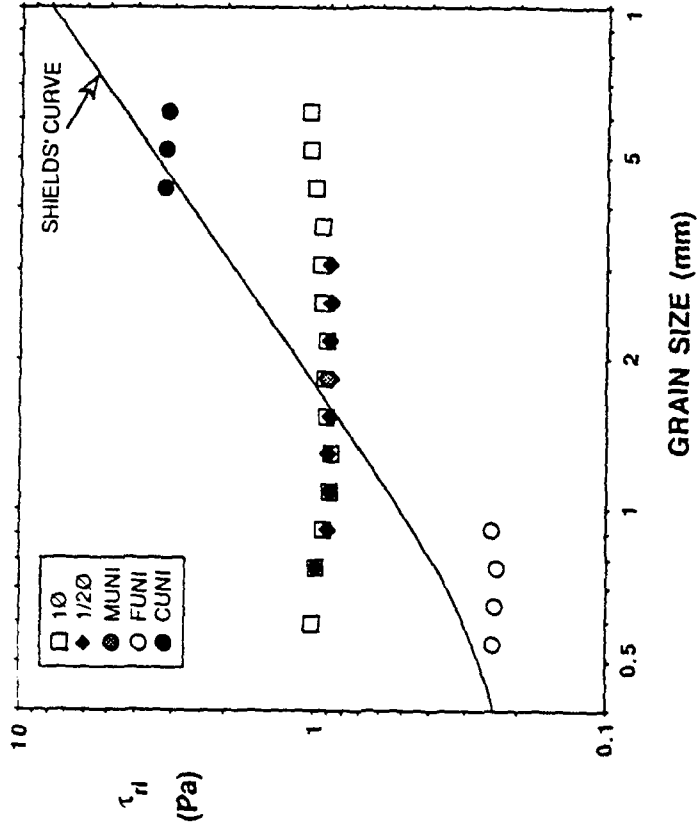
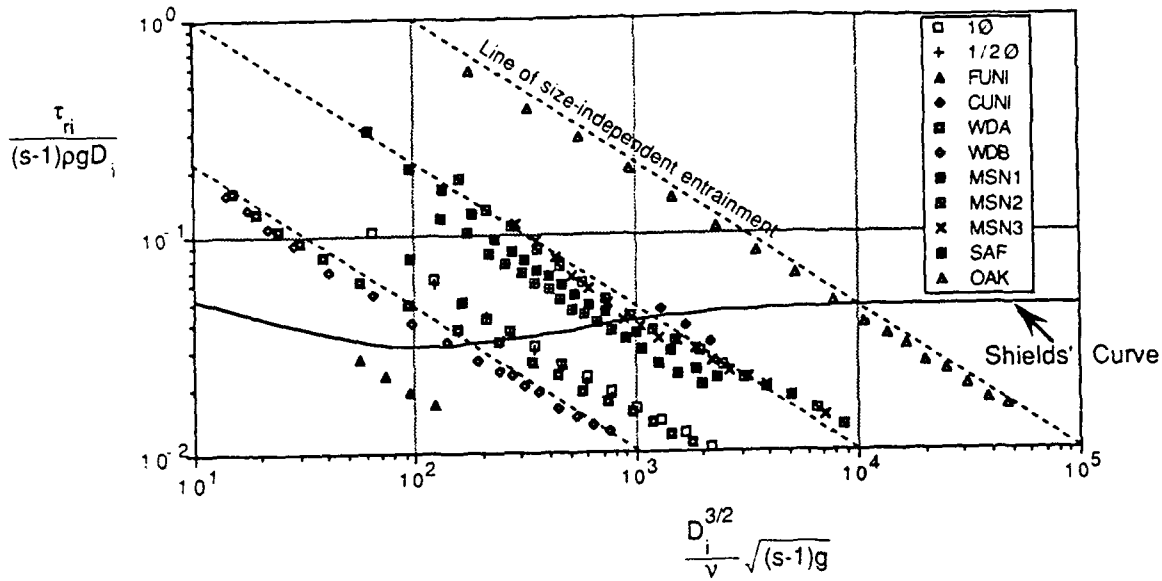


Figure 3: Reference Shields parameter vs.  $S^*$ :  
Unimodal and weakly bimodal sediments



After Wilcock and Southard (1988)  
Data Sources given in Table 1

Figure 4: Reference Shields' Parameter for  
Use of mixtures shown in Figure 3.

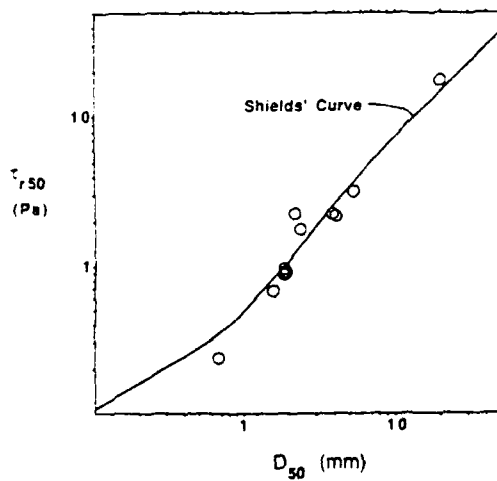


Figure 5: Reference shear stress for unimodal and bimodal sediments

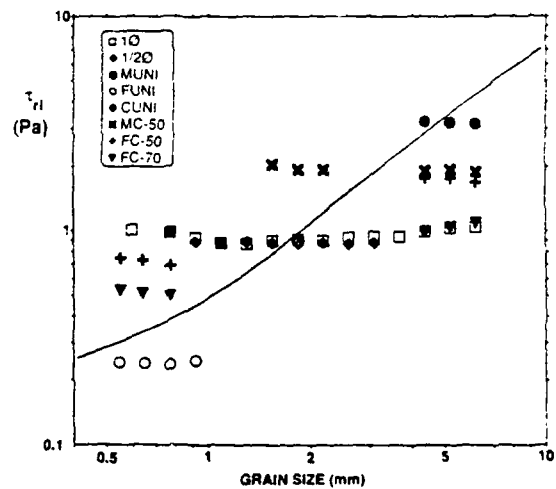


Figure 6a:  $1\phi$  Fractional Transport Rates  
Dimensionless plot, undistorted axes

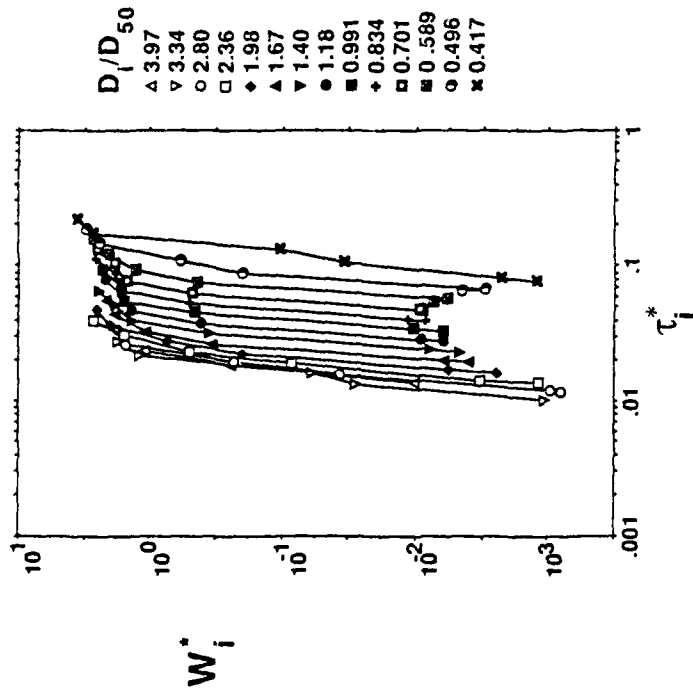


Figure 6b:  $1\phi$  Fractional Transport Rates  
Dimensional Plot

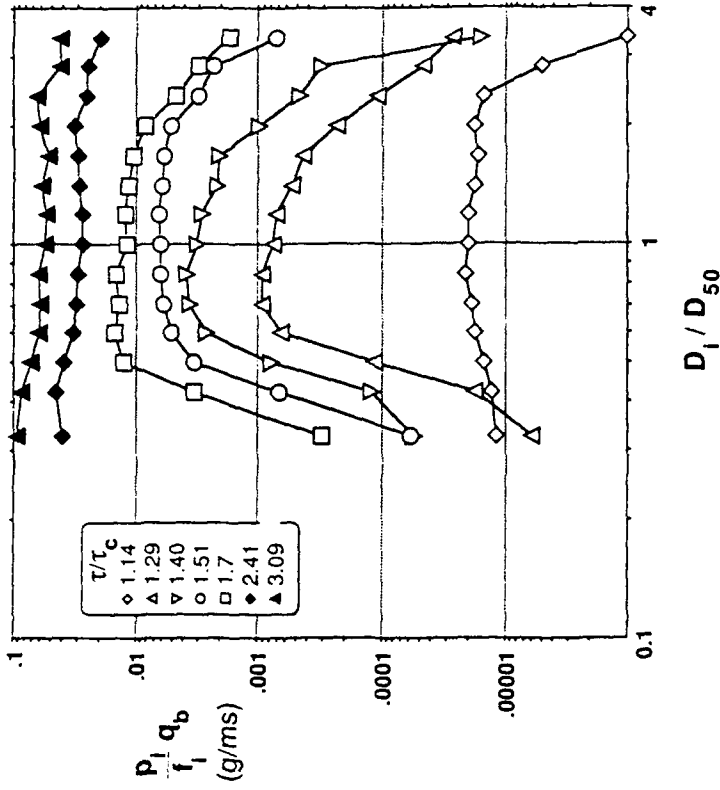


Figure 7. 1/2φ Fractional Transport Rates

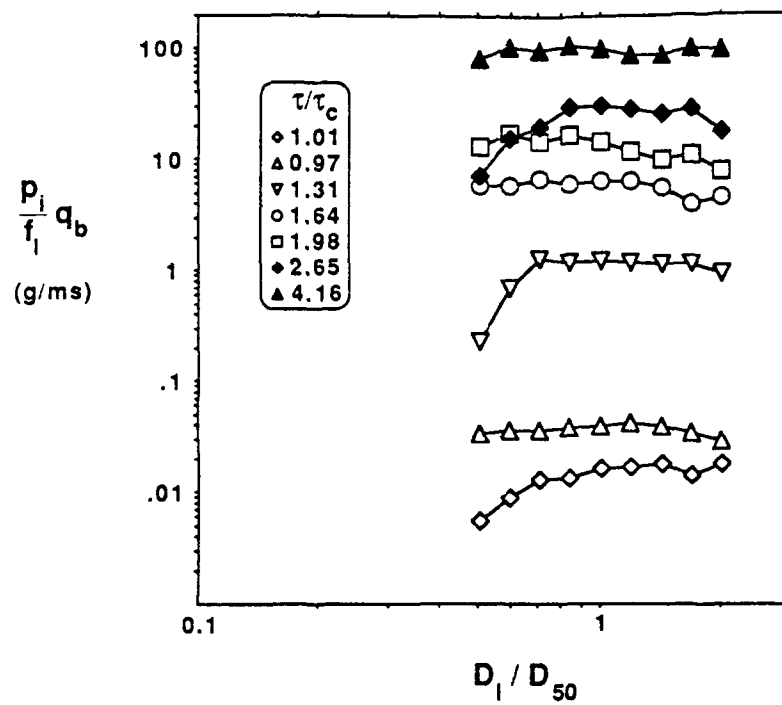


Figure 8. Oak Creek Fractional Transport Rates

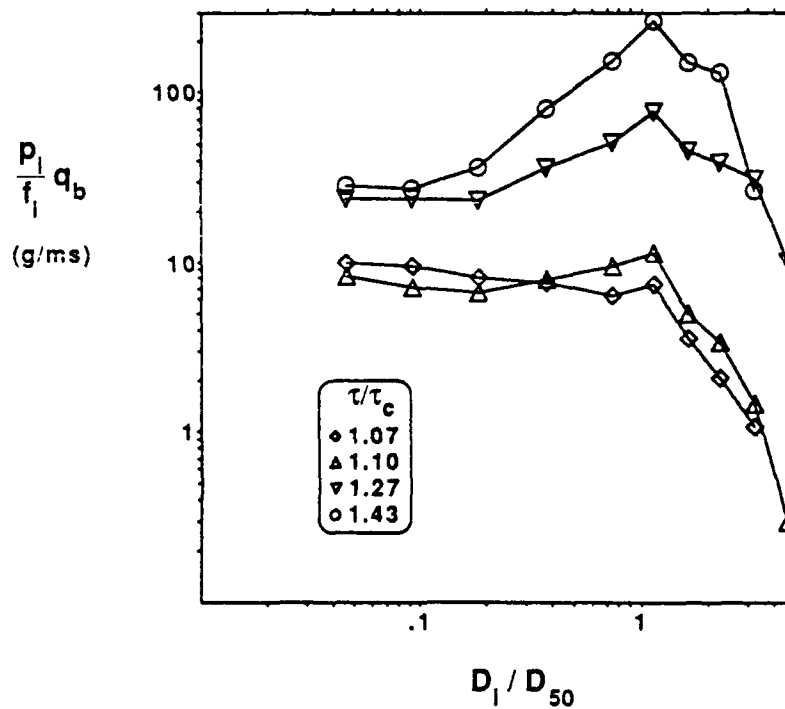


Figure 9: Fractional Transport Rates of the Bimodal Mixtures

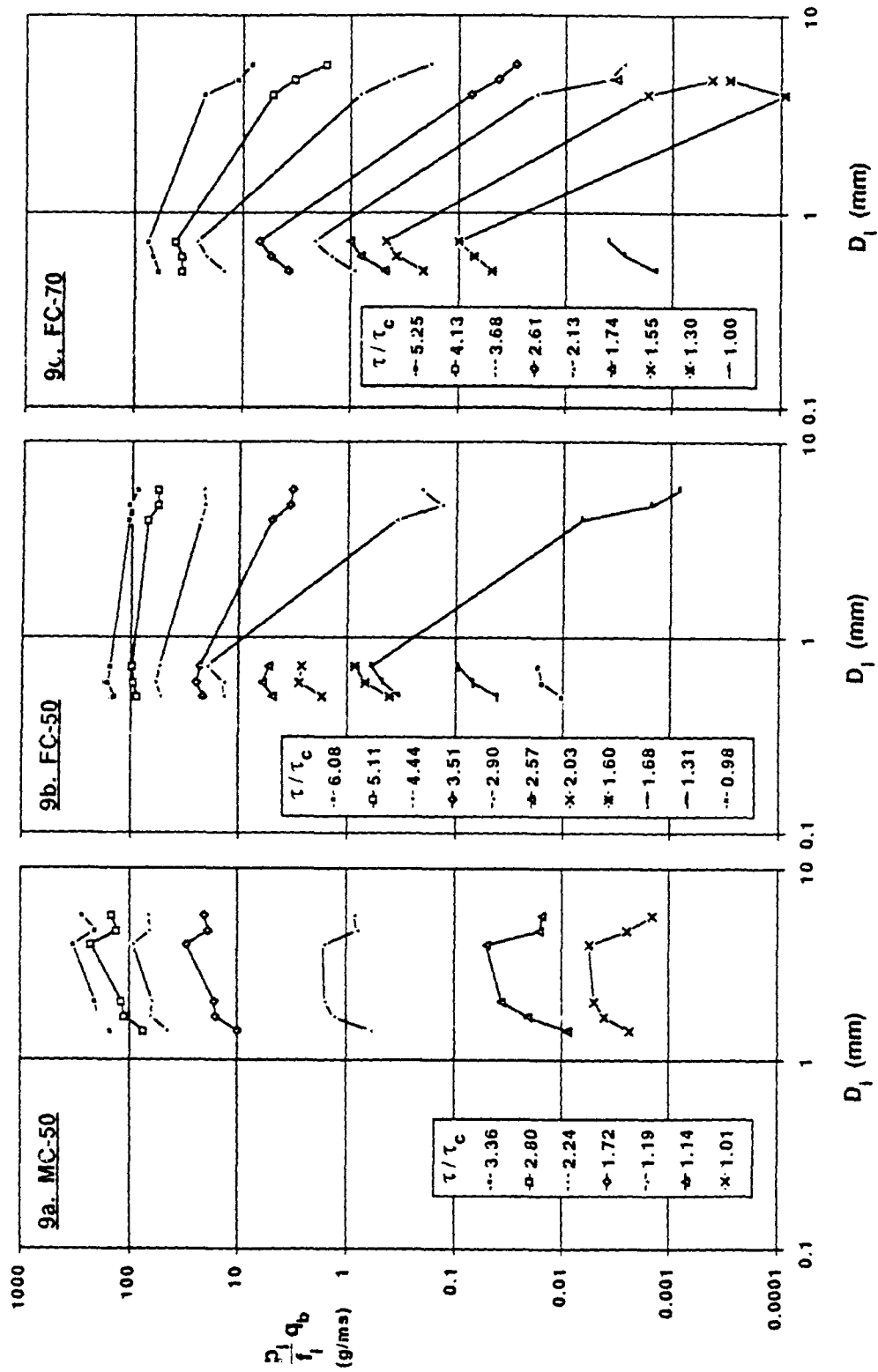


Figure 10. Ratio of bed-form spacing to height in unimodal sediment

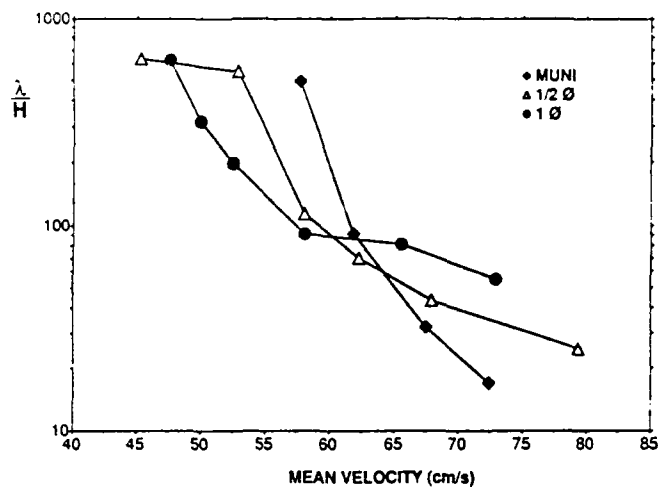


Figure 11. Variation of armor composition with  $\tau/\tau_c$  for the  $1 \phi$  sediment  
Percentage of fine and coarse sediment on the bed at the end of runs

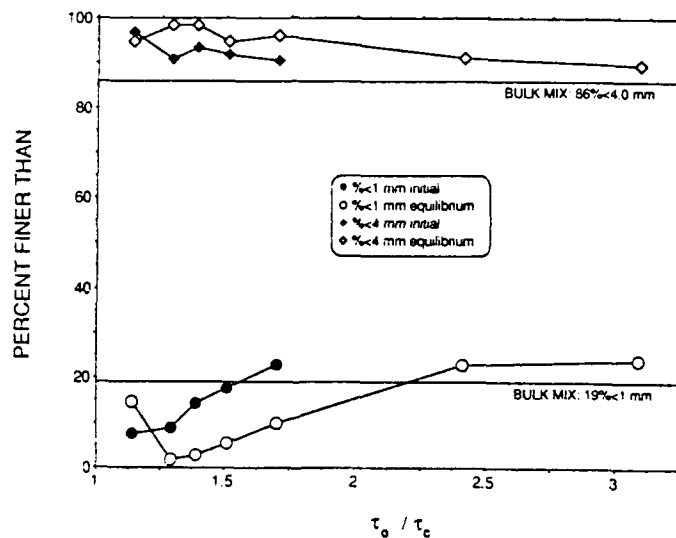
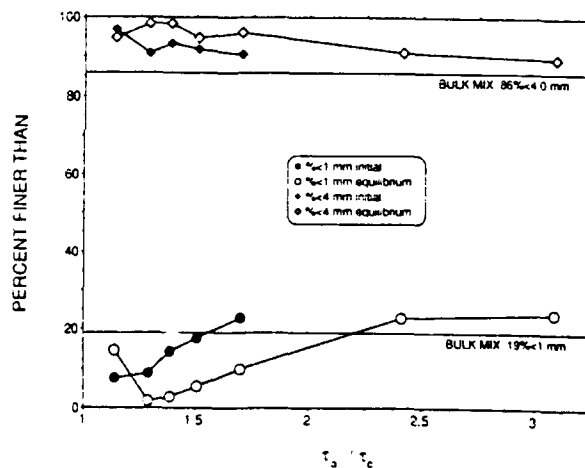


Figure 12. Variation of bed-load composition with  $\tau/\tau_c$  for the  $1 \phi$  sediment  
Percentage of fine and coarse sediment in transport at the end of runs



*THE JOHNS HOPKINS UNIVERSITY • BALTIMORE, MARYLAND 21218*

*PETER R. WILCOCK (301) 338-5421 (FAX: (301) 338-8996; BITNET: WILCOCK@JHUVMI)  
DEPARTMENT OF GEOGRAPHY AND ENVIRONMENTAL ENGINEERING*

May 30, 1990

Dr. Paolo Billi  
Dipartimento di Ingegneria Civile  
Universita Di Firenze  
Via S. Marta, 3  
50139 FIRENZE  
ITALY

Tel: 55-4796-225

Dear Dr Billi:

Enclosed is a substitute Page 20 for my Gravel-Bed Rivers Workshop manuscript. The rest of the manuscript should have arrived (along with my registration) by Friday, June 1. Please replace page 20 of the manuscript you have received with the enclosed page. Thank you.

Sincerely,



Peter R. Wilcock  
Assistant Professor



Figure 10. Ratio of bed-form spacing to height in unimodal sediment

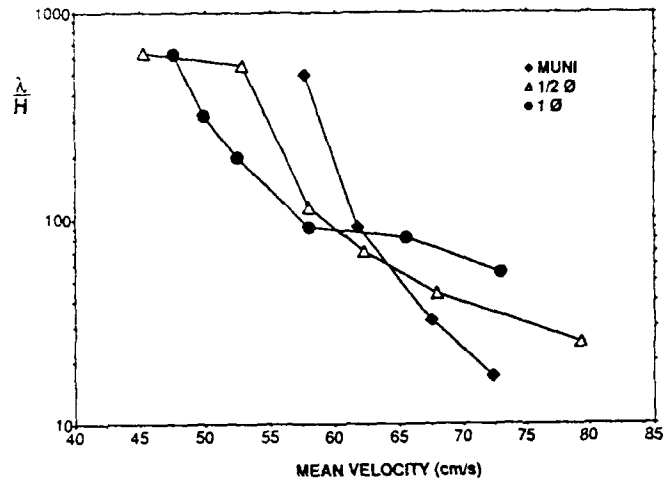


Figure 11. Variation of armor composition with  $\tau/\tau_c$  for the 1Ø sediment  
Percentage of fine and coarse sediment on the bed at the end of runs

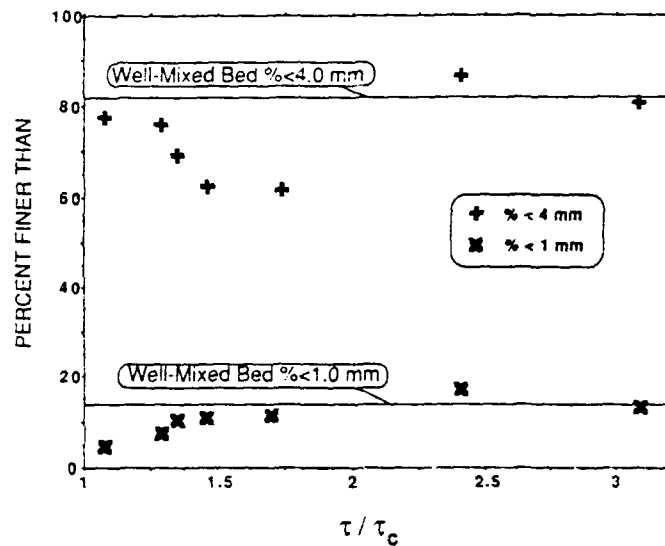
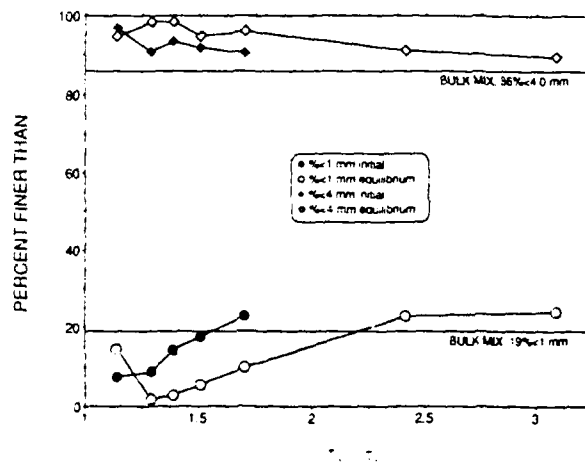


Figure 12. Variation of bed-load composition with  $\tau/\tau_c$  for the 1Ø sediment  
Percentage of fine and coarse sediment in transport at the end of runs



## Fractional Transport Rates of Bed Load on Goodwin Creek

Roger A. Kuhnle  
National Sedimentation Laboratory  
U.S. Department of Agriculture  
Agricultural Research Service  
Oxford, Mississippi 38655  
U. S. A.

### ABSTRACT

Transport rates of eight size fractions of bed material were studied on Goodwin Creek from 1984 - 1988. It was found that  $D_{50}$  of the sediment in transport increased in size from 0.77 to 7.77 mm with increasing bed shear stress, the slopes of the transport rates of individual size fractions vs. bed shear stress ( $W_i^*$  vs.  $\tau_{*i}^*$ ) decrease with decreasing grain size, and reference bed shear stresses of individual grain sizes were dependent on relative size as well as absolute size (the plot of  $\tau_{*i}^*$  vs.  $D_i/D_{50}$  had a slope of -0.80). Agreement between mean measured transport rates from Goodwin Creek and several published transport relations was poor. A technique for calculating bed load transport separating the sand and gravel fractions is proposed.

### INTRODUCTION

The Goodwin Creek Research Watershed is a 21.4 km<sup>2</sup> instrumented watershed that is operated by the USDA National Sedimentation Laboratory in Oxford, Mississippi. The purpose of the watershed is to provide data needed to estimate the impact of upstream land use and watershed processes on sediment supply and transport in stream channels and how this affects channel stability.

The ability to measure or predict the rate of bed load transport of a stream is an important part of the research program at Goodwin Creek. An accurate determination of the rate of bed load in transport is necessary to calculate net erosion from upstream areas as well to assess the effects of the transported sediment on downstream reaches of the channel. Improving our ability to accurately predict bed load transport rates on Goodwin Creek and also on other streams was the reason this study was undertaken.

In most studies of fractional transport rates in gravel-bed streams, peak bed load transport rates have been below 0.3 kg s<sup>-1</sup> m<sup>-1</sup> (e.g. Parker et al., 1982; Andrews, 1983; Tacconi and Billi, 1987; Wilcock and Southard, 1989). One exception is the study of Ashworth and Ferguson (1989) in which peak measured rates were up to 3.5 kg s<sup>-1</sup> m<sup>-1</sup>. Goodwin Creek, with bed shear stresses in excess of seven times the critical value and maximum measured cross-sectionally averaged bed load transport rates of 3.0 kg s<sup>-1</sup> m<sup>-1</sup>, offers another data set from a very active gravel-bed stream.

Most bed load transport relations in the literature characterize the importance of the bed material by one sediment size, usually the median size of the bed material. A few transport relations, most notably that of Einstein (1950), have taken into account the whole sediment mix. Parker, Klingeman, and McLean (1982) concluded that in some gravel bed streams one size fraction may in fact be

sufficient to characterize the transport of the bed material. The transport relation of Parker et al. (1982) was found to not adequately predict bed load transport on Goodwin Creek. The Goodwin Creek data show that a procedure which uses two transport relations, one for the sand and one for the gravel portions of the sediment yielded calculated transport rates close to those measured. The intermediate complexity of this two part relation may yield adequate transport rate predictions in instances where using one grain size has failed and where using data on a larger number of size fractions is not warranted.

#### FORMULATION OF THE PROBLEM

The concept of equal mobility as pertaining to fractional transport of bed material sediment in gravel-bed streams has been much discussed and debated since it was proposed by Parker et al. (1982). Equal mobility shall be defined here as consisting of two parts: equal entrainment mobility, and equal transport mobility. Equal entrainment mobility is defined as the case when all the sediment sizes in the bed material begin to move at the same flow strength. Equal transport mobility is defined as the case when all sediment sizes are transported according their relative proportion in the bed material (or the size distributions of the bed material and bed load are identical). If one condition of equal mobility for a given channel is fulfilled it does not imply that the other one is. For example Wilcock and Southard (1988) found that near perfect equal entrainment mobility was present in their laboratory flume runs, however, equal transport mobility was approached only at the highest flow strengths used in their flume experiments (Wilcock and Southard, 1989).

The transport of mixed size sediments in an alluvial stream channel is a complicated problem. As soon as movement of the bed sediment begins the size distribution of the bed surface changes as a function of the flow strength. The bed surface size distribution has been shown to be coarsest at low flow strengths and to become finer at higher flow strengths (Kuhnle, 1989). Superimposed on this process is the formation and growth of bed forms which may coexist with the mobile bed pavement for some flows or destroy it at higher flows (Wilcock and Southard, 1989). The flow strengths at which individual sizes of the bed material begin to move is another complex part of this problem. Several studies have found very close approximations to equal entrainment mobility (e.g. Parker et al., 1982; Andrews, 1983; Wilcock and Southard, 1988), while others have found that there is still an effect of relative size at entrainment conditions (e.g. Ashworth and Ferguson, 1989; this study).

A better understanding of the problem may be gained by considering the important variables which control the process:

$$q_{bi} = F(\tau_0, d, \rho, \mu, \rho_s, g, D_i, D_i/D_{50}) \quad (1)$$

where  $q_{bi}$  = the bed load transport rate of one size fraction in mass per time per unit width,  $\tau_0$  = the boundary shear stress,  $d$  = mean flow depth,  $\rho$  = the density of the fluid,  $\mu$  = dynamic viscosity of the fluid,  $\rho_s$  = the density of the sediment,  $g$  = acceleration of gravity,  $D_i$  = the size of a particular fraction of the sediment,  $D_i/D_{50}$  = grain size relative to the median grain size ( $D_{50}$ ), and  $F$  symbolizes a functional relationship. These nine variables can be represented by six dimensionless groups:

$$\frac{((\rho_s/\rho)-1)gq_{b1}}{\rho_s u_*^3 f_i} = F \left[ \frac{\tau_0}{(\rho_s - \rho)gDi}, \frac{d}{D_i}, \frac{g^{1/3} D_i}{\nu^{2/3}}, \frac{\rho_s}{\rho}, \frac{D_i}{D_{50}} \right] \quad (2)$$

where  $\nu = \mu/\rho$ ;  $\tau_0 = \rho g R S_0$ ;  $u_* = (\tau_0/\rho)^{1/2}$ ;  $S_0$  = slope of energy grade line;  $R$  = hydraulic radius;  $f_i$  = fraction of the  $i^{\text{th}}$  size contained in the bed material. Equation 2 can be referred to in short-hand notation

$$W_i^* = F(\tau_i^*, d_i^*, D_i^*, \rho_s/\rho, D_i/D_{50}) \quad (3)$$

If equal mobility is assumed, the variables  $W_i^*$  and  $\tau_i^*$  may be replaced by  $W^*$  and  $\tau_{50}^*$ , which use  $q_b$  and  $D_{50}$ , respectively, and represent the entire sediment mix. The variable  $D_i/D_{50}$  may be dropped and the variables  $D_i^*$  and  $d_i^*$  may be replaced by  $D_{50}^*$  and  $d_{50}^*$ .

For some gravel-bed streams the assumption of equal mobility is a good approximation of reality, however, for Goodwin Creek data the hypothesis of equal mobility breaks down at low flow strengths when not all of the bed material grain sizes are in motion. This is probably because the bed sediment has a significant mode in the sand size range. For gravel-bed streams with sand above some critical percent in the bed material, transport models may be expected to under-predict for low flow strengths. Possibly a better way to treat a gravel-bed stream with a bimodal distribution in the bed material may be to treat the sand and gravel portions as two separate entities each with their own characteristic grain size that interact with each other in different ways depending on the relative proportions present in the bed material and on the strength of the transporting flow. Within the sand and gravel fractions all sizes are assumed to be equally mobile.

It is the hypothesis of this report that when there is a significant sand mode in a gravel bed stream, then the transport rate can be adequately represented by using a two part transport relation: one for the sand material and one for the gravel material. These two transport functions each have a weighting coefficient:

$$w_s = F(f_s) \quad (4)$$

$$w_g = F(f_g) \quad (5)$$

where  $f_s$  and  $f_g$  are the fraction of sand and gravel in the bed material, respectively, and

$$q_b = w_s(\text{TRS}) + w_g(\text{TRG}) \quad (6)$$

with TRS - a transport relation for sand and TRG - a transport relation for gravel. For the limited range of conditions considered here it will be assumed that

$$\text{TRS} = F(\tau_{50s}^*) \quad (7)$$

$$TRG = F(r_{50g}^*)$$

(8)

with the subscripts '50s' and '50g' standing for the median sizes of the sand and gravel portions of the bed material, respectively.

#### STUDY AREA

The Goodwin Creek Research Watershed is located in the bluff-hills region of north central Mississippi, a region that is characterized by relatively steep slopes and a wide variety of erosion and sedimentation problems. The watershed includes fourteen gauging stations in the form of concrete "V" shaped supercritical flow flumes. These structures serve dual functions as grade control and gauging structures but were designed primarily to facilitate measurements of flow rates and sediment transport rates. Detailed descriptions of the watershed, its instrumentation, and the sediment sampling programs are contained in Bowie and Sansom (1986), Willis et al. (1986), and Kuhnle et al. (1988).

The channels on the watershed are ephemeral with only low base flows occurring most of the time. Flow in the channels sufficient to move the coarsest bed sediment has occurred an average of 12.1 times per year (1985-1988), usually during runoff events caused by the intense rainfall of the convective storms common to this region. As a result of the flow deriving from convective storms flow hydrographs tend to be steep with only rare periods of steady flow in the channels.

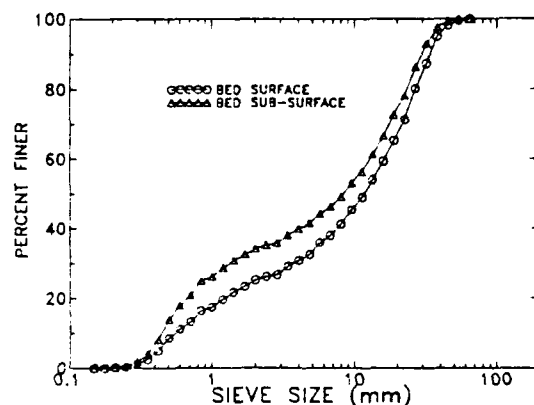


**Fig. 1.** Grain size distribution for bed material sediment of Goodwin Creek, station 2. Each curve is an average of 10 samples.

All samples considered here were collected at station no. 2 of the watershed. The drainage area upstream of station 2 is 17.9 km<sup>2</sup>. The channel at station 2 is about 25 m wide and 3.0 m deep. The surface layer (sampled at the thickness of the largest grains, 64 mm) of the bed material at station 2 has a  $D_{50} = 11.7$  mm and the subsurface material has a  $D_{50} = 8.3$  mm (Fig. 1). Both bed surface and sub-surface size distributions have prominent modes at 26.9 and 0.5 mm. The mean bed slope of the reach upstream of station 2 is 0.0033.

### SAMPLING EQUIPMENT

The supercritical flow measuring structure at station 2 is a "V" bottom concrete structure with 5:1 side slopes for 4.7 m each side of the center and 2:1 slopes thereafter. The structure has a 4 percent longitudinal slope which gives supercritical flow for all expected discharges and establishes fixed relationships between depth of flow and flow discharge rate within the supercritical section. The high flow velocities inhibit sediment deposition and provide a bottom reference for sediment transport measurements. Bed load has been sampled at station 2 using modified Helley-Smith (MHS) samplers (Helley and Smith, 1971; Druffel et al., 1976) suspended from foot bridges at the upstream end of the supercritical flow flume.

The entrance nozzle of the MHS samplers has been redesigned from a square 7.62 cm orifice to a trapezoidal shape to rest firmly on the sloping floor surface of the supercritical flume without any void area beneath the orifice. The area of the inlet orifice is 58.06 cm<sup>2</sup>, which is the same as the original Helley-Smith sampler. The ratio between the outlet and inlet orifices of the MHS samplers is 3.54. The MHS sampler is attached to a rigid strut suspension on a foot bridge over the upstream end of the concrete flume. This sampling arrangement eliminates the problems of sampler location and of sampling on uneven bed surfaces. A quick-release clasp on the 0.25 mm mesh sampler bag allows samples to be collected with a maximum frequency of about one every 2 minutes.

The hydraulic efficiency of the MHS sampler has been investigated in a laboratory flume at the National Sedimentation Laboratory. The channel used was 0.71 m wide, flow depths were all about 0.4 m, and mean flow velocities ranged from 0.4 to 1.2 m s<sup>-1</sup>. The hydraulic efficiency of the MHS sampler was evaluated by first taking velocity profiles 2.5 cm inside the inlet orifice of the sampler and at the same vertical and horizontal locations 0.61 m upstream of the inlet orifice. The velocities were measured with a pitot tube with a horizontal length of 0.46 m that was inserted through a slit in the top of the collection bag of the sampler. The pitot tube was connected to a differential pressure transducer that was sampled by a portable computer. Flow visualization using dye injection into the inlet orifice of the sampler demonstrated that the slit in the bag had a negligible effect on flow through the bag. Velocities were taken at five vertical locations in the sampler as close as possible to the two end walls and at three equally spaced locations at the interior of the orifice. Five velocities were taken at each vertical, equally spaced from the highest and lowest position within the sampler orifice. The velocities at each point were calculated from averages of 60 samples spaced 1 sec apart of the voltage output of the pressure transducer. Discharges through the inlet orifice and through an equal volume in the free stream were calculated for the area around each velocity measurement. Velocities that were adjacent to the walls of the sampler were weighted by the zero velocity assumed at the wall.

Hydraulic efficiencies were very close to 1.4 x that of the free stream for mean flow velocities from 1.22 to 0.85 m s<sup>-1</sup>. For mean flow velocities of 0.64 and 0.44 m s<sup>-1</sup> the hydraulic efficiency was 1.2 x the free stream (Table 1). This is somewhat less than the 1.5 x reported by Druffel et al. (1976) for the standard model of the Helley-Smith sampler. No attempt was made to measure bed load sampling efficiencies of the MHS sampler. Hubbell et al. (1985) calculated

that the standard version of the Helley-Smith sampler over-sampled by a factor of about 1.5. This is presumably due to the fact that the hydraulic efficiency is also 1.5 and the width of sediment sampled would have been greater than the width of the sampler. Some scouring of the bed may also have occurred at the sampler location due to its high hydraulic efficiency (Pitlick, 1988). Scouring of the bed with the MHS samplers could not have occurred due to the concrete flume base that was used in this study as a sampling platform. Furthermore the sediment moving through the supercritical flume is moving at a high velocity on the smooth bottom and much of it may have had enough inertia such that it would not be expected to be drawn into the MHS sampler from a width greater than that of the sampler. In any case a bed load sampling efficiency ratio of one was assumed for this study.

Table 1. Summary of Hydraulic Efficiency Tests of MHS Sampler.

Flow discharge ( $\text{m}^3 \text{ s}^{-1}$ )	Flow depth (m)	Mean channel flow velocity ( $\text{m s}^{-1}$ )	Mean flow vel. through orifice ( $\text{m s}^{-1}$ )	Mean flow vel. free stream ( $\text{m s}^{-1}$ )	Hydraulic efficiency ratio
0.347	0.398	1.23	1.45	1.04	1.39
0.291	0.392	1.05	1.20	0.88	1.37
0.234	0.391	0.85	0.97	0.70	1.39
0.177	0.393	0.64	0.68	0.57	1.20
0.121	0.393	0.43	0.48	0.40	1.20

#### SAMPLING TECHNIQUES

Sampling with the MHS samplers consisted of lowering the sampler to the flume bottom for a measured time interval such that the sampler fills approximately one-third full. For the period 1985 - 1986 samples were collected only at the centerline of the supercritical flow flume. Beginning in 1987 lateral samples across the right side of the 1:5 sloping section of the flume were taken at each flow strength. Each set of lateral samples was collected starting at the flume centerline and at 1.5 m lateral intervals ending either at the water's edge or the first sample with negligible sediment. These lateral samples were taken sequentially as close together in time as possible. Each set of lateral and center samples was analyzed together to give one mean cross section transport rate. Lateral samples were only collected on the right side of the structure. It was assumed that the distribution of sediment on the other side of the structure was the same. Each sample was stored in a labeled sample can for later drying, weighing, and sieving at the laboratory.

#### DATA TRANSFORMATION

The MHS sampling was conducted from November of 1984 to September of 1988. From that period 488 samples were analyzed from 21 separate transport events. A total of 187 sets of lateral samples were collected from 12 of these events with 301 samples collected only at the centerline for the other 9 events. Mean cross section transport rates and mean cross section size distributions were calculated for each of the lateral sets of samples. This was done by summing the area under

the sampled lateral transport rates connected by straight lines (Fig. 2) and computing a weighted average for the sediment size distribution. The lateral samples were divided into 3 groups based on depth of flow in the supercritical flume (0.3-0.6 m, 0.6-0.9 m, > 0.9 m) and least-squares linear relations between the mean cross section rate per unit width and the sampled rate at the center of the flume were calculated for each group. The data and least squares line are shown for flume depths > 0.9 m in Figure 3. In order to reduce the effect of outlying points on the least squares equation, points that were more than 2 standard deviations away from the fitted line were dropped and the regressions were repeated. A total of four points were dropped from the regressions by this procedure. The linear relations between mean cross section rate per unit width and sampled rate at the flume centerline of the flume (Table 2) were then used to convert the 301 centerline samples to mean cross section rates per unit width.

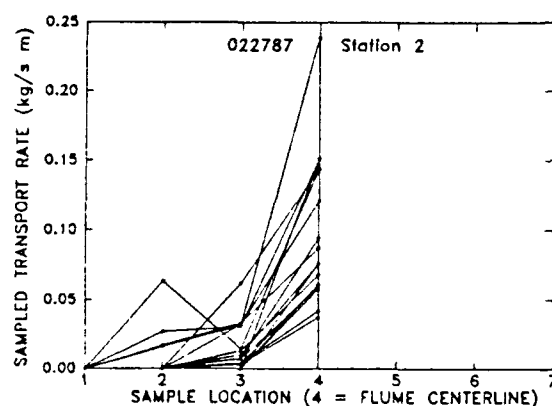


Fig. 2. Plots of lateral sample sets from 2/27/87 transport event. The distance between each sample location is 1.5 m. Lateral samples were taken only on one side of the flume centerline.

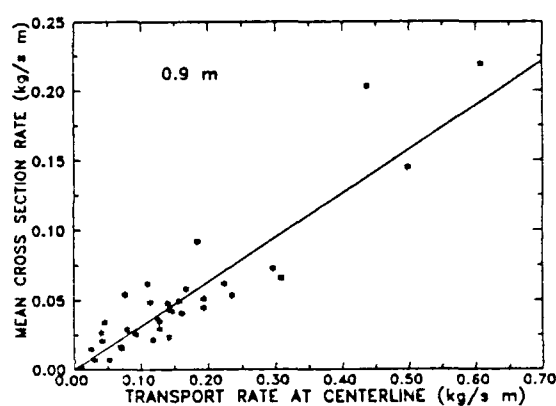


Fig. 3. Example of data used to calculate linear relations between sampled rate at flume centerline and mean cross section rate. The data for flume depths > 0.9 m is shown.

Table 2. Summary of Linear Equations Used to Convert Centerline Samples

Flume depth range (m)	# points	#points removed from regression	slope	R squared
0.3 - 0.6	85	0	0.3050	0.90
0.6 - 0.9	40	2	0.2628	0.76
> 0.9	35	2	0.3162	0.85

The bed shear stress ( $\tau_0$ ) for each mean cross section transport rate was calculated at the mid-point of the sample collection times using a mean hydraulic radius vs. flow depth relation from 10 surveyed channel cross sections and water



surface slope data from a 106 m long straight reach 63 m upstream from the supercritical flow flume. Water surface slopes were calculated for each sample time using the data from 4 USGS bubble gauges connected to pressure transducers in a 91 m length of the 106 m long surveyed channel reach. Data from the four bubble gauges was collected every minute by the remote telemetry system of the watershed.

#### DATA ANALYSIS

##### Transport Samples

Bed load transport rates calculated from the MHS data taken at station 2 are shown in Fig. 4. A mean transport rate curve for the data was defined by averaging all of the samples in  $5 \text{ N m}^{-2}$  wide strips from 10 to  $40 \text{ N m}^{-2}$ . The data was averaged to eliminate the natural variability of the bed load transport processes for gravel (Hubbell, 1987; Kuhnle and Southard, 1988; Kuhnle et al., 1989; Whiting et al. 1988) and to define the mean transport rate for a given flow strength. For flow strengths up to  $40 \text{ N m}^{-2}$  the number of transport samples collected is assumed to be sufficient to obtain representative average values for transport samples taken in that range of flow strength. Above  $40 \text{ N m}^{-2}$  not enough samples have been collected to define an accurate mean value and thus this data was not used in this study.

Weighted means of the median size of sediment in transport were also calculated for  $5 \text{ N m}^{-2}$  wide strips of bed shear stress (Fig. 5). The median size of each sample was weighted by the mass of the transport sample. For a given bed shear stress the median sizes of individual transport samples ranged from a fraction of a mm to nearly 20 mm (Kuhnle et al., 1989). The  $D_{50}$  values ranged from 0.84 to 7.77 mm.

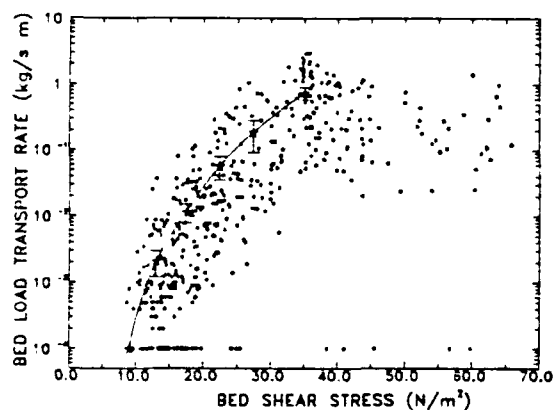


**Fig. 4.** Plot of 488 bed load samples from #2. Star points are average values from all data in each  $5 \text{ N m}^{-2}$  wide interval of bed shear stress. Error bars are the 95% confidence interval for the population mean. Solid line is a cubic spline equation fit between the points. Zero values plotted as  $10^{-4}$ .

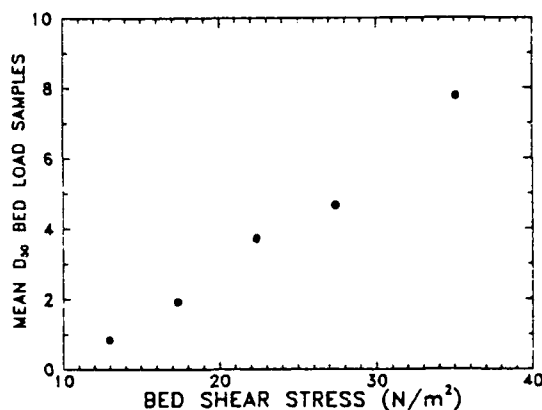


**Fig. 5.** Mean weighted  $D_{50}$  of bed load samples versus bed shear stress.

### Fractional Transport Rates

It was necessary first to determine how the size distributions of the 301 centerline samples related to the mean cross section size distributions. When the weighted average size distribution for each set of lateral samples was calculated and compared to the size distribution of the corresponding centerline sample, it was found that the centerline and weighted average size distributions were nearly the same. Therefore the size distributions of the 301 centerline samples were taken as being equal to the mean cross section size distributions of the bed load. The transport rate of each of the eight size fractions was then calculated for the 488 transport samples. These samples were then averaged in increments of  $5 \text{ N m}^{-2}$  of bed shear stress using the same technique used to average the total bed load transport rate samples.

Eight size fractions of the bed load MHS transport data from station 2 were considered. Figures 6 and 7 show plots of  $W_i^*$  vs.  $\tau_{i1}^*$  and  $\tau_{i1}^*$  vs.  $D_i/D_{50}$ , respectively. The subscript 'i' denotes that the mean diameter of that particular size fraction has been used as the characteristic grain size in that dimensionless parameter. The slopes of the lines in Figure 6 show a progressive decrease with decreasing size (Table 3). The dimensionless reference bed shear stress was defined as  $\tau_{i1}^* = \tau_{i1}^*$  when  $W_i^* = 0.002$  (Parker et al., 1982). The reference bed shear stress can be taken as a surrogate for critical bed shear stress. The slope of the line in Figure 7 is -0.8 which is somewhat less than the -1 value needed for perfect equal entrainment mobility.

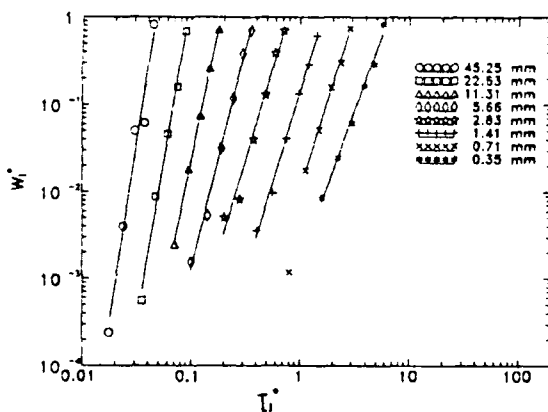


Fig. 6. Transport rates for eight size fractions of Goodwin Creek. One point for the 0.71 mm size fraction was not used in the transport relation.

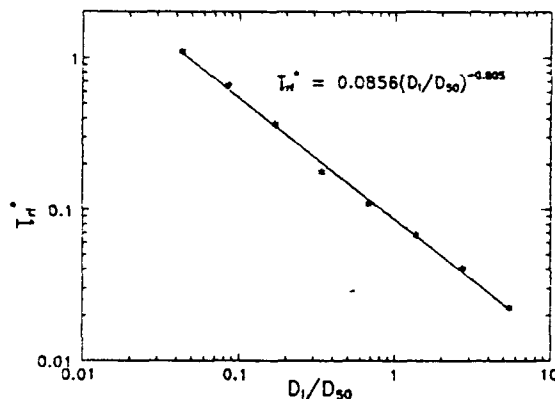


Fig. 7. Dimensionless reference bed shear stress versus relative grain size.

The mean ratios of the fraction of the  $i^{\text{th}}$  size range in the bed load -  $p_i$ , to the fraction of the  $i^{\text{th}}$  size range in the sub-surface bed material -  $f_i$  are plotted against bed shear stress in Figure 8. The relative proportion of the transport rate of each size fraction is shown in Figure 9. Figures 8 and 9 show that the finer sizes are over represented and the coarser sizes are under

represented in the bed load for low bed shear stresses with all  $p_i/f_i$  values tending toward one (equal transport mobility) at higher bed shear stresses.

Table 3. Least Squares Fit to  $W_i^* = a(\tau_{*i})^b$ , and  $\tau_{*i}^*$ .

geometric mean size of fraction (mm)	b	a	$\tau_{*i}^*$
45.25	8.27	$9.36 \times 10^{10}$	0.0223
22.63	7.46	$4.79 \times 10^7$	0.0406
11.31	6.11	$2.83 \times 10^4$	0.0674
5.66	5.07	$1.45 \times 10^2$	0.1099
2.83	4.21	$2.80 \times 10^0$	0.1787
1.41	4.19	$0.13 \times 10^0$	0.3664
0.71	3.99	$1.03 \times 10^{-2}$	0.6627
0.35	3.51	$1.40 \times 10^{-3}$	1.0972

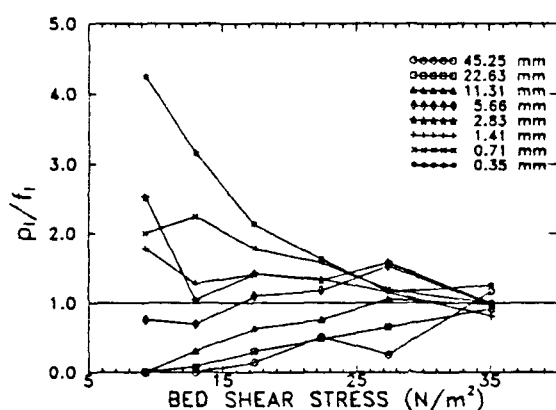


Fig. 8. Ratio of fraction of  $i$ -th size sediment in bed load to fraction of  $i$ -th size sediment in bed material sub-surface versus flow strength.

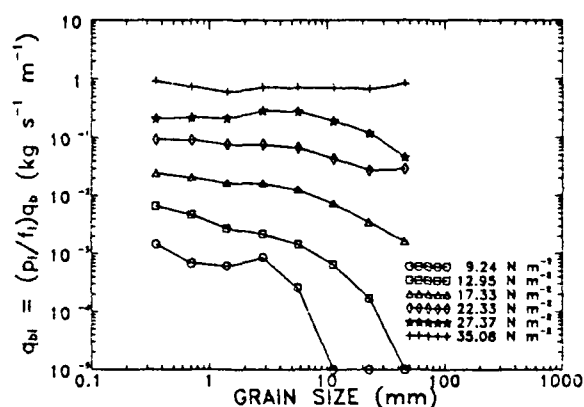


Fig. 9. Fractional transport rates for six flow strengths. Zero values plotted as  $10^{-5}$ .

#### Prediction of Bed Load Transport Rate

The accurate prediction of gravel bed load transport rates on natural streams is a difficult task (e.g. Parker et al., 1982; Gomez and Church, 1989). The published transport relationships of Meyer-Peter and Müller (1948), Parker et al. (1982), and Bagnold (1980) were compared to the mean transport relationship of Goodwin Creek graphically shown in Figure 4. None of the three transport relationships used does an adequate job of predicting bed load transport on Goodwin Creek (Fig. 10). The bimodal nature of the bed material at Goodwin Creek may be one of the reasons for the failure of the published transport relations. To test the feasibility of this hypothesis a transport relation which is composed of two parts was formulated for the Goodwin Creek data.

Instead of formulating new transport relations for sand and gravel, two existing transport relations were used with weighting coefficients derived from the Goodwin Creek data. The two transport relations used were Yalin (1963) for sand, and Parker et al. (1982) for gravel. The boundary between sand and gravel was defined as 2 mm.

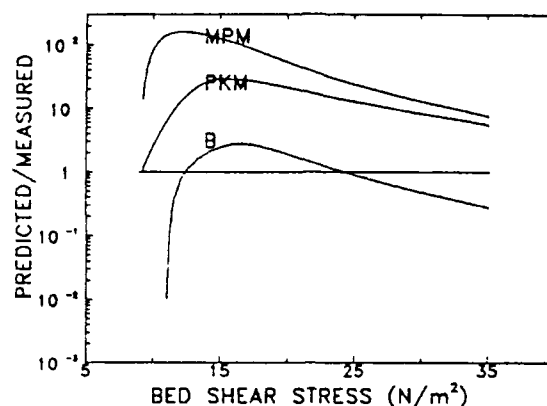


Fig.10. Three transport relations compared to mean Goodwin Creek relation. The horizontal line at 1.0 equals perfect agreement. B - Bagnold (1980), PKM - Parker, Klingeman, McLean (1982), MPM - Meyer-Peter and Müller (1948).

The calculation of critical bed shear stress values for the two transport equations was based on the bed surface grain size distribution. The critical bed shear stress used for the sand ( $\tau_{cs}$ ) was  $9.0 \text{ N m}^{-2}$ , which was empirically derived from the data. The critical bed shear stress used for the gravel fraction ( $\tau_{cg}$ ) of the load was  $17.24 \text{ N m}^{-2}$ . This value was slightly larger than the reference bed shear stress value calculated for the 45.25 mm size fraction.

A critical part of this two part transport relation is the value of the two weighting factors. After empirically fitting the weighting factors that yielded a best fit with the transport data it was determined that these values were close to the portions of sand and gravel contained in the bed surface material. These values were used ( $w_s = 0.25$ ,  $w_g = 0.75$ ) with the two transport relations to calculate the sand and gravel load (Table 4).

Table 4. Bimodal Transport Model Comparison with Goodwin Creek Data

$\tau_0$	net calc. sand	ratio sand	net calc. gravel	ratio gravel	total calc. sand+gravel	ratio total
( $\text{N/m}^2$ )	( $\text{kg/s m}$ )	(calc/meas)	( $\text{kg/s m}$ )	(calc/meas)	( $\text{kg/s m}$ )	(calc/meas)
9.00	0.0000	----	0.0000	----	0.0000	----
12.95	0.0032	1.95	0.0000	0.00	0.0032	1.54
17.33	0.0127	1.84	0.0008	0.16	0.0135	1.16
22.33	0.0293	1.02	0.0302	1.05	0.0595	1.04
27.37	0.0512	0.75	0.2370	2.02	0.2882	1.55
35.08	0.0931	0.38	0.8804	1.79	0.9735	1.32

### Discussion

Recent work has shown that the reference shear stress (a surrogate variable for the critical shear stress for movement) of an individual size fraction in a bed with a mixture of sizes is dependent on its relative size as well as its absolute size. Work by Miller and Byrne (1966), Li and Komar (1986), Komar and Li (1986), and Wiberg and Smith (1987) have shown that the interaction of the different sizes in a mix act to reduce or even eliminate the differences in the values of reference bed shear stress of the various sizes. The current understanding of the reduction of the reference shear stresses of the different sizes concerns the different pivot angles of the grains (which are inversely related to relative grain size) and the relative protrusion of the grains into the boundary layer of the flow (which causes a greater force to be exerted on the larger grains for a given flow). When equal entrainment mobility is reached a plot of dimensionless reference bed shear stress vs. relative size (Fig. 7) will have a slope of -1. In fact several researchers have reported data from field streams (Parker et al., 1982; Andrews, 1983; Andrews and Erman, 1986) and from laboratory flumes (Wilcock and Southard, 1988) with slopes very near -1. Ashworth and Ferguson (1989) and the data of White and Day (1982) analyzed by Wilcock and Southard (1988) had slopes of -0.74 and -0.81, respectively. These last two values, which were very close to that calculated for Goodwin Creek, indicate that the larger grains in the sediment mixes still required larger bed shear stresses for movement than the smaller ones. Reasons for this difference may be related to the shape of the size distribution of the bed material sediment.

Deviations from equal transport mobility were also found for bed load transport on Goodwin Creek. The slopes of the transport relations of the size fractions from 0.35 to 2.83 mm are only slightly different from one another, while the slopes of the transport relations for sizes above 2.83 mm show a larger deviation among them (Table 3). The combination of the larger grains needing a greater bed shear stress for entrainment and having a steeper sloping transport rate relation than the smaller grains yields unequal transport mobilities until high bed shear stresses are reached. The pattern of the slope variations of the Goodwin Creek data is very similar to that found by Parker et al. (1982) for Oak Creek. The entrainment mobility of Goodwin Creek, however, is different from that of Oak Creek.

The patterns of transport mobility of the different size fractions for Goodwin Creek data (Fig. 9) are similar to those from laboratory flume experiments of Wilcock and Southard (1989, Fig. 4, p. 1646). The lowest transport rates of both data sets show that the coarse grains are under represented in the transport. For intermediate flows the Goodwin Creek data shows only coarse grains under represented in the bed load not both coarse and fine grains under represented in the bed load shown by the flume data. Both data sets approach perfect equal transport mobility at the highest flows.

The two part transport relation used to calculate bed load transport rate on Goodwin Creek should be taken only as one possible way to deal with gravel-bed streams with bimodal bed material size distributions. The prediction of reference bed shear stresses for the sand and gravel parts of this model is one problem which needs to be studied further. For sand the empirically derived reference bed shear stress could be approximated from the relation:  $\tau_{x50} = 0.045$ ,

with  $D_{50}$  of the bed surface used. The reference bed shear stress for gravel could be approximated from the equation:  $\tau_{r90}^* = 0.03$ , with  $D_{90}$  of the bed surface used. In other words the interaction of the two size fractions causes different grain size information to be needed for calculating entrainment and transport rates. These two equations are only for one stream and may not hold for other cases.

Much work also remains to be done in order to determine values of the two weighting coefficients for cases other than Goodwin Creek. The two logical endpoints of this model would be a stream in which there is no sand in the bed material where  $w_s = 0$ , and  $w_g = 1$ , and one in which there is no gravel in the bed material where  $w_s = 1$ , and  $w_g = 0$ . An experimental program is currently in progress at the Sedimentation Laboratory to test if this technique works for bed material size distributions that cover the range from pure sand to pure gravel.

#### Conclusions

1. Fractional transport data from Goodwin Creek have shown that deviations from equal entrainment mobility exist on the stream. Bed surface armoring processes have not removed all of the differences in the reference bed shear stresses ( $\tau_{ri}^*$ ) of the size fractions present in the bed material.

2. For low flow rates on Goodwin Creek the coarse fractions of the sediment were under represented in the transport ( $p_i/f_i < 1$ ), the fine fractions were over represented in the transport ( $p_i/f_i > 1$ ), and equal transport mobility is approached as bed shear stresses increase.

3. A two part transport model has been shown to be a possible way to predict transport on gravel-bed streams with significant sand present in the bed material (bimodal size distribution). For Goodwin Creek the weighting factors needed for this model can be taken as the proportion of sand and gravel sediment in the bed surface layer. Within certain ranges the proportions of sand and gravel will likely be important for other streams with bimodal bed material size distributions. Prediction of reference bed shear stresses for this model will probably need to take into account the size distribution present at the surface of the bed of the stream. Dimensionless parameters scaled to  $D_{50}$  and  $D_{90}$  of the bed surface size distribution were used to arrive at the empirically derived values for reference bed shear stress for the sand and gravel fraction, respectively. It is not known if these parameters will hold for other situations.

#### References

- Andrews, E. D. (1983). 'Entrainment of gravel from naturally sorted riverbed material', *Geol. Soc. Amer. Bull.*, 94, 1225-1231.
- Andrews, E. D., and Erman, D. C. (1986). 'Persistence in the size distribution of surficial bed material during an extreme snowmelt flood', *Water Resour. Res.*, 22(2), 191-197.
- Ashworth, P. J., and Ferguson, R. I. (1989). 'Size-selective entrainment of bed load in gravel bed streams', *Water Resour. Res.*, 25(4), 627-634.

- Bagnold, R. A. (1980). 'An empirical correlation of bedload transport rates in flumes and natural rivers', *Proc. Royal Soc. London*, A372, 453-473.
- Bowie, A. J., and Sansom, C. W. (1986). 'Innovative techniques for collecting hydrologic data', *Proc. 4th Federal Interagency Sedimentation Conf.*, Las Vegas, Nevada, 1-59 -1-69.
- Druffel, L., Emmett, W. W., Schneider, V. R., and Skinner, J. V. (1976). 'Laboratory hydraulic calibration of the Helley-Smith bedload sediment sampler', U. S. Geological Survey Open-File Report 76-752, Bay St Louis, Miss., 63pp.
- Einstein, H. A. (1950). 'The bed-load function for sediment transportation in open channel flows', U. S. Department of Agriculture Soil Conservation Service, Technical Bulletin No. 1026, 78pp.
- Gomez, B., and Church, M. (1989). 'An assessment of bed load sediment formulae for gravel bed rivers', *Water Resour. Res.*, 25(6), 1161-1186.
- Helley, E. J., and Smith, W. (1971). 'Development and calibration of a pressure-difference bedload sampler', U. S. Geological Survey Open-File Report, Menlo Park, Calif., 18pp.
- Hubbell, D. W. (1987) 'Bed load sampling and analysis', in *Sediment Transport in Gravel-Bed Rivers*, edited by C. R. Thorne, J. C. Bathurst, and R. D. Hey, John Wiley, New York, 89-118.
- Komar, P. D., and Li, Z. (1986). 'Pivoting analyses of the selective entrainment of sediments by shape and size with application to gravel threshold', *Sedimentology*, 33, 425-436.
- Kuhnle, R. A. (1989). 'Bed surface size changes in gravel-bed channel', *ASCE Jour. Hydraulic Eng.*, 115(6), 731-743.
- Kuhnle, R. A., and Southard, J. B. (1988). 'Bed load transport fluctuations in a gravel bed laboratory channel', *Water Resour. Res.*, 24(2), 247-260.
- Kuhnle, R. A., Willis, J. C., and Bowie, A. J. (1988). 'Measurement of bed load transport on Goodwin Creek, northern Mississippi', *Proc. Eighteenth Mississippi Water Resources Conf.*, edited by E. J. Hawkins, Jackson, MS, 57-60.
- Kuhnle, R. A., Willis, J. C., and Bowie, A. J. (1989). 'Variations in the transport of bed load sediment in a gravel-bed stream, Goodwin Creek, northern Mississippi, U.S.A.', *Proc. Fourth International Symposium on River Sedimentation*, Beijing, China, 539-546.
- Li, Z., and Komar, P. D. (1986). 'Laboratory measurements of pivoting angles for applications to selective entrainment of gravel in a current', *Sedimentology*, 33, 413-423.
- Meyer-Peter, E., and Müller, R. (1948). 'Formulae for bedload transport', paper presented at Third Conf. Int. Assoc. Hydraul. Res., Stockholm.

Miller, R. L., and Byrne, R. J. (1966). 'The angle of repose of a single grain on a fixed rough bed', *Sedimentology*, 6, 303-314.

Parker, G., Klingeman, P. C., and McLean, D. G. (1982). 'Bedload and size distribution in paved gravel-bed streams', *Proc. ASCE Jour. Hydraul. Div.*, 108(HY4), 544-571.

Pitlick, J. (1988). 'Variability of bed load measurement', *Water Resour. Res.*, 24(1), 173-177.

Tacconi, P., and Billi, P. (1987). 'Bed load transport measurements by the vortex-tube trap on Virginio Creek, Italy', in *Sediment Transport in Gravel-Bed Rivers*, edited by C. R. Thorne, J. C. Bathurst, and R. D. Hey, John Wiley, New York, 583-616.

White, W. R., and Day, T. J. (1982). 'Transport of graded gravel bed material', in *Gravel-Bed Rivers*, edited by R. D. Hey, J. C. Bathurst, and C. R. Thorne, John Wiley, New York, 181-213.

Whiting, P. J., Dietrich, W. E., Leopold, L. B., Drake, T. G., and Shreve, R. L. (1988). 'Bedload sheets in heterogeneous sediments', *Geology*, 16, 105-108.

Wiberg, P. L., and Smith J. D. (1987). 'Calculations of the critical shear stress for motion of uniform and heterogeneous sediments', *Water Resour. Res.*, 23(8), 1471-1480.

Wilcock, P. R., and Southard, J. B. (1988). 'Experimental study of incipient motion in mixed-size sediment', *Water Resour. Res.*, 24(7), 1137-1151.

Wilcock, P. R., and Southard, J. B. (1989). 'Bed load transport of mixed size sediment: fractional transport rates, bed forms, and the development of a coarse bed surface layer', *Water Resour. Res.*, 25(7), 1629-1641.

Willis, J. C., Darden, R. W., and Bowie, A. J. (1986). 'Sediment transport in Goodwin Creek', *Proc. 4<sup>th</sup> Federal Interagency Sedimentation Conf.*, Las Vegas, Nevada, 4-30 - 4-39.

#### NOTATION

The following symbols are used in this paper:

$D_{50}$  = median grain size;

$D_i$  = mean grain size of the  $i^{\text{th}}$  grain size subrange;

$D_i^* = g^{1/3} D_i / \nu^{2/3}$ ;

$D_{50}^* = g^{1/3} D_{50} / \nu^{2/3}$ ;

$d$  = mean flow depth;

$d_i^* = d / D_i$ ;



$$d_{50}^* = d/D_{50};$$

$F$  = a functional relationship;

$f_g$  = fraction of gravel in bed material;

$f_s$  = fraction of sand in bed material;

$f_i$  = fraction of the  $i^{\text{th}}$  size sediment contained in the bed material;

$g$  = acceleration of gravity;

$p_i$  = fraction of  $i^{\text{th}}$  size sediment contained in bed load;

$q_{bi}$  = bed load transport rate of  $i^{\text{th}}$  size fraction in mass per time per unit width;

$q_b$  = total bed load transport rate in mass per time per unit width;

$R$  = flow cross-sectional area/wetted perimeter = hydraulic radius;

$S_0$  = slope of the energy grade line;

TRS = bed load transport relation for sand;

TRG = bed load transport relation for gravel;

$u_* = (\tau_0/\rho)$  = bed shear velocity;

$W^* = ((\rho_s/\rho)-1)gq_b/\rho_s u_*^3$  = dimensionless total bed load;

$W_i^* = ((\rho_s/\rho)-1)gq_{bi}/\rho_s u_*^3 f_i$  = dimensionless bed load in  $i^{\text{th}}$  size range;

$w_g$  = weighting coefficient for transport relation for gravel;

$w_s$  = weighting coefficient for transport relation for sand;

$\mu$  = dynamic viscosity of fluid;

$\nu = \mu/\rho$ ;

$\rho$  = density of the fluid;

$\rho_s$  = density of the sediment;

$\tau_0 = \rho g R S_0$  = bed shear stress;

$\tau_{cs}$  = critical bed shear stress for sand portion of bed material;

$\tau_{cg}$  = critical bed shear stress for gravel portion of bed material;

$\tau_{50}^* = \tau_0/((\rho_s-\rho)gD_{50})$  = dimensionless bed shear stress for median size of bed material

$\tau_i^* = \tau_0/(\rho_s - \rho)gD_i$  - dimensionless bed shear stress for  $i^{\text{th}}$  size range;

$\tau_{ri}^*$  - dimensionless reference bed shear stress for  $i^{\text{th}}$  size range,  
 ( $\tau_i^* = \tau_{ri}^*$  when  $W_i^* = 0.002$ );

$\tau_{r50}^*$  - dimensionless reference bed shear stress for  $D_{50}$  of bed surface sediment;

$\tau_{r90}^*$  - dimensionless reference bed shear stress for  $D_{90}$  of bed surface sediment;

$\tau_{50s}^*$  - dimensionless bed shear stress using median grain diameter of sand  
 fraction;

$\tau_{50g}^*$  - dimensionless bed shear stress using median grain diameter of gravel  
 fraction;

3rd International Workshop on Gravel-Bed Rivers  
"DYNAMICS OF GRAVEL-BED RIVERS"  
FIRENZE 24-28 SEPTEMBER 1990

MONITORING OF PARTICLE MOVEMENT ON  
VIRGINIO GRAVEL-BED STREAM

TACCONI P.\*, RINALDI M.\*\*\*, MORETTI S.\*\*\*, MATTEINI M\*\*

- \* Istituto di Ingegneria Ambientale - Universita' di Perugia
- \*\* Dipartimento di Scienza della Terra - Universita' di Firenze

## ABSTRACT

A continual operation bedload measurement station was installed near Baccaiano in the Virginio gravel-bed stream, which has a grain-size about  $D_{50} = -5 \phi$  and a straight shape with alternate bars. The slope of the stream at this point is about 0.008 and the basin has an area of 40 km<sup>2</sup>. The introduction of a marked sample of about 3000 pebbles, upstream the measurement station, makes possible to study the relationships between bedload transport with the pebbles passage through the station itself and furthermore with their position in the bed after each flood.

The results of this study confirm the pulsating rate of the bedload transport and its poor correlation with grain-size distribution and discharge. For each grain-size classes the distance travelled by the pebbles, their embedding and, in some cases, their mean velocity, was measured.

## 1. INTRODUCTION

The main part of the bed-load transport in a gravel-bed river has a grain-size considerable inferior to that characteristic of its river bed.

The most coarse grain-sizes, constituting as a rule only a small part of the ground bed-load transport, are an important contributory factor in the river-bed dynamics since they form the base of the channel, and the bars and riffles are generally formed by them. The means and quantity of pebbles transported in a gravel-bed river are little known. Its measurement is very difficult and apart from the little data measured in experimental basins and that gathered in laboratory water-channels, it has been almost impossible to measure on a large scale with a great enough level of accuracy and using present-day methods, in natural river-beds Emmett 1981; Tacconi, 1982).

The results obtained experimentally in natural river-beds between bed-load transport and other parameters such as discharge or hydraulic features of the current, are much lower than expected (Billi and Tacconi, 1987).

The variability of the coarse sediment transport is very high and it is characterized by a pulsating nature linked more to morphological-sedimentary features of the river-bed than to variations in discharge. (Klingeman e Milhous, 1970; Hayward and Sutherland, 1974; Meade et Al., 1981; Reid et Al., 1985; Tacconi and Billi, 1987).

## 2. GENERAL DESCRIPTION OF RIVER-BED AND EXPERIMENTAL STATION

Virginio Creek, situated in the Arno basin in Tuscany near Baccaiano, was equipped with a measurement gauge in continual operation for bed-load ( $\varphi > -1$ ) supplied with a vortex tube trap and readmission system for sediment in the downstream river-bed. The basin upstream has a surface area of 40 km, in which are present marine pliocene deposits composed of silts, sands, pebbles and used for cultivating grain, vines and olive trees. It has a mediterranean climate with an average annual precipitation of 900 mm.

The river-bed upstream from the measurement station is straight with alternating bars, joined to riffles and pools with banks covered by thick vegetation. The average size width-wise with a high-water level is 12 m with a gradient of 0.008.

The results of the studies made at the measurement station up until 1985 have published (Tacconi and Billi 1987; Billi and Tacconi 1987). In brief, the studies carried out have shown for Virginio Creek:

- the extreme variability of coarse sediment transport;
- its pulsating nature with a cycle of about 30';
- the low correlation between sediment and liquid transport discharges;
- the different means of transport for high discharges where the river-bed completely mobilizes itself forming a conveyor belt with solid discharge occurring in a single event like the total

- discharge measured over several consecutive years;
- the successive and progressive evolution of the bed with the formation of alternating bars and the development of the armour in the low-water channel, the close similarity between grain-size in the bedload transport and the subarmour.

The present note refers to the measurements and to the studies carried out in 1985. In this period there were only four flood events studied and, indeed along with an exceptional period of drought, the Local Authorities started the work of dredging the river-bed which they claimed necessary. In spite of its ineffectiveness, this work transformed the river-bed in a channel of trapezoidal sections destroying its natural shape and rendering for a certain amount of time any significant measurements impossible.

### 3. METHODOLOGY

The operations possible for measuring sediment transport at the measuring station are the following:

- 1) Analysis and control of transverse sections in river bed section under study.
- 2) Grain size measurements of armour and subarmour.
- 3) Continual measurement of bedload transport during flood events ( $\varphi > -1$ ).
- 4) Drawing of sample and grain size analysis of bedload transport during flood events.
- 5) Continual visual analysis of bedload transport with analysis of any further marked pebbles (transit time, grain size, weight followed by immediate reintroduction in down-stream river-bed).
- 6) Introduction of a marked sample upstream from measuring station in section under control.
- 7) Direct survey in river-bed of the cloud formed by sample distribution downstream from point of introduction, and both up and downstream from measurement station both before and after the subsequent flood events.
- 8) Other operations such as the measurement of liquid discharge of suspended sediment transport, velocity, etc..

#### 3.1 Observations and Measurements

The experiment made in 1988 consists of the introduction of a marked sample into a section 250 m upstream from the measurement station and its subsequent analysis: - evolution of river-bed; - measurement of bedload transport; recording of passage made by clasts in marked sample during the floods from the measurement section; - measurement of the distances travelled by all visible clasts (not those buried in river-bed) in each grain-size class of marked sample after the 4 flood events.

For operational purposes, not all the observations and measurements sediment transport during the events under study continued throughout the entire duration of the event.

### 3.2 Features of the River-bed at the time of Experiment

The means adopted, the nature and the quantity of the bedload transport depend to a larger extent on the state of the river-bed before the event than on the liquid discharge (Tacconi, Billi, 1987).

As mentioned in the introduction, the river-bed under study was subjected to maintenance works by the Local Authorities in 1986. The trapezoidal section that was artificially formed after the various flood events causing considerable sediment discharge, was again modified in Spring 1988 and the river-bed returned to its initial natural form (proving the ineffectiveness, if not the damage, of the Authority's dredging); the river-bed developed once more its former straight form with bars alternating with the low flow channel, and an apparent armour and sequences of riffles and pools.

The marked sample was introduced in a section 250 metres upstream from the section for measuring sediment discharge. A lateral bar on the left bank was present here placed almost 30 m from the introduction section. The low water channel was 4 m wide and was recognizable from the rest of the bed through the presence of a lateral step measuring about 10 cm; the grain-size of the river-bed examined corresponding with the lateral bars was the following:

#### Armour

Mean Diameter ( $\phi$ ) = -5.961852

Standard Deviation ( $\phi$ ) = .6869485

Skewness = .5583912

Kurtosis = 3.413433

D10 ( $\phi$ ) = -5.045822

D10 (mm) = 33.03268

D50 ( $\phi$ ) = -6.024881

D50 (mm) = 65.11334

D90 ( $\phi$ ) = -6.831544

D90 (mm) = 113.8937

#### Subarmour

Mean Diameter ( $\phi$ ) = -4.929065

Standard Deviation ( $\phi$ ) = 1.28711

Skewness = 1.393888

Kurtosis = 5.186635

D10 ( $\phi$ ) = -3.276591

D10 (mm) = 9.690636

D50 ( $\phi$ ) = -5.17537

D50 (mm) = 36.13613

D90 ( $\phi$ ) = -6.284161

D90 (mm) = 77.9329

About the low-level bed, the armour grain size was measured just before the observation period.

Mean Diameter ( $\phi$ ) = -6.383727

Standard Deviation ( $\phi$ ) = .6338497

Skewness = .6787533

Kurtosis = 3.149776

D10 ( $\phi$ ) = -5.505165

D10 (mm) = 45.41713

D50 ( $\phi$ ) = -6.480906

D50 (mm) = 89.31964

D90 ( $\phi$ ) = -7.181181

D90 (mm) = 145.1279

The sample was introduced by throwing the clasts at random across the whole low-water channel, 4 meters wide in a cross-wise strip 2 meters wide.

### 3.3 Features of the marked sample

The preparation of the marked sample was preceded by a preliminary survey that involved sampling channel and bars sediments in the river-bed tract upstream the measuring station.

The marked sample was prepared and called "Grain size", sizing between  $-4 \phi$  and  $-7 \phi$ , and composed of 3935 pebbles weighing a total of 337 kg.

Besides this "grain-size", a "morphometric" sample was introduced composed of 300 pebbles sizing between  $-4.5 \phi$  and  $-5.5 \phi$ , representative of the three forms in Folk's classification (spheric, discoidal, elongated).


The pebbles were examined in the same river-bed to ensure identical lithological features (limestones) of those normally present in bedload transport and they were subsequently given eposidic colour using two yellow colour components.

The individual clasts of the morphometric sample were numbered and coloured red enabling close study of their movements; the morphometric sample was introduced in order to study the effect of pebble morphometry on mobility; that study is not included here.

TABLE I  
CHARACTERISTICS OF MARKED SAMPLE  
GRAIN SIZE SAMPLE (YELLOW)

$\phi$	N° Clasts	Weight kg	Mean Weight
$-4 \div -4.5$	2000	20	10
$-4.5 \div -5$	1000	28	28
$-5 \div -5.5$	500	32	64
$-5.5 \div -6$	250	50	200
$-6 \div -6.5$	125	80	640
$-6.5 \div -7$	60	127	2117
$-4 \div -7$	3935	337	85.6

MORPHOMETRIC SAMPLE (RED)

$\phi$	N° Clasts	Weight kg	Morphometry
$-4.5 \div -5.5$	100 100 100	 8.5	Elongated Discoidal Spheric



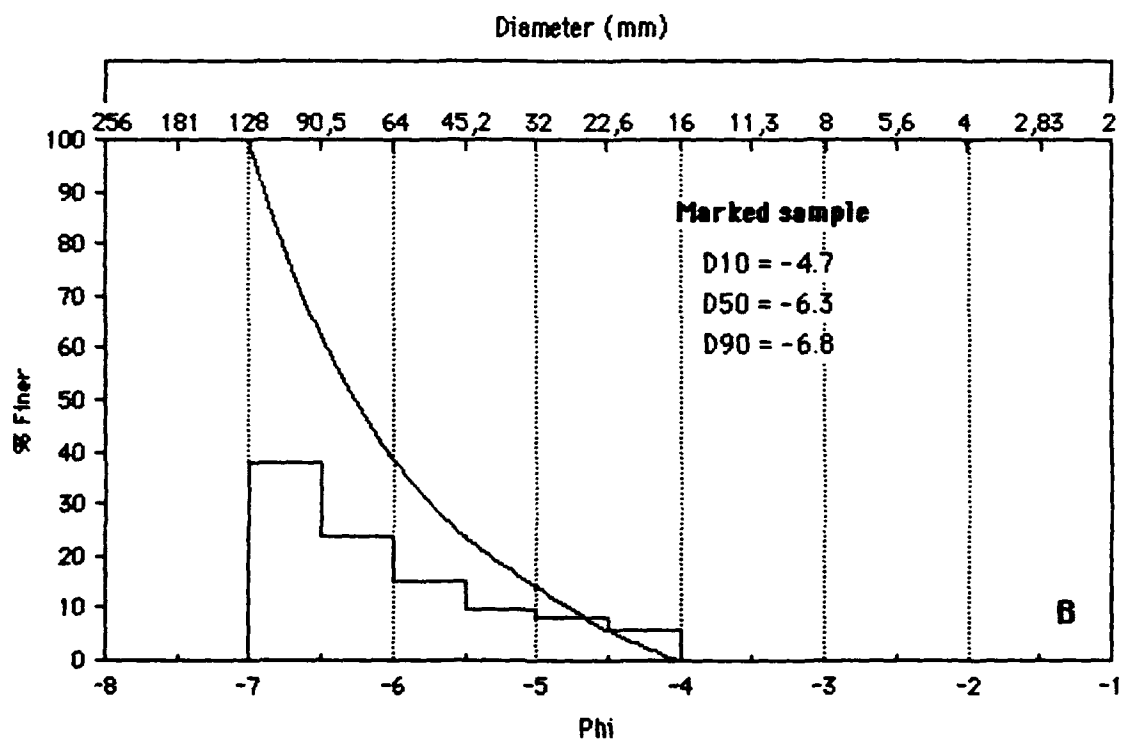
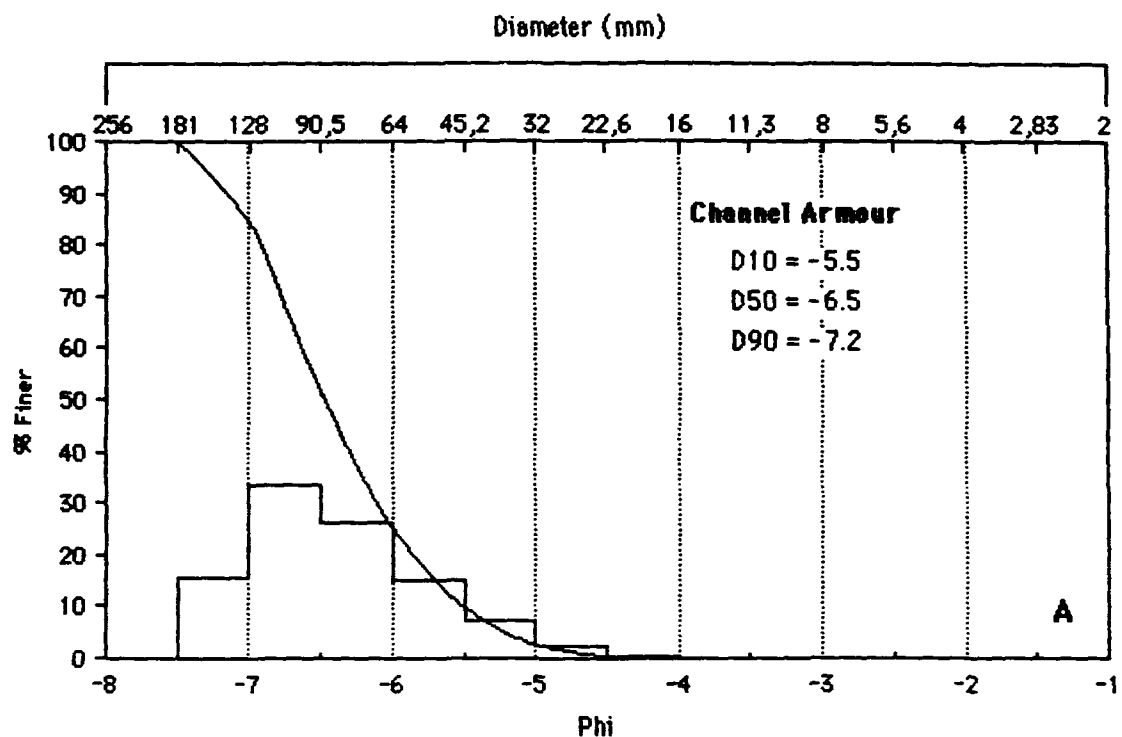


Fig.1. Granulometric distribution of the armour channel (A) and of the marked sample (B).

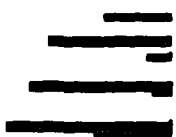


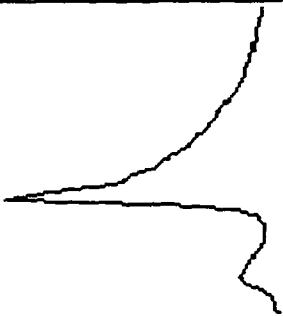


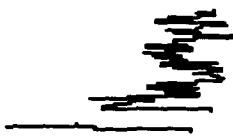

Flood number	1	2	3	4
Date	13/4/88	20/5/88	28/5/88	5/6/88
Rainfall	No measurements			No measurements
Discharge				
Bedload	No measurements			Total Bedload : 450 kg
Peak Discharge (mc/s)	3	17	6	4,9
Max Bedload (kg/min)		580	125	
Pebbles Mobility	Observations	345	331	184
	Range	1 - 666	1 - 744	2 - 776
	Mean	234,6	246,4	192,2

Fig. 2

#### 4. OBSERVED FLOOD EVENTS

The sizes measured for each of the four flood events are concisely drawn up in Fig. 2.

The main hydrological features and solid discharge for each flood are subsequently described.

##### 4.1 Flood n° 1 - 14.04.1988

This is a low intensity event with a maximum discharge of about 3 mc/sec; and duration of 1440 minutes. The sediment discharge was not measured.

##### 4.2 Flood n° 2 - 20.05.1988

This is the highest intensity flood of the four observed and it is associated to four main precipitation events.

A first peak of about 4 mc/sec was registered followed by the main peak with a discharge of 17 mc/sec.

The recording of the sediment discharge is not complete; in fact when the measuring station was put into use, some marked pebbles were found that must have travelled along a section of the order of 250 m.

Moreover, 30 minutes after the start of the recordings, due to operational problems connected with the high rate of bedload transport, measuring was stopped for 50 minutes. A maximum bedload transport of 580 kg/min and 2110 kg in 5 minutes was recorded.

This is the highest level of sediment discharge ever recorded at the measuring station from its installation.

The total sediment discharge measured was about 43260 kg. After this interruption, measuring continued for more than 48 hours during which further data was not drawn. The characteristic events measured are indicated in Fig. 3.

##### 4.3 Flood n° 3 - 28.05.1988

Inspite of its weaker intensity, the recording of data for this flood event comprises all the sizes.

The length of the flood wave is 420 minutes, with a peak discharge of 6 mc/sec.

The maximum sediment discharge measured is 125 kg/min while the total sediment discharge is 2780 kg.

A few isolated arrivals of bedload may be noted that have preceded the sediments' real state of continual motion.

During the principle event of sediment discharge following the first isolated episodes, the initial condition of sediment movement is easily recognizable, with a liquid discharge of little more than 2 mc/sec (Fig. 4).

The sediment discharge is exhausted quickly in this event after the peak period of liquid discharges.

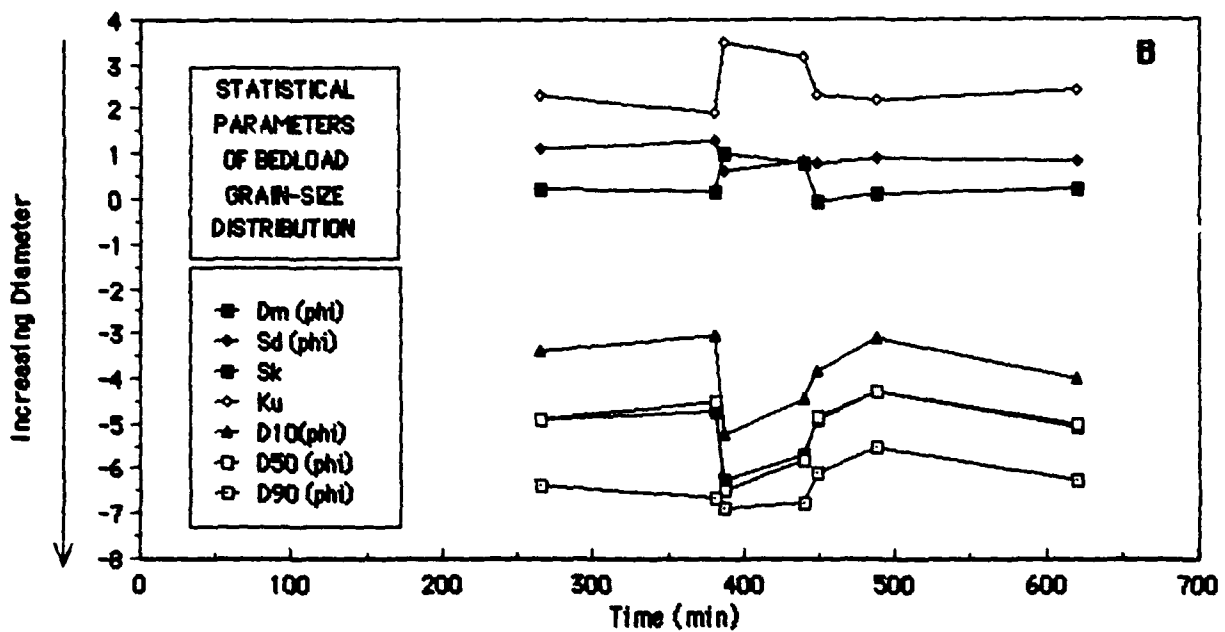
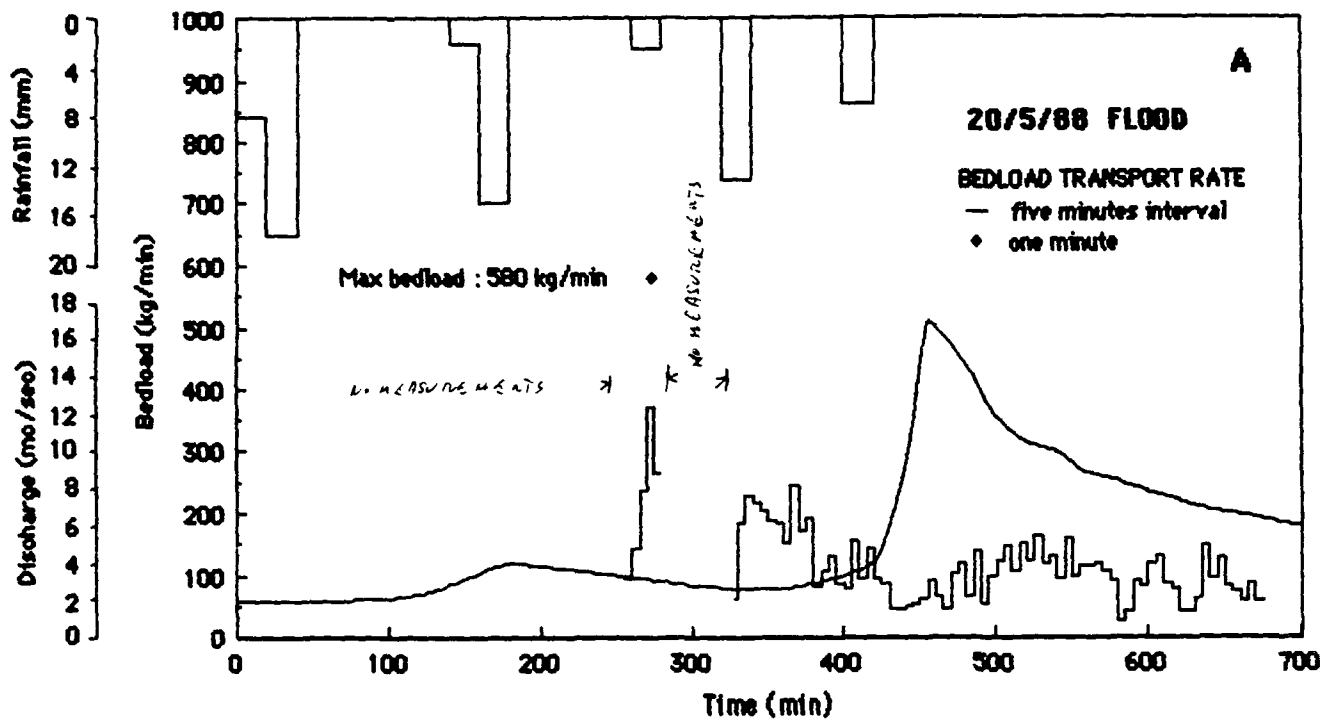


Fig.3. 20/5/88 flood : A) rainfall, discharge and bedload;  
 B) statistical parameters range for the bedload samples.  
 Dm: mean diameter; Sd: standard deviation; Sk: Skewness; Ku: Kurtosis;  
 D10,50,90: diameters for 10,50,90 percentiles.

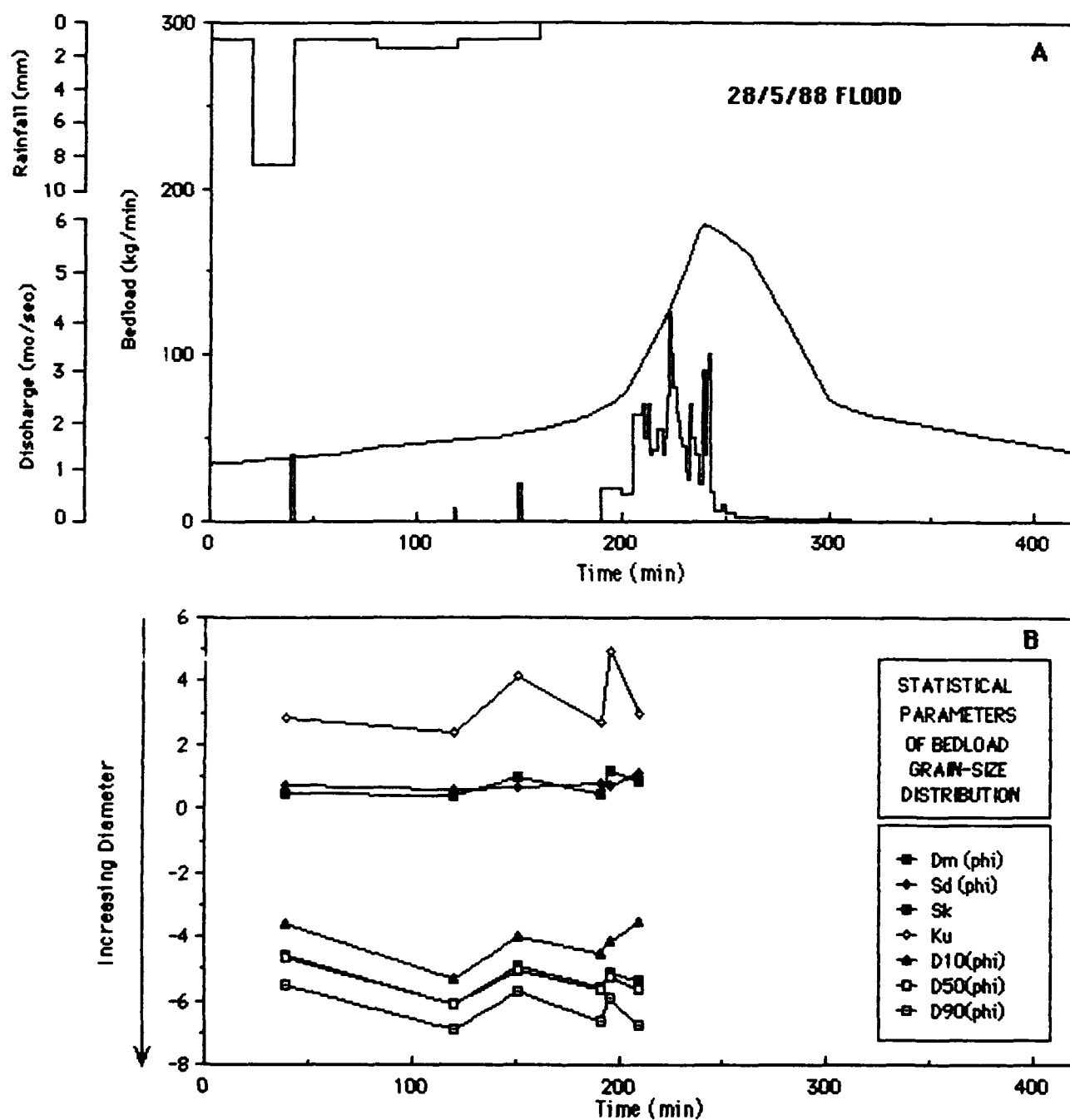


Fig.4. 28/5/88 flood : A) rainfall, discharge and bedload;  
 B) statistical parameters range for the bedload samples.  
 Dm: mean diameter ; Sd: standard deviation; Sk: Skewness; Ku: Kurtosis;  
 D10,50,90: diameters for 10,50,90 percentiles.

#### 4.4 Flood n° 4 - 05.06.1988

This event lasts a considerable amount of time, with a peak discharge of 4.9 mc/sec. Although data measuring the sediment discharge continuously is not available, it was observed that at the end of the event the vortex-tube-trap contained 450 kg of material instead of its maximum capacity of 700 kg. The material trapped inside may be put down to the total bedload transport.

This material was moreover composed of fine sediments and "mud balls", linked to a few pebbles of medium-sized dimension. This data leads one to think of an event characterized by a prevailing suspended sediment transport, linked to a prolonged washing away from its sides. The modest amount of bedload may be explained by a higher level of armouring of the river-bed that remained stable with relatively high discharges.

One supposing is also connected to the particular shape of the hydrogramme that does not present abrupt variations in the discharge even in the growth stage.

Moreover it could be a bedload due to lateral armour of material deposited and remaining stable on the armour. This can be supported by mean of the marked pebbles analysis; in fact the number of marked pebbles after flood n° 4 is much less than before, this can be due to the pebbles burying the previous ones.

#### 5. MOVEMENT OF THE MARKED PEBBLES

As we have already noted, both the "grain-size" and the "morphometric" part of the marked sample was introduced into the river-bed by randomly throwing into a section 250 m upstream from the measuring station.

In order not to create obstacles in the current, the sample was distributed over a strip 1 m wide. The marked clasts together with the riverbed clasts were moved about during the following floods, remaining partly buried under the river-bed and partly visible on the surface, embedded amongst the other clasts or leaning over and free to move about.

The visible clasts on the river-bed and partly visible on the surface, embedded were examined after the various floods determining their dimension and the distance they had travelled.

During the periods in which the bedload was measured, the clasts were recorded on their arrival and then thrown immediately back into the river-bed downstream from the measuring station; during the periods in which the measuring station was not in operation, the same clasts together with the bedload passed freely on from the measuring station.

This situation enabled us to follow "the cloud" of clasts even in the section downstream from the measuring station and determine its characteristics taking into account the maximum distance it had travelled down. The position of the clasts relative to each individual flood is demonstrated in Fig. 5 (Enclosed in text).

### 5.1 "Grain-size Sample"

It is noted how the flood n° 1 brought about only a slight redistribution of the marked sample with a maximum shifting of about 18 m from its introduction point (Fig. 5).

This small flood did not determine at all the bedload discharge or determined only a very small amount. Although measurements are not available for this bedload, this flood is significant since it moves the marked sample about placing the clasts in a position that is closer to their natural condition; in other words, the flood already places the sample in the optimal situation for determining successive measurements that are not distorted by its very presence.

The flood n° 2 caused the greatest movement of marked pebbles as a result of the greater amount of sediment discharge; the marked clasts were discovered on the surface up to 666 m away the introduction point.

Following the floods n° 3 and n° 4 the maximum distance in which the marked pebbles were found was 744 m and 776 m respectively. Whilst the barycentre of the pebble cloud resulted in being a certain distance away from the introduction point: 235 m after the 2nd flood; 246 m after the 3rd flood and 192 after the 4th flood.

The total number of pebbles found after each flood is the following:

2nd flood n° 345; 3rd flood n° 331; 4th flood n° 184

The river-bed survey continued for another 1000 m downstream from the last pebble found in the river-bed, consequently the part of the sample that was not raised must have been buried in the bed of that channel section.

### 5.2 "Morphometric Sample"

As we mentioned with reference to the "Grain-size" sample, a sample composed of 300 clasts with  $\varphi$  composed between  $-4.5$  to  $-5.5$  coloured red and individually numbered was introduced. The number of findings in the river-bed of such clasts is as follows:

2nd flood n° 13; 3rd flood n° 15; 4th flood n° 5

Having being numbered individually, it was possible to follow the movements of each single clast with greater precision away from the introduction point, and the distances between the 2nd and 3rd and those between the 3rd and 4th makes it possible to distinguish which pebbles out of the 300 present had remained on the surface and which ones embedded. The mean distance travelled by the clasts in "morphometric" sample is:

flood n° 2 = 247 m; flood n° 3 = 292 m; flood n° 4 = 252 m

The results are printed in Table 2.

Table 2 - Passage of Clasts in the "Morphometric" Sample

1	2	3	4	5	6	7
42	54.5	74		19		
100	88	202		114		
54	105	298		193		
75	142	151	227	9	76	0.608
6	202	300		98		
38	52	57	57	5	0	0
19	71	77		6		
69	312	421		109		
52	375	632		259		
73	195	195		0		
47	280	291		11		
61	477	495		18		
3	491	559	576	68	17	0.136
56		184	232		48	0.384
34		208	233		25	0.200

- 1) Number of Marked Pebble
- 2) Position after the flood of 20.05.88
- 3) Position after the flood of 28.05.88
- 4) Position after the flood of 05.06.88
- 5) Passage taken in the flood of 20.05.88
- 6) Passage taken in the flood of 28.05.88
- 7) Mean velocity (m/min) of marked pebbles during the flood of 28.05.88

## 6. OBSERVATIONS AND DISCUSSIONS

### 6.1 Observations of Bedload

The two events that we have bedload transport measures for confirm the phenomena's extreme temporal variability and its impulsive nature.

As we have already observed in past flood events, (Tacconi, Billi 1987) once the critical initial discharge has been overcome, the movements of the fluid and sediment discharges appear to continue on their own during the floods and generally the peak sediment discharges precede the highest fluid discharges. Once begun, the movement, across a partial or total mobilization of the armour, seems to trigger an its successive partial stabilization and remobilization of the river-bed matter, yet which is still the subject of study and discussion.

During the Flood n° 3 a few instantaneous arrivals of bedload may be noted, which greatly precede the initial situation of sediment motion, generalized and continued in time.

These arrivals could be linked to:

- partial lateral erosion of bars a/o banks;
- lateral contributions from tributaries;



- movement of clasts deposited over armour during terminal stage of preceding flood (20/5).

The limited duration and intensity of the main transport event after this probably excludes and actual disintegration in the armour but leads one to think of its settling in the same way suggested for the preceding impulsive arrivals.

## 6.2 Marked Sample Transport

There are many observations to be made here, yet we should remember that during the Flood n° 4 in the section of river-bed under study, there was an anomalous situation in relation to the others, that concerned the depositing of sediment in the presence of a very low bedload transport.

### 6.2.1 Number of Rediscovered Pebbles

#### - Grain-size Sample -

The first observation regards the number of pebbles rediscovered in the river-bed after floods (Tab. 3). This number after the flood n° 2 is equal to 8.8% of the total; after the flood n° 3, it is equal to 8.4% of the total and after the flood n° 4, 4.7% of the total. This last percentage may be explained through the phenomena of depositing sediment described earlier. This means that 91.2% of the pebbles after the flood n° 2 remained embedded; after the flood n° 3, 91.6% of the pebbles remained embedded, and after the flood n° 4, 95.3% of the marked pebbles. The rate of embedment is very high.

If we look at this phenomena with relation to each grain-size class, we see how this rate is very high for the small grain-sizes and diminishes according to exponential law with the rise of the clasts' dimensions. (Tab. 3 and Fig. 6).

One of the causes for this in Virginia Creek could be the smaller chance of being embedded during the transport of larger pebbles together with sorting and the formation of the armour; on the other hand, their greater exposure to the current makes them more easily transported which in turn justifies their relatively high mobility in relation to the smaller grain-sizes.

These are only a few suppositions that need verification made in the face of a far larger number of observations.

The percentage in terms of the weight of the clasts rediscovered after the flood n° 2 is 34.3% (115752 g); after the flood n° 3, it is 31.3% (105449 g); after the flood n° 4 it is 29.2% (98572 g).

During the measurement of the bedload in the flood n° 2 in the face of a bedload transport of 43260 kg, the transited sample (from the measurement section in that period (PC), was 24150 g, equal to 0.0558% of the bedload measured.

$$PC/TS \times 1000 = 0.0558 \quad (1)$$

Table 3

Clast rediscovered after the floods - Grain-seize Sample

	$\varphi$						
	-4÷-4.5	-4.5÷-5	-5÷-5.5	-5.5÷-6	-6÷-6.5	-6.5÷-7	-4÷-7
N° of clasts in Sample	2000	1000	500	250	125	60	3935
Total weight of clasts in sample (g)	20000	28000	32000	50000	80000	127000	337000
After the Flood n° 2 of 20.05.1988							
Number of clasts rediscovered	72	73	74	45	36	36	345
Weight of clasts rediscovered (g)	720	2044	4736	9000	23040	76212	115752
Percentage of clasts rediscovered	3.6	7.3	14.8	18.0	28.8	60.0	8.0
Percentage of clasts embedded	96.4	92.7	85.2	82.0	71.2	40.0	91.2

After the Flood n° 3 of 28.05.1988							
Number of clasts rediscovered	57	99	60	48	36	31	331
Weight of clasts rediscovered (g)	570	2772	3840	9600	23040	65625	105449
Percentage of clasts rediscovered	2.9	9.9	12.0	19.2	28.8	51.6	8.4
Percentage of clasts embedded	97.1	90.1	88.0	80.8	71.2	48.4	91.6

After the Flood n° 4 of 05.06.1988							
Number of clasts rediscovered	30	35	34	28	21	36	184
Weight of clasts rediscovered (g)	300	980	2040	5600	13440	76212	98572
Percentage of clasts rediscovered	1.5	3.5	9.0	11.2	16.8	60.0	4.7
Percentage of clasts embedded	98.5	96.5	91.0	88.8	83.2	40.0	95.3

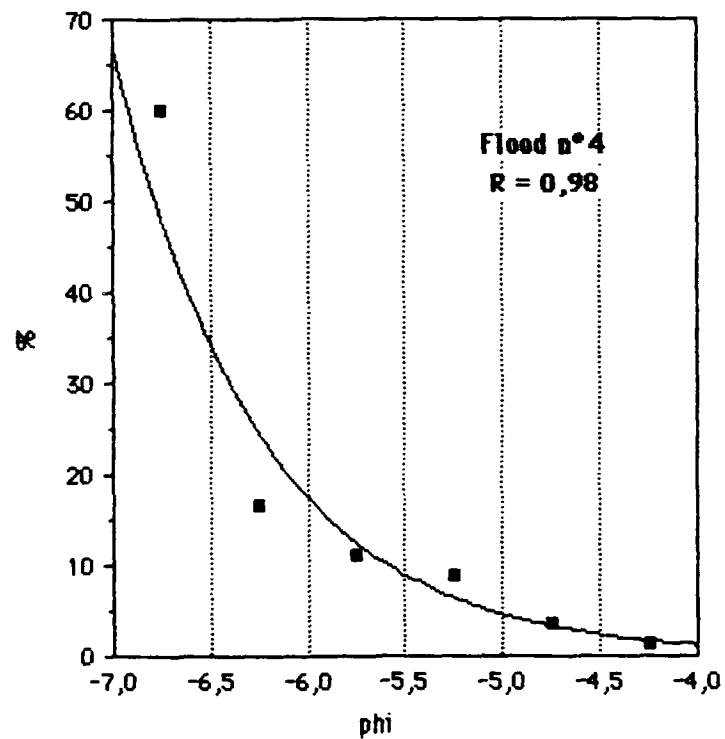
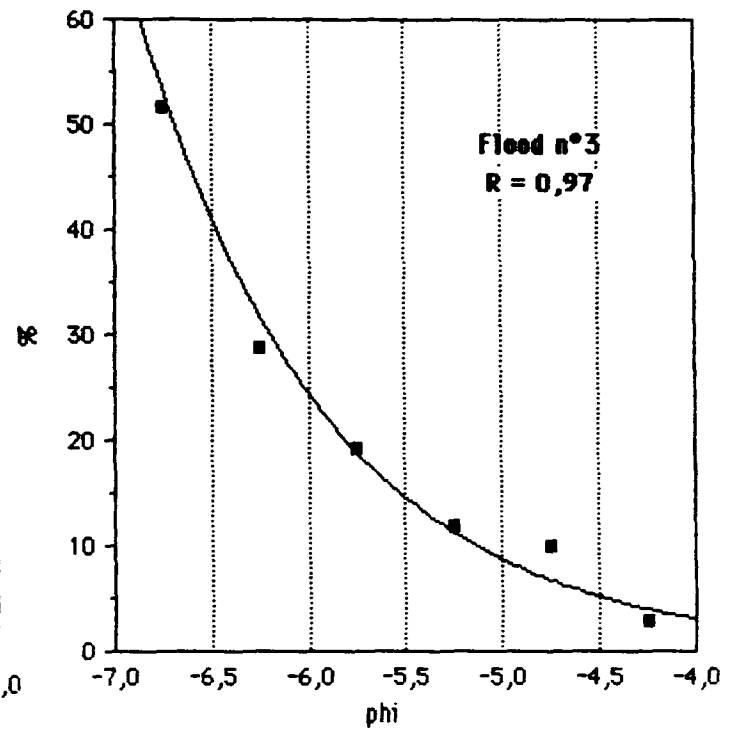
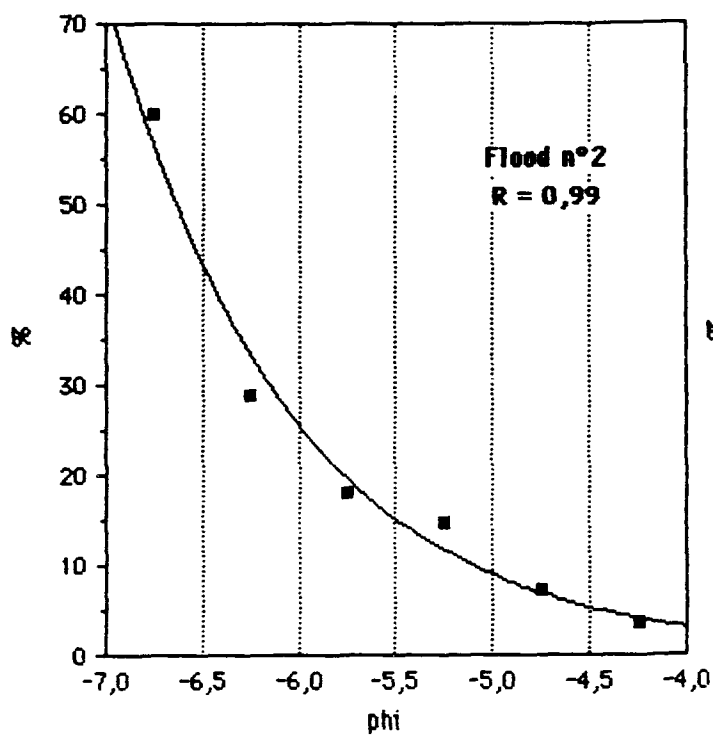


Fig.6. Phi : size of marked pebbles; % : number pebbles renvenued (in %) in respect of the total marked sample for each grain-size class.

- Morphometric sample -

The total number of pebbles in the morphometric sample is 300 units. After the flood n° 2, 13 pebbles (4.3%) were visible, after the flood n° 3, the preceding 13 pebbles remained on the surface and 2 more pebbles that had been embedded arrived making a total of 15 (5%); the flood n° 4 determined the embedment of 10 pebbles and since there were no new only 5 pebbles remained visible (1.6%).

In Fig. 5 the pebbles of the morphometric sample are indicated together with the identification number and their morphometry.

6.2.2 Position (Shifting) of marked pebbles

- Grain-size sample -

A synthetic view of the clasts' movements in the grain-size sample is shown in Fig. 7 while in Table 4 the statistical parameters of their movements are displayed subdivided into grain-size classes.

The scattering of data is very high; in Fig. 7 the positions of the pebbles subdivided by grain-size classes are shown.

Regarding the three floods observed, in all the grain-size classes there are pebbles that have practically not moved after the floods. The average distances away from the introduction point are almost alike for the grain-size classes, inferior to  $D_{50}$  with a slight rise with the increase in  $\varphi$  and a sharp decrease when  $\varphi$  is greater than  $D_{50}$ .

There is a similar behaviour, though less accentuated, in the maximum distances (Fig. 8). The surface of the river-bed where marked pebbles were found after the flood n° 2 is almost 2660 m<sup>2</sup>. If we take as the occupied surface of a visible pebble in the river-bed that corresponding to the circle with diameter  $\varphi$ , the total surface area covered by the marked pebbles ( $\Sigma\varphi$ ), inside this area, where they are distributed, is 0.76 m<sup>2</sup> equal to 0.0336% of the total surface area.

$$\Sigma\varphi/S \times 100 = 0.0336 \quad (2)$$

- Morphometric Sample -

By means of the number marked on each single clast in the morphometric sample, it was possible to follow the individual movements and the exposure (both on the surface and on those embedded) for each clast after the floods.

Unfortunately the sample, included in a single class of  $\varphi$  (-4.5÷-5.5  $\varphi$ ) was composed of a limited number of components (300) and therefore no statistics may be gathered. The data draw is similar to that of the grain-size sample. In the flood n° 3 where the bedload measurement is complete, it was possible to measure the average velocity of the few clasts available, that varies from 0 to 0.608 m/min. (Table 2).

Table 4

Statistical data of the position in relation to the introduction point of clasts in the Grain-size sample

after the flood n° 2 of 20.05.1988	$\varphi$						
	-4+-4.5	-4.5+-5	-5+-5.5	-5.5+-6	-6+-6.5	-6.5+-7	-7+-7
N° of marked clasts gathered	72	73	74	45	36	36	345
Distance from the introduction point - mean (m)	245.4	284.3	301.8	192.2	249.4	80.7	234.7
Distance from the introduction point - median	208.0	226.0	279.5	144.0	204.5	54.5	203.0
Distance from the introduction point - minimum	1.0	2.0	1.0	1.0	2.0	1.0	1.0
Distance from the introduction point - maximum	662.0	666.0	665.0	658.0	584.0	495.0	666.0
Distance from the introduction point - st. dev.	193.3	186.9	210.0	185.5	180.2	94.5	194.4
Distance from the introduction point - variance	37367	34961	44104	34393	32459	8930	38565

after eh flood n° 3 of 28.05.1988	$\varphi$						
	-4+-4.5	-4.5+-5	-5+-5.5	-5.5+-6	-6+-6.5	-6.5+-7	-7+-7
N° of marked clasts gathered	57	99	60	48	36	31	331
Distance from the introduction point - mean (m)	276.7	265.6	307.0	197.5	221.9	112.8	246.4
Distance from the introduction point - median	233.0	225.0	303.0	161.5	166.5	111.0	207.0
Distance from the introduction point - minimum	7.0	1.0	1.0	2.0	1.0	4.0	1.0
Distance from the introduction point - maximum	723.0	744.0	699.0	674.0	602.0	498.0	744.0
Distance from the introduction point - st. dev.	166.3	195.6	193.7	178.6	173.8	100.6	185.7
Distance from the introduction point - variance	27671	38289	37528	31914	30189	10127	34492

after the flood n° 4 of 05.06.1988	$\varphi$						
	-4+-4.5	-4.5+-5	-5+-5.5	-5.5+-6	-6+-6.5	-6.5+-7	-7+-7
N° of marked clasts gathered	30	35	34	28	21	36	184
Distance from the introduction point - mean (m)	244.1	268.1	198.5	152.8	178.3	107.9	192.2
Distance from the introduction point - median	224.5	215.0	187.5	139.0	183.0	103.0	182.0
Distance from the introduction point - minimum	3.0	2.0	3.0	2.0	3.0	2.0	2.0
Distance from the introduction point - maximum	776.0	745.0	744.0	726.0	510.0	505.0	776.0
Distance from the introduction point - st. dev.	198.3	216.4	175.7	165.2	135.8	107.5	178.8
Distance from the introduction point - variance	39322	46840	30887	27304	18454	11548	31963

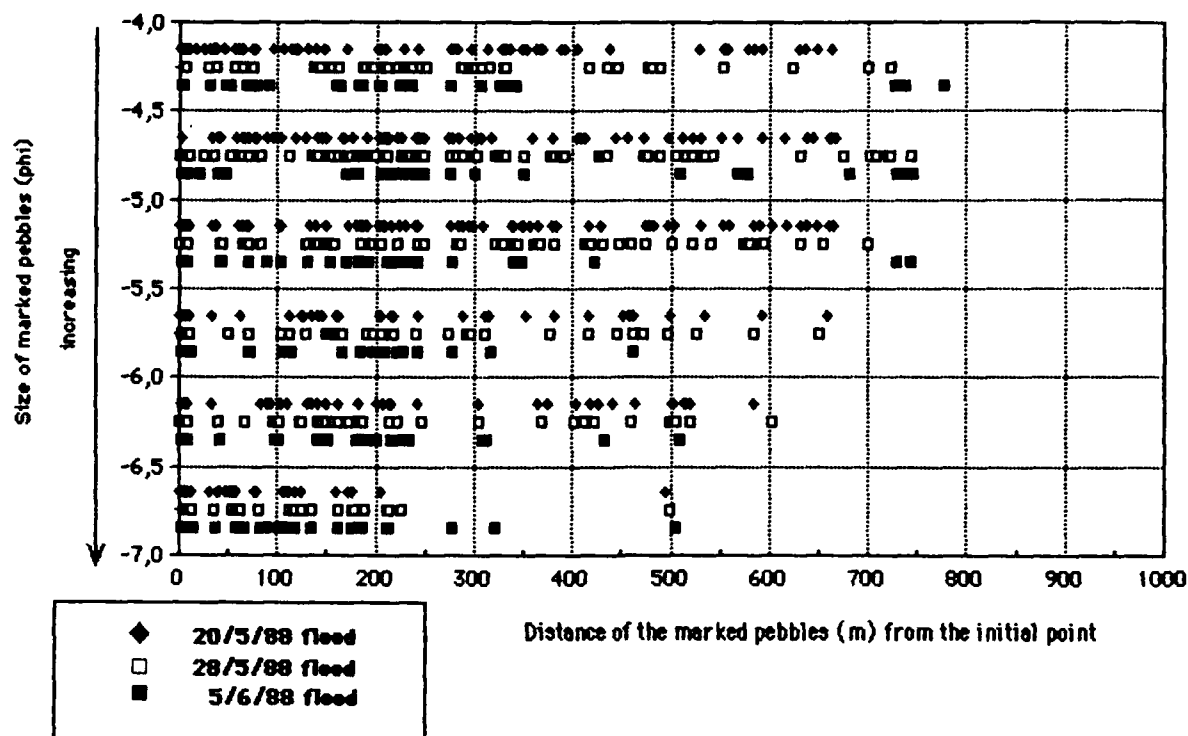


Fig.7 Distribution of the marked pebbles after the floods  
in respect of their relative size.

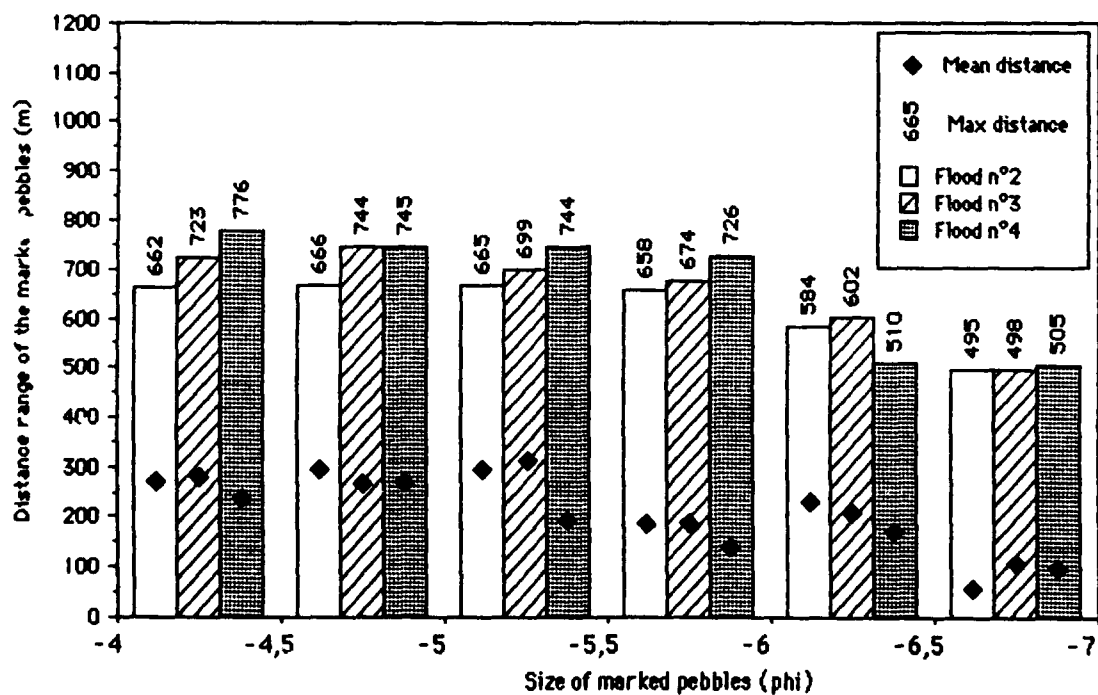


Fig. 8 - Distance Range of the Marked Pebbles (m) in respect of  
their relative size

## 7. FINAL REMARKS AND FUTURE RESEARCHES

The coarse bedload transport in the Virginio stream seems a more complex phenomena then the fine one. Apart from extreme case, the bedload transport takes place during very short periods during the floods, and it has a poor correlation with bedload transport during a flood could be indicated as the amount of pebbles going through a section by the distance travelled by them.

Because of the variability of the situations in which each single clast is encountered during the transport (free, in clusters, embedded, in the bars, in the bed etc.) the distance travelled by the clasts, during the observed floods, it is relatively short and the mean velocity at which they moved has a rate 2 - 3 times less then the water velocity which, during a flood in the examined part of the stream, can reach 6÷8 m/sec.

The measurements and the observations done in the Virginio stream, with many difficulties, are not enough to fully explain the bedload transport in such a stream.

The future researches should be supported and integrated by mean of trough model studies to simulate the recorded events under a more controlled conditions. These researches will study in detail the bedload and furthermore they will deal with the following subjects:

- 1) defining the relationships between bedload transport and bed dynamic;
- 2) establishing an indirect methodology to measure the bedload transport by mean of marked samples introduction in the bed and shifting measurements.

About this last point, the Authors are very interested because of the (1) and (2) give similar figures; in other words that means the marked sample dispersion in the bedload measured by the station it is on the same rate of the sample superficial dispersion after the recorded events.

## Acknowledgements

This research is part of a study on "Problems of solid transport in natural water channels" supported by the Ministry of the University for Scientific Research (MPI 40% funds) and by the National Research Council "Natural Group for Hydrological Catastrophes". The authors wish to thank both organizations.

## References

- BILLI, P., and TACCONI, P., (1986) - Bedload Transport Processes Monitored at Virginio Creek Measuring Station, Italy - Int. Geomorphology Part. I, J. Wiley and Sons LTD, pp. 549-559.
- EMMETT, W.W., (1981) - Measurement of Bed Load in Rivers - Proc. of the Florence Symp., IAHS, Publ. n. 133, pp. 3-15.

- HAYWARD, J.A., and SUTHERLAND, A.J., (1974) - The Torlesse Stream Vortex-tube Sediment Trap - J. Hydrol., 13, 1, pp. 41-53.
- KLINGEMAN, P.C., and MILHOUS, R.T., (1970) - Oak Creek Vortex Bed Load Sampler", 17th Annual Pacific North-West Meeting of the Am. Geophys. Union, University of Puget Sound, Tacoma, Washington, October 1970, 17 pp.
- MEADE, R.H., EMMETT, W.W., and MYRICK, R.M., (1981) - Wavelike Movement of Bed Load, East Fork River, Wyoming, U.S.A. - Abstracts, Conf. on Modern and Ancient Fluvial Systems, Sedimentology and Processes, University of Keele, UK, p. 81.
- REID, I., FROSTICK, L.E., and LAYMAN J.T., (1985) - The Incidence and Nature of Bed Load Transport During Flood Flows in Coarse Grained Alluvial Channels - Earth Surf. Proc. and Landforms, 10, pp. 33-44.
- TACCONI P., (1982) - La misura del trasporto solido nei corsi d'acqua - Atti Conv. conclusivo P.F. Cons. suolo, CNR, Roma, pp. 103-128.
- TACCONI, P., BILLI P., (1987) - Bedload Transport Measurements by the Vortex-tube Trap on Virginio Creek - Italy in Sediment Transport in Gravel-bed Rivers, J. Wiley Sons LTD, London, pp. 583-615.



# VIRGINIO CREEK

## marked sample distribution following four flood events

### schematic map



### granulometric distribution of marked sample

(phi)	symbol	number of pebbles
- 4.0	●	3000
- 4.5	⊙	1000
- 5.0	☆	500
- 5.5	⊗	250
- 6.0	○	125
- 6.5	●	60

### sample shape (after Folk)

shape	symbol	number of pebbles
elongated	▬	100
compact	■	100
platy	▲	100

A A cross section

stream flow  
→

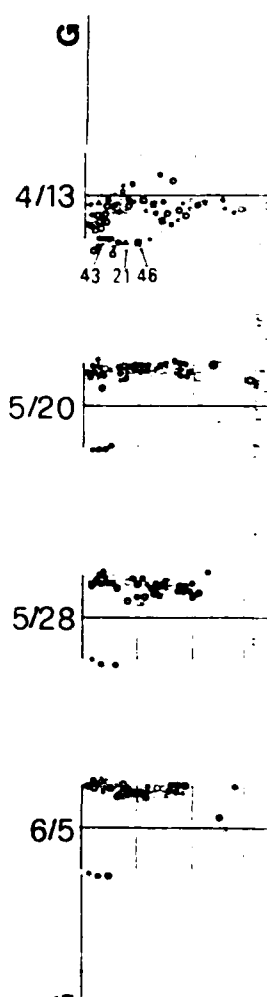


Fig. A

1. Distribution of marked pebbles in the stream bed and in the floodplain  
2. Distribution of marked pebbles in the stream bed and in the floodplain  
3. Distribution of marked pebbles in the stream bed and in the floodplain

# tribution od events

ap

Fig. 5B

50 meters

of marked sample

er of pebbles

2000

1000

500

250

125

60

iber of pebbles

100

100

100

cross section

stream flow

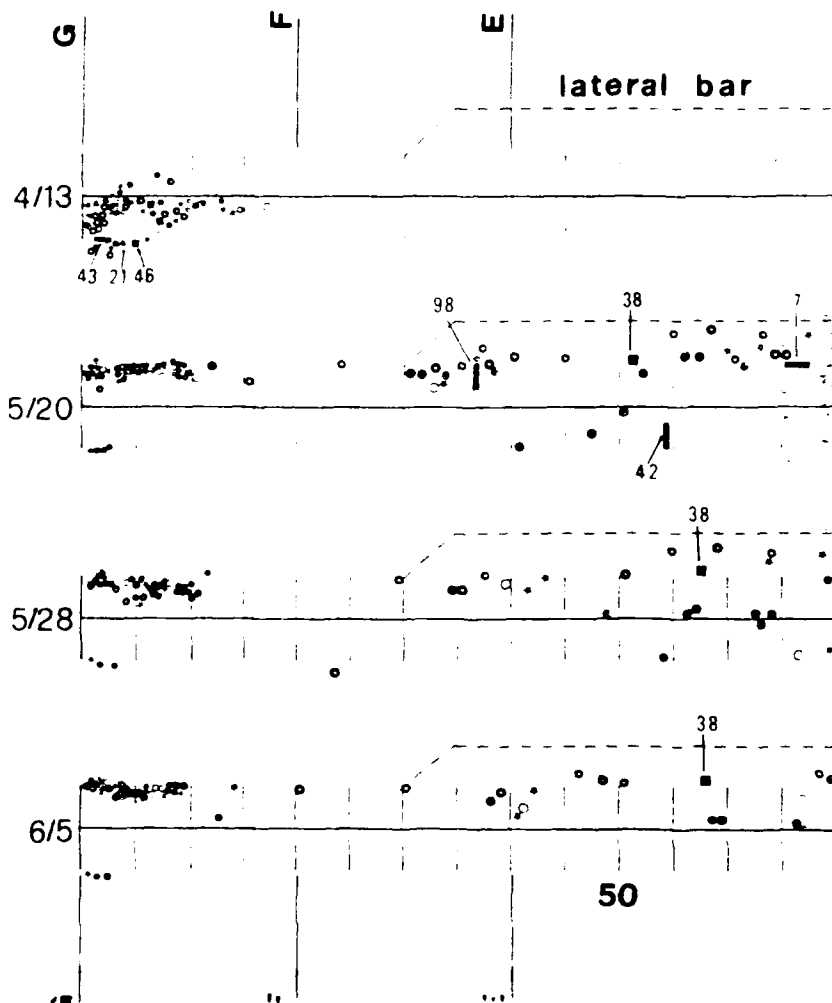


Fig 5C

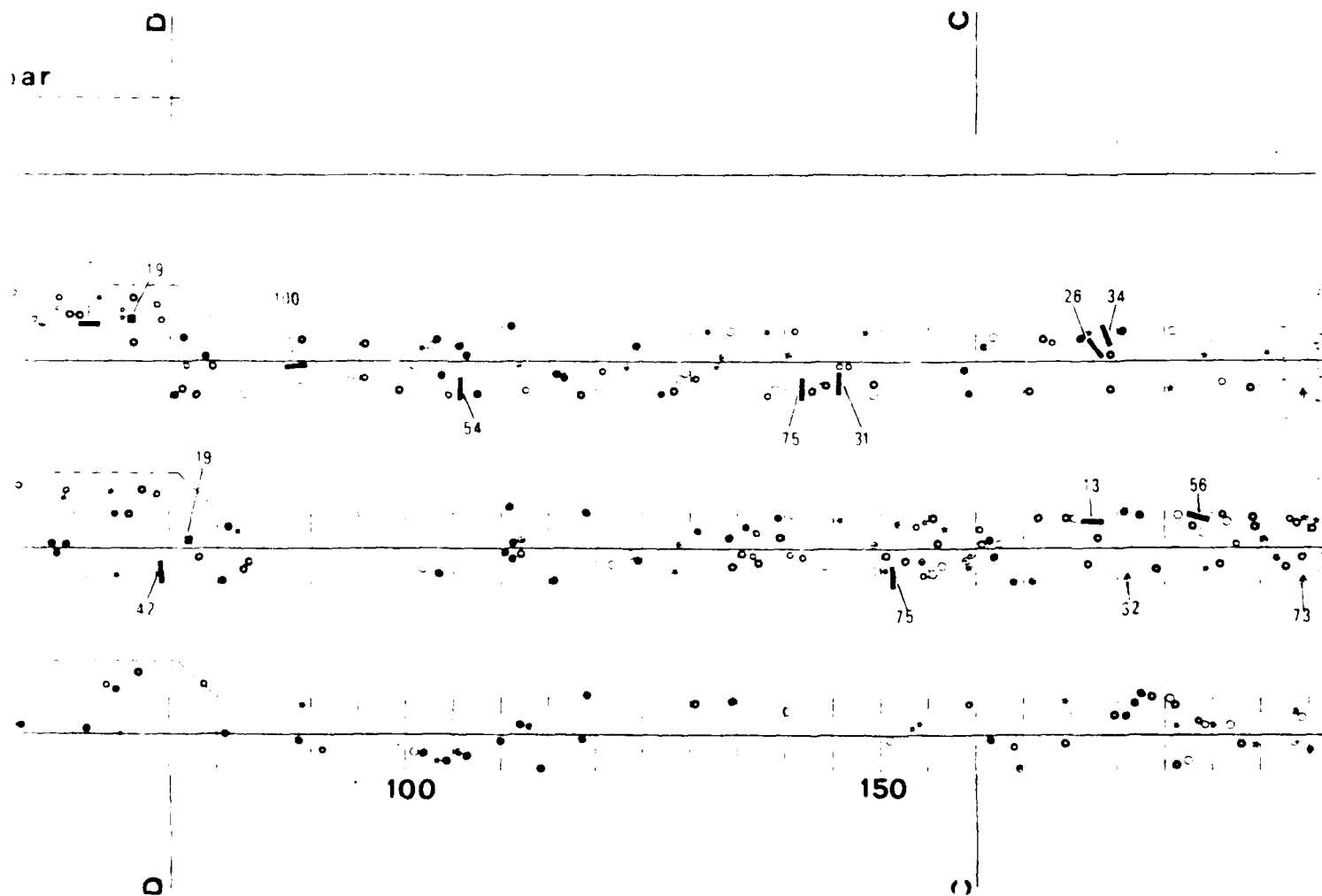


Fig. 5-D

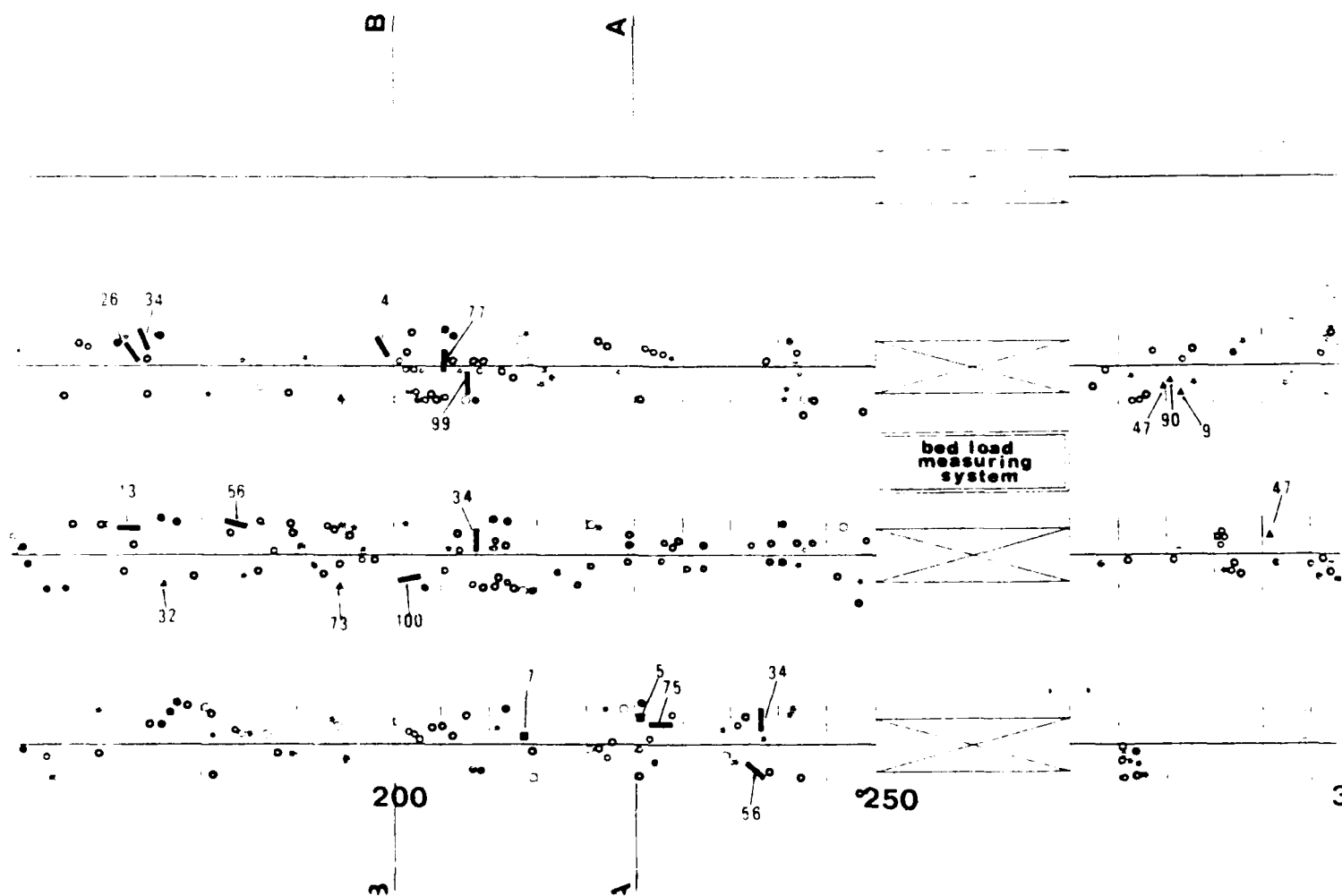


Fig 5E

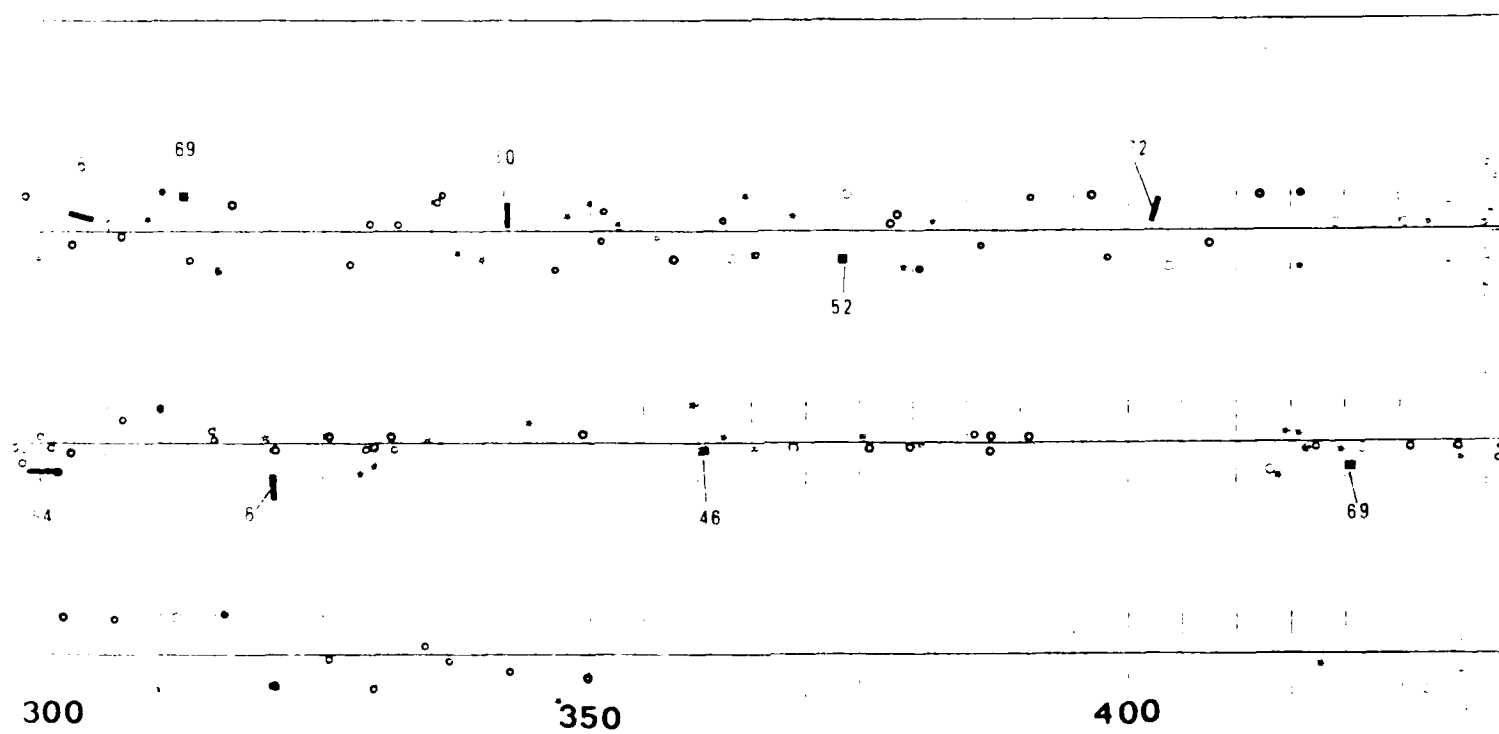


Fig. 5F

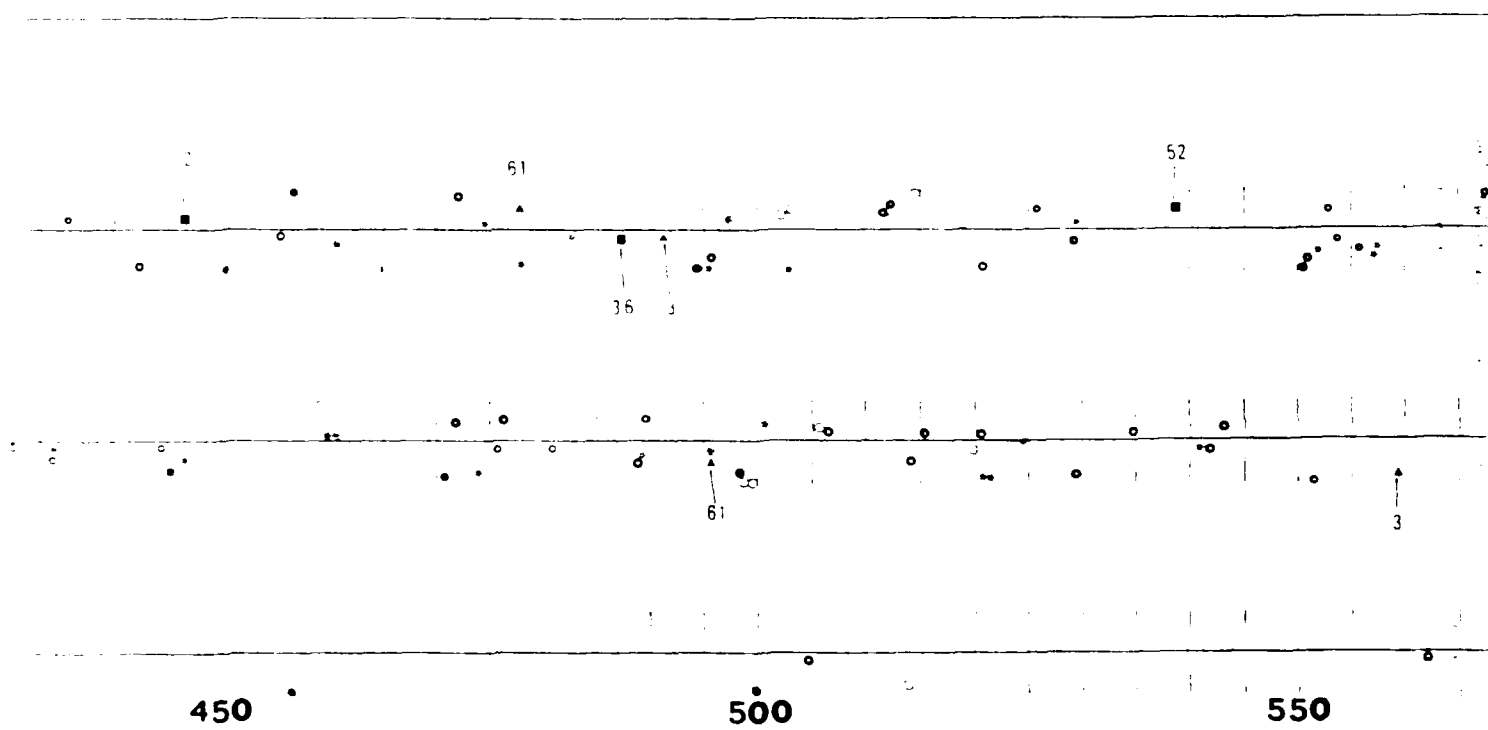


Fig. 56.

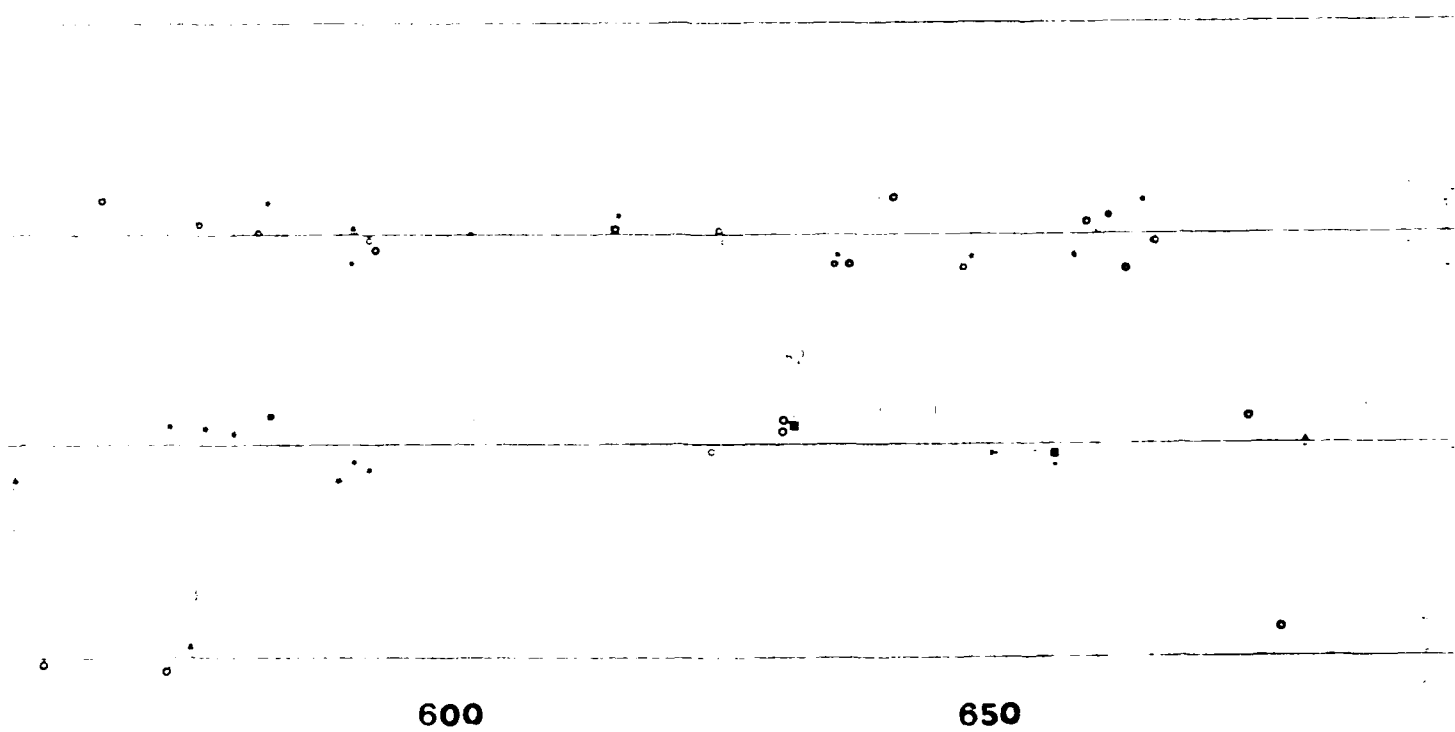
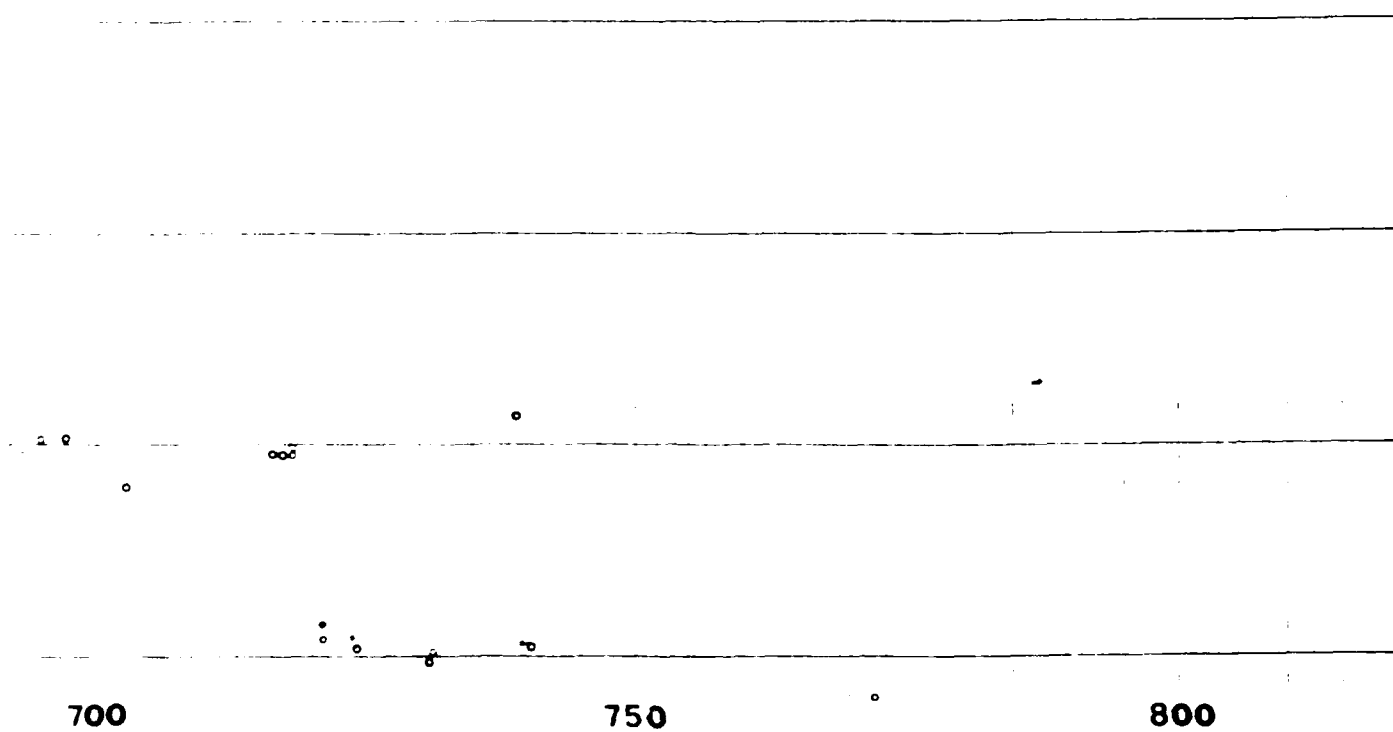


Fig. 5 H

..





# THE MOVEMENT OF INDIVIDUAL GRAINS ON THE STREAMBED

MARWAN A. HASSAN and MICHAEL CHURCH

Department of Geography  
University of British Columbia  
Vancouver, British Columbia  
Canada, V6T 1W5

## ABSTRACT

We examine the movement of ensembles of coarse clasts at low transport intensities, using all available results. The study confirms the lack of relation between the distance of movement of individual stone and their size, and emphasizes the stochastic nature of bedload movement. The distribution of distances of movement follows the Einstein-Hubbell-Sayre compound Poisson model or a simple Gamma model for small displacements. For larger displacements, bars interrupt passage of the particles. The mean distance of movement is largely independent of mean grain size for particles smaller than the surface  $D_{50}$ . For larger particles, distance declines to zero very rapidly. The relation between the mean distance of movement and excess stream power reveals the scatter typical of all transport relations. All the results remain noisy so that samples larger than several hundred stones are needed to finally discriminate the characteristics of particle displacements.

Submitted to: 3rd International Workshop on Gravel-Bed Rivers;  
"Dynamics of Gravel-Bed Rivers"

May 31, 1990

## INTRODUCTION

Sediment transport consists fundamentally of movements of individual particles. H. A. Einstein initiated the modern study of grain displacements, but the topic has not been much pursued because of the difficulty to track and recover suitably large samples of grains. Recently, methods based on radioactivity, magnetism and radio telemetry have changed the situation. The motion of grains is not continuous, but consists rather of a series of steps and rest periods. Altogether, the movement of individual stones appears to be a statistically random phenomenon (Einstein, 1937). This behaviour is similar to the random fluctuations of the local velocity. Einstein (1971) asserted that it should be possible to integrate them into a description of the total pattern of motion of the sediment.

To investigate the motion of individual stones, Einstein (1937) conducted a flume study using marked particles. He found no relation between distance of movement and particle size. Assuming that the rest periods and the actual movements are independent and each negatively exponentially distributed, Einstein described the probability that individual particle would move a certain distance for a known number of steps as a Gamma variate. The distribution of particle displacements after a known interval of time and any number of steps is, then, a compound Poisson process. Using a different approach Hubbell and Sayre (1964) developed the same results.

Flume experiments by Einstein and by Hubbell and Sayre (1964, 1965), and field data from a sand bed river collected by Sayre and Hubbell (1965) showed that the exponential distributions described the travel distances relatively well. Other investigators (cf. Grigg, 1970; Yang and Sayre, 1971) suggested that step length itself followed the Gamma distribution. Substantially more complex statistical models have subsequently been proposed (cf. Shen and Todorovic, 1971; Vukmirovic and Wilson, 1977), but they incorporate information requirements that are not yet feasible to satisfy in the field.

Einstein's theory and subsequent similar approaches have gained relatively little attention and have had relatively little impact on sediment transport research. Nordin (1971) mentioned a few possible reasons for the ignorance of Einstein's work. Among them were the fact that his thesis was written in German and was translated only in the 1960s (by W. W. Sayre), that the practical confirmation and application of such an approach was not clear at that time, and that his famous bedload equation (i.e., 1950) overshadowed it. There may be a more fundamental reason. The arguments in Einstein's thesis are kinematic, and lead to no useful prediction of sediment transport based on summary flow data. But that is what most workers in the field have pursued. However, there is no conflict between Einstein's stochastic

theory and one that seeks an empirical or a quasi-deterministic correlation between mean flow conditions and bulk sediment movement. The sediment transport rate is the product of the virtual rate of travel of the individual particles and the mean depth of the active cross-section of the bed, where the "virtual rate of travel" is the mean distance of movement of the bed material during a known interval of time. In other words, the rate of transport is determined by the average characteristics of the individual displacements of the moved particles, which may very well be correlated with mean flow conditions.

In gravel bed streams, tracer programmes were started in the early 1960s (Takayama, 1965a) in attempts to evaluate bedload movement. Instead of describing the process, most of the investigators concentrated on the expected relation between the distance of movement and particle size (e.g., Keller, 1971; Schick and Sharon, 1974; Butler, 1977; Carling, 1987; Ashworth and Ferguson, 1989). Others examined the influence of the sedimentological characteristics of the bed on the movement of individual particles (cf., Laronne and Carson, 1976; Brayshaw et al., 1983). Most of the tracer work confirms the lack of relation between distance and grain size, mentioned more than 50 years ago by Einstein (1937).

The entrainment, transport and deposition of sediment are affected by a large number of interrelated variables. These can be grouped into three categories: flow, material and channel form (Fig. 1). Some material and channel morphology variables have not been satisfactorily quantified. Prominent amongst these are the bed surface structures that characteristically develop in heterogeneous gravels. Bed structure includes microstructures, packing and armouring. "Microstructure" refers to the specific arrangement of a number of clasts whereby they constrain each other from movement. Imbrication is the best known example. Combined effects of the three categories change over space and time. Under the same conditions of flow and channel morphology, bed material may exhibit a wide range of structure and packing. Accordingly, quantities, distances, and other attributes of the moving sediment vary. Figure 1 indicates the complexity of the resulting sediment transport process.

In this paper we present descriptions of displacement characteristics of coarse particles, based on relatively large samples with high recovery rates. The material moves as bedload in a "low intensity" transport regime. That is, individual grain movements are isolated events, and the characteristic, coarse surface layer remains in place (cf. Parker and Klingeman, 1982). On the basis of these results, we seek a general description for the pattern of individual grain movements and we examine the possibility for there to be a scale-free sediment transport relation based on mean travel distance. We will show that effects produced by the channel form and material variables substantially complicate the results in river channels beyond those described from experimental studies.

## THE DATA

Data presented in this paper were obtained in various studies (Table 1). They derived from observations of painted and magnetically tagged stones. The rivers examined cover a wide range of bed texture and structure, and channel morphology. In addition, they cover a wide range of hydrological regimes, from flash floods in the desert to the opposite extreme of gradually varied snowmelt floods. For more descriptive material about the study rivers, see the cited references (Table 1).

In most of the field studies painted stones were used and the data are limited to the surface exposed particles only. In many of these studies, the recovery rate is low. Therefore, the recovered particles do not represent the entire sample, part of which will have become buried. The studies which used magnetically tagged stones include buried particles, in addition to exposed ones, with relatively high recovery rates. In these studies the recovered particles do represent the entire sample.

In most cases the tracer stones were larger than the bed material, but generally they represent reasonably the sizes that make up the surface layer. In the first event of each study, the tracer particles are initially placed on the bed surface and are not incorporated into the bed structure, so they move more readily than normal bed material.

## DISTANCE OF MOVEMENT AND PARTICLE SIZE

Under controlled conditions in his flume, Einstein (1937) tracked the movement of painted material ranging in size between 3 and 40 mm. Some of his experiments were made using a very narrow range of sizes. Table 2 shows that, for material of the same size and under similar flow conditions, some stones moved long distances whilst others remained stationary. Stelczer (1981) similarly followed the movement of single, or few, stones in the Danube River. He relocated particles after 6 or 24 hours. Table 2 shows that a single stone, under similar flow conditions, moved varying distances in successive steps. These results demonstrate clearly the stochastic nature of the entrainment and movement of individual particles in gravel bed rivers.

The consequent lack of relation between distance of movement and particle size has been reported in many field studies. However, most of these studies used tracers with a relatively narrow range of sizes, always coarser than the bulk bed material. A wide range of sizes might still reveal some relation. Figure 2 illustrates three cases. In Nahal Hebron the range of sizes was narrow and the data do not show any particular trend. In contrast, there is the appearance of an envelope over widely graded Harris Creek data suggesting that large particles

travel shorter distances. Data of Allt Dubhaig are intermediate in both respects. All the data show that stones may move any distance beneath the envelope, so that functional relations between size and distance do not occur for individual particles.

#### THE INFLUENCE OF PARTICLE SITUATION

Random entrainment of individual stones is due to the turbulent flow and the arrangement of individual grains which varies widely over the bed. In gravel bed rivers grains may lean upon each other in many ways.

At the end of a flow event, some of the particles are found free from constraint on the bed surface, others are locked within the surface layer and the rest are buried within the scouring layer. These three groups define the final situation of particles after a competent flow event and the initial situation before the next event. The initial situations affect the flow required for entrainment. This might ultimately influence the travel distance of a stone during a flow event, hence the mean distance of movement of each group. On the other hand, the final situation might reflect the average distance of movement of a group, since buried -- and perhaps locked -- particles probably stop moving before ones which remain free.

Competent flow events change the particle position relative to the local bed surface elevation (Hassan, in press). Some of the initially exposed particles (free and locked) are buried, and a portion of the buried ones become exposed. Transition frequencies for 282 particles in Nahal Hebron are given in Table 3. The frequencies are related to flow magnitude. Similar results have been obtained from Carnation Creek, but as yet our results are insufficient to tell whether a general model may describe the phenomenon.

Table 4 summarizes the mean distance of movement of particles classified according to their initial or final situation from all discriminating observations known to us. In the initial event after stones placement in Nahal Hebron and Carnation Creek, particles which were buried at the end of the event had moved farther, on average, than the free ones. The reverse result was obtained from other recorded events. Grouping particles according to their final situation revealed results similar to those based on the initial situation. Although the differences between the groups are not statistically significant, there is a consistent tendency for the locked and the buried particles to move shorter distances than the free surface stones, except in some initial events. In addition, there appears a tendency for post-event locked and buried stones to have moved proportionally less far than ones classified in these groups before the event. This outcome is interpreted to indicate that stones trapped during the event may be definitively stopped at any time -- perhaps after only a small distance of movement.

The mean distance of movement of particles buried during the 23.1.83 event of Nahal Hebron and the single event of Carnation Creek, both initial events after placement of stones on the surface, was higher than for the other groups. This result occurs because burial of initially exposed particle implies the occurrence of scour, transport and fill. On the other hand, many exposed stones remained that way because they were marooned in relatively inactive parts of the bed. The outcome is produced, then, by the unnatural distribution of stones within the scour layer before the event.

#### DISTRIBUTION OF DISTANCE OF MOVEMENT

The distribution of particle displacements is available for complete flood events for several of the streams of Table 1. The range in grain size of the tracer particles is relatively restricted, so the influence of grain size should not strongly affect the results (cf. fig. 2c). Two questions can be asked about the movement of grains; first, what is the characteristic displacement of the bed material, and second, what is the distribution of the entire sample after every flow event. The first question is concerned with the virtual rate of travel. In this case we deal with the moved particles only. The second question is concerned with the evolution of the streambed. In this case, the entire sample of tracer material should be considered, including the stones that did not move.

Figure 3 shows observed distributions for both cases. The data are, in general, highly skewed -- usually monotonic. Although the event distributions tend to be very irregular, distinct secondary modes appear in some examples.

The statistical model of Einstein-Hubbell-Sayre (hereafter referred to as E-H-S) for grain displacements can be examined in light of these data. Einstein represented the model as

$$f_t(X) = \exp(-X/T) \sum (X^n T^{n+1}) / n!(n+1)!$$

in which  $T = t/t_0 = 2\langle x \rangle^2 / \langle x_s^2 \rangle$  is the number of average rest periods in the event (a scaled event time);

$X = x/x_0$  is the number of average step lengths (a scaled distance);

$x_0 = \langle x_s^2 \rangle / 2\langle x \rangle$  is the average step length;

$t_0 = t(\langle x_s^2 \rangle / 2\langle x \rangle^2)$  is the average resting time;

$\langle x \rangle$  is the average displacement

$\langle x_s^2 \rangle$  is the variance of the displacement.

The fitted distributions are displayed in figure 3, and the similarity between the observations and these distributions was examined using the  $\chi^2$  test at the  $\alpha = 0.01$  level (chosen, in light of the noisy data, to bias the test toward acceptance of the null hypothesis). Results are reported in table 5.

Five of the nine tests indicate that the E-H-S model provides a satisfactory description of particle movements (Table 5a). The successful descriptions derive from simple rainstorm floods of moderate magnitude and small mean movement (Allt Dubhaig; Nahal Hebron; Okawa; among others), whereas unsuccessful descriptions are associated with long, complex snowmelt events (Seale Brook; Harris Creek) and major, multi peak rainstorm flows (Carnation Creek; Nahal Hebron 23.1.83) during which stones travel farther. Results for the distribution of all stones (Table 5b) are the same, except that two of the Japanese streams now have unsuccessful fits. In these channels there was a very high proportion of zero displacements

In events with moderate displacements and simple distributions, it is possible to suppose that most stones move only 1 to 2 times, so that a simple Gamma distribution might adequately describe the distribution of movements. We tested this proposal under the same conditions as our previous test (Fig. 3; Table 5). The pattern of successes is similar to that for the more realistic E-H-S model, except that Seale Brook now is successfully predicted. There are some spectacular improvements in goodness-of-fit.

The unsuccessful cases tend to have long tails (a few stones travel a long way), and to exhibit a secondary mode of displacement lengths, very pronounced in the case of Carnation Creek. The implication is that a trap exists for mobile stones after some moderate displacement, but that a good many stones may bypass it. The trap locations are channel bars, the major accumulations of mobile channel-bed sediments. We have confirmed this by direct test in Nahal Hebron and by observation of stone recovery positions in Carnation Creek. In a more detailed investigation Hassan, Church and Schick (in review) showed that truncation of the long tail in some cases produces successful statistical descriptions of the short range displacement using either the E-H-S or Gamma models.

We conclude that the movement and pattern of displacement (dispersion) of bed material can be described in the short range for individual flow events by relatively simple statistical models of a random process, as originally proposed by H.A. Einstein. However, when displacement distances become comparable with the "morphological scale" of the channel, the movement of the individual stones ceases to be completely random. The large scale features of the channel distinctly influence the transport phenomenon. A more complex stochastic model will be necessary to explain this phenomenon. It will be a salutary model in that it must incorporate a description of the principal sedimentary features of the river channel -- a consequence of sediment movement that is wholly lacking in contemporary descriptions of sediment transport.

### MEAN DISTANCE OF MOVEMENT AND MEAN SIZE

To examine the possibility to establish a practical correlation between particle characteristics and sediment movement, we studied the relation between the mean distance of movement and the mean size. The analysis was restricted to free, surface particles only (a particle must be freed before it can be moved). For free particles the common assumption is that the travel distance is proportion to  $1/D$ , where  $D$  is the grain size. This relation does not hold for locked or buried stones. The data examined here cover a wide range of flow events and grain sizes, so we scaled both variables.

Despite the scaling, the data still exhibit scatter (Fig. 4), which may be due to errors in measurements and to relatively small sample sizes. In general, the scaled distance of movement does decrease with the scaled size, declining rapidly when the scaled size is greater than about 2. The average armour ratio of the data is equal to 2. In other words, when the size of the material is larger than the median size of the surface material, mobility declines rapidly. This result agrees with Einstein's (1950) assertion that the hiding factor is important for material finer than the median size of the surface material, and is consistent with the very steep envelopes in figure 2. Figure 4 also indicates that travel distance is nearly independent of grain size for smaller grain sizes for which hiding factors and traps (comprising openings between the larger particles) are apt to promote a highly stochastic process.

### MEAN DISTANCE AND STREAM POWER

Sediment transport rate is the product of the virtual rate of travel and the depth and width of the active layer on the streambed. Here we present the correlation between distance of travel and a measure of flow conditions on an event basis. We used Bagnold's (1966) specific stream power as a matter of convenience and we calculated the "excess stream power" using Bagnold's (1980) methods.

Figure 5 presents all of the available data. The threshold values vary substantially and may be supposed to represent the combined effects of particle inertia and structural constraints to entrainment. The variation might also be a result of errors, especially in hydrological measurements. It is typical of the variability found in all displays of bed material transport. The functional relation between the mean distance of movement and excess stream power is  $\langle L \rangle = 1.3 (w - w_0)^{1.2}$ , where  $\langle L \rangle$  is the mean distance of movement and  $(w - w_0)$  is the excess stream power. Figure 6 also shows an upper envelope line for nearly all of the data. The envelope line is interpreted to represent the relation when bed structure exercises no significant influence over the threshold condition.



For comparison the figure shows some observations of gravel movement on a sand bed (Leopold et al., 1966). In sand bed rivers there is no structural constraint to movement. Individual large clasts may be transported rapidly over the sand (Fahnestock and Haushild, 1962), although individual stones may episodically become buried. For these data a poorly defined functional relation is  $\langle L \rangle = 78 (w - w_0)^{0.9}$ . The distances of movement of gravel on a sand bed are an order of magnitude larger than on a gravel bed.

It is interesting to speculate that, for a transport function  $q_b \propto (w - w_0)^{1.3}$ , these results imply that the mobile (scour) layer increases as  $(w - w_0)^{0.3}$  in gravel bed channels, and as  $(w - w_0)^{0.6}$  in sand bed channels.

#### SUMMARY

We have examined the displacement characteristics of coarse bed material moving as bedload in the "low intensity" transport regime. The study confirmed the lack of a simple, general relation between the distance of movement and particle size. However, observations using a wide range of stone sizes indicate that distances travelled by large particles decline rapidly. Flume and field data under similar flow conditions demonstrate the stochastic nature of bed material movements. Grouping particles according to their initial or final situation before or after a flow event indicates that free particles generally move greater distances than locked or buried ones.

The compound Poisson model of Einstein-Hubbell-Sayre and a simple Gamma model for the distribution of movements were tested against observed distributions of particle displacements from natural streams. Both models fit the data reasonably well for small mean displacements, but for larger displacements bars act as traps and the distribution is no longer completely random.

The relation between the scaled mean distance of travel and the scaled mean size indicates that travel distance is largely independent of grain size for particles smaller than  $2D_{50}$  of the subsurface material. For larger particles, distance declines to zero very rapidly. The discriminating point of particle behaviour closely approximates the mean armour ratio in the study streams.

The correlation between the mean distance of movement and the excess stream power is similar to that normally obtained for sediment transport. The distance of movement of gravel on a sand bed is an order of magnitude larger than on a gravel bed.

The field data remain very noisy, and further research is needed to characterize all aspects of the particle displacements. The bed characteristics and the morphological elements of the

channel influence the statistical homogeneity and the randomness of the process. This explains part of the variability in the data. The other part is the outcome of the inherently high variance. To overcome this problem, Stelczer (1981) and Hassan, Church and Schick (in review) recommended very large samples in order to ascertain the statistical characteristics of particle displacements.

The bedload consists of movements of individual particles, yet the characteristics of the individual particles alone do not explain the complexity of the interaction between flow, material and channel (Fig. 1). As demonstrated in this paper, structure, morphology and sedimentology of the bed exercise important influence over the bedload movement. A successful model should consider all of these factors.

ACKNOWLEDGMENTS: Special thanks are extended to the following people for providing their original data, which made possible the syntheses in this paper: P.J. Ashworth; P.A. Carling; M.A. Carson; W.W. Emmett; J. Lekach; A.P. Schick; and O. Slaymaker.

#### REFERENCES

- Ashworth, P.J. (1987) 'Bedload transport and channel changes in gravel bed rivers', Ph.D. thesis, Univ. Stirling, 352pp.
- Ashworth, P.J. and Ferguson, R.I. (1989). 'Size-selective entrainment of bedload in gravel bed streams', *Water Resour. Res.*, 25, 627-634.
- Bagnold, R.A. (1966). 'An approach to the sediment transport problem from general physics', U.S. Geol. Surv. Prof. Paper 422-I, 37pp.
- Bagnold, R.A. (1980). 'An empirical correlation of bedload transport rates in flumes and natural rivers', *Proc. Roy. Soc. (London)*, Ser. A, 372, 453-473.
- Brayshaw, A.C., Frostick L.E. and Reid, I. (1983). 'The hydrodynamics of particle clusters and sediment entrainment in coarse alluvial channels', *Sedimentology*, 30, 137-143.
- Butler, R. (1977). 'Movement of cobbles in a gravel bed stream during a flood season', *Geol. Soc. Amer., Bull.*, 88, 1072-1084.
- Carling, P.A (1987). 'Bed stability in gravel streams, with reference to stream regulation and ecology', in *River channels; Environment and Process*, Richards, K. (ed), Inst. British Geographers, Spec. Pub. 17, pp. 321-347.

- Chamberlin, T.W., editor, (1988) 'Applying 15 Years of Carnation Creek Results', Workshop January 13-15, 1987, Nanaimo, British Columbia, Canada, Proc. 237pp.
- Church, M., Wolcott, J.F. and Fletcher, K.W. (in press). 'A test of equal mobility in fluvial sediment transport', Water Resour. Res.
- Einstein, H.A. (1937). 'Bedload transport as a probability problem', Ph.D. thesis, in Sedimentation, Shen, H.W. (ed), 1972, Colorado State Univ., App. C.
- Einstein, H.A. (1950). 'The bedload function for sediment transportation in open channel flow', U.S. Dept. Agric., Tech. Bull. 1026.
- Einstein, H.A. (1971). 'Probability, statistical and stochastic solutions', in Stochastic Hydraulics, Chiu C.L. (ed), Univ. Pittsburgh, pp. 9-27.
- Fahnestock, R.K. and Haushild, W.L. (1962). 'Flume studies of the transport of pebbles and cobbles on a sand bed', Geol. Soc. Amer., Bull., 73, 1431-1436.
- Grigg, N.S. (1970). 'Motion of single particles in alluvial channels', Proc. Am. Soc. Civ. Engrs., J. Hydraulics Div., 96, 2501-2518.
- Hassan, M.A. (1988). 'The movement of bedload particles in a gravel bed stream and its relationship to the transport mechanism of the scour layer', Ph.D. thesis, Hebrew Univ. of Jerusalem, 203pp. (In Hebrew)
- Hassan, M.A. (in press). 'Bed material and bedload movement in two ephemeral streams', 4th Intl. Conf. on Fluvial Sedimentology, Barcelona, Spain, October 2-4, 1989. Proc.
- Hassan, M.A., Church, M. and Schick, A.P. (in review) 'On the distance of movement and burial depth of coarse particles in gravel bed streams'.
- Hubbell, D.W. and Sayre, W.W. (1964). 'Sand transport studies with radioactive tracers', Proc. Am. Soc. Civ. Engrs., J. Hydraulics. Div., 90, 39-68.
- Hubbell, D.W. and Sayre, W.W. (1965). 'Discussion: Sand transport studies with radioactive tracers', Proc. Am. Soc. Civ. Engrs., J. Hydraulics. Div., 91, 139-148.
- Keller, E.A. (1970). 'Bed movement experiments, Dry Creek, California', J. Sed. Petrol., 40, 1339-1344.

- Laronne, J.B. (1973). 'A geomorphological approach to coarse bed material movement in alluvial channels, with special reference to a small Appalachian stream', M.Sc. thesis, McGill Univ.
- Laronne, J.B. and Carson, M.A. (1976). 'Interrelationship between bed morphology and bed material transport for a small gravel bed channel', *Sedimentology*, 23, 67-85.
- Leopold, L.B., Emmett, W.W. and Myrick, R.M. (1966). 'Channel and hillslope processes in semi-arid area, New Mexico', U.S. Geol. Surv. Prof. Paper 352-G, 193-253.
- Nordin, C.F. (1971). 'Sediment transport-bedload: general report', in *Stochastic Hydraulics*, Chiu C.L. (ed), University of Pittsburgh, pp. 379-391.
- Parker, G. and Klingeman, P.C. (1982). 'On why gravel bed streams are paved', *Water Resour. Res.*, 18, 1409-1423.
- Sayre, W.W. and Hubbell, D.W. (1965). 'Transport and dispersion of labeled bed material: North Loup River, Nebraska', U.S. Geol. Surv. Prof. Paper 433-C, 48pp.
- Schick, A.P. and Sharon, D. (1974). *Geomorphology and Climatology of an Arid Watershed*, Dept. Geography, Hebrew Univ. of Jerusalem, 161pp.
- Shen, H.W. and Todorovic, P. (1971). 'A general stochastic model for the transport of sediment bed material', in *Stochastic Hydraulics*, Chiu C.L. (ed), Univ. Pittsburgh, pp. 489-503.
- Slaymaker, H. O. (1972). 'Patterns of present sub-aerial erosion and landforms in mid-Wales', *Inst. British Geographers, Trans.*, 55, 47-68.
- Stelczer, K. (1981). 'Bedload Transport; Theory and Practice', *Water Resources Pubs.*, Littleton, Colorado, 295pp.
- Takayama, S. (1965a). 'Bedload movement in terrential mountain streams', *Tokyo Geog. Papers*, 9, 169-188. (In Japanese)
- Takayama, S. (1965b). 'Sediment transport in the Rivulets near Kaifu-Ura, Niigata Prefecture', *Geog. Rev. Japan*, 38, 29-42. (In Japanese)
- Vukmirovic, V. and Wilson, G., Jr, (1977). 'Bed load movement as a random process', in *Hydraulic Problems Solved by Stochastic Methods*, Hjarth, P., Jonsson, L. and Larsen, P. (eds), *Water Resources Pubs.*, Westwood, Colorado, ch. 14.
- Yang, C.T. and Sayre, W.W. (1971). 'Stochastic model for sand dispersion', *Proc. Am. Soc. Civ. Engrs., J. Hydraul. Engrg.*, 97, 265-288.

Table 1

Data of gravel bed rivers with particle travel measurements

Stream	Grain size (mm) subsurface D50	tracers	Number of events	Tracer method	Number placed	Recovery rate %	Source
Cobble gravel channels, Israel							
Nahal Hebron	35	45-180	4	magnet	282	90-93	Hassan (1988)
Nahal Og (West Bank)	15	45-180	2	magnet	250	55-56	
Sandy gravel channel, Israel							
Nahal Yael	10	pebbles-cobbles	8	paint			Iekach & Schick (pers. comm.)
Welsh upland cobble channels							
Nant Calefwr		cobbles	1	paint	35	85-100	Slaymaker (1972)
Nant Y Grader 9A	36	cobbles	2	paint	35	85-100	
Nant Y Grader 9B	34	cobbles	2	paint	35	85-100	
English upland cobble channels							
Carl Beck	50	15-130	2	paint	120	98	Carling (pers. comm.)
Great Eggeshope	20	15-130	1	paint	85	78	
Scottish upland cobble channel							
Allt Dubhaig 1	34	11-147	4	paint	279	49-73	Ashworth (1987)
Allt Dubhaig 2	26	41-238	4	paint	150	35-92	
Allt Dubhaig 3	29	27-153	4	paint	170	36-93	
Allt Dubhaig 4	29	26-170	4	paint	135	30-88	
Allt Dubhaig 5	15	24-135	3	paint	143	80-96	
Gravel bed river in Japan							
Fukogawa	35	22-128	5	paint	300	61-98	Takayama (1965a, b)
Iiyakawa	35	22-128	5	paint	500	08-81	
Okawa	40	22-128	5	paint	500	42-81	
Gravel bed rivers in Canada							
Carnation Creek	25	16-180	1	magnet	250	80	This study*
Harris Creek	20	06-512	1	magnet & lithology		75	
Seale Brook	40	06-250	1	paint		05	Larone (1973)
Danube River, Hungary							
		11-32		radioactive	few	100	Stelczer (1981)
Flume							
		17-24		paint	649		Einstein (1937)

\* Reach described in Church et al. (in press)

\*\* Reach described in Chamberlin, ed. (1988)

Table 2

Flume and field data of tracer particles under similar flow conditions

Flume (Einstein, 1937; plates 2, 3, 4, 5, 6, and 7)

Number of stones	Number of measurements	$\langle x \rangle$ (m)	$x_s$ (m)	Size range (mm)	Duration (mins.)
	649	11.77	7.67	17-24	5
	643	9.08	7.07	17-24	60
	619	9.57	4.91	17-24	20
	344	7.86	6.93	< 17	5
	334	13.92	5.46	< 17	6
	291	20.91	6.60	> 24	3

Danube River (Stelczer, 1981; App. 1, table 22)

1	8	12.84	17.75	24.4	360
1	9	4.56	7.79	29.8	360
1	11	8.57	6.31	13.1	360
1	11	4.98	6.33	15.1	360
1	11	1.02	1.72	26.1	360
4	16	18.63	9.44	22-32	360
5	60	5.97	11.56	11-16	360
5	18	6.47	11.98	22-32	1440

$\langle x \rangle$  mean distance of movement

$x_s$  standard deviation of the distance of movement

Table 3

Transition frequencies for burial/ exposure of coarse clasts in Nahal Hebron (N = 282)

Event	Date	19.1.83*	23.1.83	17.10.84	8.11.86
	$Q_{max} (m^3 s^{-1})$	9.2	33.0	18.0	49.8
Exposed By Event			0.10	0.14	0.10
Remain Exposed		0.66	0.27	0.21	0.18
Total Exposed After Event		0.66	0.37	0.35	0.28
Exposure Frequencies			0.29	0.22	0.15
Buried By Event		0.34	0.39	0.16	0.17
Remain Buried			0.24	0.49	0.55
Total Buried After Event		0.34	0.63	0.65	0.72
Burial Frequencies		0.34	0.60	0.43	0.49

\*first event after clast placement on the surface

Table 4

Mean distance of movement of particles grouped according to their initial or final position before or after the event.

Initial Position					Final position		
Event	Position	<x> (m)	x <sub>S</sub> (m)	N	<x> (m)	x <sub>S</sub> (m)	N
Nahal Hebron							
19.1.83	Free	10.2		221	9.9	14.9	135
	Locked				10.7	15.3	86
23.1.83	Free	57.9	35.2	126	51.0	35.5	72
	Locked	63.5	35.5	73	47.2	36.7	52
	buried	No Data			70.8	33.4	138
19.1.83&	Free	69.3	37.7	126			
23.1.83**	Locked	73.2	37.2	73			
	Buried	79.9	32.3	51			
17.10.84	Free	18.1	18.9	65	16.4	17.0	65
	Locked	11.5	15.0	52	9.2	13.9	57
	Buried	3.7	9.8	144	5.2	13.7	139
8.11.86	Free	95.8	159.2	67	159.7	157.2	49
	Locked	54.9	124.1	34	54.6	111.9	19
	Buried	57.2	124.1	149	37.5	112.8	182
Nahal Og							
8.11.86	Free <sup>+</sup>	146.5	137.9	140	217.8	182.7	34
	Buried				134.3	119.2	106
6.1.87	Free <sup>+</sup>	19.7	47.0	24	21.0	83.4	27
	Buried	12.5	63.2	74	11.9	50.4	71
Seale Brook							
Spring 1972?	Free	86.5	51.85	242	93.3	63.6	88
	Locked				81.2	72.4	54
Carnation Creek							
Jan. 1990	Free <sup>+</sup>	52.6	45.8	183	36.2	42.8	72
	Buried				60.4	45.7	111

<sup>+</sup> includes a few locked particles

\*\* in the initial situation, two means represent the 23.1.83 event. For the buried group we measured only the combined distance of the two first events for notations see table 2

Table 5

Statistical characteristics of particle movements in field events.

River	a) Moved particles only					b) All particles						
	$\langle x \rangle$	$x_s^2$	T	$x^2_E$	n	$x^2_G$	$x^2_{0.01}$	$\langle x \rangle$	$x_s^2$	T	$x^2_E$	$x^2_{0.01}$
Dubhaig 2	22.8	370.2	2.81	9.4	1.05	11.3	21.7	17.5	375.6	1.63	5.9	26.2
Dubhaig 3	18.8	347.0	2.04	15.9	0.85	9.73	21.7	12.6	310.5	1.02	7.4	24.7
Fukogawa	17.8	234.4	2.71	19.5	1.19	14.2	23.2	10.7	216.4	1.05	8.1	24.7
Hayakawa	37.8	2642.0	1.08	19.0	0.57	39.4	23.2	30.0	2334.8	0.77	32.7	26.2
Okawa	5.23	10.63	5.15	9.5	2.04	14.3	18.5	2.29	11.36	0.92	83.8	27.7
Carnation Creek	52.59	2096.7	1.32	301.0	0.98	131.2	27.9	51.0	2118.8	2.46	223.0	26.2
Seale Brook	86.5	2689.1	5.57	41.1	1.14	13.3	24.7					
Harris Creek	92.9	9254.4	1.87	56.3	0.79	83.1	30.6	58.2	7814.6	1.28	148.1	30.6
Nahal Hebron												
23.1.83	53.9	1172.4	6.20	20.9	2.06	26.7	20.1	51.1	1172.4	4.46	235.1	18.5
17.10.84	19.4	300.3	2.51	18.0	0.73	4.7	18.5	16.9	316.8	1.80	18.6	20.1
8.11.86	166.1	23483.5	2.35	19.4	1.03	17.4	23.2	142.0	29261.5	1.38	16.7	23.2

for notations see text



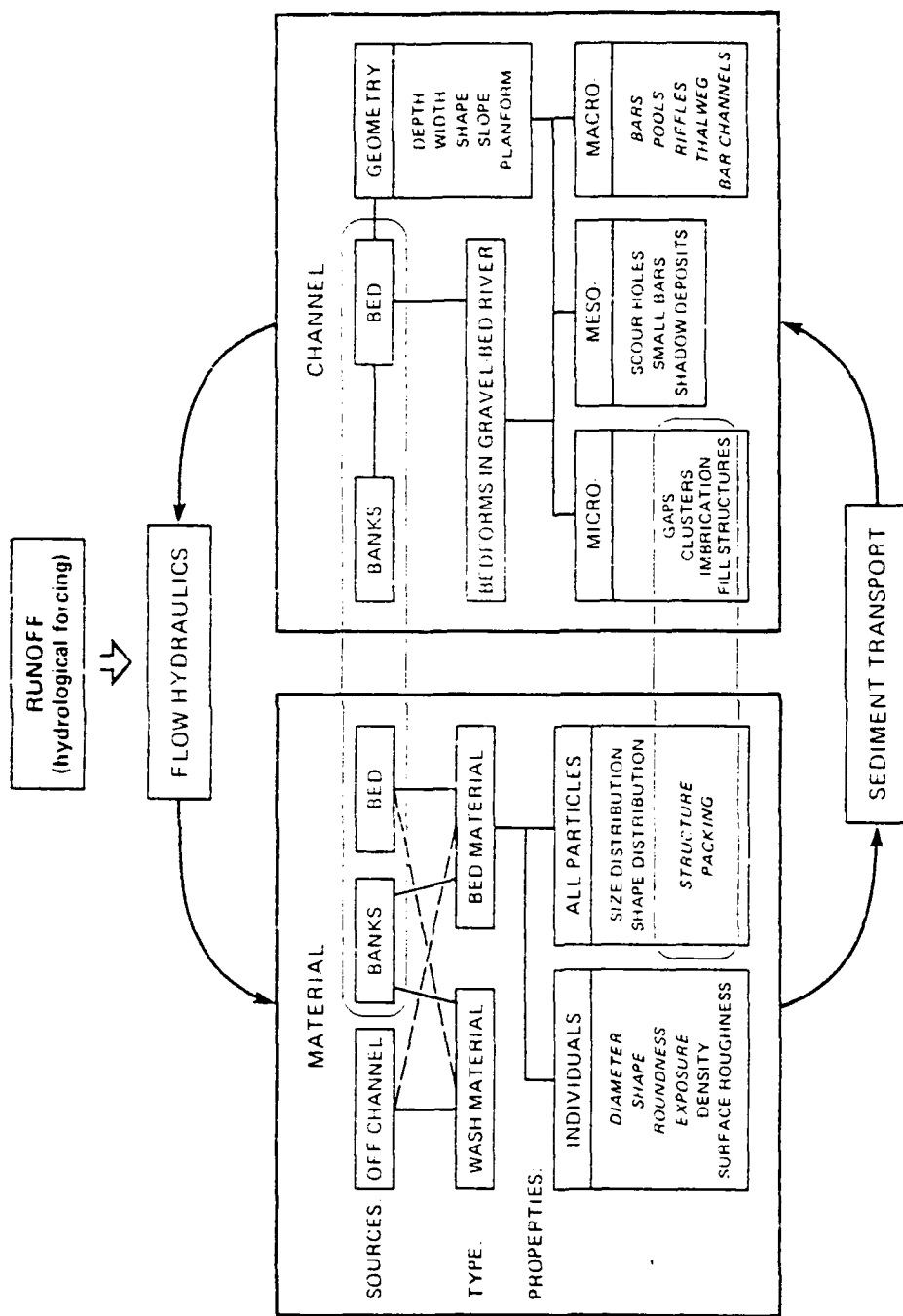


Fig. 1: Relation amongst material, flow and channel properties in gravel bed rivers.

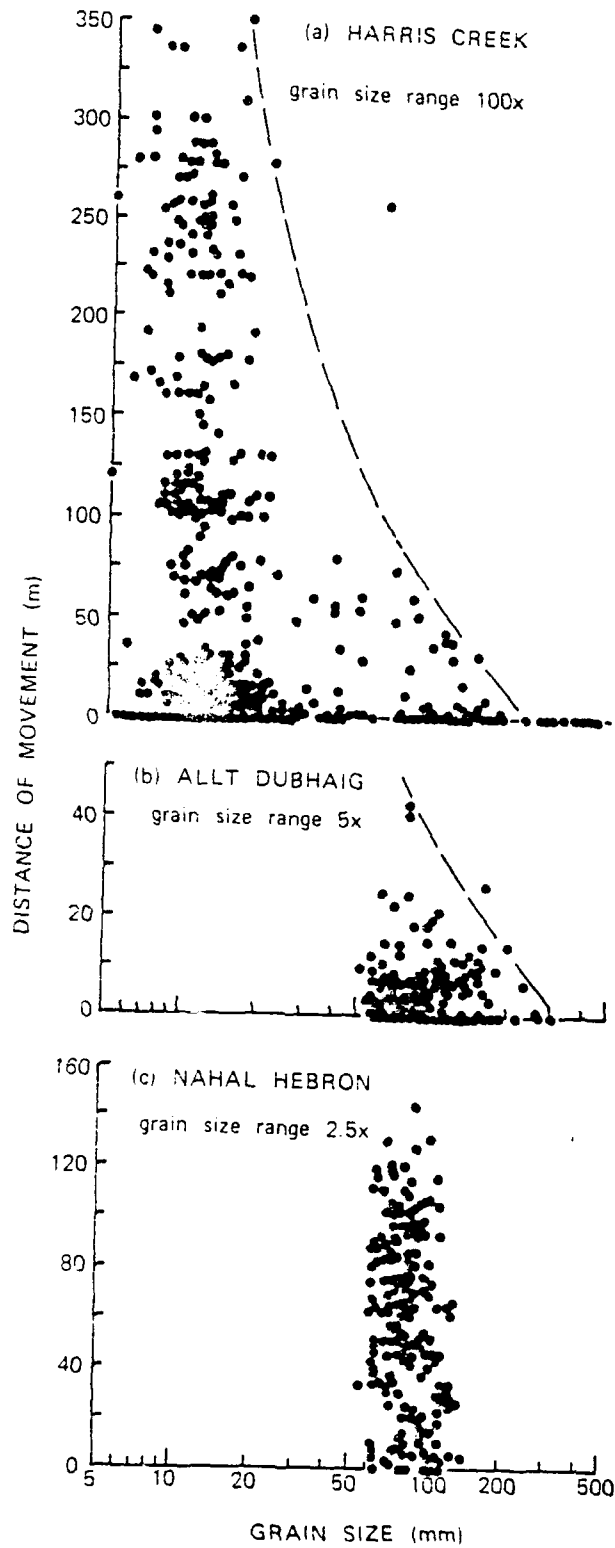


Fig. 2: Distance of travel versus particle size in (a) Harris Creek; (b) Allt Dubhaig River (data of P. J. Ashworth) and (c) Nahal Hebron. The semilogarithmic plot allows stones that did not move to be plotted.

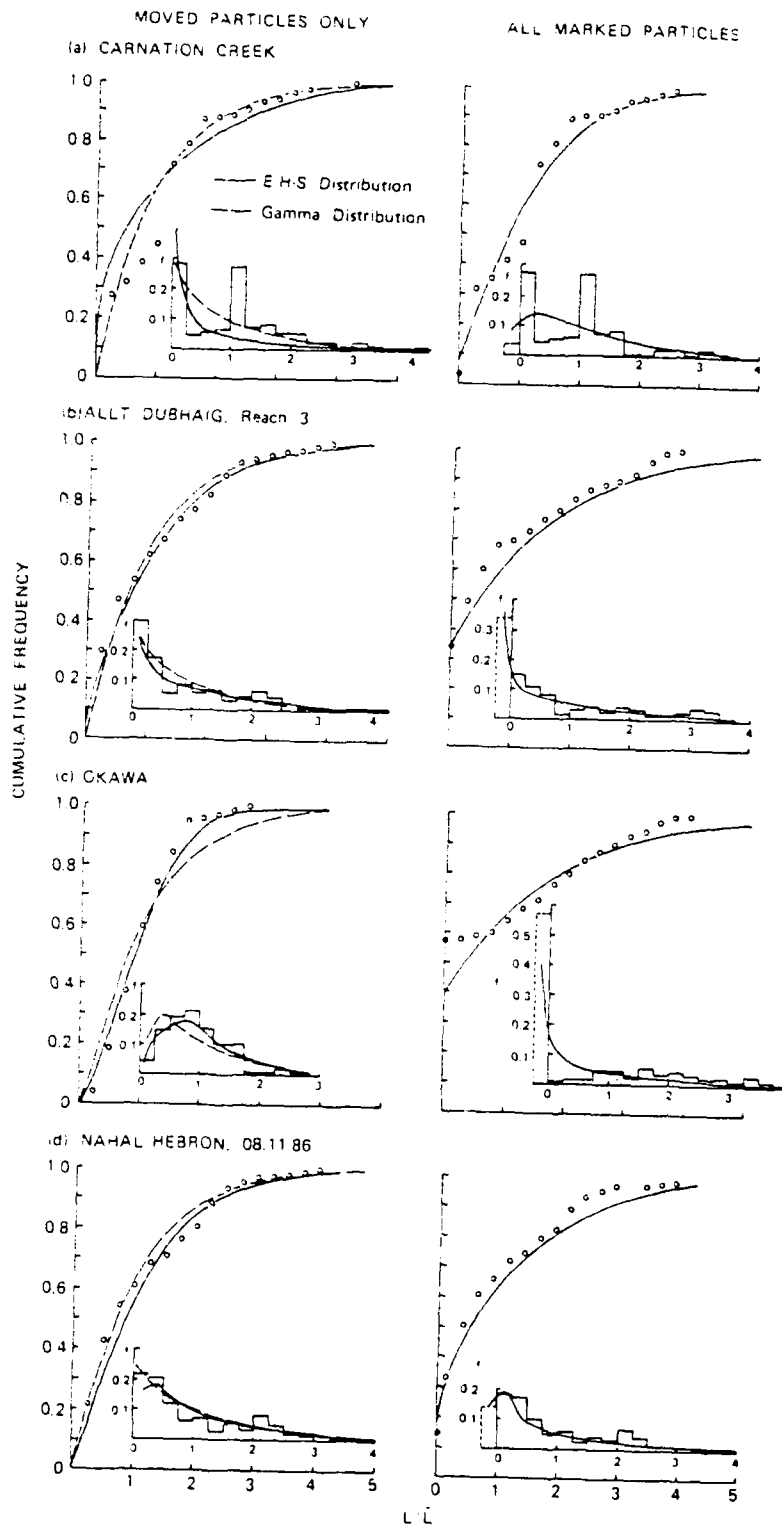


Fig. 3: Particle displacements of moved and of all particles. The data were scaled by dividing the distance of movement of each particle by the mean of the event. Then the scaled data were grouped within interval equal to 0.25 of the mean travel distance for the examined event.

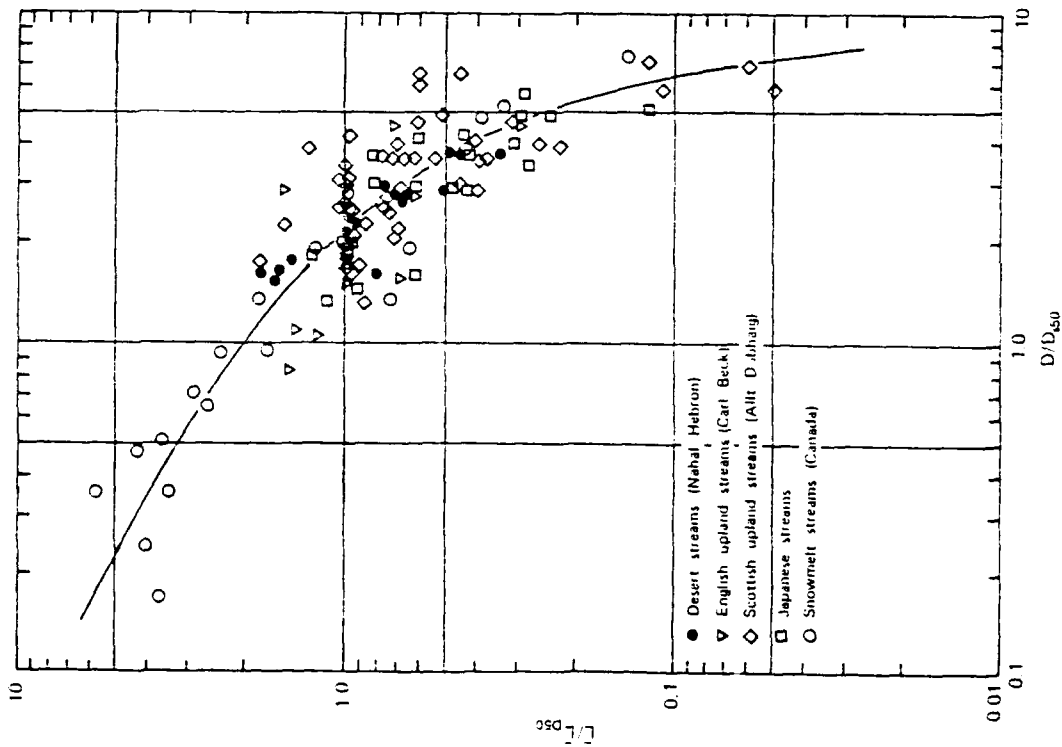


Fig. 4: Relation between scaled mean distance of movement and scaled mean particle size. Distance is scaled by the mean distance of movement of the median size group of the surface material ( $<D_{50}>$ ). Grain size is scaled by the median size of the subsurface material. Data are grouped by half phi intervals. Groups containing less than 10 stones were excluded.

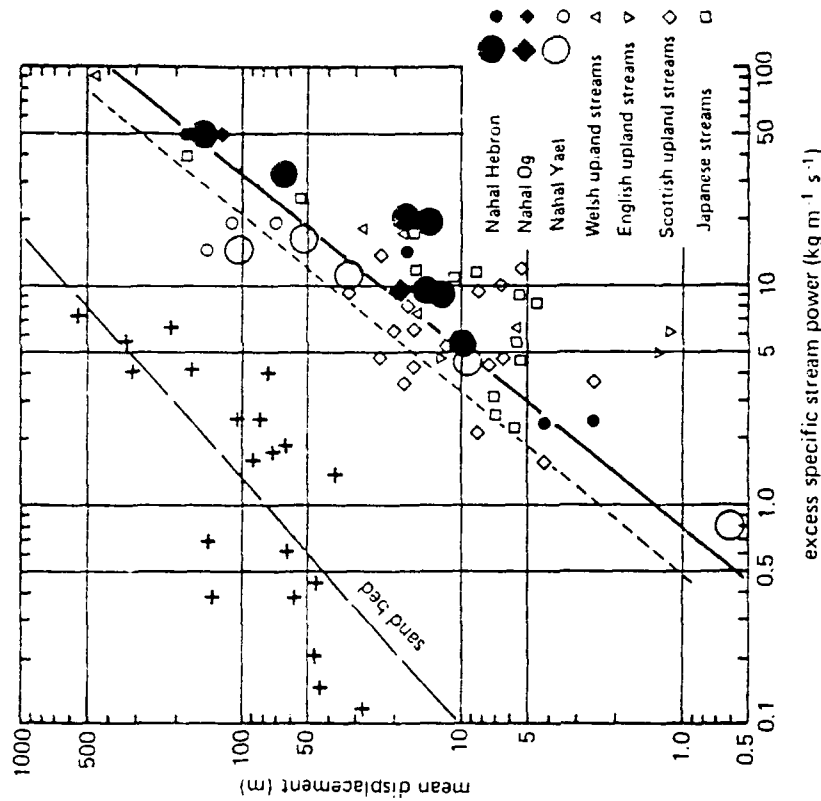


Fig. 5: Relation between mean distance of movement and excess stream power estimated for the peak flow during flood events. Large symbols indicate particles moved and deposited by previous flows (i.e., in naturalistic positions before entrainment). The solid line is the best functional relation; the dashed line is an envelope curve for most of the data. For comparison, a relation for cobbles placed in sand bed streams is shown. The mean relation is affected by four additional points outside the limits of the diagram.

Workshop on Gravel-bed Rivers

Florence, 24-28 September 1990

MODELLING SEDIMENT TRANSPORT: DOMINANT FEATURES TO BE  
SIMULATED IN DIFFERENT HYDROLOGICAL AND MORPHOLOGICAL  
CIRCUMSTANCES

by Giampaolo Di Silvio  
Professor, Istituto di Idraulica "G.Poleni",  
University of Padua

1. Introduction

Sediment transport computations are generally needed to simulate fluvial morphological processes, and in particular to predict bottom aggradation and degradation.

Aggradation and degradation processes are sometimes dramatic for gravel-bed rivers. As sediment transport in mountain rivers is comparatively more intense and more variable (both in space and in time) than in lowland watercourses, not only morphological changes may be extremely large, but the reaction time of these streams is usually very quick.

In these circumstances, a correct evaluation of sediment transport becomes crucial. On the other hand this evaluation can be made by considering only the most significant parameters that control the processes under investigation, renouncing the description of less relevant aspects.

In this respect an important distinction should be made according to the time- and space-resolution required by the analysis. For example, an overall analysis at basin-scale (100+1000 km<sup>2</sup>) needs the entire network of main streams

(slope smaller than 5-10%) to be reproduced in the model, although with a rather coarse resolution (reaches having 200-500 m length). In this case, by averaging over the reach length, a number of simplifications can be introduced, both from the waterflow and from the sediment transport point of view.

By contrast, a detailed investigation on the silting of a small reservoir or on the sediment-trapping by a selective check-dam, requires a relatively small extension of the model (one kilometer or less), but with a space-resolution of few meters; in this case the hydrodynamic description should be much more detailed, as well as the sedimentological processes taken into consideration.

By the same token, as far as time-resolution is concerned, the analysis at basin scale mentioned before can be made either for a long period of years (e.g. to study the progressive aggradation and degradation of a torrent, respectively upstream and downstream of an artificial reservoir) or just for few hours (e.g. to study the sudden aggradation of a torrent overfed by landslides and debris flow during an exceptional storm). In the first case, by averaging the pulsations of waterflow and sediment input over the hydrological cycle, the annual sediment transport can be considered slowly variable from year to year; while in the second case the discharge and all the other parameters should be considered rapidly variable during the flood. Again, depending upon the required time-resolution (years or minutes), different simplifications may be brought into the model.

In any case, regardless the time- and space-scale of the processes to be reproduced, sediment transport of mountain rivers is basically controlled by the non-uniformity of transported material and bottom material.

A number of problems related to non-uniform grainsize distribution will be mentioned in the following sections. A four-layer conceptual model for the transport of a non-

uniform grainsize material at small space- and time-resolution will be subsequently presented. The possibility of simplifying the model will be finally discussed.

## 2. Composition of bed- and transported-material.

Intuition suggests that fine particles are more mobile than coarse particles, and indeed all the experimental formulae show that the transport rate  $T(d)$  of a uniform material increases if its grainsize,  $d$ , decreases.

What about if a certain grainsize class,  $d_i$ , belongs to a mixture? If one assumes that the movement of each class is not affected by the presence of the others, the transport rate of a given class should be equal to the product  $\beta_i \cdot T(d_i)$  where  $T(d_i)$  is the transport rate of the same class computed as uniform material and  $\beta_i$  is the percentage of the same class present in the bottom. In this hypothesis, the granulometric composition of the transport results to be much finer than the granulometric composition of the bottom as the ratio

$$\beta_i T(d_i) / \sum (\beta_i T(d_i))$$

is much larger than  $\beta_i$  for finer diameters and much smaller than  $\beta_i$  for coarser diameter.

In a mixture, however, the mobility of different grainsizes is strongly equalized by the fact that finer particles are protected by the larger ones, and therefore are less subjected to the waterflow than in a uniform-size bed. To take into account this equalizing effect, different correction procedures ("hiding-and-exposure" coefficients) have been proposed (Egiazaroff, Day, Ranga-Raju, etc.). In the limit-case of equal mobility of all the grainsize classes, the composition of the river bottom is equal to the composition of the transported material.

According to some authors, an almost equal mobility is reached in many cases, especially in presence of relatively fast velocity and small grainsizes. It should be stressed, however, that there is no need to assume that the granulometry of the bottom and the granulometry of the feeding material must be necessarily the same when the equilibrium is reached. The two granulometries become equal only if all the grainsize classes have equal mobility, but more frequently this is not the case, as shown by several laboratory experiments, where the bottom composition appears to be much coarser than that of the transport. This difference is confirmed by the material forming the bed of mountain rivers, which almost invariably is much coarser than the material of the landslides feeding the transport, as well as coarser than the material trapped in a reservoir intercepting the torrent.

### 3. Vertical distribution of bottom granulometry.

Another aspect related to the hiding-and-exposure effect mentioned in the previous section is the so called pavement. As defined by Parker (1982), pavement is the upper layer of the movable bed, which appears to be generally coarser than the underlaying bottom material (subpavement). Since the particles of the pavement are susceptible to movement (they are in fact transported by the waterflow), the notion of pavement is completely different from that of armouring which designates a completely immobile (at least below certain hydraulic critical conditions) protective layer.

Although the coarser particles of the pavement are not permanently at rest, still they exert a sort of shielding on the smaller particles of the subpavement. In this respect, the formation of pavement can be seen as a "vertical hiding", which seems to be much more effective than the "horizontal hiding" exerted by the coarse grains on the finer ones in their lee. In fact, this last mechanism can



be probably neglected when compared to the shielding action exerted by the pavement.

If the "vertical hiding" is sufficiently strong, the granulometry of subpavement may be equal to the granulometry of the transported material (equal mobility conditions) although the pavement granulometry is coarser. This is what has been found by Parker in the Oak Creek. Even for the material of the subpavement, however, there is no need to be equal to the transported material. Recent experiments (Di Silvio e Brunelli, 1989) have indicated that, while the pavement appears to be coarser than the subpavement, the composition of the transported material is still much richer of fine particles than the last one.

#### 4. Distinction between bedload and suspended transport.

Since suspended and bedload transport in equilibrium conditions depend on the same hydraulic and sedimentological parameters, it may be attractive to aggregate the two modes of transport into a "total" solid discharge, as proposed by many formulae.

A distinction between bedload and suspended transport, however, may be important in non-equilibrium conditions. As a matter of fact, the most relevant difference between the two modes of transport consists in the average travel length of individual particles: while the grains transported as bed load move each time by short steps proportional to their diameter,  $d$ , the grains transported in suspension travel over much longer distances proportional to  $Uh/w$ , that is decreasing with their size.

As the average travel length is obviously related to the distance required by the transport to reach the equilibrium with the local waterflow characteristics (adaptation distance), this distance results to be practically zero for bedload, while may be extremely long for fine particles transported in suspension.

For a general purpose model, then, is preferable to keep separated the two modes of transport. We shall see later in which circumstances the aggregation is possible.

5. The four-layer conceptual model for the transport of non-uniform material.

For explaining all the features mentioned in the previous sections, both in equilibrium and non-equilibrium conditions, it is expedient to consider the cross section of a river subdivided in the following four layers (Fig.1):

- (1) Waterstream, containing particles exclusively transported in suspension;
- (2) Bottom layer, containing particles basically transported as bedload;
- (3) Mixing-layer containing particles that are presently not in movement, but are liable to frequent vertical movements (entrainment to and settlement from the upper "transport" layers)
- (4) Intrusion layer, containing particles liable to occasional vertical movements to and from the upper "transport" layers.

The particles below the intrusion layer are never disturbed, unless a general degradation of the bottom takes place.

The actual river bottom is represented by the instantaneous surface which separates moving particles and particles that, in any given instant of time, are at rest; a time-averaging operation over the bottom disturbances provides the average bottom surface, between transport layers (1 and 2) and storage layers (3 and 4).

Note that, by definition, the total volume concentration of sediments in the storage layers is equal to (1-n), being

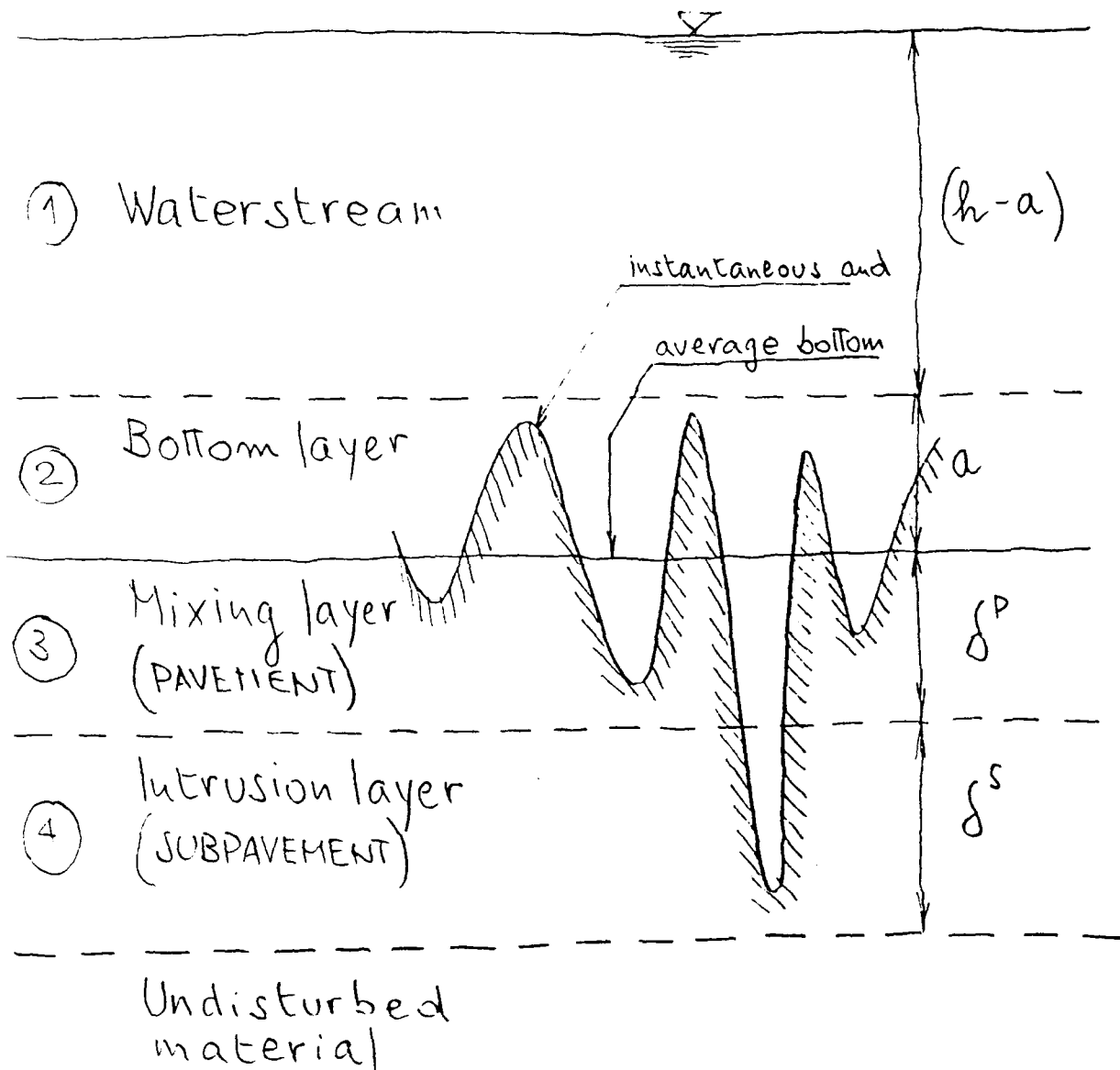


Fig. 1 - Four layer conceptual model for the transport of non-uniform material. Particles move in layers 1 and 2 (transport layers) and are temporarily at rest in layers 3 and 4 (storage layers).

n the porosity. In the transport layers, by contrast, even very close to the bottom the total concentration is a few orders of magnitude smaller (except in case of mass movements, e.g. debris-flow, that are not considered here).

The thickness of the bottom layer,  $a$ , and of the mixing layer,  $\delta^P$ , are related to the average of bottom disturbances: namely to a representative height of the bedforms or to a representative grainsize for a flat bed.

The thickness  $\delta^S$  of the intrusion layer, by contrast, is related to the deviation from the average of the same bottom disturbances. For a normal distribution of disturbances, the ratio  $\delta^S/\delta^P$  is a constant.

The four-layer model described here is quite similar to the three-layer model presented elsewhere (Armanini and Di Silvio, 1986). The fourth (intrusion) layer has been added later to explain a vertical flux below the mixing layer, observed in some experiments (Armanini and Di Silvio, 1989).

The existence of an intrusion layer was first considered by Ribberink (1987), who associated it with the less frequent deepest troughs of the dunes. As it will be seen in the next section, the same mechanism is also capable to explain the formation of a coarser mixing layer (pavement) above a finer intrusion layer (subpavement) in a gravel bed river, as shown in Fig. 3.

#### 6. Longitudinal transport and vertical fluxes.

As said before, longitudinal movement can occur only in the transport layers. However, between the transport layers (1) and (2) and the storage layers (3) and (4), upward fluxes (pick-up) and downward fluxes (settlement) take continuously place.

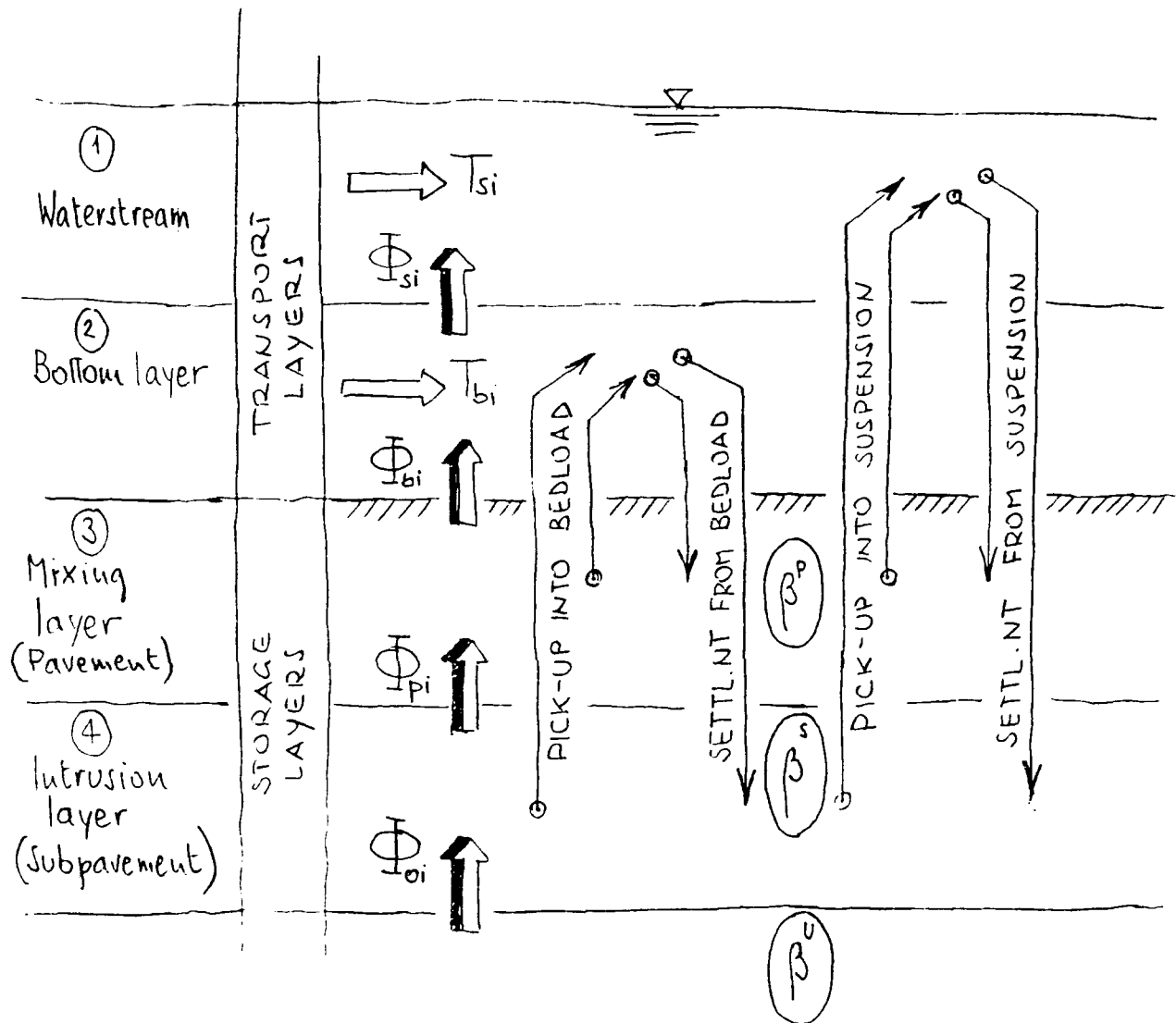


Fig. 2 - Transport and vertical fluxes of non-uniform sediments (i-th grainsize class) in non-equilibrium conditions

With reference to Fig. 2, the following balance equations may be written for the i-th grainsize class:

$$\frac{\partial T_{si}}{\partial x} + \frac{\partial C_{si}h}{\partial t} = \Phi_{si} \quad (1)$$

$$\frac{\partial T_{bi}}{\partial x} + \frac{\partial C_{bi}a}{\partial t} = \Phi_{bi} - \Phi_{si} \quad (2)$$

$$\frac{\partial \beta_i^P \delta^P}{\partial t} = \Phi_{pi} - \Phi_{bi} \quad (3)$$

$$\frac{\partial \beta_i^S \delta^S}{\partial t} = \Phi_{oi} - \Phi_{pi} \quad (4)$$

where  $T_{si}$  and  $T_{bi}$  are respectively the suspended and bedload transports;  $C_{si}$  and  $C_{bi}$  are the average concentrations in the waterstream and in the bottom layer;  $\beta_i^P$  and  $\beta_i^S$  are the percentages of the i-th grainsize class in

the mixing layer (pavements) and in the intrusion layer (subpavement);  $\Phi_{si}$ ,  $\Phi_{bi}$ ,  $\Phi_{pi}$  and  $\Phi_{oi}$  are the net vertical fluxes between adjacent layers (pick-up minus settlement). The concentrations  $C_{si}$  and  $C_{bi}$  in eqs. 1 and 2 can be expressed in terms of  $T_{si}$  and  $T_{bi}$ ; in any case the storage terms containing these quantities are negligible with respect to the others.

Note that, in equilibrium conditions, all the net vertical fluxes should be zero (pick-up is equal to settlement). In a general situation, the net vertical fluxes may be expressed in the following way:

$$\Phi_{si} = (\beta_i T_{ci} - T_i) / L_i^* \quad (5)$$

$$\Phi_{bi} = \Phi_{si} + \frac{\partial}{\partial x} (m_i \beta_i T_{ci}) \quad (6)$$

$$\begin{aligned} \Phi_{pi} = & \left[ (1-f_i) \beta_i^S T_{ci} - (1-\sum f_i) T_i \right] \frac{1}{L_i^*} + \\ & + \frac{\partial}{\partial x} \left[ \frac{1-f_i}{1-\sum f_i} m_i \beta_i^S T_{ci} \right] - \frac{\partial z}{\partial t} \beta_i^{S,P} \end{aligned} \quad (7)$$

$$\Phi_{oi} = -\frac{\partial z}{\partial t} \beta_i^{U,S} \quad (8)$$

where  $T_i$  is the actual total transport (bed and suspension) of the  $i$ -th grainsize class;  $T_{ci}$  is the total transport capacity of the same class, assumed as monogranular;  $m_i = T_{bi}/T_{ci}$  is the percentage of  $T_{ci}$  moving as bedload;  $\beta_i^P$ ,  $\beta_i^S$ ,  $\beta_i^U$  are respectively the percentage of

the  $i$ -th class in the mixing layer (pavement), in the intrusion layer (subpavement) and in the undisturbed sediment below the bottom;  $Z$  is the bottom elevation. In aggradation conditions ( $\partial z/\partial t > 0$ ) it is  $\beta^{S,P} \equiv \beta^P$  and

$\beta^{U,S} \equiv \beta^S$ , while in degradation conditions ( $\partial z/\partial t < 0$ ) it is

$\beta^{S,P} \equiv \beta^S$  and  $\beta^{U,S} \equiv \beta^U$ . The quantity  $L_i^*$ , representing the

adaptation distance of the suspended transport for the  $i$ -th grainsize class, is given by

$$\frac{L_i^* w_i}{U h} = \frac{a}{h} + \left(1 - \frac{a}{h}\right) \exp \left[ -1.5 \left(\frac{a}{h}\right)^{-1/6} \frac{w_i}{u^*} \right] \quad (9)$$

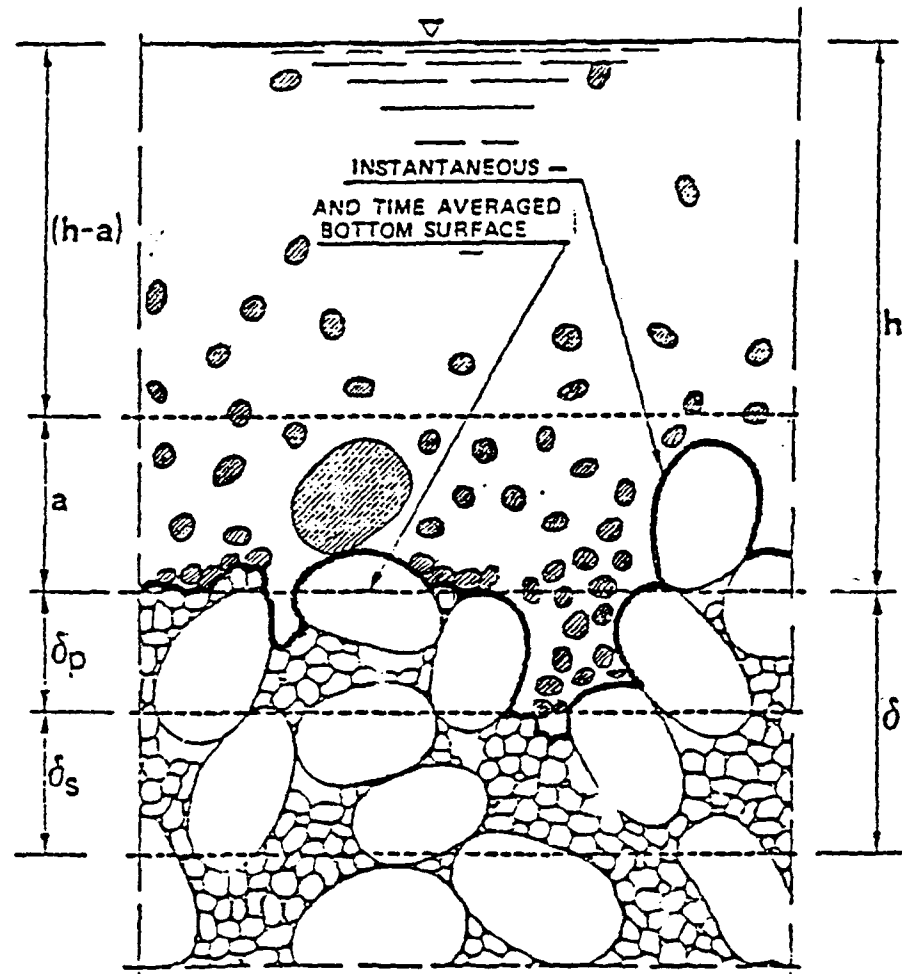


Fig. 3 - The four-layer model explains the formation of coarser pavement,  $\delta^p$ , above a finer subpavement,  $\delta^s$ , as a consequence of differential exchange between moving particles (dashed) and particles at rest (white).



where  $U$  is the flow velocity  $u^*$  the friction velocity and  $w_i$  the particle falling velocity for a diameter  $d_i$ .

The "equivalent" composition of the bottom is given by

$$\beta_i = f_i \beta_i^p + (1-f_i) \beta_i^s \quad (10)$$

where  $f_i$  and  $(1-f_i)$  respectively represent the relative importance of pavement and subpavement as far as the transport of the  $i$ -th grainsize class is concerned. The weight parameter  $f_i$  (see following section 7) is related to the different aptitude of different particle sizes transported by the stream, to exchange with the pavement rather than with the subpavement.

The total (bed and suspension) transport capacity  $T_{ci} = T_{bci} + T_{sci}$  for a monogranular material and the ratio  $m_i = T_{bci}/T_{ci}$ , for a given monogranular material of diameter  $d_i$ , are supposed to be known functions of hydrodynamics (for example, the van Rijn formulae). The weight parameter  $f_i$ , taking care of the bottom stratification, is also supposed to be a known function of the grainsize and hydrodynamic conditions (the definition of this function, based on experiments, is presently under way).

When appropriate initial and boundary conditions are respectively prescribed along the river (bottom composition) and at its upper end (sediment input), the solution of equations (1 to 8) provide the unknown quantities ( $T_i$ ,  $\beta_i^p$ ,  $\beta_i^s$  and  $Z$ ) as a function of space and time. At each time-step, the (generally unsteady) waterflow along the river is to be computed according to the present values of bottom elevation and bottom roughness. For evaluating the bottom roughness in unsteady conditions, the adaptation of the bedforms may be as well taken into account (for example, by Nakagawa and Lamberti procedure).

## 7. Formation and evolution of pavement and subpavement.

The model described in the previous section is able to explain the existence of pavement and subpavement, as a consequence of the vertical exchange between the particles contained in these two layers and the particles transported by the waterflow. The vertical exchange is controlled by the weight parameter  $f_i$  that appears in eqs. 5, 6, 7 and 10.

On the whole, as the large irregularities of the bottom surface are less frequent than the small ones, the exchange of the transported material is more active with the pavement than with the subpavement ( $\sum f_i > 0.5$ ). However,  $f_i$  tends to be even larger for finer particles because of their aptitude to remain trapped in the lower layer; as a consequence, in equilibrium conditions, the pavement results to be richer of coarser particle than the subpavement. On the other hand, the composition of the transport results to be finer than the composition of the subpavement, as soon as the ratio (see eq. 7):

$$\frac{T_i}{\sum T_i} = \frac{(1-f_i)\beta_i^S T_{ci}}{\sum (1-f_i)\beta_i^S T_{ci}} \quad (11)$$

is larger than  $\beta_i^S$  for fine diameters and smaller than  $\beta_i^S$  for coarse diameters.

Note that, should  $f_i$  being independent from the grainsize, the granulometry of subpavement would be equal to the one of pavement (no vertical hiding), and the mobility of any grainsize of the mixture would be the same as for uniform material. By contrast, should the product  $(1-f_i) T_{ci}$  being independent from the grainsize, the granulometry of subpavement would be equal to the one of transport (equal mobility), while the granulometry of the

pavement would be much coarser (very different vertical hiding).

The weight parameter  $f_i$ , in other words, would define the ratio  $\left(\beta_i^S/\beta_i^P\right)$  in equilibrium conditions, as well as the efficiency of the pavement as a shield for sediments underneath;  $f_i$  is a function of grainsize diameter and flow characteristics and plays a role similar to the "hiding coefficient" mentioned in sections 2.

It is to be noted, however, that the shielding effect exerted by the pavement in equilibrium conditions may be different when net vertical fluxes are present (in principle, according to eqs. 3 and 4, each composition  $\beta_i^S$  and  $\beta_i^P$  evolves independently from the other). In this respect, the physical meaning of  $f_i$  seems to be more general than a simple hiding coefficient.

#### 8. Possible simplifications of the model.

As mentioned in the introduction, the model can be substantially simplified (both for the waterflow and for the sediment transport) depending upon the space- and time-resolution required by the problem.

For morphological computations at basin scale (100-1000 km<sup>2</sup>) river reaches of 100-500 meters may be taken as elementary space-steps ( $\Delta x$ ) for a reasonably detailed description of the hydrographic network. Due to the irregular geometry of mountain rivers, the variation of water velocity from reach to reach is generally more relevant than the corresponding variations due to the river evolution. In these conditions, a quasi-uniform flow may be assumed in each river reach for any given water discharge. The local bottom slope may be assumed to be affected by the

differential aggradation or degradation of adjacent reaches, or even be considered constant in time.

Strong simplifications can also be brought in the sediment transport equations (1 to 8). As the space-step  $\Delta x$  is usually larger than the adaptation length  $L_i^*$  for all the grainsize classes, also suspended transport (besides bedload transport) can be considered immediately adapted to the local hydraulic conditions. In this hypothesis ( $T_{si} = \beta_i T_{sci}$ ) there is no need to discriminate between the two modes of transport, so that layers (1) and (2) of Fig. 1 may be aggregated in one single layer and a total solid discharge ( $T_i = \beta_i T_{ci}$ ) may be considered.

Another possible simplification of the model, for a mountain river subject to changes of its bottom elevation, is to consider the vertical flux  $\Phi_{pi}$  between pavement and subpavement (eq.7) being negligible with respect to the other vertical fluxes. In this hypothesis, the ratio  $\left(\beta_i^P / \beta_i^S\right)$

between the compositions of the two layers is supposed to be the same as in equilibrium conditions; there is no need to distinguish between layers (3) and (4), provided that the shielding effect of pavement is taken into account by a proper "hiding" coefficient.

By aggregating waterstream and bottom layer into one transport layer and by aggregating pavement and subpavement into one bottom layer, the traditional two-layer model without suspension space-lag, initially proposed by Hirano (1971), is obtained. It is to be noted, however, that these approximations are not acceptable anymore, either when the space-lag of suspended transport is comparable with the space resolution required by the model (e.g., for studying the silting of a reservoir), or when the flux between pavement and subpavement cannot be neglected (e.g. to study the intrusion of polluted sediments under the river bed).

A different type of simplification can be introduced in the model when long-term morphological changes are to be simulated (e.g., to predict the effects of a new construction in the river over the period of decades). In this case, equations (1 to 8) are integrated over one or more seasonal cycles and the long-term sediment conservation equations are obtained. In the averaging operation several residue terms, due to the non-linearity of the equations, are neglected; this approximation, however, is not critical for most of practical cases.

Examples of application of the simplified two-layer model, both for long-term and short-term simulations, are given by Di Silvio and Peviani (1989).

### 3. References.

- 1) Armanini, A. and Di Silvio, G.: "A one-dimensional model for the transport of a sediment mixture in non-equilibrium conditions", J. of Hydraulic Res., vol.26, 1988, n.3. See also Gruppo Nazionale Idraulica, Excerpta, vol.3, 1988.
- 2) Armanini, A. and Di Silvio, G.: "On the coexistence of bedload and suspended transport for a uniform grainsize material", Int. Symp. on Sediment Transport Modeling, ASCE, Hydr. Div., New Orleans, Aug. 14-18, 1989.
- 3) Di Silvio, G. and Brunelli, S.: "Experimental investigation on bedload and suspended transport in mountain streams", Int. Workshop on Fluv. Hydr. of Mount. Regions, Trent, Italy, October 3-6, 1989.
- 4) Di Silvio, G. and Peviani, A.: Modelling short- and long term evolution of mountain rivers: an application to the torrent Mallero (Italy). Int. Workshop on Fluv.

Hydr. of Mount. Regions, Trent, Italy, October 3-6,  
1989.

- 5) Lamberti, A. and Menduni, G.: "A mathematical model for simulation of loose granular bed response to varying discharges", Gruppo Nazionale Idraulica, Excerpta, vol.2, 1987.
- 6) Ribberink, J.S.: "Mathematical modelling of one dimensional morphological changes in rivers with non-uniform sediment", Rep. n.87-2, Delft Univ. of Techn., Sept. 1987.
- 7) Parker, G., Dhamotharan, S. and Stefan, H.: "Model Experiments on Mobile, Paved and Gravel Bed Streams". Water Resources Research, vol. 18, n.5, October 1982.
- 8) Parker, G. and Klingeman, P.C.: "On Why the Gravel Bed Streams are Paved". Water Resources Research, vol. 18, n. 5, October 1982.

# NUMERICAL MODELING OF GRAVEL MOVEMENT IN CONCRETE CHANNELS

Ronald R. Copeland and William A. Thomas

US Army Engineer Waterways Experiment Station  
Vicksburg, Mississippi, USA

## INTRODUCTION

Corte Madera Creek drains an area of approximately 28 square miles in Marin County, California. The creek discharges into San Francisco Bay about 9 miles north of the Golden Gate. In 1972 the US Army Corps of Engineers completed three units of a proposed four-unit project on Corte Madera Creek extending from San Francisco Bay through the cities of Corte Madera, Larkspur, Kentfield, and Ross, a distance of about 4.5 miles (Figure 1). The first 2.9 miles of the project consist of an earth channel. The next mile of the project consists of a 33-ft-wide concrete channel with a stilling basin at the downstream end. The first 1,000 ft of the channel has a mild slope of 0.0007. The remainder of the concrete channel has a steep slope of 0.0038, and is designed for supercritical flow. These segments have been constructed. The final unit, Unit 4, of the project was to be an additional 3,000 ft of concrete channel. Construction of Unit 4 was delayed due to litigation, environmental concerns, and strong public opposition.

The existing channel in the Unit 4 reach has a capacity of about 3,000 cfs. Flows greater than this overtop the bank and flood adjacent businesses and residences. Additional flooding problems occur because channel capacity in the downstream reaches of the concrete channel is reduced due to the accumulation of sands and gravels. This accumulation reduces conveyance and increases the composite channel roughness.

The largest recorded flood flow on Corte Madera Creek occurred in January 1982. This flood had an estimated peak of 7,200 cfs at the Ross gage and a recurrence frequency greater than 100 years. Another flood occurred in March 1983, with an estimated peak of 3,480 cfs and a recurrence interval of about 6 years. This event was the third largest flood of record. Both of these floods resulted in damages to homes and businesses adjacent to Corte Madera Creek.

In December 1983, the Corps of Engineers was requested to reinstate the project. After extensive local coordination, engineering analysis of the data, and experience obtained from the recent floods, a new plan for Unit 4 was developed by the US Army Engineer District (USAED), Sacramento. This plan consisted of channel improvements, floodwalls, and a sediment trap.

A numerical model study was performed to evaluate the deposition pattern in the concrete channel and to determine the effectiveness of the sediment trap in reducing or eliminating the deposition problem. The effect of the

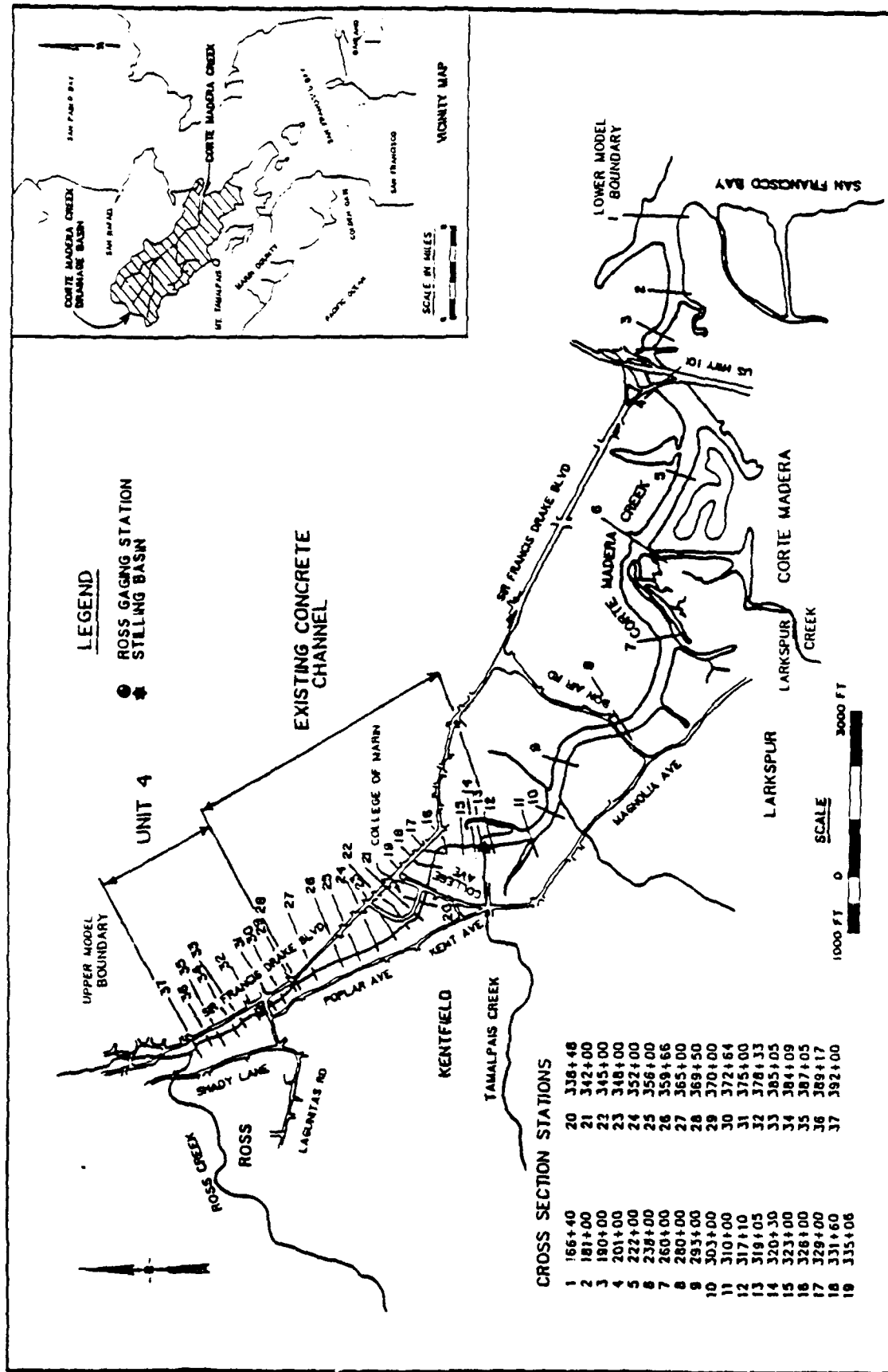


Figure 1. Cross section locations



accumulated sediment on channel roughness was evaluated. Critical to this study was the adequacy of channel wall heights in the existing concrete channel.

## THE MODEL

### Description

The TABS-1 one-dimensional sedimentation program was used to develop the numerical model for this study. Development of this computer program was initiated by Mr. William Thomas at the US Army Engineer District, Little Rock, in 1967. Further development at the US Army Engineer Hydrologic Engineering Center (USAHEC) by Mr. Thomas produced the widely used HEC-6 generalized computer program for calculating scour and deposition in rivers and reservoirs (USAHEC 1977). Additional modification and enhancement to the basic program by Mr. Thomas at the US Army Engineer Waterways Experiment Station (WES) led to the TABS-1 program currently in use (Thomas 1980, 1982). The program produces a one-dimensional model that simulates the response of the riverbed profile to sediment inflow, bed material gradation, and hydraulic parameters. The model simulates a series of steady-state discharge events and their effects on the sediment transport capacity at cross sections and the resulting degradation or aggradation. The program calculates hydraulic parameters using a standard-step backwater method assuming subcritical flow. The program assigns critical depth for water-surface elevation if the backwater calculations indicate transitions to supercritical flow. However, for supercritical flow, hydraulic parameters for sediment transport are calculated assuming normal depth in the channel.

For numerical sedimentation models to completely simulate the behavior of a stream channel, computations would have to account for all of the basic processes of sedimentation: erosion, entrainment, transportation, deposition, and compaction of both the bed and the streambanks for the complete range of particle sizes found in nature. The state of the art has not yet advanced to such a complete simulation. The computer program used in this study, TABS-1, is a state-of-the-art program for use in mobile bed channels. It is designed to calculate aggradation and degradation of the streambed profile. When applied by experts using good engineering judgement, the TABS-1 program will provide good insight into the behavior of mobile bed channels such as Corte Madera Creek.

Particle sizes from sand to gravel are involved in Corte Madera Creek, which complicates the simulation because particle size controls the fundamental processes in river sediment behavior. The time scale of interest is from a single flood event to the life of the project. The long-term trends can be evaluated from a statistical analysis of the gage records, but a great deal of variation in water and sediment runoff occurs from one storm event to the next because of the stochastic nature of the hydrologic cycle. The approach for bridging these gaps is to formulate (a) a procedure that includes the statistical nature of the boundary conditions - the uncertainty in forecasting future hydrology and sediment yield is probably more significant than gaps in modeling the physics of the mobile boundary processes so far as the accuracy of results is concerned; and (b) a computer program that emulates the physical processes in the project reach sufficiently well to quantify how the

sedimentation processes will respond to changes in the boundary conditions and/or to changes in the project geometry or roughness.

Although the sedimentation processes are complex, procedures for describing most of them have been published. The TABS-1 computer program includes those procedures. Where gaps exist between the available procedures, TABS-1 contains logic that bridges those gaps. In summary, it is state-of-the-art technology for calculating the aggradation and degradation in mobile bed channels, and because it has given reliable results at similar projects, it is expected to give reliable answers to the questions being addressed here.

#### Channel Geometry

The numerical model extends from sta 166+00 near the mouth of Corte Madera Creek at San Francisco Bay to sta 392+00, which is just downstream from the confluence of Ross Creek. Reach lengths in this model were generally about 2,000 ft downstream from the stilling basin and about 300 ft upstream. Cross-section locations are shown in Figure 1.

#### Hydrographs

Discharge hydrographs are simulated in the numerical model by a series of steady-state events. The duration of each event is chosen such that changes in bed elevation due to deposition or scour do not significantly change the hydraulic parameters during that event. At relatively high discharges, durations need to be short: time intervals as low as 1 hour were used for Corte Madera Creek. At low discharges, the time interval may be extended. Time intervals up to 3 days were used in this study. The hydrograph used in the adjustment and circumstantiation of the study was based on historical data from the US Geological Survey's (USGS) gage on Corte Madera Creek at Ross. The effect of breakout flows were incorporated into the model.

#### Bed Material

The numerical model requires that an initial volume and gradation be specified for the bed material. This was accomplished in the concrete channel reach by specifying a bed material depth of zero for the initial condition. The gradation of deposited material is then calculated by the model's sorting and armoring algorithm. The bed material gradation in the natural channel, upstream from the concrete channel, was determined from the average of four samples collected in January 1985 by the Sacramento District (Figure 2). These samples were taken in the vicinity of the Ross gage. This gradation was used to determine equilibrium sediment transport capacity at the upstream boundary of the numerical model.

#### Channel Roughness

Hydraulic roughness is influenced by grain size or bottom roughness, bank or sidewall roughness, bed form, water depth, changes in channel shape, and changes in flow direction or distribution due to bends and confluences. In the one-dimensional numerical model these effects are accounted for by the Manning's roughness coefficient. Acceleration and deceleration of flow are accounted for with expansion and contraction coefficients. The roughness coefficient may vary significantly with discharge and time. The influence of

where

$R'_b$  = hydraulic radius of the bed attributed to grain roughness

$D_{84}$  = particle size of which 84 percent of the bed is finer

In order for sand and gravel to influence the bottom roughness, a minimum bed thickness was required in the model. If this requirement was not met, the model assigned a  $D_{84}$  value that is representative of concrete. The minimum thickness was the larger of 4 mm or two times the grain size for which the percent coarser fraction covered the bed to a thickness of two grain diameters.

The Limerinos equation accounts primarily for the grain roughness. Additional bed roughness can be caused by the form roughness that occurs with a movable bed. Calculations using the Brownlie equation (Brownlie 1983) for upper regime flow showed an increase in the Manning's roughness coefficient of 0.010 due to form roughness. In the numerical model, the bed roughness coefficient was increased to account for form roughness if both the minimum bed thickness and the critical shear stress were exceeded. The Shields equation was used to determine critical shear stress.

$$\tau_c = \theta(\gamma_s - \gamma_w)D_{50} \quad (3)$$

where

$\tau_c$  = critical shear stress

$\theta$  = Shields parameter

$\gamma_s$  = specific weight of sediment

$\gamma_w$  = specific weight of water

Various investigations have established a range for the Shields parameter between 0.03 and 0.06 when median grain diameter is used in the equation. In order to provide a continuous transition for the increase in roughness coefficient for form roughness, the following procedure was adopted. If the calculated shear stress was less than critical shear stress using a Shields parameter of 0.03, then the bed was assumed to be immobile and no adjustment was made to the Limerinos bed roughness. If the calculated shear stress was greater than the critical shear stress using a Shields parameter of 0.06, then the Limerinos bed roughness was increased by 0.010 to account for form roughness due to the movable bed. The roughness increase was linearly interpolated for conditions between these limits.

The sidewall roughness in the composite roughness equation accounted for the roughness height of the wall itself. An appropriate roughness coefficient was determined by simulating high-water marks from the January 1982 flood. The wall roughness should be somewhat higher than for finished concrete because of tubeworm and barnacle deposits. A value of 0.018 was chosen.

Initially, calculated water-surface elevations in the lower portion of

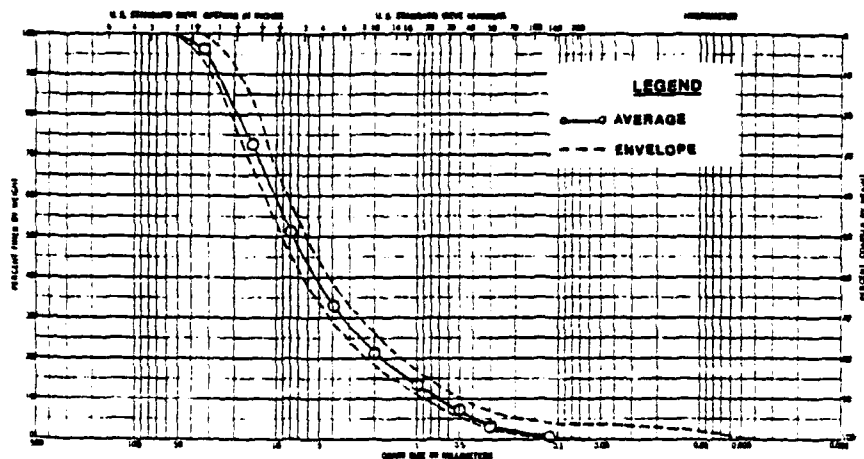


Figure 2. Bed material gradations, vicinity of Ross gage

grain or bottom roughness on hydraulic losses is known to decrease with increases in depth. Resistance due to bed forms can decline dramatically when the bed forms are washed out and replaced by a plane bed. An attempt to account for these problems was made in this study by developing an algorithm that calculated composite roughness coefficients based on roughness attributed to the bed, sidewalls, and bed movement.

Determining composite roughness in the concrete channel is complicated by the accumulation of sand and gravel on the channel bottom. A composite roughness coefficient was calculated using the following formula:

$$n = \left[ \frac{P_w n_w^{1.5} + P_b n_b^{1.5}}{P_w + P_b} \right]^{2/3} \quad (1)$$

where

$P_w$  - perimeter of the wall

$n_w$  - roughness coefficient of the wall

$P_b$  - perimeter of the bed

$n_b$  - roughness of the bed

The bed grain roughness was calculated using the Limerinos equation (Limerinos 1970):

$$n_b = \frac{0.09256 (R'_b)^{1/6}}{1.16 + 2.03 \log \left[ \frac{R'_b}{D_{94}} \right]} \quad (2)$$

the concrete channel were significantly lower than the reported high-water marks for the January 1982 flood. To correct this discrepancy, the roughness was increased by 0.004 to account for losses due to channel bends in the downstream reach, below sta 342+00. With this revision, calculated water-surface elevations and high-water marks were much closer, but the calculated values were still slightly lower than high-water marks. These water-surface comparisons are shown in Figure 3. Differences in reported and calculated values for

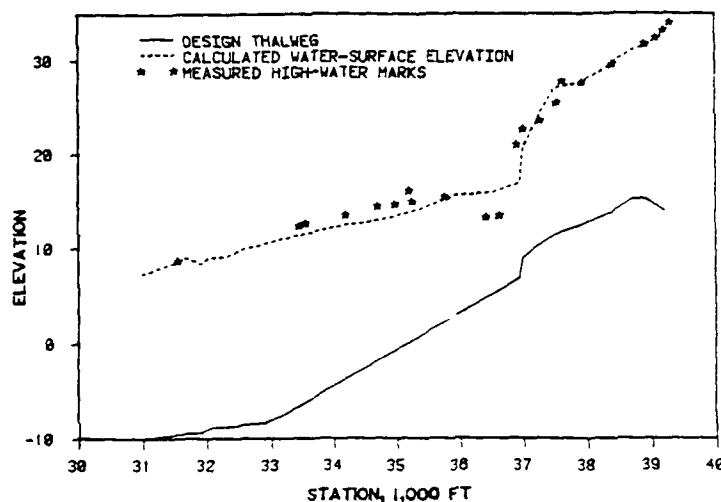


Figure 3. Maximum water-surface elevations, 4 January 1982

the high-water marks taken along the channel may be attributed primarily to losses at bridges at College Avenue and College of Marin. The assigned roughness coefficients were within the upper range used in engineering practice for this type channel, and therefore, further increases in roughness coefficients were deemed unreasonable.

#### Sediment Inflow

Measured sediment inflow data for Corte Madera Creek are inadequate to determine a reliable sediment inflow rating curve for the entire range of discharges considered in this study. USGS collected suspended load samples at the Ross gage during water years 1978-1980. The samples were analyzed to determine particle size distributions. Twenty-three events were reported with water discharges varying between 47 and 1,560 cfs. The highest measured flow was well below the design flood peak of 6,900 cfs. In addition to the suspended load measurements, seven bed-load samples were collected during water year 1978 at the Ross gage. Particle size distributions of these samples were also reported. Water discharges when the samples were collected varied between 47 and 1,180 cfs. The measured data were insufficient to determine a reliable sediment inflow rating curve for the model.

An initial sediment inflow rating curve was developed based on an optical fit of measured data for water discharges less than 2,000 cfs and on equilibrium transport for higher discharges. Equilibrium transport was calculated using the SEDTRAN transport function (described in the section on transport function) and a bed material gradation determined from four samples collected in 1985 in the vicinity of the Ross gage.

The sediment inflow rating curves were adjusted during the adjustment phase of the study. In general, the concentrations of sands were increased, but the concentrations of coarse gravels were decreased. Sediment inflow within the range of sampled data was generally unchanged. Calculated transport of coarse and very coarse gravel did not agree with sampled transport; therefore, sediment inflow concentrations for these coarsest particles were based on equilibrium calculations in the numerical model. The justification for the adapted sediment inflow rating curves is based on successful simulation of measured deposition in the concrete channel as discussed in the section on "Adjustment and Circumstantiation."

### Transport Function

A modification of the Laursen equation (Laursen 1958) was developed for use in this study. The Laursen function is desirable because it was developed for size class analysis and considers parameters essential to both bed and suspended sediment loads. The modified Laursen equation (labeled SEDTRAN) incorporated data for transport of gravels in addition to the sand data used to develop the original Laursen function.

The SEDTRAN function calculates the hydraulic radius due to grain roughness using the Limerinos equation. This value (instead of the depth as proposed by Laursen) is then used to calculate the grain shear stress:

$$\tau'_o = \frac{\rho V^2}{58} \left( \frac{D_{50}}{R_b} \right)^{1/3} \quad (4)$$

where

$\tau'_o$  = grain shear stress

$\rho$  = water density

$V$  = water velocity

This equation is dimensionally homogeneous and can be applied with any consistent set of units.

Bed-load transport is a function of the ratio of applied to critical shear stress. In the SEDTRAN function this is expressed by the parameter

$$(\tau'_o/\tau_{ci}) - 1 \quad (5)$$

where  $\tau_{ci}$  is the critical shear stress for the  $i^{\text{th}}$  grain size. The critical shear stress varies with particle size, larger particles having greater critical shear stress. Paintal (1971) determined that the critical shear stress, as used in Equation 5 to determine sediment transport, also varied with applied shear stress. When the dimensionless shear stress ( $\tau^*$ ) was less than 0.05, he found that the critical shear stress decreased significantly:

$$\tau_o^* = \frac{\tau_o}{(\gamma_s - \gamma_w) D_i} \quad (6)$$

where

$\tau_o$  = applied shear stress

$D_i$  = geometric mean diameter of the  $i^{\text{th}}$  size class

This variation in critical shear stress is accounted for in SEDTRAN by varying the Shields parameter between 0.039 and 0.020. The higher value, recommended by Laursen (1958), was used when  $\tau_o^*$  was greater than 0.05. The lower limit was determined by Andrews (1983). The effect of this change is that initiation of motion for coarser particles occurs at lower shear stresses, and the transport potential of coarser particles is increased.

The SEDTRAN function uses the ratio of grain shear velocity (instead of total shear velocity) to grain fall velocity as the important parameter influencing suspended sediment transport. A functional relationship between this ratio and other parameters was determined by Laursen (1958) based on river and flume data. Due to the reformulation of Laursen's parameters, a new functional relationship was developed for SEDTRAN. The relationship is based on data from both rivers and flumes. The functional relationship and data scatter are shown in Figure 4. Flume data gathered under more controlled conditions have significantly less scatter than the river data.

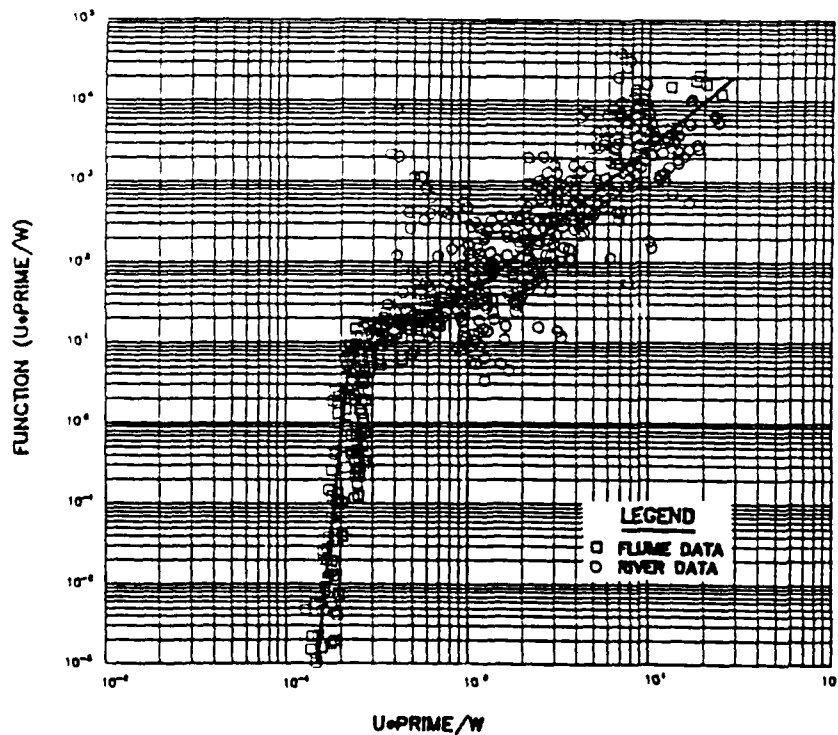


Figure 4. Function ( $U^*_{PRIME}/W$ ) for sediment transport function

Sediment concentration is calculated by SEDTRAN using the following formula:

$$C = 0.01 \gamma_v \sum_i P_i \left( \frac{D_i}{y} \right)^{7/6} \left[ \frac{\tau'_o}{\tau_{ci}} - 1 \right] f \left( \frac{U'_*}{\omega_i} \right) \quad (7)$$

where

C = concentration in weight per unit volume

$P_i$  = fraction of grain size class in the bed

y = water depth

$\tau'_o$  = bed grain shear stress

$U'_*$  = grain shear velocity  
\*

$\omega_i$  = fall velocity

$f \left( \frac{U'_*}{\omega_i} \right)$  = function defined in Figure 4

This function is considered to be a refinement to Laursen's original equation and is based on a wider range of physical data. The primary benefit is that it moves coarser gravels better than other functions. However, for the coarsest gravels (greater than 16 mm) the function still does not transport as much material as was sampled in Corte Madera Creek.

#### MODEL ADJUSTMENT AND CIRCUMSTANTIATION

##### Adjustment to Deposition Surveys

The historical hydrograph between October 1972 and July 1982 was simulated with the numerical model. This represents the time period between completion of the existing concrete channel and the first available survey of channel deposition. The survey was completed the summer after the flood of record on Corte Madera Creek. Average depths were determined from the surveyed deposition profile in the V-shaped bottom portion of the channel and an average-depth profile was developed for comparison with calculated profiles from the numerical model. Surveyed and calculated deposition profiles are compared in Figure 5. The numerical model overestimated deposition in the mild-sloped reach of the concrete channel, but reproduced both the depth and longitudinal extent of deposition in the steep-sloped portion of the channel.

The hydrograph between October 1972 and August 1984 was simulated with the numerical model. Another deposition survey was taken and bed material samples were collected in August 1984. The time period between the first



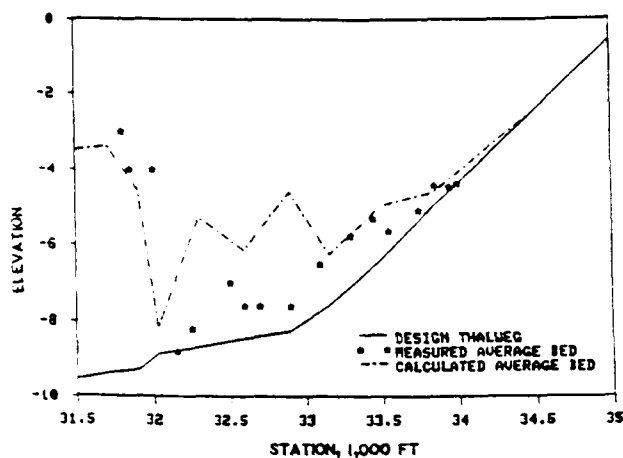


Figure 5. Aggradation in concrete channel, October 1972 to April 1982

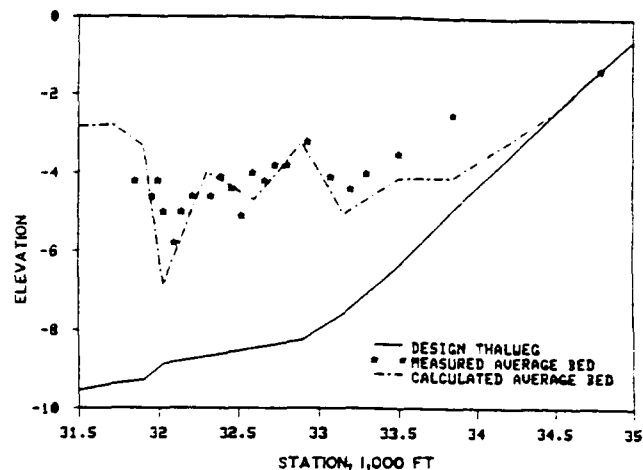


Figure 6. Aggradation in concrete channel, October 1972 to August 1984

survey, which was taken in July 1982, and August 1984 was a relatively high runoff period. The runoff hydrograph at the Ross gage peaked at 2,690 cfs. The calculated and surveyed deposition profiles are compared in Figure 6. The model satisfactorily simulated deposition in the mild-sloped portion of the channel, but underestimated deposition in the steep-sloped portion of the channel. During this 2-year period, both the calculated and surveyed profiles showed that the depth of deposition increased in the concrete channel. Bed material samples were collected at sta 335+06, which is the College Avenue Bridge, and at sta 341+00, which is 250 ft upstream of the College of Marin Bridge. Calculated gradations at model cross sections in this reach were compared to the average gradation of these two samples. The sample gradations were found to be considerably finer than the calculated gradations. It was determined from sensitivity studies (discussed in a subsequent section) that an increase in sediment inflow would result in an increase in the coarseness of the calculated gradation and that a decrease in sediment inflow would result in a finer calculated gradation. In order to improve the comparison between measured and calculated gradations, the sediment inflow into the model was adjusted. Gravel inflow was decreased and inflow of fine sands increased. The adjusted sediment inflow rating curves improved the comparison between sampled and calculated bed material gradations, but the calculated gradation was still coarser. Sampled and calculated bed material gradations for August 1984 are shown in Figures 7a and 7b, respectively. Further reduction in the gravel inflow was not deemed appropriate because it would deviate too much from the measured sediment inflow data and because it would reduce the correlation between measured and calculated depths of deposition.

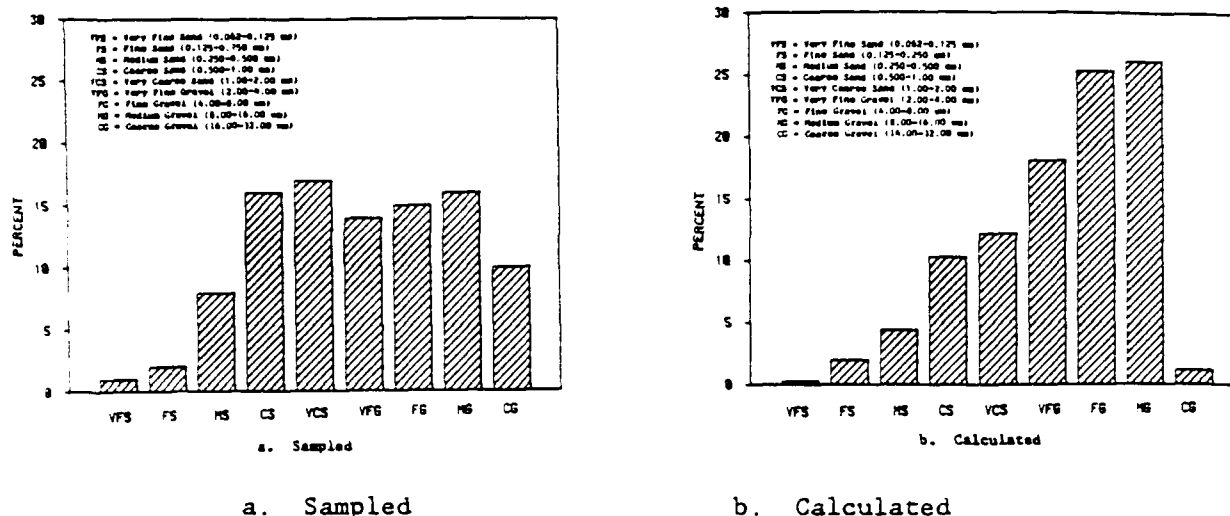


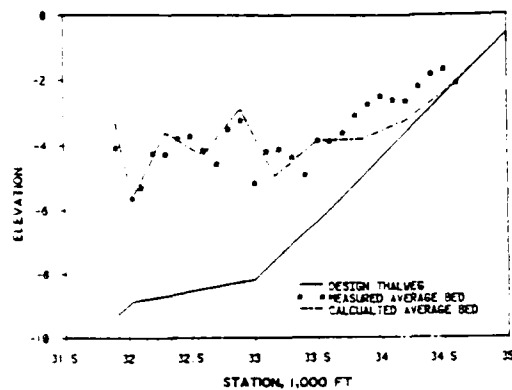
Figure 7. Bed material gradations in the vicinity of College Avenue, August 1984

#### Model Circumstantiation

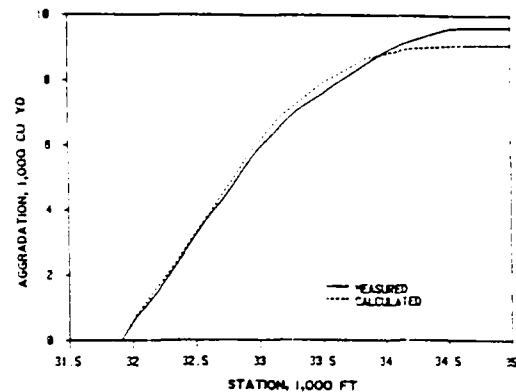
At this point in the study the numerical model was considered to be adequately adjusted for the prediction of general deposition patterns in Corte Madera Creek. Circumstantiation of the model was accomplished by continuing the historical simulation to January 1986, when another deposition survey was taken. The period between August 1984 and January 1986 had relatively high runoff with the largest peak being 2,600 cfs. Surveyed and calculated deposition profiles and accumulated deposition are compared in Figure 8. The January 1986 deposition profile (Figure 8a) shows little change from the August 1984 deposition profile (Figure 6). The model continued to reproduce an accurate profile downstream of the College Avenue Bridge, but underestimated deposition upstream. The model was very successful in predicting the quantity of total deposition in the channel.

A significant runoff event occurred in February 1986, when an estimated peak discharge of 4,150 cfs occurred at the Ross gage. Bed material samples were collected at three locations in the concrete channel upstream from the College of Marin Bridge in March 1986. A deposition survey in the concrete channel was taken in May 1986. Bed material samples were collected at 15 locations between sta 326+00 and 337+50 in May 1987, and three samples were taken laterally across the channel at sta 337+00 in September 1987. The period between May 1986 and May and September 1987 had relatively low runoff, with a maximum peak discharge of 2,500 cfs and only 5 days when the average daily flow exceeded 100 cfs. Due to the small amount of runoff between May 1986 and the collection of the bed material samples in 1987, it was deemed reasonable to compare these measurements with calculated gradations.

Calculated and surveyed deposition profiles and accumulated deposition for the October 1972 - May 1986 simulation are compared in Figure 9. Based on field surveys, 2,800 cu yd of material were removed from the concrete channel during the February 1986 flood. This compares with a removal of about

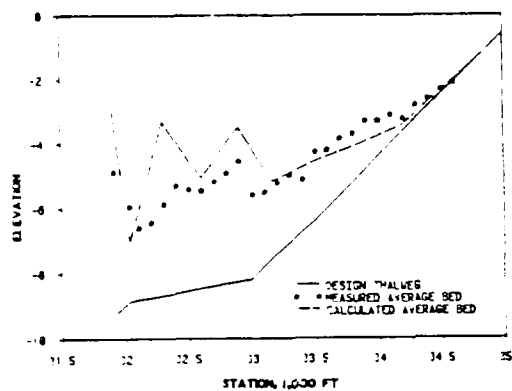


a. Profile

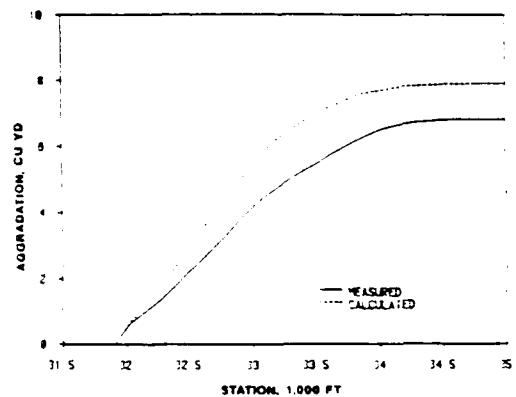


b. Accumulated

Figure 8. Aggradation in concrete channel, October 1972 to January 1986



a. Profile



b. Accumulated

Figure 9. Aggradation in concrete channel, October 1972 to May 1986

1,200 cu yd calculated in the model. The result is consistent with the comparison of field surveys and calculated deposition profiles after the flood of January 1982, which also showed more material removed in the prototype. These results indicate that the model, using average sediment inflow rating curves, underestimated the ability of the concrete channel deposits to degrade during floods. This behavior in the model may be attributed to one or more of the following factors:

- a. The sensitivity study demonstrated the importance of sediment inflow concentrations on the resultant deposition. It is possible that sediment inflow concentrations during the two flood events were significantly different from the long-term averages developed from the measured data. The measured sediment inflow data were taken between 1978 and 1980, which were fairly normal runoff years with a maximum peak discharge of 2,910 cfs.
- b. Model roughness in the concrete channel may be too high. The

high roughness values used in the model were chosen in order to match high-water marks from the January 1982 flood. These high roughness values reduce the velocity and thus the scouring potential of the flow.

- b. Model roughness in the concrete channel may be too high. The high roughness values used in the model were chosen in order to match high-water marks from the January 1982 flood. These high roughness values reduce the velocity and thus the scouring potential of the flow.
- c. Flow breaks away from the Corte Madera channel upstream from the concrete channel during flood flows. If the flow remaining in the channel is underestimated, then the model will show a reduced scouring potential.

Bed material gradations from samples taken in 1934-1987 are compared in Figure 10. Lateral and longitudinal variations in bed material gradations are

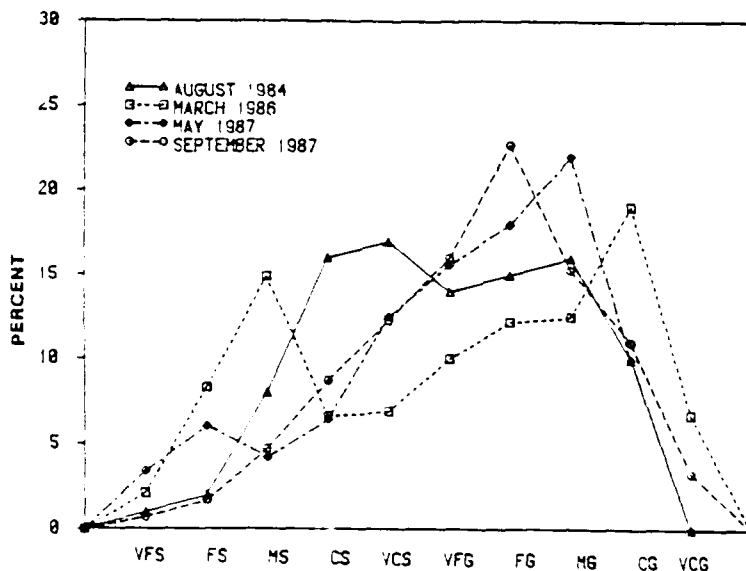
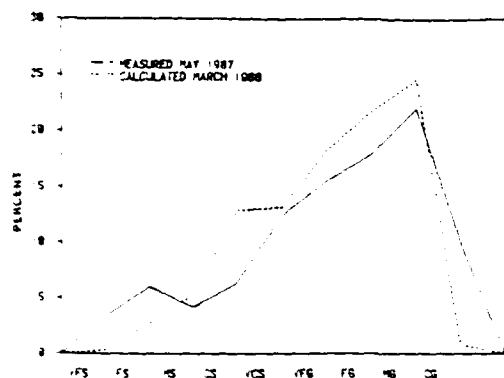


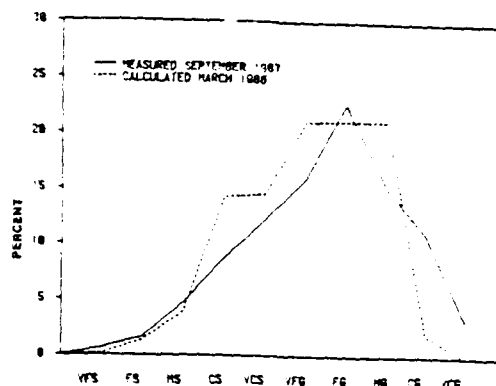
Figure 10. Sampled bed material gradations

not unusual in gravel bed streams. Therefore, average bed material gradations determined from a large sample population will be more reliable. The March 1986 gradation is finer than the other gradations. These data came from three samples between sta 340+50 and 321+00. One sample compared favorably with 1987 data; the other two had bimodal distributions. Ten samples between sta 326+00 and 337+50 were used to obtain the May 1987 gradation. Three samples, varied laterally at sta 336+80, were used to obtain the September 1987 gradation. Bed gradations calculated at the end of the 14-year simulation are compared to the 1987 sample gradations in Figure 11. This comparison is much better than the comparison of measured and calculated gradations in 1984. The calculated bed material gradations are well within the scatter of prototype data, and model performance can be considered reliable.

The numerical model can be used to evaluate the proposed channel improvements for Unit 4 on Corte Madera Creek. It is recognized that the



a. Between stilling basin  
and College of Marin bridge



b. Between College Avenue  
and College of Marin bridges

Figure 11. Bed material gradation

reliability of model predictions is somewhat limited due to the uncertainty related to prototype sediment inflow concentration and variations in bed material gradation data. The model was successful in simulating the longitudinal extent and general quantity of deposition in the concrete channel. Bed material gradations were reproduced fairly accurately. These gradations are important because they influence the roughness of the channel bed. The model predicted degradation during flood events. Because predicted quantities of degradation were less than the measured quantities, the model will provide conservative results with respect to the ability of the channel to maintain a sediment-free bed with the addition of the sediment basin in Unit 4.

#### Sensitivity Study

The sediment inflow rating curves used in the adjusted numerical model were based on suspended and bed-load samples taken at water discharges less than 2,000 cfs and on equilibrium transport calculations, with some adjustment to better simulate deposition surveys and sampled bed material gradations. Due to the critical importance of sediment inflow on deposition in the concrete channel, the sensitivity of the adjusted numerical model to sediment inflow was tested. The average values for sediment inflow were increased by a factor of 1.5 and decreased by a factor of 0.5 in the sensitivity study. These values were still within the range of measured data. Results of a historical simulation from October 1972 to August 1984 are compared in Figure 12. As expected, the sediment inflow rating curve influences the deposition profile in the concrete channel. The uncertainty and significance of sediment inflow must be considered when interpreting study results.

#### Test of Design

The proposed design for Unit 4 on Corte Madera Creek was incorporated into the numerical model and the following design conditions were used for testing the sedimentation effects in the proposed channel: (a) concrete channel and sediment trap maintained to design invert elevations at the start of the flood season, (b) the 1982 flood season, with the 100-year frequency flood replacing the 4-5 January flood, for a design hydrograph; (c) roughness

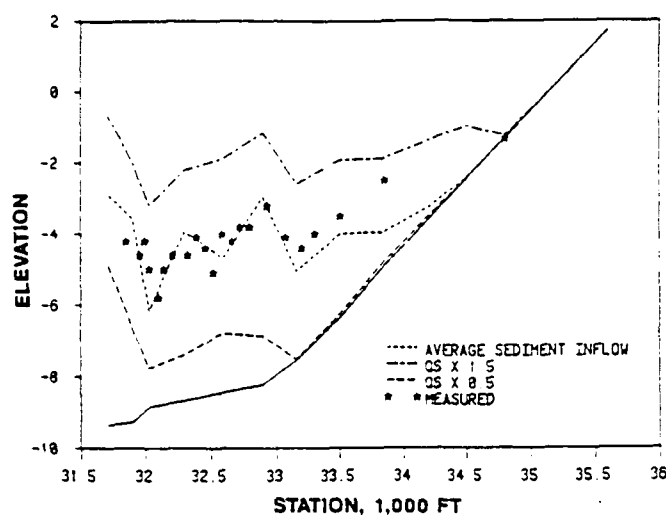
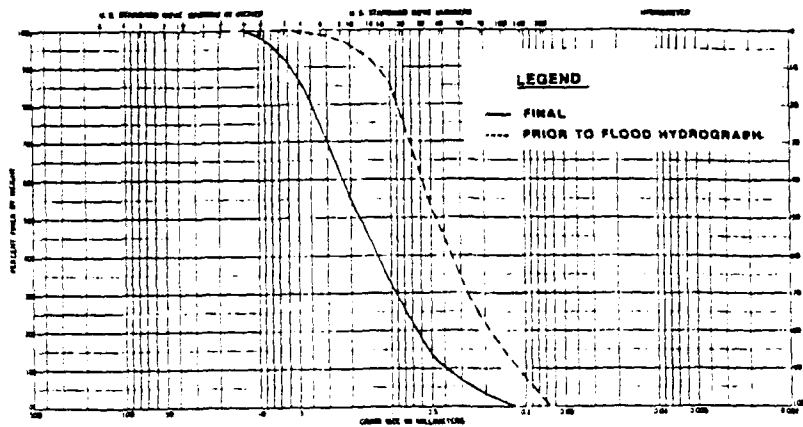


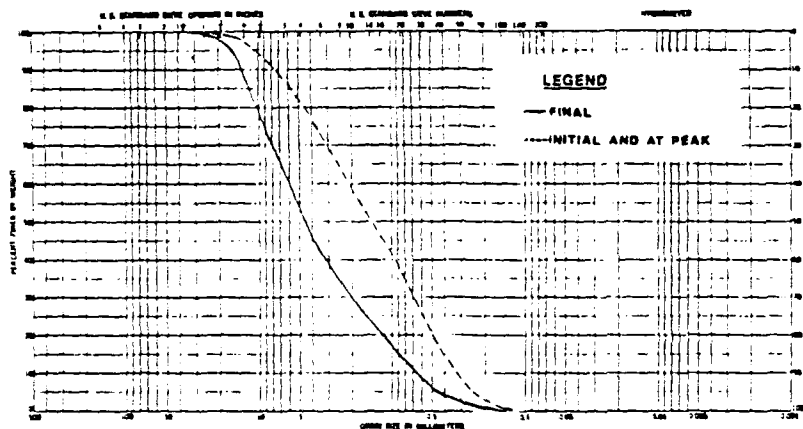
Figure 12. Sensitivity of model to sediment inflow, measured and calculated aggradation, August 1984

coefficients in the concrete channel determined from the January 1982 simulation; and (d) sediment inflow based on long-term average inflow determined by reproducing measured deposition in the channel.

The design channel operated satisfactorily in the numerical model test with the design hydrograph. About 900 cu yd of sand accumulated in the concrete channel during the antecedent flow period. The sediment trap had accumulated about 2,000 cu yd of material just before the start of the flood hydrograph. At the peak of the flood, 3,900 cu yd were stored in the sediment trap, 60 percent of which was sand and 40 percent gravel. Most of the sediment that had deposited in the concrete channel prior to the flood peak had washed out by the time the discharge reached 5,000 cfs. Calculated deposition in the concrete channel at the peak was less than 0.05 ft and can be considered to represent bed load. The  $D_{84}$  of this material was less than 2 mm, so no increase in roughness was calculated by the model's roughness algorithm. Maximum calculated water-surface elevations for the design flood were below the existing wall between the stilling basin and sta 328+00, about 1 ft higher than the existing wall at College Avenue, and about 2.4 ft higher than the existing wall at sta 342+00. The TABS-1 model does not account for bridge losses; therefore, design water-surface elevations will be higher. HEC-2 backwater calculations by Sacramento District indicated that about 0.7 ft of head loss can be expected by the combined College Avenue and College of Marin bridges. Flows subsequent to the flood peak deposited material in the concrete channel. Some of this material came from the sediment trap. At the end of the flood season, 2,800 cu yd of sediment were deposited in the trap and 4,500 cu yd in the concrete channel. The channel deposits at the end of the season were considerably coarser ( $D_{84} = 5$  mm) than deposits from the antecedent flow ( $D_{84} = 1$  mm). The material deposited in the trap at the end of the season was also coarser ( $D_{84} = 12$  mm) than deposits at the peak and from the antecedent flow ( $D_{84} = 6$  mm). Calculated gradations of the channel and trap deposits are shown in Figure 13. Bed changes during the passage of the test hydrograph are shown for three concrete channel sections in Figure 14.



a. Sta 329+00



b. Sediment trap

Figure 13. Bed material gradations

#### CONCLUSIONS

Channel roughness in the concrete channel is affected by gravel deposits. A comparison of backwater calculations and high-water marks from the January 1982 flood demonstrated that the average Manning's roughness coefficient in the concrete channel with gravel deposits was on the order of 0.030 at the flood peak. Sinuosity, grain roughness on the channel bottom, and tubeworm and barnacle growth on the channel walls were insufficient to account for a composite roughness of this magnitude. The additional roughness was attributed to form roughness due to the movable gravel bed. Criteria, which included a minimum thickness and applied shear stress, were established to determine when adding form roughness to the composite channel roughness would be appropriate. A conceptual framework, considered appropriate for making comparative analyses of sedimentation in Corte Madera Creek, was developed to emulate the complicated physical processes as much as possible, given state-of-the-art knowledge. Using this framework, with the design flood conditions, a roughness coefficient of 0.022 was calculated for a channel free from sediment deposits. This value increased to 0.028 when there was sufficient gravel

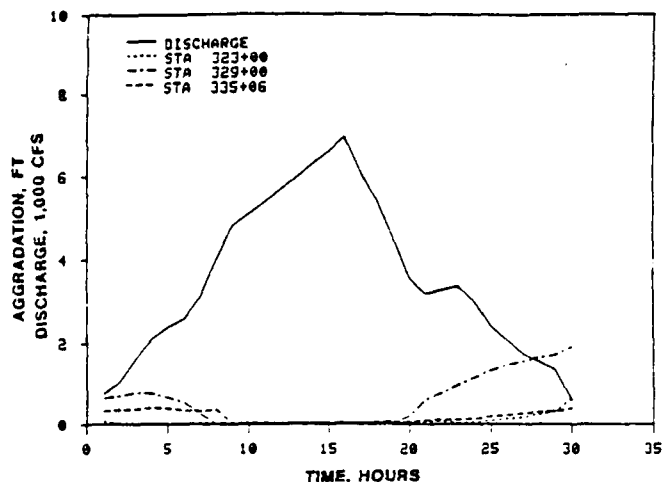


Figure 14. Aggradation in concrete channel with passage of design flood hydrograph

in the movable bed layer, either by increased antecedent flow or deletion of the sediment trap, to cause a calculated increase in roughness. When sediment deposits were not removed prior to the design flood, a value of 0.030 was calculated due to a thicker and coarser deposit.

Using average sediment inflow rating curves, the numerical model generally reproduced both measured deposition quantities and sampled gradations over a 14-year historical period. Sensitivity tests demonstrated that sediment inflows of 1.5 and 0.5 times the average would produce deposition considerably different than measured quantities. Therefore, long-term simulations using average sediment inflow are considered fairly reliable.

Probable variations in sediment inflow during a flood event make short-term predictions less reliable than long-term predictions. However, the sensitivity tests demonstrated that increasing the average sediment inflow by 50 percent did not result in an increase in calculated roughness coefficient. Results from the sensitivity study relieve some possible concern related to sediment inflow uncertainty and its effect on channel roughness.

The proposed sediment trap collects both sand and gravel. The numerical model calculated a trap storage of 3,900 cu yd, 60 percent sand and 40 percent gravel, at the peak of the design flood; about 2,000 cu yd of this material was deposited by flow preceding the peak. The effective storage capacity of the trap is not the same as the volume excavated below the existing bed profile, because during floods, sufficient sediment transport potential exists to maintain some sediment movement through the trap. The numerical model results using the design histogram demonstrated that the trap was effective in reducing channel deposition from flow preceding the peak and in reducing the coarseness of both the bed deposit and the bed load at the flood peak. This resulted in a reduction of about 1 ft in the computed water-surface elevation in the concrete channel downstream from sta 342+00. Deposition in the concrete channel at the end of the flood season was about the same, with or without the trap.



#### ACKNOWLEDGMENTS

The tests described and the resulting data presented herein, unless otherwise noted, were obtained from research conducted for the US Army Engineer District Sacramento, by the US Army Engineer Waterways Experiment Station, Vicksburg, MS. Permission was granted by the Chief of Engineers to publish this information.

#### REFERENCES

- Andrews, E.D. (1983). 'Entrainment of gravel from naturally sorted riverbed material', *Geological Society of America Bulletin*, 94, 1225-1231.
- Brownlie, William R. (1983). 'Flow depth in sand-bed channels', *Journal, Hydraulics Division, American Society of Civil Engineers*, 109 (HY7), 959-990.
- Keulegan, G. (1938). 'Laws of turbulent flow in open channels', *Journal of Research, US National Bureau of Standards, Research Paper* 1151, 21, 707-741.
- Laursen, Emmett M. (1958). 'The Total Sediment Load of Streams', *Journal, Hydraulics Division, American Society of Civil Engineers*, 84 (HY1), 1530-1 to 1530-36.
- Limerinos, J.T. (1970). 'Determination of the Manning coefficient from measured bed roughness in natural channels', *Geological Survey Water-Supply Paper* 1909-B, US Geological Survey, Washington, DC.
- Paintal, A.S. (1971). 'Concept of critical shear stress in loose boundary open channels', *Journal of Hydraulic Research*, No. 1, 90-113.
- Thomas, W.A. (1980). 'Mathematical modeling solutions', *Applications of Stochastic Processes in Sediment Transport*, H. W. Shen, H. Kikkawa, eds., Water Resources Publications, Littleton, CO.
- \_\_\_\_\_. (1982). 'Mathematical modeling of sediment movement', *Gravel Bed Rivers*, R.D. Hey, J.C. Bathurst, and C.R. Thorne, eds., Wiley, New York.
- US Army Engineer District, Sacramento. (1987). 'Corte Madera Creek flood control project, Marin County, California, supplement No. 1, unit No. 4,' Design Memorandum No. 2, Sacramento, CA.
- US Army Engineer District, San Francisco. (1966). 'Corte Madera Creek, Marin County, California', General Design Memorandum, San Francisco, CA.
- US Army Engineer Hydrologic Engineering Center. (1977). 'Users Manual HEC6 generalized computer program scour and deposition in rivers and reservoirs', US Army Corps of Engineers, Davis, CA.
- \_\_\_\_\_. (1982). 'Users manual HEC2 water surface profiles', US Army Corps of Engineers, Davis, CA.

Yang, C.T. (1973). 'Incipient motion and sediment transport', *Journal, Hydraulics Division, American Society of Civil Engineers*, Proceedings Paper No. 10067, 99 (HY10), 1679-1704.

\_\_\_\_\_. (1984). 'Unit Stream Power Equation for Gravel', *Journal, Hydraulics Division, American Society of Civil Engineers*, Proceedings Paper No. 19353, 110 (HY12), 1783-1797.

## RIVER BED ADJUSTMENTS IN A STEEP STEP-POOL SYSTEM

(Lainbach, Upper Bavaria)

Peter Ergenzinger

## Introduction

Bed adjustments by scour or fill are responsible not only for the buffered hydraulics of discharge even under very unsteady flood waves but also for the related bed load transport. Despite recent advances our knowledge about these phenomena is still somewhat restricted, especially with regard to extremely coarse-grained step-pool rivers. In the case of field studies during non-uniform unsteady floods much remains to be done. Whenever there is bed load transport, it is not sufficient to survey river sections only before and after a flood. Nor can the dynamics of roughness be determined from the average grain-size distribution of bed material. The newly developed "Tausendfuessler" can be used to measure both geometry and roughness, even during floods. First results of this approach are presented from Lainbach in Upper Bavaria.

## Test site

The Lainbach catchment, the experimental site of the Geographical Institute of the University of Munich, is situated about 70 km south of Munich close to the monastery of Benediktbeuern at the northern border of the Alps. The experimental reach lies below the confluence of Schmiedlaine and Kotlaine. The reach is 150 m long and the related area of the catchment is 18.8 km<sup>2</sup> in size. In this region floods occur either during snowmelt or after thunderstorms in July or August. The bed load originates mainly from a more than 100 m thick Quaternary fill of glacial sediments in the central parts of the basin (Becht, 1989). Mass movements and related debris flows transport the material into the river system.

The steep Lainbach is called a "Wildbach" for there are many steps, rapids and pools along the river, and extreme discharges occur with related extreme rates of solid material transports. Kotlaine and Lainbach are buttressed by many small dams (Wildbachverbauung) creating an extreme fall-pool system. Only this measuring site and the Schmiedlaine still preserve the natural conditions of a typical step-pool system (Whittaker and Jaeggi, 1982). This more natural step-pool sequence at the experimental reach is depicted in fig. 1.

#### Grain size distribution

The grain size distribution of the river bottom material ranges from boulders with b-axis up to 2 m to sandy material in some small pools in the lee of these boulders. The inner channel is paved by cobbles, coarse pebbles are common for the bars, and boulders are restricted to steep step sites.

To match the very different scales of grain sizes different techniques must be employed. Coarse grain sieving was done according to Ibbeken (1974). The paved surfaces were investigated by the "photo-sieving" technique of Ibbeken and Schleyer (1986). In order to include the steps with the boulders a photogrammetric method was used.

At the 5 and 110 meter marks of the experimental reach (fig. 2) volume samples of more than 300 kg were sieved, resulting in the following grain size parameters (Ergenzinger, Stüve 1989):

Tab. 1: Comparison of grain-size parameters created by sieving and photo-sieving

		D <sub>50</sub> (mm)	D <sub>84</sub> (mm)
5 meter mark	sieving	75	135
	photo-sieving	160	280
110 meter mark	sieving	60	120
	photo-sieving	120	205

Both samples are from pool reaches. The coarseness of the photo-sieving samples are the result of pavement processes. Compared to the grain-size distribution created by sieving, the  $D_{94}$  equals the  $D_{50}$  of the pavement.

Along the step reaches the boulders must be taken into account. During floods with more than  $8 \text{ m}^3 \text{ s}^{-1}$ , the boulders are submerged and then become "singular roughness elements" (Bathurst ). To describe this situation, vertical and oblique photos were taken along the whole measuring site with a special photogrammetric camera. For all boulders and cobbles with b-axis bigger than 120 mm the grain-size and the position were measured by Peter Stüve, using the Rollei picture analysis system MR 2. For this interpretation the experimental reach was differentiated into step- and pool-reaches according to fig. 1. The remaining area not covered by boulders and cobbles was filled up according to the grain-size distribution given by photo-sieving. The representative grain size parameters resulting from these combined distributions are shown in figure 2 and table 2.

Table 2: Representative grain size parameters for steps and pools of the experimental reach

			$D_{50}$ (mm)	$D_{94}$ (mm)
1. Step:	5 - 30 m:	MR 2 and p-s. at 5 m	650	1380
2. Pool:	30 - 55 m:	MR 2 and p-s. at 5 m	320	645
3. Step:	55 - 80 m:	MR 2 and p-s. at 110 m	805	1710
4. Pool:	80 - 110 m:	MR 2 and p-s. at 110 m	290	535

The steeper the step the coarser the grain size distribution. The parameter  $D_{94}$  is shifted by the boulders up to 1.7 meters. With one exception these boulders were never in motion during the last two years. The steps are the most stable reaches of the river bottom, whereas the pools changed their shape during every flood, and most of the surface material was replaced several times.

The different grain-size investigations resulted in a wide range of so-called representative parameters. In order to decide which one is "representative" for this Wildbach a new device, the "Tausendfuessler", was installed at the 110 m mark of the experimental reach, in a pool section.

The "Tausendfuessler" device and its application for measuring river bed adjustments

By scour and fill river beds are adjusted to discharge. Since most adjustments occur during the most unsteady and non-uniform runoff conditions, the observation and measurement of these changes in geometry are invisible and difficult to measure. The Tausendfuessler is a simple device for measurements of the changing river cross sections and was developed and applied for the first time at Squaw Creek in Montana (USA) in 1988. To measure the conditions of bed and water surface at always the same spots and along the same length intervals, a log or a tube is installed horizontally across the river and holes are drilled vertically every 10 cm (fig. 3). A measuring rod is driven through each hole and the distance between the horizontal log or tube and the upper end of the rod is measured. Depending on the stability of the installation it is possible to locate the points again with a precision of 0.5 to 1 cm. At Lainbach the first Tausendfuessler is installed at the 110 meter mark and consists of three tubes. Tube 1 is 1.65 m upstream of tube 3, and very close to tube 3, on the upward side, there is the parallel tube 2 (distance 0.15 m). The aim of this installation was to investigate first, the investigation of small scale variabilities along the tubes 3 and 2 and, second, the local changes in bed slope by comparing tube 1 and 3. Since late summer 1989 two measuring bridges have been installed across a step and a pool section. Now it is no longer necessary to wade along the Tausendfuessler during flood. But since one total observation along one section lasts about 45 minutes the sequences of measurements are still too long.

The flood of July 2/3 1989 peaked close to  $10 \text{ m}^3\text{s}^{-1}$  and lasted more than 30 hours due to the rainfall conditions (fig. 4). At the pool runoff was always subcritical with the maximum Froude number

close to 0.85. During flood, 9 measurements at tube 3 were made. The changing bed conditions are shown by the stripped area in fig. 5. The first and the last profiles of the sequence are shown separately. They stay close only at the right bar. The maximum extent of river channel changes during flood for all 9 sections defines a band of maximum scour and fill. With more than 25 cm, this band is especially thick at the inner channel and on the left bar close to the left bank. On average there are 15 cm of scour and accretion, resulting in 1.87 m<sup>2</sup> of changed river section.

In order to describe these adjustments in more detail, the river bottom was divided into the inner channel (6.5 m to 11.5 m) and the two bars (1.5 to 6.5 m and 11.5 to 13.5 m). By means of the 9 sections the adjustments in geometry can be represented in 8 steps of different time length. For each time interval the measured scour and fill and the absolute total of differences in area were determined. In order to compare the resulting figures, they were converted from m<sup>2</sup> per time interval to mm per hour by dividing them by the corresponding river width and time interval between the different measurements (fig. 6).

In accordance with the hydrograph showing peak runoff at 2 a.m. and a secondary maximum at 4 p.m. next day there was intensive erosion at the very beginning of flood on both parts of the section. Afterwards the development of the adjustments was more differentiated. The inner channel was first filled, then just after peak flow slightly eroded, but maximum erosion occurred at the end after the second flood wave. By contrast, the bar was intensively eroded just after peakflow, but stabilized afterwards, and fill was dominant after the second peak during recession. The discussion of these reactions and adjustments will be postponed until more is known about the related changes in hydraulics and roughness.

The  $k_3$  concept and the determination of changing roughness conditions.

Measuring the depth of the river bottom every 10 cm by the Tausendfuessler not only reveals the changing geometry of the river bed, but results can also be interpreted for the changing roughness conditions. Since it is impossible to obtain bed surface samples under flood conditions a more indirect technique must be used to describe the changing roughness conditions. Roughness creates turbulence mainly due to vertical differences of the river bottom. Furthermore, in the case of coarse material river bottoms the common distinction between grain and form roughness is very difficult to apply. The same coarse particle can create form roughness under low flow conditions and grain roughness under high flow conditions. This is especially true for boulders. To overcome these artificially defined differences the concept of  $k_3$  roughness was created:  $k_3$  roughness is defined as maximum difference in height across three neighbouring points at 10 cm intervals. The aim is to define a representative number which reflects the turbulence created by vertical differences across one third of a meter. This length was chosen because the impact of larger cobbles can be measured on both sides of the obstacle over this distance. In order to describe the  $k_3$  situation of a certain section of the river bed, the sweeping maximum differences of height across 3 decimeters were determined (fig. 7).

At Lainbach the averages of these sweeping maximum differences were determined for the above defined two parts of the cross section. The aim is to obtain the different roughnesses during a flood both on the bars and in the inner channel. The  $k_3$  values changed between 28 and 45 mm. In the inner channel low  $k_3$  numbers occurred at the very beginning, just before peak, and before the secondary peak of the flood wave. These low  $k_3$  numbers were always due to a small but very effective layer of pebbles infilling the gaps between the pavement cobbles. Rather rough conditions existed during peak runoff and during the recession after the secondary peak. The bar developed similarly except that at the very beginning and during the secondary peak flow the bar had a higher  $k_3$  number than the inner channel. Again the highest  $k_3$  number



occurred during recession. The  $k_3$  numbers differ from the  $D_{50}$  of the grain-size distribution and amount to only about one tenth of the measured b-axis. Nevertheless the  $k_3$  numbers change by a factor close to two during a single flood wave.

The changing roughness conditions can be described by the data of relative roughness ( $R_r = d / k_3$  with  $d$  = average water depth). Since grain size has been replaced by the more dynamic  $k_3$  the resulting data of relative roughness change quite dramatically. Especially in the inner channel the phases with reduced  $k_3$  numbers are phases with rather high values for relative roughness. Due to greater water depth in the inner channel the values of relative roughness are always higher here in comparison with the bar.

The good correspondence of relative roughness with Darcy-Weissbach roughness is rather astonishing ( $f_0 = (8 g d S) : v^2$  with  $S$  = slope). By transferring  $f_0$  to  $1/f_0^{1/2}$  (fig. 8) a similar distribution to that of relative roughness is obtained. The dynamics of roughness changes of different parts of a river are easily described if the related water depths and the differences in height of the river bottom are known. This is easier to measure than for instance, the slope of the different parts of the section. The "Tausendfuessler" approach is useful not only to measure the changes in geometry but also to determine the related changes in roughness.

#### The dynamics of the river and bed adjustments

During flood velocity profiles were measured by current meter across the "Tausendfuessler" section. The resulting data were used to determine stream power and mobility number. The mobility number reflects the big changes in geometry and roughness at the beginning and at the end of the flood far better than stream power (fig. 9). The mobility number ( $Fr = v^2 : (g k_3)$ ) does not include slope as a parameter, and grain size is replaced by  $k_3$  in order to include more of the changing conditions of the river bottom.

The relationship between roughness and mobility number is straightforward (fig. 10). There is some bias between the reactions on bars and inner channel. The gradient of Darcy-Weissbach roughness increases more rapidly on bars than in the inner channel. On the bottom of the inner channel big changes in roughness at the start of flood are not reflected by high mobility numbers. These are effects of a temporary input of bed load which does not correspond with the local dynamics of runoff.

The changes of mobility numbers for the inner channel and bar and their relationship with the changing geometry of the "Tausendfuessler" section can be studied by comparing the figures x and y. If the heavy erosion at the very beginning of flood is excluded the important changes occur during the phases when the mobility number is higher than 2. The very rapid changes of erosion and fill during the rising stage of the hydrograph is not reflected by similarly changing mobility numbers. During the periods of maximum gradient of the mobility numbers there was accretion in the inner channel at the rising limb and erosion at the falling limb. The same tendency is true for the bar but here the high gradient mobility numbers with erosion occurred just after peak flow of the flood. If the amount of change in geometry is compared with the related mobility numbers (fig. 11) the tendency is quite clear: excluding the first and the last observations at the very start and during the last phases of recession there is growing change with growing mobility numbers. But the extent of change can vary and there is no rule relating it to scour or accretion. At the pool below the "Tausendfuessler" there are very important changes in pool geometry at the beginning and towards the end of flood. This results in excessive amounts of erosion related to a rather low mobility of below 2 and rather small amounts of accretion during recession when the mobility number is still close to 13. These biases are related to phases when the impact of bed load created by erosion of the river bed just above the site is especially important.

## Results

The new "Tausendfuessler" device measures the changing conditions both of geometry and of roughness during a flood wave. The dynamics of river bed adjustments are quite complicated, for there are many possibilities of negative or positive feed-back. In step-pool systems like the Lainbach the pools are very sensitive areas which react quickly to runoff changes. In contrast the neighbouring step areas are stable and no big change occurs during low or average floods. This is due to the remarkable difference in grain size between the two different parts of the river long profile.

The dynamics of roughness changes of different parts of a section during a flood can be studied with the help of the  $k_3$  concept. The study of grain-size distribution of the superficial material is replaced by the determination of differences in height above the local level. Bottom height is measured every 10 cm, and by determining the maximum height difference between 3 neighbouring measurements it is possible to obtain the moving differences and the related averages. What is striking that even during the rising limb of the flood there are phases with low  $k_3$  numbers created by incoming pebble material. The  $k_3$  numbers are used to replace grain size for the calculation of relative roughness and mobility numbers.

The extent of change of the cross section due to scour and/or fill was determined by the comparison of different "Tausendfuessler" measurements. There are extreme reactions again at the very start of flood when the mobility numbers are rather low. For the flood the reaction measured as change in mm per hour shows quite a good relationship with the mobility numbers, but there is no change to determine the phases of erosion or accretion by means of the mobility number .

As long as the input of bed load material from the river above the measuring site is unknown, the resulting reaction of the river bed during the unsteady conditions of a flood cannot be precisely determined. A very important factor here is the availability of

rather coarse material sufficient to reduce scour and to change the local geometry of the river bed. Since availability is very important for step-pool rivers more studies are needed focusing on the sources of coarse material and their distribution along the river.

## References

- Bathurst, J.C. 1987: Flow resistance in boulder-bed streams  
in: Hey, R.D., Bathurst, J.C., Thorne, C.R. (ed.)  
Gravel-bed rivers: 403-465, Chichester
- Chin, A. 1989: Step pools in stream channels  
in: Progress in Physical Geography  
13, 3: 391-407, Chichester
- Ergenzinger, P., Stüve, P. 1989: Räumliche und zeitliche  
Variabilität der Fließwiderstände in einem  
Wildbach: Der Lainbach bei Benediktbeuern in  
Oberbayern.  
Göttinger Geogr. Abhandlungen, 86: 61-79
- Hey, R.D. 1979: Flow resistance in gravel-bed rivers  
Journal of the Hydraulic Division HY4: 365-79
- Ibbeken, H. 1974: A simple sieving and splitting device for  
field analysis of coarse grained sediments.  
Journal Sed. Petrology, 44, 939-946
- Ibbeken, H., Schleyer, R. 1986: Photo-sieving, a method for grain-  
size analysis of coarse grained,  
unconsolidated bedding surfaces. Earth Surface  
Processes and Landforms, 11, 59-77.
- Whittaker, J.G. 1987: Sediment transport in step-pool streams  
in: Thorne, C.D., Bathurst, J.C., Hey, R.D. (ed.)  
Sediment transport in gravel-bed rivers:  
545-79, Chichester
- Whittaker, J.G., Jaeggi, M. 1982: Origin of step-pool systems  
in mountain streams  
Journal of the Hydraulics Division 108: 758-73

Figures:

fig. 1: Longitudinal profile and the average slopes of the steps and pools of the experimental reach

fig. 2: Grain-size distribution for distinctive parts of the experimental reach

1 and 3: grain-size distribution for step reaches

2 and 4: grain-size distribution for pool reaches

5 and 6: grain-size distribution according to photo-sieving at 5 and 110 m

7 and 8: grain-size distribution according to sieving at 5 and 110 m

fig. 3: Tausendfuessler device: Differences of height of the river bottom are measured by rods at 10 cm intervals. The sweeping maximum differences of height across 3 decimeters are representative numbers for roughness height

fig. 4: Hydrograph of flood at Lainbach 2/3.7.1989

fig. 5: Maximum extent of 9 Tausendfuessler section measured during the flood in comparison with the section before and after flood

fig. 6: River bed adjustments during flood. Comparison of the total number of river bed changes during flood with the resulting amounts of scour and accretion of the bars and the inner channel

fig. 7: An example for the sweeping values of maximal differences across 3 decimeters

fig. 8: Changes of roughness of inner channel and the bars during flood. a.:  $k_3$  roughness  
b.: Relative roughness  
c.: Darcy-Weissbach roughness

Fig. 9: Runoff dynamics during flood of 2/3.7.1989

a.: Hydrograph

b.: Stream power

c.: Mobility number

Fig. 10: Relationship between mobility number and Darcy-Weissbach friction

Fig. 11: Relationship between mobility number and the total number of river bed changes

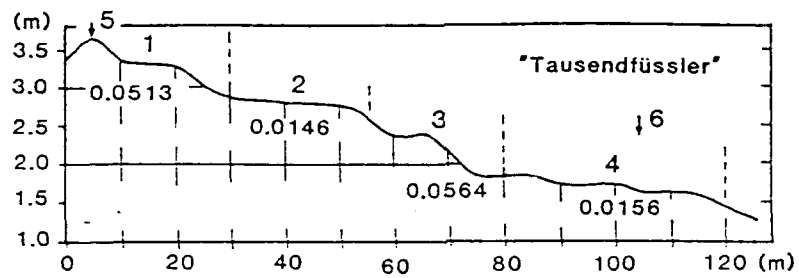


fig. 1: Longitudinal profile and the average slopes of the steps and pools of the experimental reach



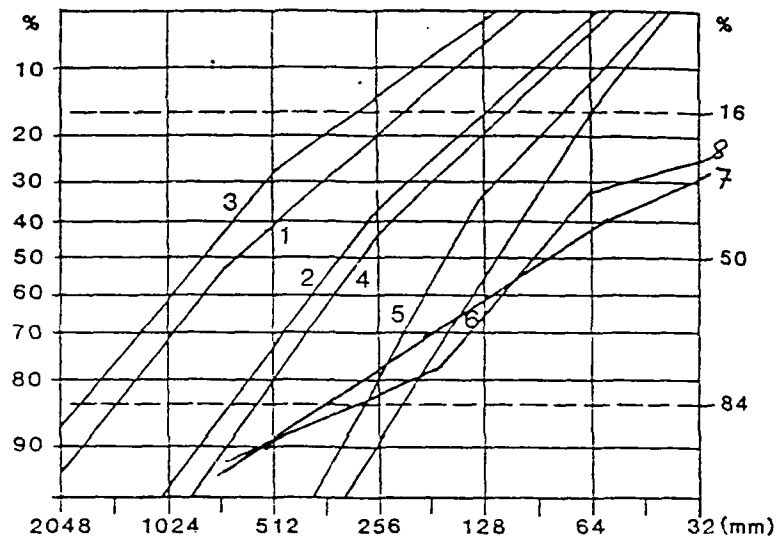


fig. 2: Grain-size distribution for distinctive parts of the experimental reach

1 and 3: grain-size distribution for step reaches

2 and 4: grain-size distribution for pool reaches

5 and 6: grain-size distribution according to photo-sieving at 5 and 110 m

7 and 8: grain-size distribution according to sieving at 5 and 110 m

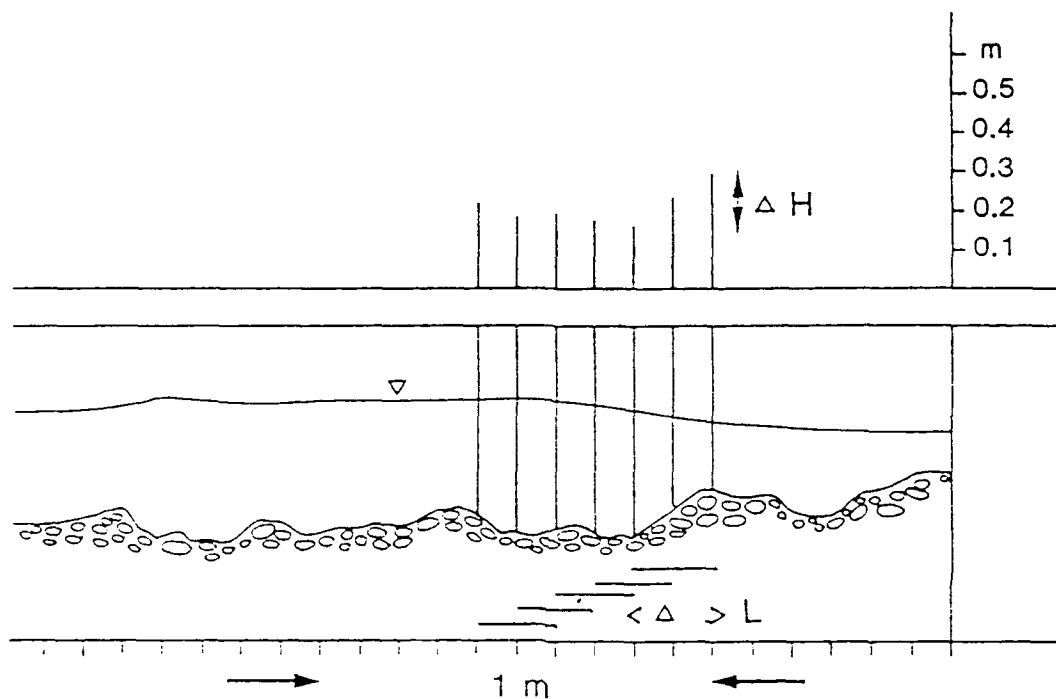


Fig. 3: Tausendfuessler device: Differences of height of the river bottom are measured by rods at 10 cm intervals. The sweeping maximum differences of height across 3 decimeters are representative numbers for roughness height

# FLOOD AT LAINBACH 2/3.7.1989

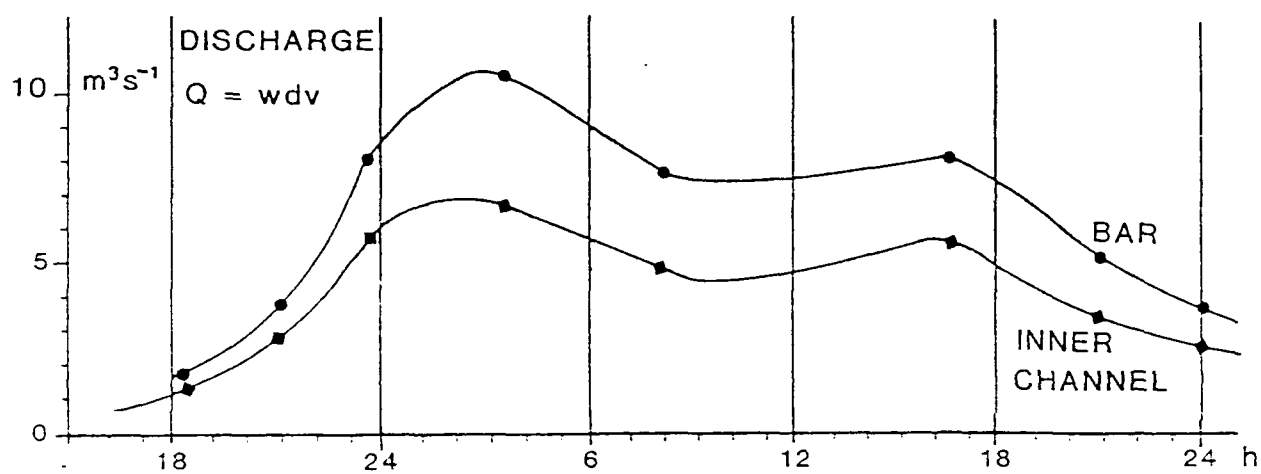


fig. 4: Hydrograph of flood at Lainbach 2/3.7.1989

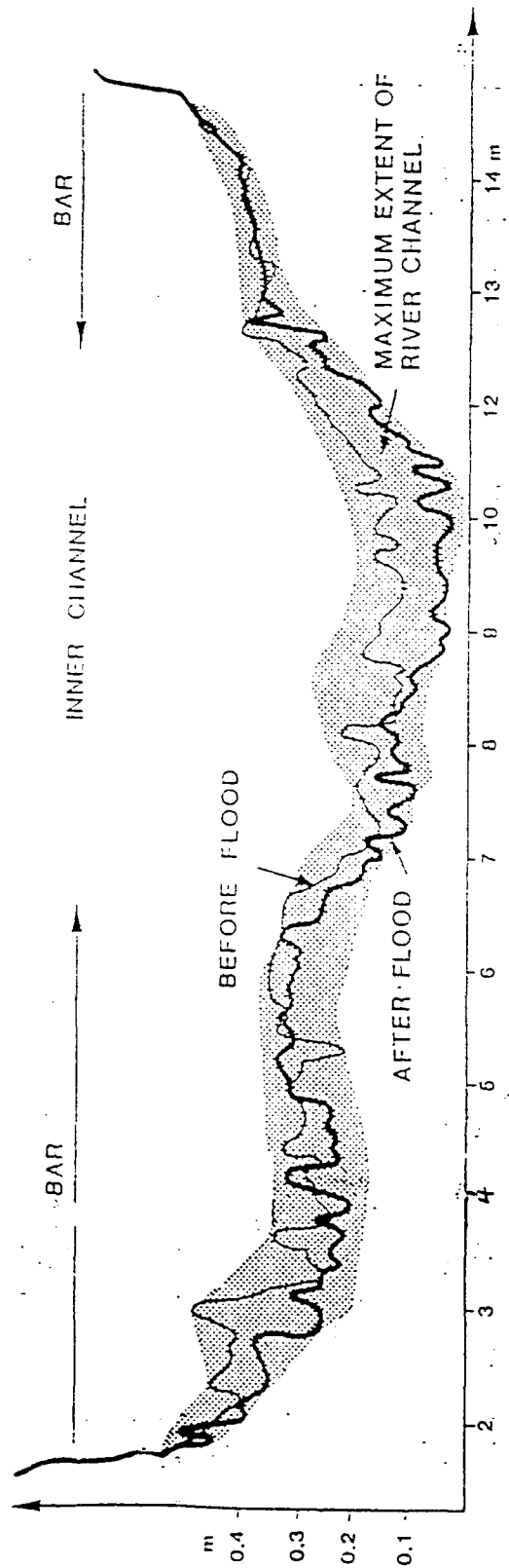


fig. 5: Maximum extent of 9 Tausendfuessler section measured during the flood in comparison with the section before and after flood

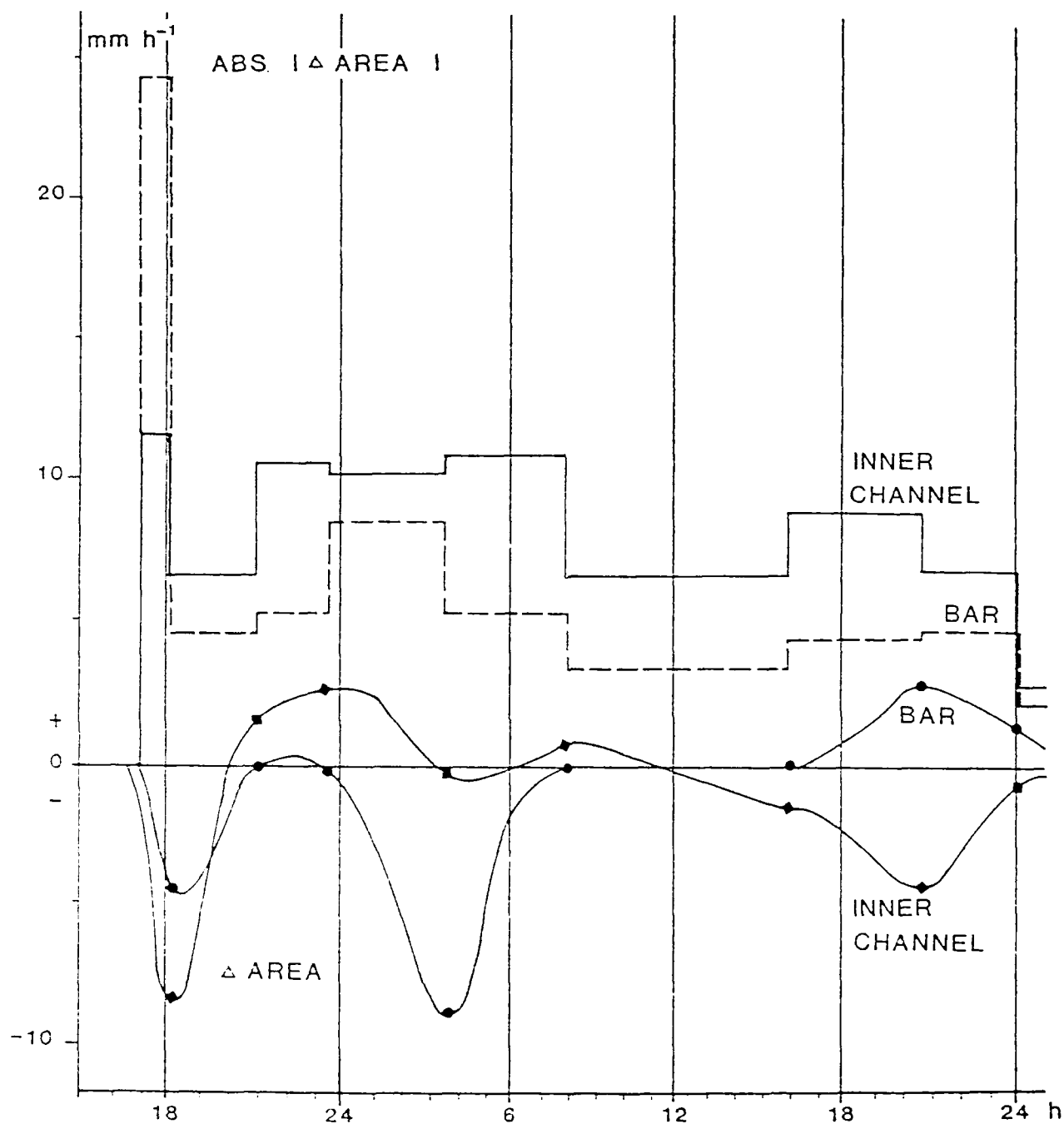


fig. 6: River bed adjustments during flood. Comparison of the total number of river bed changes during flood with the resulting amounts of scour and accretion of the bars and the inner channel

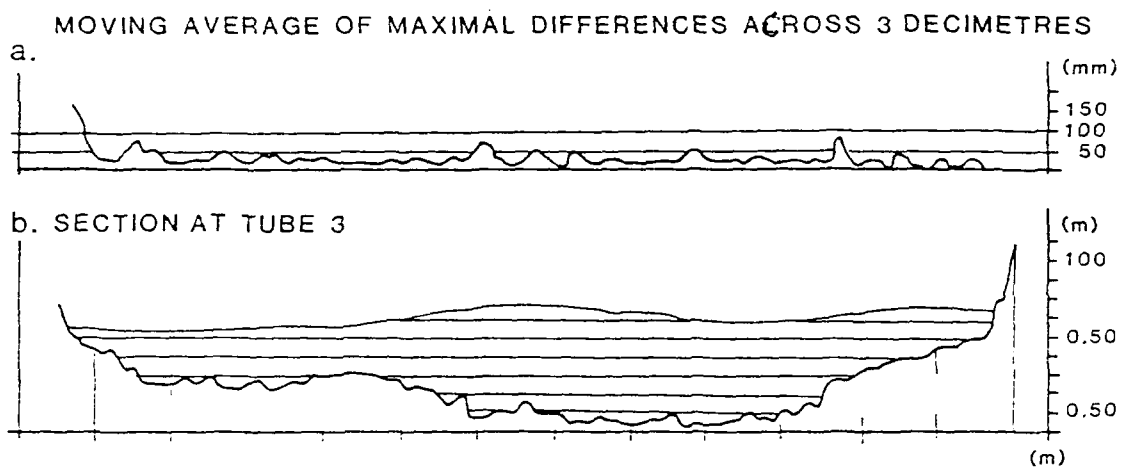
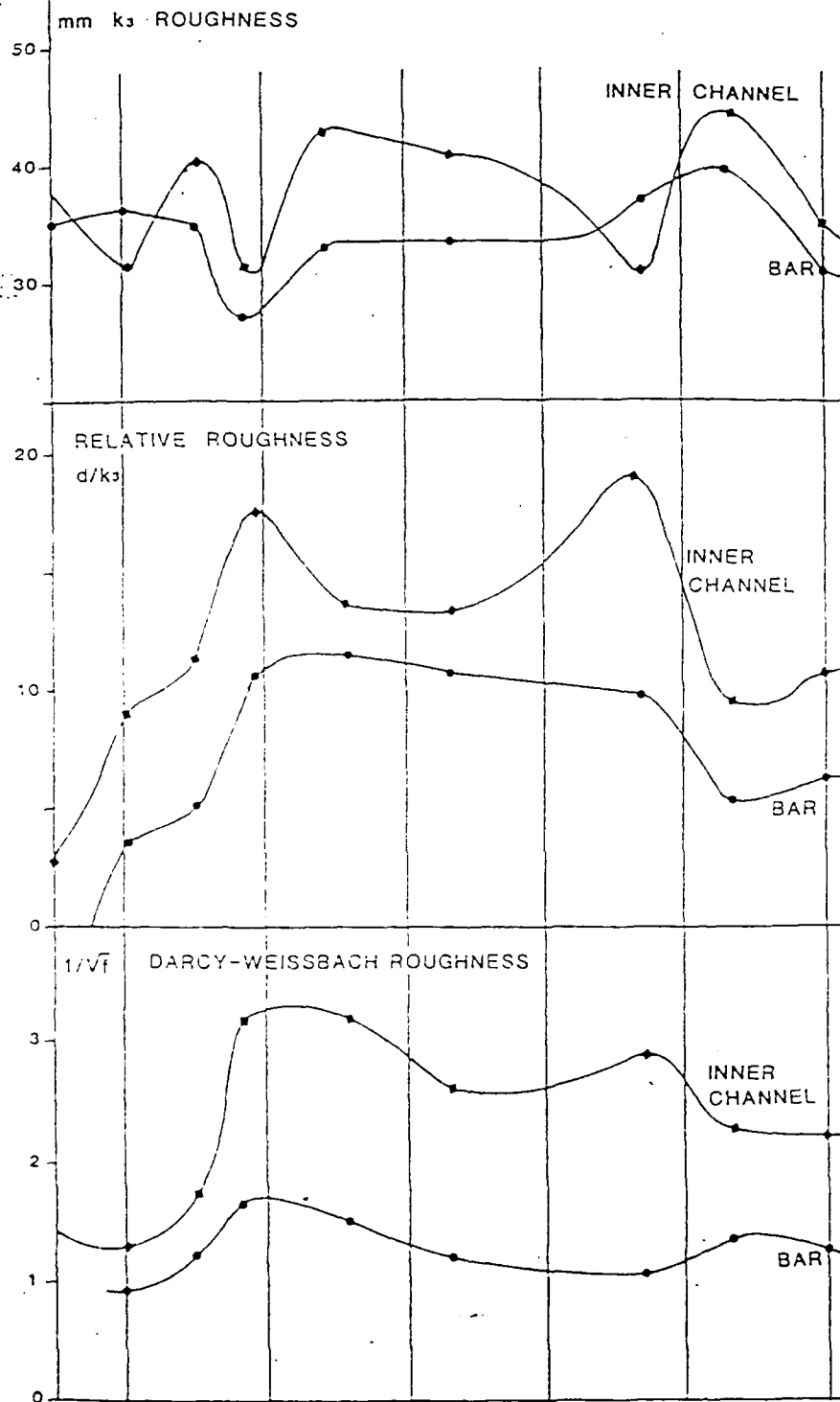


fig. 7: An example for the sweeping values of maximal differences across 3 decimeters

FLOOD AT LAINBACH 2./3.7.1989



3: Changes of roughness of inner channel and the bars during flood.  
a.:  $k_s$  roughness  
b.: Relative roughness  
c.: Darcy-Weissbach roughness

FLOOD AT LAINBACH 2/3.7.1989

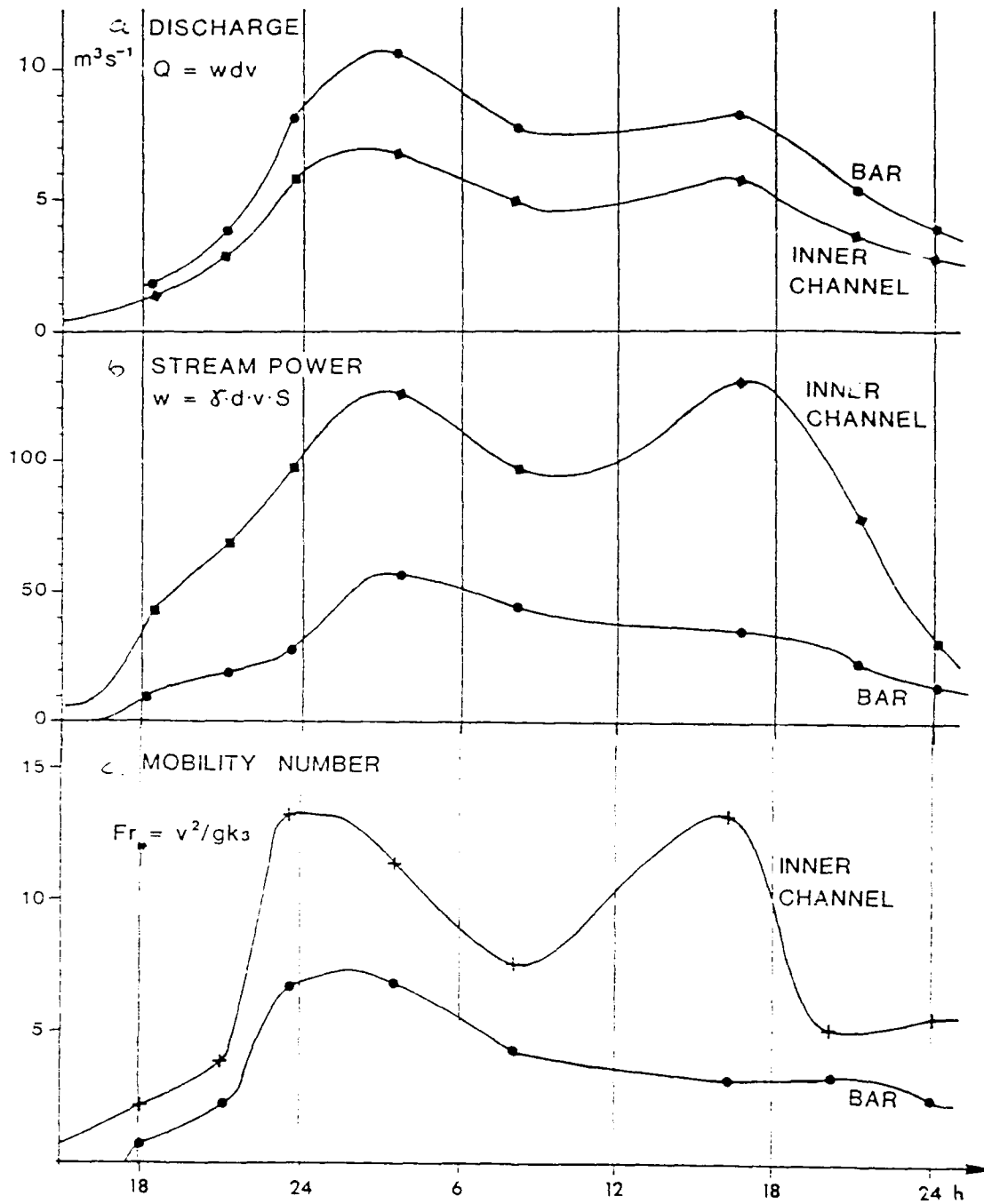


Fig. 9: Runoff dynamics during flood of 2/3.7.1989

- a.: Hydrograph
- b.: Stream power
- c.: Mobility number



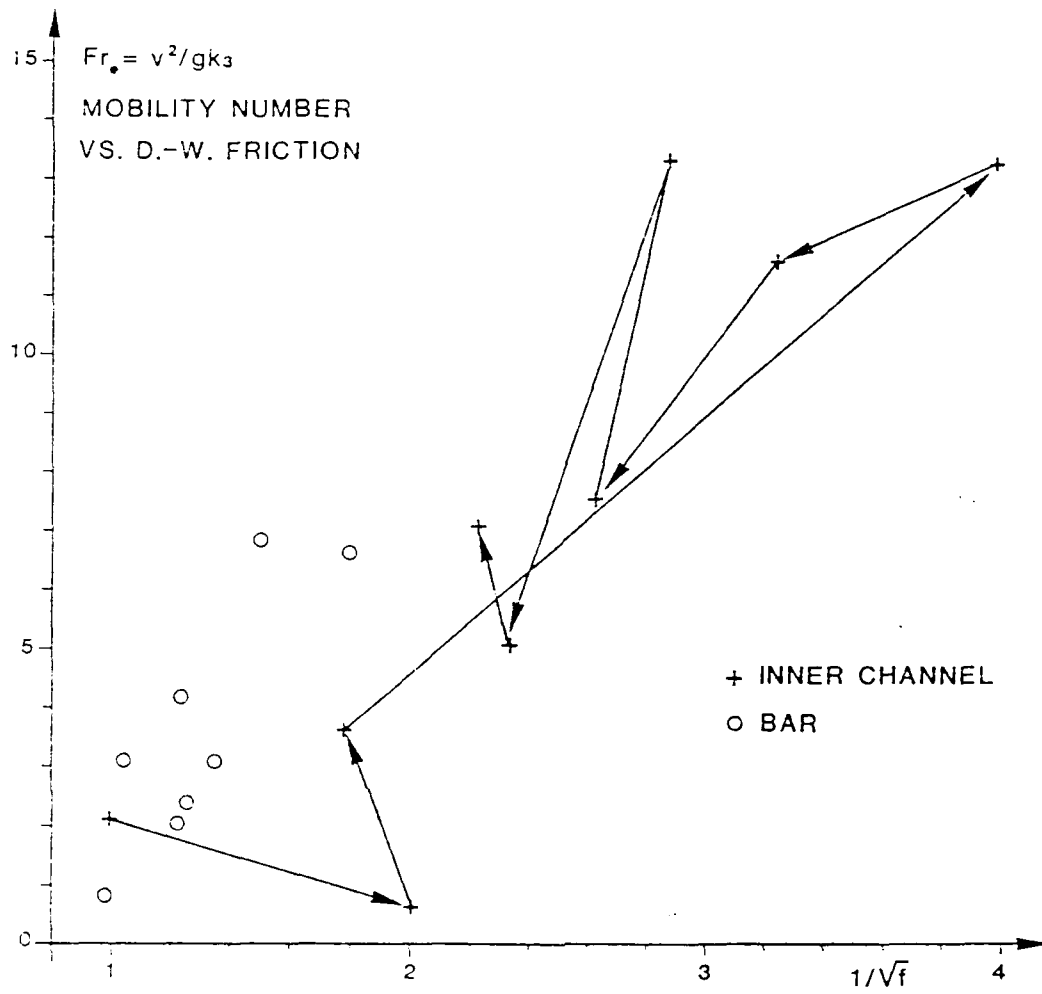


Fig. 10: Relationship between mobility number and Darcy-Weissbach friction

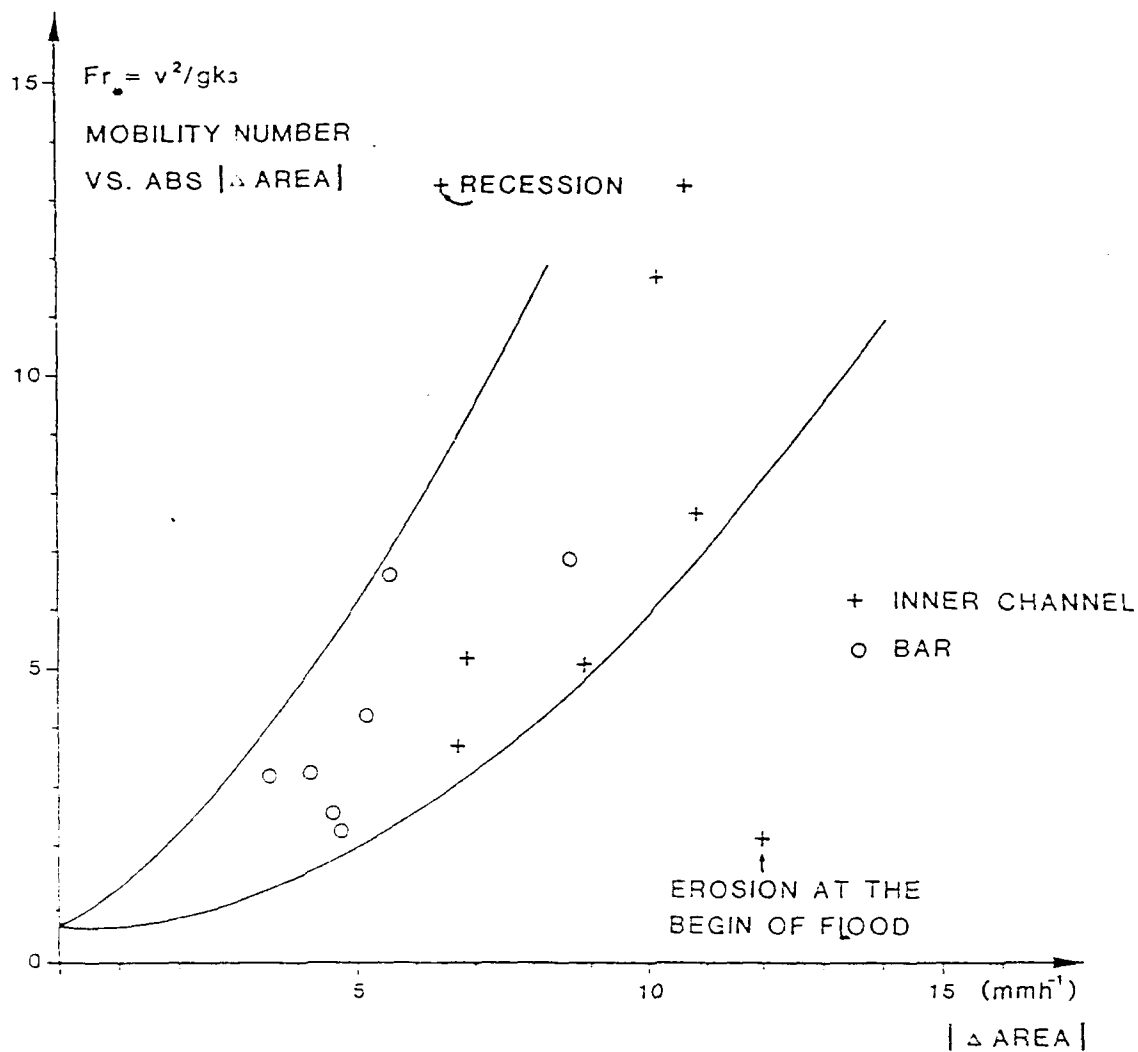


Fig. 11: Relationship between mobility number and the total number of river bed changes

C. FRIZ, G. GIADA, V. VILLI

Long term sediment budget in an alpine catchment

INTRODUCTION

Since 1983, hydrological and geomorphological observations of the Missiaga basin situated in the Belluna Dolomites, on the hydrographic left of the Cordevole River have been effected (Fig. 1).

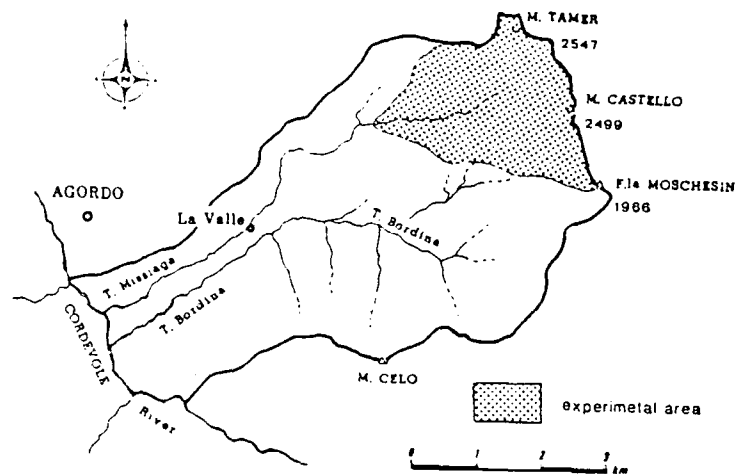


Fig. 1 Location of the study site



The results obtained up to now, above all for those regarding the transport of solid material, have been encouraging, in that it has been possible to define the relationships, even though only empirically, between the quantity of material transported ( $m^3$ ) and the significant hydrologic parameters, such as, for example the peak discharge and the quick flow volumes.

These results are, however, limited because of the short observation period which does not allow for making temporal extrapolations and the physiographic nature of the basin situated, as it is, in the mountainous dolomite region.

Nevertheless, being aware of the limits of their validity has meant that, at the same time as data was being acquired about the volume of material removed from the basin on each during hydrological events, research into the indirect quantitative evaluation of the erosion was also begun.

This problem is rather complex, given that all cases must be dealt with individually as function of the morphological evolution of the ridge and the possibility of being able to reproduce such modification graphically (PELLEGRINI, 1984).

From an operational point of view in fact, the indirect quantitative evaluation of the erosion is resolved by calculating the volume between the real topographical surface and an artificially constructed reference surface relating to a predetermined moment in the morphological evolution of the area being studied.

Therefore, placing the reference surface within a certain time period, is of primary importance, and that must, of necessity, lead to taking great care when making assessments of a geomorphological nature.

#### METODOLOGY

In the case of the Missiaga-Bordina basin it was held that an overall indirect estimate of erosion could not but begin from the immediate postglacial period. During that period in fact, after the widespread settling phenomena and the receding of the Cordevole glacier, the erosion processes began which have resulted in the present day morphological configuration of the basin.

This choice was also conditioned by the fact that it was

unnecessary to specify the nature or define the erosion processes which the basin had been submitted to, given that these occurred probably under constantly changing climatic and environmental condition.

Thus, after giving a general outline of time period within which the volume of material that was removed was estimated, it was decided to make use of C14 analysis of tree trunks in an upright position and still present on the banks of the Cordevole river, in order to obtain absolute chronological dating for greater precision. The remains of the tree trunks were found in a tract of the Cordevole river-bed where an alluvial fan formed by material originating from the enormous mass of detritus in the Missiaga-Bordina valley, barred the course of the Cordevole, giving rise to the Agordo Lake. On the basis of the above mentioned absolute dating, it can be said that such event occurred about 5900 B.C., therefore around the superior preboreal period (VENZO S., 1977).

An analysis of the bibliographic data together with the survey data has meant that a reasonably accurate reconstruction of the topographic nature of the Missiaga-Bordina basin has been possible for the end of the Wurmian period (Fig. 2)

Substantial modifications took place in the basin during the immediate postglacial period as a result of the grandiose phenomena which occurred as well as the large quantity of detritus transported and accumulating downstream.

However, it remains a fact that, during the late Wurmian period the depression was gradually filled by a large mass of detritus, the volume of which is difficult to quantify.

It was however, possible to determine the quantity of detritus which was removed from the accumulation and transported downstream to form the already mentioned alluvial fan. From the field survey, sufficient objective data were obtained to reconstruct, with a high degree of precision, the topography of the basin during the phase of maximum accumulation, such as to realise the chart reproduced in figure 3, which was taken as the original reference surface for the successive calculation of the volumes removed.

On the basis of the morphological elements described above, the quantification of the volume between this reconstructed topographic surface and the actual present day (Fig. 4) was carried out by means of the computerized system DIGCON. This system first realizes the discretization of the area under examination by superimposing a regularly sized grid, in which the altitude of each node is found by interpolation starting from the digitized level curves.

The grid consists of the intersection of all level curves

with two groups of profiles which are at right angles to each other in a N-S and E-W direction. The interdistance between the profiles obviously define the basic mesh size on the grid itself.

The altitude in each node, as already mentioned, is deter-

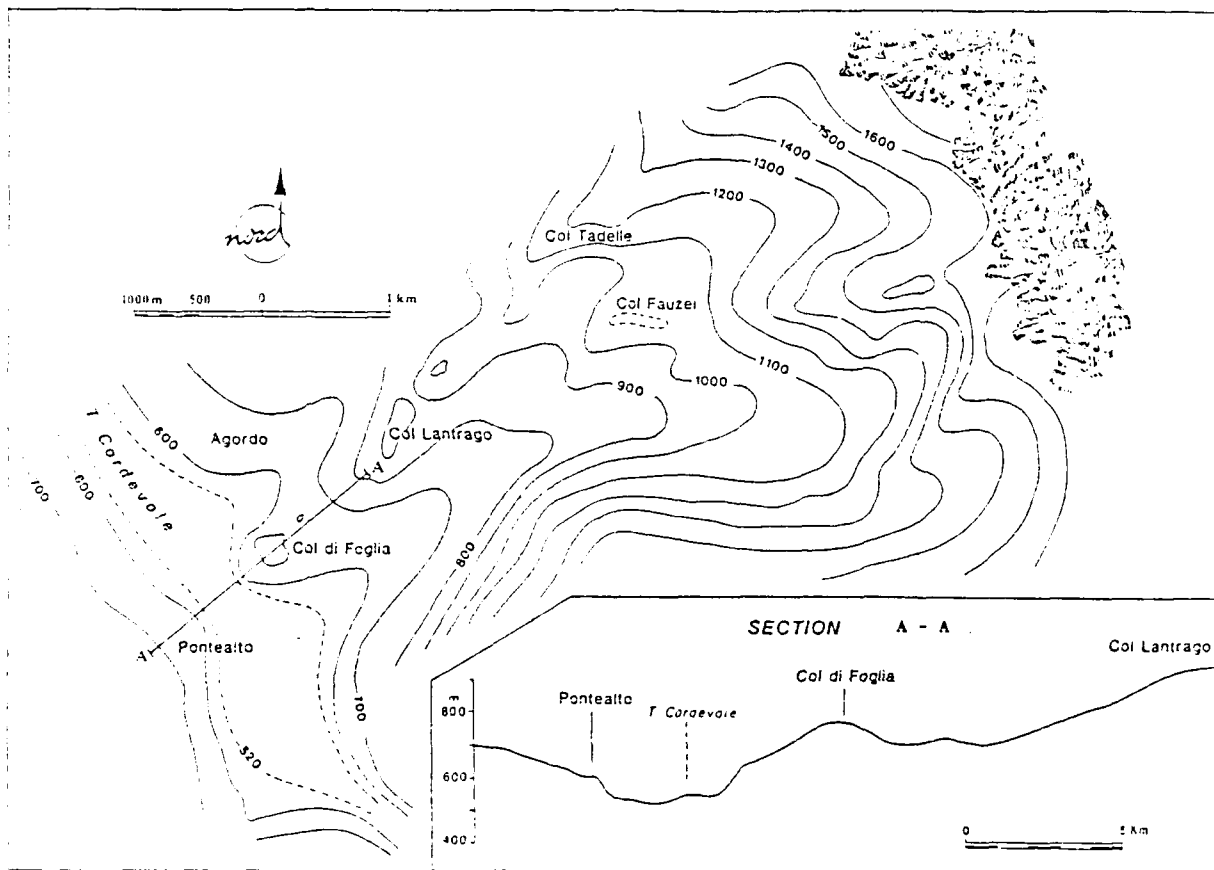


Fig. 2 The Missiaga-Bordina valley at the end of Wurmian period

mined by linear interpolation separately along the two right angled profiles that characterize it. Whenever the calculated

values do not coincided ( which can happen when in the two right angled direction, the slope and/or distances between the intersections are different) then the weighted average of the determining values are calculated, the inverse distance of the nearest intersections in the two right angled directions being used as a weighting factor.

The sizes of mesh, or rather the interdistances between the profiles, bearing in mind the peculiarity on the morphological element which must be show and the actual topographical situation was chosen as 100m.

Finally, by comparing the actual and postglacial digital model, it was possible to estimate, for every mash, the volume of the parallepipedon whic had as its base the mesh, and the arithmetic mean of the four different values of the altitudes at the nodes as its height.

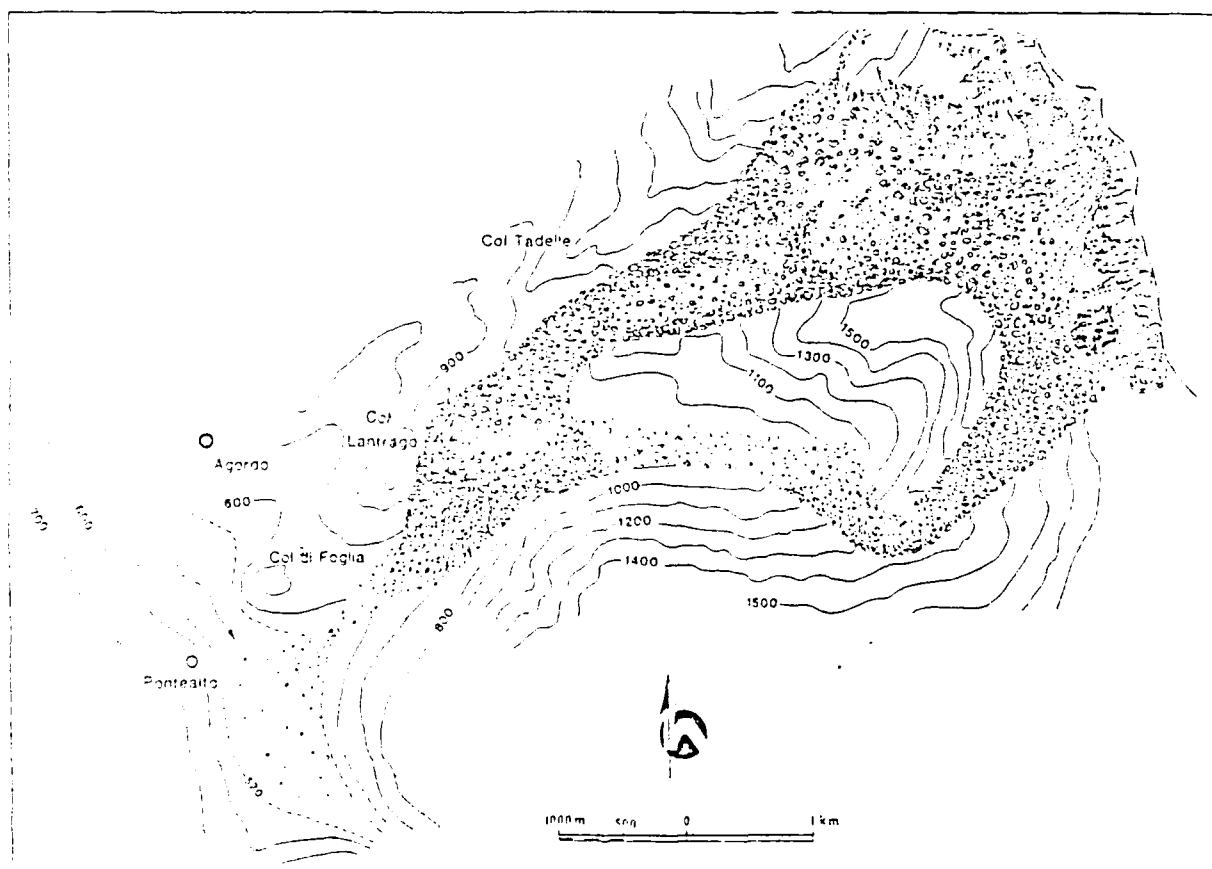


Fig. 3 The Missiagia-Bordina valley quite filled (about 8000 years ago)

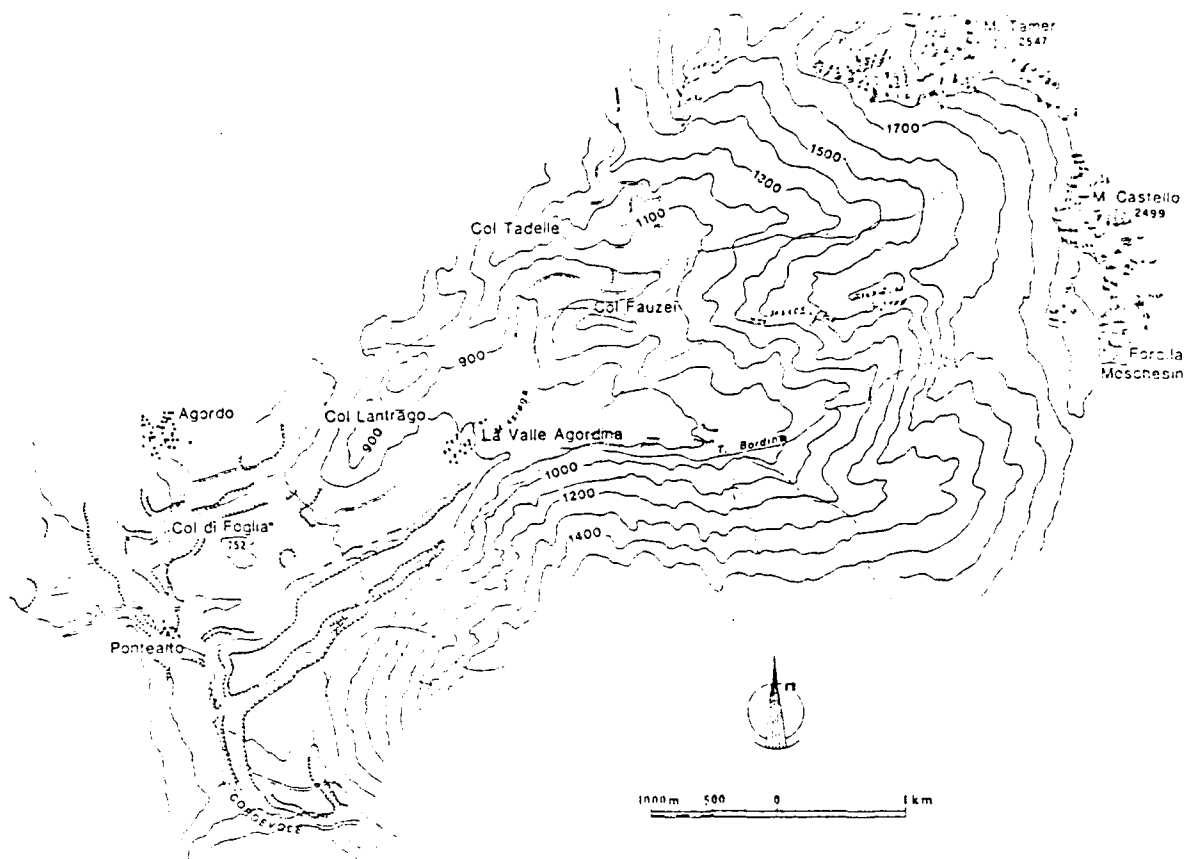


Fig. 4 Actual topography of the Missiaga-Bordina valley

## RESULTS

The algebreic sum of the single volumes then gave the overall results of 1.1 milliard m<sup>3</sup>

It should be kept in mind that:

- the Missiaga-Bordina basin that was filled up covers an area of 9.08 sq.km;
- on the basis of the chronological data furnished by the C14 analysis, the erosion of the detritus could have begun about 8000 years ago, which means that the average annual unitary loss is 15.143 m<sup>3</sup>/sq.km, a value which demonstrates unequivocally the force of the erosion processes in wearing away the detritus whic had accumulated in the Missiaga-Bordina valley.



It is not possible to compare this average value with the data relating to the transport of solid material during the accumulation of this in the upper part of the Missiaga basin, given that it can not be assumed that the condition which brought this about were homogeneous.

However that under present geomorphologic and climatic conditions, the transport of solid material into the basin under examination amounts to about 120 m<sup>3</sup>/sq.km/yr.

This is an unitary value that is congruent with many of data furnished by CATI (1981, see table) deduced from the filling up of natural and artificial alpine lakes (Fig. 5).

Basin	lake	Drainage basin	Filling in m <sup>3</sup> /km <sup>2</sup> /yr
1 Cordevole	Alleghe	246	171 (1933-1943)
2 Boite Piave	Vodo	353	118 (1958-1976)
3 Avisio (Adige)	Stramentizzo	740	130 (1951-1970)
4 Valsura (adige)	Alborello	190	149 (1953-1970)
5 Piave	Pieve Cad.	690	775 (1946-1974)
6 Cellina	Barcis	388	875 (1955-1972)
7 Canale	Mis	109	4000 (1963-1971)

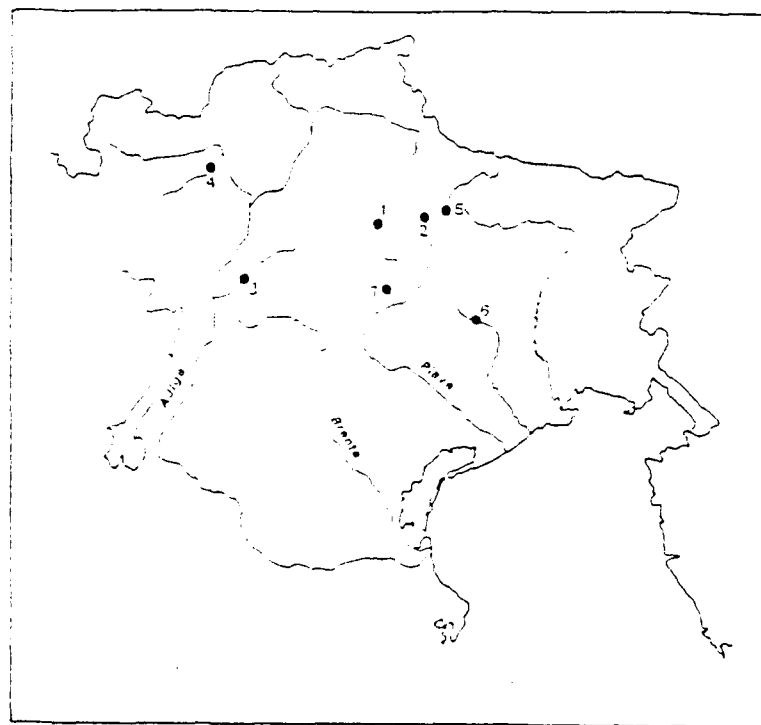


Fig. 5 Location of the mentioned lakes

With respect to the others, the average value of the transport of solid material seen in the Missiaga basin, is decidedly modest. While keeping in mind the temporal dissimilarity of the observation period, the figure relating to the Missiaga basin may seem surprising. However, the geomorphological situation of this basin, characterized by a narrow valley sole and sides covered by detritus is, from certain point of view, similar to the morphological situation of the Missiaga-Bordina basin in the past, thus lending it credibility.

#### REFERENCES

- ANSELMO, A., MARCHI, L., TECCA, P., VILLI, V. (1989). 'Sediment transport in a small watershed of Dolomite Mountains. Associazione It. di Idronomia. Quaderni di Idr. 9, 69-81.
- CATI, L. (1981). 'Idrografia e idrologia del Po', Ministero LL.PP., Servizio Idrogr. Pubbl. 19.
- FRIZ, C. and VILLI, V. (1990). 'Aspetti morfogenetici della conca di Agordo con particolare riferimento all'evoluzione quaternaria del bacino Missiaga-Bordina (Belluno, Italia). Mem. Sc. Geol. Univ. Padova. In press.
- PELLEGRINI, G.B. (1984). 'Valutazione quantitativa dell'erosione di un bacino idrografico mediante l'analisi tridimensionale del rilievo. Geogr. Fis. e Din. Quater., 6(1), 61-72.
- VENZO S. (1977). 'I depositi quaternari e del Neogene superiore nella bassa pianura del Piave da Quero al Montello e del Paleopiave nella valle di Soligo. Mem. Ist. Min. e Geol. Univ. di Padova., 30, 1-64.

C. FRIZ, L. GIADA, V. VILLI

LA VALUTAZIONE QUANTITATIVA DELL'EROSIONE IN UN BACINO  
IDROGRAFICO: ASPETTI METODOLOGICI E OPERATIVI

PREMESSA

Dal 1983 sono in corso osservazioni idrologiche e geomorfologiche nel bacino attrezzato del rio Missiaga situato nello dolomiti bellunesi, in sinistra idrografica del Cordevole (fig. ).

I risultati finora conseguiti, soprattutto per quel che riguarda il trasporto solido, sono stati incoraggianti, essendosi potuto definire delle relazioni, sia pur empiriche tra quantita' del materiale trasportato (in  $m^3$  e parametri idrologici significativi come ad esempio le portate al colmo di piena ed i volumi del quick flow.

Il limite pero' di questi risultati e' costituito dalla brevità del periodo di osservazione che non consente estrapolazioni temporali e dalla tipicità fisiografica del bacino propria dell'area montuosa dolomitica.

La consapevolezza di tali limiti di validità tuttavia, ha fatto sì che di pari passo con la acquisizione di dati relativi ai volumi di materiale di volta in volta asportato dal bacino da singoli eventi di piena si iniziasse una ricerca avente per obiettivo la valutazione quantitativa indiretta

dell'erosione.

Tale argomento presenta una certa complessita' dovendo essere trattato caso per caso in funzione della evoluzione morfologica subita dal rilievo e della possibilita' di poterla tradurre graficamente (PELLEGRINI, 1984).

Dal punto di vista operativo infatti la valutazione quantitativa indiretta dell'erosione si risolve calcolo del volume compreso tra la superficie topografica attuale ed una superficie di riferimento ricostruita relativa ad un momento prefissato dell'evoluzione morfologica dell'area in studio.

La collocazione temporale dunque della superficie di riferimento rappresenta un elemento di primaria importanza che deve necessariamente scaturire da attente considerazioni di carattere geomorfologico.

#### VALUTAZIONE QUANTITATIVA INDIRETTA DELL'EROSIONE NEL BACINO MISSIAGA-BORDINA

Nel caso del bacino Missiaga-Bordina si e' ritenuto che la stima indiretta globale dell'erosione non potesse decorrere che dal tardoglaciale.

In quel periodo infatti dopo i diffusi fenomeni di collasso seguiti al ritiro del ghiacciaio del Cerdavole, sono iniziati i processi erosivi che hanno portato all'attuale configurazione morfologica del bacino. Inoltre, dal punto di vista operativo tale scelta consente di poter prescindere dal dover specificare la natura e definire l'intensita' dei processi erosivi che hanno operato nel bacino, essendosi

verificati in condizioni climatiche ed ambientali verosimilmente mutevoli.

Per definire nel modo piu' rigoroso l'intervallo di tempo entro il quale realizzare il bilancio globale dell' erosione, del bacino Missiaga-Bordina, ci si e' avvalsi tuttavia anche delle datazioni cronologiche assolute fornite da analisi  $C^{14}$  su resti di tronchi d'albero in posizione di crescita ancora presenti nel greto del torrente Cordevole. Questi resti affiorano infatti in un tratto d'alveo dove, una conoide costituita da materiali provenienti dall'enorme ammasso detritico stabilitosi nella valle Missiaga-Bordina, ha sbarrato il corso del Cordevole, dando origine al lago di Agordo.

Tali avvenimenti sulla base delle citate datazioni assolute si sarebbero verificati 5900 anni a.C., quindi all'incirca nel preboreale superiore e prima dello stadio di Daun (VENZO S. 1977).

#### La valle Missiaga Bordina nel Postglaciale

L'analisi congiunta dei dati bibliografici e di campagna ha permesso di ricostruire con buon grado di verosimiglianza i caratteri topografici del bacino del Missiaga-Bordina al termine del wurmiano.

Le modificazioni morfologiche nel bacino nell'immediato postglaciale sono state sostanziali in seguito ai grandiosi fenomeni verificatisi e all'ingente trasporto ed accumulo dei detriti cosi' originatisi verso valle.

Sta di fatto che la depressione valliva tardowurmiana e'

stata via via invasa da una massa abnorme di materiali detritici il cui volume risulta difficilmente quantificabile.

Cio' che invece e' stato possibile determinare e' la quantita' di detrito rimosso dall'accumulo e trasportata verso valle. Sempre dai rilevamenti di campagna sono emersi dati oggettivi per ricostruire con sufficiente precisione la topografia del bacino in fase di massimo accumulo, cosi' da consentire la realizzazione della planimetria di fig. che e' stata cosi' assunta come superficie di riferimento originaria per il successivo calcolo dei volumi asportati.

#### Calcolo del volume eroso

La quantificazione del volume compreso tra questa superficie topografica l'attuale (fig. ) e' stato effettuato con una procedura informatica denominata DIGCON. Tale procedura realizza anzitutto una discretizzazione della zona esaminata. Tutto cio' con la sovrapposizione ad essa di una griglia a maglie regolari, nella quale la quota di ogni nodo e' ricavata mediante un procedimento di interpolazione a partire dalle curve di livello digitate.

Piu' in particolare detta griglia e' costituita dall'intersezione dell'insieme delle curve di livello con due famiglie di profili ortogonali. Le distanze tra i profili e le interdistanze tra i profili definiscono ovviamente le dimensioni della maglia elementare.

La quota in ogni nodo, come si e' gia' accennato viene

determinata per interpolazione lineare, e per cui si hanno i due profili ortogonali che la individuano. Qualora i valori calcolati non coincidano (puo' verificarsi quando nelle due direzioni ortogonali le pendenze e/o le distanze tra le intersezioni sono diverse) si calcola la media ponderata dei valori determinati, usando come peso l'inverso della distanza dalle intersezioni più vicine nelle due direzioni ortogonali.

Le dimensioni della maglia, ovvero l'interdistanza tra i profili, tenuto conto della particolarita' dell' elemento morfologico da rappresentare e' stata scelta di 100 m.

Il confronto tra i modelli digitali attuale e postglaciale infine ha consentito di stimare in corrispondenza ad ogni maglia il volume del parallelepipedo avente per base la maglia e per altezza la media aritmetica dei quattro valori di differenza di quota nodali.

La somma algebrica dei singoli volumi ha fornito infine il risultato complessivo risultato di 1,1 miliardi di m<sup>3</sup>.

Tenendo conto che:

- l'area del bacino Missiaga Bordini interessata dal riempimento e' di 9.08 km<sup>2</sup>
- che l'avvio della fase erosiva sul corpo del riempimento, sulla scorta dei dati forniti dalle analisi cronologiche C<sup>14</sup> puo' essere fatto risalire a circa 8000 anni fa, risulta una perdita unitaria media annua di 15,143 m<sup>3</sup>/km<sup>2</sup>, valore che evidenzia in modo inequivocabile l'energia con

cui i processi erosivi hanno smantellato l'accumulo detritico formatosi nella valle Missiaga-Bordina. Un confronto tra detto valore medio ed i dati inerenti il trasporto solido in corso di acquisizione nella parte superiore del bacino Missiaga non e' possibile, mancando il presupposto della omogeneita' delle condizioni che li hanno determinati.

Le valutazioni volumetriche effettuate dal 1984 indicano in ogni modo che nelle attuali condizioni geomorfologiche e climatiche il trasporto solido nel bacino in studio ammonta a circa  $120 \text{ m}^3/\text{km}^2/\text{anno}$ . Si tratta di un valore unitario che e' del tutto congruente con molti dei dati forniti da CATI (1981, vedi tabella) dedotti dall'interrimento di laghi naturali ed artificiali alpini.

Bacino	Nome del lago	Bacino $\text{km}^2$	Interrimento $\text{m}^3/\text{km}^2/\text{anno}$
Cordeyole	Alleghe	246	171
Boite(Piave)	Vodo di Cadore	353	118
Adige(Adige)	Stranentizzo	740	130
Valsura(Adige)	Alborelo	190	149
Piave	Pieve Cadore	690	775
Cellina	Barcis	388	875
Canale	Mis	109	4000

Rispetto ad altri invece il valore medio del trasporto solido riscontrato nel Rio Missiaga appare decisamente modesto. Pur tenendo conto della inomogeneita' temporale dei periodi di osservazione, del tutto sorprendente puo' apparire il dato relativo al bacino del Mis. La situazione geomorfologica di questo bacino tuttavia, caratterizzata da un fondovalle stretto e versanti ricoperti da detriti richiama,



per certi aspetti, situazioni morfologiche pregresse del  
bacino Missiaga-Bordina, rendendo così credibile il dato  
fornito.

# CAUSES AND NATURE OF RIVER PLANFORM CHANGE

**J.M. HOOKE**, Department of Geography, Portsmouth Polytechnic, U.K.  
**C.E. REDMOND**, National Rivers Authority, Thames Region, London

## Introduction

Research on changes in planform of gravel-bed rivers over the past 20 years has done much to elucidate their dynamic nature and characteristics. Even so, the assumption still seems to be prevalent that, given stability of conditions, meandering channels, after an initial development phase would show an equilibrium of form as measured by standard meander parameters. Various models have been produced (e.g. Brice 1974, Hooke and Harvey 1983, Keller 1972, Kondrat'yev 1968) showing evolutionary sequences in meander bends, even so, where trends in characteristics such as sinuosity are detected over long periods of time, the channel system is suggested to be in a transient state (Hickin 1983). Although conceptual frameworks (eg. Schumm 1979, Brunson and Thornes 1989) incorporate such transience and the existence of intrinsic thresholds seems to be accepted, there is still a tendency to search for triggers to phases of change. That the most active meanders may show evolution of characteristics is not taken as a basic premise.

This paper aims to examine the evidence for the extent of autogenesis in meander change by discussing the hypotheses on causes of meander changes and the expected responses from each, examining how the evidence helps to substantiate or eliminate any of these hypotheses and discussing whether it is indeed possible to distinguish one cause from another.

## Possible causes of change

Four major explanations of change can be identified and these can be divided into two major groups of causes which may be termed allogenic and autogenic (Lowin, 1977). Under the allogenic causes are human activities, particularly landuse and climate. Under autogenic are intrinsic thresholds and chaos theory. On the basis of theoretical models, hardware models and experiments, and from field studies, the expected responses can be identified though, of course, these are rarely very specific because of the problems of indeterminacy and number of variables in the system, as highlighted by Hey (1978). Schumm (1969) long ago identified the likely direction of change of major channel variables in response to changes in discharge or sediment load.

### **Anthropogenic changes:**

A wide range of human activities can affect stream channels, both directly and indirectly, and can alter either the discharge regime or the sediment load or a combination. Even the alteration of discharge may be complex and several flow parameters may be needed to characterise the change in magnitude, frequency and occurrence of flows. The combination of water and sediment alterations may be even more complex and may be

difficult to predict yet the relative balance and timing of discharge and sediment alterations will have a crucial effect on the channel response. Nevertheless, general tendencies in behaviour can be recognised. For any specific alteration, it is expected that the main impacts occur downstream though some effects can then work back upstream eg. a steepening or lowering of the channel in the form of a headcut. This can lead to a complex response over time for any specific location. The impact will vary with the spatial distribution and extent of the human activity eg. a landuse alteration may be widespread and relatively synchronous or it may be more patchy. Urbanisation will tend to be localised.

#### **Climatic change:**

Similarly, the effects of precipitation and temperature can lead to complex combined effects on runoff regime, especially through the intermediary of vegetation. The effects on the channel would be expected to be widespread in the catchment unless different parts of a large catchment have rather different climatic regimes.

Both of these types of allogenic alteration lead to modifications in the basic force element of the system ie. the discharge. In terms of response, the resistance factor of the varying channel characteristics along the length of the stream must then be taken into account. Obviously, change in planform will only take place if the banks are erodible and less resistant than the bed. It can be hypothesised that, given a change such as urbanisation in a catchment and assuming that it has altered the discharge regime downstream, the channel should adjust. The different types and scales of adjustment may then provide an indication of the sensitivity of various channel sections to such alterations. A declining effect on runoff regime with distance from the urbanised area and as its proportion of the catchment alters may be expected and thus a similar response in terms of channel change. Departures from this, eg. where individual reaches show markedly different responses, may then be attributed to local site factors placing constraints on the types of adjustment possible. Basically, the response from climatic change would be expected to be much more widespread and more synchronous than that to landuse and land practice alterations (cf Cooke and Reeves, 1976).

Temporal coincidence of activities is no proof of a cause and effect link since there may be a lag in response, the change may bring the system nearer the threshold for response but further slight alteration may push it over. However, if an alteration such as landuse or climate was the basic cause of change then some associated phasing of the channel response may be expected. Differences in temporal pattern might also be expected with much greater synchronicity in the case of climatic causes. However, the rate of propagation of effects and the problems of complex response need to be considered.

#### **Intrinsic thresholds:**

If channel changes are in response to intrinsic thresholds in the channel system then some association of zones and types of change with the spatial distribution of physical characteristics should be identifiable. The situation is complicated, however, by changes in those physical characteristics over the longer-term either because of the channel shifting and thus, for example, encountering different materials, or as a result of the channel behaviour itself eg. deposition altering slope in the longterm. Again the

situation is complicated because of the number of variables which may alter but certain key ones have been identified from experiments and case studies. The crossing of these thresholds can themselves lead to spatial propagation of the effects and complex response. However, given good enough historical information and rapid enough changes it should be possible to identify the spatial and temporal patterns of change and elucidate the dynamics.

#### **Chaos theory:**

This suggests that the behaviour of systems is markedly non-linear and very sensitive to initial conditions. It is therefore difficult to relate the behaviour of a system to physical determinants but if the behaviour over time is analysed then certain patterns and consistency of behaviour become apparent.

#### **Evidence**

Historical data at a number of different dates over a reasonably long historical period for a number of river channels may allow us to elucidate some of these patterns. The spatial distribution of changes needs to be examined at a number of different scales and the temporal sequence for each reach needs to be analysed. A number of methods have been used to provide suitable evidence.

1. To identify the distribution of channel changes over wide areas and to investigate whether there is any kind of regional or general spatial pattern, the courses of channels of rivers have been compared at two dates, c.1870 and c.1970. This has been done for a sample of streams in lowland England and for most streams draining from upland England. Changes already identified in the literature have also been collated. Only those changes greater than one channel width and therefore well above any possible map inaccuracy and only those which are not directly due to channelisation of the stream have been included.
2. The changes along particular streams and in particular reaches, especially the most active reaches have been compiled in greater detail, first by comparison of O.S. maps at two dates at 1/10560 then by compilation of maps at 1/2500 for several dates.
3. To test the relationship between changes and possible physical determinants, physical characteristics have been measured through stable and unstable reaches on certain rivers. From previous work it is hypothesised that the changes are not related in a simple manner to conventional factors and therefore complex combinations and patterns of variation have been examined.
4. It is recognised that physical determinants at the reach scale such as bank materials may not be the only determinants and that precise quantification of all characteristics may not be possible or suitable so a classification of various catchment, reach and site characteristics has also been carried out. The aim of this work is to identify constraints on channel change as much as causes of instability.

5. The fifth type of procedure is to produce time plots and phase diagrams of the channel behaviour to examine whether patterns are present which are not otherwise apparent and which it may not be possible to tie in specifically to physical determinants.

### Distribution of changes

#### **National scale:**

Figure 1 is a map of the planform changes found from map comparisons, as described above. This shows some interesting distributions. First, it can be seen that almost all the changes are in zones fringing the uplands. In the reconnaissance survey it was soon found that most channels in the lowlands were stable or had been channelised. Some may have changed slightly but shifts of channel location were below the channel width threshold for significant change. This is not to say there are no significant changes at all in the lowlands.

The reaches which have shown marked change over the past 100 years are mostly in the so-called 'piedmont' zone (Newson, 1982). The channels in these reaches have certain characteristics: they are downstream of the bedrock reaches of the uplands and are flowing in valleys with a floodplain formed from alluvium; the material tends to be highly erodible because it is still relatively coarse, with a high gravel and sand component, compared with greater clay content farther downstream; the gradients are sufficiently steep for stream power to be high but the streams are large enough to have developed a regularity of form as portrayed by meanders and pools and riffles.

However, active lateral movement does not occur on all streams in the piedmont zone and the distributions should be examined in relation to the hypothesised causes of change. If the changes were due to climatic change alone then changes might be expected everywhere or at least widespread in a region. The fact that the changes are much more localised but tending to be in a certain zone implies that there are constraints on change and that thresholds are operating.

If the changes are a response to human activities then one would expect a close relationship in spatial pattern. Very many of the basins have been affected in some way by landuse change, urbanisation, reservoirs or water abstraction. Analysis of the type of change might then show if the response was indeed in the direction expected from such changes and this will be examined below. The situation is complicated with multiple human modifications in many basins. Examination of the timing of changes may help to see if there is any association. Turning the argument round though, many case studies have shown the types of changes to be expected from specific basin and channel alterations. Perhaps we should rather ask why have certain channels not changed in planform when they have been affected by major human activities such as urbanisation? Again this points to the operation of strong thresholds and may allow us to identify reaches vulnerable to planform adjustment and other reaches which will adjust by other variables. This has important implications for channel management and impact prediction.

### **Basin scale:**

Various patterns of distribution of planform alteration can be seen along the channels and these relate to degree of activity (rate of change) and type of change. On some rivers there are long reaches that are stable then long reaches which are markedly unstable (Fig. 2). One of the striking aspects is that there is little transition between the two, with completely stable reaches adjacent to very unstable reaches. Again this points to the operation of thresholds but that once the thresholds are crossed channel pattern then alters very rapidly.

The second type of distribution is where reaches, including the whole path round bends, are affected but there is a series of short unstable reaches separated by stable ones. This implies some specific site controls and measurement of characteristics down though such sections should allow those controls to be identified. The system must be near the threshold for instability. The River Culm in Devon exhibits such a distribution (Hooke, 1977).

The third type of distribution is where whole reaches are not changing but rather erosion is confined to meander apices and change overall is very limited. Rates of erosion in such reaches are usually low. Such sites may allow the identification of critical force-resistance relations in specific terms.

### **Types of change**

An important aspect of the distribution of changes is the differentiation of types of change. It has already been indicated that certain theoretical frameworks predict distinctive planform responses depending on the direction of alteration of runoff and sediment load. A major indicator of channel response and one which is easy to measure without encountering the difficulties of meander definition is sinuosity. Increase in peak discharge is expected to decrease sinuosity because of a tendency to increase meander wavelength and therefore straighten the channel. Decrease in discharge would have the converse effect.

If change is in response to a climatic modification then it might be expected that whole rivers and even whole regions would show the same general tendency or direction of type of change. Of course the effects of a climatic change do depend on the runoff response which varies with the lithological, soil, topographic and landuse characteristics of the area but the change should not be in different directions within a region. If a whole catchment is tending to show a particular type of change but this differs from that of neighbouring catchments then this would imply that the impetus to change is confined to that catchment. This points to landuse change as being a significant factor.

Where different reaches of the same channel are behaving in contrasting manner then other explanations need to be found. It is possible that the different reaches are in fact related to some different landuse changes along the channel eg. afforestation in the uplands, then urbanisation farther down, but many examples are found where reaches close to each other in the same type of catchment are exhibiting different types of change. This implies that the changes may be part of the same phenomenon, simply at

different stages or that the period of evidence simply captures a particular phase of activity but that trends would be different if a longer period and more evidence was available.

58 rivers in England have been classified according to whether they show a net increase, net decrease or no change in sinuosity over the past 100 years. Of the 58 rivers, 22 shown an increase, 23 a decrease and 13 no change in sinuosity. Little regional differentiation is present except a rather greater proportion increasing or not changing in sinuosity in the NE and E Pennines and more decreasing in sinuosity in the Welsh Borderlands.

To understand the changes in more detail the types of change need to be classified. Changes on individual bends have also been classified according to the typology in Figure 3. Analysis of historical sequences from large-scale maps and aerial photographs on several rivers, but particularly the Dane (Hooke and Harvey 1983) has revealed a common sequence of meander development and this is presented as a graphical model in Figure 4 (Hooke 1989).

Examples of the different types of distribution can be found. For instance, taking five active meandering rivers in SE Devon and classifying the type of movement on bends, it is found that some whole rivers are behaving differently from others. The Creedy is predominantly migrating; the Otter, Axe and Yarty are growing and the Culm is mixed in type. In NW England an example of apparently contrasting behaviour can be found by comparing the neighbouring rivers of the Bollin and the Dane. According to Mosley (1975) a reach of the river Bollin downstream of Wilmslow has shown a marked decrease in sinuosity since about 1935 with numerous cutoffs. A 14km reach of the River Dane has in the past 150 years shown an increase in channel length of 10% with growth being an important component of change on individual bends.

### Temporal distribution

If the historical evidence shows that change began at a particular time then this implies that sometime earlier (how much depending on the lags in the system) there had either been an alteration of the inputs to the channel system or that an intrinsic threshold had been crossed. The latter idea may be particularly difficult to test since there are problems in reconstructing conditions, eg. local channel slope or bank materials, at that time. Even the former hypothesis poses problems of investigation since it is notoriously difficult, though not impossible, to reproduce land-use patterns on a catchment basis, let alone land-use practices. There are cases where channel change seems to have begun at a particular period eg. on the Bollin (Mosley, 1975), Skirden Beck, Lancashire (Thompson, 1984). In the case of the Bollin, Mosley investigated a number of possible causes including rainfall change and concluded the changes were probably due to urbanisation and possibly agricultural drainage due to the spatial and temporal coincidence of patterns. Further evidence on changes elsewhere on the Bollin and alternative explanations of the changes will be put forward later.

What is remarkable when many of the channel changes in Britain are examined, particularly those in the least modified catchments is that channel development seems to have been taking place from the date of the earliest evidence. In some cases this is 1840 and several channels in different parts of the country show evidence of a much lower sinuosity channel at that time. That this is not an artefact of the maps or due to channel straightening is confirmed by field evidence of the courses. This general trend of increasing planform development is substantiated by the evidence of the floodplains and terraces. In several of these valleys the floodplain is of restricted width and does not occupy the whole valley floor. It is bordered by alluvial terraces but these are highly erodible. Almost all the floodplain can be dated to channel movement within the period of map evidence and the field evidence strongly supports the idea that these are first generation floodplains. The floodplains are bounded by distinct and fresh looking terraces. In the case of the Dane the base of the depositional sequence has been dated to 4500-1200BP (Hooke et al 1990) but this is succeeded by a major aggradational phase forming the upper part of the terrace deposit. The origins of this are still unclear and there is some evidence which points towards medieval forest clearance and increase in agriculture as being the major cause. However, the increasing evidence that several valleys may be showing the same sequences and the increasing number of dates showing a high degree of coincidence (Richards, 1987, Macklin, 1989) may point towards a greater influence of climate change than has hitherto been invoked in Britain. Further work on the sequences in different parts of Britain is vitally needed and the work such as that of Macklin (pers. comm.) on the Little Ice Age is of crucial importance.

#### Environmental and physical characteristics

The aim of this part of the research has been to investigate whether planform changes and subdivision of type seem to be associated with particular conditions at the basin, valley and reach scale. If it is not possible to find common factors it may at least be possible to identify constraints, factors that prevent planform change (eg. bedrock gorges).

The problem with much analysis of physical controls on channel behaviour is that it often ignores the environmental factors because of their scale and also ignores many potentially important influences because they are so difficult to quantify. A classificatory approach has therefore been taken and the analysis is based on presence or absence of particular features and their combinations. Forms were devised, based on the work of Kellerhals et al (1976) and the categories included are listed in Table 1a. For each category or characteristic a choice of codes was available eg. terraces (Table 1b). Where there may be a mixture of characteristics up to three choices were allowed given in order of proportion eg. valley vegetation (Table 1c). These forms were completed in the field for 30 different reaches of actively shifting channel on 11 rivers. Of course, this only gives an indication of present conditions.

Techniques for analysis of this type of data are still fairly limited but certain associations became apparent. Channels have been classified into stable, slightly unstable, moderately unstable and highly unstable with respectively 8, 7, 4 and 11 in those classes. A strong association appears between degree of instability and type of pattern. Stable



channels tend to be slightly sinuous or irregular in pattern whereas all highly unstable channels are regular meanders or tortuous. No stable but well developed meanders were found and likewise the less developed patterns did not seem to be altering rapidly. This is not as obvious as it might seem and it raises the question of how low sinuosity and irregular patterns make the transition to unstable tortuous patterns. Another association which emerged clearly and is not as obvious as it might seem is that there is a strong positive relationship between degree of lateral instability and number and continuity of terraces. If lateral erosion is so rapid then it might be expected that terraces are not acting as a constraint on lateral development. What it does imply is that these reaches

already shown that the most complete sections of terraces are likely to be in these piedmont zones due to burial and height range downstream. However, the association between recent channel change and the longer-term development merits further work. The classification also shows that stable reaches occur not just where valleys are restricted but in wide valleys as well. Highly unstable reaches are mostly in wide valleys but they also have a number of constrictions. Changes are strongly associated with the most erodible bank materials as might be expected but again the classes are not exclusive. Composite banks of silt overlying either gravel or cobbles is very common on the highly unstable reaches but do not occur on any of the stable channels. Again, as would be expected, stable channels have good or very strong bank vegetation but highly unstable channels have no banks in these categories of cover. However, vegetation can be a response rather than a cause.

#### **Reach scale:**

Preliminary analysis of the distribution of channel changes had indicated that there was not a simple relationship to controls conventionally advocated, eg. slope, bank materials. The aim was to investigate whether more complex and subtle combinations of conditions were acting as thresholds to change. Various physical characteristics have been measured in the field down through stable and actively changing sections. Conventional physics demands that erosion is dependent on force on the bank at a point exceeding a threshold value which is dependent on the material of the bank. The tendency in the past has been to look at absolute force of resistance eg. power or % silt-clay. However, the force-resistance threshold may be crossed by combinations of factors varying spatially in a very complex way.

Measurements have been made on sections of the Rivers Teme, Arrow and Lugg in the Welsh Borderlands but clear patterns have not yet emerged. One of the reasons for lack of association in characteristics is that the change is a phenomenon acting over time whereas these factors are measured spatially at one point in time. It can therefore be suggested in the model that threshold conditions for change may have been reached at some location within the reach sometime in the past but the changes have since been propagated both upstream and downstream. Constraints then act at a lower level to prevent change and restrict the active reaches spatially. However, the abruptness of the changing reaches and their patterns of distribution imply that channels are very sensitive to alterations in conditions.

### Alternative explanation

One of the remarkable aspects emerging from the work on sequences of change in meanders is in fact the consistency of change in different environments and the high degree of systematic change in situations where materials, flow patterns, etc. are varying. However, it has been shown that it is remarkably difficult to relate the channel behaviour to physical determinants.

Much of the historical evidence shows that once certain thresholds, which remain difficult to identify, are crossed the channel instability then takes off. The channel becomes increasingly unstable and there seems to be a positive feedback effect. This can be seen both at the reach scale and the individual bend scale. The model of meander development described earlier shows a take-off point when rapid growth suddenly occurs. This appears to have some relationship to form (Hooke and Harvey 1983), as depicted by path length and curvature.

Analysis of the evidence of time sequences of meander changes shows that apparently different types of behaviour may be part of an autogenic sequence. This is particularly well illustrated by a reach of the River Bollin (Fig. 5). At present in a reach of this active and freely meandering river, upstream of Wilmslow, cutoffs are occurring and if the changes over the past 10-20 years are measured then a net decrease in sinuosity is seen. However, if the longer-term sequence from 1840 is compiled then it is seen that there has been a gradual increase in sinuosity until recently. It is also seen that the rate of change has increased. Cutoffs have taken place in recent years as the bends have reached the stage of development such that they intersect. The greater the rate of erosion then the sooner this point is reached. The neighbouring catchment of the River Dane which had apparently contrasting behaviour over the period 1840-1980 is now showing a similar trend with cutoffs occurring. Once a cutoff occurs then this makes room for meander development to take place again and this will go on until another cutoff occurs. Therefore once this phase is reached sinuosity may show an oscillating pattern over time. This is supported by evidence from the Welsh Borderland rivers. The River Teme is the most active channel and has an apparently chaotic sequence of changes but if sinuosity over time is tabulated then an oscillatory tendency is seen. That the crucial threshold may be related to sinuosity is seen by the association between activity and sinuosity (Table 2). This also emerged from the coding classification discussed earlier on a wider range of channels where there was a close association between degree of instability and type of channel pattern. It also emerged from that analysis that all the highly unstable reaches in that sample showed a net change in sinuosity and that, although increases in sinuosity appeared in all classes of instability, decreases in sinuosity are mostly in the highly unstable class. This indicates the trend for cutoffs, high instability and tortuous patterns to be the end of a sequence.

Work by Hooke (1987) was an intuitive attempt to analyse morphology relations, and time paths in phase space though not placed explicitly within the chaos and dynamical theory framework. Indeed the data there could be reinterpreted as supporting chaos theory in that similar trajectories are seen but they differ according to the starting point and physical conditions in the bend. In Figure 6 there is a suggestion of an attractor.

The accelerating activity of the channel as sinuosity increases may provide an explanation for the increasing rate of erosion found on Devon rivers (Hooke, 1977, Hooke and Kain, 1982). Although a wide variety of possible causes was investigated none seemed to provide an adequate explanation. It now appears that it may simply be part of the inherent trend of meanders.

Although it is hard to move away from the physical determinacy inculcated in us by conventional physics, explanations based much more on the recognition of non-linear behaviour, positive feedback and of systematic behaviour in apparently different circumstances may offer an explanation of some channel changes. It is already well established that the relationship between rate of erosion and channel curvature is markedly non-linear (Nanson & Hickin, 1983, Hooke, 1987). Ultimately we should still be able to relate these changes to what is happening in terms of force and resistance at any point in the bend but this may be so difficult to measure and model over the 3-d form of a bend let alone a series of bends that the ideas of chaos theory provide a viable alternative approach.

That this type of explanation may be adequate in itself is supported by some computer simulations of meander development. For example, Ferguson's (1984) model is based simply on a non-linear relation between rate of erosion and curvature, with no process basis directly, and yet it replicates some of the changes seen in nature.

### Conclusions

The importance of an historical perspective and analysis of time paths in understanding and explaining river behaviour has been demonstrated. There is a need for analysis at different spatial scales and for both an environmental and process-based approach. Undoubtedly human activities have had an impact on river channels but the possibility of profound influence of climate within the historical period even in Britain should not be rejected. Superimposed on this is the strong evidence for autogenesis in meander development which leads to particular sequences of form and phases of activity even if other causes provide the impetus. Physical conditions provide at least some limits on planform development. The actual distribution of changes is a complex mosaic of these different patterns but the degree of autogenesis may be greater than is often recognised.

### BIBLIOGRAPHY

- Brice, J.C. (1974) Evolution of meander loops. Geological Society of American Bulletin 85, 581-86.
- Brunsdon, D. and Thornes, J. (1979) Landscape sensitivity and change, Trans IBG, 4, 463-484.
- Cooke, R.U. and Reeves, R.W. (1976) Arroyos and Environmental Change in the American South-West. Oxford, Oxford University Press.

- Ferguson, R.I. (1984) 'Kinematic model of meander migration', in Elliott, C.M., editor, River Meandering, ASCE, New York, 942-51.
- Hey, R.D. (1978) Determinate hydraulic geometry of river channels. American Society of Civil Engineers. Journal of Hydraulics Division, 104, 869-85.
- Hickin, E.J. (1978) Hydraulic factors controlling channel migration. In Davidson-Arnott, R. and Nickling, W., editors, Research in Fluvial Systems, Norwich: Geo Abstracts, 59-66.
- Hickin, E.J. (1983) River channel changes: retrospect and prospect. In Collinson, J.D. and Lewin, J., editors, Modern and Ancient Fluvial Systems, Oxford: Basil Blackwell, 61-83.
- Hooke, J.M. (1977) The distribution and nature of changes in river channel pattern. In Gregory, K.J. editor, River Channel Changes, Chichester: John Wiley, 265-80.
- Hooke, J.M. (1984) Changes in river meanders. Progress in Physical Geography, 8, 473-508.
- Hooke, J.M. (1987) Changes in meander morphology. In International Geomorphology, 1986, ed. V. Gardiner, Wiley, Chichester, pp.591-609.
- Hooke, J.M. (1989) The linkages between bank erosion and meander behaviour in gravel-bed rivers. Paper presented at American Geophysical Union conference, Baltimore. Abstract in EOS, 70(15), 329.
- Hooke, J.M. and Kain, R.J.P. (1982) Historical Change in the Physical Environment: A Guide to Sources and Techniques. Sevenoaks: Butterworths.
- Hooke, J.M. and Harvey, A.M. (1983) Meander changes in relation to bend morphology and secondary flows. In Collinson, J.D. and Lewin, J., editors, Modern and Ancient Fluvial Systems, Oxford: Basil Blackwell, 121-32.
- Hooke, J.M. and Redmond, C.E. (1989) River channel changes in England and Wales. J. Inst. of Water and Environmental Management, 3, 328-335.
- Hooke, J.M., Harvey, A.M., Miller, S.Y. and Redmond, C.E. (1990) The chronology and stratigraphy of the alluvial terraces of the River Dane valley, Cheshire, N.W. England, Earth Surface Processes and Landforms, Vol. 15.
- Keller, E.A. (1972) Development of alluvial stream channels: a five-stage model. Geological Society of America Bulletin 83, 1531-40.
- Kellerhals, R.M., Church, M. and Bray, O.L. (1976) Classification and analysis of river processes. J. Hydr. Div., ASCE, 102, 813-829.
- Kondrat'yev, N.Ye. (1968) Hydromorphic principles of computations of free meandering and sign and indexes of free meandering. Soviet Hydrology 4, 309-35.

- Lewin, J. (1972) Late-stage meander growth. Nature - Physical Science 240, 116.
- Lewin, J. (1977) Channel pattern changes. In Gregory, K.J., editor, River Channel Changes, Chichester: John Wiley, 167-84.
- Macklin, M.G. (1989) Holocene River Alluviation in Britain. Paper presented at 2nd International Geomorphology Conference, Frankfurt.
- Mosley, M.P. (1975) Channel changes on the River Bollin, Cheshire, 1872-1973. East Midland Geographer 6, 185-99.
- Nanson, G.C. and Hickin, E.J. (1983) Channel migration and incision on the Bearton River. Journal of the Hydraulics Division, ASCE, 109, 327-37.
- Newson, M. (1981) 'Mountain streams', in Lewin, J. (ed) British Rivers, Allen and Unwin, London, 59-89.
- Richards, K.S. (1987) 'Fluvial geomorphology', Progress in Physical Geography, 11, 432-457.
- Schumm, S.A. (1969) River metamorphosis. American Society of Civil Engineers, Journal of Hydraulics Division, 95, 255-273.
- Schumm, S.A. (1979) Geomorphic thresholds; the concept and its applications, Trans IBG, 4, 485-515.
- Thompson, A. (1985) Channel patterns and channel change on upland streams of the Bowland Fells, in Guide to Field Excursions in Northwest England. (Ed: A.M. Harvey) B.G.R.G.

Table 1

Variables in classification database of reach  
and channel characteristics

	Fieldname	Variable description
<u>River data</u>		
1	RIVER	name
2	AREA	region in England
3	PERCENT	% of reach length shifted course
4	TERRAIN	type of terrain
<u>Valley reach</u>		
5	VALLEYVEG	vegetation type
6	VALLEYTREE	type of trees
7	VALLEYUSE	valley landuse
8	GEOLOGY	type of deposits
9	BEDROCK	type of bedrock
<u>Valley wall</u>		
10	WALLVEG	wall vegetation
11	WALLTREE	type of trees
<u>Terraces</u>		
12	TERRACES	extent, none-continuous
13	LEVELS	how many terrace levels
<u>Channel-valley relation</u>		
14	VALLEYTYPE	classification of type
15	NOVALLEY	fan etc.
16	UNDERFIT	yes/no
17	CONSTRICT	lateral constriction
18	VERTICAL	upgrading/degrading
19	LATERAL	relationship to valley walls/ high terraces
<u>Valley flat</u>		
20	VALLEYFLAT	presence of
21	EXTENT	width
22	FLATVEG	vegetation
23	FLATTREE	tree type
24	FLATUSE	valley flat land use

Table 1 (Continued)

<u>Channel</u>	Fieldname	Variable description
	25 PATTERN	channel pattern
	26 ISLANDS	presence of + type
	27 BRAIDING	braiding index
	28 FLOW	type of flow
	29 BARS	type
	30 BELTWIDTH	from map data
	31 WAVELENGTH	from map data
	32 SINUOSITY	from map data
	33 OBSTRUCT	natural destruction's in channel
<u>Lateral activity</u>		
	34 DEGREE	degree of obstruction
	35 ACTIVITY	lateral activity
	36 STABILITY	lateral stability
	37 BENDS	changes on bends
	38 SINCHANGE	changes in sinuosity
<u>Channel banks and bed</u>		
	39 ALLBANK	alluvial bank material
	40 NONBANK	non-alluvial bank material
	41 HEIGHT	of banks
	42 VEGBANK	vegetation cover
	43 BED	present of bedrock in channel bed
<u>Bed rock</u>		
	44 BASEROCK	predominant bed material
	45 BASETYPE	rocktype at channel base
	46 ERODE	erodibility

Table 1b

Coding for Terraces

Terraces

Terrace presence:

0	none
1	indefinite
2	fragmentary
3	continuous

Table 1c

Coding for Valley Vegetation

Vegetation:

0	0	0	not applicable
1	1	1	almost none
2	2	2	grass
3	3	3	shrubs
4	4	4	individual trees
5	5	5	sparsely forested (0-25%)
6	6	6	moderately forested (25-75%)
7	7	7	heavily forested (75-100%)
8	8	8	swamp or marsh
9	9	9	crops

Table 2

**Sinuosity of Stable and Changing River Reaches  
on Two Rivers**

<u>River</u>	<u>Degree of Change</u>	<u>Sinuosity of Reaches</u>
Teme	Stable	1.15, 1.2, 1.0, 1.18
	Migrating	1.2, 1.19, 1.22, 1.07, 1.06
	Extensive change	1.4, 1.42
	'Chaotic' change	2.04
Arrow	Stable	1.1, 1.18, 1.2
	Isolated change	1.41
	Extensive change	1.53

**Figure Captions**

- Figure 1      Survey of river planform changes in England and Wales.
- Figure 2      Example of stable and unstable reaches, River Clywedog, Clywed, N. Wales.
- Figure 3      Types of meander change (Hooke, 1984).
- Figure 4      Model of meander change (Hooke, 1989).
- Figure 5      Sequences of changes on the River Bollin, near Wilmslow, Cheshire, N.W. England.
- Figure 6      Rares of movement plotted against sinuosity showing sequences of movement for individual bends (Hooke, 1987).



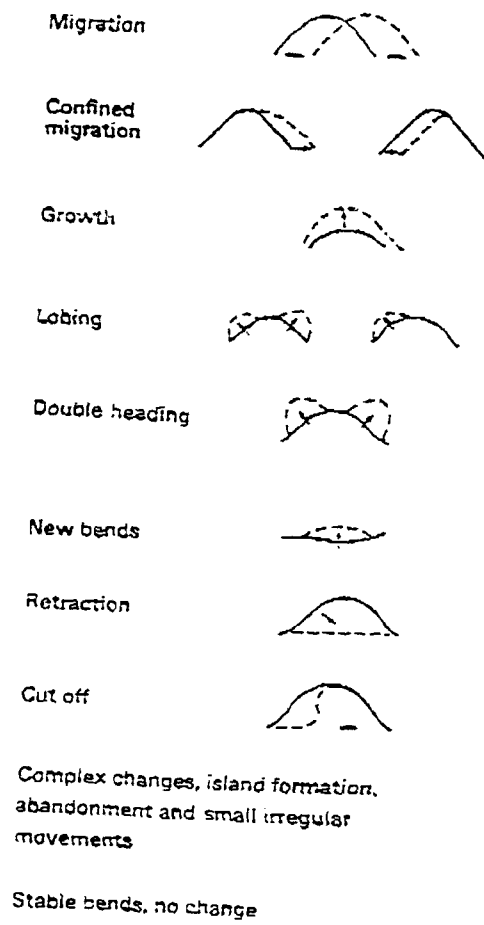


Fig. 3

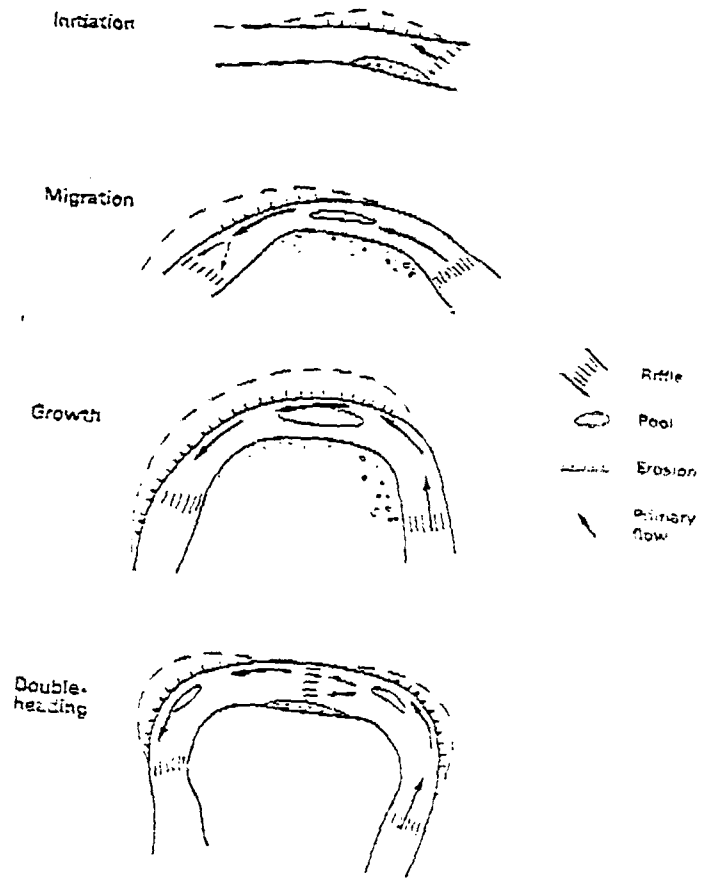
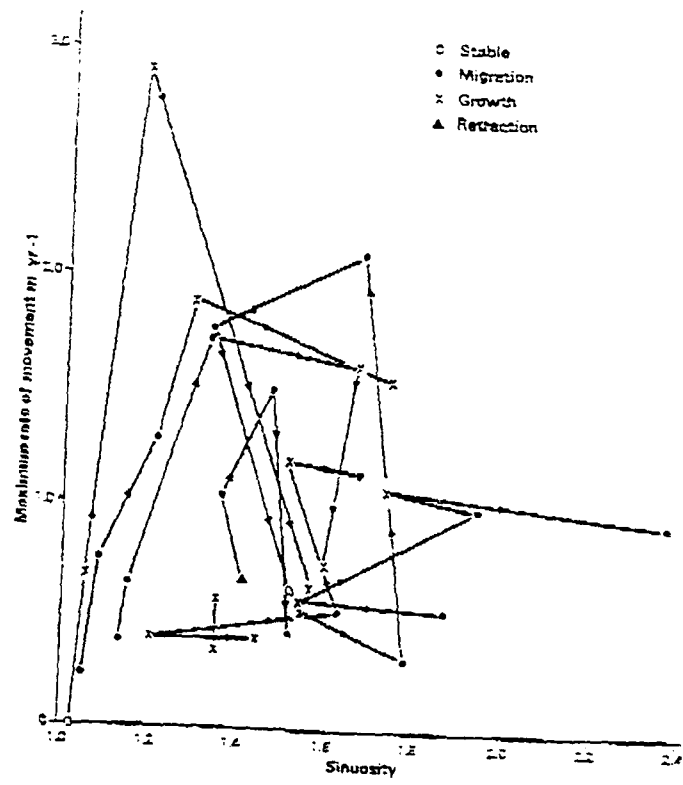
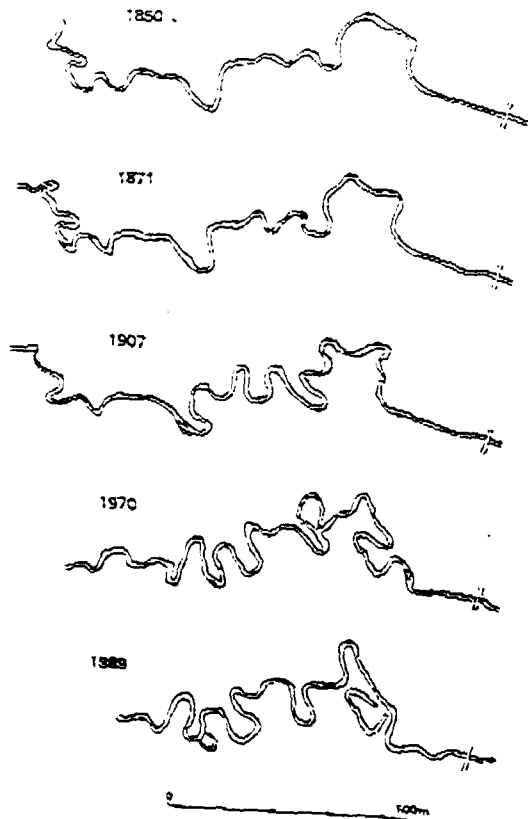


Fig. 4



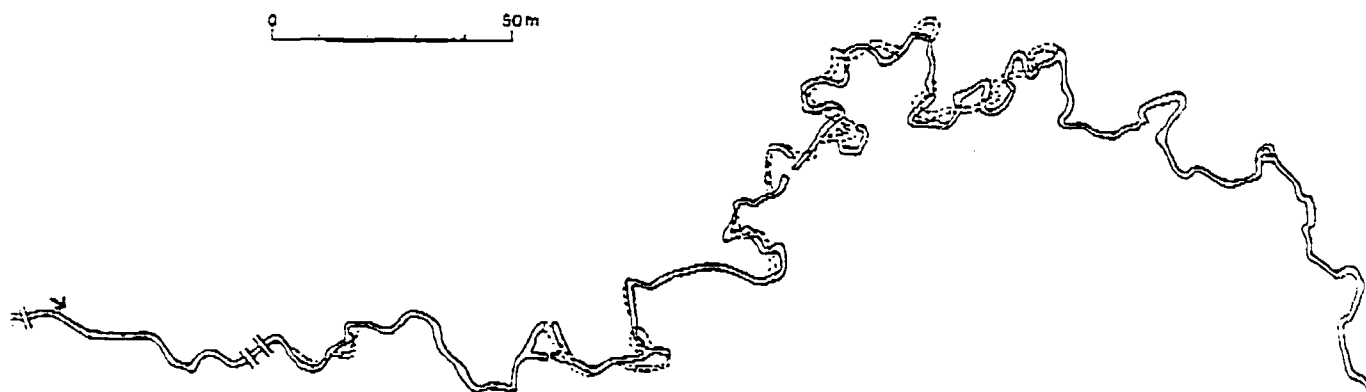
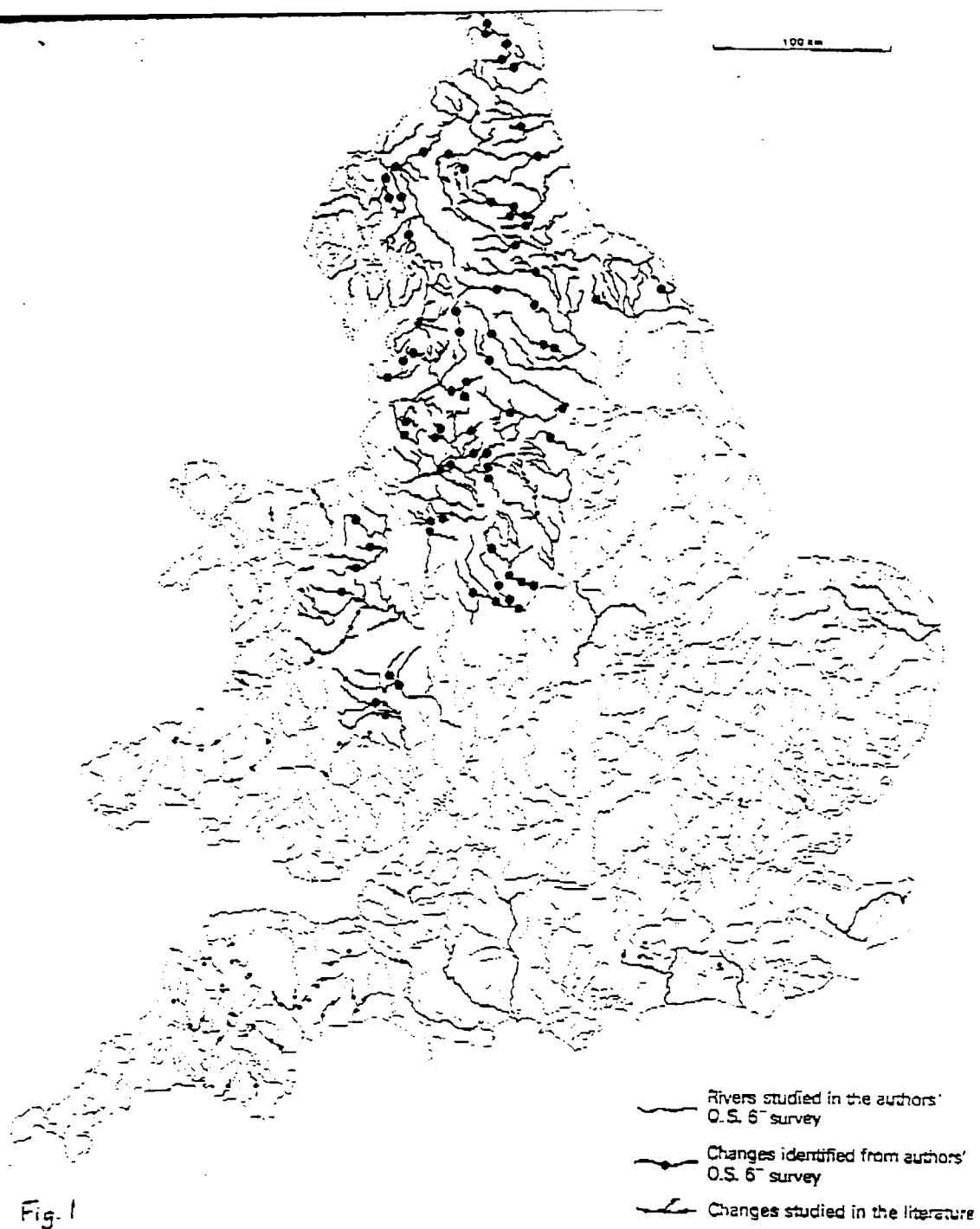


Fig. 2

**HISTORIC FLOODS AND VERTICAL ACCRETION  
OF FINE-GRAINED ALLUVIUM IN THE LOWER TYNE VALLEY,  
NORTH EAST ENGLAND**

By

Mark G Macklin  
Barbara T Rumsby  
Malcolm D Newson

Department of Geography  
The University of Newcastle  
NEWCASTLE UPON TYNE  
NE1 7RU  
UK

**Abstract**

Historical documentation of floods together with sedimentological and trace metal analysis of fine-grained flood sediments have been used to construct a flood record for the River Tyne a gravel-bed river in northern England over the last 100 years. Upsection changes of trace metal concentrations in vertically accreted alluvium have been related to lead and zinc ore production in the Tyne basin and used to date flood events. Exceptionally high (by British standards) vertical accretion rates ( $2.4 \text{ cm a}^{-1}$ ) in the lower Tyne Valley allow individual flood events to be recognised and dated. However, significant differences between documentary and sedimentary-based estimates of the frequency of inundation emerge when these two records are compared. This is shown to be the result of bias in archive sources toward recording large overbank events and the censoring of the alluvial stratigraphic record, as the result of variations in sediment supply and channel entrenchment, to reflect progressively less frequent and larger floods.

## INTRODUCTION

The paradox of flood prediction is that, as the need for accuracy increases (e.g. where sensitive areas need to be protected against flooding of a high recurrence interval) the database provided by hydrometric recordings of river discharge becomes proportionally smaller in relation to that interval. Considering the relatively recent introduction of scientific hydrometry, hydrologists in most regions of the world have turned to documented and monumented historical records (McEwen, 1987) as well as rainfall-runoff models (Anderson and Burt, 1985) to help improve prediction. Arguably the most appropriate, and certainly the most generally available means for extending the flood series beyond the period of instrumentation, however, is the stratigraphic record of alluvial deposits in river valleys (Costa, 1978). The inherent advantages of using alluvial sediments for investigating flood histories in river basins are essentially two fold: first they are not limited by climatic regime or location, and second provided that sediment units can be dated, they can be used over any time period. Palaeoflood hydrology (cf. Stedinger and Baker, 1987), utilising procedures from geobotany, sedimentology, stratigraphy and geomorphology, is particularly useful for estimating the magnitudes and frequencies of rare and large floods, which is often very difficult using conventional flood frequency analysis.

For more than a decade North American geomorphologists have been successfully employing alluvial stratigraphic analysis in flood reconstruction over Holocene and historical timescales both in semi-arid (Webb *et al.*, 1988) and humid (Costa, 1974; Knox, 1987a) regions of the USA. In Europe, however, although extensive use has been made of documentary sources to extend the flood record beyond the period of gauging (e.g. Decamps *et al.*, 1989), geomorphological investigations of floods have by and large focused on the impact of single "extraordinary" events which usually attract attention by virtue of spectacular floodplain erosion and deposition (Acreman, 1983; Brown, 1983; Carling, 1986; Harvey, 1986; McEwen and Werritty, 1988; Newson and Macklin, 1990). To our knowledge no investigation has used the alluvial record to reconstruct historic flood histories in a major British or, for that matter, continental European watershed. In the study reported here historical reports of floods together with sedimentological analysis of textural discontinuities in fine-grained, vertically accreted alluvium are used to construct a flood record of the River Tyne in northern England over the last 100 years.

## STUDY AREA

### Flood histories

Following a major flood on the 26th August 1986 bank erosion at Low Prudhoe (NZ 088637) (Fig. 1) in the lower Tyne Valley, 15 km west of Newcastle upon Tyne, revealed extensive sections in the floodplain of the River Tyne. Floodplain sediments were found to be composed of 2-3m of finely-laminated sands and silty sands overlying 2m of sandy gravels. Preliminary granulometric analysis of prominent coarser sand layers in the upper fine-grained alluvial unit showed them to have similar physical properties to sands deposited overbank on the Tyne floodplain during the August 1986 flood (Macklin and Dowsett, 1989). This suggested that sediments at this site could provide a valuable record of recent major floods in the lower Tyne Valley.

The River Tyne is a gravel-bed river with mean and maximum recorded discharges of  $44 \text{ m}^3 \text{ s}^{-1}$  and  $1497 \text{ m}^3 \text{ s}^{-1}$  measured at Bywell (NZ 038617), 5 km west of Low Prudhoe. Although the first gauging station in the catchment was completed as early as 1939 (Barrasford NY 920733 in the North Tyne), systematic instrumented records of river flow are only available after 1950. Although unusually good exposure of alluvium at Low Prudhoe initially prompted sedimentological and

stratigraphic based studies of recent floods in the lower Tyne Valley, floodstones on the Rectory steps at Ovingham (Fig. 2) marking the heights of the great floods of 1771 (the largest on record) and 1815, together with good archive records (newspapers, local books and journals, meteorological publications) of major floods in the Tyne catchment since 1699 (Archer, unpublished), make Low Prudhoe an excellent site at which to compare documentary and sedimentary flood records.

#### **River channel change and vertical accretion processes**

Over the last 130 years or so, the thalweg of the Tyne at Low Prudhoe has moved very little (Fig. 2a), but since the early 1950's its channel has narrowed appreciably most notably in a 500m reach downstream of Ovingham Bridge, within which the study section is located. Channel narrowing has been primarily the result of incision which elevated former lateral gravel bars above the level of the low flow channel and enabled them to be colonised by vegetation. These sites subsequently became the forms of fine sediment deposition resulting in the infilling of site channels and attachment of bars to the former river bank. Rates of incision and bed erosion increased considerably in the late 1950's and 1960's following gravel extraction from the river bed, and is still continuing today necessitating regular upgrading of the footings of Ovingham Bridge.

The well-bedded sands and silty sands exposed in the river bank at Low Prudhoe are believed to have been formed by vertical accretion. This deposit has a similar surface morphology (asymmetric in cross section with its highest point located adjacent to the channel, see Fig. 2b) and stratigraphy (see below) to shrub and herb covered alluvial benches located within the present Tyne channel which accrete fine sediment to the level of the contemporary floodplain. These are not levees or overbank splays but resemble alluvial benches described by Page and Nanson (1982) and Taylor and Woodyer (1978) in several Australian and Canadian rivers and defined as, "actively accreting flat-topped bodies of sediment occurring along the banks of a stream channel" (Woodyer *et al.*, 1979). Initial sedimentation at the study section was therefore under sub-bank full flow conditions with fine sediment deposition confined within the channel banks. Later sediments, as the result of progressive vertical accretion, would have tended to be deposited under flow conditions closer to bankfull and also by overbank floods. Thus a considerably proportion of fine-grained alluvium at Low Prudhoe represents the vertical component on within-channel sedimentation and is of a somewhat different origin to "overbank fines" (usually of silt and clay size and deposited some distance from the channel) more frequently described on British floodplains (eg Lambert and Walling, 1987).

#### **Geology and metal mining history**

The Tyne upstream of Low Prudhoe has a drainage area of 2198 km<sup>2</sup> and is fed by two major tributaries (Fig. 1); the River South Tyne (drainage area 800 km<sup>2</sup>) that drains the northern flank of the Northern Pennines, and the River North Tyne (drainage area 1118 km<sup>2</sup>) whose catchment comprises the Newcastle Fells and southern part of the Cheviot Hills. Both sub-catchments are primary underlain by sedimentary rocks (sandstones, limestones and shales) of Carboniferous age though small outcrops of igneous rocks (Whin Sill) are found in the lower reaches of the North and South Tyne Valleys and also in the headwaters of the River North Tyne (Cheviot granite).

The predominance of sandstone rock types within the Tyne catchment, both in pre-Quaternary lithologies and Pleistocene glacial deposits, results in a large sand component in Tyne flood sediments (Macklin and Dowsett, 1989; Newson, 1989). A high rate of "run-out" of fine-grained sediment especially from the Northern Pennine Uplands during major floods supplies abundant material for overbank

deposition on floodplains in the lower parts of the basin (Macklin and Dowsett, 1989). This enables some fine-grained alluvial stratigraphic units to be traced considerable distances through the Tyne drainage system, and allows flood histories in headwater and lowland river reaches to be compared.

The headwater tributaries of the South Tyne, most notably the Rivers Allen, Black Burn and Nent (Fig. 1), drain the northern part of the North Pennine Orefield, once the most productive metalliferous region in the UK (Dunham, 1944). A smaller area of mineralisation is also found between Haydon Bridge and Hexham (Fig. 1), close to the confluence of the North and South Tyne. There are no significant metal-bearing deposits in the North Tyne basin (Smith, 1923). The principal base metal minerals are galena (PbS) and sphalerite (ZnS) and both contain significant concentrations of trace metals including cadmium, copper and silver (Young *et al.*, 1987).

In common with many other river systems in Britain draining metal mining areas (Lewin and Macklin, 1987), effluent from the extraction and processing of lead and zinc ores resulted in the release of large quantities of fine-grained, metal-rich waste into the River Tyne. Although sediment-borne metals caused serious contamination of riparian agricultural land downstream of mining areas, and gross pollution of many water courses, they do however provide a distinctive source of "labelled" sediment. Furthermore, as the development and history of metal mining in the Tyne basin is known in some detail from the end of the seventeenth century (Raistrick and Jennings, 1965), heavy metals are important stratigraphic markers, especially within sequences of vertically accreted fine-grained alluvium (Klimek and Zawilinska, 1985; Knox, 1987b; Lewin and Macklin, 1987 and Macklin, 1985) such as those exposed at Low Prudhoe.

## **FIELD SAMPLING AND LABORATORY ANALYSES OF FLOOD SEDIMENTS**

Fine-grained alluvial sediments in the upper part of the river bank section at Low Prudhoe were sampled using Kubiena tins. In the laboratory the 2.4m long monolith was cleaned, drawn and sub-samples (135 in total) taken from every distinct layer for metal analyses and organic matter determinations. Additional material for grain size analysis was collected from the coarser, more prominent sand units (13 samples). Sediment colour was described using Munsell notation.

All samples were air dried, passed through a 2 mm sieve and heavy metal contents were estimated from the amounts of metals brought into solution by digesting sediment samples in nitric acid. Metal (lead, silver and zinc) concentrations were determined using atomic absorption spectrophotometry (Phillips SP2900 with computer) involving direct aspiration of the aqueous solution into an air-acetylene flame. The organic content of sediments was taken as the loss of weight on ignition (L.O.I.) at 450 °C. Particle size distributions were obtained using standard dry sieving methods with sieves graded at 0.25  $\phi$  intervals. Mean grain size, sorting, skewers and kurtosis were determined graphically following Folk and Ward (1957).

## **SEDIMENTARY PROPERTIES OF FLOOD DEPOSITS AND DATING FLOOD EVENTS AT LOW PRUDHOE**

### **Sedimentary sequence and grain size characteristics of flood sediments**

Flood events in fine-grained alluvial deposits at Low Prudhoe are represented by layers of generally flat bedded sands and silty sands (Fig. 3), which on the basis of grain size (following Niggli, 1935 and Pettijohn, 1975) and colour can be assigned to one of three sedimentary categories. Grain size curves for these flood sediment types are shown in Fig. 4.

- 1 Medium-fine sand (type 1 flood unit): yellow brown in colour (10 YR 5/4), mean grain size between 2.1 and 2.7  $\phi$ , mean L.O.I. 2.4% and with generally less than 5% silt and clay.
- 2 Fine-very fine sand (type 2 flood unit): dark yellowish brown in colour (10 YR 3/4), mean grain size between 2.7 and 3.3  $\phi$ , mean L.O.I. 3.3% and with between 5-10% silt and clay.
- 3 Silty fine- very fine sand (type 3 flood unit): dark brown in colour (7.5 YR 3/4), mean grain size 3.3  $\phi$ , mean L.O.I. 3.7% and with more than 10% silt and clay.

Following Knox (1987a), textural discontinuities formed by layers of medium-fine (type 1 flood unit) and fine- very fine sand (type 2 flood unit) that reverse the overall "fining upward" sequence are interpreted as the deposits of large floods. Finer-grained silty sands (type 3 flood unit) are believed to represent lower magnitude floods or sediment deposited on the falling stage of a large flood event. Where coarser type 1 or 2 flood deposits overlie finer-grained type 3 flood units boundaries are generally sharp and sometimes marked by angular unconformities (eg 80 and 120 cm), probably produced by scour at the initial stages of a flood (cf. Jahns, 1947). In contrast, where finer flood sediment (type 3 flood unit) overlies type 1 or 2 flood deposits (eg 100 and 170 cm) bounding surfaces are more usually gradational, fining-upwards over 1-2 cm. In such cases finer sediment is believed to have been deposited on the falling limb of a flood hydrograph producing a flood "couplet" similar to flood units identified by Mansfield (1938), Farrell (1987), Klinek (1974) and Knox (1987a). On the other hand, sharp, non-gradational transitions from type 1 or 2 to type 3 flood units are the product of one or, more probably, several lower magnitude events. Higher percentages of organic material towards the top of many silty fine- very fine sand units suggest incipient soil development and slower accumulation rates. Complex grading is also evident within several of the sediment units (eg 222-205, 187-185, 135-128, 118-102, 60-48, 42-32 cm) believed to have been deposited by larger floods. This is likely to have resulted from changing flow conditions during a multi-peaked hydrograph (Taylor and Woodyer (1978), varying sources of sediment or periodic upstream bank collapse during a flood event (Osterkamp and Costa, 1987). Mudcracks (eg 118 cm), scour hollows (eg 183-180, 42-40 cm) and other pre-existing surface irregularities are also useful for differentiating between flood units and using these, together with other sedimentological criteria defined above, 25 large (identified by reversals in the normal fining-upward sequence) flood events would appear to be represented in the alluvial profile at Low Prudhoe. Vertical variations in the mean size and summary movement statistics of the thickest and best developed major flood units are plotted in Fig. 4. In general, flood units become finer, relatively better sorted and more platykurtic upsection. Moment statistics also pick out major textural discontinuities, corresponding with significant changes in flood unit thickness, at 185 cm, 120 cm and 35 cm. In the lower unit (230-185 cm) grain size decreases upsection with flood units becoming more poorly sorted and platykurtic. Between 185 and 120 cm this trend continues although flood units are generally more leptokurtic. In the upper sequence (120-35 cm) coarser, well sorted, leptokurtic flood sediments at the base are followed by progressively finer, less-well sorted and platykurtic flood deposits. Although graphical moment statistics confirm the basic facies architecture and stratigraphy of the Low Prudhoe section, they are less useful for identifying the upper and lower boundaries of flood units which can only be delineated by very careful logging of the profile. Establishing precisely the number, thickness and sedimentary characteristics of major flood units is of paramount importance for reconstructing the history of flooding at a site.

### Trace metal dating of flood sediments

Vertical changes in sediment trace metal concentration at Low Prudhoe have been related to metal ore production in the Tyne basin and used to provide age estimates for flood events (Figs. 5 and 6). Water used in ore-processing, heavily laden with fine-grained metal-rich sediment, was usually discharged directly into the nearest stream. Thus although major lead and zinc mines in the Tyne catchment lay some distance from Low Prudhoe, the fine-grained nature of the mining waste enabled it to be transported rapidly downstream (particularly during major floods) thereby minimising the time interval (probably ranging from a few weeks to less than a year) between the release of metals from upstream mining operations and their incorporation in vertically accreted alluvium downstream within the lower Tyne Valley.

As has been shown in mining age alluvium elsewhere in the Tyne basin (Macklin, 1986; Macklin and Lewin, 1989; Macklin and Smith, 1990), especially high zinc levels and zinc/lead ratios in sediments between 96-118 cm mark the peak of zinc extraction in the Allendale and Alston moor ore fields between 1897 and 1915 (Fig. 6). With a sharp reduction in zinc concentrations above 120 cm following the rapid decline of zinc mining in the region after 1915 (Dunham, 1944). Comparatively low lead levels ( $<1000 \text{ mg kg}^{-1}$ ) below 90 cm indicate sedimentation at Low Prudhoe post-dates the main phase of lead production in the Tyne basin that ended in 1880, confirming age estimates provided by sediment zinc concentrations. Above 90 cm lead concentrations rise in response to the revival of lead mining in the 1920's and 1930's. Peaks in lead production in 1927, 1933 and 1937 are reflected by increased lead concentrations in flood sediments and decreased zinc/lead ratios at 56, 28 and 24 cm. Most lead veins in the Tyne basin are argentiferous (Dunham, 1948) and, as one would expect, changes in silver concentration generally follow those of lead. To summarise, trace metal dating of fine-grained alluvial sediments at Low Prudhoe, somewhat unexpectedly, indicate that the major part of the sequence was deposited over a comparatively short period of time (c.50 years) between 1890 and 1937.

### FLOOD FREQUENCIES AT LOW PRUDHOE 1890 - 1990: A COMPARISON OF THE DOCUMENTARY AND SEDIMENTARY FLOOD RECORD IN THE LOWER TYNE VALLEY

On the basis of dating control provided by sediment heavy metal analyses, and in the knowledge that archive sources tend to record larger spatially extensive floods (Archer, 1987) flood units evident in the Low Prudhoe section were assigned as far as possible to documented floods since 1890 in the Tyne Valley (Table 1, Fig. 5). Not all flood units, however, could be related to recorded flood events and in these cases chemostratigraphic dating control provided general bounded time limits. In Fig. 7 floods documented in the Tyne basin between 1890 and 1989 are plotted with the sedimentary flood record (where present) over the same period and compared below on a decade by decade basis.

#### 1890-1899

The sedimentary sequence for this period contains many more flood events than are documented in archive records (Fig. 7 and Table 1). This can be explained by a small height difference between the depositional surface and river bed at this time resulting in more frequent inundation by sub-bankfull flows. Although the accretionary surface at Low Prudhoe was probably flooded several times a year (as indicated by the large number of flood units dated to the 1890's), individual flood units are relatively thin (2-3 cm) and suggest deposition by relatively low magnitude events. Indeed, very few of these floods were sufficiently large to merit being



recorded by contemporary commentators. Thicker, coarser layers, however, probably correspond to higher magnitude floods (eg those of 1891 and 1892).

#### 1900-1919

Sedimentary and documentary based flood records are more closely matched than in the previous decade. After 1900 (c.182 cm) the thickness of individual flood units increases significantly (>10 cm) as do zinc concentrations. Both reflect the input of large quantities of metal-rich fines into the South Tyne system during the peak period of zinc mining, 1898-1915. Lower zinc levels between 160-140 cm probably mark a temporary fall in zinc production between 1906 and 1910. Though this coincides with, and may well have been accentuated by, the North Tyne floods of 1907 and 1911 that would have introduced fine sediment with low metal concentrations into the River Tyne.

#### 1920-1929

Six large floods are evident in the part of the Low Prudhoe profile dated to the 1920's (c.100-30 cm), one less than recorded in archive sources. Flood units are generally coarser (medium-fine sand) and thicker than those of earlier decades but low metal concentrations indicate that metal mining was not the source of this sediment. A marked reduction in the supply of mining-related fine material, following the closure of many mines at the end of World War I, appears to have been compensated by fine sediment generated from bank erosion (noted by commentators) during a series of very large floods in 1923, 1924 and 1926. Flood units with higher zinc concentrations and zinc/lead ratios (eg 60-50 cm) were probably derived from reworking of earlier metal contaminated alluvium located some distance upstream.

#### 1930-1949

Although the documentary record for this period shows the frequency of large floods remained high (particularly during the early to mid 1930's) only two distinct flood units, dated to 1933 and 1947, can be recognised. Thus by the early 1930's the alluvial surface at Low Prudhoe appears to have accreted to a level above the channel thalweg that could only be over-topped by floods of a much higher magnitude and reduced frequency than before.

#### Post 1949

Since 1947 only two exceptional floods have inundated the Low Prudhoe section, those of 1955 (the largest flood in the Tyne since 1771) and August 1986 (the largest flood since 1955). River bed incision (up to 2m, Fig. 2b), which probably began sometime in the 1940's, transformed the alluvial bench at Low Prudhoe (a site of rapid vertical accretion between 1890 and 1937) into a low terrace. Many reaches of the Rivers South Tyne and Tyne, similar to the Tyne at Low Prudhoe, have incised since World War II (Macklin and Lewin, 1989; Macklin and Smith, 1990) in response to gravel extraction from channels (gravel was dug from the bed of the Tyne immediately upstream of Ovingham Bridge in the 1950's and 1960's) and bed erosion following the 1947 and 1955 floods. Widespread channel degradation also occurred during the August 1986 flood (Newson and Macklin, 1990), although a thin (2-3 mm) and patchy veneer of fine sand was deposited overbank at Low Prudhoe during this event. Four years on bioturbation processes have mixed this deposit with earlier sediment, to the extent that it is now very difficult to recognise as a distinct flood unit both in its original thickness and distribution.

In summary, the documentary flood record of the River Tyne between 1890 and 1949 shows an increase in flood frequency between 1890-1909 and 1920-1939 with

relatively few floods in the decades 1910-9 and 1940-9. Flooding over this period (1890-1949) follows changing hydrometeorological conditions in north east England with rainfall maxima recorded in the region during the late nineteenth century and again between 1920-1939 (Harris, 1985).

Most of the flood units deposited before 1900 appear to have resulted from sub-bankfull flows many of which will not have been reported by local commentators or newspapers. The similar number of floods between 1900 and 1929 evident in both the stratigraphic and documented flood record, however, suggests type 1 and 2 flood units were deposited during overbank events that inundated both the depositional bench at Low Prudhoe and the Tyne Valley flow. Since 1930 an increase in the relative height of this surface above the river bed (resulting initially from sediment accretion and later by channel incision) has effected a "censoring" of the alluvial stratigraphic record to reflect progressively less frequent and larger floods. Today continuing river bed incision has enlarged the Tyne channel at Low Prudhoe to a size that can accommodate floodwaters and sediment in all but the very largest floods.

We believe the disparity between the stratigraphic and documentary flood records at Low Prudhoe over the last 100 years reflects the latter's bias towards recording large overbank floods. Archive sources will therefore inevitably under-represent the actual number of flood events recorded in the stratigraphic record, especially when a depositional surface is of low elevation and subject to inundation by low magnitude floods. Deposition of fine-grained flood sediment within the Tyne channel (which in this particular study forms the basis of the paleoflood record) though reflecting in a systematic way changes in flood flow magnitude and frequency (controlled primarily by climate) has also been strongly influenced by variations in sediment supply (associated with upstream bank erosion rates and, in the case of the Tyne, input of mining waste) and entrenchment of the channel over the period of investigation. It is therefore imperative that sediment availability and the vertical tendency of a channel reach are evaluated, and quantified, before stratigraphic evidence at a site is used to extend the flood series in a river basin.

#### VERTICAL ACCRETION RATES AT LOW PRUDHOE 1890-1990

Rates of vertical accretion at Low Prudhoe from the end of the nineteenth century up to the present have been calculated by comparing the thickness of flood sediment accumulated between dated stratigraphic horizons (Fig. 7). There is a fairly close inverse relationship between organic matter in vertically accreted sediments and sedimentation rates (Table 2), similar to that found by Knox (1987b) in Upper Mississippi floodplain sequences. Alluvial surfaces that are characterised by slow rates of sedimentation tend to accumulate organic matter in an incipient soil A horizon, whereas surfaces experiencing rapid alluviation normally accumulate relatively small amounts of organic matter (cf. Knox, 1987b).

Between 1890 and 1937 vertical accretion rates at Low Prudhoe were high averaging  $4.8 \text{ cm a}^{-1}$ . Since the 1930's, however, average yearly sedimentation rates have decreased by an order of magnitude to less than  $0.4 \text{ cm a}^{-1}$  at the present day (Fig. 7). Nevertheless, rates of recent fine-grained vertical accretion in the lower Tyne Valley are unusually high for British rivers (Table 3) and match rates recorded in some of the major river systems of Europe, North America and Australia reviewed by Bridge and Leeder (1979). The large sand load of the Tyne, derived from Carboniferous sandstone lithologies in its catchment and augmented by fine grained metal mining waste, appear to be the major causative factors. However, closer examination of the few river basins in Britain in which longer-term fine-grained sedimentation rates have been estimated show most are underlain by shale or clay lithologies where alluvium has been deposited overbank rather than within-channel as at Low Prudhoe. This, together with divergent catchment land-use histories, may

explain the generally low floodplain sedimentation rates recorded in the silt and clay suspended load rivers of lowland southern England (eg lower Severn, Avon, Ripple Brook, Culm) compared with much higher rates found to be more typical of river systems developed on sandstone lithologies in northern Britain (eg Swale and Tyne). Indeed, high vertical accretion rates would appear to be essential for the preservation of flood-related bedding structures and units in the alluvial stratigraphic record, whereas these features would tend to be destroyed by bioturbation and pedogenic processes at floodplain sites with lower rates of deposition.

## CONCLUSIONS

Our studies of fine sediment deposition in the lower Tyne Valley represent the most detailed investigation of longer-term vertical accretion yet undertaken in a major British river. From a methodological viewpoint we have confirmed the utility of trace metals for dating fine-grained alluvial sequences in large mineralised catchments. While the identification of systematic differences between sedimentary and documentary based estimates of flood frequency in the lower Tyne highlights the important contribution fluvial geomorphologists can make to developing and refining historical flood information. Hitherto hydrologists have questioned lengthy extensions of flood data (much beyond a hundred years) because of possible climatic changes introducing non-stationarity into data series. The Tyne study reveals another source of non-stationarity; changes in river bed and sedimentation levels that may alter the flood-carrying capacity of a channel, and therefore the frequency of inundation and the flood hazard at a site. This is an important second-order effect when considering the non-stationarity introduced by climatic change and is of paramount importance in locating protection works. Significant recent channel bed level changes in the lower Tyne also to a large extent invalidates using floodstones to accurately calculate discharges and return periods of extreme floods. This constraint to historical flood reconstruction may well apply to many other northern British rivers. If, as predicted, the next 100 years is a period of profound climatic change it may well be that river engineers will need to know considerably more about the spatial and temporal patterns of channel capacity change as well as their controls.

Finally, our investigations highlight at least two lines of future research with respect to deposition of fine-grained alluvium and floods on British and European floodplains. Firstly, the recognition of significant vertical accretion of fine sediment within river channels suggest that fine sediment members of historic and Holocene meandering rivers that are generally described as overbank deposits may need to be re-interpreted. The higher sand component in within-channel fines, together with regular textural reversals, may be useful criteria by which they can be distinguished from floodplain sediments deposited solely by overbank flood events. Secondly, with the development of luminescence sediment dating techniques (Smith *et al.*, 1990), sedimentological-based estimates for flood frequency at a site using sequences of vertically accreted alluvium (as outlined in this paper) could be employed over longer Holocene timescales. O.S.L. dating of flood units in sand members of late and middle Holocene alluvial fills in the lower Tyne Valley is now in progress to assess the potential of this approach.

## ACKNOWLEDGEMENTS

The authors wish to thank Mr David Archer for access to unpublished data on historical floods in the Tyne catchment and also Mr Watts Stelling for undertaking sediment heavy metal analyses. BTR is grateful to NERC for the provision of a postgraduate studentship.

## REFERENCES

- Acreman, M.C. (1983), 'The significance of the flood of September 1981 on the Ardesie Burn, Wester Ross', *Scottish Geog. Mag.*, **99**, 150-160.
- Anderson, M.G. and Burt, T.P. (eds.) (1985), *Hydrological forecasting*. John Wiley & Sons, Chichester, 604 pp.
- Archer, D. (1987), 'Improvement in flood estimates using historical flood information on the River Wear at Durham', *National Hydrology Symposium*, University of Hull, British Hydrological Society.
- Bridge, J.S. and Leeder, M.R. (1979) 'A simulation model of alluvial stratigraphy', *Sedimentology*, **26**, 617-644.
- Brown, A.G. (1983), 'An analysis of overbank deposits of a flood at Blandford Forum, Dorset, England', *Revue de Geom. Dyn.*, **32**, 95-99.
- Brown, A.G. (1987), 'Holocene floodplain sedimentation and channel response of the Lower River Severn, UK', *Zeitschrift für Geom.*, **31**(3), 293-310.
- Brown, A.G. and Barber, K.E. (1985), 'Late Holocene palaeoecology and sedimentary history of a lowland catchment in central England', *Quaternary Res.*, **24**, 87-102.
- Carling, P.A. (1986) 'The Noon Hill flash floods; July 17th 1983. Hydrological and geomorphological aspects of a major formative event in an upland landscape', *Transactions of the Inst. Brit. Geog. N.S.*, **11**, 105-118.
- Costa, J.E. (1974) 'Stratigraphic, morphologic, and pedologic evidence of large floods in humid environments', *Geology*, **2**, 301-303.
- Costa, J.E. (1978) 'Holocene stratigraphy in flood frequency analysis', *Water Res. Res.*, **14**, 626-632.
- Decamps, H. Fortune, M. and Gazelle, F. (1989) 'Historical changes of the Garonne River, Southern France', in: Petts, G.E. (ed.), *Historical Change of Large Alluvial Rivers: Western Europe*, John Wiley and Sons, Chichester, p.249-267.
- Dunham, K.C. (1944). 'The production of galena and associated minerals in the northern Pennines; with comparative statistics for Great Britain', *Transactions Ins. of Min. and Met.*, **53**, 181-252.
- Dunham, K.C. (1948), *Geology of the North Pennine Orefield. Vol 1. Tyne to Stainmore.*, Memoir Geological Survey UK, HMSO, London, 347 pp.
- Farrell, K.M. (1987), 'Sedimentology and facies architecture of overbank deposits of the Mississippi River, False River Region, Louisiana', in: Ethridge, F.G., Flores, R.M. and Harvey, M.D. eds., *Recent Developments in Fluvial Sedimentology*, Society of Economic Palaeontologists and Mineralogists, Special Publication No. 39, p.111-120.
- Folk, R.L. and Ward, W. (1957), 'Brazos River bar: a study of the significance of grain-size parameters', *Journal of Sed. Pet.*, **27**, 3-26.

- Harris, R. (1985), 'Variations in the Durham rainfall and temperature record', in, Tooley, M.J. and Sheail, G.M. (eds.), *The Climatic Scene*, George Allen and Unwin, London, p.39-59.
- Harvey, A.M. (1986), 'Geomorphic effects of a 100 year storm in the Howgill Fells, Northwest England', *Zeitschrift für Geom.*, 30 (1), 71-91.
- Jahns, R.H. (1947), *Geologic features of the Connecticut Valley, Massachusetts, as related to recent floods*, U.S. Geological Survey Water Supply Paper 996, 158p.
- Klimek, K. (1974), 'The structure and mode of sedimentation of flood-plain deposits in the Wisloka valley (South Poland)', *Studia Geom. Carp. -Bal.*, 8, 135-151.
- Klimek, K. and Zawilinska, L. (1985), 'Trace elements in alluvia of the Upper Vistula as indicators of palaeohydrology', *Earth Surf. Proc. and Land.*, 10, 273-280.
- Knox, J. (1987a), 'Stratigraphic evidence of large floods in the upper Mississippi Valley', in, Mayer, L. and Nash, D. (eds.), *Catastrophic Flooding*, The Binghamton Symposia in Geomorphology, International Series, No. 18, Allen and Unwin, p.155-180.
- Knox, J. (1987b), 'Historical valley floor sedimentation in the Upper Mississippi valley', *Annals of the Ass. of Amer. Geog.*, 77, 224-244.
- Lambert, C.P. and Walling, D.E. (1987), 'Floodplain sedimentation: a preliminary investigation of contemporary deposition within the lower reaches of the River Culm, Devon, UK', *Geografiska Ann.*, 69A(3-4), 393-404.
- Lewin, J. and Macklin, M.G. (1987), 'Metal mining and floodplain sedimentation in Britain', in, Gardiner V. (ed.), *International Geomorphology 1986*, Part 1, Wiley, Chichester, p.1009-1027.
- Macklin, M.G. (1985), 'Flood-plain sedimentation in the upper Axe Valley, Mendip, England', *Transactions of the Inst. of Brit. Geog. N.S.*, 10, 235-244.
- Macklin, M.G. (1986) 'Channel and floodplain metamorphosis in the River Nent, Cumberland', in, Macklin M.G. and Rose J. (eds.), *Quaternary river landforms and sediments in the Northern Pennines, England. Field Guide*. British Geomorphological Research Group/Quaternary Research Association, p.19-33.
- Macklin, M.G. and Dowsett, R.B. (1989), 'The chemical and physical speciation of trace metals in fine grained flood sediments in the Tyne basin, north-east England', *Catena*, 16(2), 135-151.
- Macklin, M.G. and Lewin, J. (1989), 'Sediment transfer and transformation of an alluvial valley floor, the River South Tyne, Northumbria, UK', *Earth Surf. Proc. and Landf.*, 14, 233-246.
- Macklin, M.G. and Smith, R.S. (1990), 'Historic vegetation succession of alluvial metallophyte plant communities in the Tyne basin, north-east England, UK', in, Thornes J.B. (ed.) *Vegetation and Geomorphology*, Wiley, Chichester, p.239-256.

- McEwen, L.J. (1987), 'The use of long-term rainfall records for augmenting historic flood series: a case study on the upper Dee, Aberdeenshire, Scotland', *Transactions of the Roy. Soc. of Edin: Earth Sci.* 78, 275-285.
- McEwen, L.J. and Werritty, A. (1988), 'The Hydrology and long-term Geomorphic Significance of a Flash Flood in the Caingorm Mountains, Scotland', *Catena*, 15 (3/4), 361-377.
- Mansfield, G.R. (1938), 'Flood deposits of the Ohio River, January-February 1937. A study of sedimentation', in, Grover, N.C., *Floods of the Ohio and Mississippi Rivers January-February 1937*, U.S. Geological Survey Water Supply Paper 838.
- Newson, M.D. (1989), 'Flood effectiveness in river basins: progress in Britain in a decade of drought', in, Beven K. and Carling P.A., *The hydrology, sedimentology and geomorphological implications of floods*, John Wiley & Sons, Chichester, p.151-169.
- Newson, M.D. and Macklin, M.G. (1990), 'The geomorphologically effective flood and vertical instability in river channels - a feedback mechanism in the flood series for gravel - bed rivers', *River Flood Hydraulics*, John Wiley, London.
- Niggli, P. (1935), 'Die Charakterisierung der Klastischen Sedimente nach Kornzusammensetzung', *Schweiz. Min. Pet. Mitt.*, 15, 31-38.
- Osterkamp, W.R. and Costa, J.E. (1987), 'Charges accompanying an extraordinary flood in a sand-bed stream', in, Mayer, L. and Nash, D. (eds.), *Catastrophic Flooding*, The Binghamton Symposia in Geomorphology, International Series, No. 18, Allen and Unwin, p.201-224.
- Page, K. and Nanson, G. (1982), 'Concave - bank benches and associated floodplain formation', *Earth Surf. Proc. and Landf.*, 7, 529-543.
- Pettijohn, F.J. (1975), *Sedimentary Rocks*, 3rd ed, New York, Harper and Row.
- Raistrick, A. and Jennings, B. (1965), *A history of lead mining in the Pennines*. Longmans, London, 347 pp.
- Shotton, F.W. (1978), 'Archaeological inferences from the study of alluvium in the lower Severn - Avon valleys', in, Limbrey S. & Evans J.G. (eds.), *Man's Effect on the Landscape: The Lowland Zone*. Council for British Archaeology Research Report 21, p.27-32.
- Smith, B.W., Rhodes, E.J., Stokes, S., Spooner, N.A. and Aitken, M.J. (1990) 'Optical dating of sediments: initial quartz results from Oxford', *Archaeometry*, 32, 19-31.
- Smith, D.G. (1983), 'Anastomosed fluvial deposits: modern examples from Western Canada', in, *Modern and Ancient Fluvial Systems*, Collinson, J.D. and Lewin, J. (eds.), International Association of Sedimentologists Special Publication 6, Blackwells, Oxford, pp.155-168.
- Smith, D.G. and Putnam, P.E. (1980), 'Anastomosed river deposits: modern and ancient examples in Alberta, Canada', *Canadian Journal of Earth Science* 17, 1396-1406.

- Smith, S. (1923). *Lead and Zinc ores of Northumberland and Alston Moor. Vol. XXV. Special Report on the Mineral Resources of Great Britain, Memoirs of the Geological Survey UK, HMSO, 111 pp.*
- Smith, S.A. (1989) Sedimentation in a meandering gravel-bed river: the River Tywi, South Wales. *Geological Journal* 24, 193-204.
- Stedinger, J.R. and Baker, V.R. (1987), 'Surface Water Hydrology: Historical and Paleoflood Information', *Reviews of Geophy.*, 25 (2), 119-124.
- Taylor, G. and Woodyer, K.D. (1978), 'Bank deposition in suspended-load streams', in, Miall, A.D. (ed.), *Fluvial Sedimentology*, Canadian Society of Petroleum Geologists Memoir 5, Calgary, Alberta, Canada, p.257-275.
- Thompson, R. and Oldfield, F. (1986) *Environmental Magnetism*, Allen and Unwin, London.
- Webb, R.H., O'Connor, J.E. and Baker, V.R. (1988), 'Palaeohydrologic reconstruction of flood frequency on the Escalante River, South-Central Utah', in, Baker, V.R., Kochel, C.R. and Patton, P.C. (eds.), *Flood Geomorphology*, John Wiley and Sons, New York, p.403-418.
- Wolfenden, P.J. and Lewin, J. (1977), Distribution of metal pollution in floodplain sediments. *Catena* 4, 309-317.
- Woodyer, K.D., Taylor, G. and Crook, K.A.W. (1979), 'Depositional processes along a very low-gradient, suspended-load stream: the Barwon River, New South Wales', *Sedimentary Geol.*, 22, 97-120.
- Wymer, J.J. (1968), *Lower Palaeolithic Archaeology in Britain*, John Baker, London.
- Wymer, J.J. (1976), The interpretation of Palaeolithic cultural and faunal material found in Pleistocene sediments, in, *Geo-archaeology*, Davidson, D.A. and Shackley, M.L. (eds.), Duckworth, London, pp.327-34.
- Young, B. Bridges, T.F. and Ineston, P.R. (1987), 'Supergene cadmium mineralisation in the Northern Pennine orefield', *Proceedings of the York. Geol. Soc.* 46(3), 275-278.

YEAR	DAY & MONTH	YEAR	DAY & MONTH	YEAR	DAY & MONTH
1891	24 AUGUST	1930	26 JULY	1960	10 OCTOBER
1892	2 SEPTEMBER	1931	7 NOVEMBER	1962	3 APRIL
1892	3 NOVEMBER	1933	1 FEBRUARY	1962	27 AUGUST
1895	3 AUGUST	1934	17 MARCH	1962	11 SEPTEMBER
1900	6 OCTOBER	1934	14 APRIL	1963	21 NOVEMBER
1900	27 OCTOBER	1936	14 DECEMBER	1964	8 DECEMBER
(5) 1903	9 OCTOBER	1938	8 OCTOBER	1965	30 JULY
1904	24 NOVEMBER	1939	9 JANUARY	(6) 1967	17 OCTOBER
(10) 1906	30 MAY	1939	1 DECEMBER	1968	23 MARCH
1907	9 JUNE	1941	17 FEBRUARY	1968	13 SEPTEMBER
1911	14 MAY	(3) 1947	22 APRIL	1975	30 AUGUST
1912	- JUNE	1948	20 AUGUST	1976	21 JANUARY
1919	1 NOVEMBER	1953	12 NOVEMBER	1977	26 JANUARY
(9) 1923	13 NOVEMBER	1954	3 APRIL	1978	28 DECEMBER
(4) 1924	30 DECEMBER	(7) 1954	18 OCTOBER	1979	29 MARCH
(8) 1926	20 SEPTEMBER	1954	2 DECEMBER	1979	26 NOVEMBER
1927	23 JULY	(1) 1955	10 JANUARY	1981	3 MARCH
1927	21 SEPTEMBER	1956	17 FEBRUARY	(2) 1986	26 AUGUST
1929	10 AUGUST	1956	28 AUGUST	1990	4 FEBRUARY
1929	16 NOVEMBER	1958	12 FEBRUARY		

Table 1 Documented floods in the River Tyne 1891 - 1990 as recorded in local newspapers, books, journals and meteorological publications

The ten largest floods and their probable ranks are also indicated



DEPTH (cm)	DATE	SEDIMENTATION RATE (cm a-1)	MEAN LOI (%)
— 0 —	1990	0.3	4.2
— 10 —	1950	0.8	5.5
— 18 —	1940	1.2	5.3
— 30 —	1930	7.0	2.9
— 100 —	1920	5.0	3.1
— 150 —	1910	3.0	3.3
— 180 —	1900	5.0	3.1
— 230 —	1890		

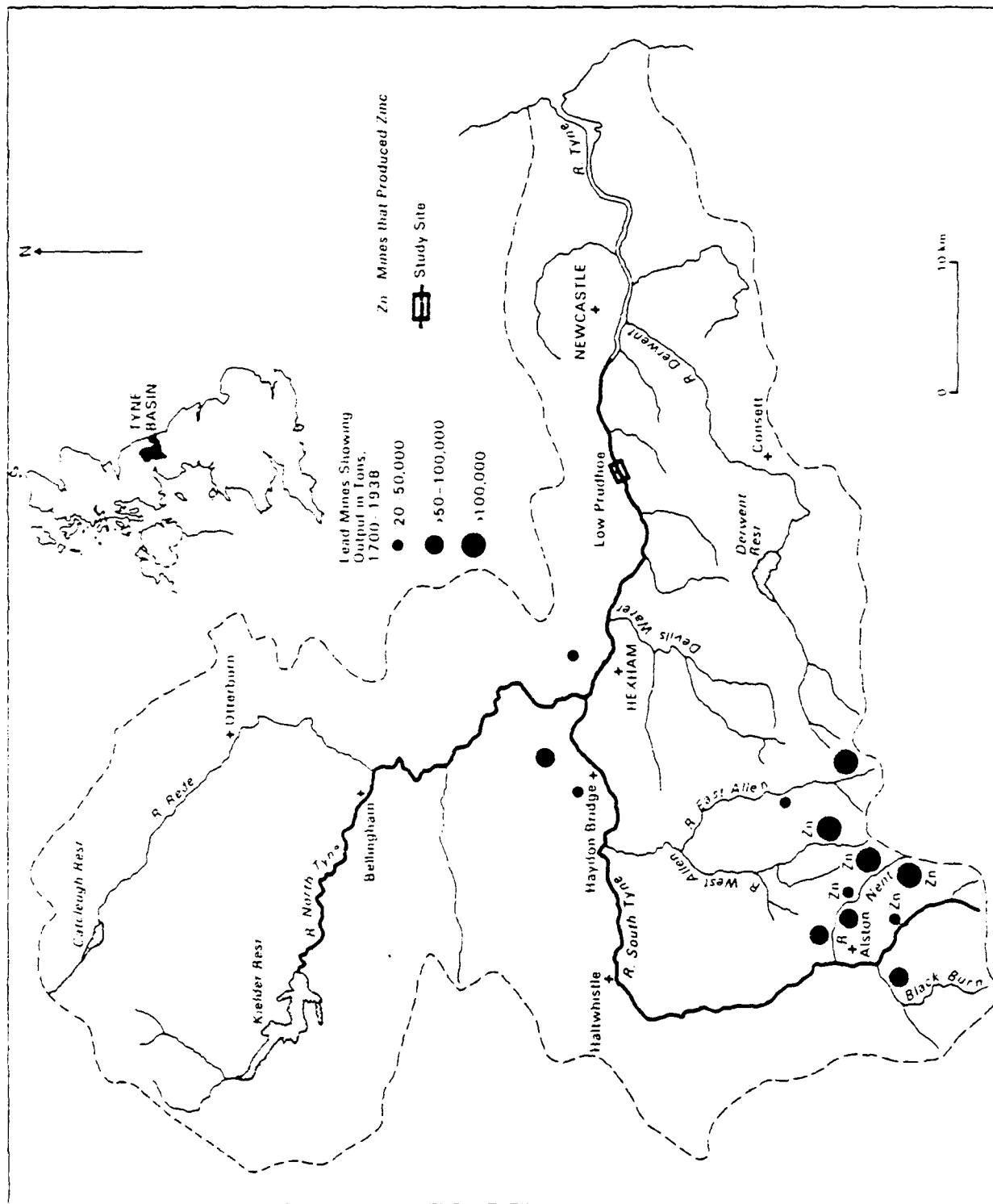
Table 2 Rates of fine-grained vertical accretion at Low Prudhoe 1890-1990

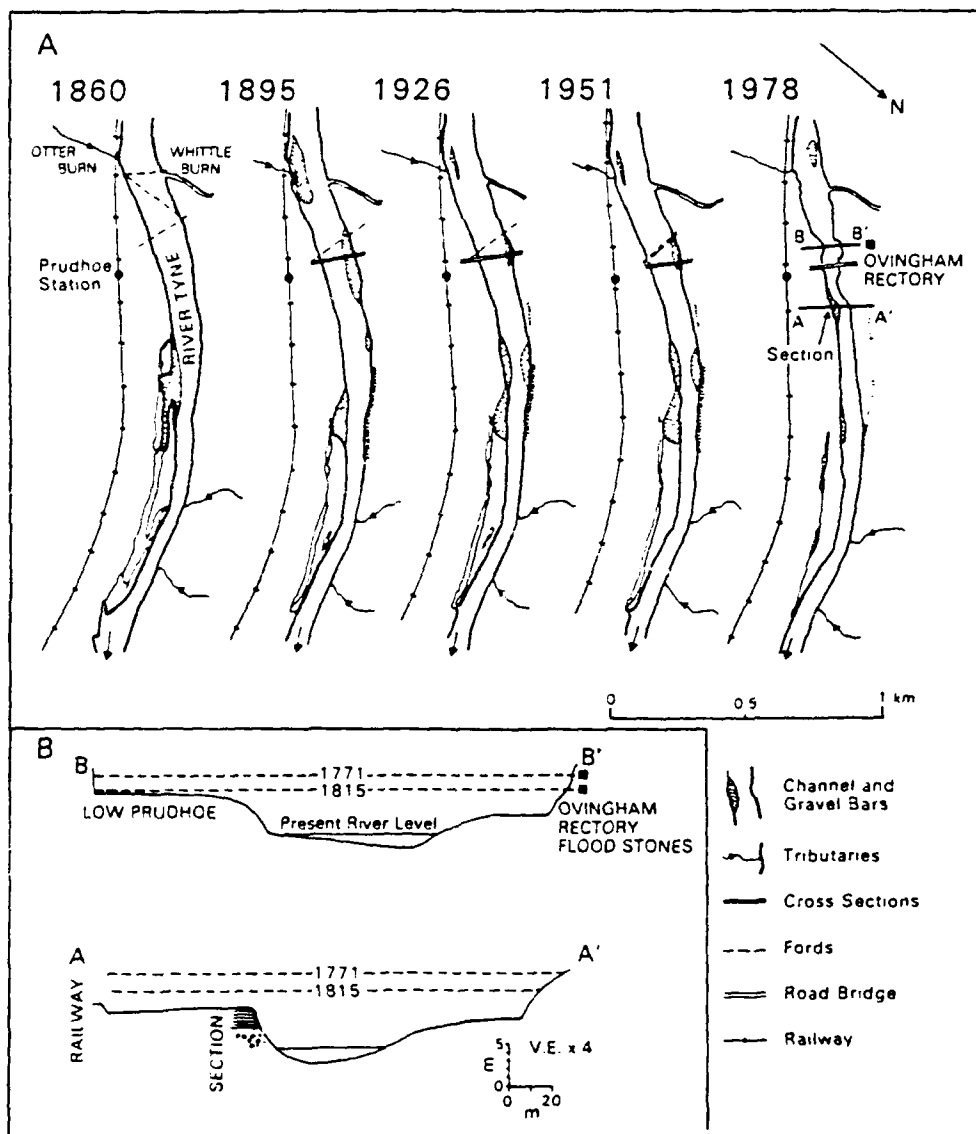
Table 3 Fine-grained vertical accretion rates in selected British river basins

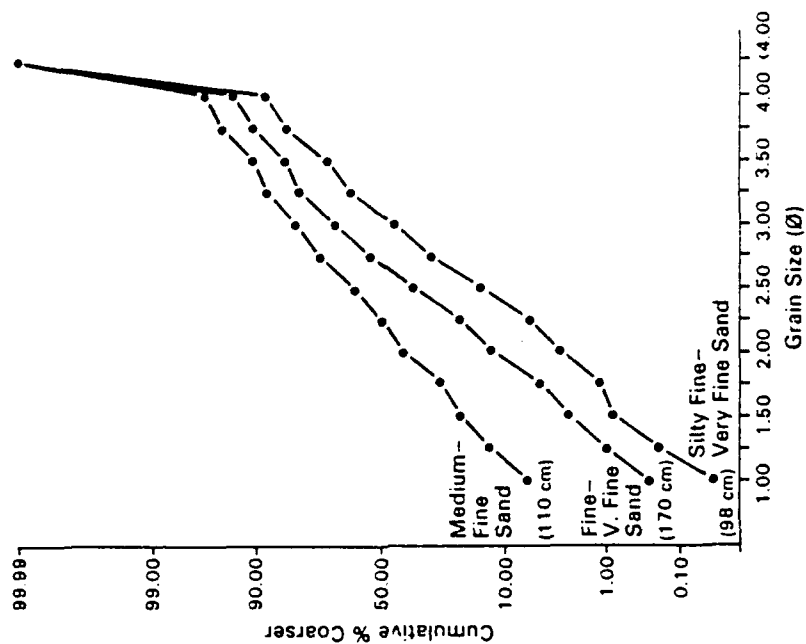
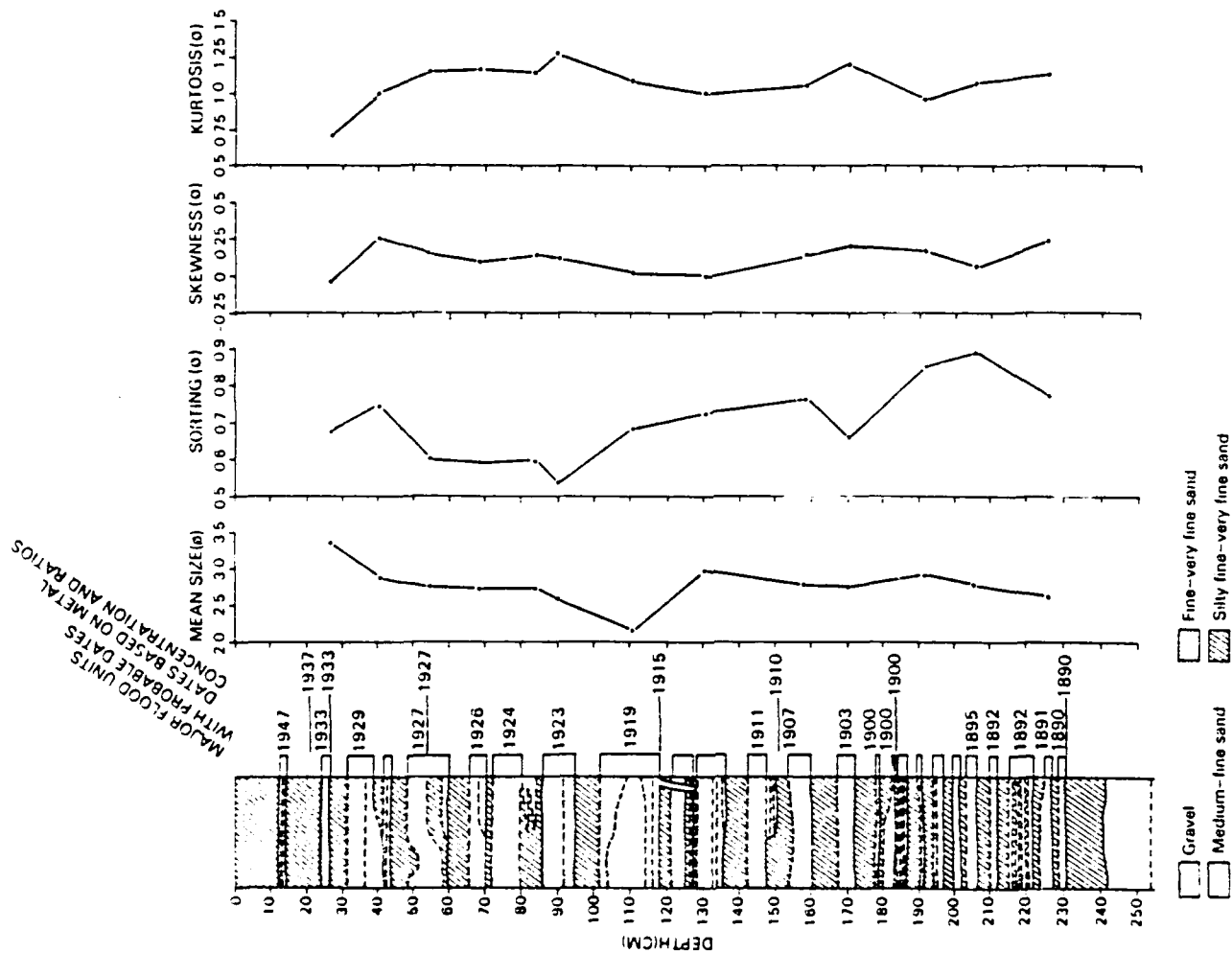
AUTHOR	RIVER BASIN	CATCHMENT AREA (km <sup>2</sup> )	SEDIMENTATION RATE (cm a <sup>-1</sup> )	TIME SCALE OF DEPOSITION (yr BP)
BROWN, 1987	SEVERN, UK	10000	0.14	0-10000
<b>THIS STUDY</b>	<b>TYNE</b>	<b>2198</b>	<b>2.37</b>	<b>0 - 97</b>
SHOTTON, 1978	AVON	1870	0.50	0 -3000
BRENNAN AND MACKLIN, UNPUBLISHED	SWALE	550	0.53	0 - 130
MACKLIN, 1985	AXE	31	0.54	0 - 312
BROWN AND BARBER, 1985	RIPPLE BROOK	19	0.05	0 -2500
-----				
BROWN, 1985	STOUR	620	10.20	MAXIMUM DEPTH OF OVERBANK DEPOSITION IN 1979 FLOOD
MACKLIN AND NEWSON, UNPUBLISHED	SWALE	550	13.00	MAXIMUM DEPTH OF OVERBANK DEPOSITION IN 1986 FLOOD
LAMBERT AND OVERBANK WALLING, 1987	CULM	276	0.05	AVERAGE  SEDIMENTATION 1983-1984

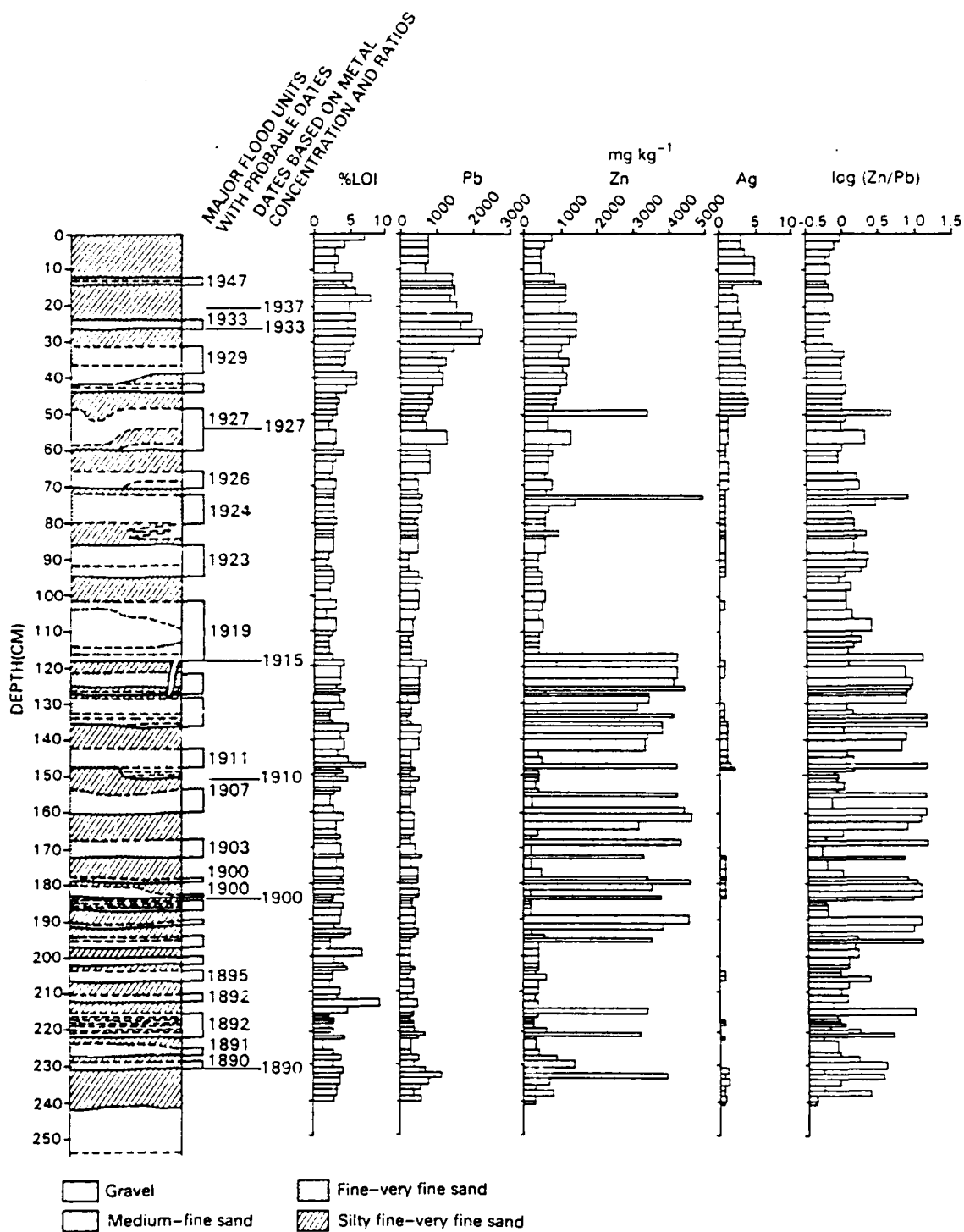
### List of Figures

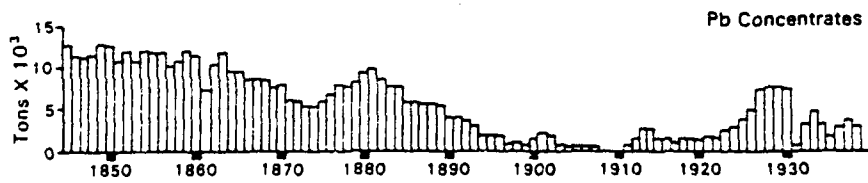
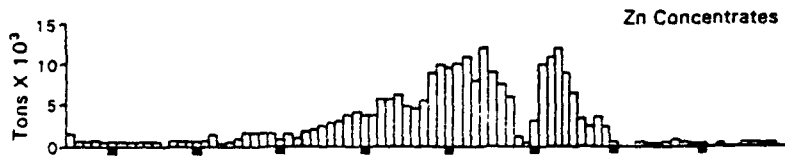
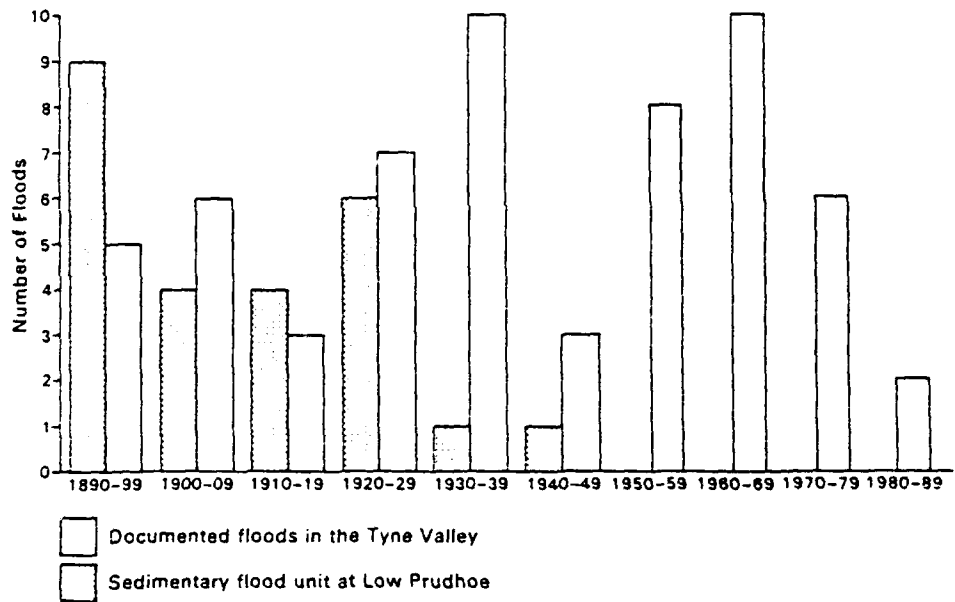
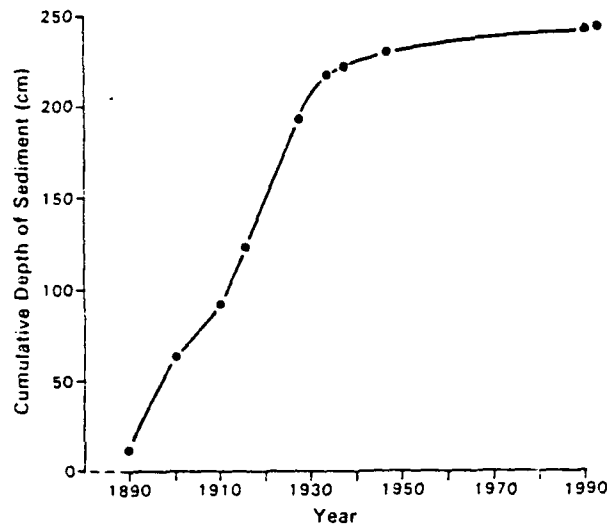
- Figure 1                      The Tyne basin showing location of study reach at Low Prudhoe, drainage network and metal mines.
- Figure 2                      (a) Maps showing channel change at Low Prudhoe between 1860 and 1978, and location of section.  
(b) Channel cross sections upstream and downstream of Ovingham bridge. Relative heights of 1771 and 1815 floods are indicated.
- Figure 3                      Sedimentary log and summary moment statistics of vertically accreted alluvium at Low Prudhoe.
- Figure 4                      Grain size curves for type 1 (medium-fine sand), type 2 (fine-very fine sand) and type 3 (silty fine-very fine sand) flood units.
- Figure 5                      Metal concentrations and organic matter content in vertically accreted alluvium at Low Prudhoe showing major flood units with their probable dates.
- Figure 6                      Lead and zinc production in the Tyne basin 1845 - 1938 (after Dunham, 1944).
- Figure 7                      Comparison of floods documented in the lower Tyne Valley (between 1890 and 1949) and the sedimentary flood record at Low Prudhoe.
- Figure 8                      Sediment-accumulation curve for Low Prudhoe 1890-1990.













3rd International Workshop on Gravel-Beds Rivers,  
Firenze, 24-28 September 1990

Martin N.R. JAEGGI

Laboratory of Hydraulics, Hydrology and Glaciology  
of the Federal Institute of Technology Zurich  
ETH-Zentrum, CH-8092 Zurich

EFFECT OF ENGINEERING SOLUTIONS ON SEDIMENT TRANSPORT

Abstract

The scope of engineering works on rivers are flood capacity, navigability and water use. Channel stability is a necessary condition for these purposes. The concept of a static stable channel or a dynamic equilibrium between sediment supply and channel geometry is usually the base of river training methods. Very often an overcapacity of sediment transport was induced by regulation works, which was necessary for a certain time to create the desired channel shape. Long term evolution often resulted in substantial erosion, what called for additional drop structures. At lower slopes an apparent equilibrium is possible, what means that non-equilibrium conditions will induce geometrical changes only over an extremely long period. On steeper slopes, buffers (e.g. between sills) usually reduce the effects of long term changes.

1. Natural Gravel Bed Rivers

Natural alluvial rivers with gravel bed do form their channel in their own deposits or in ancient fluvial or glacial deposits. In the first case, they are usually aggrading (see fig. 1). Erosion is more common in the upper reaches of such rivers, although often limited by rock outcrops. Fig. 2 shows an example of a degrading reach, which lies upstream of a gorge which is incised in a rock barrear, which had originally formed a lake. This incision is followed by a degradation process in the lake deposits.

The width of these rivers normally adjusts to a value which corresponds nearly to conditions of beginning of motion for a low frequency flood discharge (Parker, 1976).

Natural gravel bed rivers are usually braided, as shwon in Fig. 1 and 2. Smaller rivers with coarser bed material tend to meander. Straight reaches are found in boulder bed channels.

Therefore, natural gravel bed rivers are not stable, but shift their channels as a consequence of their planform, and are aggrading or degrading. Except for steep mountain gullies, these processes can be expected to be slow because of the large channel width and the associated low bed shear stresses.



Fig. 1 Rakaia River (New Zealand) near its mouth, in an aggrading reach



Fig. 2 Rakaia River (New Zealand) in its middle reach, where it is incising in old lake deposits

## 2. Static and Dynamic Equilibriums - Scope of river Engineering Work

Land reclamation, flood protection, navigation, and use of water power all need stable channels. This stability must be warranted by a dynamic equilibrium between sediment transport capacity and sediment supply (Zanke, 1972). Meyer-Peter and Lichtenhahn (1963) claim the search for such an equilibrium to be the main objective of river engineering works.

If there is no or negligible sediment supply to a river reach, equilibrium there can be only a static one. The discharge should always remain smaller than the one responsible for beginning of motion. In gravel bed rivers, critical conditions of an armour layer become dominant (Guenther, 1971).

In general, river training works tend to produce narrow and straight channels in order to increase transport capacity. In eroding channels the bed resistance is increased or drop structures are inserted to reduce the channel slope and thus transport capacity (e.g. see Ashida 1987).

It is interesting to note that there is almost no discussion about equilibrium in sand bed channels. Janssen et al. (1979) consider fixation of a channel against the natural migration associated with planforms as the only stabilisation scope. It seems that owing to the very low slopes a major difference between transport capacity and sediment supply does not necessarily create major problems. In trained gravel bed channels with slopes of the order of 0.1 to 1.0 ‰, such differences can lead to rapid fill or scour as a result of change in slope, what in turn leads to a loss of flood capacity or collapse of bank protections. Channel narrowing reduces substantially the sediment storage capacity; so that aggradation and degradation processes will be substantially faster in the trained than in the natural channel.

## 3. Effect of a Channel Geometry Change on Sediment Transport Capacity

### 3.1 Theoretical background

All the particles which are relevant for the formation and alteration of a gravel bed channel move as bedload. Even the finer bedload particles may not be involved in this process. Considering bed load transport capacity of a channel, care has to be given to the representative grain sizes.

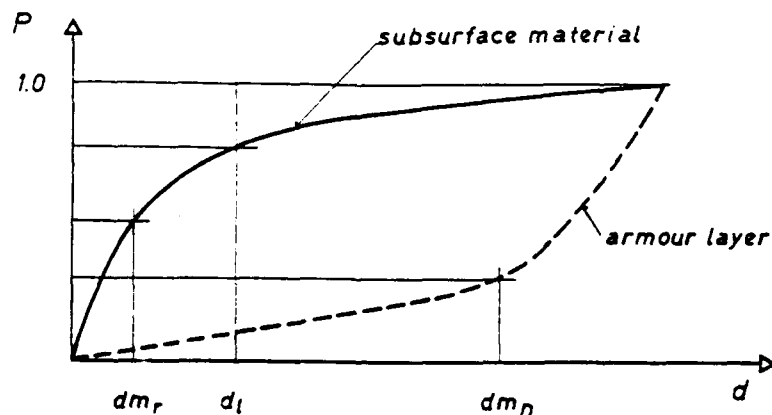


Fig. 3 Grain size distribution of gravel bed, and of the armour layer. Mean grain size  $d_{mr}$  of moving bedload and mean grain size of armour layer  $d_{mD}$ .

Fig. 3 shows a typical grain size distribution of a gravel bed and of possible armour layer. Numerical simulation has shown that a reduced mean grain size of the subsurface material and the mean grain size of the armour layer can be used as the characteristic grain sizes (Hunziker and Jaeggi, 1988).

The reduced mean grain size is supposed to represent the moving bedload material and is defined by

$$d_{mr} = \frac{\sum_{i=1}^n \Delta p_i \cdot d_i}{\sum_{i=1}^n \Delta p_i} \quad (1)$$

where  $d_i$  is the mean grain size of a fraction.  $\Delta p_i$  the proportion of this fraction in the mixture measured by weight, and  $n$  the number of fractions finer than a limiting diameter  $d_L$ .  $d_L$  is normally characterized by a sudden change of the gradient in the grain size distribution curve.

The mean grain size of the armour layer corresponds to the usual definition

$$d_{mD} = \sum \Delta p_{Di} \cdot d_i \quad (2)$$

which this time extends over all the fractions.  $\Delta p_{Di}$  represents the proportion of a fraction in the armour layer and can be calculated by Gessler's (1965) procedure of others.  $d_{mD}$  is commonly approximated by  $d_{90}$ .

Sediment transport theory allows to define a sediment transport capacity for given channel cross section, slope, grain-size and discharge. A generalized version of a transport formula for gravel bed rivers, applicable over a wide range of slopes (Smart and Jaeggi, 1984), is

$$Q_{TC} = \left( \frac{\alpha}{(\rho_s/\rho_w - 1)} \right) \beta Q J^{1.6} \left( 1 - \frac{1}{\eta} \right) \quad (3)$$

where  $Q_{TC}$  [ $m^3/s$ ] is the bedload transport capacity over the full width,  $\rho_s$  [ $kg/m^3$ ] and  $\rho_w$  [ $kg/m^3$ ] the densities of sediment and water,  $Q$  the water discharge, and  $J$  the slope.  $\alpha$  is a coefficient determined experimentally to be  $4 \leq \alpha \leq 4.8$ , it may be considered as a variable in a somewhat wider range to account for the problem of fitting a single equation to numerous transport experiments.  $\beta$  is an efficiency factor.  $\beta = 1$  corresponds to ideal condition in a laboratory flume with negligible wall drag. In straight single channels with plane bed wall drag reduces  $\beta$  to  $0.7+0.9$ . In strongly meandering or braided channels  $\beta$  may decrease to be  $0.1+0.3$ , but will definitely not reduce to zero. Finally

$$\eta = \frac{\theta}{\theta_{cr}} = \frac{h_m J}{(\rho_s/\rho_w - 1) d_{mr} \theta_{cr}} \quad (4)$$

with  $\theta_{cr} \approx 0.05$  and  $h_m$  being a representative flow depth in the bedload carrying parts of the channel.

Armouring is considered by a value of

$$\eta_D = \left( \frac{d_{mD}}{d_m} \right)^{0.67} \quad (5)$$

For  $\eta \leq 1$  there is no motion, for  $1 \leq \eta \leq \eta_D$  material of size  $d$  supplied from upstream can be moved downstream, and for  $\eta \geq \eta_D$  bed erosion is possible and thus supply of sediment from the bed in the absence of upstream supply.

If  $Q(t)$  is a duration curve of a river, then

$$W = \int_0^T Q dt \quad (6)$$

is the total water yield over a period  $T$ , usually taken as one year. Using eq. (3) over the whole discharge range, then one gets bedload yield over the same period  $T$ :

$$GF = \beta \cdot J^{1.6} \frac{\alpha}{(\rho_s/\rho_w - 1)} \int_0^T Q \left(1 - \frac{1}{\eta}\right) dT = A \int_0^T Q \left(1 - \frac{1}{\eta}\right) dT \quad (7)$$

Fig. 4 shows that the integral part corresponds to an "effective part" of the water yield over the period  $T$  for sediment transport. The reduction is due to the beginning of motion conditions expressed by  $1/\eta$ . Potential erosion yield only is given for the period  $T_D$  for which  $\eta_D$  is exceeded. This is characterized by  $F_1$  and thus the corresponding minimum transport capacity by  $A \cdot F_1$ . Considering sufficient supply from upstream, the period  $T_0$  with  $\eta \geq 1$  must be considered. The corresponding area is the  $F_1 + F_2$  and the maximum transport capacity  $A(F_1 + F_2)$ .

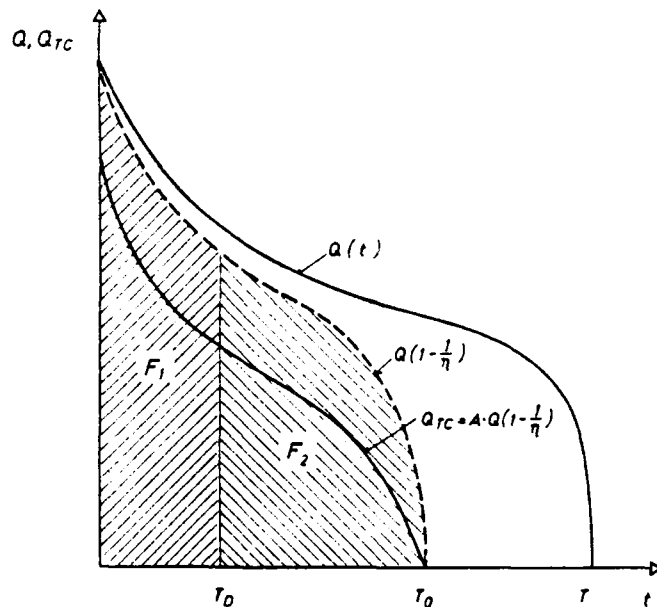


Fig. 4 Definition of maximum  $(A \cdot F_1 + A \cdot F_2)$  and minimum transport capacity  $(A \cdot F_1)$  over a period  $T$ .  $T_0$  is the part of the period for which  $\eta \geq 1$ ,  $T_D$  with  $\eta \geq \eta_D$ , and  $T_{1D}$  with  $\eta \geq 2 \eta_D$ .

### 3.2 Discussion

A change in channel geometry (cross-section or alignment) results in a change of transport capacity (yields) as defined by eq. (7). Such a change may vary the slope, the efficiency factor  $\beta$ , or the area  $F$  by  $\Delta F$  as a function of a variation of  $\eta$ . The change of one parameter may be dominant, but all of them may vary.

For two channel geometries, and in particular a material and an artificial one, transport capacities expressed in terms of annual yields can be defined and compared. According to the particular situation, maximum or minimum values on one of each may be considered. The ratio of transport capacities leads to an expression

$$\frac{GF_i}{GF_j} = \frac{\beta_i J_i^{1.6}}{\beta_j J_j^{1.6}} \frac{F_i}{F_j + \Delta F} \quad (8)$$

$F_i$  and  $F_j$  may represent  $F_1$  or  $F_1 + F_2$ , according to the particular situation.  $\Delta F$  is dependent on the variation of the period with bedload transport (increase or decrease of  $T_0$ ) and the change in the function  $Q(\eta)$ . Equation (8) allows to discuss, at least approximatively, the change in "efficiency" (parameter  $\beta$ ) compared to a change in slope and the shift due to alteration in the condition for beginning of motion.

Another advantage of the discussion of transport capacities based on  $\beta$ ,  $J$  and  $F$  or  $\Delta F$  is that this expression (8) is not dependent on the fit of a transport formula to experimental results. This is described by the parameter  $\alpha$  not appearing in this discussion.

A variation of the morphological conditions changes mainly  $\beta$ . Channel narrowing associated with a change from a braided river to a plane bed channel results in an increase for  $\beta$  from about 0.2 to 0.9. The change in  $\eta$  may be small compared to this if the slope does not change and  $\eta$  for the braided river was defined in the main bed load carrying channels. This shows the order of magnitude of a change produced by an engineering solution in the sediment regime of a river.

A disequilibrium probably exists along a river a channel. Expression (8) allows to find out within which limits transport capacity can be varied with variation of channel geometry to obtain a continuous sediment transport, what is the objective of engineering solutions. It may well be that along a channel a desired continuity of identical transport capacities cannot be realised, e.g. for a continuously decreasing slope. This limits the application of a dynamic equilibrium concept.

Many other kinds of comparative calculations based on equation (8) can be imagined, which can visualize the effect of engineering solutions. In particular, changes in geometry resulting from other needs than sediment regime can be evaluated.

## 4. Training Works and Sediment Transport

### 4.1 Generalities

Straightening of a river course and narrowing of the cross-section is normally the consequence of major river training schemes. An increase in slope and a width reduction normally result in an increase of transport capacity. Fig. 5 show the relation between annual bedload yield (function of the discharge duration curve) and channel width for different slopes.

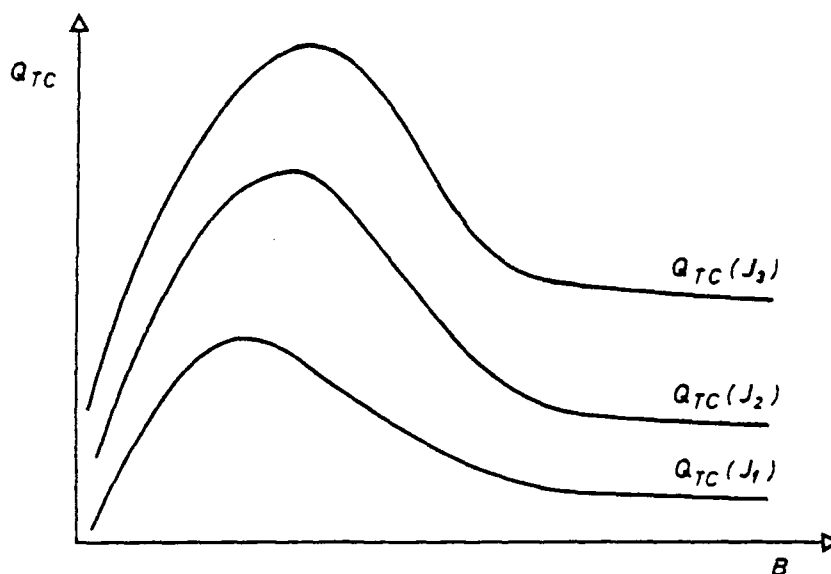


Fig. 5 Bedload yield as a function of channel width for different slopes ( $J_3 \geq J_2 \geq J_1$ ) for given discharge duration curve

Obviously, an increase in slope means the shift from one curve to the upper one and thus an increase in transport capacity. In a certain range of channel widths, narrowing also produces an increase of sediment transport capacity. For very narrow channels, the opposite could happen, because of wall drag. For very wide channels, due to the braided pattern, transport capacity is almost independent of channel width. Finally, for given slope and duration curve, there is always a maximum of transport capacity (annual yield) which cannot be exceeded by any change of cross-sectional geometry.

Trained rivers have very often a channel width which corresponds to this maximum of transport capacity. Further narrowing of the section does therefore not induce a further increase in transport capacity. A reduction from natural width (braided channel) to an "optimum" width (corresponding to maximum transport capacity) induces a substantial increase in transport capacity. This is equivalent to an increase of the efficiency parameter  $\beta$ , discussed above, from about 0.2 to a value near 1.0. A width reduction is almost irrelevant on transport capacity if it for both widths the channel is braided. This latter case was characteristic for some of the early training works where the natural aggradation rate was not altered, but the deposition area reduced and thus the bed elevation rate increased (Jaeggi, 1989).

#### 4.2 Overcapacities induced by River Regulation

An accelerated aggradation was the major fear of river engineers during the 19th century. If the river started to degrade after a regulation scheme was applied, this was considered to be a success. For this to happen, overcapacities had to be accepted. At that time, it was not possible, or not economic, to excavate the full desired channel cross-section. This work was left over to the river erosion. Since normally one objective of river training work was to lower flood levels, if possible even below ground level, this resulted in a potential erosion volume which corresponds to many annual bedload yields.

Normally, regulation works were executed upstream and extended over years and decades. As fig. 6 shows, the reach where a training scheme was finished delivered an extra load which saturated the overcapacity in the downstream reach. Only because of this overcapacity the downstream reach was able to evacuate natural supply plus the extra load. It is only a

certain time after this extra delivery had stopped, after the training works even in the tributaries were finished, that an erosion exceeding the originally accepted amount was the consequence. The river was still completing the natural supply by an extra load from the river bed. Many regulated Alpine rivers show such an erosive behaviour.

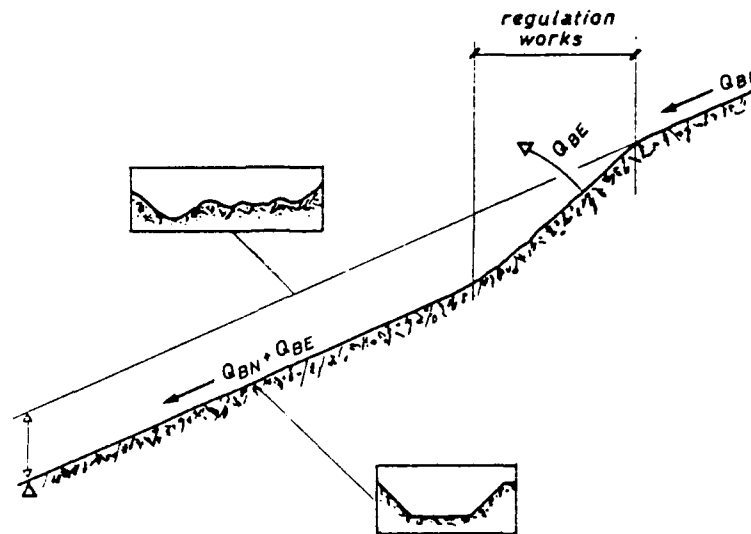


Fig. 6 Lowering of river bed, the aim of many river regulations, producing an extra load of sediment. The reach downstream of the construction site is maintained in equilibrium by the natural supply plus the extra supply

#### 4.3 The River Danube Downstream of Vienna

From a multiple channel river the Danube near Vienna has been transformed in a more or less single thread channel for navigation purposes in the 19th century. Between this main channel and the remote flood protection dykes a natural habitat had been preserved or even redevelopped, which had become internationally famous. Upstream of Vienna, after World War II a series of hydro-power schemes again designed for improvement of the navigation have been developed. Downstream of Bratislava (CSFR) the scheme of Gabčíkovo is now almost completed. Some years ago the building of the Hainburg power plant was supposed to fill the gap. National and international protests finally prevented that these scheme was realised and the river forest in the remnant flood plain was protected.

Since the last centuries regulation, but now with increased speed because of the hydro-power development in the upstream reach and gravel dredging for improvement of the navigation, the Danube erodes its bed. The project of building a power plant in Vienna would even increase the problem in the downstream reach. This was investigated recently with the aid of a numerical simulation (VAW, 1989).

It came out that the rate of erosion is reasonably small, despite the general trend of incision. The local erosion in the upper reaches (what means downstream of the last power plant) is sufficient to nearly saturate the deficit in transport capacity for a long time. Again, a comparatively steep downstream reach can thus be held in equilibrium over decades until the supply to this reach decreases. The incision rate is slow because the annual minimum transport capacities (yields), which are relevant for erosion, are small compared to the volumes involved. As fig. 7 shows, it would need over 80 years to erode the bed between 0.3 and 1.1 m.



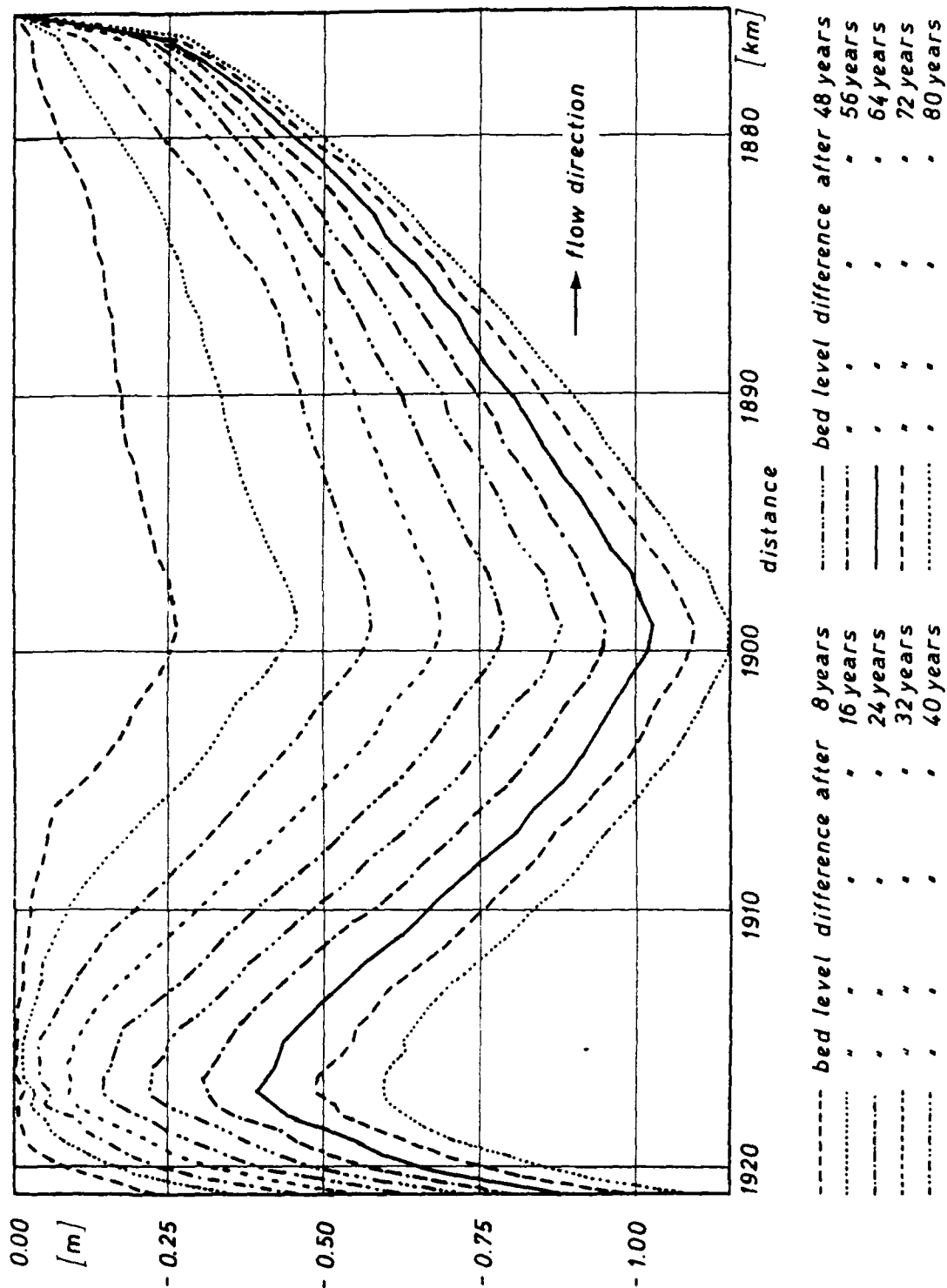


Fig. 7 Bed level differences calculated in the Danube between Vienna (km 1921) and the Austro-Czechoslovakian border (km 1875) in a 80 year simulation

#### 4.4 The Emme River

The Emme river is a tributary of the Aare river in Switzerland. Over about 60 km it has been trained in the second half of the last century and the first thirty years of this century. The valley slope is 0.8 ‰ in the upper, 0.6 ‰ in the middle, and 0.4 ‰ in the lower reach.

An evolution as described in section 4.2 occurred in this river. After completion of the lower parts of the scheme, the desired erosion was observed. Often, it was considered to be too slow and dredging plants were installed to speed up the process. However, after the extra supply from the regulation works progressing upstream was diminishing, bed erosion as shown in fig. 6, associated with a lowering of bed slope started. Drop structures were built to stop this process and to protect local structures like bridges and water intakes. After about 80 years about one third of the total head in the regulated river reach corresponds to the sum of the drops of these structures. Investigation of the bedload regime (Hunziker and Jaeggi, 1988; Jaeggi, 1989) has shown that the bed erosion had not stopped since the regulation scheme was applied and was still nowadays a consequence of the original overcapacity. Assuming that the actual training works would not be destroyed by further erosion, it would need another 50 years to reach some sort of equilibrium conditions. The actual situation and such a future evolution is shown in fig. 8. The actual sediment regime is therefore far away from an equilibrium one, with a two and a half fold increase of the yield along the channel.

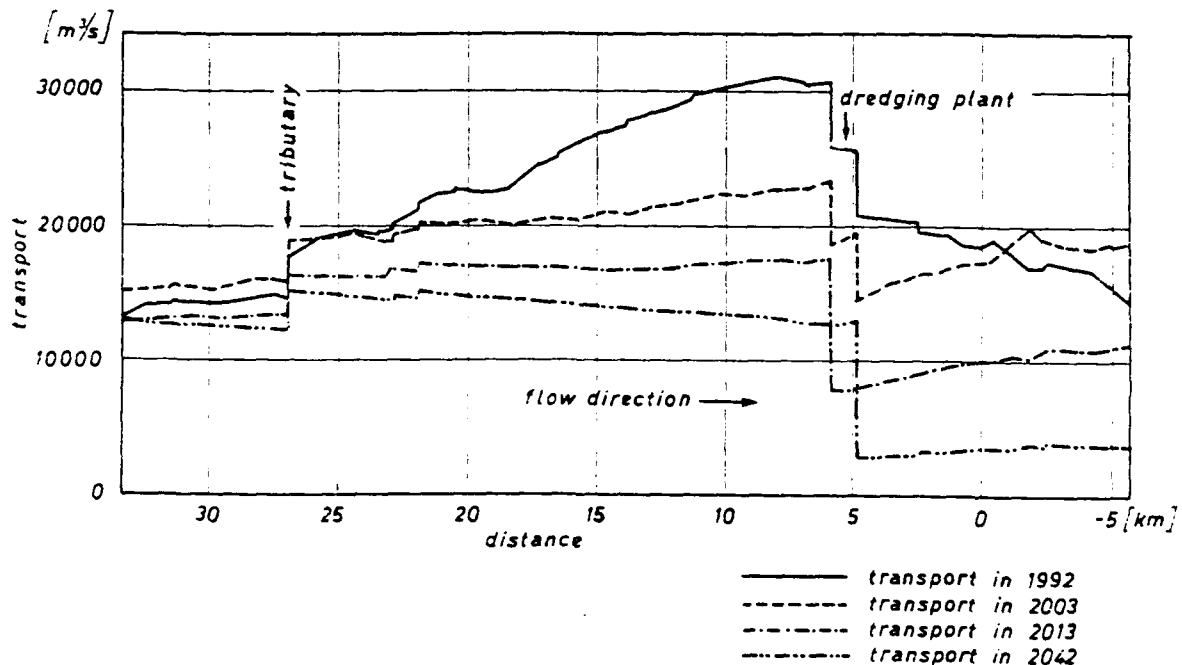


Fig. 8 Actual transport situation along the Emme river and future evolution (for idealised conditions)

## 5. Discussion of the Long Term Equilibrium

Analysis of transport capacity along a river reach, would very probably lead to a diagnosis of disequilibrium. The question is how to cope with this situation.

### 5.1 The Apparent Equilibrium

If transport capacities are small, for small slopes and/or coarse bed material, then a non-equilibrium situation does not mean that an immediate adjustment is induced. Channel geometry may be apparently stable, although transport capacities and sediment supply do not correspond. The Danube downstream of Vienna reacts very slowly to the reduction to zero of the sediment supply. A final equilibrium stage would be reached only after centuries. From one year to the other, theoretical bed level changes are in the order of millimeters or centimeters. This may be called the apparent equilibrium.

### 5.2 The Quasi-Equilibrium

On a differential scale, the equilibrium conditions are fulfilled. A difference between local transport capacity and sediment supply to a limited reach is compensated by local erosion or aggradation. On a larger scale, this local compensation may maintain a longer reach in equilibrium over a certain time period. One example is the regulated reach being fed by the extra load of erosion out of a freshly trained reach. As for erosion, in case of too low capacities a local buffer may take over the aggradation rate and supply a smaller rate to a downstream reach which is then in equilibrium with this small rate.

Although it is obvious that a long term scale the situation will change, such a quasi-equilibrium may well be stable over years or decades.

### 5.3 Concept of Buffers

#### 5.3.1 Aggrading Reaches

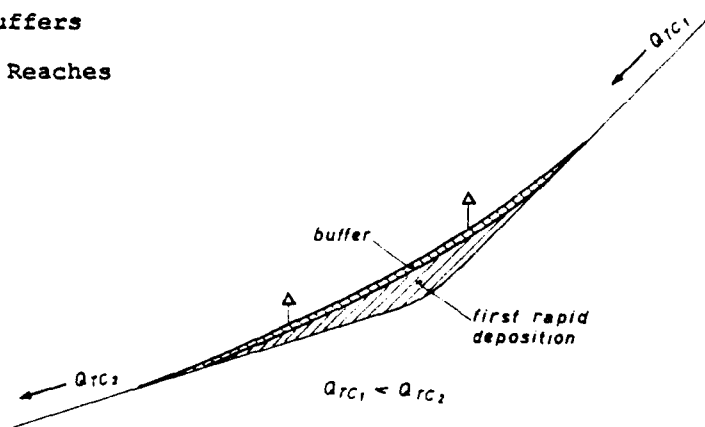


Fig. 9 Concept of a buffer in an aggrading reach

Naturally, the slope of alluvial rivers is decreasing downstream, and therefore normally also transport capacity. In case of an apparent equilibrium, aggradation is very slow because it spreads over a long distance. The potential aggradation volume (see fig. 9) can be viewed as a buffer. Assuming that the aggradation rate is constant, this means that there must be a constant decrease in transport capacity. In case of change in slope, as in fig. 10, it can be expected that a first quick aggradation fills up a first volume and allows that a linear buffer to take over the

loads of following years. In a situation like shown for the Danube, a buffer defined by a considerable length may take over many annual loads with a small change in bed level. A regulation scheme which leads to such an aggradation, or cannot prevent it, is still economic, if the effect of aggradation e.g. on flood capacity is felt only after a period of fifty or hundred years. After that period, a new scheme may be applied.

Fig. 9 applies to natural rivers as well. It may be noted again that regulation schemes which had failed had, in such situations, just reduced the channel width and so the width of the buffer. Thus, a natural slow aggradation rate was changed to a dramatic one.

### 5.3.2 Degrading Reaches

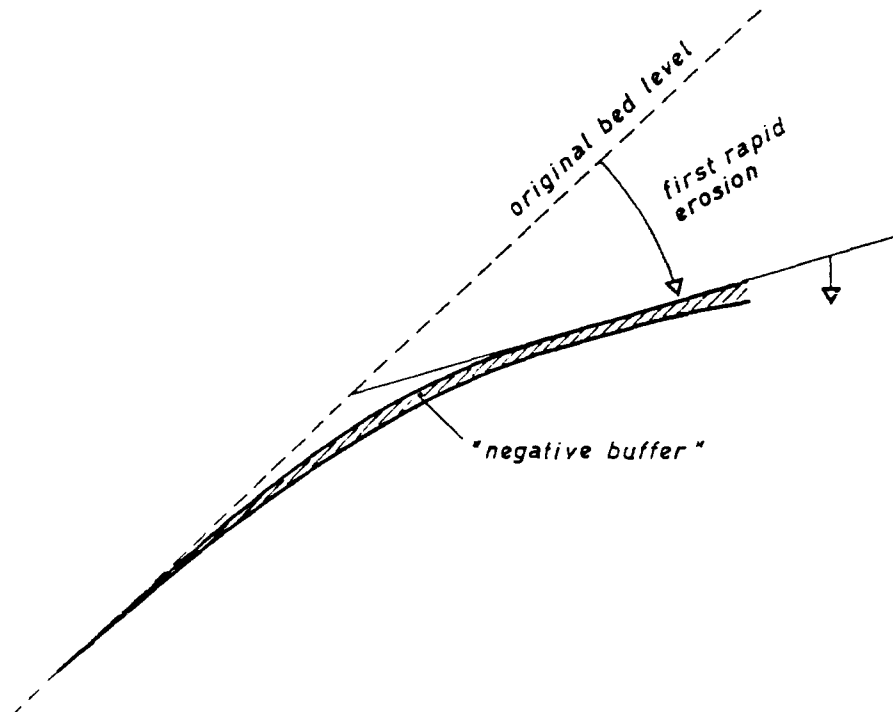


Fig. 10 Buffer in degrading reaches

A change in the transport capacity or the sediment supply may produce an erosion trend as shown in fig. 10. After a first rapid erosion again a transition reach develops whose contribution to the supply to the downstream reach may become substantial. Such an evolution was shown to happen in the Danube river after reduction of sediment supply. Again, this sort of negative buffer may have a sufficient influence so that a change in channel geometry becomes necessary only in a remote future.

### 5.3.3 Stepped Channels (artificial and natural)

Most of the steeper regulated rivers do form a sequence of artificial drop structures, as described for the Emme river. Steep natural river from step-pool systems (Whittaker, 1987) which have again a buffering effect on sediment transport.

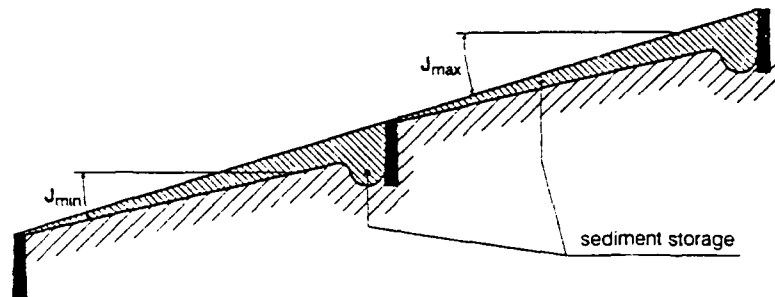


Fig. 11 Buffers in stepped channels

In both cases, the crest of the steps defines maximum transport capacity, which is function of the valley slope. This is never or rarely reached, because of natural or artificial overcapacity. A flatter slope between the steps defines a minimum transport capacity, corresponding to flow conditions for which the system is still stable with respect of scouring the steps. If the natural supply to the system is within the range defined by this two slopes, then the system remains stable. It is therefore insensitive to variations in sediment transport, which would just fill and empty the buffers. It is not surprising that this system of including overcapacity and erosion control is quite popular.

It should be noted that Fig. 11 can strictly be applied only for spacings of the steps of several hundreds of meters and more. For smaller spacings, the concept applies to the energy line but not the bed level. This takes then more a scour form. The scour is still a buffer, but its shape depends not only on the energy line and the filling of the buffer, but on local flow conditions also.

## 6. Dredging

Dredging is a solution often applied to cope with discontinuities of transport capacity along a channel reach. Since a maximum of transport capacity exists irrespective of any change in geometry it may often be the only solution in case of large discrepancies.

Dredging is delicate if a certain transport rate downstream of the intervention point is required. Very often, an erosion problem results. In the presence of large buffering areas, the river's reaction to excessive or insufficient dredging quantities is slow. Problems with dredging in the Alpine Rhine (Meyer-Peter/Lichtenhahn, 1963, Lichtenhahn, 1972) may be viewed as an example of such a situation. There, after a last change in the regulation scheme, accomplished in 1954, a dredging company had to be paid for the excavation work. In the sixties, dredging became commercially interesting and the dredged quantities excessive. The subsequent erosion led to the collapse of the road bridge Buchs-Schaan in 1970.

## 7. Conclusions

River engineering solutions often change dramatically the sediment regime of a river. Often, such a change was the scope of the scheme. A dynamic equilibrium between sediment supply to a reach and transport capacity along the reach was considered to be the optimum solution. Effectively, buffers in long and wide river reaches or defined by artificial steps play an important role in sediment balance. Long term changes which are function of the behaviour in this buffers may lead to new conditions, in apparantly stable river reaches.

# Computing Bed-load Discharge and Channel Adjustment in a Cobble Bed River for Flood Control Channel Design

by

Brad R. Hall<sup>1</sup>, William A. Thomas<sup>1</sup>, and Monte L. Pearson<sup>2</sup>

The Hydraulics Laboratory, US Army Engineer Waterways Experiment Station, has computed the existing condition sedimentation regime of the Truckee River at Reno, NV, in support of channel design modifications for flood control. The sedimentation analysis was complicated by the cobble-sized bed materials found in the channel, several existing bridges in the study area that significantly affect the channel hydraulics at flood discharge, and water diversion drop structures that provide local storage zones for bed-load transport.

Bed-load measurements on the Truckee River at the upstream end of the study reach were not available. The inflowing sediment load was determined by calculating the equilibrium sediment transport rate for a range of water discharges for a reach of the Truckee River within the study area called the equilibrium reach. The equilibrium reach is geomorphically stable and exhibits characteristics in channel planform, bed material, and channel banks that are similar to that portion of the Truckee River immediately upstream of the study area.

The one-dimensional sediment transport model "Sedimentation in Stream Networks," TABS-1, was used to quantify sedimentation processes. Sedimentation model adjustment was completed by comparing observed rating curve changes due to channel aggradation with computed shifts in the rating curve. Average annual and design flood sedimentation were quantified with the TABS-1 model.

## INTRODUCTION

### Study Area

The Truckee River study reach is located near Reno, NV, and extends from the Vista gage at approximately River Mile (RM) 43.9 to just upstream of the Booth Street bridge at RM 53.0. A map of the study area is shown in Figure 1. The Truckee River is a perennial stream characterized by pool and riffle channel morphology. Several bridge crossings and water diversion structures are found in the study reach. Man-made channel modifications, especially within the upper 3 miles of the study reach, have limited the amount of channel migration. Bed material size decreases through the reach, and the channel bed is armored at base flow discharge.

---

<sup>1</sup>. Research Hydraulic Engineer, Hydraulics Laboratory, US Army Engineer Waterways Experiment Station, 3909 Halls Ferry Road, Vicksburg, MS 39180

<sup>2</sup>. Senior Research Scientist, Geotechnical Laboratory, US Army Engineer Waterways Experiment Station, 3909 Halls Ferry Road, Vicksburg, MS 39180

## Approach

The Hydraulics Laboratory, US Army Engineer Waterways Experiment Station, computer program "Sedimentation in Stream Networks," TABS-1, was used to quantify channel response to hydrologic variations. The Hydraulics Laboratory developed TABS-1 as a research tool to incorporate new and enhanced sediment transport technology in the widely used HEC-6 moveable-bed model (US Army Engineer Hydrologic Engineering Center, 1977). A detailed description of the assumptions, limitations, and data requirements for the TABS-1 model is provided in Appendix A of Copeland and Thomas, 1989. The study reach of the Truckee River lacks sampled bed-load transport rates, suspended sediment concentrations, and morphological surveys documenting lateral and vertical river channel migration to permit the normal numerical model adjustment and verification. This study combined a theoretical treatment of sediment transport with observed channel morphology to quantify channel bed dynamics associated with gravel and boulder streams. In addition to quantifying instantaneous sediment transport rates, the analysis allowed evaluation of channel bed aggradation and degradation response to long-term hydrologic sequences.

## FIELD DATA

### Hydrological and Geometric Data

There are three United States Geological Survey (USGS) stream gages in the Truckee River study reach (Figure 1). The gages and the period of record for streamflow data at each gage are listed in the following tabulation.

USGS Stream gages in the study reach.

<u>Gage</u>	<u>Drainage Area, square miles</u>	<u>Period of Record</u>
Truckee River at Reno, NV USGS Gage No. 10348000	1067	1907 - present
Truckee River near Sparks, NV USGS Gage No. 10348200	1070	1977 - present
Truckee River at Vista, NV USGS Gage No. 10350000	1431	1900 - present

Channel geometry was developed from channel and overbank surveys completed in 1975. Bridge geometry was surveyed in 1989 including low and high chord profiles and bridge pier location and orientation.

### Sampled Sediment Transport

An extensive review of several technical libraries indicates that no measurements of bed-load transport have been documented for the project reach of the Truckee River. Sampling of suspended sediment concentration by the USGS in the Truckee River in the Reno, NV, area has occurred on a sporadic basis. Provisional records from the USGS provide the concentrations listed in Table 1. Suspended sediment concentration and river discharge have been sampled at the McCarran Boulevard bridge (RM 47.7) as part of separate water



quality and water supply studies (Table 2).

#### Bed Material Samples and Gradation

Twenty sediment samples were collected from the channel bed, bars, and bank at 15 locations spaced along the 9-mile study reach in June 1989. Samples were taken near the water's edge, from the channel bed, and from locations on point- and mid-channel bars. Bed material sample locations are plotted in Figure 2 along with a channel thalweg survey and computed water surface profile for a flood discharge of 25,000 cfs. Wolman count (Wolman, 1954) bed surface material gradations were collected (Water Engineering and Technology, Inc., 1989) providing an estimate of the surficial coverage of the channel bed by coarse grain sediments (i.e., cobbles) which are generally omitted in bulk material samples. Profiles of the percent finer for each sediment size class sampled in the grab samples and the Wolman counts used for the numerical model application are given in Figures 3 and 4, respectively. Grain size classifications follow the American Geophysical Union standard recommended by Lane, 1947.

#### Channel Characteristics

Field observations in 1989 of the project area indicate that the Truckee River can be generally considered as three separate and distinctive reaches in terms of channel and bed characteristics. These reaches are identified as (a) the reach from the upstream limit of the study area to the Highway 395 bridge, (b) from Highway 395 bridge to just downstream of the McCarran Avenue bridge, and (c) the reach from the McCarran Avenue bridge to the downstream limit of the study area at the Vista gage. Each reach is characterized by distinctive bed material sizes and channel characteristics.

The reach upstream of Highway 395 bridge is an armored pool and riffle channel. The river channel is incised into the coarse sediments of the Tahoe and Donner Lake outwash deposits. The large boulders of the Tahoe and Donner Lake formations are apparently armoring the bed causing an irregular series of riffles and pools whose distribution is controlled by the intersection of the Truckee River with boulder beds in the underlying deposits. The channel is relatively straight with local high energy gradients in the boulder riffles. Within this reach, bridge abutments and piers have caused local scour and deposition in the "downtown" subreach (RM 51.7 to RM 52.2). There is a noticeable absence of boulders in the river channel in the downtown subreach. Excavations adjacent to the channel indicate that boulders are present in the alluvial materials adjacent to the subreach, indicating that either the boulders were removed from the river channel since the existing channel improvements were constructed, or gravel and cobble sediments have deposited and covered the boulders in the lower energy gradient region upstream of the bridges. With the exception of the downtown subreach, the principal geomorphic activity of the Truckee River in this reach appears to be gradual bed degradation and winnowing of the finer (sand and gravel) materials encountered in the outwash deposits. As the Truckee continues to degrade slowly in this reach, the bed will maintain an armor of cobbles and boulders derived from the outwash deposits.

From the Highway 395 bridge to McCarran Avenue bridge, the Truckee River exhibits a slightly meandering planform with a marked decrease in the size of

the bed material. Several types of bars occur including point-, alternate-, and mid-channel bars. This reach is apparently a sediment storage reach where the coarse bed load that passes through the upstream reach is gradually deposited in several river bars. The bars are armored by gravels and cobbles. The distribution of the alternate and point bars suggest that the coarser point bars are formed and maintained by higher discharges and the alternate bars by more frequent lower stage flows (Water Engineering and Technology, Inc. 1989). This reach is generally experiencing slow lateral migration through point bar growth and bank migration.

Downstream of McCarran Avenue Bridge, the Truckee River changes to a gently meandering channel which is incising into fine-grained cohesive alluvium. This alluvium consists of slack-water deposits of silty clays that were most likely deposited during an earlier blockage of the Truckee River at Vista. The bed consists of irregularly distributed scour pools incised into the cohesive deposits. Gravel material appears infrequently on the bed, which generally consists of sand or a clean erosional flute in the underlying silty clays. The number of bars decreases considerably in this lower reach as the channel generally decreases in sinuosity. Steep channel banks may be unstable locally as indicated by several large rotational slides.

#### SEDIMENTATION ANALYSIS

##### Stability of the Truckee River at Reno Stage-Discharge Curve

The stage-discharge rating curve developed by the USGS for the Truckee River at Reno, NV, gage (No. 10348000) was reviewed for any significant changes in the rating. The gage is located near the Highway 395 bridge at approximately RM 50.6. The measurements indicate a very stable stage-discharge relationship through 1977. After 1977, a slight increase in stage over time for low discharges can be detected. The rating curves used through 30 September 1977, 3 February 1982, and 17 February 1986 are compared in Figure 5. The rating curves indicate that for discharges less than 1,000 cfs, the stage has increased approximately 0.5 ft at the gage. The increase in stage for a given discharge rapidly diminishes for discharges greater than 1,000 cfs. Possible reasons for the change in the stage-discharge relationship are (a) a gradual channel aggradation at the gage location, and/or (b) changes in the relative roughness characteristics of the channel at discharges less than 1,000 cfs, and/or (c) changes in the channel morphology that has altered the stage-discharge relationship. The specific reason for the change in stage-discharge relationship cannot be determined from the rating curve records. However, if the change can be attributed to channel aggradation, the aggradational trend indicates that channel fill is occurring at a sluggish rate and that the aggradational trend does not significantly effect the stage discharge relationship for discharges greater than 10,000 cfs.

##### Sedimentation Model

Two modifications were made to the TABS-1 model for this study. The first accounts for the presence of bridge piers and girders in the geometric calculations for additional wetted perimeter and reduced flow area at bridge cross sections. The calculations are similar to the "normal bridge" method in the HEC-2 Water Surface Profile model (US Army Engineer Hydrologic Engineering

Center, 1982). The second modification allows for increasing the maximum transportable grain size in the computations. The maximum transportable grain size in previous versions of TABS-1 was 64 mm. A significant amount of the bed material in the study area is of a diameter greater than 64 mm. Thirteen grain size classes between 0.0625 mm and 512 mm were used in this study.

#### Hydraulic Roughness

Estimates of the sediment transport potential are dependent upon the proper designation of the hydraulic roughness. The roughness coefficients used for the channel portion of the hydraulic calculations were estimated with the analytical roughness predictors contained in the "Hydraulic Design Package for Flood Control Channels" (SAM). The SAM algorithm was developed at the Hydraulics Laboratory and computes a Manning's  $n$  value based on bed material grain size distribution and the relative roughness of the bed material to the channel hydraulic conditions. The Manning's  $n$  is calculated using the roughness predictors developed by either Brownlie (1983) or Limerinos (1970). The Limerinos relationship is better suited to roughness prediction for coarse grained channels with no significant bed forms. The computed values of Manning's  $n$  are 0.029 for the river reach from Vista gage (RM 43.9) to the Steamboat Creek confluence (RM 45.2), 0.035 from Steamboat Creek to the Lake Street Bridge (RM 51.9), 0.030 from Lake Street Bridge to Arlington Street Bridge (RM 52.3), and 0.035 upstream of Arlington Street Bridge.

#### Determination of Inflow Sediment Load

Since bed-load measurements on the Truckee River at the upstream end of the study reach were not available, the sediment inflow to the study area was determined by calculating the equilibrium sediment transport rate for a range of water discharges for selected reaches of the Truckee River where sediment transport is in equilibrium with the bed materials. This reach of river is termed the "equilibrium reach." For gravel and cobble transport the portion of the Truckee River from approximately RM 50.5 to 51.5 exhibits similar characteristics in channel planform, bed material, and channel bank characteristics as that portion of the Truckee River immediately upstream of the study area. For bed-load transport of sand, the downstream limit of the study area (RM 43.9 to RM 45.3) is used for the equilibrium transport calculations. The locations of these reaches are shown in Figure 6.

Determining the equilibrium bed-load quantity requires an iterative application of TABS-1 on the equilibrium reach until the estimated inflowing load for all size classes to the equilibrium reach is approximately equal to the average transport capacity (by size class) in the reach with only minor amounts of aggradation and degradation. Excessive scour should not be computed in equilibrium reach calculations since excessive scour indicates that the coarse bed materials are being removed from the bed and the channel is not armoring. The bed gradation at the end of the equilibrium reach calculations should be similar to the bed material gradation at the beginning of the simulation. If this condition is met, then the bed material gradation is in equilibrium with the computed transport rate.

#### Equilibrium Bed-load Transport of Gravels and Cobbles

Several sediment transport functions were tested for the equilibrium bed-load

calculations. The Meyer-Peter and Muller (MPM) bed-load equation (Meyer-Peter and Muller, 1948) provided the most consistent bed elevation variation and uniform transport rate by size class for the equilibrium reach, and was chosen for this study. The equilibrium sediment load for discharges of 1,000, 10,000, and 30,000 cfs for a simulated duration of 30 days at 0.1-day time-steps was computed. The calculated equilibrium bed load of gravel and cobble in the equilibrium reach for discharges of 1,000, 10,000, and 30,000 cfs is shown in Figure 7.

Published research on critical shear stress values for gravel transport indicates that there is a wide variability in the recommended method and appropriate value of critical shear stress. The equation used in this study to calculate dimensionless shear stress is:

$$\tau^* = \frac{\gamma R S}{(\gamma_s - \gamma) D}$$

where  $\tau^*$  is the dimensionless critical shear stress,  $\gamma$  is the specific weight of water,  $R$  is the hydraulic radius,  $S$  is the slope of the energy gradient,  $\gamma_s$  is the specific weight of the sediment, and  $D$  is the nominal grain diameter of the sediment particle. A practical application of the MPM bed-load transport equation in a steep gravel-bed river is given in Carson and Griffiths (1989). They determined that raising the value of  $\tau^*$  in the MPM equation from 0.047 to 0.059 gave the best agreement for observed gravel transport on a braided gravel-bed river on a channel slope of 0.0048. Wiberg and Smith (1987) developed a method of computing  $\tau^*$  based on grain size and near-bed hydrodynamic characteristics for coarse, mixed grain size bed sediments. Their results indicate that the value of  $\tau^*$  for sediments with the characteristics of Truckee River riffles is in the range of 0.03 to 0.06. Boulder transport due to a dambreak flood surge on the Rubicon River in California was analyzed by Scott and Gravlee (1968). They determined the maximum tractive force at several locations by measuring the diameter of the maximum size boulder moved by the flood surge, the water surface slope, and the depth of flow. The value of  $\tau^*$  for cobble and boulder transport measured by Scott and Gravlee varied between 0.025 and 0.08. Due to the variability of analytically computed and field measurements of  $\tau^*$  on gravel and boulder bed rivers, and the cited references that indicate that critical shear stress should be increased for determining bed-load transport of gravel, the recommended value of  $\tau^*$  of 0.047 in the MPM bed-load transport equation was retained for computing bed-load sediment transport.

#### Equilibrium Bed-load Transport of Sands

Negligible amounts of sediments smaller than coarse sand (0.5 mm) are present in the bed material samples upstream of the gravel and cobble equilibrium reach (RM 50.5 to 51.5). Thus bed material transport of sediments this size class and smaller could not be determined from the equilibrium reach calculations described in the previous paragraphs. To estimate the quantity of sediment smaller than coarse sand entering the upstream end of the study reach and moving as bed load in the downstream end of the study reach, additional calculations were performed for the Truckee River between Steamboat Creek (RM 45.3) and the Vista gage (RM 43.9). To be consistent with the mode (i.e., bed load) of sediment transport being simulated through the upstream

end of the study reach, the Meyer-Peter and Muller transport function was used. Additional fine sediment may be transported through the study area as suspended load, but sampled suspended load data indicate that the flow has sufficient energy to pass the suspended load through the study reach as wash load. The suspended sediment data sampled at the Sparks gage (RM 50.4), McCarran Boulevard (RM 47.7), and the Vista gage (RM 43.9) are compared in Figure 3. Regression analysis indicates insignificant differences in the water discharge versus concentration data for each gage. The hydraulic characteristics vary from a channel slope of approximately 0.005 at the Truckee River at Sparks gage to approximately 0.0005 at the Truckee River at Vista gage, indicating that the suspended sediment is actually wash load and does not need to be considered in the analysis of channel bed profile changes.

Bed material samples from channel bars at RM 45.6 indicate that 10 percent of the material is finer than 0.5 mm. Preliminary calculations using total load sediment transport equations (e.g., Tofalletti, Laursen) indicate that transport of material smaller than 0.5 mm would pass through the upper end of the study area as suspended load. Thus, the sediment load for medium sand, fine sand, and very fine sand determined in this reach can be added to the load calculated for gravel and cobble sediment inflow to the study area. The total (sand, gravel, and cobble) bed-load inflow rating curve developed using the MPM relationship is plotted in Figure 9. The equilibrium reach bed load was adjusted by comparing computed long term channel response with observed prototype channel conditions. The procedure by which the bed-load inflow transport rate was adjusted is described in the following paragraphs.

#### Long-Term Channel Response

A water discharge-exceedence frequency hydrograph that approximates the average annual hydrograph for the Truckee River at Reno for 1977-1986 was developed. The average annual hydrograph and water surface elevation at the Vista gage are tabulated below.

#### Average Annual Hydrograph Characteristics

<u>Water</u> <u>Discharge, cfs</u>	<u>Exceedence</u> <u>Frequency</u>	<u>Vista Gage</u> <u>Elevation, feet</u>
5480.	0.10	4378.5
2450.	0.20	4375.0
1410.	0.33	4373.5
707.	0.46	4373.0
375.	1.00	4372.5

#### Estimate of the Average Annual Bed Load

The hydrologic conditions for 1977-1986 for the study reach was simulated to compare computed with measured shifts in the stage-discharge rating curve for the Truckee River at Reno gage (Figure 5). Computed bed elevation changes at the end of the 9-year simulation period are plotted in Figure 10. The results indicate that extensive deposition occurs at the downstream portion of the study area. The computed rating curve shift for the 9-year simulation period for the Truckee River at Reno gage also indicates aggradation at the gage location in excess of the measured gage shift.

The simulation results using the equilibrium reach bed load (Figure 9) indicate that the computed bed-load transport into the study area is excessive. The total bed-load transport rating curve was adjusted downward until reasonable agreement between computed and observed sediment deposition quantities and zones, as measured by bed elevation changes through the study area after the 9-year simulation period, and comparable changes in both magnitude and trend in the observed shift of the stage-discharge rating curve for the Truckee River at Reno gage were obtained. The bed-load sediment inflow rating curve was reduced to 33 percent of the bed-load transport rate computed from the equilibrium reach. Further reduction of the bed-load inflow rate resulted in excessive scour at the upstream end of the model. The adjusted bed-load inflow rate used for existing condition simulations is plotted along with the equilibrium reach bed-load rating curve in Figure 9.

The computed rating curve shift for the Truckee River at Reno gage using the adjusted bed-load inflow rating curve is given as follows.

<u>Water</u> <u>Discharge, cfs</u>	<u>Computed</u> <u>Shift, ft</u>	<u>Observed</u> <u>Shift, ft</u>
707.	1.4	0.5
1410.	0.8	0.3
2450.	0.1	0.2
5480.	0.0	0.1

Computed bed elevation changes for the study reach after the nine year simulation period are plotted in Figure 11. Another way to display model results is to show the accumulated weight of sediment passing each cross-section. Computed accumulated bed load through the study reach after 1 year and after 9 years simulation time are plotted in Figure 12. Storage of bed material upstream of the three irrigation diversion drop structures between RM 49.1 and 50.1 during the first year of simulation is evident by the reduction in accumulated bed load in this region. This results in scour and associated increase in bed load downstream of the drop structures from approximately RM 49 to RM 48. After nine years simulation time, the storage of sediment upstream of the drop structures is filled and the channel bed is armored downstream of the drop structures, resulting in relatively uniform transport of bed load from the upstream limit of the study area at RM 53 downstream to approximately RM 48. Downstream of RM 48, a relatively uniform reduction in the total bed-load transport rate from RM 48 to RM 44 is computed, indicating sediment deposition and channel aggradation in this reach.

The 9-year simulation indicates that significant amounts of deposition occur downstream of McCarran Avenue Bridge at RM 47.7. Extensive bar development is not apparent in the prototype at this location. Sediment storage in the prototype is observed primarily between Highway 395 and the McCarran Avenue bridge. Possible reasons for this discrepancy between the computed and observed conditions are errors in the computed hydraulic conditions downstream of RM 47.7 resulting in computed sediment transport being too low, or errors in the computed hydraulic conditions between Highway 395 and McCarran Avenue Bridge resulting in computed sediment transport capacity being too high in this reach.

The 9-year sedimentation analysis of the study reach provides a means for estimating the average annual bed-load transport at several locations. The

TABS-1 results indicate sediment storage between RM 47.3 and RM 44.4. The average annual bed load at the upstream study limit, RM 47.3, RM 44.4, and the downstream study limit are given in Table 3. The computed average annual bed-load inflow to the study reach is approximately 51,000 tons per year. Sampled suspended sediment concentration combined with average annual flow-exceedence statistics yields an average annual suspended sediment discharge of 250,000 tons per year. The computed bed-load discharge is approximately 17 percent of the total sediment discharge. The computed average annual trap efficiency for bed load of the study reach is 71 percent.

#### Single Event Analysis

The 100-year recurrence interval flood simulation was completed to assess the quantity and location of sediment scour or deposition within the project reach for the design flood. To minimize the effects of initial bed material and bed profile gradations, the flood hydrograph was appended to the end of the 9-year simulation of average annual hydrographs. The differences in bed elevations and sediment scour or deposition between the end of the 9-year spin-up hydrograph and the 100-year flood hydrograph were used to quantify 100-year flood sedimentation parameters. Computed bed elevation changes at the end of the 100-year flood hydrograph are plotted in Figure 13. The accumulated bed load passing each cross section in the study reach at the end of the 100-year flood is plotted in Figure 14. The 100-year flood simulation results indicate the following:

- a. Passage of the inflowing sediment load through the downtown reach to approximately RM 51.8.
- b. Channel scour and associated increase in sediment load from 50.8 through 51.8. The scour is primarily due to channel adjustment and armoring to the high water discharge.
- c. Transport of the increased load to RM 49.
- d. Gradual trapping and reduction of the sediment load from RM 49 to RM 47.
- e. Transport of the reduced load out of the study reach.

#### SUMMARY AND CONCLUSIONS

Assessment of channel stability on instantaneous hydraulic conditions (e.g., shear stress, depth-averaged velocity, and stream power) does not consider long-term sediment transport conditions, and does not address the effects of sediment inflow to the study area on channel stability. Channel changes result from the balance of sediment transport into a reach, the sediment transport capacity of the reach, and the sediment availability in the reach. Simulation of the sediment transport through the project reach is required to address the sediment balance and subsequent channel stability.

Sediment transport theory was combined, using the TABS-1 numerical model, with evidence developed from field reconnaissance to quantify the bed-load inflow rating curve for the Truckee River at Reno, NV. The technique used is called the equilibrium reach method, and develops the sediment load based on sediment

transport theory, channel thalweg stability, and bed material gradation stability. Multi-year simulations using the equilibrium reach bed-load inflow resulted in excessive deposition, as indicated by the field reconnaissance and geomorphological analysis, at the downstream end of the numerical model. To compensate for this discrepancy, the bed-load inflow rating curve was adjusted downward to 33 percent of the equilibrium reach sediment inflow. TABS-1 simulation using the adjusted sediment load inflow rating curve resulted in reasonable agreement between observed and computed stage-discharge rating curve shifts; however, the model computed excessive sediment deposition downstream of the prototype sediment deposition zone. Additional adjustments are needed to reduce degradation between RM 53 and 51 and aggradation between RM 46 and 44. However, the study approach allows a reasonable estimate of annual sediment yield for flood control channel design. The bed-load inflow value of 51,000 tons per year may be high, but the design value is bracketed between that and the calculated outflow of 15,000 tons per year.

#### ACKNOWLEDGMENTS

The tests described and the resulting data presented herein, unless otherwise noted, were obtained from research conducted under the Civil Works Program of the United States Army Corps of Engineers by the US Army Engineer Waterways Experiment Station, Vicksburg, MS. Permission was granted by the Chief of Engineers to publish this information.

#### REFERENCES

- Brownlie, W. R. (1983). 'Flow depth in sand-bed channels', *Journal of the Hydraulics Division*, American Society of Civil Engineers, 109(7), 959-990.
- Carson, M. A. and Griffiths, G. A. (1989). 'Gravel transport in the braided Waimakariri River: mechanisms, measurements and predictions', *Journal of Hydrology*, 109, 201-220.
- Copeland, R. R. and Thomas, W. A. (1989). 'Corte Madera Creek sedimentation study', Technical Report HL-89-6, US Army Engineer Waterways Experiment Station, Vicksburg, MS.
- Lane, E. W. (1947). 'Report of the subcommittee on sediment terminology', *Transactions*, American Geophysical Union, 28, 936-938.
- Limerinos, J. T. (1970). 'Determination of the Manning coefficient from measured bed roughness in natural channels', US Geological Survey Water Supply Paper 1989-B, US Government Printing Office, Washington, DC.
- Meyer-Peter, E. and Muller, R. (1948). 'Formulas for bed-load transport', *Report on the Second Meeting of International Association for Hydraulic Research*, Stockholm, Sweden, 39-64.
- Scott, K. M. and Gravlee, G. C. (1968). 'Flood surge on the Rubicon River, California - hydrology, hydraulics and boulder transport', US Geological Survey Professional Paper 422-M, US Government Printing Office, Washington, DC.



US Army Engineer Hydrologic Engineering Center. (1977). 'HEC-6, Scour and deposition in rivers and reservoirs users manual', Davis, CA.

US Army Engineer Hydrologic Engineering Center. (1982). 'HEC-2, Water surface profiles users manual', Davis, CA.

Water Engineering and Technology, Inc. (1989). 'Geomorphic analysis of Truckee River from RM 56 to RM 43', Draft Report, US Army Engineer District, Sacramento, CA.

Wiberg, P. L. and Smith, J. D. (1987). 'Calculations of the critical shear stress for motion of heterogenous sediments', *Water Resources Research*, 23(8), 1471-1480.

Wolman, M. G. (1954). 'A method of sampling coarse river bed materials', *Transactions, American Geophysical Union*, 35, 951-956.

Table 1. Sampled suspended sediment concentration, USGS data base

Truckee River near Sparks, NV USGS Gage No. 10348200

<u>Date</u>	<u>Water discharge, cfs</u>	<u>Concentration, mg/l</u>
5 Feb 1980	346	26
28 Feb 1980	790	23
12 Mar 1980	533	14
20 Mar 1980	480	14
4 Apr 1980	479	5
10 Apr 1980	563	9

Truckee River at Vista, NV USGS Gage No. 10350000

<u>Date</u>	<u>Water discharge, cfs</u>	<u>Concentration, mg/l</u>
9 May 1979	1600	18
20 Dec 1981	7500	950
13 Mar 1983	5500	884

Table 2. Sampled suspended sediment concentration,  
Truckee River at McCarran Boulevard.

<u>Date</u>	<u>Water discharge, cfs</u>	<u>Concentration, mg/l</u>
17 Dec 1985	347	5
21 Jan 1986	682	9
20 Feb 1986	14000 *	1345
25 Mar 1986	3430 *	1407
15 Apr 1986	2699	93
5 May 1986	2814	57
12 May 1986	2636	22
21 May 1986	2407	32
10 Jun 1986	1266	31
7 Jul 1986	628	32

\* estimated water discharge from Truckee River at Reno USGS stream gage records

Table 3. Average annual bed load of the Truckee River

<u>Location</u>	<u>Bed load, Tons per Year</u>			<u>Total</u>
	<u>Sand</u>	<u>Gravel</u>	<u>Cobble</u>	
RM 53.1	28,960	22,040	17	51,000
RM 47.3	24,420	20,130	0	44,550
RM 44.4	14,150	2,690	0	16,840
RM 43.9	12,820	1,940	0	14,760

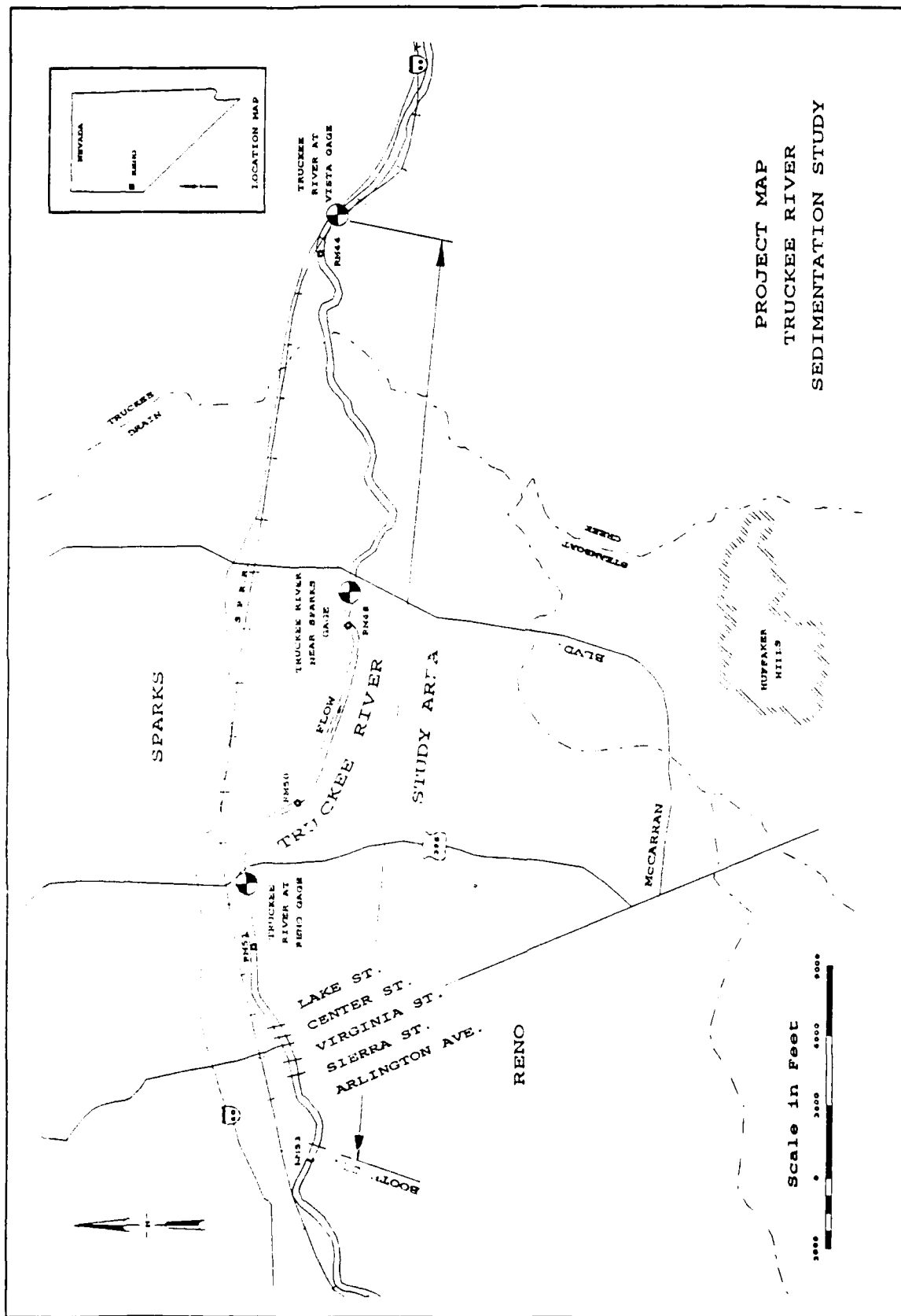


Figure 1. Vicinity map.

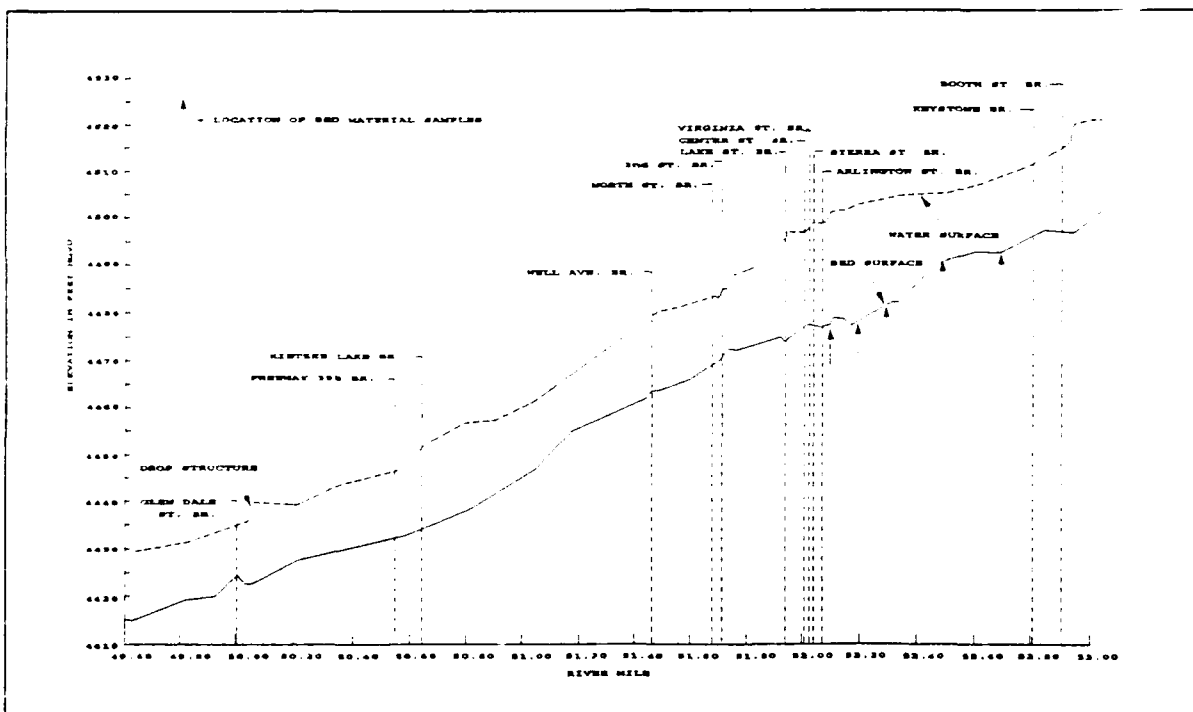
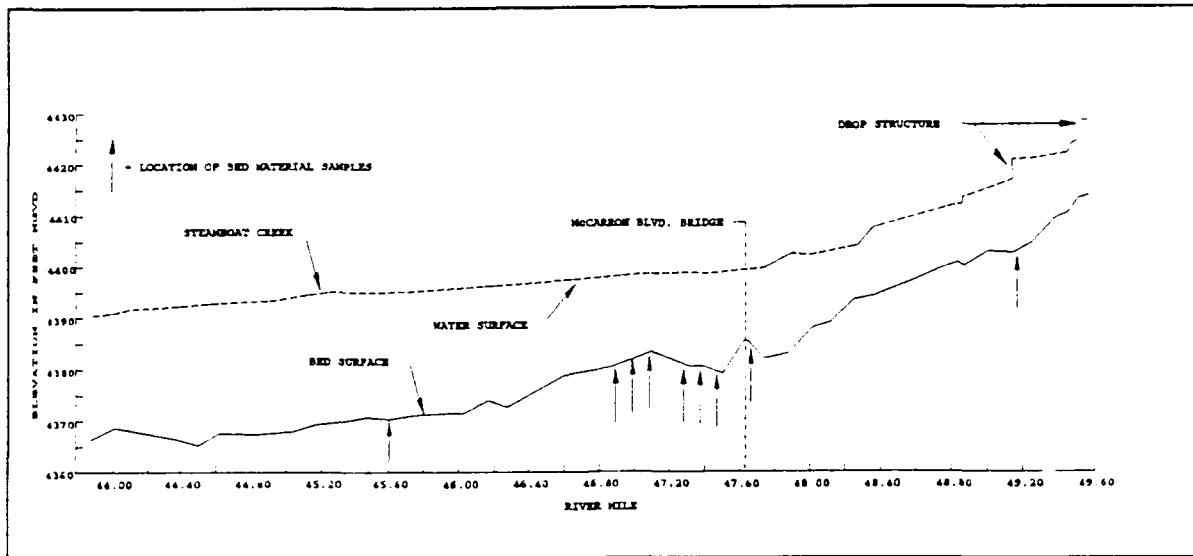


Figure 2. Bed material sample locations.

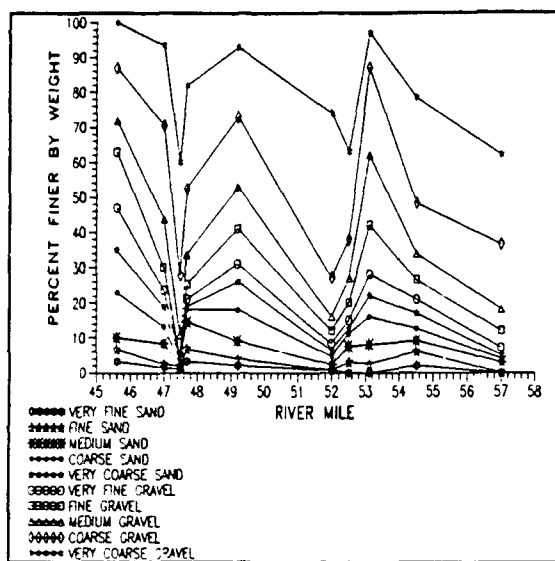


Figure 3. Bed material sample gradations.

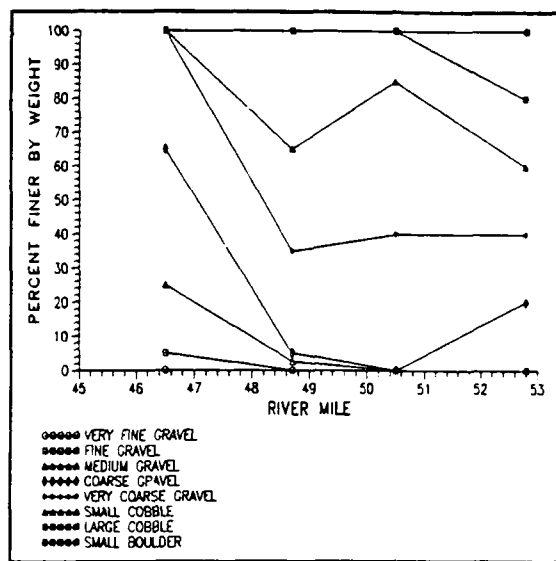


Figure 4. Wolman count material gradations.

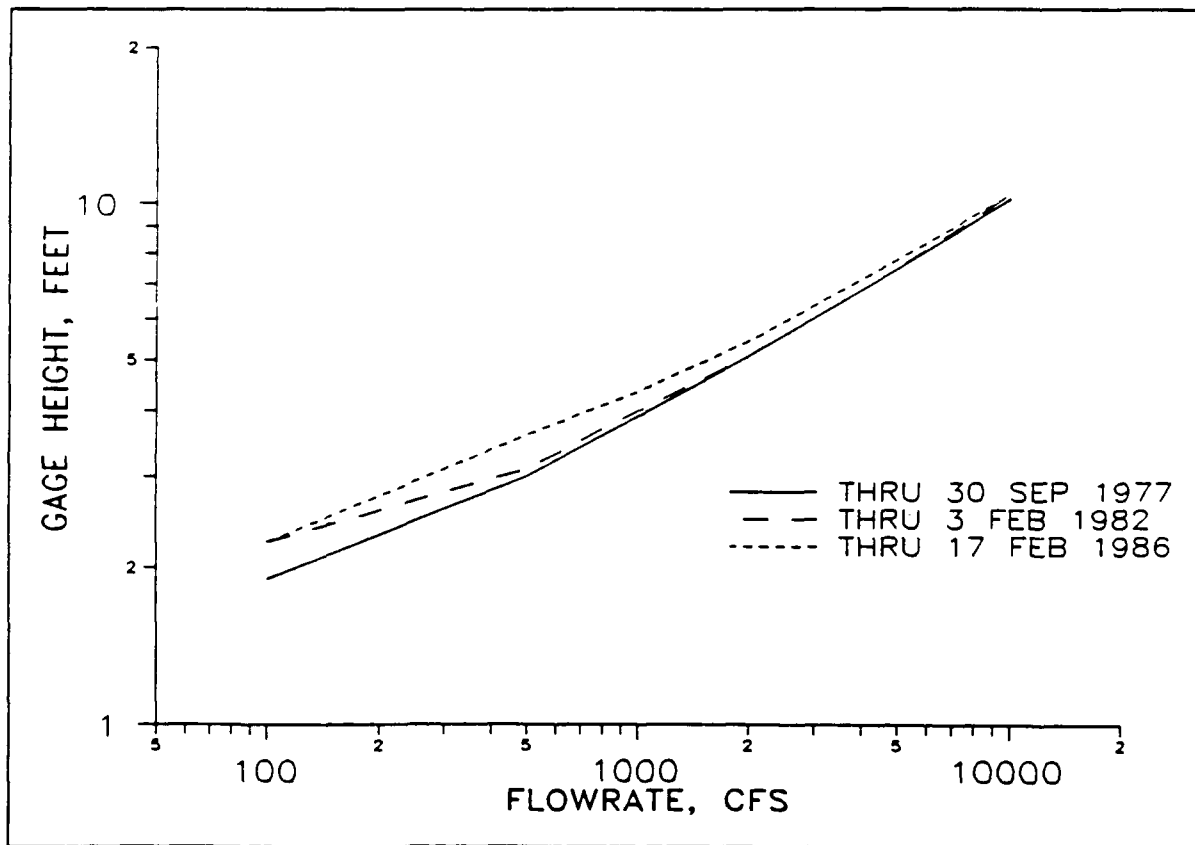
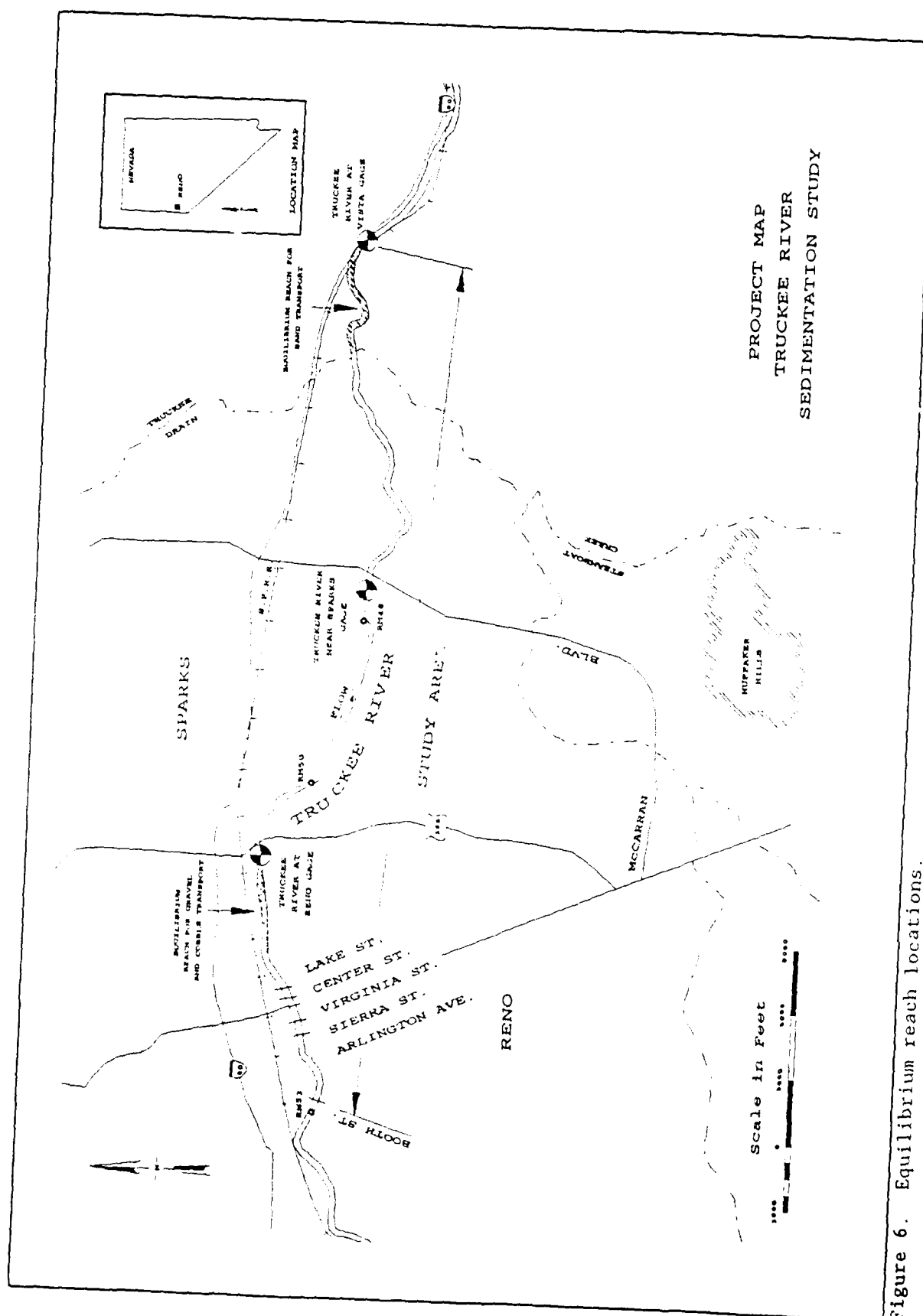


Figure 5. Stage-discharge rating curve, Truckee River at Reno, Nevada



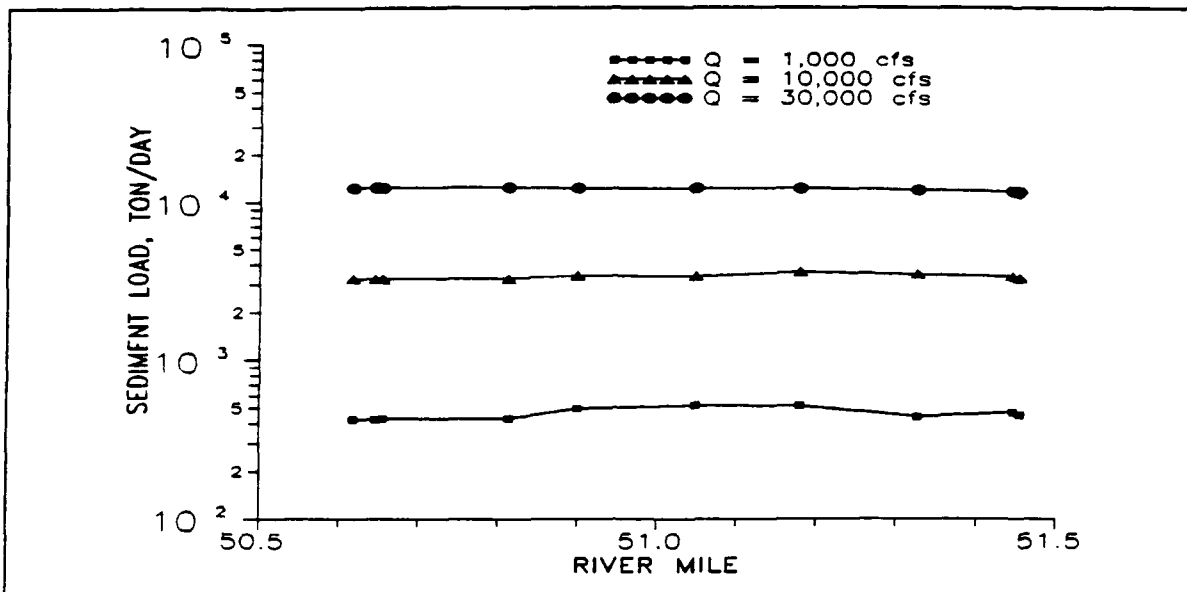


Figure 7. Equilibrium reach bed-load transport.

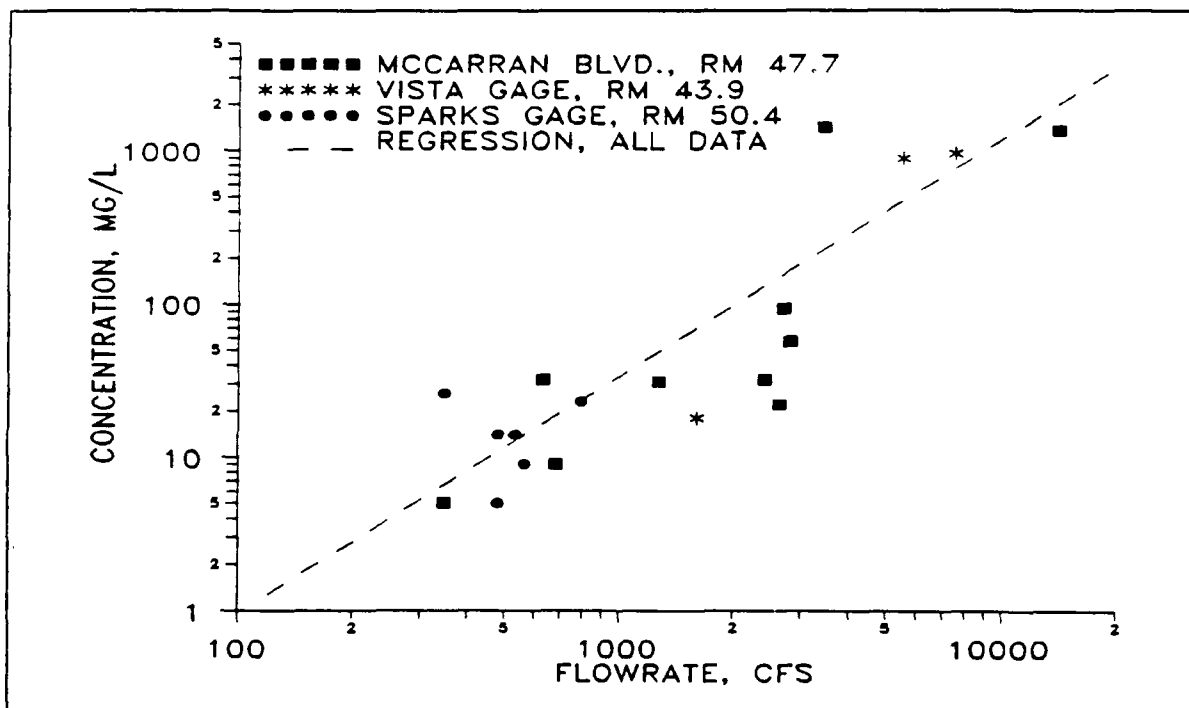


Figure 8. Sampled suspended sediment concentration.

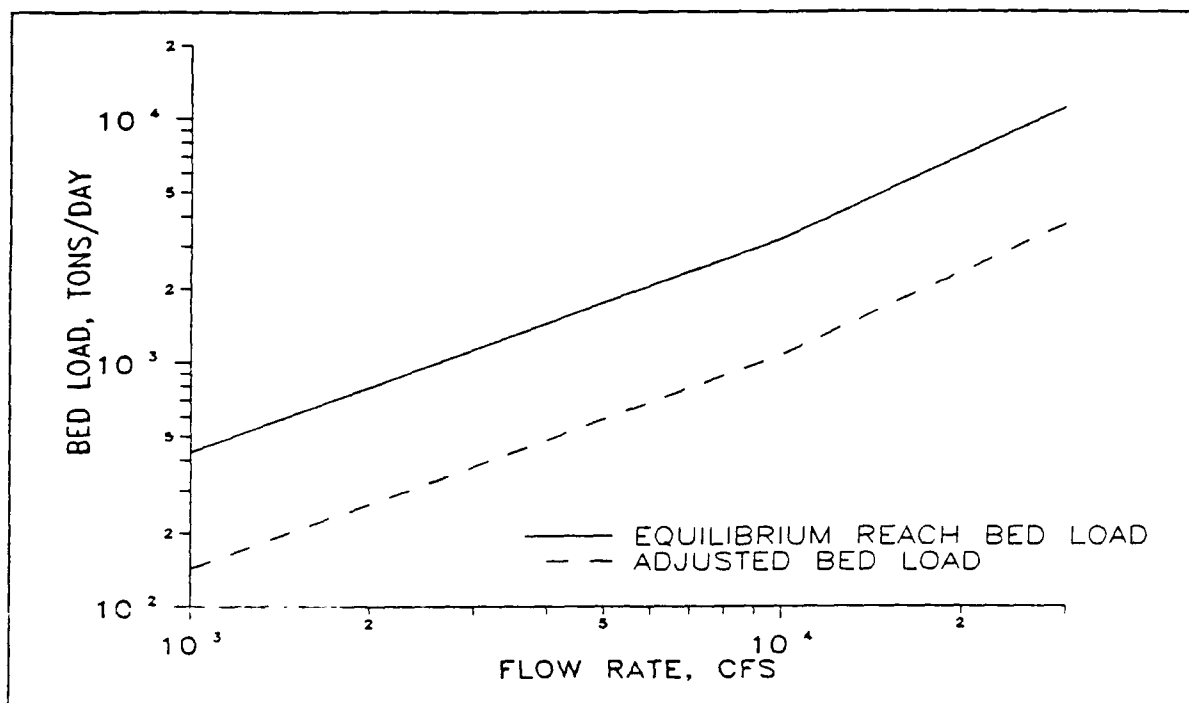


Figure 9. Bed-load inflow rating curves.

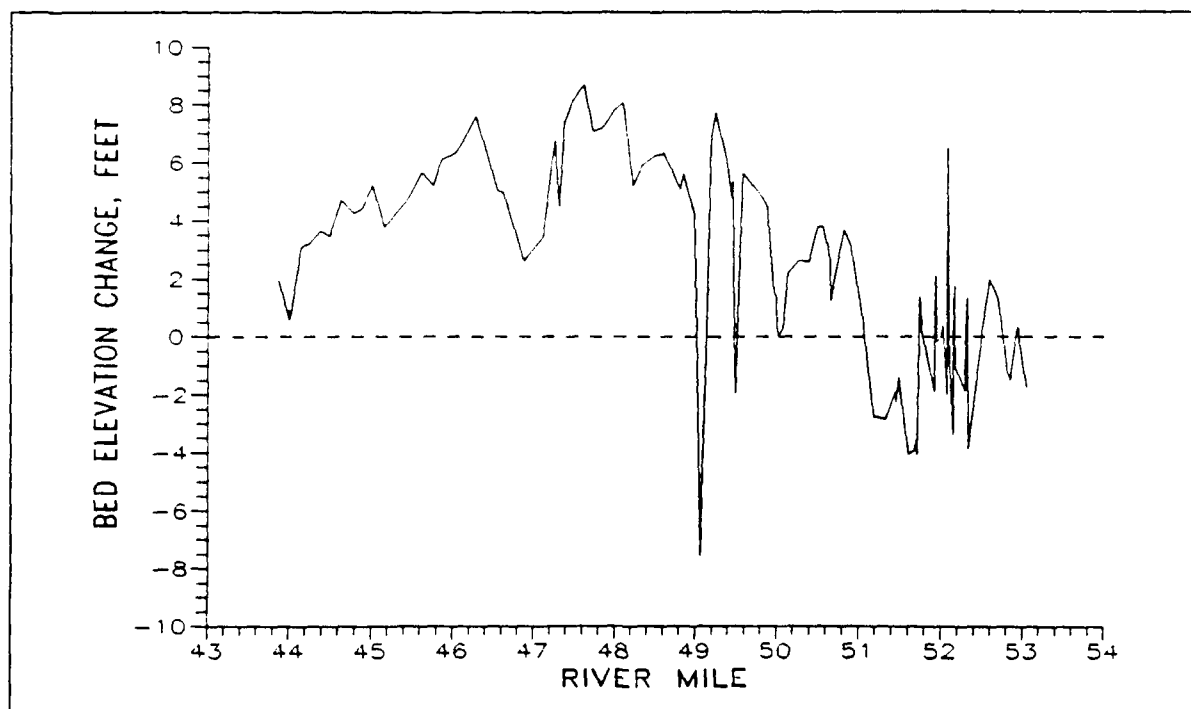


Figure 10. Bed elevation change, equilibrium reach bed-load inflow.



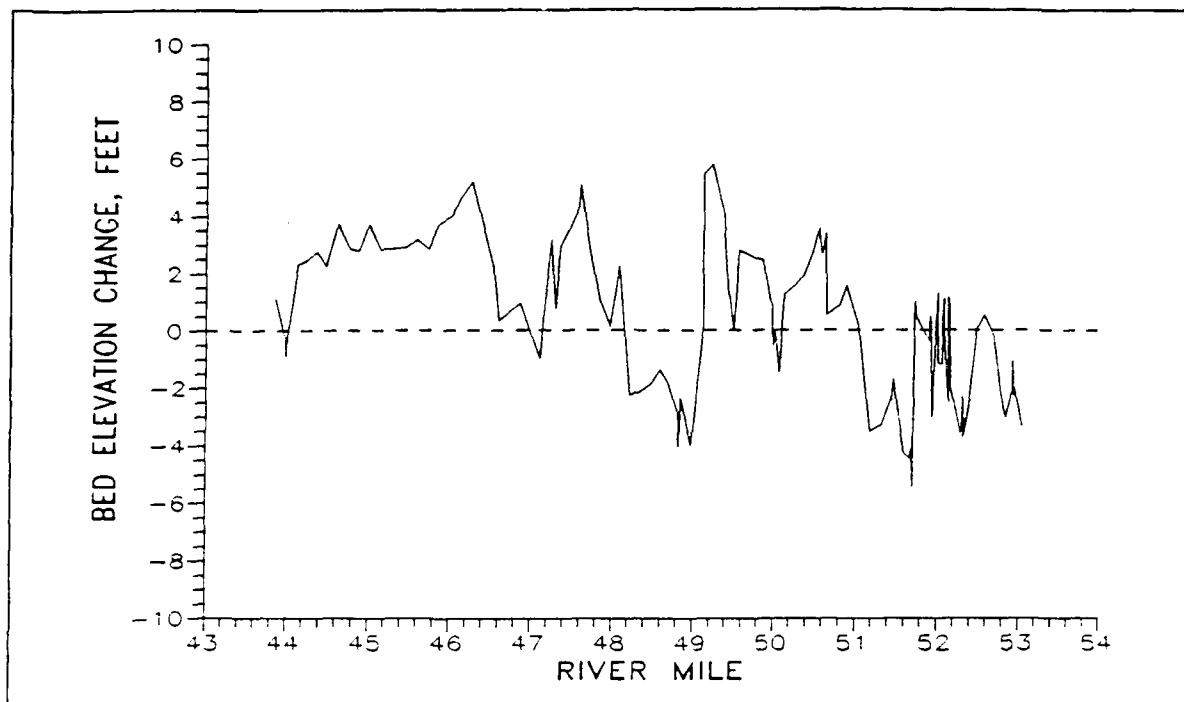


Figure 11. Bed elevation change, adjusted bed-load inflow.

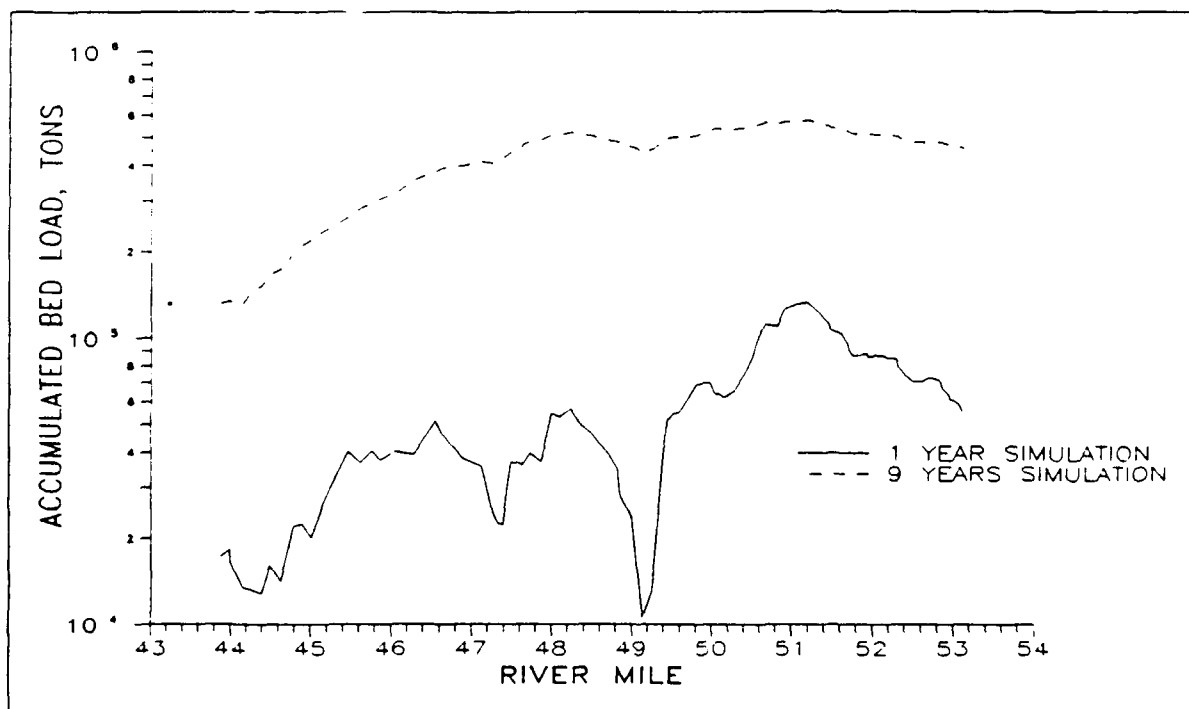


Figure 12. Accumulated bed load, adjusted bed-load inflow.

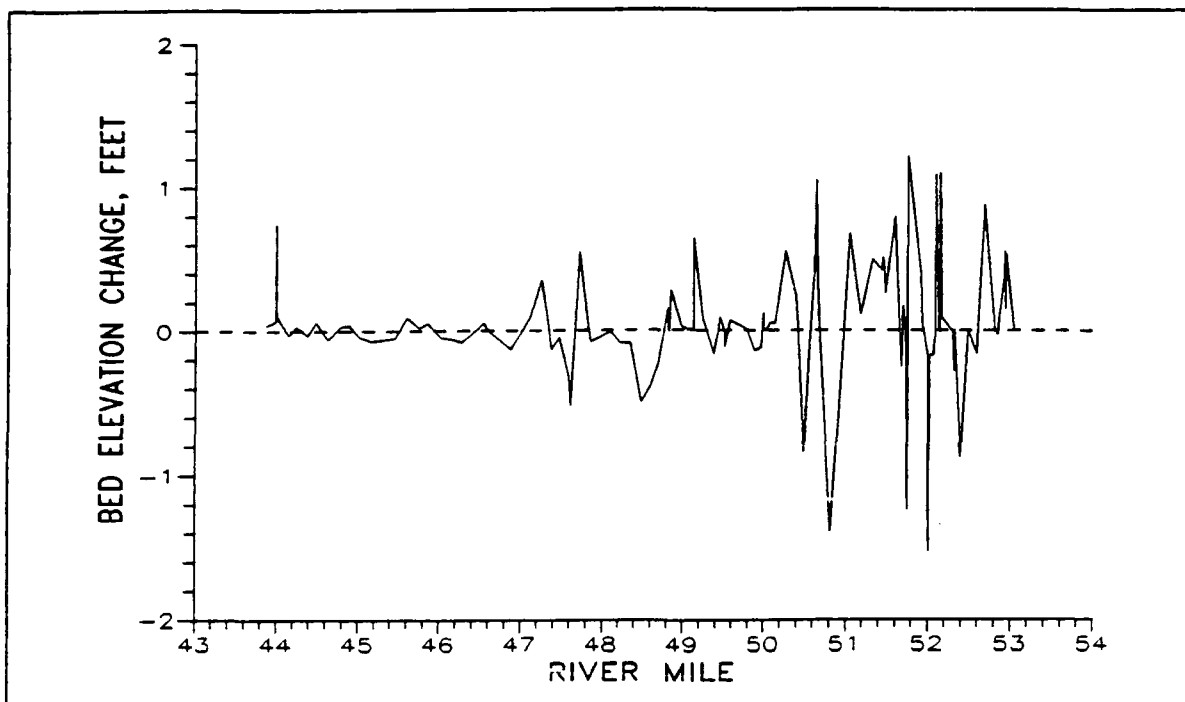


Figure 13. Bed elevation change, 100-year flood.

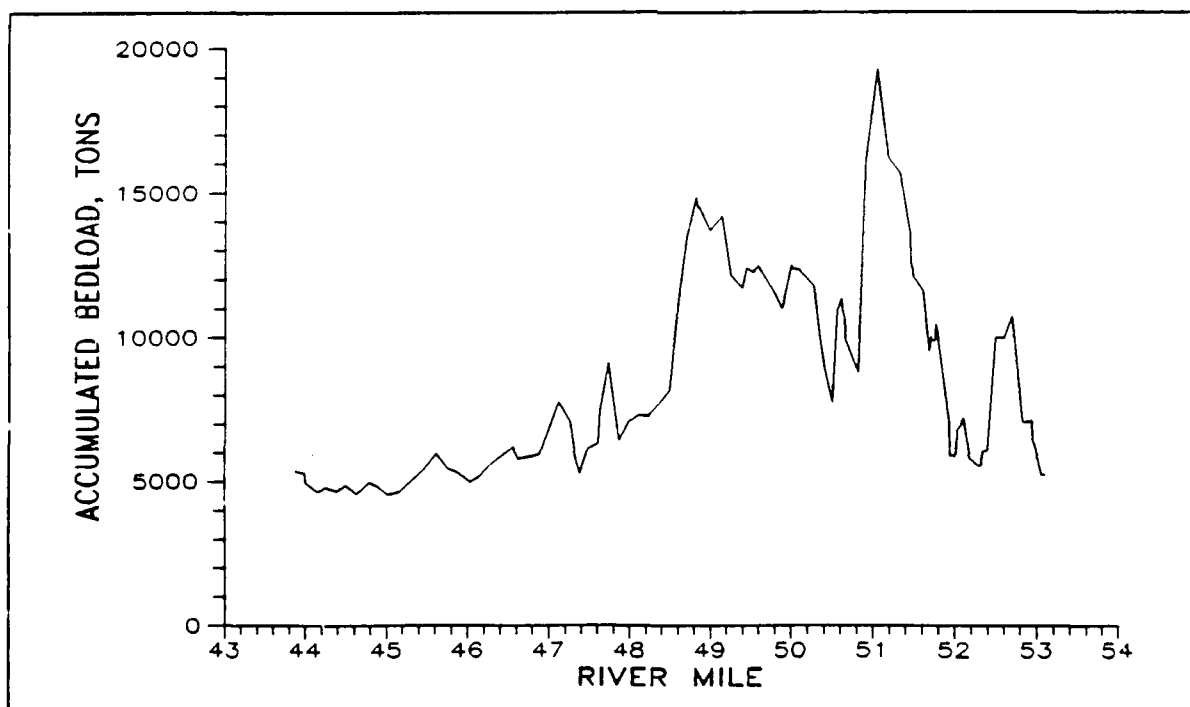


Figure 14. Accumulated bed load, 100-year flood.